This special issue of the *General Physiology and Biophysics* contains invited and peer-reviewed papers presented at the international scientific conference entitled *"Current Trends in Physiological Sciences"* held on 17–18 December 2008 in Belgrade, Republic of Serbia. It was organized under the auspices of the *Federation of European Physiological Societies*. The conference was organized through activity of the *Serbian Physiological Society* to honor Professor Richard Burian (1871–1954). He was the founder of the Institute of Medical Physiology, School of Medicine, University of Belgrade and one of the most internationally recognized physiologists at the beginning of the 20th century. Guest editors for this special issue were Vladimír Štrbák (Bratislava, Slovak Republic), Dragan Djurić (Belgrade, Republic of Serbia) and Vladimir Jakovljević (Kragujevac, Republic of Serbia). *Serbian Physiological Society* and the organizers of this conference express their gratitude to the *Institute of Molecular Physiology and Genetics* of the *Slovak Academy of Sciences*, editors of the *General Physiology and Biophysics*, and to the honorary chairman of the conference Vladimír Štrbák for their understanding and invaluable support.

Content of Special Issue

Editorial

PROFESSOR RICHARD BURIAN (1871–1954) FOUNDER OF THE INSTITUTE OF MEDICAL PHYSIOLOGY SCHOOL OF MEDICINE UNIVERSITY OF BELGRADE

A life dedicated to creative work, of high ideals, combined with a search for knowledge, truth, and giving of community service, benevolence and philanthropy.

The name of Professor Richard Anton Burian, the founder of the Institute of Medical Physiology, Belgrade, holds an honored place in the School of Medicine. He was born on 8th January, 1871 in Vienna, where he graduated from the School of Medicine (in 1894). In the period from 1895 to 1897, he published 4 papers while working as an assistant to Professor Neusser's clinic on physiological and chemical problems, and at the University chemical laboratory of Professors Liben and Mautner. In 1897, he transferred, by invitation, to the University of Leipzig, where he investigated physiological and chemical problems. He graduated in 1899 with the title *"Die dissimilations purine der sangetiere"* and after publication of his work entitled *"Due Dussunukatuibsozrube der Sazgetuere"*, he became an Assistant Professor of Physiology in 1900, under Professor Evald Hering who put him in charge of the teaching related to metabolism. During 1903, Richard Burian was proposed for a full Professorship (Physics) at *Hochschule für Bodenkultur* in Vienna. However, at Professor Dorn's invitation, Richard Burian spent the winter of 1903/4 at the famous Zoo-Oceanographic Institute in Naples. He became the head of a newly founded Department of Physiology there and after being made Professor in 1911, he stayed until the beginning of the First World War (1914). He gathered at this Institute, thanks to his commitment and enormous experience, a great number of famous scientists who had been doing research on sea invertebrates (Fuchs, Sulze, Goldchmidt, Scaffidi, Baner, Sulima). During this time, Richard Burian was named a full Professor of Medical Chemistry at the University of Innsbruck (1910) and a full professor of Physiology at the College of Veterinary Medicine in Vienna (1912).

With the outbreak of war, Richard Burian returned to Leipzig where he helped his old teacher, Professor Hering, by taking over the whole of the teaching of Physiology at the School of Medicine. Here he remained until 1916. Then, Richard Burian left Leipzig due to tensions related to the bringing of Professor Garten (from Gissen) to the the School of Medicine in Leipzig.

Although he came to Yugoslavia at the invitation of the School of Medicine in Ljubljana (today Slovenia), and though a full Professor of different disciplines at Vienna, Innsbruck, Hannover and Leipzig, it was not until 1920 that he was made, at the insistence of Professor Milan Jovanovic-Batut, a full Professor of Physiology at the newly founded School of Medicine in Belgrade.

During the winter of 1922/1923, at the School of Medicine in Belgrade, Richard Burian started with his lectures in German. However, after two years, he gave all his lectures in the Serbian language. As well as organization of all the teaching, his main concern was the setting up of the Institute of Physiology and Histology. For this purpose he was given the former building of the English-Serbian Children's Hospital. It is due to his wealth of experience, incredible energy and tremendous effort, that the Institute of Physiology and Histology was opened in 1927.

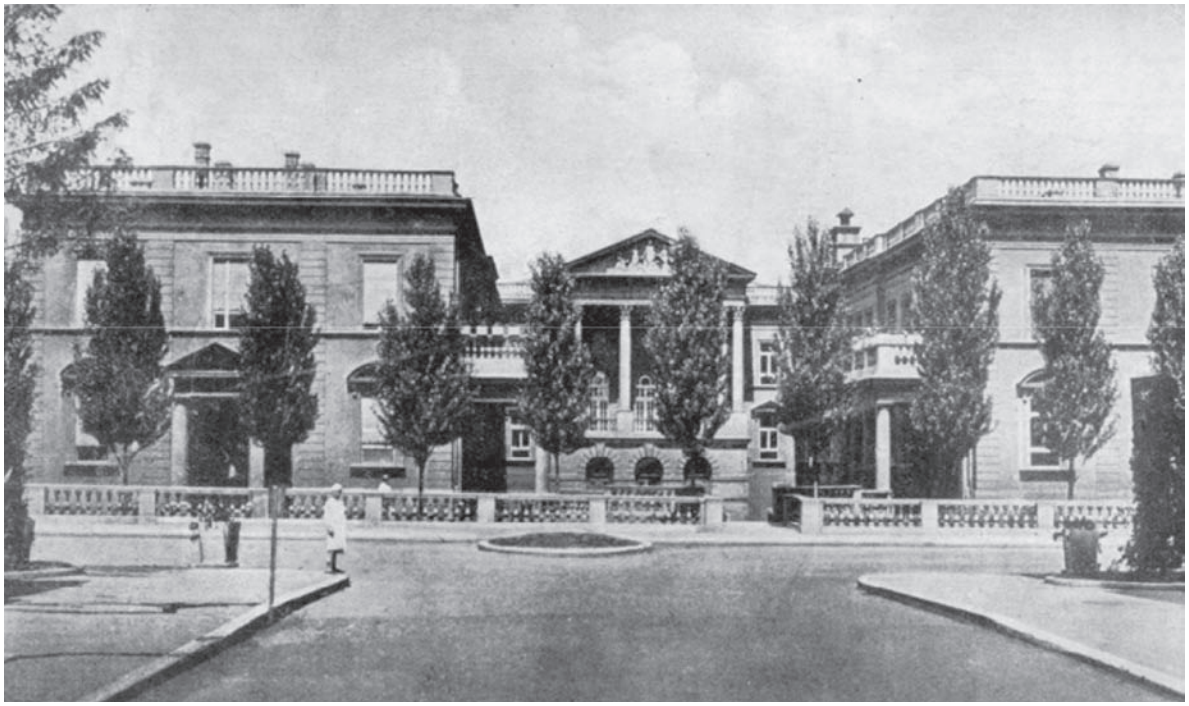

In the first few years, within the Institute of Physiology (today – the Institute of Medical Physiology), scientific research was progressing in several departments. These included Physico-Chemistry, Chemical Physiology, Microchemistry, Electrophysiology (which contained facilities for photographic recording), Graphics working with the operating theatres. These were all supported by an academic library and a mechanical workshop. In addition to the lecture theatres and laboratories, due to the commitment of Richard Burian and the generous memorial fund of Dr. Elsie Inglis of London, it was possible to build several departments for experimental work. In 1916, Dr. Elsie Inglis was the first woman to receive the highest Serbian decoration – The Order of the White Eagle. She was a member of "the Scottish Women's Hospital" (the name refers to the Military-Medical Unit that was set up during the First World War as a gesture of help from the women of Scotland to the Serbian people). In memory of this great friend of the Serbian people, in 1929, a memorial table was placed in the central hall of the Institute of Medical Physiology, at the initiative of Professor Richard Burian.

Apart from being one of the founders of the School of Medicine in Belgrade and the Dean or Vice-Dean between 1923 and 1934, Prof. Burian was also involved with the creation of both the School of Veterinary Medicine (1936), and the School of Pharmacy of Belgrade (1939), of which he was the first head, respectively. These two schools were housed in the same building. He was elected as a corresponding member of the Serbian Royal Academy of Science in 1926. Due to the tremendous effort of Prof Burian, the Serbian School of Medicine and Physiology was able to keep pace with the corresponding institutions in Europe from their conception.

The personality of Richard Burian, together with his reputation in science, and authority as a professor, attracted numerous associates not only at the Institute of Physiology in Belgrade, but also with other Professors of Physiology within Belgrade (the School of Veterinary Medicine, the School of Pharmacy and the School of Agriculture). He also collaborated well with other schools of medicine in former Yugoslavia: Professors Milutin Neskovic, Ilija Djuricic and Bozidar Nikolic in Belgrade, Aleksandar Sabovljev in Sarajevo, Radmilo Anastasijevic in Novi Sad, and Aleksandra Volkanoska in Skopje.

Professor Richard Burian retired in 1938, but he continued with his experiments at the Institute of Physiology until the beginning of the Second World War. Sadly, on 6th April 1941, one of the first Nazi bombs to land on Belgrade destroyed, and

then set on fire the architecturally beautiful building. This was a disaster as the creative work of Professor Richard Burian accumulated over many years was destroyed instantly. However, forty books with signatures of the Burian family members were found beneath the ruins of the Institute. These included books by Chekhov, Tolstoy, Goethe, Seneca and numerous others from the 19th century, together with about 200 professional books in German, French and English. Also saved were numerous scientific articles that he had obtained through personal contacts.

ЗГРАДА ХИСТОЛОШКОГ И ФИЗИОЛОШКОГ ИНСТИТУТА ПОСЛЕ БОМБАРДОВАЊА 1941

The attitude of the family Burian towards the country and Serbian people during the war under the Nazi occupation is best illustrated by an example from the diaries/memoirs of Professor Aleksandar Kostic. From these Prof. Kostic noted that at a quiet suggestion from his wife Mrs. Kostic, that they, the family Burian, as Austrians, would probably have better treatment concerning supplies of food and in general, Richard Burian reacted: "What do you mean, *chere amie*, we are not, for God's sake, *"Folksdeutchers"* but Yugoslavs. We are that now and that's what we are going to stay in the future!"

When Belgrade was liberated in October 1944, students of Professor Burian and especially a major of the national-liberation army, Assistant Professor Aleksandar Sabovljev, remembered their old and lonely professor. Prof Sabovljev (later professor and founder of the School of Medicine in Sarajevo – today Bosnia and Herzegovina) provided him with the room in the former Main Military Hospital (today the Military Medical Academy) where he had complete care. After his recovery, Professor Burian stayed with his step-son who lived in Belgrade. After many invitations from his son, Herman, in 1947 Prof. Burian emigrated to the USA, to the small town of Hanover near Boston. His son Herman Martin Burian (born in Naples, 1906–1974) (received M.D. from University of Belgrade in 1930, came to U.S. 1936, professor at Dartmouth 1936–1945, then moved to Iowa City) was appointed Professor of Ophthalmology at the University of Iowa in 1951 (Iowa City, U.S.). Prof. Burian hoped that he would come back to Belgrade some day and continue with his research. Sadly this was not to be and he died in Iowa City on April 6th, 1954. He led a life that was dedicated to high ideals. He was an excellent intellectual in the real sense of the word. He handed down his love towards literature of the world classics, music and philanthropy to his family.

Richard Burian was engaged in experimental research in many fields. These included metabolism of purines, methodology of nerve and muscle research in mollusks, contraction of damaged muscle, function of neuromuscular synapses, function of kidney and genito-urinary system, function of biological membranes and the physiology of swallowing.

Professor Richard Burian was a recipient of several medals and honors: the Order of the Romanian Crown of 3rd class (in 1931), the Order of Saint Sava of 2nd class (in 1934) and the Order of the Yugoslav Crown of 2nd class (in 1936). In memory and respect of the founder and first director, the Institute of Medical Physiology of the School of Medicine bears his name. At the suggestion of the School of Medicine in Belgrade, (in 1971) one street in Belgrade bears the name of the physiologist Professor Richard Burian. He was an inspiration, both as a scientist and philanthropist.

Selected references

Richard Burian. Über Sitosterin. Ein Beitrag zur Kenntniss der Phytosterine. Monatshefte für Chemie/Chemical Monthly, Volume 18, Number/December, 1897

Richard Burian und Heinrich Schur. Über die Stellung der Purinkörper im menschlichen Stoffwechsel. Arch f d ges Physiol. 80, 241–350, 1900

Richard Burian und Heinrich Schur. Das quantitative Verhalten der menschlichen Harnpurinausscheidung. Nochmalige Feststellung und kritische Prüfung unserer bisherigen Ergebnisse, zugleich Antwort auf O. Loewi's Einwände. Pflügers Archiv European Journal of Physiology, Volume 94, Numbers 5–6/February, 1903

Richard Burian. Chemie der Spermatozoen. I. Reviews of Physiology, Biochemistry and Pharmacology, Volume 3, Number 1/March, 1904

Richard Burian. Über die oxydative und die vermeintliche synthetische Bildung von Harnsäure in Rinderleberauszug. Zeitschrift für Physiologische Chemie 43, 497–531, 1904/05

Richard Burian. Ein letztes Wort zu den Permanganatversuchen von Kutscher und Seemann. Zeitschrift für Physiologische Chemie 45, 351–354, 1905

Richard Burian. Chemie der Spermatozoen. II. Reviews of Physiology, Biochemistry and Pharmacology, Volume 5, Number 1/December, 1906

Richard Burian. Funktion der Nierenglomeruli und Ultranitration. Pflügers Archiv European Journal of Physiology, Volume 136, Number 1/December, 1910

Dragan M. Djurić, MD, PhD
Professor of Physiology

Institute of Medical Physiology
"Richard Burian" School of Medicine
University of Belgrade
Višegradska 26/II
11000 Belgrade
Republic of Serbia
E-mail: drdjuric@eunet.*rs*

Ethanol and magnesium suppress nickel-induced bursting activity in leech Retzius nerve cells

Dhruba Pathak[1], Srdjan Lopicic[1], Marija Stanojevic[1], Aleksandra Nedeljkov[1], Dragan Pavlovic[2], Dusan Cemerikic[1] and Vladimir Nedeljkov[1]

[1] *Institute for Pathological Physiology, Medical Faculty Belgrade, Serbia*
[2] *Ernst Moritz Arndt University, Greifswald, Germany*

Abstract. In the present study we have examined effects of ethanol and magnesium on Ni^{2+}-induced bursting of leech Retzius cells. Saline with 3 mmol/l $NiCl_2$ induced spontaneous bursting activity, characterized by rapid depolarizations to a plateau level during which bursts of action potentials occurred. To test for the mechanism of bursting initiation external Na^+ was completely removed. Removal of external Na^+ in presence of 3 mmol/l $NiCl_2$ terminated the bursting activity. Application of 2% ethanol solution significantly decreased the bursting frequency, duration and amplitude of depolarization plateaus, and the number of spikes per plateau. Solution containing 10 mmol/l Mg^{2+} almost completely abolished the oscillatory activity of the neurons and completely suppressed action potential generation. We conclude that ethanol and magnesium suppress Ni^{2+}-induced epileptic activity.

Key words: Bursting — Leech Retzius neuron — Ethanol magnesium

Introduction

Epileptic seizures are based on paroxysmal depolarization shifts (PDS) which are synchronized in many neurons. Mechanisms underlying PDS and seizures are still not understood (Üre and Altrup 2006). Essential mechanisms of epileptic activity are thought to be identical in whatever part of the human or animal nervous system it appears (Altrup 2004). Invertebrate models have proved to be quite useful for the understanding of some processes in the central nervous system. Since invertebrate neurons are easily accessible to experimentation, it has been possible to explore in detail the basic mechanisms controlling neuronal excitability using these cells and to make some useful predictions about electrophysiological mechanisms that may be present in the central neurons (Lewis et al. 1986).

The nervous system of the leech is a valuable model system for investigating the cellular basis for epileptiform activity. As in other invertebrate preparations, it has been possible to identify many of the individual neurons comprising the relevant neuronal circuits and to determine their cellular and synaptic properties (Angstadt 1999). The largest neurons in the leech central nervous system are Retzius cells which exhibit stable resting membrane potential and which are nonbursting neurons with a low spontaneous firing rate (Beck et al. 2001).

Rhythmical epileptiform bursting activity can be induced in the Retzius neurons by several exogenous agents, such as neutral red, various pyrethroids (Leake 1982) and by the convulsants, penicillin or bemegride (Prichard 1972). Furthermore, epileptiform activity can be induced by FMRF-amide or related peptides, by the injection of phorbol ester, and by lowering external Ca^{2+} concentration through reducing $CaCl_2$ in bath media with or without EGTA, the use of EGTA alone, and by replacement of external Ca^{2+} by Ba^{2+}, Co^{2+}, and other inorganic Ca^{2+}-channel blockers, such as Ni^{2+}, Mn^{2+}, Cd^{2+}, La^{3+} and Zn^{2+} (Angstadt et al. 1998). This epileptiform activity has been observed not only in Retzius neurons, but in nearly all neurons in leech ganglia, perhaps synchronized by electrical coupling. In Na^+-free Ringer solution epileptiform activity induced by Ni^{2+} becomes eliminated, suggesting that sodium influx plays a major role in its generation (Angstadt and Friesen 1991).

Correspondence to: Vladimir Nedeljkov, Institute for Pathological Physiology, Medical Faculty Belgrade, Dr. Subotica 1/II, 11000 Belgrade, Serbia
E-mail: nedeljkovvladimir@hotmail.com

Anticonvulsant effects of ethanol have been revealed by a number of *in vivo* studies in various electrically- and chemically-induced seizures tests (Zuk et al. 2001; Hillbom et al. 2003). Similarly, magnesium has an anticonvulsant effect in preeclampsia and eclampsia (Sibai 1990), and magnesium levels are shown to be significantly lower in patients with seizures (Sinert et al. 2007). *In vitro* and *in vivo* experiments have also provided evidence for the ability of magnesium to affect seizures, showing the anticonvulsant effect of magnesium (Standley et al. 1995; Wang et al. 2004).

Since ethanol and magnesium both show inhibitory effect on epileptiform activity, by influencing ion channel function and synaptic transmission, we have undertaken a study to test whether they could modulate this Ni^{2+}-induced Na^{+}-dependent bursting activity, which greatly resembles the electrophysiological properties of neurons during seizures.

Materials and Methods

The experiments were performed at room temperature (22–25°C) on Retzius nerve cells in the isolated segmental ganglia of the ventral nerve cord of leech *Haemopis sanguisuga*. The method of dissection has been previously described (Beleslin 1971), and complies with institutional research council guidelines.

Dissected segments of 3 ganglia were immediately transferred to 2.5 ml plastic chamber with leech Ringer and fixed by means of fine steel clips. The plastic chamber was then placed in grounded Faraday's cage mounted on a fixed table in a manner that prevents vibrations. Identification and penetration of the cells was performed in the cage under a stereomicroscope. The Retzius cells were identified by their position on the ventral surface of the ganglion, their size, and their bioelectrical properties.

Prior to the experiments, the chamber was flushed with fresh Ringer solution, microelectrode dipped into the solution and allowed 20–30 min for equilibration. To change the solution, the chamber was continuously flushed with a volume of fluid at least 5 times that of the chamber volume. The superfusion was usually completed in 10–15 s.

Electrical methods (electrophysiological recordings)

The membrane potential was recorded using standard single-barrel glass microelectrodes. Micropipettes were pulled from thick wall capillaries with internal filament (O.D. 1.5 mm, I.D. 0.6 mm, World Precision Instruments) on a vertical puller (Narishige, Japan) and then filled with 3 mmol/l KCl shortly after being pulled. The tip diameter of the electrodes was less than 1 μm, tip potentials were less than 5 mV, and the microelectrode resistance was 15–25 MΩ in standard Ringer solution (for composition see solutions).

The recordings were amplified using high input impedance amplifier (model 1090, Winston Electronics). Microelectrodes were connected to the amplifier *via* an Ag-AgCl wire. The ground electrode was an Ag-AgCl wire in a separate chamber filled with Ringer solution connected to the experimental chamber by a 3 mmol/l KCl 3% agar bridge. The recordings were displayed on a two-channel oscilloscope (Hameg, Germany) and permanently recorded on a pen recorder (Linseis, Selb, Germany), and a thermal printer (Hameg, Germany).

Solutions

The Ringer solution used in these experiments had the following composition (in mmol/l): NaCl 115.5, KCl 4, $CaCl_2$ 2, NaH_2PO_4 0.3, Na_2HPO_4 1.2 (pH = 7.2). In Ni^{2+}-containing solutions 3 mmol/l $NiCl_2$ was added. In Na^{+}-free solutions NaCl was completely replaced by an equal amount of tris(hydroxymethyl)aminomethane-Cl (Tris), Na_2HPO_4 and NaH_2PO_4 were omitted, and pH adjusted to 7.2 with HCl. Absolute ethanol (Merck) was added to the Ringer solution to produce a final concentration of 2% ethanol. In magnesium containing saline 10 mmol/l $MgCl_2$ was added and NaCl was reduced by 15 mmol/l.

Data analysis

All results are expressed as means ± S.E.M. Comparison between mean values was made using Student's *t*-test; *p* values of less than 0.05 were considered significant.

Results

Ni^{2+}-induced bursting activity of Retzius neurons of H. sanguisuga

The resting membrane potential of the Retzius neurons in standard Ringer solution was –40.7 ± 1.6 mV (n = 18 cells), and spontaneous action potentials of amplitude, shape and duration usual for leech Retzius cells (amplitude 20–50 mV, duration 6–8 ms) were generated at a low frequency (≈1 Hz, Fig. 1A). Superfusion with Ringer solution containing 3 mmol/l of Ca^{2+} channel blocker Ni^{2+} (Ni-Ringer) induced a small depolarization of the membrane potential followed by spontaneous bursting activity, characterized by rapid depolarizations to a plateau level during which bursts of action potentials occurred. The plateaus spontaneously ended by rapid repolarizations followed by interplateau intervals that over time gave way to the next rapid depolarization (Fig. 1B,C). Over the 2–7 min upon superfusion by Ni-Ringer the plateau depolarizations increased in frequency, duration, amplitude, and number of spikes per plateau, eventually reaching final

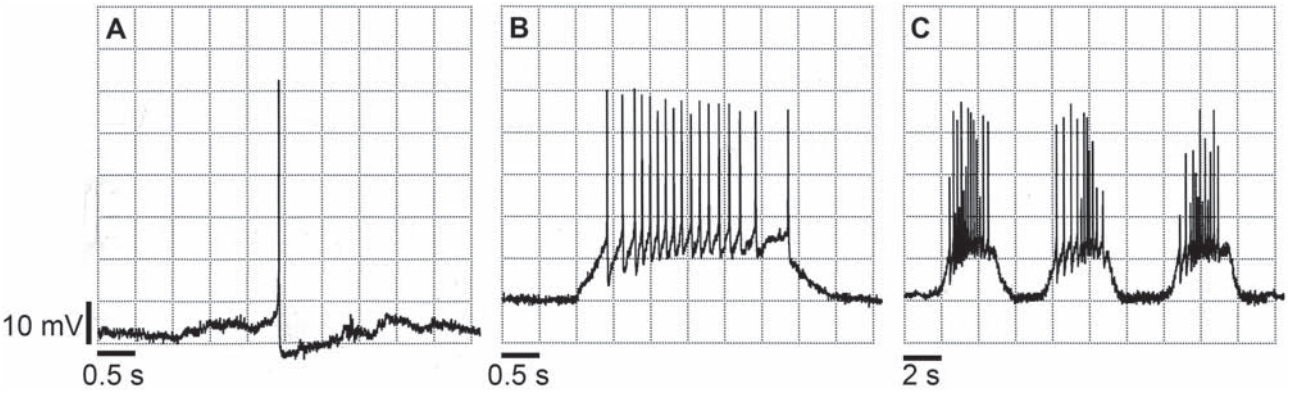

Figure 1. Spontaneous and bursting activity of leech Retzius neuron as recorded by thermal printer. **A.** Spontaneous firing of single action potentials in standard Ringer solution. **B.** A plateau of depolarization with burst of action potentials induced by 3 mmol/l $NiCl_2$. **C.** Same as B on a different time scale.

levels shown in Table 1. These levels were sustained for as long as Ni-Ringer was applied (Fig. 2). All further experiments were performed, and appropriate measurements taken, only when this final and stable level had been reached.

Bursting activity seized and the cells recovered within several minutes of washout with standard Ringer solution.

Dependence of Ni^{2+}-induced bursting activity on Na^+

Bursting activity induced in *Hirudo medicinalis* by Co^{2+}, Ni^{2+} (Angstadt and Friesen 1991), and other transitional metal ions (Angstadt et al. 1998) has been reported to be sodium-dependent (Angstadt and Friesen 1991). To examine whether the same holds for our preparation (*H. sanguisuga*), we have replaced Na^+ entirely by Tris in the Ni-Ringer solution (Tris-Ni-Ringer).

Bursting activity of 6.9 ± 0.7 plateaus per minute was induced by 3 mmol/l Ni^{2+} in Retzius neurons having a resting membrane potential of –39.7 ± 4.6 mV (n = 4 cells). Upon the stabilization of bursting activity Ni-Ringer was replaced by Tris-Ni-Ringer. Removal of external Na^+ in presence of 3 mmol/l Ni^{2+} induced a rapid hyperpolarization of the cell membrane. Within the first 2–3 min, the membrane potential partially depolarized and remained at a stable level for the remainder of Tris-Ni application. During the whole period of Tris-Ni application, the bursting activity was completely abolished since no plateaus of depolarization occurred. After washout with Ni-Ringer containing the normal concentration of Na^+, the cell membrane potential fully recovered and bursting activity resumed as before (Fig. 3).

Table 1. Characteristics of the Ni^{2+}-induced bursting activity of the Retzius neuron after stabilization

Parameter	Value	n
Spikes/plateau	7.09 ± 0.48	35
Plateau duration (s)	4.20 ± 0.16	45
Plateau amplitude (mV)	11.43 ± 0.54	47

Data shown as mean ± S.E.M.; n, number of plateaus used for measurements.

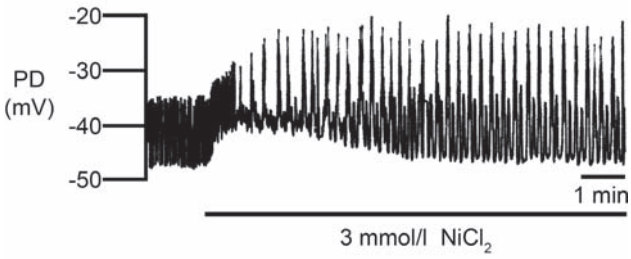

Figure 2. A trace from pen recorder showing bursting activity of leech Retzius neuron induced by 3 mmol/l $NiCl_2$. Application of Ni^{2+} is followed by initial depolarization and initiation of bursting activity. After 5 min membrane potential and bursts reach stable level that is sustained for the remainder of the recording. PD, membrane potential.

Effects of 2% ethanol on Ni^{2+}-induced bursting activity

In this set of experiments Ni-Ringer-induced bursting activity stabilized at 6.9 ± 0.7 plateaus per minute (n = 7 cells, resting membrane potential –41.0 ± 3.2 mV). Replacement of Ni-Ringer with 2% ethanol solution containing 3 mmol/l Ni^{2+} (EtOH-Ni-Ringer) led to a minor depolarization and a highly significant decrease in frequency of bursting activity to 2.9 ± 0.7 plateaus per minute ($p < 0.01$, Fig. 4A). Ethanol also adversely affected the duration and amplitude of the plateaus as well as the number of spikes per plateau (Fig. 4B). Plateau duration was reduced from 4.6 ± 0.5 s to 3.06 ± 0.36 s ($p < 0.05$, n =

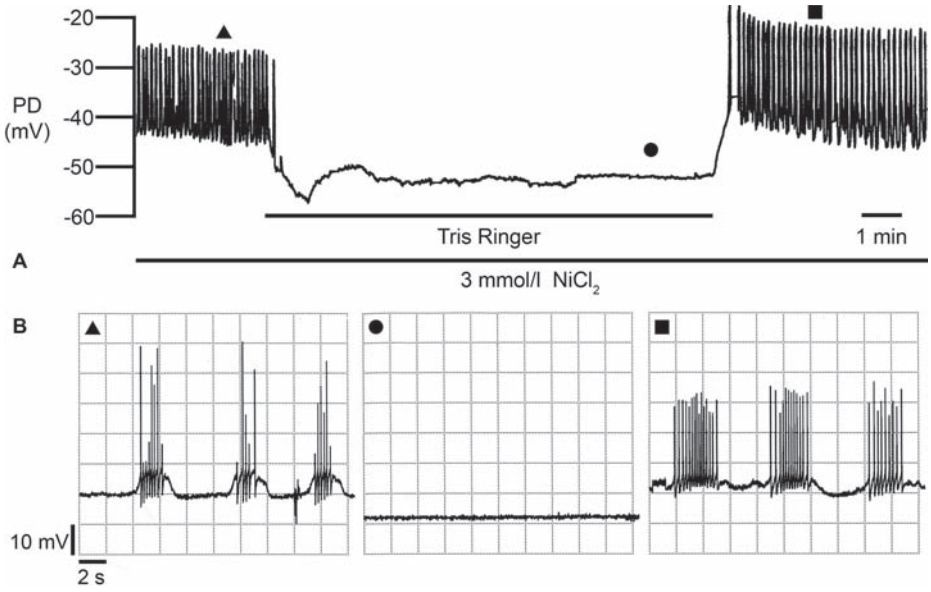

Figure 3. Effect of Tris Ringer on bursting of leech Retzius neuron. **A.** Trace from pen recorder. Upon application of Tris Ringer membrane potential transiently hyperpolarizes and bursting is completely terminated. Washout restores both membrane potential and bursting activity. Presence of $NiCl_2$ is maintained throughout the experiment. **B.** Thermal printer recordings of representative points from plate A. PD, membrane potential.

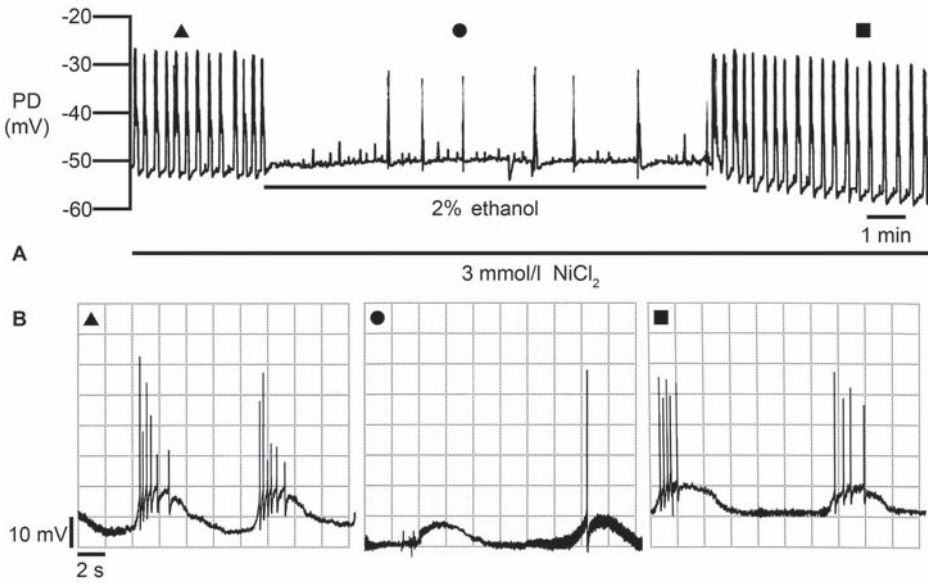

Figure 4. Effect of 2% ethanol on bursting of leech Retzius neuron. **A.** Trace from pen recorder. Upon application of ethanol frequency of bursting is diminished. Washout of ethanol restores bursting activity. Presence of $NiCl_2$ is maintained throughout the experiment. **B.** Thermal printer recordings of representative points from plate A. Ethanol reduces duration and amplitude of plateaus as well as number of spikes per plateau (● vs. ▲). PD, membrane potential.

48 plateaus) and the amplitude was diminished by 3.1 ± 0.4 mV from 9.7 ± 0.7 to 6.7 ± 0.6 mV ($p < 0.01$, $n = 48$ plateaus). During the application of EtOH-Ni-Ringer, action potentials rarely occurred during plateaus of depolarization, and average number of spikes per plateau was reduced from 5.8 ± 0.6 to 0.7 ± 0.2 ($p < 0.01$, $n = 30$ plateaus, Fig. 5). After washout with Ni-Ringer membrane potential fully recovered in all seven cells, and bursting activity resumed at near control values.

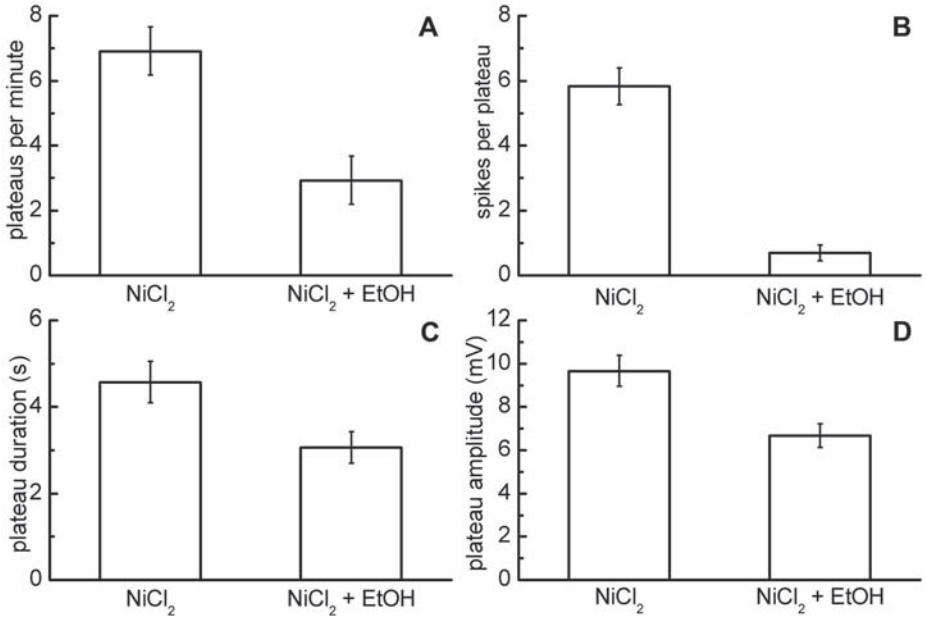

Figure 5. Graphic representation of effect of ethanol on frequency (A, $n = 7$ cells), number of spikes per plateau (B, $n = 30$ plateaus), plateau duration (C, $n = 48$ plateaus), and amplitude (D, $n = 48$ plateaus) of leech neuron bursting induced by $NiCl_2$. Error bars represent ± S.E.M.

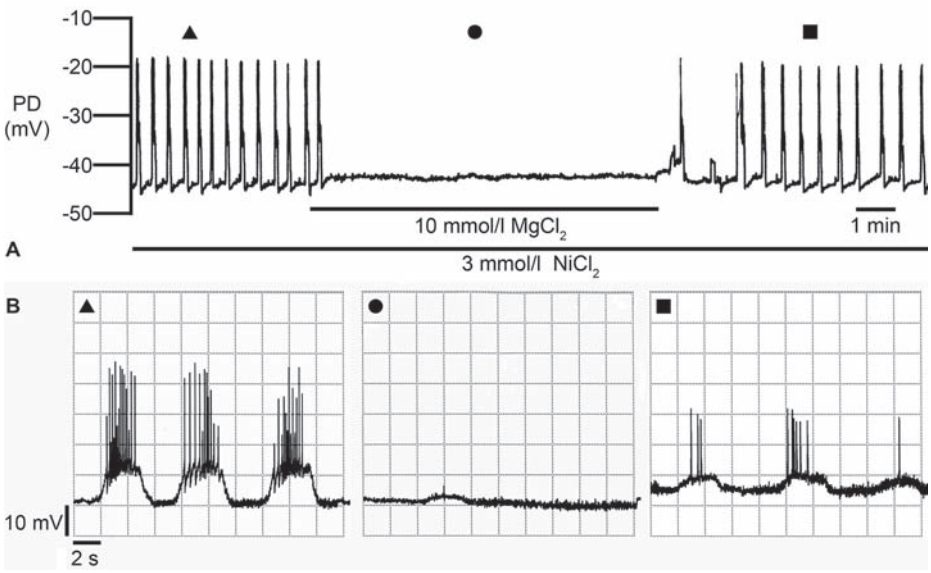

Figure 6. Effect of 10 mmol/l Mg^{2+} on bursting of leech Retzius neuron. **A.** Trace from pen recorder. Application of $MgCl_2$ apparently terminates the bursting. Washout of Mg^{2+} restores bursting activity. Presence of $NiCl_2$ is maintained throughout the experiment. **B.** Thermal printer recordings of representative points from plate A. Middle trace (●) reveals a plateau of depolarization diminished in duration and amplitude which does not elicit spikes. PD, membrane potential.

Effects of 10 mmol/l Mg^{2+} on Ni^{2+}-induced bursting activity

The effect of Mg^{2+} on Ni^{2+}-induced bursting activity is illustrated in Fig. 6. Oscillatory activity induced in Retzius cells in these experiments ($n = 7$, resting membrane potential –40.0 ± 3.4 mV) had the frequency of 5.7 ± 1.0 plateaus per minute. Superfusion with saline containing 10 mmol/l Mg^{2+} and 3 mmol/l Ni^{2+} (Mg-Ni-Ringer) almost completely eliminated the oscillatory activity of the neuron, reducing it to 0.2 ± 0.1 plateaus per minute ($p < 0.01$, Fig. 6A). Dur-

ing this period action potential generation was completely abolished, and plateaus of depolarization occurred only sporadically, i.e. we have recorded only four plateaus in all seven cells with combined duration of Mg-Ni-Ringer application spanning more than 70 min. The plateau duration was reduced from 3.9 ± 0.1 to 2.7 ± 0.3 s ($p < 0.01$, $n = 4$), and plateau amplitude was diminished by 4.5 ± 1.2 mV from 12.5 ± 0.3 to 8.0 ± 1.0 ($p < 0.05$, $n = 4$). One of the plateaus is shown in Fig. 6B. Washout with Ni-Ringer led to restoration of bursting activity.

Discussion

Na^+-dependent bursting and mechanism of burst initiation in H. sanguisuga

Many epileptic conditions are considered to be idiopathic and the related seizures of unknown origin. It does appear that different types of seizures are caused by differing mechanisms. Most membrane potential oscillations, burst firing, and seizure activity described to date are Ca^{2+}-dependent as they require influx of Ca^{2+} through voltage-gated Ca^{2+} channels. However, in some cases rhythmic bursting and seizures are produced in low or zero Ca^{2+} environments. It has been shown that in the avian Edinger Westphal nucleus in repetitively firing cells removal of extracellular calcium increases the frequency of action potential discharge (Fujii 1992), that low and zero Ca^{2+} solutions cause development of spontaneous, rhythmic and synchronous bursting discharges in rat hippocampal slices (Wang et al. 2004) and supraoptic nucleus neurons (Li and Hatton 1996), and also that low calcium levels can cause, or at least contribute to myoclonic seizures, infantile spasms, and seizures concurrent with Down syndrome (Thiel 2006).

Similar bursting activity can be induced in Retzius neurons of the leech *H. medicinalis* by block of Ca^{2+} currents with transitional metal ions such as Co^{2+}, Ni^{2+}, and others, Ni^{2+} being the most potent of them (Angstadt et al. 1998). The following mechanism has been proposed for the initiation of this Na^+-dependent bursting: block of voltage dependent Ca^{2+} influx suppresses Ca^{2+} dependent outward currents, namely calcium activated potassium current ($I_{K(Ca)}$) unmasking the effects of persistent inward Na^+ current resulting in a rapid depolarization, and supporting a maintained depolarizing plateau (Angstadt and Friesen 1991; Angstadt 1999).

In the present study we have used 3 mmol/l Ni^{2+} solution to induce bursting activity in the Retzius neurons of the leech *H. sanguisuga*. All characteristics of bursting in our model (bursting frequency, plateau duration and amplitude) are in keeping with results of Angstadt (1991) on *H. medicinalis*. Also, in our experiments the onset of oscillatory activity was preceded by membrane depolarization, a result consistent with block of tonic $I_{K(Ca)}$. Furthermore, we have shown that bursting of Retzius neurons in *H. sanguisuga* is also Na^+-dependent, as bursting is completely abolished in Na^+-free solution, and the pattern of changes induced by removal of Na^+ is virtually identical to that shown by Angstadt (1999). Therefore we conclude that the same mechanism as the one described by Angstadt for *H. medicinalis* leads to bursting initiation in *H. sanguisuga*.

Ethanol inhibits Ni^{2+}-induced bursting

Our results show that 2% ethanol suppresses Ni^{2+}-induced bursting activity of Retzius cells by lowering the frequency of bursts, and reducing the duration and amplitude of plateaus of depolarization, as well as the number of spikes per plateau. This is in agreement with pronounced antiepileptogenic and anticonvulsant effects of ethanol after acute application (Fischer and Kittner 1998).

The antiepileptogenic and anticonvulsant effects of ethanol could be explained by its effect on excitatory and inhibitory neurotransmission. There is substantial proof of ethanol action on N-methyl-D-aspartate (NMDA) (Kumari and Ticku 2000), non-NMDA, and γ-aminobutyric acid receptor function (Weight et al. 1992). It has also been shown that intoxicating concentrations of ethanol posses anticonvulsant activity through blockage of the NMDA receptor-mediated synaptic excitation (Gean 1992). However, this is an unlikely cause of ethanol suppression of bursting activity in our model, since Ni^{2+} solution used to induce bursting activity rapidly and completely blocks chemical synaptic transmission (Angstadt and Friesen 1991; Angstadt et al. 1998). Moreover, Retzius cells isolated in culture, and therefore deprived of synaptic inputs, exhibit rhythmic plateau potentials (Angstadt and Choo 1996).

A more plausible mechanism of ethanol suppression of bursting is block of voltage-dependent Na^+ channels. The acute intoxicating effects of ethanol have been widely attributed to its ability to block voltage-gated Na^+ channels (Fitzgerald and Nestler 1995). Ethanol exhibits significant inhibition of sodium current in Aplysia neurons (Camacho-Nasi and Treistman 1986), rat neurons (Harris and Bruno 1985a), and other preparations. This effect might be mediated by ethanol-induced membrane lipid disorder, secondarily affecting Na^+ channels (Harris and Bruno 1985b), or by direct action on the channel itself (Krylov et al. 2000).

Another possible avenue of ethanol effect on bursting is activation of $I_{K(Ca)}$. Studies performed in systems that likely represent relevant targets of alcohol actions in the body, such as the neurons involved in motor coordination, nociceptive and neuropeptide releasing-neurons, and growth-hormone releasing cells, at a variety of levels, and using a wide variety of approaches indicate that Ca^{2+}-activated K^+ channels

represent relevant targets in ethanol actions (Brodie et al. 2007). Open probability of Ca^{2+}-activated K^+ channels is increased 2–6 times depending on the concentration of ethanol, with a functional consequence of reduced firing frequency during ethanol application in dorsal root ganglia of rats (Gruss et al. 2001). The potentiation of Ca^{2+}-activated K^+channels by ethanol is a result of direct action on the channel itself (Dopico et al. 1999). Interestingly, this effect is especially pronounced when Ca^{2+} influx into the cell is minimal (Dopico et al. 1999), a case that corresponds very well to our model.

Since the mechanism of bursting in Retzius cells is directly related to the block of $I_{K(Ca)}$ and influx of Na^+ as described before, activation of Ca^{2+}-activated K^+ channels and block of voltage-gated Na^+ channels would clearly have detrimental effect on bursting activity.

Inhibition of Ni^{2+}-induced bursting by Mg^{2+}

Characteristic clinical features of hypomagnesemia and hypocalcemia include seizures (Baker and Worthley 2002). Further, the concentrations of cerebrospinal fluid-ionized magnesium in convulsive children is significantly lower than in non-convulsive children and is related to age-dependent changes in ionized calcium as well as decreased ionized magnesium in the developing brain (Miyamoto et al. 2004). Also, low Mg^{2+}-induced epilepsy in CA1 neurons of intact mice hippocampus is enhanced by Ca^{2+} channel blocker nifedipine (Derchansky et al. 2004). On the other hand, increasing Mg^{2+} levels suppress bursting induced by low Ca^{2+} in rat hippocampal slices (Wang et al. 2004).

Having in mind this apparent relationship of low Ca^{2+}, Mg^{2+}, and seizure generation, we have examined the effect of 10 mmol/l Mg^{2+} on Ni^{2+}-induced bursting of leech Retzius cell. Our results show that Mg^{2+} in concentration of 10 mmol/l almost completely blocks bursting activity, shortens the duration and decreases the amplitude of the plateaus in our model.

Proconvulsive and anticonvulsive effects of Mg^{2+} are mostly attributed to its modulatory action on NMDA receptors (Gean and Shinnick-Gallagher 1988). However, it has been demonstrated that block of NMDA receptors does not prevent all forms of Mg^{2+}-free-induced epileptiform activity in rats (Thomson and West 1986). Also, non-NMDA channel blocker CNQX is shown to have no effect on bursting activity induced by lowering extracellular Mg^{2+} concentration in rat hippocampal slices (Wang et al. 2004). Additionally, low Ca^{2+} and high Mg^{2+} solutions effectively block chemical synaptic transmission. Finally, as discussed before, chemical synaptic transmission bares no significance to bursting initiation in our model. Consequently, Mg^{2+} action on synaptic transmission does not seem to be an underlying mechanism of bursting termination in leech Retzius cells.

More probably, the effect of Mg^{2+} results from modulation of Na^+- and Ca^{2+}-dependent K^+ channels. Permeation across the Na^+ channels of rat hippocampal neurons is voltage- and concentration-dependently reduced by both intracellular (Lin et al. 1991), and extracellular Mg^{2+} (Sang and Meng 2002). The mechanism of this action is two-fold as Mg^{2+} changes the surface potential of the membrane and interferes with Na^+ permeation by competitively occupying Na^+ channels (Lin et al. 1991).

On the other hand, previous studies have shown a significant potentiation of Ca^{2+}-induced K^+ outward current (through Ca^{2+}-dependent K^+ channels) – after the addition of Mg^{2+} into the solution (McLarnon and Sawyer 1993). This potentiation was only observed if there had been Ca^{2+} present in the cell, but this agrees well with our results since we did not perform substitution of Ca^{2+} with Ni^{2+}, but rather an addition of Ni^{2+} to Ca^{2+} containing solution.

Thus, similarly to ethanol, there are two possible mechanisms of suppressive action of Mg^{2+} upon bursting, one affecting Na^+ channels, and the other affecting $I_{K(Ca)}$.

Concluding remarks

The chemical synapse-independent mechanism of ethanol and magnesium suppression of bursting activity by action on Na^+ channels and $I_{K(Ca)}$ proposed in this paper might have broader significance, pertaining not only to leeches, but mammalian neurons as well. It has been shown that phasic bursting in magnocellular neuropeptidergic cells is not dependent upon synaptically-mediated excitation (Hatton 1982), and that a low and zero Ca^{2+} mechanism of non-synaptic epileptogenesis exists in rat hippocampal neurons (Watson and Andrew 1995). Many anticonvulsant drugs target voltage-gated Na^+ channels (Remy et al. 2003), and Na^+ channel blocker YWI192 inhibits burst firing in CA1 neurons of animals with temporal lobe epilepsy (Jones et al. 2009). Lastly, increased excitability and rhythmic and synchronous bursting discharges that develop in rat hippocampal slices in solutions containing low Ca^{2+} are attributed to a Ca^{2+}-activated K^+ conductance (Martin et al. 2001).

It might also be noteworthy that there is an interplay of ethanol, Ca^{2+}, and Mg^{2+}. It is documented that ethanol consumption lowers both Ca^{2+} and Mg^{2+} levels in rabbits (Mahboob and Haleem 1988) and humans (Petroianu et al. 1991). Additionally, hypomagnesemia occurs in chronic alcoholism (Wu and Kenny 1996), and neurological signs which accompany ethanol ingestion are associated with rapid deficits in serum ionized magnesium (Altura and Altura 1999). It is not clear in which way combination of these disturbances leads to disease, but common sites of action postulated in this paper might shed some light on this problem as well.

Acknowledgement. This work was supported by the Ministry of Science and Technological Development of Serbia, grant No. 145085.

References

Altrup U. (2004): Epileptogenicity and epileptic activity: mechanisms in an invertebrate model nervous system. Curr. Drug Targets **5**, 473–484

Altura B. M., Altura B. T. (1999): Association of alcohol in brain injury, headaches, and stroke with brain-tissue and serum levels of ionized magnesium: a review of recent findings and mechanisms of action. Alcohol **19**, 119–130

Angstadt J. D., Friesen W. O. (1991): Synchronized oscillatory activity in leech neurons induced by calcium channel blockers. J. Neurophysiol. **66**, 1858–1873

Angstadt J. D., Choo J. J. (1996): Sodium-dependent plateau potentials in cultured Retzius cells of the medicinal leech. J. Neurophysiol. **76**, 1491–1502

Angstadt J. D., Choo J. J., Saran A. M. (1998): Effects of transition metal ions on spontaneous electrical activity and chemical synaptic transmission of neurons in the medicinal leech. J. Comp. Physiol., A. **182**, 389–401

Angstadt J. D. (1999): Persistent inward currents in cultured Retzius cells of the medicinal leech. J. Comp. Physiol., A. **184**, 49–61

Baker S. B., Worthley L. I. G. (2002): The essentials of calcium, magnesium and phosphate metabolism: Part II. Disorders. Crit. Care Resusc. **4**, 307–315

Beck A., Lohr C., Nett W., Deitmer J. W. (2001): Bursting activity in leech Retzius neurons induced by low external chloride. Pflügers Arch. **442**, 263–272

Beleslin B. (1971): Effects of different external media on the leech ganglion cells interaction. Period. Biol. **73**, 63–67

Brodie M. S., Scholz A., Weiger T. M., Dopico A. M. (2007): Ethanol interactions with calcium-dependent potassium channels. Alcohol Clin. Exp. Res. **31**, 1625–1632

Camacho-Nasi P., Treistman S. N. (1986): Ethanol effects on voltage-dependent membrane conductances: comparative sensitivity of channel populations in Aplysia neurons. Cell. Mol. Neurobiol. **6**, 263–279

Derchansky M., Shahar E., Wennberg R. A., Samoilova M., Jahromi S. S., Abdelmalik P. A., Zhang L., Carlen P. L. (2004): Model of frequent, recurrent, and spontaneous seizures in the intact mouse hippocampus. Hippocampus **14**, 935–947

Dopico A. M., Chu B., Lemos J. R., Treistman S. N. (1999): Alcohol modulation of calcium-activated potassium channels. Neurochem. Int. **35**, 103–106

Fischer W., Kittner H. (1998): Influence of ethanol on the pentylenetetrazol-induced kindling in rats. J. Neural Transm. **105**, 1129–1142

Fitzgerald L. W., Nestler E. J. (1995): Molecular and cellular adaptations in signal transduction pathways following ethanol exposure. Clin. Neurosci. **3**, 165–173

Fujii J. T. (1992): Repetitive firing properties in subpopulations of the chick Edinger Westphal nucleus. J. Comp. Neurol. **316**, 279–286

Gean P. W., Shinnick-Gallagher P. (1988): Epileptiform activity induced by magnesium-free solution in slices of rat amygdala: antagonism by N-methyl-D-aspartate receptor antagonists. Neuropharmacology **27**, 557–562

Gean P. W. (1992): Ethanol inhibits epileptiform activity and NMDA receptor-mediated synaptic transmission in rat amygdaloid slices. Brain Res. Bull. **28**, 417–421

Gruss M., Henrich M., Konig P., Hempelmann G., Vogel W., Scholz A. (2001): Ethanol reduces excitability in a subgroup of primary sensory neurons by activation of BK(Ca) channels. Eur. J. Neurosci. **14**, 1246–1256

Harris R. A., Bruno P. (1985a): Effects of ethanol and other intoxicant-anesthetics on voltage-dependent sodium channels of brain synaptosomes. J. Pharmacol. Exp. Ther. **232**, 401–406

Harris R. A., Bruno P. (1985b): Membrane disordering by anesthetic drugs: relationship to synaptosomal sodium and calcium fluxes. J. Neurochem. **44**, 1274–1281

Hatton G. I. (1982): Phasic bursting activity of rat paraventricular neurones in the absence of synaptic transmission. J. Physiol. **327**, 273–284

Hillbom M., Pieninkeroinen I., Leone M. (2003): Seizures in alcohol-dependent patients. CNS Drugs **17,** 1013–1030

Jones P. J., Merrick E. C., Batts T. W., Hargus N. J., Wang Y., Stables J. P., Bertram E. H., Brown M. L., Patel M. K. (2009): Modulation of sodium channel inactivation gating by a novel lactam: implications for seizure suppression in chronic limbic epilepsy. J. Pharmacol. Exp. Ther. **328**, 201–212

Krylov B. V., Vilin Y. Y., Katina I. E., Podzorova S. A. (2000): Ethanol modulates the ionic permeability of sodium channels in rat sensory neurons. Neurosci. Behav. Physiol. **30**, 331–337

Kumari M., Ticku M. K. (2000): Regulation of NMDA receptors by ethanol. Prog. Drug Res. **54**, 152–189

Leake L. D. (1982): Do pyrethroids activate neurotransmitter receptors? Comp. Biochem. Physiol., C. **72,** 317–323

Lewis D. V., Huguenard J. R., Anderson W. W., Wilson W. A. (1986): Membrane currents underlying bursting pacemaker activity and spike frequency adaptation in invertebrates. Adv. Neurol. **44**, 235–261

Li Z., Hatton G. I. (1996): Oscillatory bursting of phasically firing rat supraoptic neurones in low-Ca^{2+} medium: Na^{+} influx, cytosolic Ca^{2+} and gap junctions. J. Physiol. (Lond.) **496**, 379–394

Lin F., Conti F., Moran O. (1991): Competitive blockage of the sodium channel by intracellular magnesium ions in central mammalian neurones. Eur. Biophys. J. **19**, 109–118

Mahboob T., Haleem M. A. (1988): Effect of ethanol on serum electrolytes and osmolality. Life Sci. **42**, 1507–1513

Martin E. D., Araque A., Buno W. (2001): Synaptic regulation of the slow Ca^{2+}-activated K^{+} current in hippocampal CA1 pyramidal neurons: implication in epileptogenesis. J. Neurophysiol. **86**, 2878–2886

McLarnon J. G., Sawyer D. (1993): Effects of divalent cations on the activation of a calcium-dependent potassium channel in hippocampal neurons. Pflügers Arch. **424**, 1–8

Miyamoto Y., Yamamoto H., Murakami H., Kamiyama N., Fukuda M. (2004): Studies on cerebrospinal fluid ionized calcium

and magnesium concentrations in convulsive children. Pediatr. Int. **46**, 394–397

Petroianu A., Barquete J., Plentz E. G., Bastos C., Maia D. J. (1991): Acute effects of alcohol ingestion on the human serum concentrations of calcium and magnesium. J. Intern. Med. Res. **19**, 410–413

Prichard J. W. (1972): Events in leech Retzius neurons resembling the "paroxysmal depolarising shift". Neurology **22**, 439

Remy S., Urban B. W., Elger C. E., Beck H. (2003): Anticonvulsant pharmacology of voltage-gated Na^+ channels in hippocampal neurons of control and chronically epileptic rats. Eur. J. Neurosci. **17**, 2648–2658

Sang N., Meng Z. (2002): Blockade by magnesium of sodium currents in acutely isolated hippocampal CA1 neurons of rat. Brain Res. **952**, 218–221

Sibai B. M. (1990): Magnesium sulfate is the ideal anticonvulsant in preeclampsia-eclampsia. Am. J. Obstet. Gynecol. **162**, 1141–1145

Sinert R., Zehtabchi S., Desai S., Peacock P., Altura B. T., Altura B. M. (2007): Serum ionized magnesium and calcium levels in adult patients with seizures. Scand. J. Clin. Lab. Invest. **67**, 317–326

Standley C. A., Irtenkauf S. M., Cotton D. B. (1995): Anticonvulsant effects of magnesium sulfate in hippocampal-kindled rats. J. Biomed. Sci. **2**, 57–62

Thiel R. (2006): Might calcium disorders cause or contribute to myoclonic seizures in epileptics? Med. Hypotheses **66**, 969–974

Thomson A. M., West D. C. (1986): N-methylaspartate receptors mediate epileptiform activity evoked in some, but not all, conditions in rat neocortical slices. Neuroscience **19**, 1161–1177

Üre A., Altrup U. (2006): Block of spontaneous termination of paroxysmal depolarizations by forskolin (buccal ganglia, *Helix pomatia*). Neurosci. Lett. **392**, 10–15

Wang T., Wang J., Cottrell J. E., Kass I. S. (2004): Small physiologic changes in calcium and magnesium alter excitablity and burst firing CA1 pyramidal cells in rat hippocampal slices. J. Neurosurg. Anesthesiol. **16,** 201–209

Watson P. L., Andrew R. D. (1995): Effects of micromolar and nanomolar calcium concentrations on non-synaptic bursting in the hippocampal slice. Brain Res. **700**, 227–234

Weight F. F., Aguayo L. G., White G., Lovinger D. M., Peoples R. W. (1992): GABA- and glutamate-gated ion channels as molecular sites of alcohol and anesthetic action. Adv. Biochem. Psychopharmacol. **47**, 335–347

Wu C., Kenny M. A. (1996): Circulating total and ionized magnesium after ethanol ingestion. Clin. Chem. **42**, 625–629

Zuk O. V., Zinkovsky V. G., Golovenko N. Y. (2001): The pharmacodynamics of anticonvulsant and subconvulsant effects of ethanol in CBA and C57BL/6 mice. Alcohol **23**, 23–28

Acetylcholinesterase as a potential target of acute neurotoxic effects of lindane in rats

Danijela Vučević[1], Nataša Petronijević[2], Nevena Radonjić[2], Aleksandra Rašić-Marković[3], Dušan Mladenović[1], Tatjana Radosavljević[1], Dragan Hrnčić[3], Dragan Djurić[3], Veselinka Šušić[4], Macut Djuro[5] and Olivera Stanojlović[3]

[1] *Department of Pathophysiology, School of Medicine, University of Belgrade, Belgrade, Serbia*
[2] *Institute of Medical and Clinical Biochemistry, School of Medicine, University of Belgrad, Belgrade, Serbia*
[3] *Laboratory of Neurophysiology, Institute of Physiology, School of Medicine, University of Belgrade, Belgrade, Serbia*
[4] *Serbian Academy of Sciences and Arts, Belgrade, Serbia*
[5] *Institute of Endocrinology, Diabetes and Metabolic Diseases, Clinical Center of Serbia, Belgrade, Serbia*

Abstract. The aim of our study was to investigate the possible involvement of acetylcholinesterase (AchE) in mediating the early phase of acute lindane neurotoxicity in rats. Male Wistar rats (n = 48) were divided into following groups: 1. control, saline-treated group; 2. dimethylsulfoxide-treated group; 3. group that received lindane dissolved in dimethylsulfoxide, in a dose of 8 mg/kg intraperitoneally. Eight animals from each group were sacrificed 0.5 and 4 h after treatment and brain samples were prepared for further analysis. AchE activity (mitochondrial and synaptosomal fraction) was determined in cerebral cortex, thalamus, hippocampus and nc. caudatus spectrophotometrically. A significant increase in mitochondrial AchE activity was detected in cortex and nc. caudatus of lindane-treated animals 0.5 h after administration ($p < 0.05$). This rise was sustained in nc. caudatus within 4 h after treatment ($p < 0.05$). In contrast, activity of synaptosomal AchE fraction was significantly increased only in thalamus 4 h after lindane administration ($p < 0.05$). An increase in AchE activity may be involved in mediating acute neurotoxic effects of lindane, at least in some brain structures in rats.

Key words: Acetylcholinesterase — Lindane — Neurotoxicity — Rats

Introduction

Lindane (γ-hexachlorocyclohexane) is an organochlorine pesticide used extensively in agriculture and in human and veterinary medicines (Ntow 2001; Katsumata and Katsumata 2003; Mills and Yang 2003; Muscat et al. 2003; Kalantzi et al. 2004; Radosavljević et al. 2008). This environmentally persistent xenobiotic was reported to exert neurotoxic (Sahoo et al. 2000; Parmar et al. 2003; Sahaya et al. 2007), cardiovascular (Anand et al. 1995), gastrointestinal (Moreno et al. 1996), renal (Dietrich and Swenberg 1990), respiratory (Brown 1988), reproductive (Srivastava and Raizada 2000), hematological (Rauch et al. 1990), musculoskeletal (Hong and Boorman 1993), endocrine (Beard and Rawlings 1999), metabolic (Agrawal et al. 1995; Mladenović et al. 2008), immunological and lymphoreticular (Hong and Boorman 1993), hepatotoxic (Radosavljević et al. 2008), and proconvulsive effects (Martinez and Martinez-Conde 1995; Parmar et al. 2003; Kaminski et al. 2004; Vučević et al. 2008). It has been postulated that lindane achieves its behavioral effects and neurotoxicity through several mechanisms, like interfering with γ-aminobutiryc acid (GABA), Na^+,K^+-ATPase, Mg^{2+}-ATPase and acetylcholinesterase (AchE), inducing imbalance of the central monoaminergic systems, alteration of cerebral glucose uptake, induction of brain cytochrome P450s, alteration of neurotransmitter levels, etc. (Anand et al. 1998; Rivera et al. 1998; Sahoo et al. 2000; Parmar et al. 2003).

Changes in levels of brain norepinephrine and serotonin (Rivera et al. 1991) have been reported in rats administered

Correspondence to: Olivera Stanojlović, Institute of Physiology, School of Medicine, University of Belgrade, Višegradska 26/II, 11000 Belgrade, Serbia
E-mail: solja@afrodita.rcub.bg.ac.yu

acute oral doses of lindane. Decreased dopamine levels were seen in rats treated by gavage with 10 doses totaling 60 mg lindane/kg (half the LC_{50}) over a period of 30 days (Martinez and Martinez-Conde 1995). Increase in the levels of brain catecholamines, particularly norepinephrine and dopamine, and associated signs of toxicity such as mild tremor, lacrimation, salivation, and dyspnea were observed in female rats given oral doses of 100 mg/kg/day of technical-grade lindane for 7 days (Raizada et al. 1993). The activity of monoamine oxidase (MAO) in the cerebrum showed a marginal decrease, while the cerebellum and spinal cord indicated a significant increase and cdecrease in MAO, respectively. Rats treated with 20 mg technical-grade lindane/kg/day in food for 90 days exhibited increased GABA levels, increased glutamate decaarboxylase activity, and decreased glutamate levels in the brain (Nagaraya and Desiraju 1994).

Neurotransmission is regulated mainly by the release of neurotransmitter from presynaptic nerve terminals, the accumulation of neurotransmitter at the synaptic clefts, and the function of the postsynaptic receptors. Acetylcholine (Ach), in particular, is known to be rapidly hydrolyzed by AchE (Cooper et al. 2003). The duration of action of this major neurotransmitter in peripheral and central cholinergic system at the synaptic clefts depends critically on AchE activity (Prado et al. 2002). AchE belongs to a family of enzymatic proteins distributed in cholinergic neurons and widely throughout the body mainly in cholinergic nerves and erythrocytes (Prado et al. 2002; Cooper et al. 2003). Apart from its catalytic function in hydrolyzing Ach, AchE affects cell proliferation, differentiation and responses to various insults, including stress (Grisaru et al. 1999). It also performs nonenzymatic, trophic (e.g. stimulation of neuritogenesis and remodeling) and neuromodulatory (promotion of long-term functional changes in the central nervous system) functions (Gralewicz 2006).

Despite existing knowledge, the data on the AchE role in early phase of acute lindane intoxication is not reported in the curently available literature. Taking into account the absence of studies showing the influence of AchE activity on lindane neurotoxic effects, this study was aimed to investigate the possible involvement of AchE in mediating the early phase of acute neurotoxicity of this pesticide in rats.

Materials and Methods

Animals

Experiments were performed on adult male Wistar rats, weighing 170–200 g, raised at Military Medical Academy Breeding Laboratories, Belgrade. Animals were kept under standard controlled laboratory conditions (temperature 22 ± 2°C, relative humidity 50% and 12/12 h light/dark cycle with light switched on at 9 a.m.), and were housed individually with free access to standard pelleted food and tap water. All experimental procedures were in full compliance with The European Council Directive (86/609/EEC) and approved by The Ethical Committee of the University of Belgrade (Permission No. 298/5-2).

All animals (n = 48) were divided into following groups: 1. control, saline-treated (n = 16); 2. DMSO-treated (n = 16); 3. group that received lindane in a dose of 8 mg/kg intraperitoneally (i.p.) (n = 16). Before administration, lindane (Sigma-Aldrich Chemical Co., U.S.A.) was dissolved in dimethylsulfoxide (DMSO; Sigma-Aldrich Chemical Co., U.S.A.) and injected in a volume of 0.5 ml/kg body weight. The dose of 8 mg/kg was chosen since in previous studies convulsions were found to appear in rats after acute exposure to this dose (Mladenović et al. 2007). Eight animals from each group were sacrificed by decapitation 0.5 and 4 h after treatment.

Biochemical analysis

After decapitation the heads were immersed into liquid nitrogen and stored at –80°C. For the determination of enzyme activity crude synaptosomal and mitochondrial fractions of specific brain regions were prepared according to the method of Whittaker and Barker (1972) with the omission of purification step through sucrose gradient. Isolation of cerebral cortex, hippocampus, thalamus and nc. caudatus from individual animals was done quickly on ice. Isolated tissue was homogenized in ice-cold buffer, pH 7.0, containing 0.25 mmol/l sucrose, 0.1 mmol/l EDTA, 50 mmol/l K-Na phosphate buffer. Homogenates were centrifuged twice at 1000 × g for 15 min at 4°C. The supernatant was further centrifuged at 20,000 × g for 20 min. Supernatant obtained by this procedure represents crude synaptosomal fraction containing membrane vesicles (microsomes) from smooth and rough endoplasmic reticulum, Golgi and plasma membrane and all of the soluble components of the cytoplasm. The pellet was resuspended in deionized water and left for 60 min at +4°C. Finally, resuspended pellet was centrifuged at 1700 × g for 15 min. Obtained supernatant represents crude mitochondrial fraction containing mitochondria, lysosomes, peroxisomes, Golgi membranes and some rough endoplasmic reticulum. Crude synaptosomal and crude mitochondrial fractions were stored at –80°C.

AchE activity, expressed as mol/mg prot./min × 10^{-4} was assayed by spectrophotometric method of Ellman et al. (1961), using acetylthiocholine iodide as a substrate in homogenates of cerebral cortex, hippocampus, thalamus and nc. caudatus. Each sample was taken from one animal and assayed in duplicate. The rate of hydrolysis of acetylthiocholine iodide was measured at 412 nm through the release

of the thiol compound which, when reacted with 5,5`-dithiobis 2-nitrobenzoic acid (DTNB), produced the absorbing compound thionitrobenzoic acid.

Statistical analysis

For statistical purposes, one-way ANOVA was followed by Newman-Kuels test for multiple comparisons taking $p < 0.05$ as the level of significance. All the results were expressed as means ± SD.

Results

No significant changes in AchE activity were detected in any brain region in control group 0.5 or 4 h after treatment (data not shown). In addition, administration of DMSO did not induce any significant change in the activity of both AchE izoenzymes within 0.5 or 4 h in comparison with control group ($p > 0.05$) (data not shown).

The AchE activity in the crude mitochondrial fraction of cerebral cortex was significantly increased in the lindane-treated animals 0.5 h after administration of this pesticide (0.272 ± 0.018 mol/mg prot./min × 10^{-4}) ($p < 0.05$) in comparison with its basal activity measured in control group (0.191 ± 0.015 mol/mg prot./min × 10^{-4}) (Fig. 1A).

There were no significant changes in the AchE activity in the crude mitochondrial and synaptosomal fraction of hippocampus in the lindane-treated animals in comparison with its basal activity found in control group (Fig. 1B).

A significant rise in synaptosomal AchE activity was detected in thalamus of animals that received lindane (0.388 ± 0.105 mol/mg prot./min × 10^{-4}) ($p < 0.05$), 4 h after its administration in comparison with control value (0.282 ± 0.076 mol/mg prot./min × 10^{-4}) (Fig. 1C).

The AchE activity in the crude mitochondrial fraction of nc. caudatus was significantly increased in lindane-injected animals 0.5 h (4.011 ± 0.648 mol/mg prot./min × 10^{-4}) ($p < 0.05$) and 4 h (4.336 ± 0.855 mol/mg prot./min × 10^{-4}) ($p < 0.05$) after intraperitoneal application of this convulsant when compared to control value (3.117 ± 0.083 mol/mg prot./min × 10^{-4}) (Fig. 1D).

Discussion

The mode of action by which lindane alters neurotransmitter equilibrium in the brain and cause neurotoxicity is still an incompletely known territory. From a toxicological point of view, our results represent important findings, because the influence of lindane on the AchE activity has not been examined in the *in vitro* and *in vivo* experiments.

Our investigation has shown that in the lindane-treated animals 0.5 h after administration of this pesticide the AchE activity in the crude mitochondrial fraction of cerebral cortex was significantly increased ($p < 0.05$) (Fig. 1A). On the other hand, investigation reported by Gopal et al. (1992) concerning assessment of brain biochemistry has shown effects that reduced total brain ATPase and AchE activity. Another similar investigations have shown that lindane neurotoxicity include alterations in the activities of various enzymes, including Na^+, K^+-ATPase, Mg^{2+}-ATPase and AchE (Raizada et al. 1993; Martinez and Martinez-Conde 1995; Anand et al. 1991, 1998; Rivera et al. 1998; Sahoo et al. 2000; Parmar et al. 2003). Additionally, it is known that acute administration of high doses of aluminium significantly reduces AchE activity in mitochondrial and microsomal fractions of the cortex of gerbil brain (Mićić and Petronijević 2000).

As it is previously mentioned, any studies have not been conducted on lindane mechanism involving cholinergic system. In our experiment there was no significant difference between the AchE activity in the crude mitochondrial and synaptosomal fraction of hippocampus in the lindane-treated animals 0.5 and 4 h after treatment with this substance (Fig. 1B). On the other hand, AchE activity in mitochondrial and microsomal fractions of the hippocampus of gerbil brain was significantly decreased after acute administration of high doses of aluminium (Mićić and Petronijević 2000).

Ach has an important role in peripheral and central nervous system. Apart from glutamatergic, hippocampus consists of cholinergic neurons that form rich connections with numerous brain regions (Hossain et al. 2004). Besides, a large portion of the septohippocampal projection is GABAergic (Amaral and Kurz 1985) and the septal GABAergic afferents terminate exclusively on hippocampal interneurons (Freund and Antal 1988). Cholinergic activation depresses excitatory responses by increasing GABA release from interneuron terminals (Pitler and Alger 1992). It is also known that events included in the synthesis and release of Ach require acetyl coenzyme A and energy from the mitochondria in nerve terminals. It is possible that lindane caused a disturbance of mitochondrial respiration in the hippocampus which led to non significant changes in the activities of AchE fractions in the hippocampus of investigated rats in the present study.

The primary target for lindane action was suggested to be GABA receptor. Lindane binds to the picrotoxin site of ionotropic $GABA_A$ receptor, thus inhibiting its function and enhancing excitatory neurotransmission in the central nervous system. This effect was confirmed by suppression of lindane-induced convulsions by various $GABA_A$ agonists and their exacerbation by $GABA_A$ antagonists (Martinez and Martinez-Conde 1995; Anand et al. 1998). However, the effect of the lindane in the present experiment may have affected both the cholinergic and GABAergic interneurons which interact within the hippocampus. It is possible that

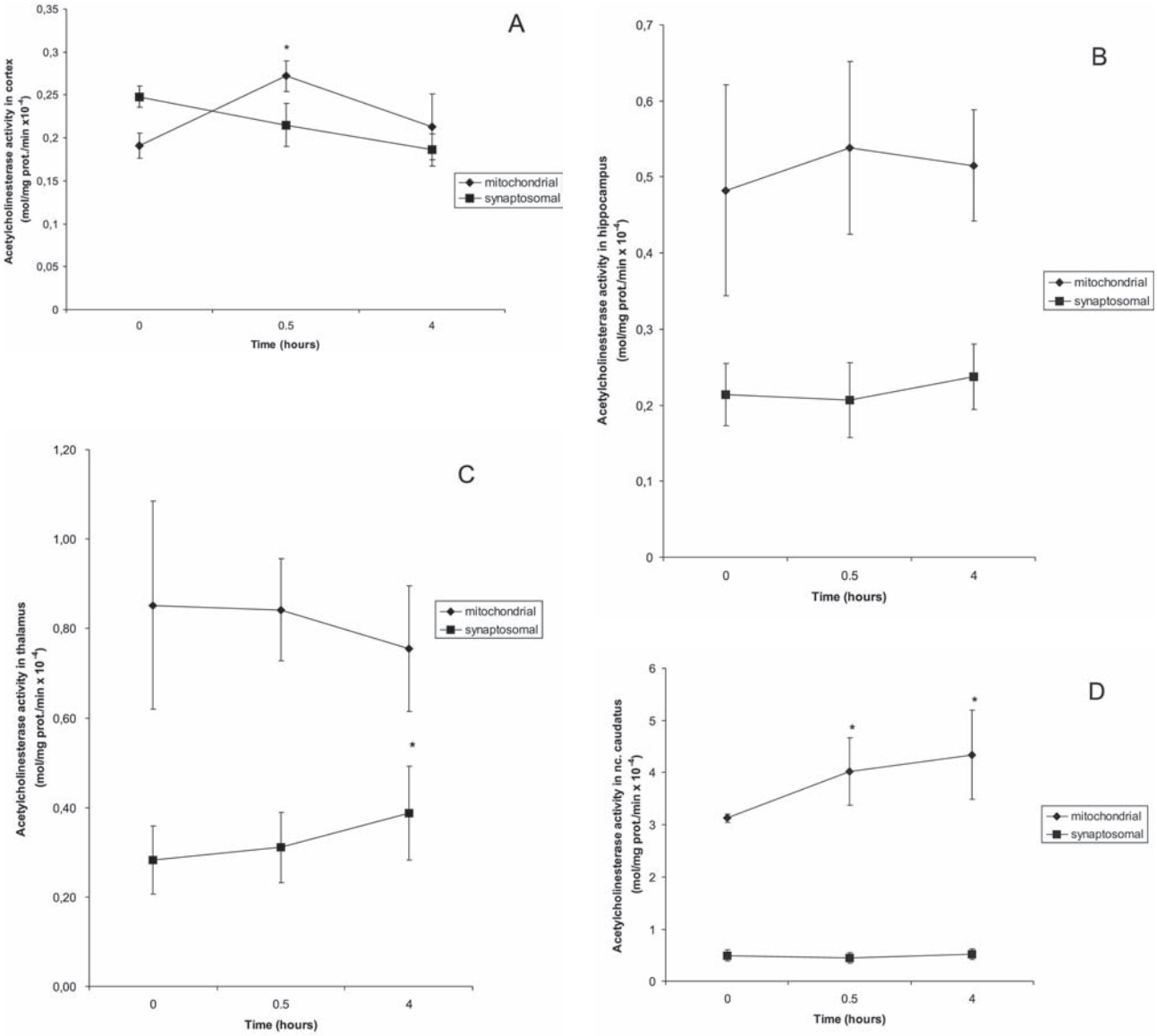

Figure 1. Acetylcholinesterase (AchE) activity in cerebral cortex (A), hippocampus (B), thalamus (C) and nc. caudatus (D) in rats 0, 0.5 and 4 h after lindane (8 mg/kg, i.p) administration. AchE activities measured in control group were considered to be its basal activities (0 h). Data are means ± SD, * $p < 0.05$ (one way ANOVA and Newman-Kuels test) in comparison with basal activity (0 h).

a lindane increases the release of Ach *via* affecting sodium channels of cholinergic nerves and also decreases the release of Ach via increasing GABA release that may, in turn, inhibit the cholinergic excitement. Additionally, Soderlund et al. (2002) clearly demonstrated that, unlike insects, mammals have multiple sodium channel isoforms that vary in their biophysical and pharmacological properties, including their differential sensitivity to pesticides. The literature, also, describe hippocampal differences in sensitivity to pesticide action in comparison with other regions of the brain (Soderlund et al. 2002; Hossain et al. 2004, 2005; Gralewicz 2006; Trevisan et al. 2008). Namely, with low doses, and after a short period of exposure, malathion induces an up-regulation of hippocampal and cortical AchE activity (Trevisan et al. 2008).

The inhibition of AchE activity in target tissues is often taken as an indication of pesticide intoxication (Kwong 2002), resulting in the hyper-stimulation of cholinergic receptors (Carr et al. 2001). In the hippocampus the activity of the antioxidant enzymes studied correlates positively with AchE activity increase (Trevisan et al. 2008). In relation to, oxidative stress has been hypothesized as an alternative

pathway for organophosphate toxicity, by either increasing reactive oxygen species production or decreasing antioxidant defenses. It is known that oxidative perturbation can be an alternative pathway for malathion toxicity in the central nervous system (Trevisan et al. 2008). Besides, the absence of AchE inhibition, suggests that the cholinergic system may not be directly involved in the toxic effects of malathion at repeated low doses. Furthermore, cerebral cortex and hippocampus were able to increase AchE, which may be considered an adaptive response. Among alternative targets, reduction of antioxidant protection, especially in the cerebral cortex, is a possible alternative route for malathion toxicity (Trevisan et al. 2008). Similarly, lindane has also been shown to be a strong oxidant causing free radical generation in tissues including brain through lipid peroxidation. This oxidant generation is accompanied by alterations in antioxidant capacity of the brain, too (Sahoo et al. 2000; Sahaya et al. 2007). It cannot be excluded that alteration of AchE activity is a contributing factor in lindane toxicity in our experiment.

A significant rise ($p < 0.05$) in synaptosomal AchE activity was detected in thalamus of animals 4 h after lindane administration (Fig. 1C). On the other hand, acute administration of high doses of aluminium significantly reduces AchE activity in mitochondrial and microsomal fractions of the thalamus of gerbil brain (Mićić and Petronijević 2000).

As shown in Fig. 1D, the AchE activity in the crude mitochondrial fraction of nc. caudatus was significantly increased ($p < 0.05$) in lindane-injected animals.

AchE was found in various molecular forms, depending on alternative splicing of its transcripts and association with structural proteins. Tetramers of the "tailed" variant (AchE-T), which are anchored in the cell membrane of neurons by the PRiMA (Proline Rich Membrane Anchor) protein, constitute the main form of AchE in the mammalian brain. In the mouse brain, stress and anticholinesterase inhibitors have been reported to induce expression of the unspliced "readthrough" variant (AchE-R) mRNA which produces a monomeric form (Perrier et al. 2005). Besides, AchE responses (cell proliferation, differentiation, responses to various insults, including stress) are at least in part specific to the three C-terminal variants of AchE, which are produced by alternative splicing of the single AchE gene. "Synaptic" AchE-S constitutes the principal multimeric enzyme in brain and muscle; soluble, monomeric "readthrough" AchE-R appears in embryonic and tumor cells and is induced under psychological, chemical and physical stress; and glypiated dimers of erythrocytic AchE-E associate with red blood cell membranes. It has been postulated that the homology of AchE to the cell adhesion proteins, gliotactin, glutactin and the neurexins, which have more established functions in nervous system development, is the basis of its morphogenic functions (Grisaru et al. 1999). Taking these facts into consideration, results of our study also suggest that competition between AchE variants and their homologs on interactions with the corresponding protein partners is possible in investigated brain structures in rats during lindane-induced neurotoxicity.

On the basis of our study, it can be concluded for the first time the possible involvement of AchE activity in mediating the early phase of acute lindane neurotoxicity in rats. However, the exact mechanism of AchE influence on lindane animal model of acute neurotoxicity will require further investigation.

Acknowledgement. This work was supported by the Ministry of Science and Environmental Protection of Serbia, grant No. 145029B.

References

Agrawal D., Subramoniam A., Afaq F. (1995): Influence of hexachlorocyclohexane on phosphoinositides in rat erythrocyte membranes and brain. Toxicology **95**, 135–140

Amaral D. G., Kurz J. (1985): An analysis of the origins of the cholinergic and noncholinergic septal projections to the hippocampus formation of the rat. J. Comp. Neurol. **240**, 35–59

Anand M., Agrawa A. K., Rehmani B. N. H. (1998): Role of GABA receptor complex in low dose lindane (HCH) induced neurotoxicity: Neurobehavioural, neurochemical and electrophysiological studies. Drug. Chem. Toxicol. **21**, 35–46

Anand M., Gupta G. S. D., Gopal K. (1991): Influence of dietary protein deficiency on EEG neurotransmitters and neurobehaviour after chronic exposure to HCH. Toxicol. Environ. Chem. **34**, 1–11

Anand M., Meera P., Kumar R. (1995): Possible role of calcium in the cardiovascular effects of prolonged administration of gamma-HCH (Lindane) in rats. J. Appl. Toxicol. **15**, 245–248

Beard A. P., Rawlings N. C. (1999): Thyroid function and effects on reproduction in ewes exposed to the organochlorine pesticides lindane or pentachlorophenol (PCP) from conception. J. Toxicol. Environ. Health **58**, 509–530

Brown D. (1988): Lindane: 13 week dermal toxicity study (with interim kill and recovery period) in the rat. Hazelton UK, North Yorkshire, England. HUK report no. 5757–5802

Carr R. L., Chambers H. W., Guarisco J. A., Richardson J. R., Tang J., Chambers J. E. (2001): Effects of repeated oral postnatal exposure to chlorpyrifos on open-field behavior in juvenile rats. Toxicol. Sci. **59**, 260–267

Cooper J. R., Bloom F. E., Roth R. H., (2003): Acetylcholine. The Biochemical Basis of Neuropharmacology. Oxford University Press, New York

Dietrich D. R., Swenberg J. A. (1990): Lindane induces nephropathy and renal accumulation of α2μ-globulin in male but not in female Fischer 344 rats or male NBR rats. Toxicol. Letters **53**, 179–181

Ellman G. L., Courtney K. D., Andres V. Jr., Feather-Stone R. M. (1961): A new and rapid colorimetric determination of

acetylcholinesterase activity. Biochem. Pharmacol. **7**, 88–95

Freund T. F., Antal M. (1988): GABA-containing neurons in the septum control inhibitory interneurons in the hippocampus. Nature **336**, 170–173

Gopal K., Anand M., Khanna R. N. (1992): Some neurotoxicological consequences of hexachlorocyclohexane (HCH) stress in rats fed on protein deficient diet. Toxicol. Environ. Chem. **36**, 57–63

Gralewicz S. (2006): Possible consequences of acetylcholinesterase inhibition in organophosphate poisoning. Discussion continued. Med. Pr. **57**, 291–302 (in Polish)

Grisaru D., Sternfeld M., Eldor A., Glick D., Soreq H. (1999): Structural roles of acetylcholinesterase variants in biology and pathology. Eur. J. Biochem. **264**, 672–686

Hong H. L., Boorman G. A. (1993): Residual myelotoxicity of lindane in mice. Fundam. Appl. Toxicol. **21**, 500–507

Hossain M. M., Suzuki T., Sato I., Takewaki T., Suzuki K., Kobayashi H. (2004): The modulatory effect of pyrethroids on acetylcholine release in the hippocampus. Neurotoxicology **25**, 825–833

Hossain M. M., Suzuki T., Sato I., Takewaki T., Suzuki K., Kobayashi H. (2005): Neuromechanical effects of pyrethroids, allethrin, cyhalothrin and deltamethrin on the cholinergic processes in rat brain. Life Sci. **77**, 795–807

Kalantzi O. I., Hewitt R., Ford K. J. (2004): Low dose induction of micronuclei by lindane. Carcinogenesis **25**, 613–622

Kaminski R. M., Tochman A. M., Dekundy A., Turski W. A., Czuczwar S. J. (2004): Ethosuximide and valproate display high efficacy against lindane-induced seizures in mice. Toxicol. Lett. **154**, 55–60

Katsumata K., Katsumata K. (2003): Norwegian scabies in an elderly patient who died after treatment with γBHC. Intern. Med. **42**, 367–369

Kwong T. C. (2002): Organophosphate pesticides: biochemistry and clinical toxicology. Ther. Drug Monit. **24**, 144–149

Martinez A. O., Martinez-Conde E. (1995): The neurotoxic effects of lindane at acute and subchronic dosages. Ecotoxicol. Environ. Saf. **30**, 101–105

Mićić D. V., Petronijević N. D. (2000): Acetylcholinesterase activity in the mongolian gerbil brain after acute poisoning with aluminium. J. Alzheimer Dis. **2**, 1–6

Mills P. K., Yang R. (2003): Prostate cancer risk in California farm workers. J. Occup. Environ. Med. **45**, 249–258

Mladenović D., Hrnčić D., Radosavljević T., Vučević D., Djurić D., Rašić-Marković A., Macut Dj., Šušić V., Šćepanović Lj., Stanojlović O. (2008): Dose-dependent anticonvulsive effect of ethanol on lindane-induced seizures in rats. Can. J. Physiol. Pharmacol. **86**, 148–152

Moreno M. J., Pellicer S., Fernández-Otero M. P. (1996): Effects of in situ and systemic lindane treatment on in vivo absorption of galactose and leucine in rat jejunum. Arch. Toxicol. **70**, 767–772

Muscat J., Britton J., Djordjevic M. (2003): Adipose concentrations of organochlorine compounds and breast cancer recurrence in Long Island, New York. Cancer Epidemiol. Biomarkers Prev. **12**, 1474–1478

Nagaraja T. N., Desiraju T. (1994): Brain regional variations in the levels of biogenic amines, glutamate, GABA and glutamate decarboxylase activity in developing and adult rats exposed chronically to hexachlorocyclohexane. Biogenic Amines **10**, 141–149

Ntow W. J. (2001): Organochlorine pesticides in water, sediment, crops, and human fluids in a farming community in Ghana. Arch. Environ. Contam. Toxicol. **40**, 557–563

Parmar D., Yadav S., Dayal M., Johri A., Dhawan A., Seth P. K. (2003): Effect of lindane on hepatic and brain cytochrome P450s and influence of P450 modulation in lindane-induced neurotoxicity. Food Chem. Toxicol. **41**, 1077–1087

Perrier N. A., Salani M., Falasca C., Bon S., Augusti-Tocco G., Massoulié J. (2005): The readthrough variant of acetylcholinesterase remains very minor after heat shock, organophosphate inhibition and stress, in cell culture and in vivo. J. Neurochem. **94**, 629–638

Pitler T. A., Alger B. E. (1992): Cholinergic excitation of GABAergic interneurons in the rat hippocampal slices. J. Physiol. (London) **450**, 127–142

Prado M. A. M., Reis R. A. M., Prado V. F., De Mello M. C., Gomez M. V., De Mello F. G. (2002): Regulation of acetylcholine synthesis and storage. Neurochem. Int. **41**, 291–299

Radosavljević T., Mladenović D., Vučević D., Petrović J., Hrnčić D., Djurić D., Lončar-Stevanović H., Stanojlović O. (2008): Effect of acute lindane and alcohol intoxication on serum concentration of enzymes and fatty acids in rats. Food Chem. Toxicol. **46**, 1739–1743

Raizada R. B., Srivastava M. K., Sarin S. (1993): Impact of technical hexachlorocyclohexane (HCH) on biogenic amines and locomotor activity of rat. Natl. Acad. Sci. Lett. (India) **16**, 73–76

Rauch A. E., Kowalsky S. F., Lesar T. S. (1990): Lindane (Kwell)-induced aplastic anemia. Arch. Intern. Med. **150**, 2393–2395

Rivera S., Rosa R., Martinez E., Sunol C., Serrano M. T., Vendrell M., Rodriguez-Farre E., Sanfeliu C. (1998): Behavioral and monoaminergic changes after lindane exposure in developing rats. Neurotoxicol. Teratol. **20**, 155–160

Rivera S., Sanfeliu C., Sunol C. (1991): Regional effects on the cerebral concentration of noradrenaline, serotonin, and dopamine in suckling rats after a single dose of lindane. Toxicology **69**, 43–54

Sahaya K., Mahajan P., Mediratta P. K., Ahmed R. S., Sharma K. K. (2007): Reversal of lindane-induced impairment of step-down passive avoidance and oxidative stress by neurosteroids in rats. Toxicology **239**, 116–126

Sahoo A., Samanata L., Chainy G. B. N. (2000): Mediation of oxidative stress in HCH-induced neurotoxicity in rat. Arch. Environ. Contam. Toxicol. **39**, 7–12

Soderlund D. M., Clark J. M., Sheets L. P., Mullin L. S., Piccirillo V. J., Sargent D., Stevens J. T., Weiner M. L. (2002): Mechanisms of pyrethroid neurotoxicity: implications for cumulative risk assessment. Toxicology **171**, 3–59

Srivastava M. K., Raizada R. B. (2000): A limited three-generation reproduction study on hexachlorocyclohexane (HCH) in rats. Food Chem. Toxicol. **38**, 195–201

Trevisan R., Uliano-Silva M., Pandolfo P., Franco J. L., Brocardo P. S., Santos A. R. S., Farina M., Rodrigues A. L. S., Takahashi R. N., Dafre A. L. (2008): Antioxidant and acetylcholinesterase response to repeated malathion exposure in rat cerebral cortex and hippocampus. Basic Clin. Pharmacol. Toxicol. **102**, 365–369

Vučević D., Hrnčić D., Radosavljević T., Mladenović D., Rašić-Marković A., Lončar-Stevanović H., Djurić D., Macut Dj., Šušić V., Stanojlović O. (2008): Correlation between electrocorticographic and motor phenomena in lindane-induced experimental epilepsy in rats. Can. J. Physiol. Pharmacol. **86**, 173–179

Whittaker V. P., Barker L. A. (1972): The subcellular fractionation of brain tissue with special reference to the preparation of synaptosomes and their component organelles. In: Methods in Neurochemistry. (Ed. R. Fried), Marcel Dekker, New York

High dose of ethanol decreases total spectral power density in seizures induced by D,L-homocysteine thiolactone in adult rats

Aleksandra Rašić-Marković[1], Dragan Djuric[1], Dragan Hrnčić[1], Helena Lončar-Stevanović[1], Danijela Vučević[2], Dušan Mladenović[2], Predrag Brkić[1], Macut Djuro[3], Ivana Stanojević[4] and Olivera Stanojlović[1]

[1] *Laboratory of Neurophysiology, Institute of Medical Physiology, School of Medicine, University of Belgrade, Serbia*
[2] *Institute of Pathophysiology, School of Medicine, University of Belgrade, Serbia*
[3] *Institute of Endocrinology, Diabetes and Metabolic Diseases, Clinical Center of Serbia, Belgrade Serbia*
[4] *Vinča Institute of Nuclear Science, Belgrade, Serbia*

Abstract. The effects of ethanol on epilepsy are very complex. Ethanol can have depressant as well as excitatory effect on different animal models of epilepsy. Systemic administration of homocysteine can trigger seizures. The aim of the present study was to examine the changes of total spectral power density after ethanol alone and together with homocysteine thiolactone in adult rats. Adult male Wistar rats were divided into following groups: 1. saline-injected, (control) C; 2. D, L-homocysteine thiolactone, H (8 mmol/kg); 3. ethanol, E ($E_{0.5}$, 0.5 g/kg; E_1, 1 g/kg; E_2, 2 g/kg) and 4. E ($E_{0.5}$, E_1, and E_2) 30 min prior to H, EH ($E_{0.5}H$, E_1H and E_2H). For EEG recordings three gold-plated screws were implanted into the skull. Our results demonstrate that ethanol, when applied alone, increased total EEG spectral power density of adult rats with a marked spectrum shift toward low frequency waves. In EH groups, increasing doses of ethanol exhibited a dose-dependent effect upon spectral power density. Ethanol increased EEG spectral power density in $E_{0.5}H$ and E_1H group, comparing to the H group ($p > 0.05$), the maximal increase was recorded with the lowest ethanol dose applied. The highest dose of ethanol (E_2H) significantly decreased total power spectra density, comparing to the H group. We can conclude that high doses of ethanol depressed marked increase in EEG power spectrum induced by D,L-homocysteine thiolactone.

Key words: Epilepsy — EEG — Ethanol — D,L-homocysteine thiolactone

Introduction

Seizures and epilepsy have been documented since the earliest civilizations, before much was understood about the nervous system at all. Epilepsy, defined by a state of recurrent, spontaneous seizures (Scharfman 2007), is a major health problem that affects 1–2% of the population worldwide. Epileptogenic processes have been associated with an imbalance between excitatory and inhibitory control systems in selective regions of the brain (Brailowsky and Garcia 1999). Available drugs reduce seizures in the majority of patients, but only 40% are free of seizures despite optimal treatment (Loscher 2002). Animal models of epilepsy had a fundamental role in our understanding of the physiological and behavioral changes associated with human epilepsy, and have led to the discovery of antiepileptic drugs that are still in use. The physiological mechanisms underlying preictal, interictal, ictal and postictal states and transitions from one state to another are far from being elucidated, that is why animal models continue to be important for many aspects surrounding epilepsy (Sarkisian 2001).

Ethanol is used as a social drug and is the second psychoactive substance most widely used in the world after caffeine. The influence of ethanol on central nervous system (CNS) depends on the dose, drinking pattern, tolerance and other factors. The effects of ethanol on epilepsy are very complex. While chronic ethanol consumption is followed by series of

Correspondence to: Olivera Stanojlović, Institute of Medical Physiology, School of Medicine, University of Belgrade, Višegradska 26/II, 11000 Belgrade, Serbia
E-mail: solja@afrodita.rcub.bg.ac.yu

seizures during the withdrawal period, acute ethanol intake exerts mainly inhibitory effects on the CNS and is usually associated with an increase of seizure threshold (Hillbom et al. 2003). Ethanol exerts important effects on membranes, voltage-gated ion channels, second messenger systems and a variety of different neurotransmitter systems such as adenosine (Concas et al. 1996), glycine (Aguayo and Pancetti 1996), acetylcholine (Coe et al. 1996), as well as monoamines and neuropeptides (Wang et al. 1996) systems.

Two major amino acid neurotransmitter systems, GABA and excitatory amino acids (glutamate and aspartate) are affected by ethanol. Numerous *in vivo* studies showed that ethanol inhibits calcium influx through N-methyl-D-aspartate (NMDA) glutamatergic receptors (Faingold et al. 1998) and enhances the inhibitory action of GABA (Davis and Jang-Yen 2001).

Homocysteine is a sulphur-containing amino acid normally present in human plasma and its concentration ranges from 1 to 15 μmol/l. Homocysteine is as one of the most potent excitatory agent of the CNS. Available data suggests that homocysteine can be harmful to human cells because of its metabolic conversion to a reactive thioester homocysteine thiolactone. Systemic administration of homocysteine or homocysteine thiolactone can trigger seizures in animals (Folbergova et al. 2000; Stanojlovic et al. 2000) and patients with homocystinuria suffer from epileptic seizures (Sachdev 2005). The various deleterious manifestations of hyperhomocysteinemia are due to overstimulation of NMDA and group I metabotropic glutamate receptors (mGluRs), oxidative stress, DNA damage and triggering of apoptosis. Normal human plasma levels of homocysteine thiolactone vary from 0 to 34.8 nmol/l and account for 0.002–0.3% total plasma homocysteine (Jakubowski 2006).

The aim of the present study was to examine the changes of total spectral power density after ethanol alone and together with homocysteine thiolactone in adult rats.

Materials and Methods

Animals

Adult (2-months-old) male Wistar rats, weighing 180–230 g, obtained from the Military Medical Academy Breeding Laboratories, Belgrade, were used in experiments. During the experiment, the animals were kept under controlled environmental conditions (21 ± 2°C, 50% humidity and a 12/12 h light/dark cycle with light switched on at 9 a.m.) and housed individually with free access to standard laboratory animal chow and tap water. Animals were divided into following groups:

1. saline-injected, (control) C ($n = 6$)
2. D,L-homocysteine thiolactone, H (8 mmol/kg, $n = 6$)
3. ethanol, E: $E_{0.5}$ (0.5 g/kg, $n = 6$), E_1 (1 g/kg, $n = 6$), E_2 (2 g/kg, $n = 6$)
4. E ($E_{0.5}$, E_1, and E_2) 30 min prior to H, EH: $E_{0.5}H$ ($n = 6$), E_1H ($n = 6$), E_2H ($n = 6$).

All the substances were applied intraperitoneally (i.p.). Each rat was used only once. D, L-homocysteine thiolactone (Sigma-Aldrich Chemical Co., USA) was dissolved in saline and after adjusting the pH to 7.0 was administered in a volume of 1 ml/100 g body weight.

All experimental procedures were in full compliance with The European Council Directive (86/609/EEC) and approved by The Ethical Committee of the University of Belgrade (Permission No. 298/5-2).

EEG

The rats were anesthetized with pentobarbital sodium (50 mg/kg, i.p.), placed in a stereotaxic apparatus and three gold-plated recording electrodes were implanted over frontal, parietal and occipital cortices (for details see Stanojlović et al. 2000, 2007). Animals were allowed at least 7 days recovery from the surgery and then acclimated to the recording environment for at least 24 h. During that period, animals were supervised and no epileptiform phenomena were noticed. The animals were placed in separate transparent plastic cages (55 × 35 × 15 cm), and observed for 120 min for the occurrence of specific behavior and EEG.

An 8-channel EEG apparatus (RIZ, Zagreb, Croatia) was used. The signals were digitized using a SCB-68 data acquisition card (National Instruments Co., Austin, Texas, USA). A sampling frequency of 512 Hz/channel and 16-bit A/D conversion were used for the EEG signals. The cutoff frequencies for EEG recordings were set at 0.3 Hz and 80 Hz for the high-pass and low-pass filters, respectively. Ambient noise was eliminated using a 50 Hz notch filter. Data acquisition and signal processing were performed with LabVIEW software developed in the laboratory (NeuroSciLaBG).

All EEG recordings in freely moving rats were visually monitored and screened for seizure activity and stored on disk for subsequent off-line analysis. EEG epochs containing artifacts, were rejected prior to further analysis. The observational period (120 min) was divided into eight 15 min intervals. From each interval, a 5 min period of EEG was chosen (near to the midpoint of the 15 min interval) during typical and characteristic vigilance state. After that, ten consecutive 12 s epochs of EEG were extracted and the mean total power spectrum density was calculated. Energies in different frequency bands were calculated integrating the power spectrum in these frequency windows. The fast Fourier transform method (linear detrending, Hanning window, 0.083 Hz resolution) was applied to obtain estimates of total spectral power densities ($\mu V^2/Hz$) and spectral power densities in δ (0.5–4 Hz); θ (4–7 Hz);

α (7–15 Hz) and β (15–30 Hz) frequency band. Relative powers were calculated by dividing the absolute amplitude within a given frequency range by corresponding measures of total amplitude.

Data analyses

Differences in total power spectral density between the groups were compared with one-way ANOVA. For data not normally distributed, Kruskal-Wallis one-way ANOVA on Ranks and a Dunns post hoc analysis (SigmaStat, SPSS Inc., Chicago, USA) was applied.

Results

The power spectra analysis showed (Fig. 1A) that there were significant differences in the mean total power spectra densities between C and E groups. Ethanol increased mean total spectral power density 15 min and 30 min after administration, in all E groups $E_{0.5}$ ($p < 0.05$, $p < 0.01$), E_1 ($p < 0.01$, $p < 0.01$), E_2 ($p < 0.01$, $p < 0.01$), respectively, compared to the C group. The highest total power density in both time points was recorded in E_1 group and it was statistically significant (for 15 min $p < 0.01$, $p < 0.05$; and for 30 min $p < 0.01$, $p < 0.01$) compared to the $E_{0.5}$ and E_2 group, respectively.

There were no differences in total power spectra densities between E and C groups, 45 and 60 min after ethanol administration. However, 75 min after ethanol administration spectral power density in all E groups were significantly higher ($p < 0.05$) compared to the C group. The highest spectral power density was recorded in E_1 group in consecutive 90, 105 and 120 time points, and it was significantly different in comparison with C group.

EEG recording 15 min after ethanol injection displayed synchronization, decreased frequency and increased amplitude of EEG and spectral power in the δ frequency range, together with an increase in the mean voltage. Additionally, a significant decrease in the highest frequency ranges was recorded 30, 45, and 60 min (Fig. 2A) after ethanol administration. The analysis of EEG frequency bands, revealed dose-dependent increase in proportion on δ rhythm recording with a decrease in proportion of β and of α rhythm.

In another series of experiments, D, L-homocysteine thiolactone in 45 min time point caused initial decrease in total spectral power density which was significantly lower ($p < 0.05$) comparing to the C group (Fig. 1B). In consecutive periods 60, 75, 90, 105 and 120 min, spectral power densities in H group were significantly higher comparing to the C group ($p < 0.05$, $p < 0.05$, $p < 0.05$, $p < 0.01$, $p < 0.05$, respectively). The increased power density was due to epileptiform activity induced by D, L-homocysteine thiolac-

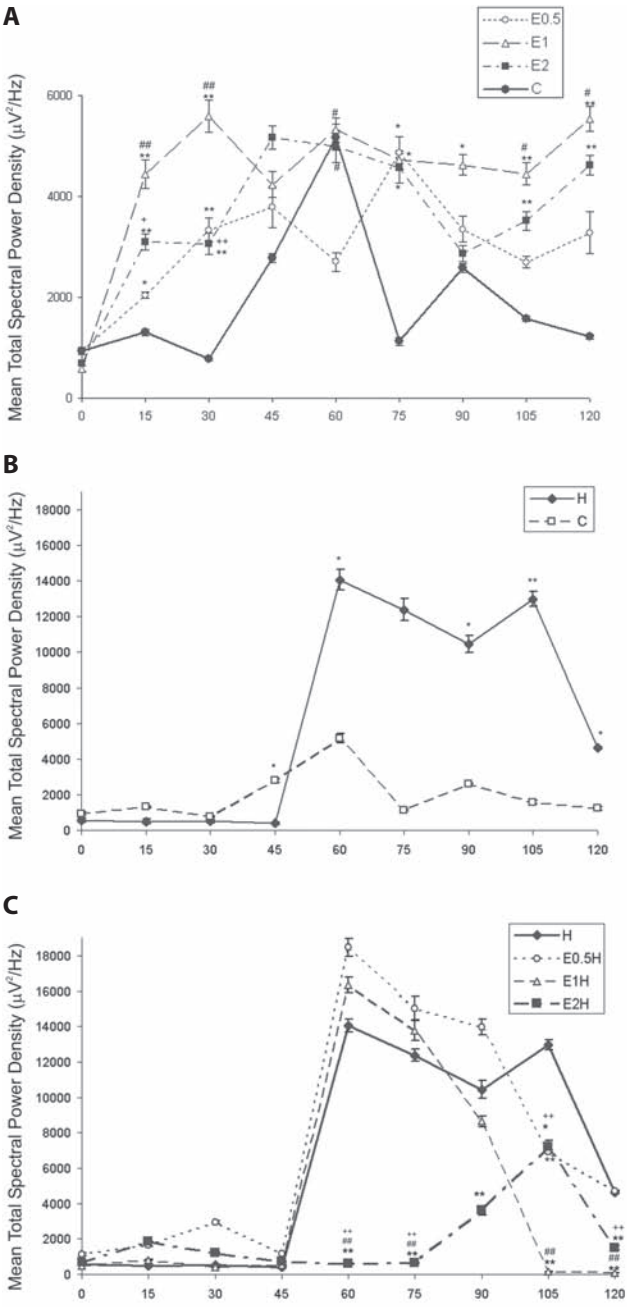

Figure 1. Time-course of EEG total spectral power densities in ethanol and control (A), D, L-homocysteine thiolactone and control (B), and ethanol 30 min prior to D, L-homocysteine thiolactone group (C). C, control group; E, ethanol groups ($E_{0.5}$, 0.5 g/kg; E_1, 1 g/kg; E_2, 2 g/kg); EH ($E_{0.5}H$; E_1H and E_2H), $E_{0.5}$, E_1, and E_2 30 min prior to H. All the substances were applied intraperitoneally (i.p.). Statistical significance was estimated by one-way ANOVA. For data not normally distributed, Kruskal-Wallis one-way ANOVA. * $p < 0.05$; ** $p < 0.01$ vs. C; # $p < 0.05$; ## $p < 0.01$ vs. $E_{0.5}$; + $p < 0.05$; ++ $p < 0.01$ vs. E_1 (A). * $p < 0.05$; ** $p < 0.01$ vs. C (B). * $p < 0.05$; ** $p < 0.01$ vs. H; # $p < 0.05$; ## $p < 0.01$ vs. $E_{0.5}H$; + $p < 0.05$; ++ $p < 0.01$ vs. E_1H (C).

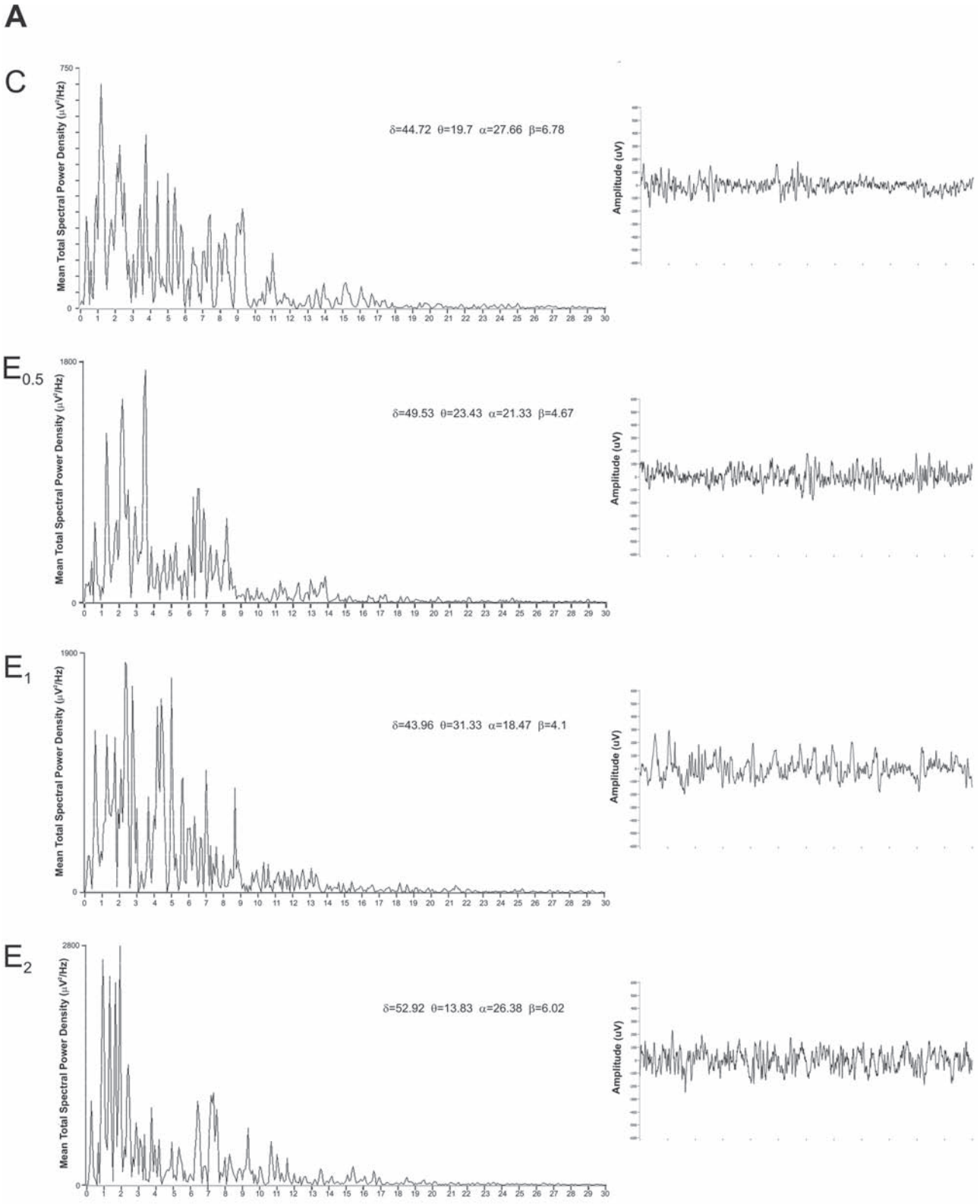
A
C
δ=44.72 θ=19.7 α=27.66 β=6.78
Mean Total Spectral Power Density (μV²/Hz)
Amplitude (uV)
E0.5
δ=49.53 θ=23.43 α=21.33 β=4.67
E1
δ=43.96 θ=31.33 α=18.47 β=4.1
E2
δ=52.92 θ=13.83 α=26.38 β=6.02

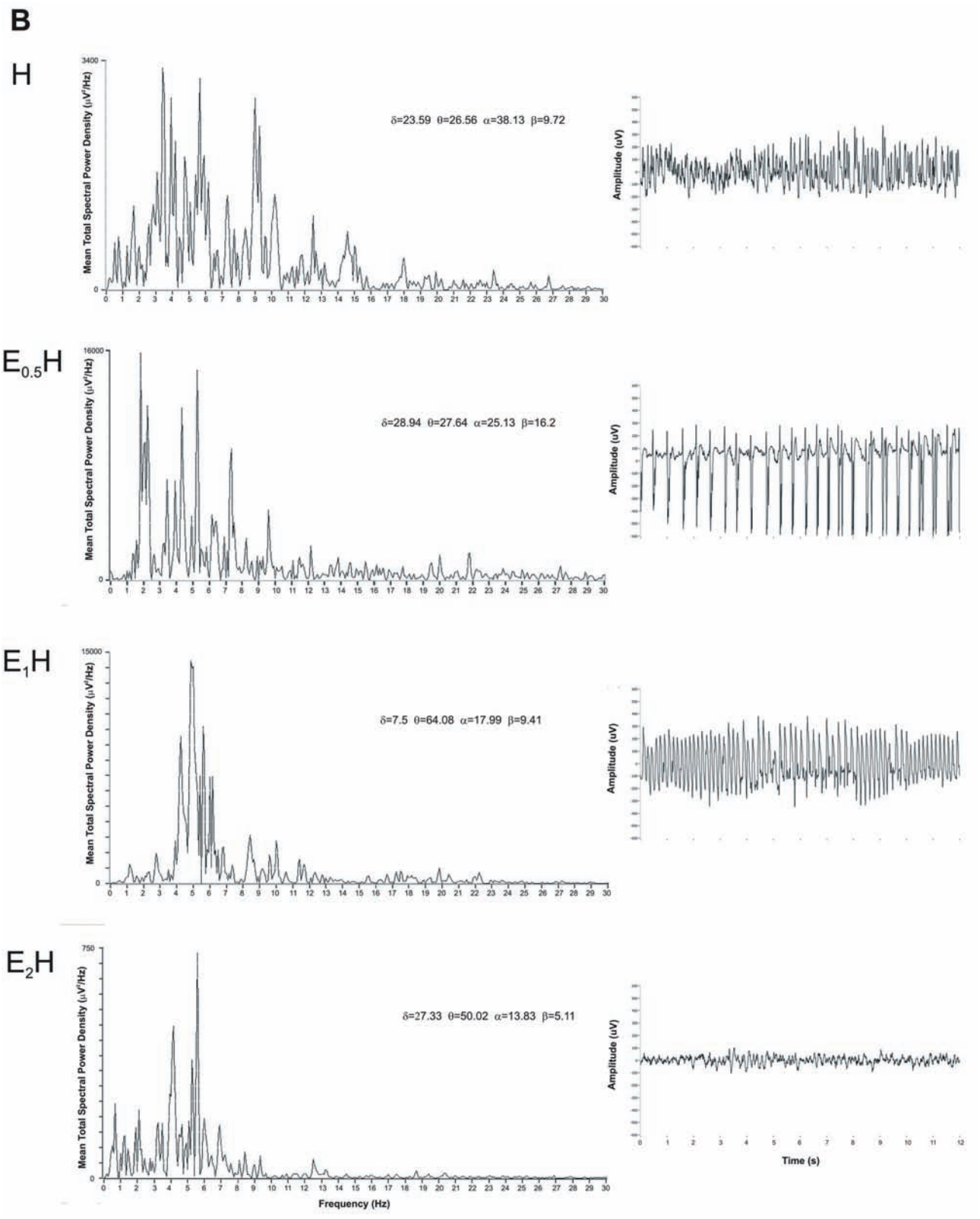

Figure 2. Representative EEG recordings and spectral power densities in the 60 min time point for ethanol and control groups (A) and for ethanol 30 min prior to D, L-homocysteine thiolactone groups (B) (see the caption for Fig. 1).

tone, with characteristic high voltage spikes and spike-wave complexes (Fig. 2B (H)).

Application of D, L-homocysteine thiolactone after ethanol, in 45 min time point, caused initial decrease in total spectral power densities in all experimental groups, although statistical significance was not attained (Fig. 1C). In the 60 min time point, lower doses of ethanol prior to homocysteine ($E_{0.5}H$, E_1H groups) increased power densities, but without statistical significance. In consecutive time points 75 and 90 min, spectral power density in $E_{0.5}H$ group decreased gradually but did not return to the basal values. The same holds true with E_1H group, in 105 and 120 min, in comparison to the H group ($p < 0.01$, $p < 0.01$), $E_{0.5}H$ group ($p < 0.01$, $p < 0.01$) and E_1H group ($p < 0.01$, $p > 0.05$), respectively. On the other hand, in E_2H group we observed significantly reduced total power density in comparison with H ($p < 0.01$, $p < 0.01$), $E_{0.5}H$ ($p < 0.01$, $p < 0.01$) and E_1H ($p < 0.01$, $p < 0.01$) group in 60 and 75 time point, respectively. This reduction of total spectral power density persisted until the end of the observational period; although a transient peak was detected in 105-time point, which was significantly lower in comparison with H group ($p < 0.05$). At the end of the observational period, spectral power density in E_2H group returned to its basal value and it was significantly lower in comparison with the H group ($p < 0.01$). The highest dose of ethanol (E_2H group) almost completely abolished spiking activity in all time points and restored baseline-like activity (Fig. 2B (E_2H group)), while lower doses of ethanol increased the amplitude of high voltage spikes (Fig. 2B ($E_{0.5}H$ group) and Fig. 2B (E_1H group)).

Discussion

In the present study, we investigated the changes of total spectral power density after ethanol alone and together with homocysteine thiolactone in adult rats. Recording electrical activity of the brain represents a measure of both brain functions and dysfunctions. The changes in the brain spontaneous activity produced by alcohol have been widely investigated by EEG.

Our results presented here demonstrate that ethanol, when applied alone, induced changes in the total EEG spectral power density of adult rats. Characteristic changes in EEG of ethanol-treated rats were accompanied by hypnotic changes. The increase in power density was most obvious 15 and 30 min after ethanol administration, and at the very end of the observational period, e.g. 105 and 120 min after ethanol administration. Interestingly, between 45 and 60 min period there were no differences in EEG power density between E and C groups, because the hypnotic effect of ethanol in E groups overlapped with sleeping period in control rats (Fig. 1A).

The first two doses employed (0.5 and 1 g/kg), showed a dose-dependent increase, while the highest dose applied decreased total power spectra. It is known that ethanol produces various changes in the EEG in both humans and animals, depending upon dose. High doses of ethanol induced a shift of the power spectrum to slower frequencies, whereas the effect of smaller doses depends on individual reaction. Increases in both slow and fast frequencies may be observed (Sauerland and Harper 1970). Our results presented here revealed a marked spectrum shift toward low frequency waves (Fig. 2A).

Together with the data of the others (Young et al. 1982; Ilian and Gevins 2001; Pietrzak and Czarnecka 2005, 2006), we have clearly demonstrated that EEG changes are associated with increased proportion of a low-frequency waves with a high amplitude, corresponding to δ and θ rhythm and accompanied by decreased proportion of α and β rhythm recording.

Ethanol and epilepsy are complexly interrelated and have been linked since Hippocrates. Alcohol-related changes in the CNS are thought to be mediated through the unbalance of excitation–inhibition with GABAergic activity being predominantly affected by alcohol. An important action of ethanol involves enhancement of the activation of the $GABA_A$ receptor, which results in hyperpolarization of the neuronal membrane by opening of the Cl^- channel and influx of Cl^- ions and the resultant inhibition of the neuron, mechanism opposing epilepsy (Faingold et al. 1998).

Acute administration of ethanol inhibits NMDA-induced ion currents *in vitro* (Lovinger et al. 1989) and *in vivo* (Simson et al. 1991), Ca^{2+} influx, cyclic GMP production (Hoffman et al. 1989), neurotransmitter release and reduces NMDA-evoked neurotoxicity (Chandler et al. 1993). In contrast to NMDA receptors, ethanol potentiates the action of serotonin (5-HT) at central 5-HT3 receptors.

Animal models have played a key role in the discovery and characterization of all significant antiepileptic drugs. It is highly likely that no single model system could be useful for all types of epilepsy. Ethanol administered by different routes and doses modified convulsive activity in bicuculine (Zhuk et al. 2001), pentylenetetrazol (Fischer and Kittner 1998), maximal electroshock (Fischer 2005) and amygdale-kindled (Kim 1995) models of epilepsy. Ethanol also raised the threshold to elicit an electrographic seizure (Cohen et al. 1993a,b). Some studies proved that ethanol induced susceptibility to audiogenic seizures in rats during the withdrawal syndrome (Faingold et al. 1998). This question seems to be matter of special interest, since ethanol is considered to be a high risk factor for epileptic patients.

D,L-homocysteine thiolactone induced significant increase in total EEG spectral power density 30 min after its administration (60 min time point, Fig. 1B) due to synchronized EEG activity which developed into high-amplitude spikes and waves, especially during the tonic phase of a maximal behavioral response. This is in agreement with

previous results which have shown that median latency to the first seizure episode in H group was 28 (21–39) min (Stanojlovic et al. 2009). The total power density remained increased, comparing to the C, till the end of the observational period, due to convulsive and epileptic activity of D, L-homocysteine thiolactone.

Homocysteine and its oxidized forms could provoke seizures and act on NMDA ionotropic glutamate receptors together with group I mGluRs, major gates for Ca^{2+} influx and intraneuronal calcium mobilization in the presence of glycine (Zieminska et al. 2003; Sachdev 2005). Increased cytosolic Ca^{2+} concentrations affect enzyme activities and synthesis of nitric oxide, a retrograde messenger that overstimulates excitatory amino acid receptors including glutamate, to convulsive threshold (Meldrum 1994). It seems that homocysteine exerts a direct excitatory effect comparable to the action of glutamate (Wuerthele et al. 1982). Homocysteine was shown to enhance either the release or uptake of other endogenous excitatory amino acids (Folbergrova 1997). Furthermore, there is some data that homocysteine sequesters adenosine, an endogenous anti-convulsant and thereby reduces the seizure threshold (Marangos et al. 1990). Homocysteine relates to an additional important issue in the management of patients with epilepsy. Most anticonvulsants (phenytoin, carbamazepine and valproic acid) lower plasma folate levels and as a result, increases homocysteine levels significantly. These data suggest that increased homocysteine levels may be related to epileptogenesis and suboptimal control of seizures in the patients with epilepsy (Sener et al. 2006).

Interestingly, in EH groups, increasing doses of ethanol exhibited a dose-dependent effect upon spectral power density. When applied in doses 0.5 and 1 g/kg, ethanol increased total power spectra in $E_{0.5}H$ and E_1H group, comparing to the H group ($p > 0.05$), the maximal increase was recorded with the lowest ethanol dose applied. The highest dose of ethanol (E_2H) significantly decreased total power spectra density, comparing to the H, and all EH groups, in all time points. At the end of the observational period, spectral power densities in E_1H and E_2H group returned to its basal value, which was not the case with the $E_{0.5}H$ group (Fig. 1C).

Action of ethanol on electrographic pattern was found to be biphasic, with potentiation of epileptiform activity in one dose range and depression in another one. Low ethanol doses causing euphoria and behavioral arousal are associated with desynchronization of the EEG, decrease in the mean amplitude, and increase in the theta and alpha activity (Lucas et al. 1986; Cohen et al. 1993a; Little 1999).

Literature data (Little 1999; Cohen et al. 1993a,b), similarly to our results, demonstrated that higher ethanol doses, led to decreased frequency and increased amplitude in the EEG.

All aforementioned data on EEG monitoring concerning the ethanol influence on homocysteine-induced epilepsy support the idea that acute ethanol treatment could represent one of the factors of the exogenous stabilization of brain excitability and that high doses of ethanol have depressed EEG power spectra effect.

Acknowledgement. This work was supported by the Ministry for Science, Technology and Environmental Protection of Serbia, grant No. 145 029B.

References

Aguayo L. G., Pancetti F. C. (1994): Ethanol modulation of the $GABA_A$- and glycine-activated Cl^- current in cultured mouse neurons. J. Pharmac. Exp. Ther. **270**, 61–69

Brailowsky S., Garcia O. (1990): Ethanol, GABA and epilepsy. Arch. Med. Res. **30**, 3–9

Chandler L. J., Newsom H., Sumners C., Crews F. (1993): Chronic ethanol exposure potentiates NMDA excitotoxicity in cerebral cortical neurons. J. Neurochem. **60**, 1578–1581

Coe I. R., Yao L. N., Diamond I., Gordon A. S. (1996): The role of protein kinase C in cellular tolerance to ethanol. J. Biol. Chem. **271**, 29468–29472

Cohen H. L., Porjesz B., Begleiter H. (1993b): Ethanol-induced alterations in electroencephalographic activity. Electroencephalogr. Clin. Neurophysiol. **86,** 368–376

Cohen S. M., Martin D., Morrisett R. A., Wilson W. A., Swartzwelder H. S. (1993a): Proconvulsant and anticonvulsant properties of ethanol: studies of electrographic seizures *in vitro*. Brain Res. **601,** 80–87

Concas A., Mascia M. P., Cuccheddu T., Floris S., Mostallino M. C., Perra C., Satta S., Biggio G. (1996): Chronic ethanol intoxication enhances [^{3}H]CCPA binding and does not reduce A_1 adenosine receptor function in rat cerebellum. Pharmac. Biochem. Behav. **53**, 249–255

Davis K., Jang-Yen W. (2001): Role of glutamatergic and GABAergic systems in alcoholism. J. Biomed. Sci. **8**, 7–19

Faingold C. L., Gouemo P., Riaz A. (1998): Ethanol and neurotransmitter interactions – from molecular to integrative effects. Prog. Neurobiol. **55**, 509–535

Fischer W. (2005): Influence of ethanol on the threshold for electroshock-induced seizures and electrically-evoked hippocampal afterdischarges. J. Neural. Transm. **112**, 1149–1163

Fischer W., Kittner H. (1998): Influence of ethanol on the pentylenetetrazole-induced kindling in rats. J. Neural. Transm. **105**, 1129–1142

Folbergová J., Haugvicová R., Mareš P. (2000): Behavioral and metabolic changes in immature rats during seizures induced by homocysteic acid: the protectie effect of NMDA and non-NMDA receptor antagonists. Exp. Neurol. **161,** 336–345

Folbergrova J. (1997): Anticonvulsant action of both NMDA and non-NMDA receptor antagonists against seizures induced by homocysteine in immature rats. Exp. Neurol. **145,** 442–450

Hillbom M., Pieninkeroinen I., Leone M. (2003): Seizures in alcohol-dependent patients. CNS Drugs **17**, 1013–1030

Hoffman P. L., Rabe C. S., Moses F., Tabakoff B. (1989): N-methyl-D-aspartate receptors and ethanol: inhibition of calcium flux and cyclic GMP production. J. Neurochem. **52,** 1937–1940

Ilian A. B., Gevins A. (2001): Prolonged neurophsiological effects of cumulative wine drinking. Alcohol **25,** 137–152

Jakubowski H. (2006): Pathophysiological consequences of homocysteine excess. J. Nutr. **136,** S1741–1749

Kim C. K., Kalynchuk L. E., Pinel J. P., Kippin T. E. (1995): Tolerance to the anticonvulsant and ataxic effects of pentobarbital: effect of an ascending-dose regimen. Pharmacol. Biochem. Behav. **52**, 825–829

Little H. J. (1999): The contribution of electrophysiology to knowledge of the acute and chronic effects of ethanol. Pharmacol. Ther. **84,** 333–353

Loscher W. (2002): Current status and future directions in the pharmacotherapy of epilepsy. Trends Pharmacol. Sci. **23**, 113–118

Lovinger D. M., White G., Weight F. F. (1989): Ethanol inhibits NMDA-activated ion current in hippocampal neurons. Science **243**, 1721–1724

Lucas S. E., Mendelson J. H., Benedikt R. A., Jones B. (1986): EEG alpha activity increases during transient episodes of ethanol-induced euphoria. Pharmacol. Biochem. Behav. **25,** 889–895

Marangos P. J., Lofturs T., Weisner J., Lowe T., Rossi E., Browne C. E., Gruber H. E. (1990): Adenosine modulation of homocysteine-induced seizures in mice. Epilepsia **31**, 239–246

Meldrum B. S. (1994): The role of glutamate in epilepsy and other CNS disorders. Neurology **44,** 4–23

Pietrzak B., Czarnecka E. (2005): Effect of the combined administration of ethanol and acamprosate on rabbit EEG. Pharmacol. Rep. **57,** 61–69

Pietrzak B., Czarnecka E. (2006): The effect of combined administration of ethanol and gabapentin on rabbit electroencephalographic activity. Basic Clin. Pharmacol. Toxicol. **99,** 383–390

Sachdev P. S. (2005): Homocysteine and brain atrophy. Prog. Neuropharmacol. Biol. Psychiatry **29,** 1152–1161

Sarkisian M. R. (2001): Overview of the current animal models for human seizure and epileptic disorders. Epilepsy Behav. **2**, 201–216

Sauerland E. K., Harper R. M. (1970): Effects of ethanol on EEG spectra of the intact brain and isolated forebrain. Exp. Neurol. **27**, 490–496

Scharfman H. E. (2007): The neurobiology of epilepsy. Curr. Neurol. Neurosci. Rep. **4,** 348–354

Sener U., Zorlu Y., Karaguzel O., Ozdamar O., Coker I., Topbas M. (2006): Effects of common anti-epileptic drug monotherapy on serum levels of homocysteine, vitamin B12, folic acid and vitamin B6. Seizure **15**, 79–85

Simson P. E., Criswell H. E., Johnson K. B., Hicks R. E., Breese G. R. (1991): Ethanol inhibits NMDA-evoked electrophysiological activity *in vivo*. J. Pharmacol. Exp. Ther. **257**, 225–231

Stanojlović O., Živanović D., Šušić V. (2000): N-methyl-D-aspartic acid and metaphit-induced audiogenic seizures in rat model of seizure. Pharmacol. Res. **42,** 247–253

Stanojlović O., Hrnčić D., Rašić A., Lončar-Stevanović H., Djuric D., Šušić V. (2007) Interaction of delta sleep-inducing peptide and valproate on metaphit audiogenic seizure model in rats. Cell Mol. Neurobiol. **27,** 923–932

Stanojlović O., Rašić-Marković A., Hrnčić D., Sušić V., Macut D., Radosavljević T., Djuric D. (2009): Two types of seizures in homocysteine thiolactone-treated adult rats, behavioral and electroencephalographic study. Cell. Mol. Neurobiol. **29**, 329–339

Wang Y., Jeng C. H., Lin J. C., Wang J. Y. (1996): Serotonin modulates ethanol-induced depression in cerebellar Purkinje neurons. Alcohol Clin. Exp. Res. **20**, 1229–1236

Wuerthele S. E., Yasuda R. P., Freed W. J., Hoffer B. J. (1982): The effect of local application of homocysteine on neuronal activity in the central nervous system of the rat. Life Sci. **31**, 2683–2691

Young G. A., Wolf D. L., Khazan N. (1982): Relationships between blood ethanol levels and ethanol-induced changes in cortical EEG power spectra in the rat. Neuropharmacology **21**, 721–723

Zhuk O. V., Zinkovsky V. G., Golovenko N. Y. (2001): The pharmacodynamics of anticonvulsant and subconvulsant effects of ethanol in CBA and C57BL/6 mice. Alcohol **23**, 23–58

Zieminska E., Stafiej A., Lazarewicz J. (2003): Role of group I metabotropic glutamate receptors and NMDA receptors in homocysteine-evoked acute neurodegeneration of cultured cerebellar granule neurons. Neurochem. Int. **43,** 481–492

Wavelet and fractal analysis of rat brain activity in seizures evoked by camphor essential oil and 1,8-cineole

Milka Ćulić[1], Goran Keković[1], Gordana Grbić[1], Ljiljana Martać[1], Marina Soković[1], Jelena Podgorac[1] and Slobodan Sekulić[2]

[1] *Institute for Biological Research "Siniša Stanković", University of Belgrade, Serbia*
[2] *Medical Faculty, University of Novi Sad, Serbia*

Abstract. We investigated the rat brain activity in acute seizures evoked by camphor essential oil or its main constituent 1,8-cineole by wavelet (primarily) and fractal analysis. Experiments were performed on anesthetized animals before and after intraperitoneal camphor oil or cineole administration. The properties of frequency bands in pre-ictal, ictal and inter-ictal stages have been determined by wavelet analysis. The domination of δ frequency band was confirmed in obtained brain activities, which participate with ≈45% of mean relative wavelet energy (MRWE) in control signals and arise up to ≈76% MRWE in energy spectrum during the ictal stage (after drug administration). Other frequency bands decreased during ictal stage and arised in inter-ictal stage. There was a dose-dependent response of cineole effect: increase in cineole concentration leaded to the higher values of relative wavelet energy (RWE) of δ frequency band while there were slight changes of the mean fractal dimension (FD) values as a measure of system complexity.

Key words: Electrocortical activity — Wavelet analysis — Fractal analysis — Camphor oil and 1,8-cineole — Epileptic seizures

Introduction

Neurotoxic effects could appear by wrong usage of essential oils and other plant preparations in alternative/traditional medicine, cosmetics and food preparations. Particularly, essential oils that have monoterpen constituents, such as camphor and 1,8-cineole, may induce epileptic seizures in humans and animals (Medvedev 1990; Grbić et al. 2006). As the wavelet transform was a powerful and suitable tool designed for analysis of non-stationary signals, a new scheme of optimum classification of epileptic seizures based on wavelet analysis of electroencephalograms has recently appeared (Ocak 2008). We already performed fractal analysis on cerebral electrocortical signals and found that during ictal stages the fractal dimension (FD) value was lower than before camphor essential oil administration as well as during interictal periods (Grbić et al. 2008). The aim of this study was to investigate the acute effect of 1,8-cineole as the main constituent of camphor essential oil and to develop a new technique to quantify the electrocortical changes by wavelet analysis. A preliminary account on this study has appeared recently (Culić and Keković 2008).

Correspondence to: Milka Ćulić, Institute for Biological Research "Siniša Stanković", University of Belgrade, Bulevar Despota Stefana 142, 11000 Belgrade, Serbia
E-mail: milkacul@ibiss.bg.ac.yu

Materials and Methods

Surgical procedure and camphor essential oil/cineole administration

The experiments were performed on adult male rats, as described in our recent study (Grbić et al. 2008), in accordance with the European Council Directive (86/609/EEC) and approved by our Institute's local Ethical Committee. The surgery was done under pentobarbitalsodium (Serva, Heidelberg) – initial dose of 35 mg/kg and subsequently ~8 mg/kg every 50–60 min when necessary, to obtain light anesthesia throughout the experiment. Each animal was mounted in a stereotaxic apparatus. Partial round-shaped craniotomies were made over the parietal cerebral cortex (P: 2.0–2.5 mm; L/R: 2.0–2.5, in respect to bregma). For inducing acute seizures, camphor es-

sential oil (Institute for Medicinal Plant Research "Josif Pančić", Belgrade, Serbia) or 1,8-cineole (Sigma, USA) were used by intraperitoneal administration. The experimental animal was injected by camphor essential oil (at doses 400/500/600 μl/kg) dissolved in 1 ml of saline or by 1,8-cineole (at doses 300/400/500 μl/kg) – in 1 ml of saline. It should be pointed out that the main constituent of the used camphor essential oil was 1,8-cineole (73.01%) while the other constituents were as follows: camphor (9.18%); α-terpineol (2.14%); borneol (1.95%); p-cymene (1.65%) and terpinen-4-ol (1.05%). All the rats survived acute experimentation and did not show any behavior peculiarities in the following days.

Recording procedure and data acquisition

Local field potentials (LFPs) of the cerebral cortex were monopolarly recorded by epidurally positioned silver ball electrodes or, intracortically, superficially positioned tungsten micro-electrodes, with a ground electrode laid over the frontal bone and temporal muscles. Cortical activity was amplified and filtered by a multichannel processor (Alpha-Omega Eng, Nazareth) with band pass filter DC (direct current) to 1 kHz and a 50 Hz notch. We used the program package SIG VIEW (Jovanović 2004) for data acquisition. The biosignals were digitized at the sampling rate of 256 Hz, filtered to avoid artifacts which occasionally appeared at 61 and 106 Hz. The biosignals were recorded sequentialy during the period about 180 min, with ~5 min interuptions; each recorded sequence lasted ~2 min.

Fractal analysis

In brief, we calculated FD values of cerebral electrocortical activity in anesthetized rats before and after camphor oil/cineole administration using Higuchi's algorithm (Higuchi 1988; Klonowski et al. 2000; Spasić et al. 2005) with slight modifications. Parameter N = 200 was equivalent to an epoch (window) duration of 781 ms and parameter $k_{max} = 8$ was the optimum choice. Individual FD values were averaged across all epochs for particular experimental conditions before and at certain time exactly after camphor oil/cineole administration to obtain the mean FD.

Wavelet analysis

The original software of discontinual wavelet analysis was developed in this study. Therefore, the mathematical basis and certain details will be described more carefully.

In the wavelet analysis (Metin 1997; Latka et al. 2003) an arbitrary signal is analyzed by quickly vanishing oscillating functions called wavelet family $\psi_{a,b}(t)$ which are generated from mother wavelet $\psi(t)$:

$$\psi_{a,b}(t) = \frac{1}{\sqrt{|a|}}\psi\left(\frac{t-b}{a}\right) \tag{1}$$

where $a, b \in R, a \neq 0$ represent the scale and shifting parameters, and t is time. The scaling parameter a is inversely related to the frequency of the analyzed signal: by increasing this parameter lower frequencies can be analyzed. The shifting parameter b controls translation of wavelet until the whole signal is covered. As a result in continuous wavelet transform appear the wavelet coefficients defined by equation:

$$C_{a,b} = \frac{1}{\sqrt{a}}\int f(t)\psi\left(\frac{t-b}{a}\right)dt \tag{2}$$

where $f(t)$ signifies the analyzed signal. For the discrete set of parameters: $a_j = 2^{-j}$, $b_{j,k} = 2^{-j}k$ the wavelet family constitutes an orthonormal basis of the Hilbert space:

$$\int 2^{j_1}\psi(2^{j_1}t - k_1)\psi(2^{j_2}t - k_2)dt = \delta(j_1 - j_2)\delta(k_1 - k_2) \tag{3}$$

For simplicity, we choose sampling time $t_s = 1$ s then arbitrary signal $f(t)$ can be decomposed into a sum of wavelet coefficients and the appropriately constituent wavelets:

$$f(t) = \sum_{j=-N}^{-1}\sum_{k} C_j(k)\psi_{j,k}(t) \tag{4}$$

where N represents number of resolutions levels. Similar to the Fourier theory, there is a concept of total energy contained in the windows consisting of N_S sampling points of a signal. It is given by the expression:

$$E_{tot} = \sum_j\sum_k \left|C_j(k)\right|^2 \tag{5}$$

In expression given above terms: $E_j = \sum_k \left|C_j(k)\right|^2$ signify energy of signal at the resolution level j given by summing all over sampled time k. Now, we are in a position to define very useful quantifier for analyzing EEG signals (Daud et al. 2005; Magosso et al. 2007) and which is called relative wavelete ernergy (RWE):

$$\rho_j = \frac{E_j}{E_{tot}}; \qquad j = -N, -N+1, \ldots, -1 \tag{6}$$

From physical point of view this quantifier can be understood as a distribution of energy trough resolution levels and time. From the above formula it can be concluded that is always fulfilled:

$$\sum_j \rho_j = \left(\sum_j E_j\right)/E_{tot} = E_{tot}/E_{tot} = 1 \tag{7}$$

By continuing in this manner, we are expressing the mean relative wavelet energy (MRWE) which represents the mean value of RWE at some stage of a signal. In the purpose of investigating the frequency bands of a signal, it is necessary to establish connection between frequency bands and resolutions levels. This can be done *via* the formula:

$$\frac{f_C \cdot N_S}{2^{j+1}} \leq \Delta f \leq \frac{f_C \cdot N_S}{2^j} \quad (8)$$

where Δf is a frequency band of j-th resolution level, f_C is "central" frequency of the mother wavelet which is used for a particular choice of Haar wavelet as the simplest and the most important from Daubeshi family wavelet (f_C = 0.996 Hz), N_S is number of sampling points (N_S = 256). We marked the frequency bands as in our previous study (Ćulić et al. 2005).

Results

The increased amplitude of electrocortical activity with occasional single and multiple spiking of high amplitude (ictal activity) without behavior changes at parietal cortical level occurred about 2–10 min after camphor essential oil or its main constituent 1,8-cineole injection and lasted for 2–3 h. The behavioral signs of camphor essential oil/cineole evoked neurotoxicity – convulsions of forelimbs/hindlimbs, were presented only sometimes, because of the supression induced by anesthesia. We compared the cerebral electrocortical activity characterized by epileptic like seizures obtained in the typical C2D rat 45 min after camphor essential oil administration and control signals (before camphor oil administration), as shown on Fig. 1a,b.

By applying the discrete Wavelet transform to those signals, general characteristics of their frequency bands were obtained, where parameter RWE determined energy spectrum of the signal. Analysis of cerebral electrocortical activity 45 min after camphor oil administration (C2D13T1) presented on Fig. 2a,b, showed the trend of increasing RWE of δ frequency and decreasing RWE of θ, α, β, γ frequency bands during of epileptic seizures, with superposed peaks from α and β band. With dashed line end of epileptic seizures has been marked. After ending the seizure, the situation is completely different: there is increasing in parameter RWE of α, β and γ frequency bands with peaks from α and β bands. In both cases, the RWE

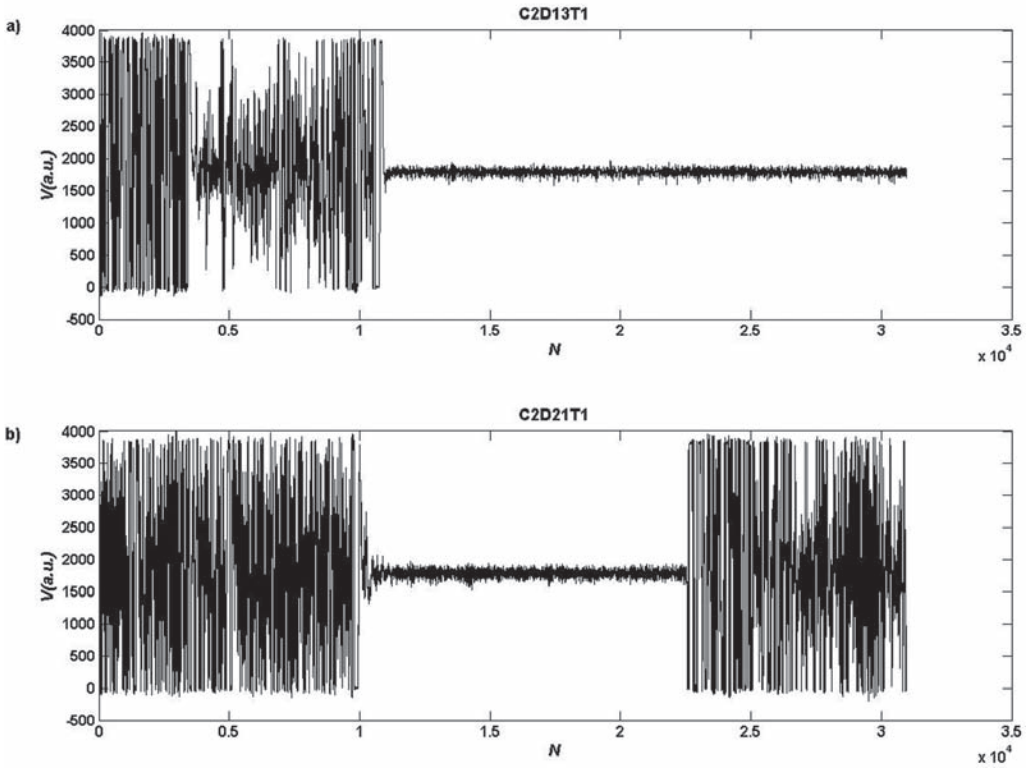

Figure 1. The characteristic signals with epileptic activity (ictal and inter-ictal): C2D13T1 – 45 min after (a) and C2D21T1 – 65 min after camphor oil administration (b). Signal intensity is expressed in arbitrary units (a.u.) of local field potential versus number of experimental points N.

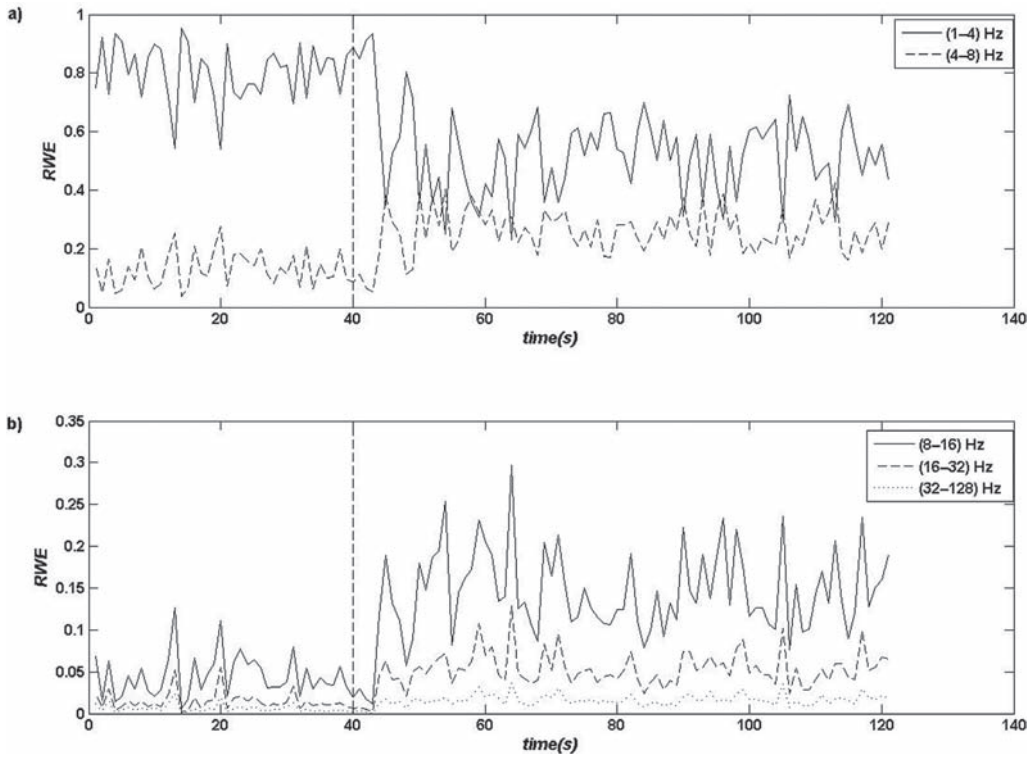

Figure 2. The distribution of parameter RWE of the signal C2D13T1: a) δ (1–4 Hz) and θ (4–8 Hz) b) α (16–32), low β (8–16 Hz) and γ (30–128 Hz) frequency bands, versus time (in seconds).

dominate in energy of spectrum of signal with characteristic values of MRWE = 0.81 during epileptic seizures and MRWE = 0.52 after epileptic seizures, which means that it is contained 52–81% in energy spectrum of the signal. Even 2 h after camphor oil administration, seizure activity has appeared and analysis of the signal C2D21T1 (Fig. 3a,b) could mark the start and end of inter-ictal stage. In this case, the value of parameter MRWE varies from 0.42 (inter-ictal stage) to 0.76 (ictal stage), which corresponds to 42–76% δ band in energy spectrum of RWE. The peaks from α and β bands could be observed in Fig. 3. However, in order to complete the analysis, it is necessary to define mean activity of all frequency bands and calculate standard devaitions. The features of various frequency bands of electrocortical activity 45 min after camphor oil administration (C2D13T1) could be observed from Table 1. During the ictal stage, δ frequency band (MRWE = 0.81 ± 0.10) increased, while θ (MRWE = 0.13 ± 0.06) slightly decreased, but activity of both bands were higher than activity of the control signal. Intensities and activities of other frequency bands decreased, except of γ frequency band where certain increase in parameter MRWE = 0.06 ± 0.05 could be noticed as compared to the control (MRWE = 0.03 ± 0.02).

Table 1. The values of parameter MRWE (±SD) of the control signal C2D02T1 and the signal C2D13T1 45 min after camphor oil administration

Frequency band (Hz)	Ictal stage MRWE		Post-ictal stage MRWE	
	Control	C2D13T1	Control	C2D13T1
1–4	0.64 ± 0.11	0.81 ± 0.10	0.71 ± 0.10	0.52 ± 0.13
4–8	0.19 ± 0.06	0.13 ± 0.06	0.16 ± 0.05	0.26 ± 0.07
8–16	0.09 ± 0.03	0.04 ± 0.03	0.08 ± 0.03	0.15 ± 0.05
16–32	0.04 ± 0.02	0.02 ± 0.01	0.03 ± 0.02	0.05 ± 0.02
32–128	0.03 ± 0.02	0.06 ± 0.05	0.02 ± 0.01	0.02 ± 0.01

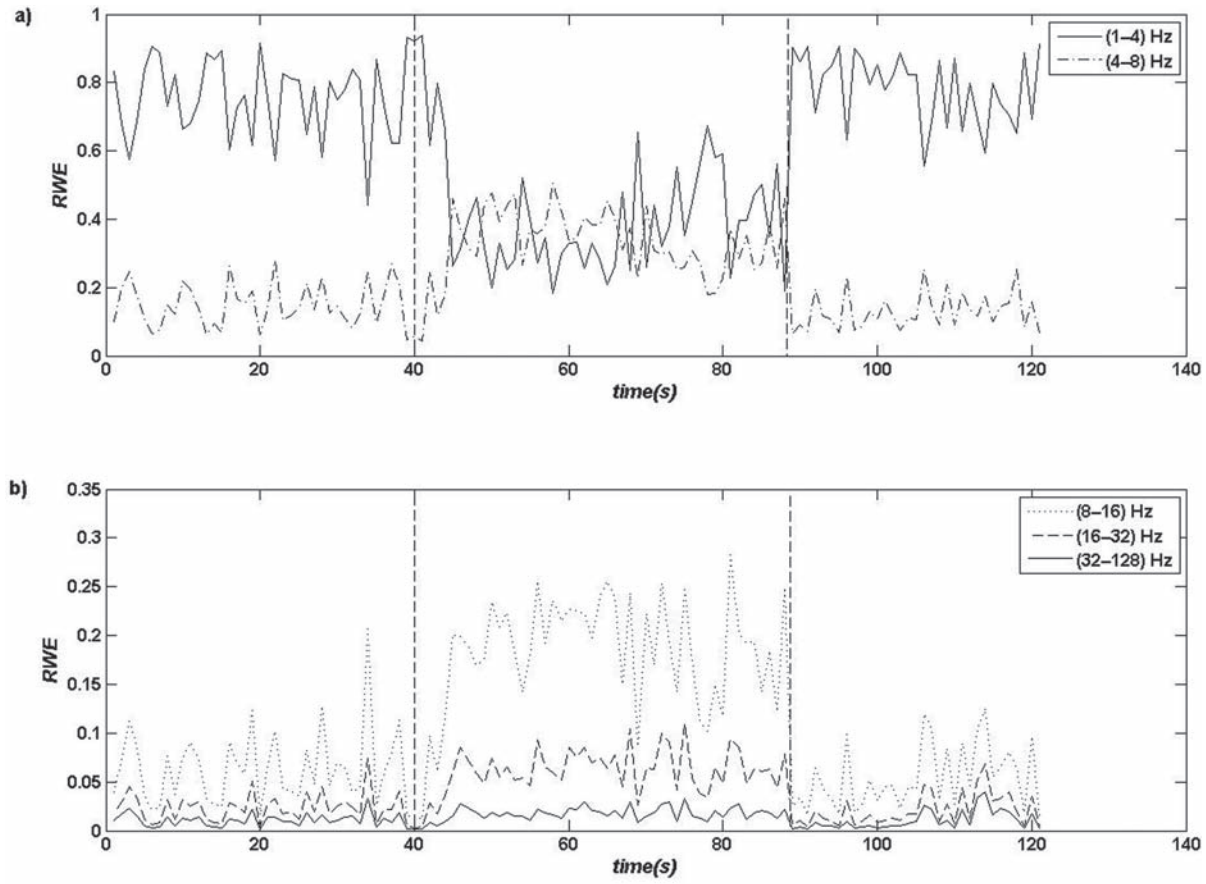

Figure 3. The distribution of parameter RWE of the signal C2D21T1: a) δ (1–4 Hz) and θ (4–8 Hz) b) α (16–32), low β (8–16 Hz) and γ (30–128 Hz) frequency bands, versus time (in seconds).

As shown in Table 2, in δ frequency band of the electrocortical activity, 65 min after cineole administration (C2D21T1), corresponding values of parameter MRWE = 0.76 ± 0.12 and its standard deviation during the ictal stage were obtained. In control signal (C2D02T1) before cineole administration, value of parameter MRWE = 0.64 ± 0.11 was lower. Likewise, parameter in θ band was MRWE = 0.15 ± 0.07 during ictal stage and MRWE = 0.19 ± 0.06 during control stage, which meant that this band was very active. The value of MRWE of higher frequency bands decreased during the ictal phase. In later post-ictal stages there was a tendency of equalizing those MRWE values with the control values, with exception of α and low β frequency band (8–16 Hz) which may be suggested as the possible indicators of inter-ictal stage. Of course, this position can not be taken as such before verification on more templates.

Table 2. The values of parameter MRWE (±SD) of the control signal C2D02T1and the signal C2D21T1 65 in after camphor oil administration

Frequency band (Hz)	Ictal stage MRWE		Inter-ictal stage MRWE	
	Control	C2D21T1	Control	C2D21T1
1–4	0.64 ± 0.11	0.76 ± 0.12	0.62 ± 0.14	0.42 ± 0.19
4–8	0.19 ± 0.06	0.15 ± 0.07	0.27 ± 0.11	0.3 ± 0.11
8–16	0.09 ± 0.03	0.06 ± 0.04	0.06 ± 0.03	0.18 ± 0.06
16–32	0.04 ± 0.02	0.02 ± 0.01	0.03 ± 0.02	0.06 ± 0.02
32–128	0.03 ± 0.02	0.01 ± 0.01	0.02 ± 0.01	0.02 ± 0.01

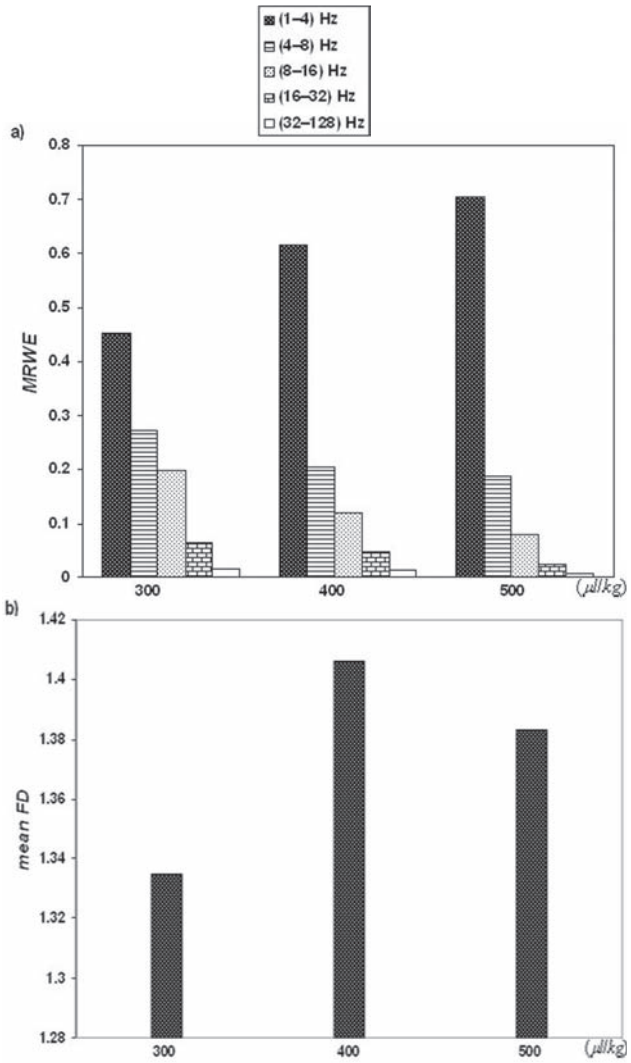

Figure 4. The influence of different doses of 1,8-cineole (300, 400, 500 μl/kg) on characteristic parameters of electrocortical activity after administration in three rats – E3, E4, E5: a) MRWE; b) mean FD.

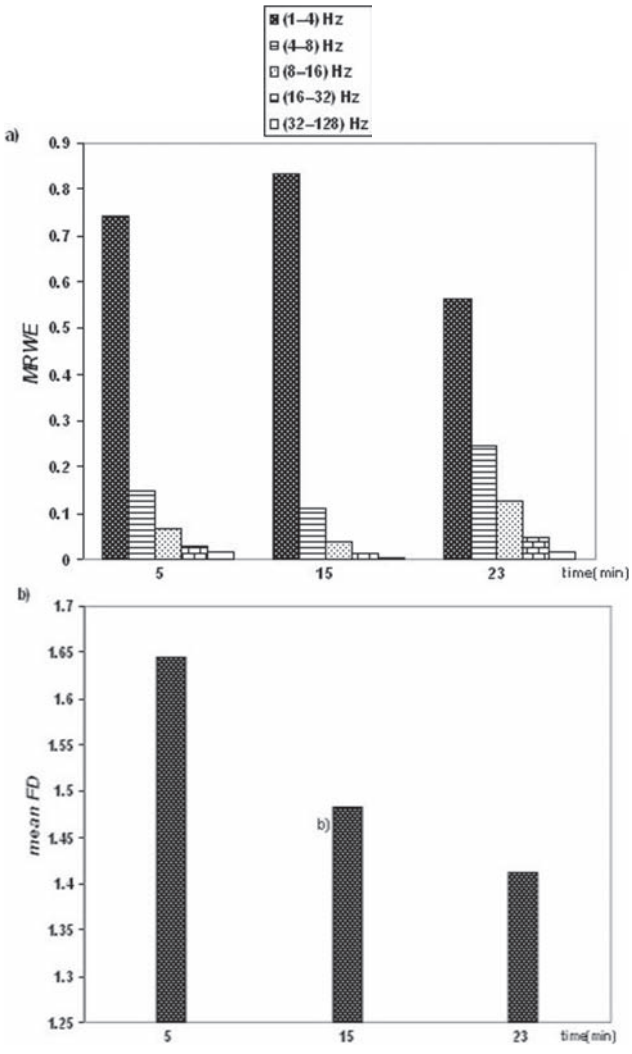

Figure 5. The distribution of characteristic parameters in terms of camphor oil induced effects: a) MRWE; b) mean FD, versus time (in minutes).

In order to complete the analytic approach to brain functioning we also calculated the FD of obtained biosignals which could be an indicator of uncontrolled electrical discharges, too. In that purpose, we compared changes of FD values with values RWE in relation to the concentration of administrated camphor essential oil/1,8-cineole. Let us first consider the distribution of RWE through energy spectrum and mean FD of signal in terms of concentration of 1,8-cineole (Fig. 4) and camphor oil (Fig. 5). There was a dose-response cineole effect: increment of cineole concentration leaded to higher value of RWE in δ frequency band. The mean FD values (as a measure of system complexity) also changed after camphor oil/cineole administration. The mean FD values followed changes in δ frequency band, but were very sensitive to changes in γ frequency band, too. Namely, the value of MRWE increased from 0.62 (after administration of 400 μl/kg of cineole) to 0.70 (after administration of 500 μl/kg of cineole), while at the same time, the FD values decreased from 1.41 to 1.38, due to changes in γ frequency band. We also monitored the changes of parameter MRWE values in time, after specified administration of camphor essential oil at the dose of 600 μl/kg (Fig. 5). The up-growth of parameter MRWE of δ band to values 0.74 indicated epileptic/like activity 5 min after camphor oil administration, which was followed by decreased MRWE of other frequency bands. At the same time, the values of mean FD was 1.64 and lower relative to the control value. Furthermore, after 15 min we have recorded the higher values of MRWE of δ

(0.83) and degradation of MRWE of γ band from 0.02 to 0.01 while mean FD value decreased to 1.48. The reasonable explanation of this behavior may be that FD as a measure of chaos in brain is relatively simple: during ictal stages, because of reduced activity of higher frequencies bands, many degrees of freedom of system are removed. But, there is another point: mean FD has maximum values, while the values of MRWE of δ and γ frequency band are increasing, at the same time.

Discussion

The electrophysiologic effects of 1,8-cineole parenterally administrated at doses of 300–500 μl/kg completely resembled the effects of camphor essential oil injections at doses of 400–600 μl/kg. This work also showed that certain properties of acute epileptic like seizures induced by camphor essential oil or by its main constituent, 1,8-cineole could be described on satisfactory way in the frame of wavelet analysis. By applying this tool, the properties of frequency bands in pre-ictal, ictal and inter-ictal stages have been determined. The domination of δ frequency band in cerebral eletrocortical activities has been confirmed and it participated with ≈45% MRWE in the control signal (before camphor oil/cineole admnistration) and arised up to ≈76% MRWE in energy spectrum during the ictal stage. Inversely, other frequency bands were decreasing during ictal stages and were rising during inter-ictal stages. This behavior could be explained by hypothesis on hierarchical organization of neural oscillations in the brain. Slow waves are trying to be in accord with higher frequency bands, but it could not happen, because there is a brain disorder in the form of uncontrolled electrical discharges or epileptic like seizures. In the post/inter-ictal stages the value of RWE of δ band is decreasing ≈32% relative to the control value but other frequency bands are increasing up to the values higher than the control values. It is especially interesting that α and low β (8–16 Hz) increased ≈173% relative to the control values and this nominates these frequency bands as possible indicators of inter-ictal stages. Also, the effects of electrocortical activity induced by different doses of 1,8-cineole or camphor essential oil were investigated. It has been shown that higher concentracions generated the higher values of parameter RWE of δ frequency band. This value is in correlation with the value of RWE of γ frequency band which has significant impact on the mean FD value as a measure of chaos in the brain.

There was a general trend of the relative increase in low frequency bands and decrease in high frequency bands during epileptic seizures in accordance with previous findings (Kharlamov 2003). This fact, once again, clearly confirms predominance of δ frequency band not only during anesthesia but the key role of slow waves in complex brain activity induced by neurotoxic drugs. There was an interesting report from Berkley (Canolty et al. 2006) who found … "the first experimental evidence that slow brain oscillations " tune in" the fast brain oscillations or γ waves. On that way different regions in the brain much easier transfer information among each other". This gives a new insight in brain functioning and introduces a very interesting hypothesis on hierarchy of oscillations in the brain. Our wavelet results in this study are in agreement with our recent studies on camphor essential oil effects on spectral changes in brain activity (Grbić et al. 2006) and fractal changes of cerebrocortical activity (Grbić et al. 2008), but we point out some advantages of wavelet analysis in possible prediction of epileptic seizures by defining the preictal stages. It has been suggested that a dimensional change in brain activity occurs before seizure onset and it is now thought to possess predictive powers (Babloyantz and Destexhe 1986). The application of nonlinear deterministic dynamics and powerful algorithms were devised to analyse the behavior of the seizure state (Schiff 1998). When principles of nonlinear dynamics are applied on the time series domain, they can yield measures of fundamental information about complex brain dynamics (Elger et al. 2000).

Acknowledgement. This study was supported by the Serbian Ministry of Science and Technological Development (project No. 143021).

References

Babloyantz A., Destexhe A. (1986): Low-dimensional chaos in an instance of epilepsy. Proc. Natl. Acad. Sci. U.S.A. **83**, 3153–3157

Canolty R. T., Edwards E., Dalal S. S., Soltani M., Nagarajan S. S., Kirsh H. E., Berger M. S., Barbaro N. M., Knight R. T. (2006): High gamma power is phase-locked to theta oscillations in human neocortex. Science **313**, 1626–1628

Ćulić M., Keković G. (2008): Electrocortical Activity of Rat Brain and Cineole Effect – Spectral and Continual Wavelet Analysis. IV Kongres of Serbian Society for Neuroscience, Kragujevac, September 11–14, (Abstract Book), pp. 330

Ćulić M., Martać Blanuša Lj., Grbić G., Spasić S., Janković B., Kalauzi A. (2005): Spectral analysis of cerebellar activity after acute brain injuri in anesthetized rats. Acta. Neurobiol. Exp. (Wars.) **65**, 11–17

Daud M. S., Yunus J. (2005): Relative wavelet energy as a tool to select suitable wavelet for artifact removal in EEG. In: Proceeding of 1st Conference on Computers, Communication, and Signal Processing, Kuala Lumpur (4–16 November)

Elger C. E., Widman G., Andrzejak R., Arnhold J., David P., Lehnertz K. (2000): Nonlinear EEG analysis and its potential role in epileptology. Epilepsia **41**, S34–38

Grbić G., Ćulić M., Martać Lj., Kesić S., Soković M., Spasić S., Đoković D. (2006): Camphor oil poisoning-spectral analysis of rat brain activity. Acta Physiol. Pharmacol. Serbica **42**, 233–238

Grbić G., Ćulić M., Martać Lj., Soković M., Spasić S., Djoković D. (2008): Effect of camphor essential oil on rat cerebrocortical activity detected by changes in fractal dimension. Arch. Biol. Sci. **60**, 547–553

Higuchi T. (1988): Approach to an irregular time series on the basis of the fractal theory. Physica D **31**, 277–283

Jovanović A. (2004): Biomedical Image and Signal Processing. School of Mathematics, University of Belgrade

Kharlamov E. A., Jukkolap I., Schmitt K. L., Kellz K. M. (2003): Electrobehavioral characteristics of epileptic rats following photothrombotic brain infarction. Epilepsy Res. **56,** 185–203

Klonowski W., Olejarczyk E., Stepien R. (2000): Nonlinear dynamics of EEG-signal reveals influence of magnetic field on the brain. Conf. Proc. IEEE Eng. Med. Biol. Soc. **4**, 2955–2958

Latka M., Was Z., Kozik A., Wes J. B. (2003): Wavelet analysis of epileptic spike. Phys. Rev. E **67**, 052902/1–052902/4

Magosso E., Ursino M., Provini F., Montagna P. (2007): Wavelet analysis of electroencephalographic and electro-oculographic changes during the sleep onset period. Conf. Proc. IEEE Eng. Med. Biol. Soc. **1**, 4006–4010

Metin A. (1997): Time-frequency and wavelets in biomedical signal processing. In: Fast Algorithms for Wavelet Transform Computation. pp. 211–222, IEEE Computer Society Press

Medvedev A. V. (1990): The long-term action of camphor on "audiosensitive" rats: electrophysiological research and mathematical modelling of the properties of the neuronal networks. Neurophysiology **22**, 193–200

Ocak H. (2008): Optimal classification of epileptic seizures in EEG using wavelet analysis and genetic algorithm. Signal Processing **88**, 1858–1867

Schiff S. J. (1998): Forecasting brain storms. Nat. Med. **4**, 1117–1118

Spasić S., Ćulić M., Grbić G., Kalauzi A., Martać Lj. (2005): Fractal analysis of rat brain activity after injury. Med. Biol. Eng. Comput. **43**, 345–348

Effect of continuous exposure to alternating magnetic field (50 Hz, 0.5 mT) on serotonin and dopamine receptors activity in rat brain

Branka Janać[1], Gordana Tovilović[2], Mirko Tomić[2], Zlatko Prolić[1] and Lidija Radenović[3]

[1] *Laboratory for Magnetobiology and Behaviour, Institute for Biological Research "Siniša Stanković", University of Belgrade, Bul. Despota Stefana 142, 11060 Belgrade, Serbia*
[2] *Department of Biochemistry, Institute for Biological Research "Siniša Stanković", University of Belgrade, Bul. Despota Stefana 142, 11060 Belgrade, Serbia*
[3] *Department of Physiology and Biochemistry, Faculty of Biology, University of Belgrade, P.O.Box 52, Studentski trg 16, 11000 Belgrade, Serbia*

Abstract. External magnetic fields (MFs) have the ability to modify motor activity of animals, complex type of behaviour connected with dopaminergic and serotonergic neurotransmissions in the brain. Thus, the purpose of this study was to examine MF-induced changes in the activity of serotonin 5-HT_{2A} receptors in the prefrontal cortex, as well as dopamine D_1 and D_2 receptors in the striatum of adult Wistar rats, considering their involvement in motor behavior regulation. Experimental animals were continuously exposed to extremely low frequency MF (ELF-MF, 50 Hz, 0.5 mT) for 1, 3, and 7 days. Subsequently, binding properties (K_d and B_{max}) of receptors were determined by *in vitro* radioligand receptor binding assays. It was shown that the affinity of serotonin 5-HT_{2A} receptors decreased and their density increased in the prefrontal cortex of rats after ELF-MF exposure. Regarding affinity, this effect was duration-dependent and most prominent after 7-day of ELF-MF exposure. In contrast to serotonin 5-HT_{2A} receptors in the prefrontal cortex, ELF-MF had no significant effect on the affinity and density of dopamine D_1 and D_2 receptors in the striatum. We can conclude that continuous exposure to ELF-MF up to 7 days affects cortical serotonergic neurotransmission, whereby intensity of these changes depends on ELF-MF exposure duration.

Key words: 50 Hz magnetic field — Serotonin 5-HT_{2A} receptors — Dopamine D_1 and D_2 receptors — Brain — Rats

Introduction

Living systems are constantly being exposed to magnetic fields (MFs) of different characteristics (type, frequency, intensity, duration). The natural MF derived from Earth (geomagnetic field) is present during the entire period of living beings evolution, and thus represents a very important ecophysiological factor. Geomagnetic field is under the direct influence of cosmic fields, mostly derived from Sun, which on regular or irregular way change its daily, annual and long-lasting activity. On the other hand, the artificial MFs are unavoidable consequence of impressive scientific and technological development. Among them, alternating MFs of extremely low frequency (ELF, 50–60 Hz) derived from power lines, household appliances, traffic and different industrial technologies deserve particular attention because of their omnipresence in human working and living environment. Magnetic induction values of these MFs are often more pronounced than the values of the natural geomagnetic field (about 20–50 μT in normal conditions).

Numerous experimental and clinical studies indicated that external ELF-MF modify different processes in the brain, including those mediated by serotonergic and dopaminergic neurotransmissions (Lai 1996; Pešić et al. 2004; Janać et al. 2005; Jeong et al. 2006; Jadidi et al. 2007). Even though there are reports that present certain MF effects on serotonergic and dopaminergic neurotransmis-

Correspondence to: Lidija Radenović, Department of Physiology and Biochemistry, Faculty of Biology, University of Belgrade, P.O.Box 52, Studentski trg 16, 11000 Belgrade, Serbia
E-mail: lidijar@bio.bg.ac.rs

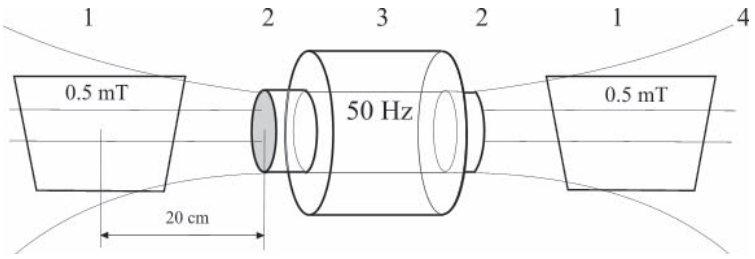

Figure 1. Schematic drawing of the MF exposure system. 1 – animal cages; 2 – magnetic poles of ferrite magnetic core; 3 – coils; 4 – magnetic force lines.

sions (Ben-Shachar et al. 1999; Massot et al. 2000; Sieron et al. 2001; Kanno et al. 2003; Sieron et al. 2004), the accurate roles of these neurotransmitter systems in MF-induced changes in the central nervous system (CNS) are not completely explained yet. Thus, the purpose of this study was to investigate effects of continuous ELF-MF (50 Hz, 0.5 mT) exposure for 1, 3, and 7 days on activity (affinity and density) of serotonin 5-HT_{2A} receptors in the prefrontal cortex, as well as dopamine D_1 and D_2 receptors in the striatum of adult rats. The main reasons for choosing these receptors were our previously published data regarding the effect of MF exposure on animal motor activity and the direct/indirect involvement of serotonin 5-HT_{2A}, dopamine D_1 and dopamine D_2 receptors in motor behavior regulation (Jackson and Westlind-Danielsson 1994; Hillegaart et al. 1996; Janać et al. 2005).

Materials and Methods

Animals

Adult (about 3-month-old) male Wistar rats, average weight 250–350 g, derived from the vivarium of Institute for Biological Research in Belgrade were used in the research. The animals were housed in groups of 4–5 per cage in standard conditions (room temperature 23 ± 2°C, relative humidity 60–70%, circadian light regime of 12 h, food and water *ad libitum*), according to the principles enunciated in the Guide for Care and Use of Laboratory Animals, NIH publication No. 85-23. They were subjected to experimental protocols approved by the local Ethical Committee.

Alternating MF source

An electromagnet with a regular laminated transformer core and pole diameter of 9.5 cm was used for generation of alternating MF. This electromagnet was supplied with a sinusoidal current (50 Hz, 40 V, 4.5 A), producing relative homogenous ELF-MF with the gradient of magnetic induction. The greatest value of magnetic induction B = 8.9 mT was measured on the electromagnetic poles by a GM05 Gaussmeter (Hirsst) using a PT2837 probe. Magnetic force lines were parallel to the horizontal component of local geomagnetic field. During the experiment, geomagnetic field deviation in the area of study (44°38' N, 20°46' E), measured by a GSM 10 proton magnetometer (Geomagnetic Institute – Grocka, Belgrade), was within the normal range. The background MF did not exceed the value of 10^{-5} mT.

Experimental procedure

At the same time, two standard polycarbonate cages (26 cm width × 43 cm length × 15 cm high) with 3–4 experimental animals were placed in the vicinity of ELF-MF source for 1, 3, and 7 days, one on the left and another on the right side of electromagnet (Fig. 1). Cages were placed on polystyrene foam and away from electromagnet to avoid possible vibration and heating. The center of each cage was at 20 cm from the electromagnetic poles and exposed to ELF-MF with an average magnetic induction of B = 0.5 mT. Control animals were submitted to the same experimental procedure with electromagnet turned off (i.e. sham exposed). Animals were sacrificed immediately after the ELF-MF/sham exposure. Dissected prefrontal cortices and corpora striata were weighed and stored at –70°C until biochemical receptor analysis.

Complete set up for ELF-MF exposure system (electromagnet with cages) was in an isolated room with the same values of temperature, relative humidity, artificial light intensity, and circadian light regime as in the vivarium. During continuous exposure to ELF-MF for 1, 3, and 7 days, animals had free access to food and water.

Preparation of synaptosomes and saturation binding assay

Membranes with serotonin 5-HT_{2A} (derived from prefrontal cortex), as well as dopamine D_1 and D_2 (derived from striatum) binding sites were prepared according to standard

procedures (Vogel 2002). Pooled tissue from three animals was homogenized (6–10 strokes, 800 rpm, Braun homogenizer) in 10 volumes of appropriate ice-cold assay buffer: 50 mmol/l Tris (pH = 7.7; ICN Pharmaceuticals, USA) for cortical, and with salts 50 mmol/l Tris, 120 mmol/l NaCl (Merck), 5 mmol/l KCl (Alkaloid, Skoplje), 2 mmol/l $CaCl_2$ (Merck), 1 mmol/l $MgCl_2$ (pH = 7.5; Merck) for striatal tissue. The homogenate was centrifuged at 40,000 × *g* for 15 min at 4°C (Beckman L7-55 ultracentrifuge, rotor Ti-50). The pellet was re-homogenized in 10 volumes of appropriate assay buffer and re-centrifuged under the same conditions. Finally, sediment was re-suspended in 20 volumes of appropriate assay buffer. Aliquots (~1.5 ml) were stored at –70°C, until use.

In vitro saturation binding assays were performed by standard pharmacological procedures described in Vogel (2002). The radioligands used for characterization of serotonin 5-HT_{2A}, dopamine D_1, and dopamine D_2 receptors were [^{3}H]-ketanserin (88 Ci/mmol; Perkin-Elmer, USA), [^{3}H]-SCH23390 (91 Ci/mmol; Amersham, USA), and [^{3}H]-spiperon (77.8 Ci/mmol; Amersham, USA), respectively. Samples in duplicate containing either cortical or striatal membranes and different concentrations (0.25–8 nmol/l for serotonin 5-HT_{2A} receptors; 60 pmol/l–2 nmol/l for dopamine D_1 and D_2 receptors) of appropriate radioligand were incubated in appropriate assay buffer at 37°C for 10 min. The reaction was terminated by addition of ice-cold buffer and rapid vacuum filtration of the individual samples through Whatman GF/B filters. The filters were washed two times with 3.5 ml of appropriate ice-cold buffer and radioactivity remained on filters was measured using liquid scintillation counter (LKB RackBeta 1219). Nonspecific binding was determined in the presence of 1 μmol/l ketanserin (Sigma Chemical, USA) in case of serotonin 5-HT_{2A} receptors, and 1 μmol/l (+)-butaclamol (Sigma Chemical, USA) in case of dopamine D_1 and D_2 receptors. Binding of [^{3}H]-spiperon to serotonin 5-HT_{2A} receptors in the striatum was prevented by adding of 50 nmol/l ketanserin to dopamine D_2 receptor saturation assay tubes. Protein concentration was determined by the method of Markwell et al. (1978).

Statistical analysis

Values of binding parameters, index of receptor affinity (K_d) and index of receptor density (B_{max}), of serotonin 5-HT_{2A} receptors, and dopamine D_1 and D_2 receptors were calculated by GraphPad Prism® software, version 4.00. Results were presented in tables as mean ± SEM of three independent trials each performed in duplicate. One-way ANOVA, followed by post hoc LSD test was used for statistical analysis of obtained data. Results were considered to be significantly different at $p < 0.05$.

Results

Upon the initial statistical analysis, no significant differences of either affinities or densities of serotonin 5-HT_{2A} receptors in the prefrontal cortex, and dopamine D_1 and D_2 receptors in the striatum among the three control groups (sham-exposed for 1, 3, or 7 days) were found (data not shown). So, all these data were cumulated and expressed as the only control values. These binding parameters were also found to be in the same range with those reported by the other authors (Papp et al. 1994; Yamada et al. 1995; Gili-Martín et al. 1997).

Activity of serotonin 5-HT_{2A} receptors in the prefrontal cortex of rats was significantly changed after ELF-MF (50 Hz, 0.5 mT) exposure ($K_d - F_{(3,8)} = 11.51$, $p < 0.01$; $B_{max} - F_{(3,8)} = 8.89$, $p < 0.01$; one-way ANOVA). Detail comparisons indicated that ELF-MF reduced the affinity (i.e. increased K_d) of serotonin 5-HT_{2A} receptors proportionally to the exposure duration (Table 1A). Alterations were statistically significant after continuous 3- or 7-day ELF-MF exposure. Density of these receptors (i.e. B_{max} value) was significantly increased in the prefrontal cortex of all animals exposed to ELF-MF (Table 1A). Increase in receptor density was not proportional to exposure duration.

In contrast to serotonin 5-HT_{2A} receptors in the prefrontal cortex, ELF-MF exposure irrespective of duration did not significantly modify the affinity or density of dopamine D_1 and D_2 receptors in the striatum (Table 1B and C). Values obtained for the affinity and density of dopamine D_1 receptors of ELF-MF exposed animals were mainly at control levels (Table 1B). On the other hand, a slight tendency toward decreasing of dopamine D_2 receptors affinity (i.e. increasing K_d) was detected after 1- and 3-day ELF-MF exposure (Table 1C).

Discussion

The main target of interaction of ELF-MFs on the biological systems is the plasma membrane, namely proteins anchored in lipid bilayer of the cell membrane functioning as ion channels, enzymes, and receptors (Bersani et al. 1997). Some of the proposed mechanisms of ELF-MFs effects are modulations in the receptor/ligand binding, receptor capping, ion transport or overall distribution of the intra-membrane proteins (Adey and Lawrence 1984; Chiabrera et al. 1991a,b; Bersani et al. 1997).

Our results revealed that continuous exposure to ELF-MF (50 Hz, 0.5 mT) for 7 days decreased the affinity of serotonin 5-HT_{2A} receptors and increased their density in the prefrontal cortex of experimental animals. These findings are in accordance with the data of Ben-Shachar et al. (1999), who showed decreased affinity of serotonin 5-HT_2 receptors in the frontal cortex of animals after 10 days of

Table 1. The effect of continuous exposure to extremely low frequency magnetic field (ELF-MF; 50 Hz, 0.5 mT) for 1, 3, and 7 days on binding parameters (affinity and density) of serotonin 5-HT_{2A} receptors in the prefrontal cortex (A), as well as dopamine D_1 and D_2 receptors in the striatum (B, C) of experimental animals

A

Serotonin 5-HT_{2A} receptors		
Treatment	K_d (nmol/l)	B_{max} (fmol/mg protein)
Control	1.06 ± 0.08	57.7 ± 8.3
ELF-MF 1 day	1.72 ± 0.23	81.0 ± 12.0*
ELF-MF 3 days	2.33 ± 0.26**	94.7 ± 7.5**
ELF-MF 7 days	2.50 ± 0.54**	71.8 ± 11.8*

B

Dopamine D_1 receptors		
Treatment	K_d (nmol/l)	B_{max} (fmol/mg protein)
Control	0.67 ± 0.10	128.1 ± 18.2
ELF-MF 1 day	0.73 ± 0.15	112.9 ± 14.0
ELF-MF 3 days	0.75 ± 0.10	110.3 ± 8.5
ELF-MF 7 days	0.64 ± 0.07	155.0 ± 20.9

C

Dopamine D_2 receptors		
Treatment	K_d (nmol/l)	B_{max} (fmol/mg protein)
Control	0.13 ± 0.04	87.5 ± 18.5
ELF-MF 1 day	0.19 ± 0.05	68.2 ± 14.0
ELF-MF 3 days	0.17 ± 0.04	84.1 ± 10.6
ELF-MF 7 days	0.11 ± 0.03	96.0 ± 19.2

Binding affinities of the receptors for the specific radioligands are represented by the dissociation constants (K_d). B_{max} values are the estimated tissue densities of the receptors. Each value represents mean ± SEM of three independent trials performed in duplicate. * $p < 0.05$ and ** $p < 0.01$ indicate significant differences compared to control animals (one-way ANOVA, followed by LSD test).

repetitive transcranial magnetic stimulation treatment. Also, our results are in some way expected, having in mind the role of the serotonergic neurotransmission in the adapted response of the CNS to different external or internal stimulus (Jacobs and Azmitia 1992).

In contrast to serotonin 5-HT_{2A} receptors in the prefrontal cortex, we showed that ELF-MF exposure had no effects on the affinity and density of dopamine D_1 and D_2 receptors in the striatum of experimental animals. However, we could not exclude the possibility that some changes exist but that they are below the detection level. Sieron et al. (2001) demonstrated reduced reactivity of central dopamine D_1 receptors after ELF-MF (10 Hz, 1.8–3.8 mT, 1 h daily) exposure for 14 days in neonatal 6-hydroxydopamine-treated rats. Reasons for this disagreement with our results could arise from differences between animals used and experimental procedures.

Alterations in the affinity and density of serotonin 5-HT_{2A} receptors detected in our experiments could be a direct result of ELF-MF influence on serotonin 5-HT_{2A} receptor protein conformation and/or indirect consequence of ELF-MF-induced changes in serotonin concentration. Massot et al. (2000) already revealed that exposure to a 50-Hz MF in the range of intensity from 0.1 to 1 mT (EC_{50} close to 0.5 mT) specifically affects serotonin 5-HT_{1B} receptors inducing structural changes of the protein and thus functional desensitization of the receptors. At the same time, they did not register effect on serotonin 5-HT_{2A} receptors and possible reasons of this discrepancy with our results could be shorter time period of MF exposure (up to 60 min) and greater susceptibility of serotonin 5-HT_{1B} receptors to the external MF. Concerning serotonin concentration, Sieron et al. (2004) found increase in the synthesis rate (turnover) of serotonin in the frontal cortex of rats after exposure to ELF-MF (10 Hz, 1.8–3.8 mT, 1 h daily) for 14 days. It is known that a quantitative increase in serotonin level at the synaptic cleft may be followed by decreased density of serotonergic receptors in the membrane (Rioux et al. 1999; Li et al. 2000). Having in mind all these facts and results obtained in our study, we consider that direct influence of ELF-MF on serotonin 5-HT_{2A} protein conformation is a more suitable hypothesis for us. In that case, decreased affinity of serotonin 5-HT_{2A} receptors in the prefrontal cortex is the initial event, while increased density of these receptors represents response of the organism on disturbed homeostatic conditions.

Serotonin 5-HT_{2A} receptors are G-protein linked molecules that are positively coupled to phosphoinositide metabolism. They are involved in numerous physiological (motor activity, pain, learning and memory) and pathophysiological (schizophrenia, psychosis, depression, anxiety, migraine) processes in the brain (Hillegaart et al. 1996; Buhot et al. 2000; Naughton et al. 2000; Sandrini et al. 2002). Reported findings already indicated that some of these processes are subjected to modification by external ELF-MFs (Wilson 1988; Lai 1996; Sienkiewicz et al. 1998; Pešić et al. 2004; Janać et al. 2005; Bao et al. 2006; Jeong et al. 2006; Jadidi et al. 2007; Liu et al. 2008). ELF-MF-induced alterations in the activity of serotonin 5-HT_{2A} receptors could affect downstream signal transduction pathways. According to the theory based on the resonance interaction between ELF-MF and intracellular signal cascades (Liboff 1985; Lednev 1991), the effects of MFs on calcium-dependent biological processes provoke extensive consequences in the organisms (Walleczek 1992; Frey 1993). In our previous study we found that exposure to ELF-MF (50 Hz, 0.5 mT) for 7 days reduced amphetamine-induced (1.5 mg/kg, i.p.) motor activity in rats (Janać et al. 2005). It is known that serotonin 5-HT_{2A} receptors are located on the pyramidal (in the large percentage) and GABAergic neurons in the prefrontal cortex (Santana et al. 2004; Wedzony et al. 2008). Also, most of these py-

ramidal neurons are projected to dopaminergic neurons of the ventral tegmental area involved in the control of motor activity (Carr and Sesack 2000). This means that serotonin 5-HT_{2A} receptors in the prefrontal cortex have modulatory influence on dopaminergic activity in the ventral tegmental area and release of dopamine in the mesocortical pathway (Bortolozzi et al. 2005). These facts and our results regarding serotonin 5-HT_{2A} receptors indicate that depressor effect of ELF-MF on amphetamine-induced hypermotor response may be a consequence of reduced mesocortical dopaminergic neurons activity. Moreover, O'Neill et al. (1999) suggested involvement of serotonin 5-HT_{2A} receptors in the behavioral responses induced by compounds that increase synaptic concentration of dopamine, such as amphetamine.

We presume that different effects of ELF-MF on cortical serotonin and striatal dopamine receptors are related to the different threshold of reactions of specific brain regions and/or neurotransmitter systems. Previously reported data support both proposed mechanisms, underlining once again very complex and non-predictable nature of external MFs (Chance et al. 1995; Ben-Shachar et al. 1997; Sieron et al. 2004; Zhang et al. 2005). It is known that the time of the physical and biological reactions have important role in the reaction of the living systems to the MFs. Thus, outcome of an experiment depends on characteristics of applied MF (frequency, intensity, impulse shape, exposure duration) and individual features of the organism (functional state, sex, age).

In conclusion, these results contribute not only to better understanding of mechanism(s) underlying observed motor activity effects, but also to the prediction and explanation of other modifications in the brain processes induced by external ELF-MF.

Acknowledgement. This study was supported by the Ministry of Science and Technological Development, Republic of Serbia (grant No. 143027 and 143032).

References

Adey W. R., Lawrence A. F. (1984): Nonlinear Electrodynamics in Biological Systems. pp. 3–22, Plenum Press, New York

Bao X., Shi Y., Huo X., Song T. (2006): A possible involvement of beta-endorphin, substance P, and serotonin in rat analgesia induced by extremely low frequency magnetic field. Bioelectromagnetics **27**, 467–472

Ben-Shachar D., Belmaker R. H., Grisaru N., Klein E. (1997): Transcranial magnetic stimulation induces alterations in brain monoamines. J. Neural. Transm. **104**, 191–197

Ben-Shachar D., Gazawi H., Riboyad-Levin J., Klein E. (1999): Chronic repetitive transcranial magnetic stimulation alters beta-adrenergic and 5-HT_2 receptor characteristics in rat brain. Brain Res. **816**, 78–83

Bersani F., Marinelli F., Ognibene A., Matteucci A., Cecchi S., Santi S., Squarzoni S., Maraldi N. M. (1997): Intramembrane protein distribution in cell cultures is affected by 50 Hz pulsed magnetic fields. Bioelectromagnetics **18**, 463–469

Bortolozzi A., Diaz-Mataix L., Scorza M. C., Celada P., Artigas F. (2005): The activation of 5-HT_{2A} receptors in prefrontal cortex enhances dopaminergic activity. J. Neurochem. **95**, 1597–1607

Buhot M. C., Martin S., Segu L. (2000): Role of serotonin in memory impairment. Ann. Med. **32**, 210–221

Carr D. B., Sesack S. R. (2000): Projections from the rat prefrontal cortex to the ventral tegmental area: target specificity in the synaptic associations with mesoaccumbens and mesocortical neurons. J. Neurosci. **20**, 3864–3873

Chance W. T., Grossman C. J., Newrock R., Bovin G., Yerian S., Schmitt G., Mendenhall C. (1995): Effects of electromagnetic fields and gender on neurotransmitters and amino acids in rats. Physiol. Behav. **58**, 743–748

Chiabrera A., Bianco B., Kaufman J. J., Pilla A. A. (1991a): Quantum dynamics of ions in molecular crevices under electromagnetic exposure. In: Electromagnetics in Medicine and Biology. (Eds. C. T. Brighton and S. R. Pollack), pp. 21–26, San Francisco Press, CA, USA

Chiabrera A., Bianco B., Kaufman J. J., Pilla A. A. (1991b): Quantum analysis of ion binding kinetics in electromagnetic bioeffects. In: Electromagnetics in Medicine and Biology. (Eds. C. T. Brighton and S. R. Pollack), pp. 27–31, San Francisco Press, CA, USA

Frey A. H. (1993): Electromagnetic field interactions with biological systems. FASEB J. **7**, 272–281

Gili-Martín E., Fernández-Briera A., Calvo P. (1997): Effects of chronic ethanol treatment and ethanol withdrawal on [3H]SCH23390 binding to rat striatal membranes. Neuropharmacology **36,** 101–106

Hillegaart V., Estival A., Ahlenius S. (1996): Evidence for specific involvement of 5-HT_{1A} and 5-$HT_{2A/C}$ receptors in the expression of patterns of spontaneous motor activity of the rat. Eur. J. Pharmacol. **295**, 155–161

Jackson D. M., Westlind-Danielsson A. (1994): Dopamine receptors: molecular biology, biochemistry and behavioural aspects. Pharmacol. Ther. **64**, 291–369

Jacobs B. L., Azmitia E. C. (1992): Structure and function of the brain serotonin system. Physiol. Rev. **72**, 165–229

Jadidi M., Firoozabadi S. M., Rashidy-Pour A., Sajadi A. A., Sadeghi H., Taherian A. A. (2007): Acute exposure to a 50 Hz magnetic field impairs consolidation of spatial memory in rats. Neurobiol. Learn. Mem. **88**, 387–392

Janać B., Pešić V., Jelenković A., Vorobyov V., Prolić Z. (2005): Different effects of chronic exposure to ELF magnetic field on spontaneous and amphetamine-induced locomotor and stereotypic activities in rats. Brain Res. Bull. **67**, 498–503

Jeong J. H., Kum C., Choi H. J., Park E. S., Sohn U. D. (2006): Extremely low frequency magnetic field induces hyperalgesia in mice modulated by nitric oxide synthesis. Life Sci. **78**, 1407–1412

Kanno M., Matsumoto M., Togashi H., Yoshioka M., Mano Y. (2003): Effects of repetitive transcranial magnetic stimulation on behavioral and neurochemical changes in rats during an elevated plus-maze test. J. Neurol. Sci. **211**, 5–14

Lai H. (1996): Spatial learning deficit in the rat after exposure to a 60 Hz magnetic field. Bioelectromagnetics **17**, 494–496

Lednev V. V. (1991): Possible mechanism for the influence of weak magnetic fields on biological systems. Bioelectromagnetics **12**, 71–75

Li Q., Wichems C., Heils A., Lesch K. P., Murphy D. L. (2000): Reduction in the density and expression, but not G-protein coupling, of serotonin receptors (5-HT_{1A}) in 5-HT transporter knock-out mice: gender and brain region differences. J. Neurosci. **20**, 7888–7895

Liboff A. R. (1985): Geomagnetic cyclotron resonance in living cells. J. Biol. Phys. **13**, 99–102

Liu T., Wang S., He L., Ye K. (2008): Anxiogenic effect of chronic exposure to extremely low frequency magnetic field in adult rats. Neurosci. Lett. **434**, 12–17

Markwell M. A., Haas S. M., Bieber L. L., Tolbert N. E. (1978): A modification of the Lowry procedure to simplify protein determination in membrane and lipoprotein samples. Anal. Biochem. **87**, 206–210

Massot O., Grimaldi B., Bailly J. M., Kochanek M., Deschamps F., Lambrozo J., Fillion G. (2000): Magnetic field desensitizes 5-HT_{1B} receptor in brain: pharmacological and functional studies. Brain Res. **858**, 143–150

Naughton M., Mulrooney J. B., Leonard B. E. (2000): A review of the role of serotonin receptors in psychiatric disorders. Hum. Psychopharmacol. **15**, 397–415

O'Neill M. F., Heron-Maxwell C. L., Shaw G. (1999): 5-HT_2 receptor antagonism reduces hyperactivity induced by amphetamine, cocaine, and MK-801 but not D_1 agonist C-APB. Pharmacol. Biochem. Behav. **63**, 237–243

Papp M., Klimek V., Willner P. (1994): Parallel changes in dopamine D_2 receptor binding in limbic forebrain associated with chronic mild stress-induced anhedonia and its reversal by imipramine. Psychopharmacology (Berl.) **115**, 441–446

Pešić V., Janać B., Jelenković A., Vorobyov V., Prolić Z. (2004): Non-linearity in combined effects of ELF magnetic field and amphetamine on motor activity in rats. Behav. Brain Res. **150**, 223–227

Rioux A., Fabre V., Lesch K. P., Moessner R., Murphy D. L., Lanfumey L., Hamon M., Martres M. P. (1999): Adaptive changes of serotonin 5-HT_{2A} receptors in mice lacking the serotonin transporter. Neurosci. Lett. **262**, 113–116

Sandrini M., Vitale G., Pini L. A. (2002): Central antinociceptive activity of acetylsalicylic acid is modulated by brain serotonin receptor subtypes. Pharmacology **65**, 193–197

Santana N., Bortolozzi A., Serrats J., Mengod G., Artigas F. (2004): Expression of serotonin$_{1A}$ and serotonin$_{2A}$ receptors in pyramidal and GABAergic neurons of the rat prefrontal cortex. Cereb. Cortex **14**, 1100–1109

Sienkiewicz Z. J., Haylock R. G., Bartrum R., Saunders R. D. (1998): 50 Hz magnetic field effects on the performance of a spatial learning task by mice. Bioelectromagnetics **19**, 486–493

Sieron A., Brus R., Szkilnik R., Plech A., Kubanski N., Cieslar G. (2001): Influence of alternating low frequency magnetic fields on reactivity of central dopamine receptors in neonatal 6-hydroxydopamine treated rats. Bioelectromagnetics **22**, 479–486

Sieron A., Labus L., Nowak P., Cieslar G., Brus H., Durczok A., Zagzil T., Kostrzewa R. M., Brus R. (2004): Alternating extremely low frequency magnetic field increases turnover of dopamine and serotonin in rat frontal cortex. Bioelectromagnetics **25**, 426–430

Vogel G. H. (2002): Drug Discovery and Evaluation-Pharmacological Assays. Springer-Verlag, Berlin

Walleczek J. (1992): Electromagnetic field effects on cells of the immune system: the role of calcium signaling. FASEB J. **6**, 3177–3185

Wedzony K., Chocyk A., Maćkowiak M. (2008): A search for colocalization of serotonin 5-HT_{2A} and 5-HT_{1A} receptors in the rat medial prefrontal and entorhinal cortices-immunohistochemical studies. J. Physiol. Pharmacol. **59**, 229–238

Wilson B. W. (1988): Chronic exposure to ELF fields may induce depression. Bioelectromagnetics **9**, 195–205

Yamada S., Watanabe A., Nankai M., Toru M. (1995): Acute immobilization stress reduces (+/–) DOI-induced 5-HT_{2A} receptor-mediated head shakes in rats. Psychopharmacology (Berl.) **119**, 9–14

Zhang J., Wang X., Wang M. (2005): Influence of time-varying magnetic field on the release of neurotransmitters in raphe nuclei of rats. Conf. Proc. IEEE Eng. Med. Biol. Soc. **6**, 6214–6216

The effect of ascorbate supplementation on the activity of antioxidative enzymes in the rat hypothalamus and adrenals

Sinisa Djurasevic, Gordana Cvijic, Jelena Djordjevic, Iva Djordjevic, Nebojsa Jasnic and Predrag Vujovic

Institute of Physiology and Biochemistry, Faculty of Biology, University of Belgrade, Studentski trg 16, 11000 Belgrade, Republic of Serbia

Abstract. We investigated the effect of vitamin C on the oxidative status in the hypothalamus and adrenal glands of rats supplemented by its two doses over a four-week period. The results obtained have shown that vitamin C exerts effects which are tissue specific. In hypothalamus, it decreased the activity of copper zinc superoxide dismutase (CuZnSOD), the concentration of hydrogen peroxide (H_2O_2), as well as the activity of catalase and the level of lipid peroxidation, thus causing effects which are obviously antioxidative. On the other hand, the changes detected in adrenals indicate that vitamin C there performs some other, specific functions. They are followed by an increase in the activity of both CuZnSOD and MnSOD, as well as with the consequent rise of H_2O_2 content. However, these changes seem not to be of pro-oxidative nature since the level of lipid peroxidation in adrenals remains unchanged as compared to the controls.

Key words: Rats — Vitamin C — Hypothalamus — Adrenals — Oxidative status

Introduction

Vitamin C (ascorbic acid, ascorbate) is a vitamin which takes part in many biochemical processes in organism. Chemically capable of reacting with most of the physiologically important radicals and oxidants (Buettner 1993) it acts as a proven hydrosoluble antioxidant (Halliwell 1996). Another important biological function of ascorbate is to serve as a cosubstrate for several hydroxylase and oxygenase enzymes, maintaining their active center metal ions in a reduced state for optimal enzyme activity (Carr and Frei 1999). One of these enzymes is dopamine β-hydroxylase (DBH), which in different neuroendocrine tissues synthesizes noradrenaline through hydroxylation of dopamine (Diliberto et al. 1987).

It is known that the level of the DBH activity highly depends on the intracellular vitamin C content (Levine 1986), which, in turn, depends on the activity of members of the family of mammalian Na^+-dependent L-ascorbic acid plasma membrane transporters (Tsukaguchi et al. 1999). There are two types of these transporters, SVCT1 and SVCT2 (Daruwala et al. 1999), and the latter is widely expressed in the brain and adrenals (Liang et al. 2001). It has been shown that mutant mice lacking SVCT2 have severely reduced (99%) ascorbic acid levels in both brain and adrenals (Sotiriou et al. 2002). While this fall in vitamin C concentration shows no implication on the brain levels of dopamine and noradrenaline, it causes marked reduction in adrenal level of DBH activity; it seems that deranged catecholamine system function in SVCT2 null mice is largely restricted to the adrenal medulla (Bornstein et al. 2003).

According to previously mentioned, we assumed that the same tissue-specific response of hypothalamus and adrenals could be achieved even in normal rats, as a result of increased vitamin C supply. Since the activity of DBH involves the accumulation of an activated oxygen intermediate, with the properties of a copper-peroxo or copper-oxo species (Evans et al. 2003), we decided to study the oxidative status of rats supplemented by two different doses of ascorbic acid over a four-week period of time. Thus, the activities of copper zinc superoxide dismutase (CuZnSOD), manganese superoxide dismutase (MnSOD) and catalase, hydrogen peroxide (H_2O_2) concentration, the level of lipid peroxidation and

Correspondence to: Sinisa Djurasevic, Institute of Physiology and Biochemistry, Faculty of Biology, University of Belgrade, Studentski trg 16, 11000 Belgrade, P.O.Box S2, Republic of Serbia
E-mail: sine@bio.bg.ac.rs

vitamin C content were determined in the hypothalamus and adrenal glands of the experimental animals, as well as their serum vitamin C level.

Materials and Methods

Design of experiment

Male rats of the Wistar strain (*Rattus norvegicus*) weighing 200 ± 45 g were used for the experiments. The animals were acclimated to 22 ± 1°C and maintained under conditions of 12-h periods of light and dark, with unlimited access to tap water and commercial rat food.

The rats were divided into three groups, each consisting of six animals. The control group consisted of rats which drank tap water. The second and the third group formed animals supplemented with a low or high dose of vitamin C dissolved in tap water.

Vitamin C supplementation

The vitamin C doses were chosen as 0.75 mg (low dose) and 25 mg (high dose) ascorbic acid/kg rat body weight per day. According to our previous experiment performed on a group of six animals during four weeks, the daily consumption of water in rats was linear in respect to their body weight, with average value of 240 ± 5 ml/kg. Therefore, both doses of vitamin C were dissolved in adequate volume of tap water every day (i.e. 3.125 mg ascorbic acid/l water and 104.167 mg ascorbic acid/l water, respectively) and administered to appropriate group of animals. This supplementation was permanent throughout four weeks.

Sample preparation

At the end of the vitamin C supplementation period, animals were killed by decapitation with Harvard guillotine without anesthesia, as recommended by the Local Ethical Committee. After this, hypothalamus and adrenal glands were removed and divided in two equal portions.

One sample of each tissue was homogenized in 9 volumes of 25 mmol/l phosphate buffered saline (PBS), pH 7.0, and centrifuged at 9000 g in a semi-preparative Sorvall Super T21 centrifuge for 20 min at 4°C. Supernatants were used for determination of catalase, CuZnSOD and MnSOD activities, as well as for the measurement of the concentration of H_2O_2e and total lipid hydroperoxides (the level of lipid peroxidation).

Another set of tissue samples, as well as blood serum, were used for determination of vitamin C content by using the similar procedure, except that 6% trichloroacetic acid was used instead of PBS.

Methods

The vitamin C concentration was determined in trichloroacetic acid samples by the method of Roe and Kuether (1943) and calculated against vitamin C standard curve absorption values.

The total superoxide dismutase activity was determined in the PBS samples by the adrenaline method of Misra and Fridovich (1972), using potassium cyanide as a CuZnSOD inhibitor for differential calculation of MnSOD activity (Weisiger and Fridovich 1973).

The catalase activity was measured in the PBS samples by the method of Beutler 1982), based on the rate of H_2O_2 degradation by the action of the catalase contained in the examined samples.

The measurement of the total lipid hydroperoxides and H_2O_2 content were both based on the ferrous ion oxidation by xylenol orange (FOX) assay (Wolf 1994). The two versions of FOX assays are described in the literature, FOX-1 and FOX-2 (Banerjee et al. 2002). The concentration of H_2O_2 was measured in PBS samples by the FOX-1 assay (Gay and Gebicki 2000) and calculated against H_2O_2 standard curve absorption values. The concentration of lipid hydroperoxides was measured in PBS samples by the FOX-2 assay (Jiang et al. 1991) with the level of lipid peroxidation in samples being expressed as a percent of lipid peroxidation level of control animal group.

Statistics

The data were expressed as means ± SEM. One-way ANOVA was undertaken for multiple range comparison, while significant differences among groups were determined by the Tukey posterior test. The probability of significance of differences was set at $p < 0.05$.

Results

In the vitamin C-supplemented rats its endogenous concentration in the serum was dose-dependently elevated, which results in its corresponding accumulation in the adrenal glands, but not in the hypothalamus of these animals (Fig. 1).

As can be seen from Fig. 2, the activity of CuZnSOD, but not the MnSOD, is depressed in the hypothalamus of rats fed with vitamin C. This probably results in decreased production of H_2O_2 and consequent decline of catalase activity in this tissue (Fig. 2). In accordance with this, feeding with vitamin C also decreases the level of lipid peroxidation in the hypothalamus (Fig. 2).

In the adrenal glands, activity of both forms of SOD was elevated as a result of vitamin C treatment (Fig. 3).

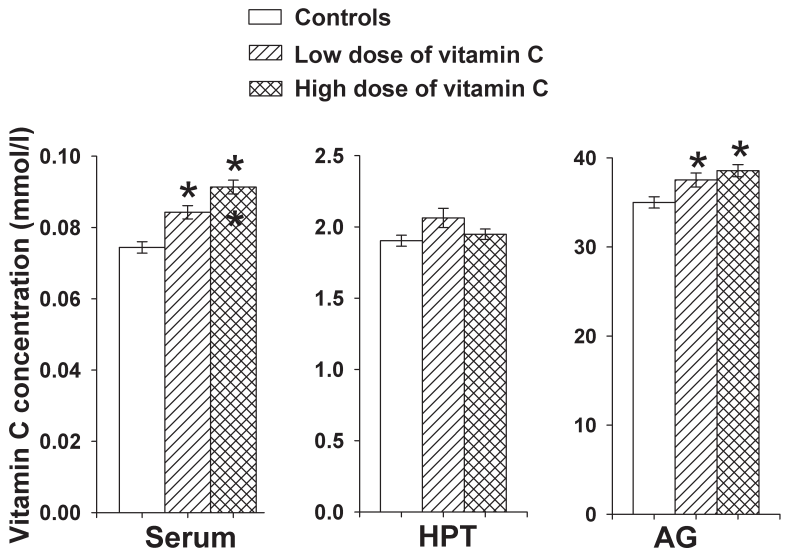

Figure 1. The effect of low and high dose of vitamin C supplementation on its concentration in rat serum, hypothalamus (HPT) and adrenal glands (AG). The data are expressed as means ± SEM. Statistically significant differences ($p < 0.05$) in relation to the control are marked with an asterisk above the columns, while statistically significant differences between two doses of the vitamin C are marked with an asterisk inside the columns.

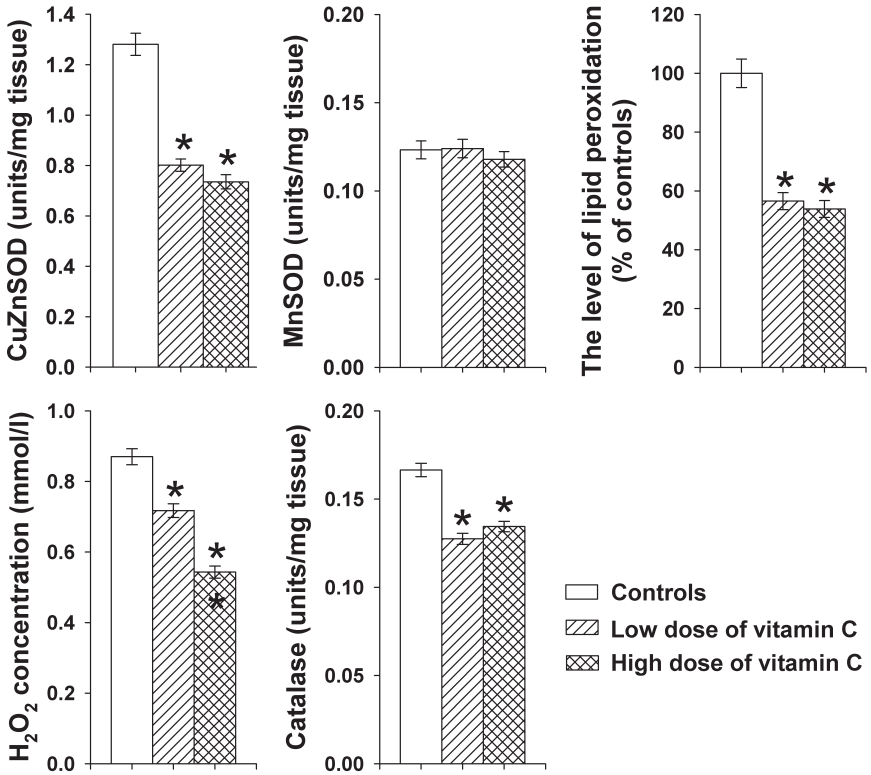

Figure 2. The effect of low and high dose of vitamin C supplementation on the oxidative status of rat hypothalamus. The data are expressed as means ± SEM. Statistically significant differences ($p < 0.05$) in relation to the control are marked with an asterisk above the columns, while statistically significant differences between two doses of the vitamin C are marked with an asterisk inside the columns.

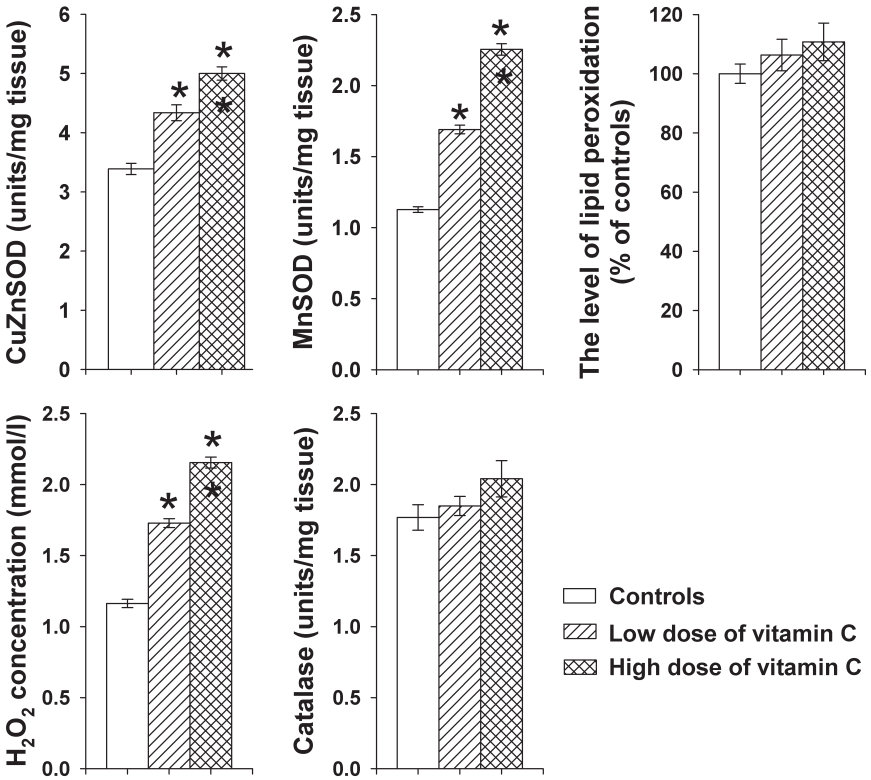

Figure 3. The effect of low and high dose of vitamin C supplementation on the oxidative status of rat adrenal glands. The data are expressed as means ± SEM. Statistically significant differences ($p < 0.05$) in relation to the control are marked with an asterisk above the columns, while statistically significant differences between two doses of the vitamin C are marked with an asterisk inside the columns.

This was followed with accompanying increase in the concentration of H_2O_2, but not with the increase in the activity of catalase, which remains unchanged under the influence of vitamin C, as well as the level of lipid peroxidation (Fig. 3).

Discussion

As can be seen from our results, vitamin C decreases the activity of CuZnSOD in hypothalamus. The mechanism of this action probably involves a removal of superoxide radical as its respective substrate (Buettner 1993), with the similar effect already described in cultured rat brain astrocytes after incubation with ascorbate (Kao et al. 2003). In accordance to this, the concentration of H_2O_2, a product of superoxide dismutases activity, is also lowered in the hypothalamus, followed with the consequent catalase activity decline. Proved with the further level of lipid peroxidation decrease, these results implicate the antioxidant effect of ascorbate in hypothalamus. This vitamin C outcome is of the exceptional importance for the neural tissue, being particularly sensitive to oxidative damage due to the high concentrations of unsaturated lipids (Sevanian and McLeod 1997). Indeed, the brain ascorbate level in anoxia-tolerant reptiles is known to be several times higher than in mammals, in order to prevent oxidative damage during reoxygenation after a hypoxic dive (Rice et al. 1995).

The ascorbic acid concentration in hypothalamus is of the order of several millimoles, which is in complete agreement with the literature data (Oke et al. 1987). Conversely, the vitamin C itself does not alter this concentration, thus making difficult to interpret its antioxidative effects in hypothalamus. Being already among the highest in the organism (Kratzing et al. 1982), the concentration of ascorbic acid in the brain is known to be under strong homeostatic regulation (Rice 2000). Realized through rapid ascorbate turnover among neural cells and blood (Spector 1977), this regulation probably combines fast neuronal SVCT2 mediate ascorbic acid uptake and simultaneously dehydroascorbic acid upset (mediated by some of the members of glucose transporters family). Thus maintained stable intracellular ascorbic acid level most likely causes the ability of dietary vitamin C to increase its brain content controversially (Hediger 2002).

In sharp contrast to hypothalamus, vitamin C supplementation in adrenals exerts completely different pattern of changes. It is not just that the activities of both forms of SODs are elevated under the influence of ascorbate, but also the concentration of H_2O_2, as a consequent product of their activity. The source of increased superoxide radical production, as a respective substrate of superoxide dismutases activity, remains to stay unclear. However, there are indications that the DBH activity may be followed by increased oxidative stress since the mechanism of dopamine hydroxylation involves the accumulation of an activated oxygen intermediate with the properties of a copper-peroxo or copper-oxo species (Evans et al. 2003). In accordance with the previous statement, the increased formation of H_2O_2 could be involved in modulation of the DBH activity. To be more specific, it is known that the enzyme activity leads to increased generation of H_2O_2 (Levin and Kaufman 1961), which in turn causes further DBH inactivation (Slama et al. 2001). Here we propose that both H_2O_2 formations during dopamine hydroxylation, as well as its inhibitory action on DBH, represent segments of the same mechanism of negative auto-regulation of the enzyme activity. In this sense, the function of appropriate peroxidase activity would be the maintenance of H_2O_2 at the optimal concentration, in agreement with our results showing that the adrenal catalase activity remains unchanged under the influence of vitamin C. Nevertheless, this mechanism seems not to be pro-oxidative, since the level of lipid peroxidation remains unchanged as compared to the controls.

Unlike hypothalamus, feeding with ascorbic acid significantly increases its adrenal concentration, confirming the glands ability to accumulate vitamin C under normal physiological conditions. This is very important for the function of adrenals as a main organism depot of vitamin C, capable of releasing it during stress response (Lahiri and Lloyd 1962; Padayatty et al. 2007) with pattern which has been shown to be stressor specific (Djordjević et al. 2006).

In conclusion, our results have shown that vitamin C exerts effects which are tissue-specific and not necessarily dose-dependent. Indeed, the fact that SVCTs are fully saturated at low extracellular ascorbic acid concentrations (Washko et al. 1989) probably explains the relative inefficiency of high vitamin C dose in animals, as it is already shown in humans (Levine et al. 1996). Also, it has been demonstrated that the use of high doses of ascorbic acid causes strong decrease in SVCT1 expression in the apical surface of the intestinal membrane (MacDonald et al. 2002), thus confirming the old thesis that the main limiting factor of the vitamin C bioavailability is its intestinal absorption (Hodges et al. 1969).

Acknowledgement. This work was supported by the Serbian Ministry of Science and Technology, grant No. 143050.

References

Banerjee D., Kumar A., Kumar B., Madhusoodanan U. K., Nayak S., Jacob J. (2002): Determination of absolute hydrogen peroxide concentration by spectrophotometric method. Curr. Sci. **83**, 1193–1194

Beutler E. (1982): Catalase. In: Red Cell Metabolism, a Manual of Biochemical Methods. pp. 105–106, Grune & Stratton, New York

Bornstein S. R., Yoshida-Hiroi M., Sotiriou S., Levine M., Hartwig H. G., Nussbaum R. L., Eisenhofer G. (2003): Impaired adrenal catecholamine system function in mice with deficiency of the ascorbic acid transporter (SVCT2). FASEB J. **17**, 1928–1930

Buettner G. R. (1993): The pecking order of free radicals and antioxidants: lipid peroxidation, α-tocopherol, and ascorbate. Arch. Biochem. Biophys. **300**, 535–543

Carr A., Frei B. (1999): Does vitamin C act as a pro-oxidant under physiological conditions? FASEB J. **13**, 1007–1024

Daruwala R., Song J., Koh W. S., Rumsey S. C., Levine M. (1999): Cloning and functional characterization of the human sodium-dependent vitamin C transporters hSVCT1 and hSVCT2. FEBS Lett. **460**, 480–484

Diliberto E. J. Jr., Menniti F. S., Knoth J., Daniels A. J., Kizer J. S., Viveros O. H. (1987): Adrenomedullary chromaffin cells as a model to study the neurobiology of ascorbic acid: from monooxygenation to neuromodulation. Ann. N. Y. Acad. Sci. **498**, 28–53

Djordjević J., Djurašević S., Vučković T., Jasnić N., Cvijić G. (2006): Effect of cold and heat stress on the rat adrenal, serum and liver ascorbic acid concentration. Arch. Biol. Sci. **58**, 161–164

Evans J. P., Ahn K., Klinman J. P. (2003): Evidence that dioxygen and substrate activation are tightly coupled in dopamine β-monooxygenase. Implications for the reactive oxygen species. J. Biol. Chem. **278**, 49691–49698

Gay C., Gebicki J. M. (2000): A critical evaluation of the effect of sorbitol on the ferric-xylenol orange hydroperoxide assay. Anal. Biochem. **284**, 217–220

Halliwell B. (1996): Vitamin C: antioxidant or pro-oxidant *in vivo*? Free Radic Res. **25**, 439–454

Hediger M. A. (2002): New view at C. Nat. Med. **8**, 445–446

Hodges R. E., Baker E. M., Hood J., Sauberlich H. E., March S. C. (1969): Experimental scurvy in man. Am. J. Clin. Nutr. **22**, 535–548

Jiang Z. Y., Woollard A. C., Wolff S. P. (1991): Lipid hydroperoxide measurement by oxidation of Fe^{2+} in the presence of xylenol orange. Comparison with the TBA assay and an iodometric method. Lipids **26**, 853–856

Kao P. F., Lee W. S., Liu J. C., Chan P., Tsai J. C., Hsu Y. H., Chang W. Y., Cheng T. H., Liao S. S. (2003): Downregulation of superoxide dismutase activity and gene expression in cultured rat brain astrocytes after incubation with vitamin C. Pharmacology **69**, 1–6

Kratzing C. C., Kelly J. D., Oelrichs B. A. (1982): Ascorbic acid in neural tissues. J. Neurochem. **39**, 625–627

Lahiri S., Lloyd B. B. (1962): The form of vitamin C released by the rat adrenal. Biochem. J. **84**, 474–477

Levin E. Y., Kaufman S. (1961): Studies on the enzyme catalyzing the conversion of 3,4-dihydroxyphenylethylamine to norepinephrine. J. Biol. Chem. **236**, 2043–2049

Levine, M. (1986): Ascorbic acid specifically enhances dopamine β-monooxygenase activity in resting and stimulated chromaffin cells. J. Biol. Chem. **261**, 7347–7356

Levine M., Conry-Cantilena C., Wang Y., Welch R. W., Washko P. W., Dhariwal K. R., Park J. B., Lazarev A., Graumlich J. F., King J., Cantilena L. R. (1996): Vitamin C pharmacokinetics in healthy volunteers: evidence for a recommended dietary allowance. Proc. Natl. Acad. Sci. U.S.A. **93**, 3704–3709

Liang W. J., Johnson D., Jarvis S. M. (2001): Vitamin C transport systems of mammalian cells. Mol. Membr. Biol. **18**, 87–95

MacDonald L., Thumser A. E., Sharp P. (2002): Decreased expression of the vitamin C transporter SVCT1 by ascorbic acid in a human intestinal epithelial cell line. Br. J. Nutr. **87**, 97–100

Misra H. P., Fridovich I. (1972): The role of superoxide anion in the autoxidation of epinephrine and a simple assay for superoxide dismutase. J. Biol. Chem. **247**, 3170–3175

Oke A. F., May L., Adams R. N. (1987): Ascorbic acid distribution patterns in human brain. A comparison with nonhuman mammalian species. Ann. N. Y. Acad. Sci. **498**, 1–12

Padayatty S. J., Doppman J. L., Chang R., Wang Y., Gill J., Papanicolaou D. A., Levine M. (2007): Human adrenal glands secrete vitamin C in response to adrenocorticotrophic hormone. Am. J. Clin. Nutr. **86**, 145–149

Rice M. E. (2000): Ascorbate regulation and its neuroprotective role in the brain. Trends Neurosci. **23**, 209–216

Rice M. E., Lee E. J., Choy Y. (1995): High levels of ascorbic acid, not glutathione, in the CNS of anoxia-tolerant reptiles contrasted with levels in anoxia-intolerant species. J. Neurochem. **64**, 1790–1799

Roe J. H., Kuether C. A. (1943): The determination of ascorbic acid in whole blood and irine through the 2,4-dinitrophenylhydrazine derivative of dehydroascorbic acid. J. Biol. Chem. **147**, 399–407

Sevanian A., McLeod L. (1997): Formation and biological reactivity of lipid peroxidation products. In: Free Radical Toxicology. (Ed. K. B. Wallace), pp. 47–70, Taylor and Francis, Washington

Slama P., Jabre F., Tron T., Reglier M. (2001): Dopamine β-hydroxylase inactivation generates a protein-bound quinone derivative. FEBS Lett. **491**, 55–58

Sotiriou S., Gispert S., Cheng J., Wang Y., Chen A., Hoogstraten-Miller S., Miller G. F., Kwon O., Levine M., Guttentag S. H., Nussbaum R. L. (2002): Ascorbic-acid transporter Slc23a1 is essential for vitamin C transport into the brain and for perinatal survival. Nat. Med. **8**, 514–517

Spector R. (1977): Vitamin homeostasis in the central nervous system. N. Engl. J. Med. **296**, 1393–1398

Tsukaguchi H., Tokui T., Mackenzie B., Berger U. V., Chen X. Z., Wang Y., Brubaker R. F., Hediger M. A. (1999): A family of mammalian Na^+-dependent L-ascorbic acid transporters. Nature **399**, 70–75

Washko P., Rotrosen D., Levine M. (1989): Ascorbic acid transport and accumulation in human neutrophils. J. Biol. Chem. **264**, 18996–19002

Weisiger R. A., Fridovich I. (1973): Mitochondrial superoxide simutase. Site of synthesis and intramitochondrial localization. J. Biol. Chem. **248**, 4793–4796

Wolf S. P. (1994): Ferrous ion oxidation in presence of ferric ion indicator xylenol orange for measurement of hydroperoxides. Methods Enzymol. **233**, 182–189

The effect of acute or/and chronic stress on the MnSOD protein expression in rat prefrontal cortex and hippocampus

Dragana Filipović, Jelena Zlatković and Snežana B. Pajović

Laboratory of Molecular Biology and Endocrinology, Institute of Nuclear Sciences "Vinča", P.O.Box 522-090, 11001 Belgrade, Serbia

Abstract. Manganese superoxide dismutase (MnSOD) is the major antioxidant in mitochondria that protect brain from neuroendocrine stress. Although MnSOD is localized in the mitochondria, the immediate subcellular distribution of MnSOD protein level in the prefrontal cortex and hippocampus of Wistar male rats exposed to acute stressors immobilization or cold, chronic stress isolation or their combinations (acute/chronic) have not been studied. Western immunoblotting revealed that acute immobilization stress resulted in an increase in mitochondrial MnSOD protein level, whereas chronic isolation compromises MnSOD protein level. Chronically stressed animals exposed to novel acute stressors showed a significant decrease in mitochondrial MnSOD protein level and reciprocal increase in this protein in the cytosolic fraction. At the same time, a significant increase in serum corticosterone level was observed after acute stressors, whereas chronic isolation led to negligable changes and caused a reduced responsiveness to a novel acute stressors. Presence of cytochrome c in mitochondrial and cytosolic fraction of both brain structures was also confirmed. Results suggest that chronic stress isolation results in mitochondrial dysfunction and MnSOD release into the cytosol.

Key words: MnSOD — Prefrontal cortex — Corticosterone — Hippocampus — Neuroendocrine stress

Introduction

Exposure to neuroendocrine stress (NES) leads to the increased release of glucocorticoids (GCs) by activation of hypothalamo-pituitary adrenal (HPA) axis. The effects of GCs in any *acute* stressful situation can be classified as *protective* for the *organism* (preserving homeostasis) against the negative sequelae of stress, while prolonged periods of exposure to elevated levels of GCs (such as occurs during chronic stress) may have deleterious biological effects, in which oxidative stress plays a major etiopathological role (Sapolsky 1992; Pardon 2007). Neurodegeneration mediated by GCs under stress conditions has been linked to an increase in generation of reactive oxygen species (ROS), which can directly damage lipids, nucleic acids and proteins (Blumberg 2004; Evans et al. 2004) resulting in mitochondrial dysfunction, cytochrome c release in the cytosol (Fujimura et al. 1999; Chong et al. 2005) and biochemical cascade that could lead to the apoptosis (Le Bras et al. 2005). The extent of NES-triggered effects and the resulting vulnerability of cells are related to the NES duration and intensity.

One of the primary intracellular sites for *in vivo* ROS production is the mitochondria (Turrens 1997). Manganese superoxide dismutase (MnSOD) is antioxidant enzyme present in the inner membrane and matrix of mitochondria (Slot et al. 1986; Okado-Matsumoto and Fridovic 2001). It is encoded in the nuclear chromatin, synthesized as a precursor in the cytoplasm, and imported posttranslationally into the mitochondrial matrix in its mature form subsequent to the removal of its 23-amino acid NH_2-terminal leader sequence by specific proteases (Wispe et al. 1989). In the presence MnSOD, superoxide radical (O_2^-) can be converted to the hydrogen peroxide (H_2O_2) which can then diffuse out of mitochondria in the cytoplasm. In the presence of high iron concentrations, H_2O_2 can form the highly reactive hydroxyl radical (HO) *via* the Fenton reaction. O_2^- can also react with nitric oxide to form the highly reactive peroxynitrite anion ($ONOO^-$), as it has been demonstrated in brain after stress (Olivenza

Correspondence to: Dragana Filipović, Laboratory of Molecular Biology and Endocrinology, Institute of Nuclear Sciences "Vinča", P.O.Box 522–090, 11001 Belgrade, Serbia
E-mail: dragana@vinca.rs

et al. 2000), causing oxidative/nitrosative damage (Liu et al. 1996; Madrigal et al. 2001).

Chronic exposure to mitochondrial ROS leads to inactivation of key mitochondrial enzymes and accumulation of mitochondrial DNA mutation (Wallace 2005). It has been shown that MnSOD knockout mice display degenerative changes in large areas of the central nervous system, especially in the basal ganglia (Lebovitz et al. 1996). Overexpression of MnSOD results in neuroprotection by reducing cellular apoptosis and decreasing brain ischemic damage (Keller et al. 1998). Recent evidence has shown that chronic isolation stress increases the activity of MnSOD, whereas it is not affected by acute stressors in the brain (Pajović et al. 2006). GCs have been shown to decrease the activity of antioxidative enzymes in the hippocampus and brain cortex, both basally and in the presence of an oxidative stressor (McIntosh et al. 1998a,b). Moreover, dexamethasone can reduce basal or cytokine-stimulated MnSOD mRNA expression, suggesting that MnSOD is under glucocorticoid regulation (Valentine and Nick 1994; Antras-Ferry et al. 1997). Consequently, a decrease in the antioxidant capacity of the brain may be responsible for the stress-related oxidative damage. A possible mechanism by which stress-hormones may contribute to oxidative damage may be due to compromised brain antioxidant defense system (Michel et al. 2007; Sarandol et al. 2007).

Taking into account the above studies, we investigated the hypothesis that 2 h of acute stress immobilization or cold, 21 day of chronic stress isolation or their combinations (homotypic chronic stress followed by as heterotypic acute stress) alter MnSOD subcellular protein level in the rat prefrontal cortex as a center of cognitive brain and hippocampus which comprises the numerous centers of emotional brain, as essential components of neural circuitry mediating stress (Jacobson and Sapolsky 1991; Mizoguchi et al. 2003). We also measured serum corticosterone (CORT) level in control and all stressed rat groups, in order to examine the biological impact of the stressor. The chronic isolation stress was chosen as the model because it is a continuous stressor which contains both psychological and physiological components (Popović et al. 2000; Chourbaji et al. 2005), and may enhance anxiety in rat (Maisonnette et al. 1993; Haller and Halasz 1999) even after 7 days of isolation (Niesink and Van Ree 1982). The immediate aim of the study was to define the kind of stress (acute, chronic or combined) which led to the most pronounced changes in serum CORT levels and MnSOD subcellular protein level.

Materials and Methods

Animal treatments

Adult Wistar male rats (2–3 months old, weighing 330–400 g) were housed in groups of four individuals per cage in a temperature 20 ± 2°C, humidity 55 ± 10% and offered water and food *ad libitum*. The light was kept on between 7:00 a.m. and 7:00 p.m. The animal experiments were approved by the Ethical Committee for the Use of Laboratory Animals of the Institute of Nuclear Sciences "Vinca", which follows the guidelines of the registered "Serbian Society for the Use of Animals in Research and Education". For experimental purposes, the animals were randomly divided into four groups: in group I four animals were kept per cage representing the unstressed animals (control, $n = 6–8$); group II was exposed to 2 h of immobilization (IM) or cold (C; 4°C) representing acute stressors (each one, $n = 6–8$); group III was exposed to chronic isolation by individual housing for 21 day (IS; $n = 6–8$), according to the model of Garzon and del Rio (1981), where the animals had relatively normal auditory and olfactory experiences but could not at any time see, touch or be touched by other colony animals; group IV was exposed to chronic IS followed by only once for 2 h of acute IM or C (4°C) stress, representing combined stressors (IS+IM, IS+C, each one, $n = 6–8$). Experiments of acute stressors were performed between 8:00 a.m. and 10:00 a.m., to avoid CORT circadian rhythm. Rats were exposed to IM action by introducing them in the prone position with all four limbs fixed to the board with adhesive tape. The head was also fixed with a metal loop over the neck area, with a consequent limitation of head motion (Kvetnansky and Mikulaj 1970). The animals exposed to C stress were initially kept at ambient temperature (20 ± 2°C) and then carefully transferred into a refrigerator room at 4°C. Following stress procedure, the whole brain was immediately removed and, the prefrontal cortex and hippocampus were dissected on ice. Tissue were frozen in liquid nitrogen and kept at –70°C.

Serum CORT assay

Immediately after stress, the animals were decapitated and the trunk blood was collected. Blood samples were centrifuged at 4°C for 20 min at 1500 × *g*, and serum was separated and kept at –70°C until CORT levels determination. Levels of serum CORT were determined using the Octeia ELISA kit (IDS, Boldon, U.K.) and the values were expressed as nanogram per milliliter. All samples were measured in duplicate in one assay. The variation between duplicate samples was less than 7%. The lower detection limit for hormone levels in this assay system is 25 ng/ml.

Mitochondria/cytosol fractionation

To prepare mitochondria and cytosol tissue protein extracts, frozen prefrontal cortex and hippocampus were weighed and homogenized in 2 vol. (w/v) of ice-cold homogenization buffer I (0.25 mol/l sucrose, 15 mmol/l TRIS-HCl (pH 7.9), 16 mmol/l KCl, 15 mmol/l NaCl, 5 mmol/l ethylenediamine-

tetraacetic acid (EDTA), 1 mmol/l ethylene glycol tetraacetic acid, 1 mmol/l dithiothreitol (DTT), 0.15 mmol/l spermine and 0.15 mmol/l spermidine supplemented with following protease inhibitors: 0.1 mmol/l phenylmethanesulphonylfluoride, 2 μg/ml leupeptin, 5 μg/ml aprotinin, 5 μg/ml antipain) by 40 strokes in the Potter-Elvehjem teflon-glass homogenizer. Samples were centrifuged at 2000 × *g,* 4°C for 10 min. The supernatant was centrifuged at 15,000 × *g*, 4°C for 20 min. The resulting mitochondrial pellet was washed by resuspension in homogenization buffer I followed by additional centrifugation at 15,000 × *g,* 4°C for 20 min and resuspended in 250 μl of lysis buffer (50 mmol/l TRIS-HCl (pH 7.4), 5% glycerol, 1 mmol/l EDTA, 5 mmol/l DTT, supplemented with mentioned protease inhibitors and 0.05% Triton X-100). The supernatant was further centrifuged at 100,000 × *g* for 60 min to obtain the pure cytosolic fraction. Protein content in the mitochondrial and cytosolic fractions was determined by the method of Lowry et al. (1951), using bovine serum albumin (BSA; Sigma-Aldrich) as reference.

Electrophoresis and Western blot analysis

Equal amounts of protein of mitochondrial and cytosolic fractions of unstressed control and all stressed groups isolated from prefrontal cortex and hippocampus were electrophoresed on a 10% sodium dodecyl sulfate-polyacrylamide gel electrophoresis and electrophoretically transferred to a polyvinylidene difluoride membrane (Bio-Rad, Hercules, CA). Membranes were blocked in a blocking buffer with 5% BSA in TRIS-buffered saline (20 mmol/l TRIS, 137 mmol/l NaCl (pH 7.6), containing 0.3% Tween 20) and incubated with a rabbit polyclonal anti-MnSOD antibody (SOD-110; Stressgen, Victoria, BC, Canada). Mouse anti-cytochrome c antibody (6H2; Santa Cruz Biotechnology) was used to confirm the presence of cytochrome c in mitochondrial and cytosolic fractions of both brain structures. Western blots were performed with horseradish peroxidase (HRP)-conjugated anti-rabbit (7074; Cell Signaling Technology) or goat anti-mouse immunoglobuline (SC-2005; Santa Cruz Biotechnology) for 2 h. To confirm a consistent protein loading for each lane, membranes were stained for β-actin (primary monoclonal mouse anti-β-actin antibody, A5316 Sigma-Aldrich, followed by HRP-conjugated secondary goat anti-mouse immunoglobuline). Antigen-antibody complexes were incubated with the LumiGLO substrate (7003; Cell Signaling Technology) for 5 min and immediately exposed to X-ray film. The immunoreactive bands were quantitated by Image software. Results were expressed as MnSOD/β-actin ratio. In the figures, the MnSOD levels in stressed animals were expressed as percentage of change in relation to those in unstressed animals taken as 100% (unstressed control). The data are expressed as means ± S.E.M. of 6–8 animals per group.

Statistical evaluation

Data were analyzed by two-way ANOVA (the factors were acute or chronic stress, and the levels for the acute stress were none, IM and C, while for the chronic stress they were none and IS). The Tukey post-hoc test was used to evaluate the differences between the groups. Statistical significance was accepted at $p < 0.05$. All data are given means ± S.E.M.

Results

Serum CORT level in unstressed control and stressed animals

The results on serum CORT level in unstressed control and all stressed rat groups are presented in Fig. 1. Two-way ANOVA analysis revealed a significant effect of acute ($F_{2.30} = 93.19$, $p < 0.001$), chronic ($F_{1.30} = 22.45$, $p < 0.001$) or combined stress ($F_{2.30} = 6.44$, $p < 0.01$) on serum CORT secretion. In the acutely stressed animals, IM acted as an extremely potent stressor, resulted in a 5-fold increase in serum CORT level ($p < 0.001$), while C stress led to a 2-fold increase in CORT level ($p < 0.01$), compared to the unstressed control (Fig. 1, left panel). In animals chronically exposed to IS, serum CORT level was

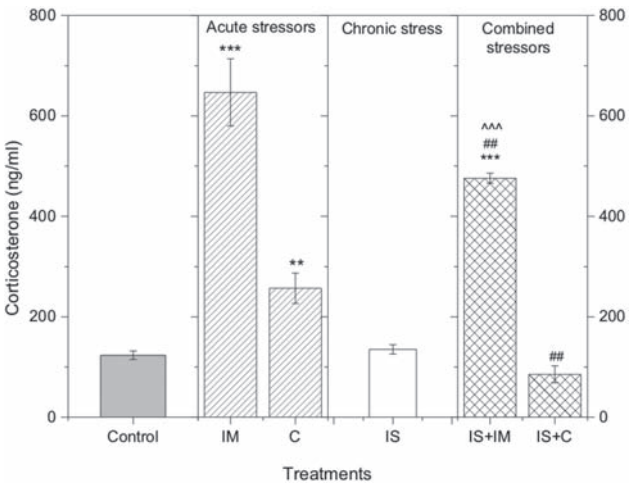

Figure 1. Changes in serum CORT levels (ng/ml) of adult Wistar male rats in unstressed control and rats exposed to acute immobilization (IM) or cold (C) stressors, chronic isolation (IS) or their combinations, as indicated. The results are expressed as mean ± S.E.M. of 6 animals per group. Symbols indicate a significant difference between: respective stress treatment and unstressed control ** $p < 0.001$, *** $p < 0.001$; combined stressors and those respective acute stressors $^{\#\#}$ $p < 0.01$; combined stress isolation followed by immobilization (IS+IM) and chronic isolation (IS) $^{\wedge\wedge\wedge}$ $p < 0.001$, by Tukey post-hoc test.

not changed ($p > 0.05$), (Fig. 1, middle panel) when compared to the unstressed control. Novel acute stressor IM showed a significant elevation of serum CORT level in the chronic IS-pretreated group and reached a 4-fold increase compared to the unstressed control ($p < 0.001$), as well as, 3-fold increase compared to the chronic IS ($^{\wedge\wedge\wedge}$ $p < 0.001$). On the other hand, consecutive exposure to acute C did not significantly alter serum CORT level ($p > 0.05$) compared of either unstressed control or chronic IS stress. When the results of the combined stressors were compared to those of acute stressors, it was observed a significant decrease ($^{\#\#}$ $p < 0.01$, Tukey post-hoc test).

MnSOD protein levels in mitochondrial or cytosolic fractions of the prefrontal cortex

An immunoreactive band of ~25 kDa corresponding to the predicted molecular mass of MnSOD protein was detected in mitochondrial and cytosolic fractions of the prefrontal cortex in unstressed control and all stressed rat groups (Fig. 2A). Two-way ANOVA analysis of mitochondrial MnSOD protein levels revealed significant effect of chronic stress ($F_{1.30} = 87.01$, $p < 0.001$), as well as, interaction effects of acute × chronic stress ($F_{2.30} = 7.64$, $p < 0.01$). Post-hoc Tukey analysis showed a significant increase in the mitochondrial MnSOD protein level following acute IM ($p < 0.01$) (Fig. 2B, left panel), whereas acute C did not change this protein level, compared to the unstressed control. In chronically stressed animals, mitochondrial MnSOD protein level was not changed in a statistically significant manner ($p > 0.05$) compared to the unstressed control (Fig. 2B, middle panel). Additional acute stress of either IM or C showed a significant decrease in the mitochondrial MnSOD protein level in the chronic IS-pretreated group ($p < 0.01$, $p < 0.05$), relative to the unstressed control. The mitochondrial MnSOD protein levels following both combined stressors were significantly decreased from their levels after acute IM or C stressors, as indicated by Tukey post-hoc test ($^{\#\#\#}$ $p < 0.01$). For the cytosolic MnSOD protein levels in the prefrontal cortex, ANOVA analysis indicated that the main effect of chronic stress ($F_{1.30} = 27.89$, $p < 0.001$) exist in these animals. No significant differences were found in cytosolic MnSOD protein level between acute stressors and unstressed control ($p > 0.05$, Fig. 2B, left panel). A trend towards an increase in cytosolic MnSOD following chronic IS (Fig. 2B, middle panel) was found but it was not statistically significant ($p = 0.24$). Exposure to novel IM or C stress led to a significant increase in cytosolic MnSOD protein levels ($p < 0.05$) in the chronic IS-pretreated group, compared to the unstressed control (Fig. 2B, right panel). Statistically significant increase in cytosolic MnSOD protein level between combined IS+IM and acute IM stress was also observed ($^{\#\#}$ $p < 0.01$, Fig. 2B, right panel).

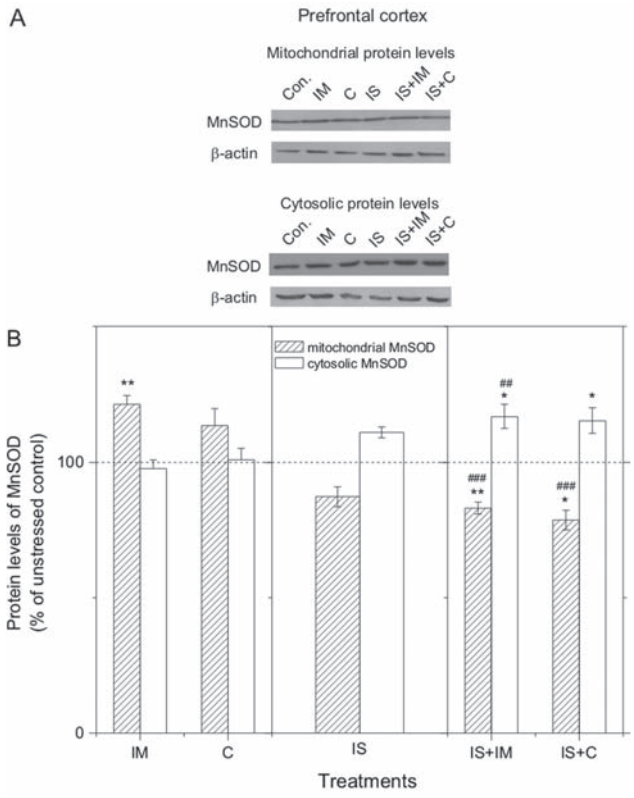

Figure 2. MnSOD protein level in mitochondrial or cytosolic fractions of the prefrontal cortex. **A.** Representative Western blots of MnSOD protein normalized to β-actin protein. **B.** Relative changes in MnSOD protein levels of rats exposed to acute immobilization (IM) or cold (C) stressors, chronic isolation (IS) or their combinations in both fractions, as indicated. The values are expressed as means ± S.E.M. of 6–8 animals. Symbols indicate a significant difference between: the respective stress treatment and unstressed control * $p < 0.05$, ** $p < 0.01$; combined stressors and those respective acute stressors $^{\#\#}$ $p < 0.01$, $^{\#\#\#}$ $p < 0.001$, by Tukey post-hoc test.

MnSOD protein levels in mitochondrial or cytosolic fractions of the hippocampus

The representative hippocampal Western blots of MnSOD protein level in unstressed control and stressed Wistar male rat groups are presented in Fig. 3A. Two-way ANOVA analysis of mitochondrial MnSOD protein levels revealed significant effect of chronic stress ($F_{1.30} = 17.66$, $p < 0.001$). Post-hoc Tukey analysis showed a significantly increase in mitochondrial MnSOD protein level following acute IM stress compared to the unstressed control ($p < 0.05$) (Fig. 3B, left panel), whereas acute C did not change the level of this protein ($p > 0.05$). In chronically stressed group, mitochondrial MnSOD protein level was unchanged compared to the unstressed control level ($p > 0.05$) (Fig. 3B, middle

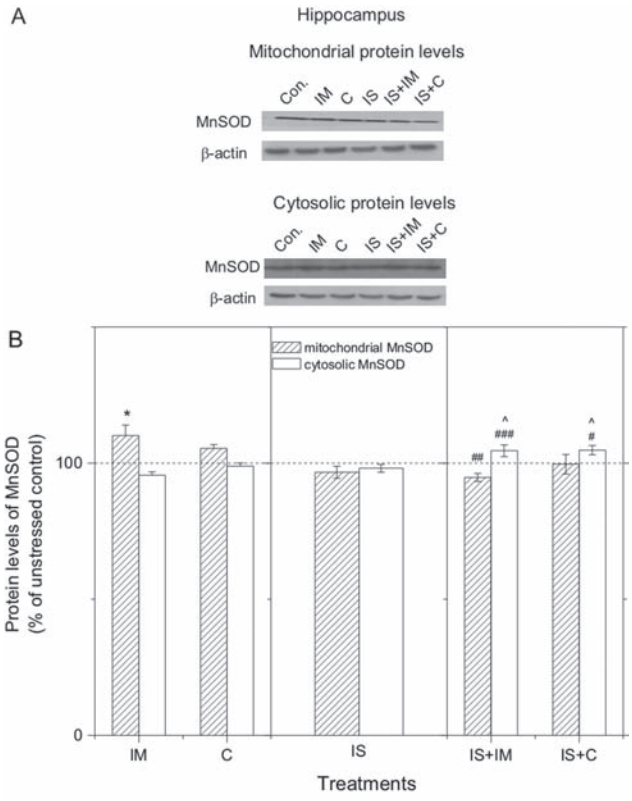

Figure 3. MnSOD protein level in mitochondrial or cytosolic fractions of the hippocampus. **A.** Representative Western blots of MnSOD protein normalized to β-actin protein. **B.** Relative changes in MnSOD protein levels of rats exposed to acute immobilization (IM) or cold (C) stressors, chronic isolation (IS) or their combinations in both fractions, as indicated. The values are expressed as means ± S.E.M. of 6–8 animals. Symbols indicate a significant difference between: acute immobilization (IM) and unstressed control * $p < 0.05$; combined stressors and those respective acute stressors $^{\#}$ $p < 0.05$, $^{\#\#}$ $p < 0.001$, $^{\#\#\#}$ $p < 0.001$; combined stressors and chronic isolation (IS) stress $^{\wedge}$ $p < 0.05$, by Tukey post-hoc test.

panel). In combined stress experiments, only IM led to decrease in the MnSOD protein level following IS compared to its level after acute IM stress ($^{\#\#}$ $p < 0.01$) (Fig. 3B, right panel). Similarly to the prefrontal cortex, we found presence of hippocampal MnSOD protein in the cytosolic fraction of unstressed control and all stressed groups (Fig. 3A). Two-way ANOVA analysis revealed significant interaction effects of acute × chronic stress ($F_{2.35} = 8.7$, $p < 0.01$). Post-hoc Tukey analysis showed a significant increase in cytosolic MnSOD level following both combined stressors (Fig. 3B, right panel) compared to either chronic IS ($^{\wedge}$ $p < 0.05$) or those acute stressors ($^{\#\#\#}$ $p < 0.001$, $^{\#}$ $p < 0.05$), respectively.

Western blots demonstrating release of mitochondrial cytochrome c

To confirm the absence of mitochondrial contamination in our preparations, the same membrane from mitochondrial and cytosolic samples was reprobed with anti-mouse cytochrome c oxidase subunit I (COX I; molecular probe 1 : 500), as the mitochondrial marker which is tightly bound to the inner mitochondrial membrane (Jin et al. 2005). The absence of COX I in the cytosolic fraction in unstressed control and all stressed groups of both brain structures confirmed that there was not contamination of mitochondria in the cytosolic fraction (Fig. 4).

As shown in Fig. 5, cytochrome c immunoreactivity was evident as a single band of molecular mass 15 kDa in the cytosolic fraction of all stressed groups of both brain structures, whereas it was barely detected in the unstressed control. The mitochondrial fractions of cytochrome c were also detected.

Discussion

This study compares the acute, chronic or combined stress models and determines the most effective stress model according to serum CORT level and subcellular distribution

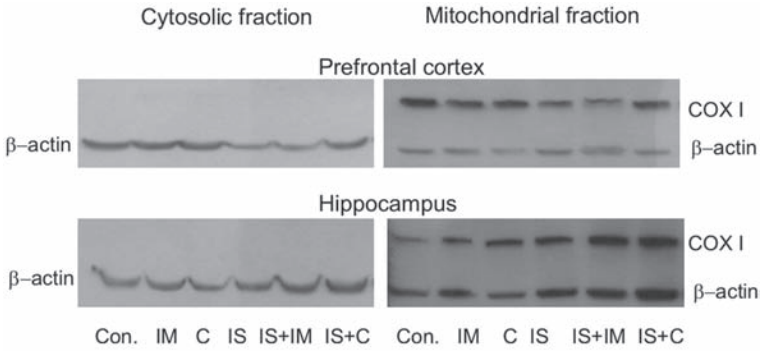

Figure 4. Cytochrome c oxidase subunit I (COX I) Western blots of mitochondrial or cytosolic fractions in unstressed control and all stressed groups from prefrontal cortex and hippocampus. β-actin was used as loading control. COX I was expressed in the mitochondrial fractions but not in the cytosolic fractions of both brain structures.

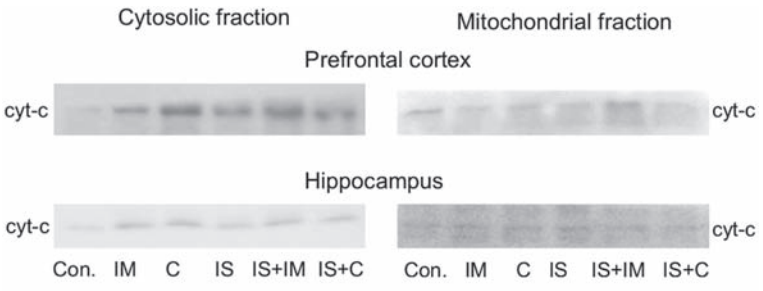

Figure 5. Cytochrome c (cyt-c) Western blots of mitochondrial and cytosolic fractions in unstressed control and all stressed groups from prefrontal cortex and hippocampus. cyt-c was detected in mitochondrial and cytosolic fractions in all stressed groups of both brain structures, whereas it was barely detected in unstressed control.

of MnSOD protein level in the prefrontal cortex and hippocampus. Western blot analysis of mitochondrial MnSOD protein level following acute IM stress showed up-regulation in both brain structures. The increased serum CORT level following both acute stressors is in accordance with previous studies (Dronjak et al. 2004; Sahin and Gümüşlü 2004) showing that serum CORT is important indicator of stress. IM as combined physical and emotional stress seems to be stronger stressor, while C is assumed to be a mild stressor, as judged by serum CORT level. Since the acute stress increases the production of ROS in the brain (McEwen 2001), increased mitochondrial MnSOD protein levels in both brain structures following acute IM are required to remove these high levels of ROS, generated under the high CORT level, and may reflect a protective response to oxidative stress, aiming to restore the cell homeostasis (Greenlund et al. 1995). Because MnSOD is localized in the inner membrane and matrix of mitochondria (Melov et al. 1999; Okado-Matsumoto and Fridovich 2001) we were surprised to find MnSOD protein level in the cytosolic fractions of unstressed control or both acute stressors of both brain structures. Absence of COX I from cytosolic fraction of unstressed control and all stressed groups showed that mitochondria fractionation procedure itself was not responsible for the release of mitochondrial MnSOD protein into the cytosolic compartment of brain (see Fig. 4). Since the MnSOD is encoded in the nuclear chromatin, synthesized as a precursor in the cytoplasm and transported to mitochondria *via* mitochondria targeting sequence, the presence MnSOD protein level in cytosolic fraction of unstressed control and following acute stressors in both brain structure, could be the results of identification of MnSOD protein that is in transit to the mitochondria after nuclear synthesis (Jin et al. 2005).

Opposite to the acute stressors, chronically stressed animals showed unchanged serum CORT level, relative to unstressed control, Furthermore, the effects of social IS on CORT level in the adult rats are not consistent among studies. Increased CORT level has been reported (Gamallo et al. 1986), whereas other groups observe no changes (Holson et al. 1991; Malkesman et al. 2006) or reduced CORT level (Sanchez et al. 1998). At the same time, chronic IS stress did not produce any significant changes in mitochondrial as well as in cytosolic MnSOD protein level of the prefrontal cortex and hippocampus, compared to the unstressed control. On the other hand, MnSOD activity data in response to the same acute or chronic stressor published by Pajović et al. (2006) were not followed by MnSOD protein expression data after either acute or chronic stressor determined in this study. The explanation for those discrepancies could be due to subcellular redistribution of the MnSOD protein in mitochondria and cytosol fraction of both brain structures examined in this study and its activity in whole extract of same brain structures performed by Pajović et al. (2006). Also, the MnSOD activity may be regulated at posttranslation level *via* phosphorylation or dephosphorylation independently of regulation of its protein synthesis (Hopper et al. 2006).

It has been shown that animals chronically exposed to a homotypic stressor display an exaggerated response of the HPA axis after exposure to heterotypic novel stressor (Marti et al. 1994; Bhatnagar and Dallman 1998). In our study, chronically isolated animals were also exposed to novel acute IM or C as heterotypic stressors. Since the chronic IS stress leads to the deregulation of glucocorticoid negative feedback mechanisms at the level of HPA axis in the prefrontal cortex and hippocampus of stressed rats (Sanchez et al. 1995; Filipović et al. 2005), novel acute stressors cannot generate appropriate answer to stimuli. This is represented by lower increase in serum CORT level than in acutely stressed animals. Our data are in agreement with the findings of Sanchez et al. (1998) who reported that 2 months of isolated rats also resulted in reduced plasma CORT concentration to 15 min of restrain stress, compared to the controls which were exposed to the acute restrain stress. Nevertheless, it is hard to say that it is a protective phenomenon, since altered activation of HPA axis is correlated with some major disorders (Tanke et al. 2008). Other possible explanation for lower

CORT levels is due to decreased secretion of corticotrophin releasing hormone that also occurs in long-term IS (Sancez et al. 1995). Moreover, novel acute IM stress produced a higher increase in serum CORT level of chronically isolated rats, comparing to the novel C stress, suggesting that response of the chronically stressed animals additionally exposed to novel acute stressors depend on the applied stress stimuli (Pacak and Palkovits 2001; Gavrilović and Dronjak 2005). At the same time, there was significant decrease in mitochondrial MnSOD protein levels in chronically stressed animals exposed to either IM or C in the prefrontal cortex, relative to the control or those levels after acute stressors, while in hippocampus it was observed only between chronic IS followed by IM and acute IM. Nevertheless, it may be claimed that our preparations reflect the average MnSOD protein changes in whole hippocampus, which could potentially mask MnSOD protein changes, and that detailed histochemical pictures would reflect protein expression more precisely. It could be speculate that chronic stress-induced changes in homeostatic mechanism could contribute to MnSOD protein inactivation by peroxynitrite (MacMillan-Crow et al. 1998; Yamakura et al. 1998; Knirsch and Clerch 2001; Filipović et al. 2007). Peroxynitrite-related MnSOD has been suggested to be related to the phosphorylation of superoxide dismutase binding proteins and to the induction of dityrosine formation and tyrosine oxidation in MnSOD. Accordingly, compromised mitochondrial MnSOD protein level could lead to the increased oxidant production within mitochondria, which could lead to nitration of other mitochondrial proteins (Madrigal et al. 2001; Cruthirds et al. 2003).

At the other side, a reciprocal increase in cytosolic MnSOD protein level between combined stressors and unstressed control in the prefrontal cortex, as well as between combined stressors and chronic or acute stressor in hippocampus, was shown. To assess whether presence of the MnSOD in the cytosol was a consequence of loss of mitochondrial membrane integrity under the combined stressors and mitochondrial MnSOD release into the cytosol, we used another mitochondrial marker, cytochrome c, to document mitochondrial damage (Jin et al. 2005). Therefore, the blots of mitochondrial/cytosolic fractions of the unstressed control and all stressed groups of prefrontal cortex and hippocampus were stripped of primary antibody and reprobed with the cytochrome c antibody. Like MnSOD, cytochrome c was observed in cytosol fraction following acute, chronic or combined stressors, whereas it was barely detected in unstressed control (Fujimura et al. 1999). It seems tempting to speculate that ROS generated under prolonged neuroendocrine stress could contribute to the release of cytochrome c to the cytosol after opening of the permeability transition pore (Yang and Cortopassi 1998; Cassarino et al. 1999; Petrosillo et al. 2001). This release may results in further ROS production by inhibition of the respiratory chain (Cai and Jones 1998). Taken together, increased cytosolic MnSOD protein level could be derived from mitochondrial MnSOD and/or inappropriate transport of newly synthesized MnSOD into mitochondria (changes in mitochondrial targeting domain). Regardless of the mechanism, the appearance of MnSOD in the cytosolic fraction clearly indicates a loss of mitochondrial membrane integrity (Cruthirds et al. 2003; Jin et al. 2005).

The results suggest that, different stress models have different degree in influences on serum CORT and MnSOD subcellular protein level in the prefrontal cortex and hippocampus. The increased mitochondrial MnSOD protein level following acute stress might reflect a protective response to increased oxidative stress. Chronic neuroendocrine stress compromises induction of mitochondrial MnSOD protein whereas its cytosolic localization is significantly increased following combined stressors. Release mitochondrial MnSOD as well as intermembrane protein cytochrome c into the cytosol could serve as biochemical markers for mitochondrial dysfunction. Moreover, mitochondrial MnSOD protein level could serve as index for discrimination of previous chronic stress exposure. The lack of MnSOD in mitochondria may lead to further biochemical cascade causing cytochrome c release (Fujimura et al. 1999), which is known to be apoptogenic (Liu et al. 1996). Further studies are necessary to clarify whether cytochrome c plays a role in inducing the mitochondrial-dependent apoptosis cascade in acute or chronic stressed rat brain.

Acknowledgement. This work was supported by the Ministry of Sciences of the Republic of Serbia, grant No. 143044B.

References

Antras-Ferry J., Mahéo K., Morel F., Guillouzo A., Cillard P., Cillard J. (1997): Dexamethasone differently modulates TNF-alpha- and IL-1beta-induced transcription of the hepatic Mn-superoxide dismutase gene. FEBS Lett. **403**, 100–104

Bhatnagar S., Dallman M. (1998): Neuroanatomical basis for facilitation of hypothalamic-pituitary-adrenal responses to a novel stressor after chronic stress. Neuroscience **84**, 1025–1039

Blumberg J. (2004): Use of biomarkers of oxidative stress in research studies. J. Nutr. **134**, 3188–3189

Cai J., Jones D. P. (1998): Superoxide in apoptosis. Mitochondrial generation triggered by cytochrome c loss. J. Biol. Chem. **273**, 11401–11404

Cassarino D. S., Parks J. K., Parker W. D. Jr., Bennett J. P. Jr. (1999): The parkinsonian neurotoxin MPP^+ opens the mitochondrial permeability transition pore and releases cytochrome c in isolated mitochondria via an oxidative mechanism. Biochim. Biophys. Acta **1453**, 49–62

Chong Z. Z., Li F., Maiese K. (2005): Oxidative stress in the brain: novel cellular targets that govern survival during neurodegenerative disease. Prog. Neurobiol. **75**, 207–246

Chourbaji S., Zacher C., Sanchis-Segura C., Spanagel R., Gass P. (2005): Social and structural housing conditions influence the development of a depressive-like phenotype in the learned helplessness paradigm in male mice. Behav. Brain Res. **164**, 100–106

Cruthirds D. L., Novak L., Akhi K. M., Sanders P. W., Thompson J. A., MacMillan-Crow L. A. (2003): Mitochondrial targets of oxidative stress during renal ischemia/reperfusion. Arch. Biochem. Biophys. **412**, 127–133

Dronjak S., Gavrilović Lj., Filipović D., Radojčić B. M. (2004): Immobilization and cold stress affect sympatho-adrenomedular system and pituitary-adrenocortical axis of rats exposed to long-term isolation and crowding. Physiol. Behav. **81**, 409–415

Evans M. D., Dizdaroglu M., Cooke M. S. (2004): Oxidative DNA damage and disease: induction, repair and significance. Mutat. Res. **567**, 1–61

Filipović D., Gavrilović Lj., Dronjak S., Radojčić B. M. (2005): Brain glucocorticoid receptor and heat shock protein 70 levels in rats exposed to acute, chronic or combined stress. Neuropsychobiology **51**, 107–114

Filipović M. R., Stanić D., Raicević S., Spasić M., Niketić V. (2007): Consequences of MnSOD interactions with nitric oxide: nitric oxide dismutation and the generation of peroxynitrite and hydrogen peroxide. Free Radic. Res. **41**, 62–72

Fujimura M., Morita-Fujimura Y., Kawase M., Copin J. C., Calagui B., Epstein C. J., Chan P. H. (1999): Manganese superoxide dismutase mediates the early release of mitochondrial cytochrome c and subsequent DNA fragmentation after permanent focal cerebral ischemia in mice. J. Neurosci. **19**, 3414–3422

Gamallo A., Villanua A., Trancho G., Fraile A. (1986): Stress adaptation and adrenal activity in isolated and crowded rats. Physiol. Behav. **36**, 217–221

Garzon J., del Rio J. (1981): Hyperactivity induced in rats by long-term isolation: further studies on a new animal model for the detection of antidepressants. Eur. J. Pharmacol. **74**, 287–294

Gavrilović L., Dronjak S. (2005): Activation of rat pituitary-adrenocortical and sympatho-adrenomedullary system in response to different stressors. Neuro Endocrinol. Lett. **26**, 515–520

Greenlund J., Deckwerth L., Johnson M. Jr. (1995): Superoxide dismutase delays neuronal apoptosis: a role for reactive oxygen species in programmed neuronal death. Neuron **14**, 303–315

Haller J., Halasz J. (1999): Mild social stress abolishes the effects of isolation on anxiety and chlordiazepoxide reactivity. Psychopharmacology (Berl.) **144**, 311–315

Holson R. R., Scallet A. C., Turner B. B. (1991): Isolation stress revisited: isolation-rearing effects depend on animal care methods. Physiol. Behav. **49**, 1107–1118

Hopper R. K., Carroll S., Aponte A. M., Johnson D. T., French S., Shen R. F., Witzmann F. A., Harris R. A., Balaban R. S. (2006): Mitochondrial matrix phosphoproteome: effect of extra mitochondrial calcium. Biochemistry **45**, 2524–2536

Jacobson L., Sapolsky R. (1991): The role of the hippocampus in feedback regulation of hypothalamic-pituitary-adrenocortical axis. Endocr. Rev. **12**, 118–134

Jin Z. Q., Zhou H. Z., Cecchini G., Gray M. O., Karliner J. S. (2005): MnSOD in mouse heart: acute responses to ischemic preconditioning and ischemia-reperfusion injury. Am. J. Physiol., Heart Circ. Physiol. **288**, 2986–2994

Keller J. N., Kindy M. S., Holtsberg F. W., St. Clair D. K., Yen H.-C., Germeyer A., Steiner S. M., Bruce-Keller A. J., Hutchins J. B., Mattson M. P. (1998): Mitochondrial manganese superoxide dismutase prevents neural apoptosis and reduces ischemic brain injury: suppression of peroxynitrite production, lipid peroxidation, and mitochondrial dysfunction. J. Neurosci. **18**, 687–697

Knirsch L., Clerch L. B. (2001): Tyrosine phosphorylation regulates manganese superoxide dismutase (MnSOD) RNA-binding protein activity and MnSOD protein expression. Biochemistry **40**, 7890–7895

Kvetnansky R., Mikulaj L. (1970): Adrenal and urinary catecholamines in rat during adaptation to repeated immobilization stress. Endocrinology **87**, 738–743

Le Bras M., Clément M. V., Pervaiz S., Brenner C. (2005): Reactive oxygen species and the mitochondrial signaling pathway of cell death. Histol. Histopathol. **20**, 205–219

Lebovitz R. M., Zhang H., Vogel H., Cartwright J. Jr., Dionne L., Lu N., Huang S., Matzuk M. M. (1996): Neurodegeneration, myocardial injury, and perinatal death in mitochondrial superoxide dismutase-deficient mice. Proc. Natl. Acad. Sci. U.S.A. **93**, 9782–9787

Liu J., Wang X., Shigenaga M. K., Yeo H. C., Mori A., Ames B. N. (1996): Immobilization stress causes oxidative damage to lipid, protein, and DNA in the brain of rats. FASEB J. **10**, 1532–1538

Liu X., Kim C. N., Yang J., Jemmerson R., Wang X. (1996): Induction of apoptotic program in cell-free extracts: requirement for dATP and cytochrome c. Cell **86**, 147–157

Lowry O. H., Rosebrough N. J., Farr A. J., Randall R. J. (1951): Protein measurement with the Folin phenol reagent. J. Biol. Chem. **123**, 265–275

MacMillan-Crow L. A., Crow J. P., Thompson J. A. (1998): Peroxynitrite-mediated inactivation of manganese superoxide dismutase involves nitration and oxidation of critical tyrosine residues. Biochemistry **37**, 1613–1622

Madrigal J. L., Olivenza R., Moro M. A., Lizasoain I., Lorenzo P., Rodrigo J., Leza J. C. (2001): Glutathione depletion, lipid peroxidation and mitochondrial dysfunction are induced by chronic stress in rat brain. Neuropsychopharmacology **24**, 420–429

Maisonnette S., Morato S., Brandão M. L. (1993): Role of resocialization and of 5-HT1A receptor activation on the anxiogenic effects induced by isolation in the elevated plus-maze test. Physiol. Behav. **54**, 753–758

Malkesman O., Maayan R., Weizman A., Weller A. (2006): Aggressive behavior and HPA axis hormones after social isolation in adult rats of two different genetic animal models for depression. Behav. Brain Res. **175**, 408–414

Marti O., Gavalda A., Gomez F., Armario A. (1994): Direct evidence for chronic stress-induced facilitation of the

adrenocorticotropin response to a novel acute stressor. Neuroendocrinology **60**, 1–7

McEwen B. S. (2001): Plasticity of the hippocampus: adaptation to chronic stress and allostatic load. Ann. N. Y. Acad. Sci. **933**, 265–277

McIntosh L. J., Hong K. E., Sapolsky R. M. (1998a): Glucocorticoids may alter antoxidant enzyme capacity in the brain: baseline studies. Brain Res. **791**, 209–214

McIntosh L. J., Cortopassi K. M., Sapolsky R. M. (1998b): Glucocorticoids may alter antioxidant enzyme capacity in the brain: kainic acid studies. Brain Res. **791**, 215–222

Melov S., Coskun P., Patel M., Tuinstra R., Cottrell B., Jun A. S., Zastawny T. H., Dizdaroglu M., Goodman S. I., Huang T. T., Miziorko H., Epstein C. J., Wallace D. C. (1999): Mitochondrial disease in superoxide dismutase 2 mutant mice. Proc. Natl. Acad. Sci. U.S.A. **96**, 846–851

Michel T. M., Frangou S., Thiemeyer D., Camara S., Jecel J., Nara K., Brunklaus A., Zoechling R., Riederer P. (2007): Evidence for oxidative stress in the frontal cortex in patients with recurrent depressive disorder – a postmortem study. Psychiatry Res. **151**, 145–150

Mizoguchi K., Ishige A., Aburada M., Tabira T. (2003): Chronic stress attenuates glucocorticoid negative feedback: involvement of the prefrontal cortex and hippocampus. Neuroscience **119**, 887–897

Niesink R. J., Van Ree J. M. (1982): Antidepressant drugs normalize the increased social behaviour of pairs of male rats induced by short term isolation. Neuropharmacology **21**, 1343–1348

Okado-Matsumoto A., Fridovich I. (2001): Subcellular distribution of superoxide dismutases (SOD) in rat liver: Cu,Zn-SOD in mitochondria. J. Biol. Chem. **276**, 38388–38393

Olivenza R., Moro M. A., Lizasoain I., Lorenzo P., Fernández A. P., Rodrigo J., Bosca L., Leza J. C. (2000): Chronic stress induces the expression of inducible nitric oxide synthase in rat brain cortex. J. Neurochem. **74**, 785–791

Pacak K., Palkovits M. (2001): Stressor specificity of central neuroendocrine responses: implications for stress-related disorders. Endocr. Rev. **22**, 502–548

Pajović S. B., Pejić S., Stojiljković V., Gavrilović Lj., Dronjak S., Kanazir D. T. (2006): Alterations in hippocampal antioxidant enzyme activities and sympatho adrenomedullary system of rats in response to different stress models. Physiol. Res. **55**, 453–460

Pardon M. C. (2007): Stress and ageing interactions: a paradox in the context of shared etiological and physiopathological processes. Brain Res. Rev. **54**, 251–273

Petrosillo G., Ruggiero F. M., Pistolese M., Paradies G. (2001): Reactive oxygen species generated from the mitochondrial electron transport chain induce cytochrome c dissociation from beef-heart submitochondrial particles *via* cardiolipin peroxidation. Possible role in the apoptosis. FEBS Lett. **509**, 435–458

Popović M., Popović N., Erić-Jovicić M., Jovanova-Nesić K. (2000): Immune responses in nucleus basalis magnocellularis-lesioned rats exposed to chronic isolation stress. Int. J. Neuroscience **100**, 125–131

Sahin E., Gümüşlü S. (2004): Alterations in brain antioxidant status, protein oxidation and lipid peroxidation in response to different stress models. Behav. Brain Res. **155**, 241–248

Sanchez M. M., Aguado F., Sanchez-Toscano F., Saphier D. (1995): Effects of prolonged social isolation on responses of neurons in the bed nucleus of the stria terminalis, preoptic area, and hypothalamic paraventricular nucleus to stimulation of the medial amygdala. Psychoneuroendocrinology **20**, 525–541

Sanchez M., Aguado F., Sanchez-Toscano F., Saphier D. (1998): Neuroendocrine and immunocytochemical demonstrations of decreased hypothalamo-pituitary-adrenal axis responsiveness to restraint stress after long-term social isolation. Endocrinology **139**, 579–587

Sapolsky R. M. (1992): An introduction to the adrenocortical axis. In: Stress, the Aging Brain, and the Mechanisms of Neuron Death. Bradford. pp. 11–27, MIT Press, Cambridge

Sarandol A., Sarandol E., Eker S. S., Erdinc S., Vatansever E., Kirli S.(2007): Major depressive disorder is accompanied with oxidative stress: short-term antidepressant treatment does not alter oxidative-antioxidative systems. Hum. Psychopharmacol. **22**, 67–73

Slot J. W., Geuze H. J., Freeman B. A., Crapo J. D. (1986): Intracellular localization of the copper-zinc and manganese superoxide dismutases in rat liver parenchymal cells. Lab. Invest. **55**, 363–371

Tanke M. A., Fokkema D. S., Doornbos B., Postema F., Korf J. (2008): Sustained release of corticosterone in rats affects reactivity, but does not affect habituation to immobilization and acoustic stimuli. Life Sci. **83**, 135–141

Turrens J. F. (1997): Superoxide production by the mitochondrial respiratory chain. Biosci. Rep. **17**, 3–8

Valentine J. F., Nick H. S. (1994): Glucocorticoids repress basal and stimulated manganese superoxide dismutase levels in rat intestinal epithelial cells. Gastroenterology **107**, 1662–1670

Wallace D. C. (2005): A mitochondrial paradigm of metabolic and degenerative diseases, aging, and cancer: a dawn for evolutionary medicine. Annu. Rev. Genet. **39**, 359–407

Wispe J. R., Clark J. C., Burhans M. S., Kropp K. E., Korfhagen T. R., Whitsett J. A. (1989): Synthesis and processing of the precursor for human mangano-superoxide dismutase. Biochim. Biophys. Acta **994**, 30–36

Yamakura F., Taka H., Fujimura T., Murayama K. (1998): Inactivation of human manganese-superoxide dismutase by peroxynitrite is caused by exclusive nitration of tyrosine 34 to 3-nitrotyrosine. J. Biol. Chem. **273**, 14085–14089

Yang J. C., Cortopassi G. A. (1998): Induction of the mitochondrial permeability transition causes release of the apoptogenic factor cytochrome c. Free Radic. Biol. Med. **24**, 624–631

Regional changes in ectonucleotidase activity after cortical stab injury in rat

Ivana Bjelobaba[1], Mirjana Stojiljkovic[1,2], Irena Lavrnja[1], Danijela Stojkov[1], Sanja Pekovic[1], Sanja Dacic[2], Danijela Laketa[2], Ljubisav Rakic[3] and Nadezda Nedeljkovic[2]

[1] *Department for Neurobiology and Immunology, Institute for Biological Research "Siniša Stanković", Belgrade, Serbia*
[2] *Institute for Physiology and Biochemistry, Faculty of Biology, University Belgrade, Serbia*
[3] *Serbian Academy of Sciences and Arts, Serbia*

Abstract. During a variety of insults to the brain adenine nucleotides are released in large quantities from damaged cells, triggering local cellular and biochemical responses to injury. Different models of brain injury reveal that the local increase in adenine nucleotides levels is followed by a compensatory up-regulation of ectonucleotidase enzymes that catalyze sequential hydrolysis of ATP to ADP, AMP and adenosine. However, recent studies imply that changes in adenine nucleotides release may also occur in the areas distant from the site of direct damage. Therefore, in the present study we have used the model of cortical stab injury to analyze extracellular ATP, ADP and AMP hydrolysis in the membrane preparations obtained from the brain regions that were not subjected to direct tissue damage. The brain regions analyzed were contralateral cortex, hippocampus, caudate nucleus, thalamus and hypothalamus. It was evidenced that cortical stab injury induced early widespread decrease in AMP hydrolysis in all brain areas tested, except in the hypothalamus, without changes in ATP hydrolysis. These findings imply that brain injury affects global extracellular adenine nucleotide and nucleoside levels, consequently affecting neuronal function in the regions distant to the primary damage.

Key words: Ectonucleotidase — Ecto-5'-nucleotidase — ATP — AMP — Adenosine — Stab injury — Brain — Rat

Introduction

Brain injury induces release of wide variety of mediators that influence local cellular and biochemical responses to injury. One such mediator is ATP which is massively released from damaged cells reaching high concentration in the extracellular space (Juranyi et al. 1999; Melani et al. 2005; Franke et al. 2006). By acting at specific purinergic P2 receptors, ATP exhibits both tissue protective (Rathbone et al. 1992b; Franke et al. 1999; Davalos et al. 2005) and destructive effects (Volonte et al. 1999; Amadio et al. 2002; Franke et al. 2006). Differential effects of ATP are likely mediated by the levels of ligand produced and the specific pattern of P2 receptors expression on target cells.

Correspondence to: Nadezda Nedeljkovic, Institute for Physiology and Biochemistry, Faculty of Biology, University Belgrade, Studentski trg 3, 11001 Belgrade, Serbia
E-mail: nnedel@bio.bg.ac.rs

Cellular responses induced by extracellular ATP are terminated by the action of ectonucleotidase enzymes. E-NTPDases (ecto-nucleotide triphospho-diphosphohydrolases; CD39), degrade ATP to ADP or directly to AMP, whereas ecto-5'-nucleotidase (CD73) converts AMP to adenosine (Zimmermann 2000). Adenosine is potent neuromodulator and neurotransmitter, acting at its own G-protein coupled P1 receptor family (Ralevic and Burnstock 1998) and eliciting diverse effects on neuronal excitability and neurotransmitter release (Jacobson et al. 1999).

It is well known that brain injury and massive ATP release induce compensatory up-regulation of ectonucleotidase enzymes. Up-regulation of ectonucleotidase activities in damaged tissue was reported in different models of epilepsy (Nagy et al. 1997; Bonan et al. 2000a,b) and ischemia (Braun et al. 1998; Villa et al. 2002). We have recently described temporal changes in ectonucleotidase activities in the damaged tissue in the model of cortical stab injury (CSI). In the model, ATP hydrolysis catalyzed by E-NTPDase was significantly

up-regulated 14 days after the injury (Nedeljkovic et al. 2006), whereas AMP hydrolysis, catalyzed by ecto-5'-nucleotidase changed in a biphasic manner, with an immediate early decrease that lasted four hours after the injury (Nedeljkovic et al. 2008), followed by a prominent increase, that persisted two weeks after the injury (Nedeljkovic et al. 2006).

Results of recent studies imply that brain injury induces global changes in brain energy metabolism, which first results in loss of ionic gradients with consequent depolarization. Under these conditions there is depletion of intracellular ATP content (Manville et al. 2007), that could be due to either intracellular degradation of ATP (Latini and Pedata 2001) or its release to the extracellular space (Melani et al. 2005). Therefore in the present study we have used the model of CSI to analyze extracellular ATP and AMP hydrolysis in the distant brain regions that were not directly affected by tissue damage.

Materials and Methods

Animals

The study was performed on 3-month-old male rats of the Wistar strain (250–350 g body weight at the time of surgery). Animals were subjected to 12-h light/dark cycle, housed 3/cage, with free access to food and water.

Surgery

All animals were treated in accordance with the principles from Guide for Care and Use of Laboratory Animals, NIH publication No. 85-23 and the protocols were approved by the Belgrade University Animal Care and Use Committee.

Animals were anesthetized with diethyl ether and placed in a stereotaxic frame. Scalp was shaven and incision was made along the midline of the scalp to expose bregma. CSI was performed as previously described (Nedeljkovic et al. 2006, 2008). In order to assess the effect of diethyl ether anesthesia on ectonucleotidase activity, another set of animals was submitted to the same procedure under the anesthesia except inflicting the stab injury (sham-operated animals, $n = 4$). Animals of both groups were placed in heated room and monitored while recovering from anesthesia. At 4 and 24 h after sham-operation or CSI, the animals were decapitated (Harvard apparatus) and brains were removed for immediate plasma membrane preparation. Intact age-matched animals ($n = 4$) were also processed as intact controls.

Plasma membrane preparation

After decapitation, brains were removed and the right (contralateral) cortices, hippocampi, caudate nuclei, thalami and hypothalami from each group were dissected and pooled for a preparation of plasma membranes. The preparation was obtained essentially following the procedure of Gray and Whittaker (1962) as previously described Nedeljkovic et al. (1998). Protein content was determined by the method prevously descibed by Markwell et al. (1978) and samples were kept on –70°C until use.

Enzyme assays

All enzyme activity assays were performed as described previously (Nedeljkovic et al. 2006) under the conditions of initial velocity and substrate saturation. The reaction medium used to assay ATP hydrolysis contained (in mmol/l): 50 Tris-HCl buffer (pH 7.4), 0.5 EDTA, 5 $MgCl_2$ in the final volume of 200 µl. The reaction medium used to assay ecto-5'-nucleotidase activity contained (in mmol/l): 100 Tris-HCl buffer (pH 7.4), 10 $MgCl_2$ in the final volume of 200 µl. Membrane preparations (20 µg of proteins for ATP hydrolysis and 50 µg for AMP hydrolysis) were added to the reaction mixture, pre-incubated for 10 min and incubated for 15 min (ATP hydrolysis) or 30 min (AMP hydrolysis) at 37°C. The reaction was initiated by the addition of ATP or AMP to a final concentration of 1.0 mmol and stopped by the addition of 20 µl of 3 mol/l perchloric acid. The samples were chilled on ice and were taken for the assay of released inorganic phosphate (Pi) (Pennial 1966).

Data analysis

The data obtained for ectonucleotidase activities were expressed as mean specific activities (nmol Pi/mg protein/min) ± S.E.M from $n \geq 3$ independent determinations performed in duplicate. Statistical evaluation was carried out using one-way ANOVA (Origin 7.0 software package). The value $p < 0.05$ was considered statistically significant.

Results

The aim of the present study was to analyze ATP and AMP hydrolysis in distant brain regions that were not subjected to direct brain damage. We used the model in which CSI was inflicted to the left cerebral cortex, whereas ATP and AMP hydrolysis were analyzed in the membrane preparations obtained from the contralateral cortex (Ctx), hippocampus (Hip), caudate nucleus (CN), thalamus (Th) and hypothalamus (HT), 4 and 24 h following injury.

Figure 1 present regional levels of ATP hydrolysis 4 and 24 h after the surgery. In all brain regions analyzed, sham operation did not affect ATP hydrolysis over the time. In the CSI group, the level of ATP hydrolysis remained unchanged over time in respect to both sham-operated and intact control animals.

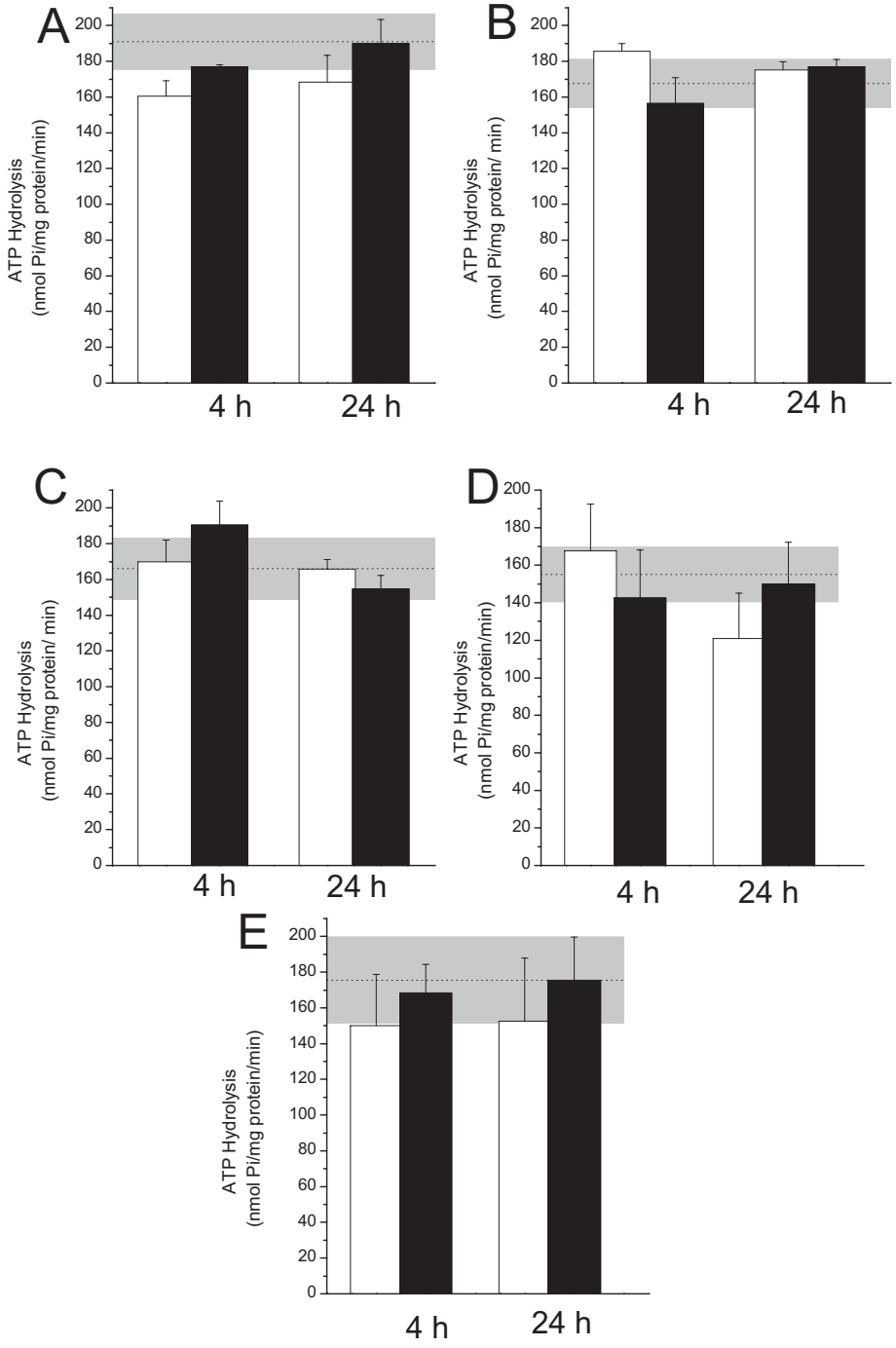

Figure 1. ATP hydrolysis (nmol Pi/mg/min) ±SEM in the plasma membrane preparations obtained from the contralateral cortex (A), hippocampus (B), caudate nucleus (C), thalamus (D) and hypothalamus (E), in sham animals (white bars) and animals submitted to CSI (black bars) 4 and 24 h after the surgery. Dot lines indicate level of ATP hydrolysis in intact control animals ±SEM (gray areas).

Figure 2 represents regional changes in AMP hydrolysis, 4 and 24 h after the sham surgery or CSI. In all brain regions analyzed, AMP hydrolysis was comparable in sham animals and in the intact controls. However, CSI induced significant decrease in AMP hydrolysis 4 h after the injury in Ctx (46.3 ± 8.7%, $p < 0.001$), Hip (27.9 ± 7.8%, $p < 0.05$) and CN (19.0 ± 6.2%, $p < 0.05$). Levels of AMP hydrolysis remained unchanged in the Th and HT.

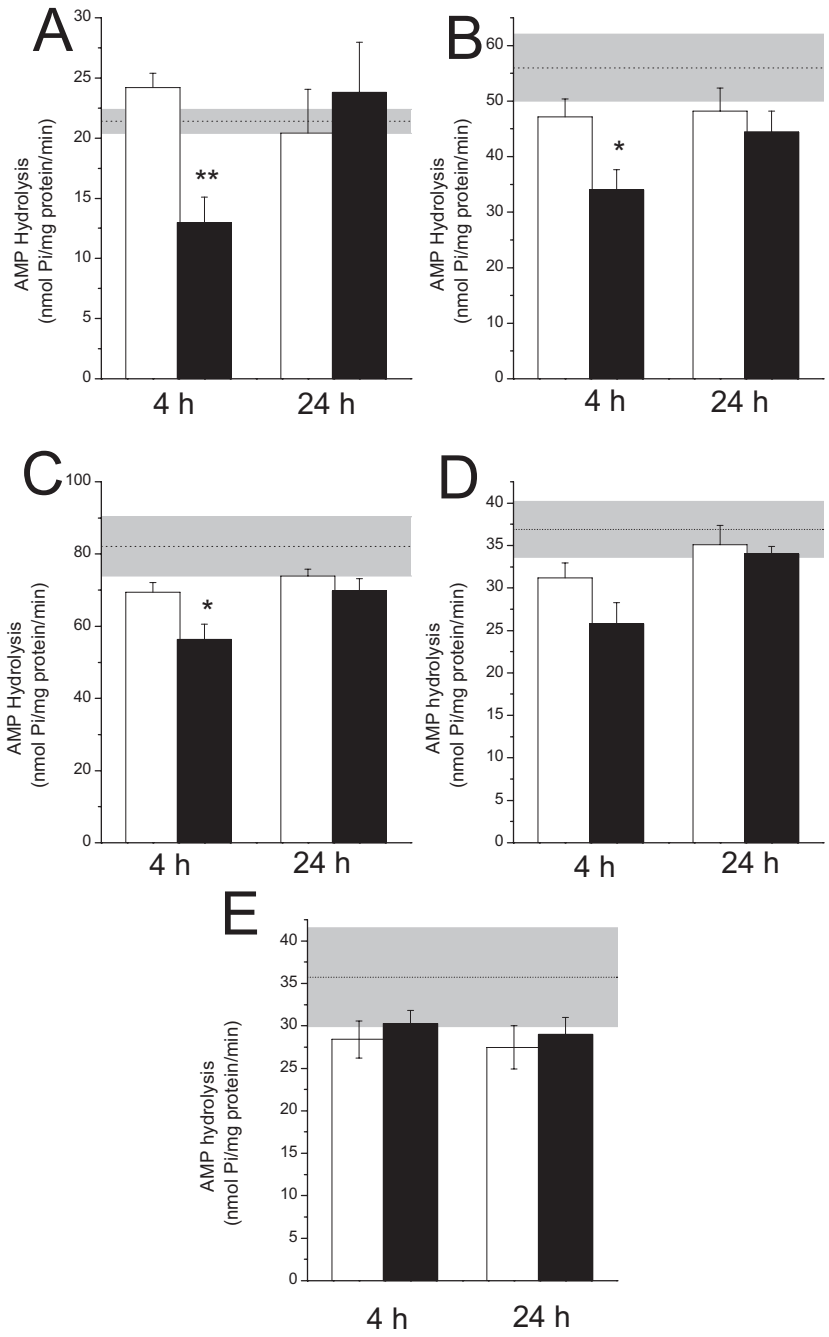

Figure 2. AMP hydrolysis (nmol Pi/mg/min) ±SEM in the plasma membrane preparations obtained from the contralateral cortex (A), hippocampus (B), caudate nucleus (C), thalamus (D) and hypothalamus (E), in sham animals (white bars) and animals submitted to CSI (black bars), 4 and 24 h after the surgery. Dot lines indicate level of AMP hydrolysis in intact control animals ±SEM (gray areas). Different from sham-operated animals, * $p < 0.05$, ** $p < 0.001$.

Discussion

It is well known that ATP induce numerous responses to injury, including early proliferation of microglia (Rathbone et al. 1992a), astrocytes (Hindley et al. 1994) and vascular endothelial cells (Rathbone et al. 1992c). Ectonucleotidase enzymes serve to terminate actions of extracellular ATP and cytotoxic effects of its massive accumulation (Volonte et al. 1999). Our previous studies scrutinized temporal changes in ectonucleotidase activities at the site of primary tissue

damage (Nedeljkovic et al. 2006, 2008). In the present study we have evaluated changes in the ectonucleotidase activities in distant cortical and subcortical brain areas in the same CSI model.

In order to isolate the effect of CSI from the effects of stress induced by anesthesia and surgical procedure, we first evaluated ATP and AMP hydrolysis in the group of animals subjected to sham operation. Results have shown that sham operation remained without effect on ATP and AMP hydrolysis in all brain regions tested.

The main finding of our study is that CSI induces early widespread decrease in AMP hydrolysis without changes in ATP hydrolysis in the cortical and subcortical regions distant to the site of direct damage. We shall discuss each in turn, along with the potential significance of altered extracellular adenine nucleotides metabolism in distant areas following injury.

Extracellular ATP is degraded by the action of several enzyme families, including E-NTPDases and ectonucleotide pyrophosphatase/phosphodiesterases, which have widespread and overlapping distribution in the rat brain (Nedeljkovic et al. 2003; Bjelobaba et al. 2006, 2007). We have previously reported that CSI induced significant up-regulation of whole enzyme chain for the extracellular hydrolysis of adenine nucleotides in remote brain areas, the effect that was observed two weeks after the injury (Nedeljkovic et al. 2006). Present study, however, revealed that during first 24 h period, CSI did not alter extracellular ATP hydrolysis, suggesting that the enzymes that hydrolyze extracellular ATP in distant regions were not affected by cortical injury.

The activity of ectonucleotidase enzymes primarily depends on the availability of their respective substrates. Extracellular ATP is thought to be released from damaged cells, reaching high concentration in the extracellular space. Accordingly, direct release of ATP in different models of brain injury has been demonstrated *in vitro* (Juranyi et al. 1999) and *in vivo* (Melani et al. 2005; Franke et al. 2006; Frenguelli et al. 2007). In the model of CSI, Franke and coworkers (2006) demonstrated immediate increase in extracellular ATP at the site of injury, which returned to its basal level within 30 min. However, the issue of extracellular ATP release in brain areas distant from the site of primary damage has not been directly examined, but our resuts revealed unaltered ATP hydrolysis during 24 h period after CSI.

On the other hand, our study revealed that CSI induced global reduction of AMP hydrolysis 4 h after the injury. Extracellular AMP hydrolysis is catalyzed by ecto-5'-nucleotidase, the enzyme widely expressed on the outer surface of different cell types throughout the brain (Bjelobaba et al. 2007; Langer et al. 2008). Observed decrease in AMP hydrolysis therefore could be linked to either decrease in ecto-5'-nucleotidase catalytic efficiency or reduction in its cell surface expression. It is known that ecto-5'-nucleotidase is competitively inhibited by extracellular ATP and ADP with K_i in the low micromolar range or below (Zimmermann 1996; Cunha 2001). However, if ATP hydrolysis sustains the basal level in distant areas following injury, as our result revealed, than catalytic inhibition of ecto-5'-nucleotidase by high ATP/ADP levels seems unlikely. Another explanation could be that injury induces secondary events in distant regions that lead to changes in the enzyme surface expression. However, since decrease in AMP hydrolysis was observed 4 h after the injury and dissapeared 24 h after the injury, transcriptional or translational down-regulation are unlikely to play a role. However, rapid time scale of the observed changes does imply another mechanism that modulates enzyme surface expression. Namely, ecto-5'-nucleotidase is a glycosylphosphatidylinositol anchored enzyme, that can be cleaved off the membrane by the action of intracellular phosphatidylinositol-specific phospholipase C (PI-PLC; Lehto and Sharom 1998, 2002). Although PI-PLC-mediated cleavage of ecto-5'-nucleotidase was evidenced in vascular endothelial cells (Kalsi et al. 2002), it remains to be seen whether the same mechanism is responsible for decrease in AMP hydrolysis in remote brain areas after CSI.

Since ectonucleotidases acts synergistically in the control of extracellular adenine nucleotides, the finding that CSI induces differential effects on ATP and AMP hydrolysis in remote areas suggests that injury alters extracellular adenine nucleotides levels and extent of their respective receptor activation. Reduction of ecto-5'-nucleotidase activity also imply accumulation of AMP in the extracellular space. This certainly affects neuronal environment, as AMP, in addition to ATP and adenosine, affects synaptic transmission and neuronal excitability (Schoen and Kreutzberg 1994). It is also noteworthy that priming P2X7 receptors, a subtype of ATP-gated receptor channel, with a very low ATP concentrations, induces dramatic increase in receptor's sensitivity to AMP (Chakfe et al. 2002) and release of interleukin-1 and TNF-α (Hide et al. 2000) from microglial cells. It was also suggested that P2X7 can even permeate AMP that could elevate intracellular AMP/ATP ratio (Menze et al. 2005). Recent discoveries suggest that increase in AMP/ATP ratio activates AMP-activated protein kinase, that is part of an ultrasensitive system, a "fuel gauge" for monitoring cellular energy stores (Hardie et al. 1999).

In summary, CSI induces early depression of AMP hydrolysis catalyzed by ecto-5'-nucleotidase without changes in ATP hydrolysis in remote cortical and subcortical areas. Implications of such alteration on neuronal function are likely to depend upon the ratio between ATP, ADP, AMP and adenosine and beneficial and damaging cellular cascades initiated by them. Since ATP and adenosine exert potent and generally opposing actions on neuronal activity and survival after injury, understanding how to tip

the balance in favor of the benefit could have clinical, as well as therapeutic importance in the treatment of brain injuries.

Acknowledgement. This study was supported by Serbian Ministry of Science and Technological Development, project No. 143005.

References

Amadio S. D. A. N., Cavaliere F., Murra B., Sancesario G., Bernardi G., Burnstock G., Volonte C. (2002): P2 receptor modulation and cytotoxic function in cultured CNS neurones. Neuropharmacology **42,** 489–501

Bjelobaba I., Nedeljkovic N., Subasic S., Lavrnja I., Pekovic S., Stojkov D., Rakic L., Stojiljkovic M. (2006): Immunolocalization of ecto-nucleotide pyrophosphatase/phosphodiesterase 1 (NPP1) in the rat forebrain. Brain Res. **1120,** 54–63

Bjelobaba I., Stojiljkovic M., Pekovic S., Dacic S., Lavrnja I., Stojkov D., Rakic L., Nedeljkovic N. (2007): Immunohistological determination of ecto-nucleoside triphosphate diphosphohydrolase 1 (NTPDase1) and 5'-nucleotidase in rat hippocampus reveals overlapping distribution. Cell. Mol. Neurobiol. **27,** 731–743

Bonan C. D., Amaral O. B., Rockenbach I. C., Walz R., Battastini A. M., Izquierdo I., Sarkis J. J. (2000a): Altered ATP hydrolysis induced by pentylenetetrazol kindling in rat brain synaptosomes. Neurochem. Res. **25,** 775–779

Bonan C. D., Walz R., Pereira G. S., Worm P. V., Battastini A. M., Cavalheiro E. A., Izquierdo I., Sarkis J. J. (2000b): Changes in synaptosomal ectonucleotidase activities in two rat models of temporal lobe epilepsy. Epilepsy Res. **39,** 229–238

Braun N., Zhu Y., Krieglstein J., Culmsee C., Zimmermann H. (1998): Upregulation of the enzyme chain hydrolyzing extracellular ATP after transient forebrain ischemia in the rat. J. Neurosci. **18,** 4891–4900

Chakfe Y., Seguin R., Antel J. P., Morissette C., Malo D., Henderson D., Seguela P. (2002): ADP and AMP induce interleukin-1-beta release from microglial cells through activation of ATP-primed P2X7 receptor channels. J. Neurosci. **22,** 3061–3069

Cunha R. A. (2001): Regulation of the ecto-nucleotidase pathway in rat hippocampal nerve terminals. Neurochem. Res. **26,** 979–991

Davalos D., Grutzendler J., Yang G., Kim J. V., Zuo Y., Jung S., Littman D. R., Dustin M. L., Gan W. B. (2005): ATP mediates rapid microglial response to local brain injury *in vivo*. Nat. Neurosci. **8,** 752–758

Franke H., Krugel U., Illes P. (1999): P2 receptor-mediated proliferative effects on astrocytes *in vivo*. Glia **28,** 190–200

Franke H., Grummich B., Härtig W., Grosche J., Regenthal R., Edwards R. H., Illes P., Krügel U. (2006): Changes in purinergic signaling after cerebral injury-involvement of glutamatergic mechanisms? Int. J. Dev. Neurosci. **24,** 123–132

Frenguelli B. G., Wigmore G., Llaudet E., Dale N. (2007): Temporal and mechanistic dissociation of ATP and adenosine release during ischaemia in the mammalian hippocampus. J. Neurochem. **101,** 1400–1413

Gray E. G., Whittaker V. P. (1962): The isolation of nerve endings from brain: an electron-microscopic study of cell fragments derived by homogenization and centrifugation. J. Anat. **96,** 79–88

Hardie D. G., Salt I. P., Hawley S. A., Davies S. P. (1999): AMP-activated protein kinase: an ultrasensitive system for monitoring cellular energy charge. Biochem. J. **338,** 717–722

Hide I., Tanaka M., Inoue A., Nakajima K., Kohsaka S., Inoue K., Nakata Y. (2000): Extracellular ATP triggers tumor necrosis factor-alpha release from rat microglia. J. Neurochem. **75,** 965–972

Hindley S., Herman M. A., Rathbone M. P. (1994): Stimulation of reactive astrogliosis in vivo by extracellular adenosine diphosphate or an adenosine A2 receptor agonist. J. Neurosci. Res. **38,** 399–406

Jacobson K. A., Hoffmann C., Cattabeni F., Abbracchio M. P. (1999): Adenosine-induced cell death: evidence for receptor-mediated signalling. Apoptosis **4,** 197–211

Juranyi Z., Sperlagh B., Vizi E. S. (1999): Involvement of P2 purinoceptors and the nitric oxide pathway in [3H] purine outflow evoked by short-term hypoxia and hypoglycemia in rat hippocampal slices. Brain Res. **823,** 183–190

Kalsi K., Lawson C., Dominguez M., Taylor P., Yacoub M. H., Smolenski R. T. (2002): Regulation of ecto-5'-nucleotidase by TNF-alpha in human endothelial cells. Mol. Cell Biochem. **232,** 113–119

Langer D., Hammer K., Koszalka P., Schrader J., Robson S., Zimmermann H. (2008): Distribution of ectonucleotidases in the rodent brain revisited. Cell Tissue Res. **334,** 199–217

Latini S., Pedata F. (2001): Adenosine in the central nervous system: release mechanisms and extracellular concentrations. J. Neurochem. **79,** 463–484

Lehto M. T., Sharom F. J. (1998): Release of the glycosylphosphatidylinositol-anchored enzyme ecto-5'-nucleotidase by phospholipase C: catalytic activation and modulation by the lipid bilayer. Biochem. J. **332,** 101–109

Lehto M. T., Sharom F. J. (2002): PI-specific phospholipase C cleavage of a reconstituted GPI-anchored protein: modulation by the lipid bilayer. Biochemistry **41,** 1398–1408

Manville J., Laurer H. L., Steudel W. I., Mautes A. E. (2007): Changes in cortical and subcortical energy metabolism after repetitive and single controlled cortical impact injury in the mouse. J. Mol. Neurosci. **31,** 95–100

Markwell M. A., Haas S. M., Bieber L. L., Tolbert N. E. (1978): A modification of the Lowry procedure to simplify protein determination in membrane and lipoprotein samples. Anal. Biochem. **87,** 206–210

Melani A., Turchi D., Vannucchi M. G., Cipriani S., Gianfriddo M., Pedata F. (2005): ATP extracellular concentrations are increased in the rat striatum during *in vivo* ischemia. Neurochem. Int. **47,** 442–448

Menze M. A., Clavenna M. J., Hand S. C. (2005): Depression of cell metabolism and proliferation by membrane-permeable

and -impermeable modulators: role for AMP-to-ATP ratio. Am. J. Physiol., Regul. Integr. Comp. Physiol. **288,** R501–510

Nagy A. K., Walton N. Y., Treiman D. M. (1997): Reduced cortical ecto-ATPase activity in rat brains during prolonged status epilepticus induced by sequential administration of lithium and pilocarpine. Mol. Chem. Neuropathol. **31,** 135–147

Nedeljkovic N., Nikezic G., Horvat A., Pekovic S., Stojiljkovic M., Martinovic J. V. (1998): Properties of Mg^{2+}-ATPase rat brain synaptic plasma membranes. Gen. Physiol. Biophys. **17,** 3–13

Nedeljkovic N., Banjac A., Horvat A., Stojiljkovic M., Nikezic G. (2003): Ecto-ATPase and ecto-ATP-diphosphohydrolase are co-localized in rat hippocampal and caudate nucleus synaptic plasma membranes. Physiol. Res. **52,** 797–804

Nedeljkovic N., Bjelobaba I., Subasic S., Lavrnja I., Pekovic S., Stojkov D., Vjestica A., Rakic L., Stojiljkovic M. (2006): Up-regulation of ectonucleotidase activity after cortical stab injury in rats. Cell Biol. Int. **30,** 541–546

Nedeljkovic N., Bjelobaba I., Lavrnja I., Stojkov D., Pekovic S., Rakic L., Stojiljkovic M. (2008): Early temporal changes in ecto-nucleotidase activity after cortical stab injury in rat. Neurochem. Res. **33,** 873–879

Pennial R. (1966): An improved method for determination of inorganic phosphate by the isobutanol-benzen extraction procedure. Anal. Biochem. **14,** 87–90

Ralevic V., Burnstock G. (1998): Receptors for purines and pyrimidines. Pharmacol. Rev. **50,** 413–492

Rathbone M. P., Christjanson L., Deforge S., Deluca B., Gysbers J. W., Hindley S., Jovetich M., Middlemiss P., Takhal S. (1992a): Extracellular purine nucleosides stimulate cell division and morphogenesis: pathological and physiological implications. Med. Hypotheses **37,** 232–240

Rathbone M. P., Deforge S., Deluca B., Gabel B., Laurenssen C., Middlemiss P., Parkinson S. (1992b): Purinergic stimulation of cell division and differentiation: mechanisms and pharmacological implications. Med. Hypotheses **37,** 213–219

Rathbone M. P., Middlemiss P. J., Kim J. K., Gysbers J. W., DeForge S. P., Smith R. W., Hughes D. W. (1992c): Adenosine and its nucleotides stimulate proliferation of chick astrocytes and human astrocytoma cells. Neurosci. Res. **13,** 1–17

Schoen S. W., Kreutzberg G. W. (1994): Synaptic 5'-nucleotidase activity reflects lesion-induced sprouting within the adult rat dentate gyrus. Exp. Neurol. **127,** 106–118

Villa R. F., Gorini A., Hoyer S. (2002): ATPases of synaptic plasma membranes from hippocampus after ischemia and recovery during ageing. Neurochem. Res. **27,** 861–870

Volonte C., Ciotti M. T., D'Ambrosi N., Lockhart B., Spedding M. (1999): Neuroprotective effects of modulators of P2 receptors in primary culture of CNS neurones. Neuropharmacology **38,** 1335–1342

Zimmermann H. (1996): Biochemistry, localization and functional roles of ecto-nucleotidases in the nervous system. Prog. Neurobiol. **49,** 589–618

Zimmermann H. (2000): Extracellular metabolism of ATP and other nucleotides. Naunyn Schmiedebergs Arch. Pharmacol. **362,** 299–309

Ribavirin administration alters ectonucleotidase activities in experimental autoimmune encephalomyelitis

Irena Lavrnja[1], Nadezda Nedeljkovic[2], Ivana Bjelobaba[1], Danijela Stojkov[1], Sanja Dacic[2], Sanja Pekovic[1], Ljubisav Rakic[3], Marija Mostarica-Stojkovic[4], Stanislava Stosic-Grujicic[5] and Mirjana Stojiljkovic[1]

[1] *Department of Neurobiology, Institute for Biological Research "Siniša Stanković", University of Belgrade, Serbia*
[2] *Institute of Physiology and Biochemistry, Faculty of Biology, University of Belgrade, Serbia*
[3] *Serbian Academy of Sciences and Arts, Belgrade, Serbia*
[4] *Institute of Microbiology and Immunology, School of Medicine, University of Belgrade, Serbia*
[5] *Department of Immunology, Institute for Biological Research "Siniša Stanković", University of Belgrade, Serbia*

Abstract. The role of extracellular purines and purinoreceptors in the pathophysiology of different neurological disorders is the focus of rapidly expanding area of research. Ectonucleotidases are the enzymes with multiple roles in extracellular nucleotides metabolism and regulation of nucleotide-based intercellular signaling. The aim of present study was to investigate the changes in the ATP, ADP and AMP hydrolyzing activities after ribavirin treatment in spinal cord during experimental autoimmune encephalomyelitis (EAE). Our results demonstrate that ribavirin itself had no significant effect on ectoenzyme activities, when tested *in vitro* and *in vivo* on spinal cord crude membrane preparation of intact animals. We observed significant increase in ATP, ADP and AMP hydrolyzing activity in the spinal cord crude membrane preparation in EAE animals at 15 days post immunization compared to control animals. The increase was registered at 28 days post immunization, as well. At same time points, ribavirin treatment decreased ATP, ADP and AMP hydrolyzing activity compared to EAE animals. In addition, no significant changes 8 days post immunization was observed between EAE-induced and ribavirin- treated EAE animals and these levels were similar to control level. Thus, we suppose that ribavirin-induced alteration in ectonucleotidase activities is rather due to its suppression of inflammation, than to its direct action on ATP, ADP and AMP hydrolysis.

Key words: Ribavirin — EAE — Rat spinal cord — Ectonucleotidase activity

Introduction

Purine nucleotides, such as ATP and adenosine, represent a ubiquitous class of extracellular signaling molecules crucial for normal functioning of the nervous system. Recently, extracellular nucleotides such as ATP and adenosine have become clearly recognized to play an important role in modulating immune processes (Dwyer et al. 2007). Extracellular ATP and ADP are important signaling molecules in inflammatory events operative through the activation of specific P2X and P2Y receptors that are expressed on many cell types (Yegutkin 2008). Activation of these receptors regulates lymphocyte and leukocyte functions such as cytokine secretion and/or migration (Langson et al. 2003; Jalkanen and Salmi 2008). On the other hand, adenosine, an end product of nucleotide hydrolysis, has potent anti-inflammatory and immunosuppressive properties (Haskó et al. 2005).

Levels of extracellular nucleotides and the generation of adenosine are tightly regulated by cell surface ectoenzymes known as ectonucleotidases (Zimmermann 2001). The most relevant ecto-enzymes involved in adenine nucleotide extracellular hydrolysis are NTPDase (E.C. 3.6.1.5, ecto-nucleoside triphosphate phosphohydrolase, ecto-NTPDase/CD39) and ecto-5'-nucleotidase (E.C. 3.1.3.5, CD73) (Colgan et al. 2006). NTPDase is a membrane-bound enzyme that

Correspondence to: Irena Lavrnja, Department of Neurobiology, Institute for Biological Research "Siniša Stanković", Bulevar Despota Stefana 142, Belgrade, Serbia
E-mail: irenam@ibiss.bg.ac.rs

hydrolyzes ATP and ADP to AMP, which is subsequently converted to adenosine by ecto-5'-nucleotidase (Birk et al. 2002; Leal et al. 2005). CD39 has been identified originally as a cell-surface glycoprotein expressed on activated B-cells after cell activation (Maliszewski et al. 1994). CD39 is also expressed on NK-cells and subsets of T-cells, vascular endothelial cells, macrophages, and dendritic cells (Kansas et al. 1991). Wang and Guidotti (1996, 1998) have shown that CD39 is expressed widely in the glial cells and neurons in the rat brain. CD73 is a 70-kDa cell surface enzyme expressed on many cell types including subsets of on subsets of B-cells and T-cells (Thompson et al. 1987; Yang et al. 2005), endothelial cells (Narravula et al. 2000), neurons (Maienschein and Zimmermann 1996) and epithelial cells (Strohmeier et al. 1997). Ecto-5'-nucleotidase activity is also found on astrocytes, oligodendrocytes, microglial cells and brain endothelial cells (Robson et al. 2006).

Multiple sclerosis (MS) is the most common chronic demyelinating disease of the CNS of unknown etiology and the major disabling neurological illness of young adults (Noseworthy et al. 2000). Several animal models have been applied for mimicking pathophysiological events in MS and experimental-induced autoimmune encephalomyelitis (EAE) is the best avaliable model so far (Gold et al. 2006). Early events in the pathogenesis of MS/EAE are associated with breakdown of blood brain barrier, massive infiltration of activated mononuclear cells to the CNS, production of different inflammatory mediators leading to demyelination (Compston and Coles 2002) and axonal loss (Bjartmar et al. 2003; Lisak 2007).

Recently, it was shown that CD39-null mice can spontaneously develop features of autoimmune diseases associated with Th1 immune deviation (Dwyer et al. 2007) and that CD73-null mouse are resistant to EAE (Mills et al. 2008), implying the significance of these enzymes in control of autoimmune response.

Ribavirin (1-β-D-ribofuranosyl-1,2,4-triazole-3-carboxamide; Virazol) is a synthetic guanosine analogue, an agent approved as a broad-spectrum antiviral drug (Sidwell et al. 1972). The mechanism of its action includes inhibition of inosine-monophosphate dehydrogenase (IMPDH), an enzyme necessary for de novo synthesis of purine nucleotides and causes interruption of cell metabolism by reducing cellular guanilate concentration (Weber et al. 2003). Earlier studies have shown that ribavirin exerts immunosuppressive activity (Peavy et al. 1980; Jolley et al. 1988; Heagy et al. 1991). We have recently described suppressive effect of ribavirin on the development of actively induced EAE in rats (Milicevic et al. 2003).

Extracellular ATP induces secretion of cytokines involved in the progression of neurodegenerative diseases, like IL-2, IFN-γ, IL-1-β and TNF-α from the activated lymphocytes (Langston et al. 2003; Bours et al. 2006), macrophages (Ferrari et al. 1997) and microglial cells (Hide et al. 2000), whereas adenosine inhibits the production of pro-inflammatory cytokines (Bours et al. 2006). The expression of pro-inflammatory cytokines is positively correlated to the disease induction and progression of EAE (Merril and Benveniste 1996) and it was shown that these cytokines induce upregulation of ecto-5'-nucleotidase on peritoneal macrophages (Savic et al. 1990) and NTPDase expression on lymphocytes (Duensing et al. 1994). We have shown in our previous study (Lavrnja et al. 2008) that ribavirin alters the balance between pro- and anti-inflammatory cytokines in favor of the latter (Lavrnja et al. 2008), which might contribute to the beneficial effect in EAE. However, the exact cellular and molecular mechanisms that underlie the suppression of EAE by of ribavirin have not been fully understood yet. Hence, the aim of this study has been to investigate whether previously described positive effects of ribavirin treatment during EAE could lead to alteration in ecto-enzyme activities *via* adenosine-mediated anti-inflammatory and neuroprotective effects.

Materials and Methods

Experimental animals

Female Dark Agouti (DA) rats, 8 weeks of age, were used throughout the experiments. The animals, obtained from the animal colony maintained at the Institute for Biological Research, were divided into groups of 5 per cage, matched by weight (130–160 g). They were housed under conventional conditions with laboratory chow and water *ad libitum,* and were watered by hand during the period of paralysis. Experimental protocols were approved by the Local Animal Care Committee and conformed to the recommendations given in "Guide for the Care and Use of Laboratory Animals" (National Academy Press, Washington D.C., 1996).

EAE was induced as described previously (Milicevic et al. 2003; Lavrnja et al. 2008). Briefly, rats were immunized by intradermal injection of 100 μl emulsion of rat spinal cord homogenate (50% w/v in saline) and complete Freund's adjuvant containing 1 mg/ml Mycobacterium tuberculosis (Sigma, St. Louis, MO, USA) divided in half and injected in both hind footpads.

Ribavirin (ICN Pharmaceutical Costa Mesa, CA, USA) was dissolved in saline and daily administered intraperitoneally (i.p., 30 mg/kg), from the day of immunization until the end of experiment. The dose of ribavirin was chosen on the basis of previous studies (Milicevic et al. 2003; Lavrnja et al. 2008). Control EAE rats received the equal volume of saline. All immunized animals irrespective of treatment were compared to intact, control rats.

Animals from EAE and ribavirin-treated and/or EAE rats were sacrificed by a decapitation on 8 dpi (day post immunization) (E8 and R8, respectively), 15 dpi (E15 and R15, respectively) or 28 dpi (E28 and R28, respectively).

Immunized animals were daily monitored for clinical signs of EAE, which were graded on scale of 0–5 as follows: 0 – no clinical signs; 1 – flaccid tail; 2 – hind limb paresis; 3 – hind limb paralysis; 4 – moribund state, 5 – death of the animal.

The influence of ribavirin administration on ectonucleotidases activity in intact animals was investigated in the independent experiment, where one group of intact animals was given ribavirin for 15 days at daily dose of 30 mg/kg i.p., while another group of intact animals served as control (data not shown).

Histochemistry

At sacrifice, lumbosacral regions of spinal cords were dissected and fixed in Bouin's solution for 48 h, then dehydrated in a series of alcohol, immersed in xylene and embedded in paraffin. Hematoxylin-eosin staining on 5 μm paraffin thick transverse sections of spinal cord sections was performed according to standard procedures.

Crude membrane preparation

After decapitation, lumbosacral segments of spinal cords were rapidly removed from EAE-induced, ribavirin-treated EAE and control, intact rats. Crude membrane preparation was isolated by homogenization of the obtained tissue in the buffer containing 0.32 mol/l sucrose and 0.005 mol/l Tris pH 7.4, followed by centrifugation at 1000 × *g* for 10 min at 4°C, as previously described for the brain tissue (Nedeljkovic et al. 2003). Resulted supernatant was centrifuged at 12,000 × *g* for additional 30 min, and pelleted membrane preparation was resuspended and homogenized in 0.005 mol/l Tris, pH 7.4. The protein contents were determined by the method of Markwell et al. (1978), using bovine serum albumin as a standard.

Ectonucleotidase assays

Rates of ATP, ADP and AMP hydrolysis were measured by colorimetric determination as previously described (Nedeljkovic et al. 1998). Briefly, the ATP and ADP hydrolyzing activity was measured in reaction mixture containing: 50 mmol/l Tris-HCl (pH 7.4), 0.5 mmol/l EDTA, 5 mmol/l $MgCl_2$, 1 mmol/l ATP or ADP and 20 μg of membrane preparations in a final volume of 200 μl. Reaction was started by the addition of ATP or ADP to the mixture and proceeded for 15 min. Medium for measuring AMP hydrolyzing activity contained: 100 mmol/l Tris-HCl (pH 7.4), 10 mmol/l $MgCl_2$, 1 mmol/l AMP and 50 μg of membrane preparations in a final volume of 200 μl. Reaction was started by the addition of AMP and allowed to proceed for 30 min. Incubations were carried out in a water bath at 37°C. Reactions were stopped by the addition of 3 mol/l perchloracetic acid. All samples were chilled on ice and used for the determination of liberated inorganic phosphate (Pi) (Penniall 1966).

In vitro assays for the estimation of ribavirin effect on ectonucleotidase activities

In these assays crude membrane preparations obtained from spinal cords of intact animals were used. Ribavirin was added to the reaction mixtures to reach 0.01, 0.1, 1 or 10 μg/ml final concentrations. ATP and AMP hydrolysis was then measured as described above.

Data analysis

All samples were run in duplicate in $n > 3$ independent determinations. The ATP and ADP hydrolyzing activities were expressed as μmol Pi/mg proteins/min ± SD. The AMP hydrolyzing activity was expressed as nmol Pi/mg proteins/min ± SD. Significance of differences between groups was determined using Student's *t*-test for paired samples. The values of $p \leq 0.05$ were considered statistically significant ($p \leq 0.05$; $p \leq 0.005$).

Results

Clinical assessment of EAE and the effect of ribavirin on EAE development

After active immunization with whole rat spinal cord homogenate in complete Freund's adjuvant, all rats (100%) in both EAE-induced and ribavirin-treated animals developed acute monophasic disease. In accordance with previous experiments (Milicevic et al. 2003; Lavrnja et al. 2008), first signs of EAE were observed at 9–10 days after the induction of disease in both groups, were increased and peaked at day 14–15 dpi and period of recovery was prolonged until day 22 Pi (data not shown). Rats treated with ribavirin developed milder form of disease as evaluated by mean maximal severity score, disease index and duration of disease in respect of EAE rats, thus confirming previously demonstrated beneficial effects of the drug (Milicevic et al. 2003; Lavrnja et al. 2008). Hematoxylin-eozin staining revealed massive infiltration in white matter in lumbosacral regions of EAE-induced animals in 15 dpi and inflammation persists until the end of experiment 28 dpi (data not shown). Ribavirin treatment reduces inflammation at both examined time points (data not shown).

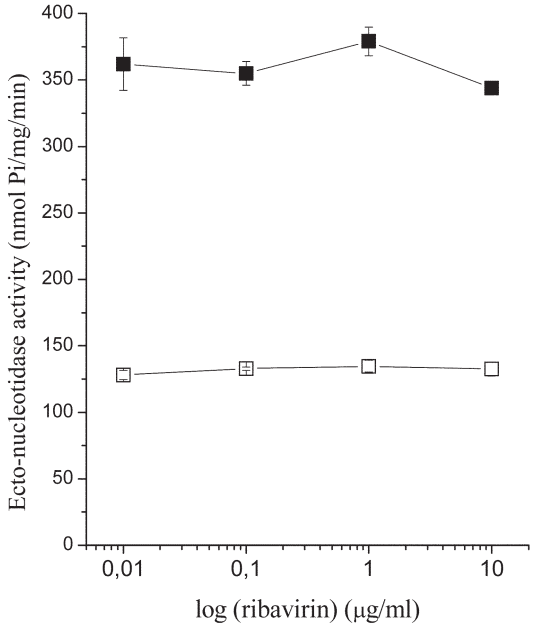

Figure 1. Effect of ribavirin *in vitro* on ATPase and AMPase hydrolysis in the crude membrane preparation of spinal cord. Ribavirin was added to the crude membrane preparation of spinal cord of control healthy animals and the results from 3 different experiments performed in duplicate of *in vitro* on ATPase (solid symbols) and AMPase (empty symbols) hydrolysis are shown. Ribavirin concentrations are given in μg/ml (0.01, 0.1, 1 and 10; logarithmic scale).

In vitro effect of ribavirin on ectonucleotidase activities in the spinal cord crude membrane preparation

In order to investigate *in vitro* effect of ribavirin on ectonucleotidase activities, we added the pure substance to the reaction mixture, in final concentrations of 0.01, 0.1, 1 and 10 μg/ml. Obtained results show that, at any concentration tested, ribavirin by itself did not significantly affect rates of ATP and AMP hydrolyses in the spinal cord crude membrane preparation of control healthy animals (Fig. 1).

Temporal changes in ATP, ADP and AMP hydrolyzing activities in spinal cords of EAE and ribavirin-treated EAE rats

Time-course changes in ATP, ADP and AMP hydrolysis in the spinal cord plasma membrane preparations obtained from control, EAE-induced and ribavirin-treated EAE animals are presented in Fig. 2. Levels of ATP-, ADP- and AMP-hydrolysis at 8 dpi in EAE-induced and ribavirin-treated EAE animals remain unchanged in respect to the corresponding control levels (Fig. 2). However, at 15 dpi, a significant increase in ATP (53%, $p < 0.001$), ADP (33%, $p < 0.001$) and AMP (43%, $p < 0.001$) hydrolysis in EAE-

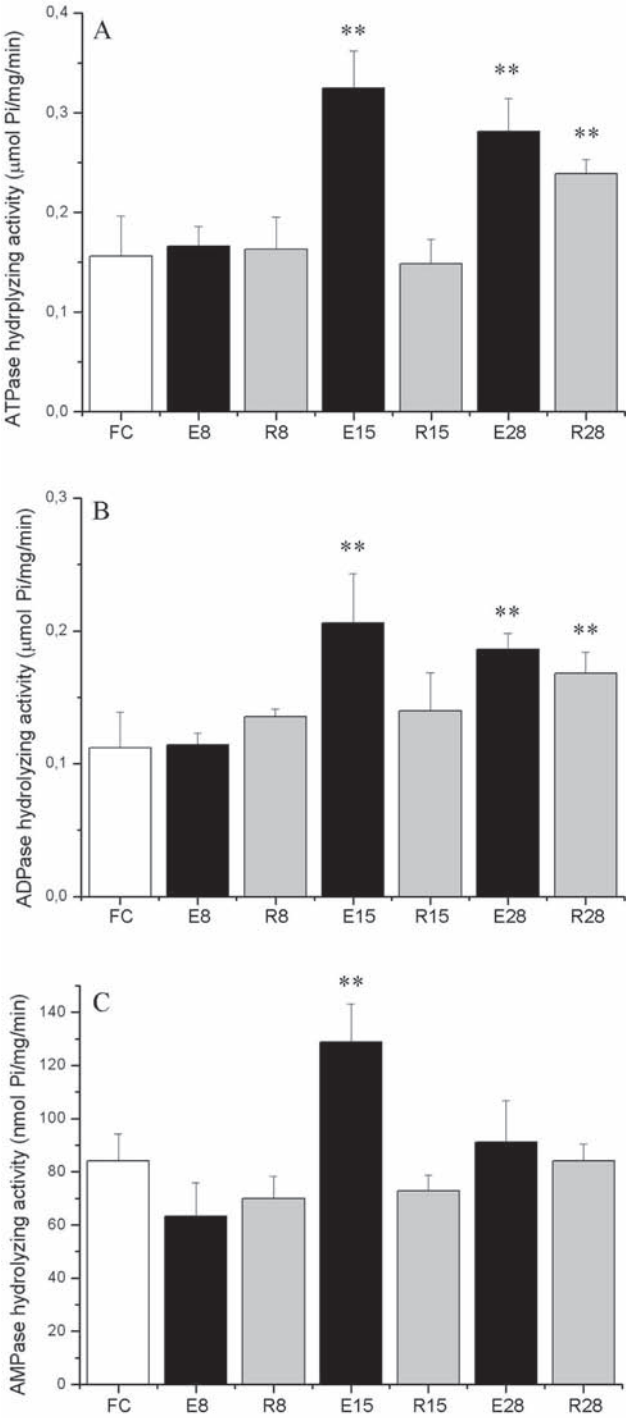

Figure 2. ATP (A), ADP (B) and AMP (C) hydrolyzing activities in the crude membrane preparations of lumbosacral segments of spinal cord of control (FC) (white bars), EAE (black bars) from 8, 15 and 28 days after immunization (E8, E15 and E28) and ribavirin-treated rats (gray bars) from 8, 15 and 28 days after immunization (R8, R15 and R28) ($n = 5$). The results are expressed as mean specific activities ± S.D. from 5 different experiments performed in duplicate. Activities obtained from EAE and ribavirin-treated animal rats were compared with control with significance levels (Student's *t*-test): ** $p < 0.005$.

induced animals was observed when compared to control group (Fig. 2). Similarly, at same time point, EAE group showed significant increase in ATP (50%, $p < 0.001$), ADP (48%, $p < 0.001$) and AMP (35%, $p < 0.001$) hydrolysis when compared to ribavirin-treated animals while no statistical difference was observed between ribavirin-treated EAE animals and control group. At 28 days after immunization, although ectonucleotidase activities in EAE-induced group decreased in relation to previous time point tested, ATP and ADP hydrolysis remained significantly increased in respect to the control group and ribavirin-treated group, ATP (42%, 33%, $p < 0.001$, respectively) and ADP (40%, 35%, $p < 0.001$, respectively) hydrolyzing activities. At same time point, AMP hydrolysis in EAE animals, although significantly decreased in respect to previous time point remained unchanged in respect to ribavirin-treated and control group (Fig. 2). No significant differences was observed in AMPase activity between ribavirin-treated EAE group in all examined times.

Discussion

In the present study we investigated the ability of ribavirin to interfere with the ectonucleotidase activities during EAE actively induced in highly susceptible DA rats (Stosic-Grujicic et al. 2004). Our results demonstrate the significant increase in ATP, ADP and AMP hydrolyzing activities in spinal cords of EAE-induced animals in the peak of disease. This increase was sustained until the end of disease. Since adenosine, the end product of ecto-enzymatic cascade has anti-inflammatory and neuroprotective effects, we analyze whether previously described beneficial effects of ribavirin in EAE (Milicevic et al. 2003) lies in alternation of ectonucleotidase activities in favor of generation of adenosine. In the present study, we have shown that ribavirin treatment significantly decreased ectonucleotidase activities to almost control levels in both examined time points.

The main findings of our study are that EAE animals express increased ectonucleotidase activities in spinal cord membrane preparations in respect to ribavirin-treated animals and the most prominent alterations coincide with clinical score and most pronounced histopathological changes (Lavrnja et al. 2008), that is in the peak of disease. Since extracellular ATP levels increase in injured tissue (Yegutkin 2008), it is possible that the up-regulation of ectonucleotidase activities in EAE animals is caused by inflammation, demyelination, axonal loss and reactive astrogliosis, common features observed in spinal cord after the induction of EAE, as we have shown in our previous studies (Milicevic et al. 2003; Stojkov et al. 2008). It has been previously shown that under inflammatory conditions, release of ATP can contribute to neurodegeneration in MS/EAE (Le Feuvre et al. 2002) and as it was already proposed, demyelination itself, could increase extracellular ATP levels and consequently lead to activation of ectonucleotidases (Spanevello et al. 2006). Thus, if inflammation and demyelination is a trigger for ectonucleotidase up-regulation, ribavirin could impede this cascade simply by preventing lymphocyte infiltration to CNS. Although the mode of action in the modulation of induced EAE is unknown, we proposed that ribavirin exerts these effects through inhibition of IMPDH and depletion of guanilate pools by inhibiting recruitment of activated lymphocytes, macrophage/microglia (Milicevic et al. 2003) and reactive astrocytes (Pekovic et al. 2005). Therefore, lower ectonucleotidase activities observed in the present study could occur as a result of ribavirin action on lymphocytes and glial cells, rather than as a result of direct action of this drug on these enzymes. Our results also demonstrated that no significant changes 8 days post immunization was observed between EAE-induced and ribavirin-treated EAE animals and these levels were similar to control level. Since no histopathological changes could be seen in both examined groups (data not shown), at this time point the absence of ectonucleotidase activities alteration confirms that it reflects tissue injury induced by the autoimmune attack.

We also tested the possibility of ribavirin to interfere with nucleotide hydrolysis. The *in vitro* effect of ribavirin on the hydrolysis of ATP and AMP was also studied. When added in the incubation mixture with the crude membrane preparation obtained from intact animals, ribavirin did not interfere neither with ATP nor AMP hydrolysis. Since ribavirin is a prodrug that must be converted to its nucleotide metabolites to exert activity (Parker 2005), we assumed that its active metabolite generated *in vivo* might be involved in decreased ectonucleotidase activities observed in this study. Therefore, we also investigated the effect of prolonged ribavirin treatment on intact animals and measured ATP and AMP hydrolyzing activities. Likewise, *in vivo* ribavirin treatment had no impact on ATP or AMP hydrolysis in the spinal cord crude membrane preparations of intact animals.

Recently, it was reported that CD73-generated adenosine restricts lymphocyte migration into draining lymph nodes (Takedachi et al. 2008), which is an absolute prerequisite for autoimmune damage to the CNS (Gold et al. 2006). On the contrary CD73 is required for efficient entry of lymphocytes into CNS during EAE (Mills et al. 2008) and lymphocyte-endothelial interaction regulates CD73 activity (Jalkanen and Salmi 2008), implying the importance of this enzyme in regulation of lymphocyte migratory pattern, an event shown to be critical step in the pathogenesis of MS/EAE (Engelhardt 2006). We previously hypothesized that ribavirin prevents the development of EAE in DA rats by inhibiting the proliferation of encephalitogenic cells in the lymph node draining the site of inoculation and affects migration of encephalitogenic T lymphocytes to the target tissue (Lavrnja et al. 2008). Therefore, the observed decrease

in ATP, ADP and AMP hydrolysis in ribavirin-treated animals in the peak and at the end of disease seems expected. Furthermore, it was previously shown that other IMPDH inhibitors like tiazofurin and mycophenolate mofetil attenuate clinical symptoms in EAE by affecting cell-cell interaction and suppressing glycosylation and the binding activity of various adhesion molecules (Tran et al. 2001; Stosic-Grujicic et al. 2002), thus participating in regulation of lymphocyte migratory pattern.

It was recently reported that CD39 is important component of $CD4^+/CD25^+/Foxp3^+$ T regulatory cells (Deaglio et al. 2007), acting through removal of proinflammatory ATP (Borsellino et al. 2007) and in concert with CD73 participates in generation of immunosuppressive adenosine (Dwyer et al. 2007), leading to the inhibition of T-cell proliferation and pro-inflammatory cytokine secretion (Bours et al. 2006; Kobie et al. 2006). Therefore, an observed increase in nucleotide hydrolysis in EAE animals could be related to compensatory response to inflammation, demyelinization and axonal loss decreasing ATP availability and consequently contributing to the production of adenosine and possibly recovery of disease.

It is proposed that CD73-generated adenosine appears to be beneficial in fight against inflammation (Thompson et al. 2004). For that reason, the primary therapeutic option with CD73 is to increase its enzymatic activity and expression. It was reported that IFN-β treatment, one of the most effective treatment in MS, increased expression of CD73 and consequently decrease the transmigration of lymphocytes through blood-brain barrier (Niemelä et al. 2008). Hence, the increased production of adenosine at least in part can contribute to the beneficial effect of IFN-β. Therefore, the observed decrease in ectoenzyme activities in ribavirin-treated animals seems unexpected. On the other hand, it is important to note that CD73 and extracellular generated adenosine are needed for the efficient migration of T-cells to CNS and mice lacking CD73 is resistant to the induction of EAE (Mills et al. 2008), implying that inhibition of CD73 could be valuable approach in treating MS.

In summary, we have shown that ribavirin can affect the ecto-nucleotidase pathway during EAE. Altered ectonucleotidase activities observed after ribavirin treatment are rather due to its suppression of inflammation and demyelination, than due to its direct action on ATP, ADP and AMP hydrolysis.

Acknowledgement. This work was financed by the Serbian Ministry of Science and Environmental Control, project No. 143005, 143029, 145066.

References

Birk A. V., Broekman M. J., Gladek E. M., Robertson H. D., Drosopoulos J. H., Marcus A. J., Szeto H. H. (2002): Role of extracellular ATP metabolism in regulation of platelet reactivity. J. Lab. Clin. Med. **140**, 166–175

Bjartmar C., Wujek J. R., Trapp B. D. (2003): Axonal loss in the pathology of MS: consequences for understanding the progressive phase of disease. J. Neurol. Sci. **206**, 165–171

Borsellino G., Kleinewietfeld M., Di Mitri D., Sternjak A., Diamantini A., Giometto R., Höpner S., Centonze D., Bernardi G., Dell'Acqua M. L., Rossini P. M., Battistini L., Rötzschke O., Falk K. (2007): Expression of ectonucleotidase CD39 by Foxp3+ Treg cells: hydrolysis of extracellular ATP and immune suppression. Blood **110,** 1225–1232

Bours M. J., Swennen E. L., Di Virgilio F., Cronstein B. N., Dagnelie P. C. (2006): Adenosine 5'-triphosphate and adenosine as endogenous signaling molecules in immunity and inflammation. Pharmacol. Ther. **112**, 358–404

Colgan S. P., Eltzschig H. K., Eckle T., Thompson L. F. (2006): Physiological roles for ecto-5'-nucleotidase (CD73). Purinergic Signal. **2**, 351–360

Compston A., Coles A. (2002): Multiple sclerosis. Lancet **359**, 1221–1231

Deaglio S., Dwyer K. M., Gao W., Friedman D., Usheva A., Erat A., Chen J. F., Enjyoji K., Linden J., Oukka M., Kuchroo V. K., Strom T. B., Robson S. C. (2007): Adenosine generation catalyzed by CD39 and CD73 expressed on regulatory T cells mediates immune suppression. J. Exp. Med. **204**, 1257–1265

Duensing S., Kirshner H., Atzpodien J. (1994): CD39 as a novel marker of *in vivo* immune activation. Blood **83**, 3826–3827

Dwyer K. M., Deaglio S., Gao W., Friedman D., Strom T. B., Robson S. C. (2007): CD39 and control of cellular immune responses. Purinergic Signal. **3**, 171–180

Engelhardt B. (2006): Molecular mechanisms involved in T cell migration across the blood-brain barrier. J. Neural Transm. **113,** 477–485

Ferrari D., Chiozzi P., Falzoni S., Dal Susino M., Melchiorri L., Baricordi O. R., Di Virgilio F. (1997): Extracellular ATP triggers IL-1 beta release by activating the purinergic P2Z receptor of human macrophages. J. Immunol. **159**, 1451–1458

Gold R., Linington C., Lassmann H. (2006): Understanding pathogenesis and therapy of multiple sclerosis via animal models: 70 years of merits and culprits in experimental autoimmune encephalomyelitis research. Brain **129**, 1953–1971

Haskó G., Pacher P., Vizi E. S., Illes P. (2005): Adenosine receptor signaling in the brain immune system. Trends Pharmacol. Sci. **26**, 511–516

Heagy W., Crumpacker C., Lopez P. A., Finberg R. W. (1991): Inhibition of immune functions by antiviral drugs. J. Clin. Invest. **87**, 1916–1924

Hide I., Tanaka M., Inoue A., Nakajima K., Kohsaka S., Inoue K., Nakata Y. (2000): Extracellular ATP triggers tumor necrosis factor-α release from rat microglia. J. Neurochem. **75,** 965–972

Jalkanen S., Salmi M. (2007): VAP-1 and CD73, endothelial cell surface enzymes in leukocyte extravasation. Arterioscler. Thromb. Vasc. Biol. **28**, 18–26

Jolley W. B., Sharma B., Chami R., Ng C., Bullington R. (1988): Long-term skin allograft survival by combined therapy with suboptimal dose of cyclosporine and ribavirin. Transplant. Proc. **20**, 703–706

Kansas G. S., Wood G. S., Tedder T. F. (1991): Expression, distribution and biochemistry of human CD39. Role in activation-associated homotypic adhesion of lymphocytes. J. Immunol. **146,** 2235–2244

Kobie J. J., Shah P. R., Yang L., Rebhahn J. A., Fowell D. J., Mosmann T. R. (2006): T regulatory and primed uncommitted CD4 T cells express CD73, which suppresses effector CD4 T cells by converting 5'-adenosine monophosphate to adenosine. J. Immunol. **177**, 6780–6786

Langston H. P., Ke Y., Gewirtz A. T. Dombrowski K. E., Kapp J. A. (2003): Secretion of IL-2 and IFN-γ, but not IL-4, by antigen-specific T cells requires extracellular ATP. J. Immunol. **170**, 2962–2970

Lavrnja I., Stojkov D., Bjelobaba I., Pekovic S., Dacic S., Nedeljkovic N., Mostarica-Stojkovic M., Stosic-Grujicic S., Rakic L., Stojiljkovic M. (2008): Ribavirin ameliorates experimental autoimmune encephalomyelitis in rats and modulates cytokine production. Int. Immunopharmacol. **8**, 1282–1290

Le Feuvre R., Brough D., Rothwell N. (2002): Extracellular ATP and P2X7 receptors in neurodegeneration. Eur. J. Pharmacol. **447**, 261–269

Leal D. B., Streher C. A., Bertoncheli Cde M., Carli L. F., Leal C. A., da Silva J. E., Morsch V. M., Schetinger M. R. (2005): HIV infection is associated with increased NTPDase activity that correlates with CD39-positive lymphocytes. Biochim. Biophys. Acta **1746**, 129–134

Lisak R. P. (2007): Neurodegeneration in multiple sclerosis: defining the problem. Neurology **68**, (Suppl. 3), S5–12; Discussion S43–54

Maienschein V., Zimmermann H. (1996): Immunocytochemical localization of ecto-5'-nucleotidase in cultures of cerebellar granule cells. Neuroscience **70,** 429–438

Maliszewski C. R., Delespesse G. J., Schoenborn M. A., Armitage R. J., Fanslow W. C., Nakajima T., Baker E., Sutherland G. R., Poindexter K., Birks C. (1994): The CD39 lymphoid cell activation antigen. Molecular cloning and structural characterization. J. Immunol. **153**, 3574–3583

Markwell M. A., Haas S. M., Bieber L. L., Tolbert N. E. (1978): A modification of the Lowry procedure to simplify protein determination in membrane and lipoprotein samples. Anal. Biochem. **87**, 206–210

Merrill J. E., Benveniste E. N. (1996): Cytokines in inflammatory brain lesions: helpful and harmful. Trends Neurosci. **19,** 331–338

Milicevic I., Pekovic S., Subasic S., Mostarica-Stojkovic M., Stosic-Grujicic S., Medic-Mijacevic Lj., Pjanovic V., Rakic Lj., Stojiljkovic M. (2003): Ribavirin reduces clinical signs and pathological changes of experimental autoimmune encephalomyelitis in Dark Agouti rats. J. Neurosci. Res. **72**, 268–278

Mills J. H., Thompson L. F., Mueller C., Waickman A. T., Jalkanen S., Niemela J., Airas L., Bynoe M. S. (2008): CD73 is required for efficient entry of lymphocytes into the central nervous system during experimental autoimmune encephalomyelitis. Proc. Natl. Acad. Sci. U.S.A. **105**, 9325–9330

Narravula S., Lennon P. F., Mueller B. U., Colgan S. P. (2000): Regulation of endothelial CD73 by adenosine: paracrine pathway for enhanced endothelial barrier function. J. Immunol. **165**, 5262–5268

Nedeljković N., Nikezić G., Horvat A., Peković S., Stojiljković M., Martinović J. V. (1998): Properties of Mg^{2+}-ATPase in rat brain synaptic plasma membranes. Gen. Physiol. Biophys. **17**, 3–13

Nedeljković N., Banjac A., Horvat A., Stojiljković M., Nikezić G. (2003): Ecto-ATPase and ecto-ATP-diphosphohydrolase are co-localized in rat hippocampal and caudate nucleus synaptic plasma membranes. Phys. Res. **52**, 797–804

Niemelä J., Ifergan I., Yegutkin G. G., Jalkanen S., Prat A., Airas L. (2008): IFN-beta regulates CD73 and adenosine expression at the blood-brain barrier. Eur. J. Immunol. **38**, 2718–2726

Noseworthy J. H., Lucchinetti C., Rodriguez M., Weinshenker B. G. (2000): Multiple sclerosis. N. Engl. J. Med. **343**, 938–952

Parker W. B. (2005): Metabolism and antiviral activity of ribavirin. Virus Res. **107**, 165–171

Peavy D. L., Koff W. C., Hyman D. S., Knight V. (1980): Inhibition of lymphocyte proliferative responses by ribavirin. Infect. Immun. **29**, 583–589

Pekovic S., Filipovic R., Subasic S., Lavrnja I., Stojkov D., Nedeljkovic N., Rakic Lj., Stojiljkovic M. (2005): Downregulation of glial scaring after brain injury: the effect of purine nucleoside analogue ribavirin. Ann. N. Y. Acad. Sci. **1048**, 296–310

Penniall R. (1966): An improved method for determination of inorganic phosphate by the isobutanol-benzene extraction procedure. Anal. Biochem. **14**, 87–90

Robson S. C., Sévigny J., Zimmermann H. (2006): The E-NTPDase family of ectonucleotidases: structure function relationships and pathophysiological significance. Purinergic Signal. **2**, 409–430

Savic V., Stefanovic V., Ardaillou N., Ardaillou R. (1990): Induction of ecto-5'-nucleotidase of rat cultured mesangial cells by interleukin-1 beta and tumour necrosis factor-alpha. Immunology **70**, 321–326

Sidwell R. W., Huffman J. H., Khare G. P., Allen L. B., Witkowski J. T., Robins R. K. (1972): Broad-spectrum antiviral activity of Virazole: 1-beta-D-ribofuranosyl-1,2,4-triazole-3-carboxamide. Science **177**, 705–706

Spanevello R. M., Mazzanti C. M., Kaizer R., Zanin R., Cargnelutti D., Hannel L., Côrrera M., Mazzanti A., Festugatto R., Graça D., Schetinger M. R. C., Morsch V. M. (2006): Apyrase and 5'-nucleotidase activities in synaptosomesfrom the cerebral cortex of rats experimentally demylinated with ethidium bromide and treated with interferon-ß. Neurochem. Res. **31**, 455–462

Stojkov D., Lavrnja I., Pekovic S., Dacic S., Bjelobaba I., Mostarica-Stojkovic M., Stosic-Grujicic S., Jovanovic S., Nedeljkovic N., Rakic Lj., Stojiljkovic M. (2008): Therapeutic effects of combined treatment with ribavirin and tiazofurin on experimental autoimmune encephalomyelitis develop-

ment: clinical and histopathological evaluation. J. Neurol. Sci. **267,** 76–85

Stosic-Grujicic S., Savic-Radojevic A., Maksimovic-Ivanic D., Markovic M., Bumbasirevic V., Ramic Z., Mostarica-Stojkovic M. (2002): Downregulation of experimental allergic encephalomyelitis in DA rats by tiazofurin. J. Neuroimmunol. **130**, 66–77

Stosic-Grujicic S., Ramic Z., Bumbasirevic V., Harhaji L., Mostarica-Stojkovic M. (2004): Induction of experimental autoimmune encephalomyelitis in Dark Agouti rats without adjuvant. Clin. Exp. Immunol. **136**, 49–55

Strohmeier G. R., Lencer W. I., Patapoff T. W., Thompson L. F., Carlson S. L., Moe S. J., Carnes D. K., Mrsny R. J., Madara J. L. (1997): Surface expression, polarization, and functional significance of CD73 in human intestinal epithelia. J. Clin. Invest. **99**, 2588–2601

Takedachi M., Qu D., Ebisuno Y., Oohara H., Joachims M. L., McGee S. T., Maeda E., McEver R. P., Tanaka T., Miyasaka M., Murakami S., Krahn T., Blackburn M. R., Thompson L. F. (2008): CD73-generated adenosine restricts lymphocyte migration into draining lymph nodes. J. Immunol. **180,** 6288–6296

Thompson L. F., Ruedi J. M., Low M. G., Clement L. T. (1987): Distribution of ecto-5'-nucleotidase on subsets of human T and B lymphocytes as detected by indirect immunofluorescence using goat antibodies. J. Immunol. **139**, 4042–4048

Thompson L. F., Eltzschig H. K., Ibla J. C., Van De Wiele C. J., Resta R., Morote-Garcia J. C., Colgan S. P. (2004): Crucial role for ecto-5'-nucleotidase (CD73) in vascular leakage during hypoxia. J. Exp. Med. **200,** 1395–1405

Tran G. T, Carter N., Hodgkinson S. J. (2001): Mycophenolate mofetil treatment accelerates recovery from experimental allergic encephalomyelitis. Int. Immunopharmacol. **1**, 1709–1723

Wang T. F., Guidotti G. (1996): CD39 is an ecto-(Ca^{2+},Mg^{2+})-apyrase. J. Biol. Chem. **271**, 9898–9901

Wang T. F., Guidotti G. (1998): Widespread expression of ecto-apyrase (CD39) in the central nervous system. Brain Res. **790**, 318–322

Weber G., Shen F., Orbán T. I., Kökeny S., Olah E. (2003): Targeting signal transduction. Adv. Enzyme Regul. **43**, 47–56

Yang L., Kobie J. J., Mosmann T. R. (2005): CD73 and Ly-6A/E distinguish in vivo primed but uncommitted mouse CD4 T cells from type 1 or type 2 effector cells. J. Immunol. **175,** 6458–6464

Yegutkin G. G. (2008): Nucleotide- and nucleoside-converting ectoenzymes: important modulators of purinergic signalling cascade. Biochim. Biophys. Acta **1783**, 673–694

Zimmermann H. (2001) Ectonucleotidases: some recent developments and a note on nomenclature. Drug Dev. Res. **52**, 44–56

The new experimental model for behavioral investigations in animal studies

Zdravko Obradovic[1], Suzana Pantovic[1], Gvozden Rosic[1], Zorica Selakovic[1] and Mirko Rosic[1,2]

[1] *Department of Physiology, Medical faculty, University of Kragujevac, Serbia*
[2] *Center for Scientific Research Serbian Academy of Science and Art and University of Kragujevac, Serbia*

Abstract. In this paper a video file based approach to evaluate position and locomotion in animal behavior experiments is described. For this purpose original software Animal Tracker for transforming a video data to a log file which is suitable for further computational analyzes, was developed. To perform analyzes from the log file, an additional software PostProc), which enables assessment of locomotion, velocity or place preferences, was created. For video recording software called DScaler was used. This is an open source software and freely available for download. The method that we describe in this paper is based on simple video equipment and supported by three software mentioned above. This method enables performing of a wide diversity of experimental designs without limitations in time duration, color and light conditions, shape and size of experimental area and/or investigated objects. As an example, results obtained from experiments with rats in an Open-field test are included. One group of animals was treated with benzodiazepine (2 $mg \cdot kg^{-1}$, single dose, subcutaneously). This easy to use system can be implemented in most laboratories without any special training and used by investigators in the field of animal behavior research.

Key words: Animal behavior — Locomotion — Displacement — Computer evaluation

Introduction

The behavioral investigation, such as locomotors activity, memory, anxiety, learning, aggression etc. has been used in various experimental designs. One of the most frequently used experimental design in this kind of investigation, defined as an Open-field activity test, represents a valid measure of marked changes in "anxiety-like" behaviors in drug-treated and genetically manipulated animals and can also be used for general assessment of animal basal locomotors activity and exploration. The first attempts in measurement of animal behavior occurred early in the previous century (Hall 1934). As the essential goal of any experiment is to obtain valid and exact results, it is obvious that in behavioral experiments this depends on the tools capable of sensitive tracking, recording and analyzing of the events. These tools came a long way from the first Open-field score tests (Giulian and Silverman 1975), in which only a plain box with a visible grid pattern, stopwatch and sharp eye of investigator were included in the setting.

Early semi-automated systems for detecting animal's movement were photocell-based. They automatically detected any breaking of the (visible) IR beam grid (Ericson et al. 1991). In the combination with a computer program, this method can be very accurate (Koob et al. 2006), but still it has some aspects of disadvantages such as: relatively expensive, complicate to set and use, possible influence of IR beams on animal, impossibility of sequential and retrospective analyzes, detection of movements on previously established grid, etc.

Newer methods for video analyses of animal movement appeared with the development of video and digital equipment (Godden and Graham 1983; Schwarting et al. 1993). Most of these systems are dependent on the specific hardware. Some low-cost web-cam based methods had been described, too (Lind et al. 2005; Togasaki et al. 2005). There is, however, some limitations even in the most sophisticated systems. For example: i) it depends on the specific light and arena color conditions; ii) limited experimental time duration; iii) sequential, retrospective analyses are not possible; iv) movements are detected on previously established grid, etc.

Correspondence to: Mirko Rosic, Department of Physiology, Medical Faculty, University of Kragujevac, Svetozara Markovića 69, 34 000 Kragujevac, Serbia
E-mail: mrosic@medf.kg.ac.yu

In this work we suggest a low-cost and easy to use combination of software and hardware for recording, tracking and analyzing of animal's movement and position. The system is based on movement tracking and it is independent of the light environment, color of the animal or the arena, animal species or shape and of the background color. The software practically can analyze any video file as long as camera can record it. This method can be used for tracking movement in absolute dark conditions due to its being equipped with IR camera, which can be useful in observing circadian rhythm.

In this study we recorded movements within 24 h, but in fact there is no limitation in time because video data can be transferred to an external memory or other computers in the intranet connection. In addition, all recorded data from video file can be analyzed within any amount of space and time sequence retrospectively and since the system is based on movement, tracking from video file it is not necessary to have previously defined grid. When data from the video file are analyzed, virtual grid can be defined by software to evaluate position of the animal within any amount of space or chosen time sequence.

In order to validate accuracy of the system we were watching video file and compared it with the data obtained from analyzing programs. This process of validation was performed randomly, for random time sequences of experiment, in all examples given in this work.

Materials and Methods

Video format of the experiment is provided using the following video equipment:

- Standard or IR camera connected to a standard PC computer with 1 GHz CPU and 256 MB of RAM memory.
- PCI TV tuner card with Philips bt878 chipset for capturing video input.
- Windows XP operating system.
- Software called DScaler for video recording (that is open source software and it is freely available for downloading at the address: http://deinterlace.sourceforge.net/). DScaler software records AVI file with XVID encoding, usually with half PAL resolution.

Especially designed software, named Animal Tracker, enables detection of animal's movement from video file input by estimating animal's positions in every video frame – that is 25 times in one second and produces the log file from captured video format. The estimation of position is done in every frame until the end of video file. In every frame the current time and the current position is logged to a file. The Animal Tracker program is made in C++ language. It has no graphical user interface and it is executed from command line. This means that the possibilities for setting changes are not offered in advance. Instead, a simple modification in parameter files allows changes of settings. It is a small executable file, and system requirements are not demanding.

Before placing an investigated subject into the arena, we took a short (1–5 s) recording of the background (empty arena). The initial recording is used to create the basic background picture of the open field. It is further used for determining the position of in investigated subject.

After importing this initial recording (with the duration of *T1* seconds) into the memory, it is represented by matrix *M1[W, H, 3, FoT1]*, where: *W* is the number of pixels at horizontal axis (camera resolution), *H* is the number of pixels at vertical axis (camera resolution), *3* is the matrix dimension of the RGB (red-green-blue) components required for representation of each frame, and *Fo* is the frame frequency per second.

Number of frames in the initial recording can be calculated as $N1 = FoT1$.

The initial background picture is represented by matrix *M2[W, H, 3]*. It is actually, one averaged frame, calculated as:

$$M2[i, j, k] = \frac{\sum_{l=1}^{N1} M1[i, j, k, l]}{N1}$$

where parameter *i* is in the range from 1 to *W*, parameter *j* is in the range from 1 to *H*, and parameter *k* has values of 1, 2 or 3 which represent RGB components, respectively.

After the initial recording, investigated subject was placed into the arena. This moment is considered as the start of the experiment, and following recording (with the duration of *T2* seconds) is represented by matrix *M3[W, H, 3, FoT2]*.

Number of experimental frames in the experimental recording can be calculated as $N2 = FoT2$.

Temporary matrix, $T_{mp}[W, H, 3]$, represents absolute values of the difference between initial background picture and actual experimental frame for each RGB component. Each element of those matrices is marked as 1 if the substantial difference exists or with 0 if the substantial difference does not exist. The Animal Tracker takes difference as substantial if pixel values in experimental frame are out of range defined by standard deviation in corresponding initial background picture. After that, the matrix $T_{mp}OB[W, H]$ is created. This matrix is the result of application of logical or operation applied pixel-wise on each matrix (R, G and B matrix), and represents the union of regions of change detected on each color matrix (R, G and B matrices). The obtained binary matrix represents area at which investigated subject is detected. We consider the mean value of coordinates of all pixels marked as 1, as the referent point *Rp*, calculated from the following equation:

$$Rp = \frac{\sum_{x_{ij} \in O} x_{ij}}{card(O)}$$

where *O* is the body of all pixels marked as 1.

In further analysis, the PostProc uses the referent point for motion evaluation. Usually, processing is a few-times faster than duration of video file. Software Animal Tracker transforms and save data to a log file. The log file contains comma separated values – frame time, and estimated animal position.

PostProc software was designed and used to analyze log files obtained from Animal Tracker. The results of processing can be analyzed in the programs options. One of the options is animal movement in 2D view for entire time of experiment. These movements are shown through position dots that are taken every 0.02 s (this time is adjustable and can be reduced if needed).

In the experiments described in this paper, we used Wistar ($n = 20$) rats, ten male and ten female, weighing between 250 and 320 g from laboratory of experimental animals of Natural Sciences Faculty. One group of ten animals was used for control experiments, and another group of ten animals was treated with benzodiazepine, (test drug; Galenika AD, Belgrade, Serbia). Animals were held in the same environment, with water and food ad libitum and same cleaning habits, in the same room in 12 : 12 h dark/light conditions (lights on at 07:30), at the temperature of 20°C.

The arena used in this work was open field arena 50 × 70 × 30 cm, made of polyester and color shift able. Open field arena was in the same room in which animals were kept to exclude additional stress of displacement. Camera was placed 230 cm above the arena. For the test, the rat was placed in a corner of the open field and allowed to move freely.

Test group of animals ($n = 10$) was treated with benzodiazepine (2 mg·kg^{-1} subcutaneously) 10 min before placing in the arena. We gave this drug in order to induce locomotion impairment, just as an example of experimental design that the system is applicable. In control group ($n = 10$), we used saline, given in exactly the same way as test drug. Control experiments were performed by applying saline and placing animals in the open field, where video file of their locomotion for 24 h was made. There were no interference by any external stimuli on the animal during the experiment and experiment was conducted in the same room the animal was kept in. After 12 h light was turned off automatically, so that 12 : 12 h dark/light conditions were achieved in experiment. After the control experiments, we preformed the test drug experiments with the same conditions and the same number of animals. Animals were in good health and no drug or other stimuli have been given to them in order to record ordinary behavior of the animals in new environment.

Experimental data were analyzed using Student's *t*-test, were $p \leq 0.05$ was considered as statistically significant.

All the experiments were performed according to EU (86/609/EEC) and Local Ethical Guidelines.

Results

After making log files by Animal Tracker, and analyzing those files by PostProc, we obtained experimental data. In Table 1, the parameters that PostProc calculate automatically are presented. These values are given for the entire control group of ten animals.

In the Fig. 1, average speed was calculated for each hour during 24 h of the control experiment. If the average speed is higher, the experimental animal is more active, and

Table 1. Parameters of animal's motion calculated automatically by PostProc

Va (m·s^{-1})	*Vmax* (m·s^{-1})	*S* (km)	*Dm* (h)	*Ds* (h)
0.86 ± 0.098	3.65 ± 0.29	18.64 ± 0.59	6.02 ± 0.61	17.97 ± 1.51

Va, average speed in meters per second; *Vmax*, maximal speed in meters per second; *S*, total distance traveled by animal in kilometers; *Dm*, duration of motion in hours; *Ds*, duration of stillness in hours.

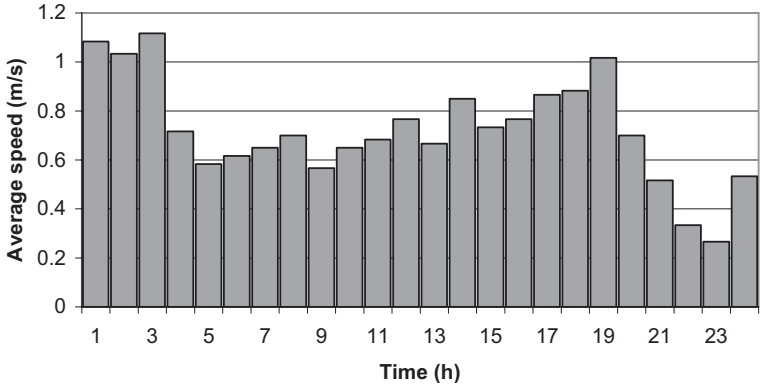

Figure 1. Average speed calculated for every hour during 24 h of the control experiment. Note that these results are obtained from one animal in control group. The data given in this figure is calculated automatically by PostProc.

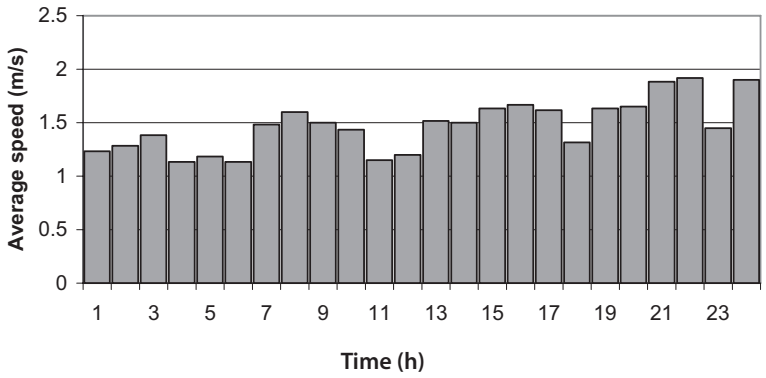

Figure 2. Average speed calculated for every 5 min during first 2 h of the control experiment with the line of activity. Note that these results are obtained from one animal in control group. The data given in this figure is calculated automatically by PostProc.

vice versa. These results are confirmed by watching the actual video recording of the experiment.

Fig. 2 represents animal's activity through its average speed calculated for every 5 min for the first two hours of the same experiment as in the Fig. 1. This period was taken to make animal's exploratory activity clearly visible.

For further analyzes of the video file, arena was divided in a virtual grid formed by lines connecting every 5 cm of the opposite sides of the open field.

In the Fig. 3, time that one of the tested animals in the control group spent in every grid section is shown. The time is displayed in minutes with accuracy of ±30 s. In the white sections the animal spent less than 1 min. Also, the grid section where the animal achieved maximal speed (*Vmax*) is marked. Fig. 3 further shows that animal spent most of the time in the corners of the arena.

In the experiment described above: i) *Vmax* was 3.16 $m \cdot s^{-1}$; ii) *Vmax* occurred in 16^{th} second of 107^{th} minute of experiment (animal was moving with this speed for 0.3 s); iii) *Vmax* occurred in F4 section of the virtual grid (Fig. 3).

In the same manner as in the control experiments we made the log file by Animal Tracker of data obtained in test drug experiments, and analyzed it by PostProc. In Table 2, we present parameters that PostProc has calculated automatically for test drug experiments. These values are given for the entire test group.

	A	B	C	D	E	F	G	H	I	J	K	L	M	N
1	65	24	34	12	5		1			7	6	11	43	57
2	54	56	13	5									45	56
3	45	23	3											23
4	12	12				*								1
5	11													2
6	2													
7	4	3	4										3	2
8	15	4	12									5	7	19
9	67	69	43	23								15	23	54
10	78	76	56	16	15	4		2		3	5	14	21	45

Figure 3. The amount of time animal spent in various grid section; ∗ = *Vmax* (maximal speed is achieved in F4 section of the grid); different numbers represent different duration of time animal spent in each section in minutes (section with less than 1 min time spent are left blank); the center of the arena is marked with black frame.

Table 2. Parameters of animal's motion calculated automatically by PostProc for test drug experiments

Va ($m \cdot s^{-1}$)	*Vmax* ($m \cdot s^{-1}$)	*S* (km)	*Dm* (h)	*Ds* (h)
0.36 ± 0.061	1.61 ± 0.16	2.86 ± 0.24	2.07 ± 0.12	21.95 ± 2.42

These results show that the values of *Va*, *Vmax*, *S* and *Dm* are significantly lower, while value of *Ds* is significantly higher in test drug treated animals comparing to the values in the control experiments.

In the Fig. 4, average speed is calculated for every hour during 24 h of test drug experiments. This figure shows that animals exploratory activity in the first 3 h of testing is significantly impaired comparing with control experiments (see Fig. 1). The significant increase in activity observed between 14^{th} and 17^{th} hour and later between 20^{th} and 24^{th} hour is still below the average speed in control experiments (see Fig. 1).

Using the parameters described above we introduced a few coefficients that can be useful for analyzing data obtained in the experiment. Since the arena can be divided in the virtual grid, and the center and periphery of the arena can be determined, one useful tool for expressing animal's exploratory activity can be introduced. We can calculate the time spent in the center of the open field and time spent in the periphery. In this study, we considered that periphery of the arena is 10 cm from the walls, and rest of the arena was treated as center.

As an example we marked amount of time spent in the center as *Tc* (see Fig. 3) and time spent at the periphery as *Tp* and then introduced the coefficient named motion distribution (*Md*) as:

$Md = Tc/Tp$

Md can be calculated for the entire experiment or for any time sequence of the experiment. In the control experiments, *Md* value (mean ± SE), is calculated in following manner:

$Tc = 11{,}176 \pm 1283$ s

$Tp = 75{,}336.6 \pm 6452$ s

$Md = Tc/Tp = 0.148 \pm 0.0043$

In the Fig. 5, *Md* values through 24 h of experiment are represented, by calculating *Md* for every hour.

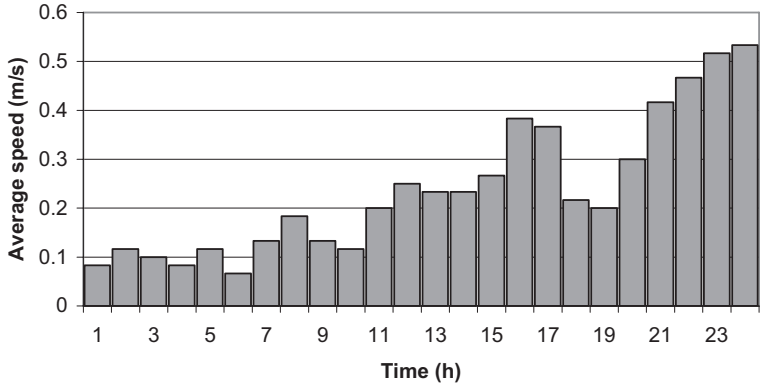

Figure 4. Average speed calculated for every hour during 24 h of the test drug experiment, with the line of activity. Note that these results are obtained from one animal in the test drug experiment. The data given in this figure is calculated automatically by PostProc.

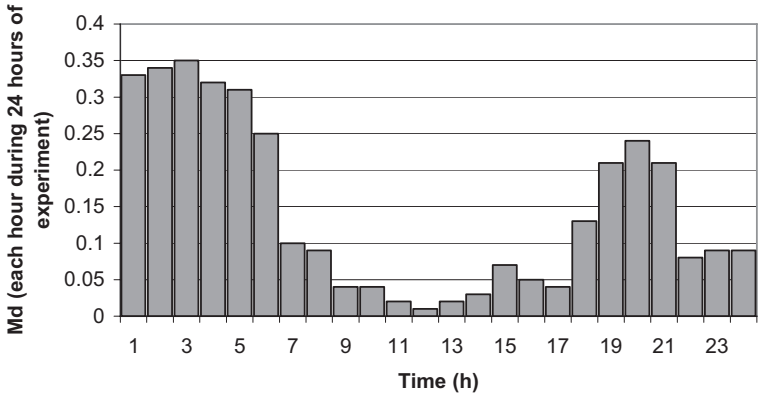

Figure 5. *Md* values through 24 h of experiment, by calculating *Md* for every hour from one control experiment. Note that these results are obtained from one animal in control group. The data given in this figure is calculated automatically by PostProc.

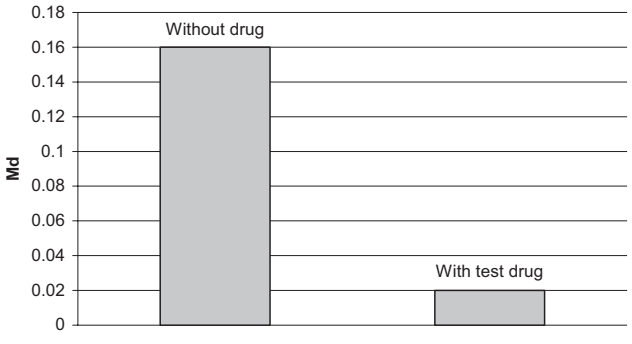

Figure 6. *Md* values from one control experiments and one test drug experiment (with benzodiazepine). Note that these results are obtained from one animal in each experimental group.

Combining with the example from control test group of the experiments, we can show *Md* correlation between one of the controls and one of the test drug experiments (Fig. 6):

Control experiment	Test drug experiment
Tc = 11,473 s	*Tc* = 1968 s
Tp = 72,114 s	*Tp* = 82,356 s
Md = *Tc*/*Tp* = 0.16	*Md* = *Tc*/*Tp* = 0.02

Significantly lower values of *Md* in test drug experiments (with benzodiazepine) indicate impairment of explorative activity.

Another parameter that we introduce is obtained by dividing duration of motion (*Dm*) with duration of stillness (*Ds*). This coefficient we named module of activity (*Am*), and it is calculated as:

Am = *Dm*/*Ds*

In the control experiments, *Am* value, mean ± SE, is calculated in this manner:

Dm = 21,678 ± 2231 s

Ds = 64,772 ± 5443 s

Am = *Dm*/*Ds* = 0.33 ± 0.0064

If *Am* is higher it indicates that animal was more active in motion. We can calculate this value for any period of time, and compare these values through out the entire experiment. In this way, *Am*, as a function of time, can be obtained. This is shown in the Fig. 7, which shows *Am* for every hour for 24 h of experiment.

To see in practice how *Am* can be used we calculated and compared *Am* for one animal from control group with one from test drug experiments (Fig. 8):

Control experiment	Test drug experiment
Dm = 22,459.7 s	*Dm* = 6234,8 s
Ds = 70,090.9 s	*Ds* = 73222,2 s
Am = *Dm*/*Ds* = 0.3	*Am* = *Dm*/*Ds* = 0.08

It is obvious that *Am* is much lower in the test drug experiments (with benzodiazepine) which indicates locomotors impairment.

Since software automatically calculates the time animal spent moving in the range between stillness (*Vo*) and average speed (*Va*) and amount of time moving in range between *Va* and *Vmax*, we introduced another potential new tool/option. The percentage of time that animal spent in a velocity range we called velocity distribution (*Vd*). The percentage of time that animal spent in a velocity range from *Vo* to *Va* we marked as Vd_1, while Vd_2 represents the percentage of the time animal spent in velocity range from *Va* to *Vmax*. We can easily calculate the time animal spends moving, not only in those two ranges but in any range of velocity that we want to observe. It can be done by simply setting ″speed limit″ to different points. This parameter can be calculated and displayed for any portion of time and for any section of space of arena partially. These values were calculated for each hour of 24 h from one of the control experiments, and displayed in the Fig. 9.

Each column in the Fig. 9 represents one hour of the experiment and two colors of the columns represent percentage of the time that animal spent moving in Vd_1 range and Vd_2

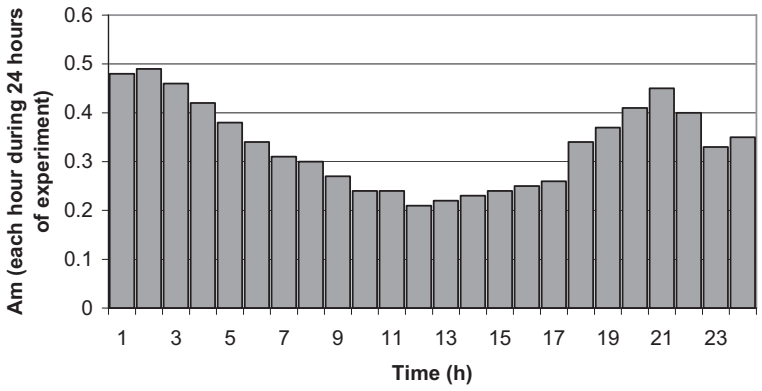

Figure 7. *Am* values through 24 h of experiment, by calculating *Am* for every hour from one control experiment. Note that these results are obtained from one animal in control group. The data given in this figure is calculated automatically by PostProc.

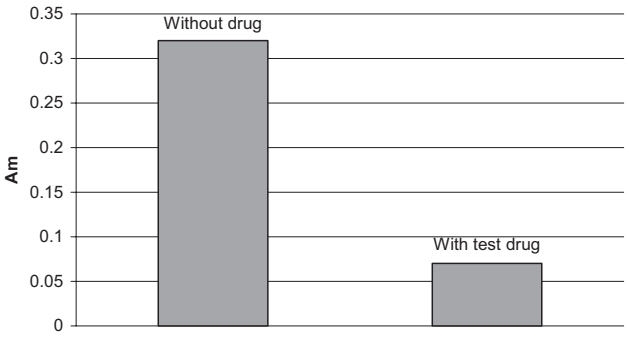

Figure 8. *Am* values from one control experiment and one test drug experiment (with benzodiazepine). Note that these results are obtained from one animal in each experimental group.

range. The highest level of Vd_2 was achieved in the first two hours and then again from 18th to 20th hour.

Discussion

Presently used systems for behavioral experiments are based on two main approaches: IR beam-based and video file-based systems.

IR beam-based systems are complicated to set and use, do not have possibility for sequentional and retrospective analyses because they detect movements on previously established grid. In addition, there is a question of possible influence of IR beam on the investigated subject (Koob et al. 2006).

The video file based systems for behavioral experiments already exist, as commercial products. These systems with graphical interface are capable to record a large number of experimental parameters (Lind et al. 2005; Togasaki et al. 2005).

The experimental model described in this work is also capable to record the same parameters as other video file based systems mentioned above, but at reasonable lower cost. In addition, our model provides the possibility for calculation of two new parameters (*Md* and *Am*). In our experimental model we implemented two separate originally developed open software (Animal Tracker and PostProc), with no common graphical interface. Almost unlimited modifications of Animal Tracker and/or PostProc are possible by simple changes in parameter files. With this possibility of modification, we are able to create various experimental models in order to meet specific requirements.

Our experiments included video files of 24 h or more, but XVID compression occupies less than 4 GB of hard drive space and can fit to only one DVD, and can be reanalyzed, or shipped to different location and distributed or stored in any desirable way. Even further, the experiment can be recorded on the computers in the intranet connection which means that the duration of experimental time is almost unlimited. Video file can be encoded with any other standard encoder, and video file can be saved with any program for video recording and filmed with any kind of camera. Also, it can be taken under almost any illumination, color or other possible criteria of filming. Animal movements are detected by separating animal and background part of the video frame and thus animal can be of any size or shape, and (most importantly) of any color. Also, the background can be in any color or shape, and the illumination can go from bright colored to almost full dark conditions. As mentioned in Introduction section, we use IR camera, and any additional equipment such as LED is unnecessary. When during 24 h of experiments light conditions in the room automatically switch from light to dark, the algorithm for detection automatically adjusts background image.

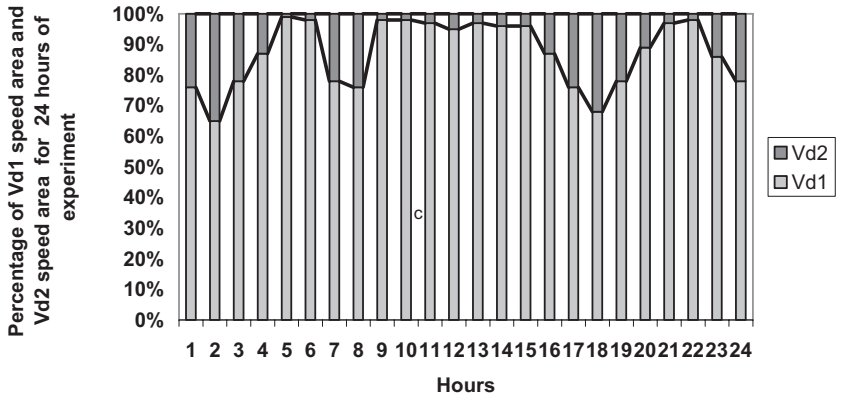

Figure 9. Percentage of time spent in Vd_1 speed range and Vd_2 speed range calculated for every hour during 24 h of experiment from one of the control experiments. Note that these results are obtained from one animal in control group. The data given in this figure is calculated automatically by PostProc.

After making video file with Animal Tracker software, PostProc is taking the position dots every 0.02 s (this time is adjustable and can be reduced if needed). These dots are connected by lines following the animal movements, producing in this way the line of total movement of the animal in the experiment. Another option of this program is to create virtual grid of any size and shape dividing arena in segments. This program also calculates the number of position dots in every segment of the grid and since position dots are taken every 0.02 s, the number of dots represent the time (amount of dots multiplied by 0.02) that animal spent in specific part of the grid. If animal stays in one place without moving, the program continuously calculates at each 0.02 s the number of dots, although graphically it is represented as one dot because animal is not moving. Furthermore, certain time sequences during the experiment can be extruded and animal's location in particular time frame can be determined, where it came from to the specific section and where it left to after this. In addition, to this there is one more option called activity. This view shows exact speed in pixels/second (this can be transformed in to $m \cdot s^{-1}$) on the y axes and the time on x axis, and can also be extruded for any time sequence of the experiment. This option gives values of duration of experiment (or duration of the time sequence we choose), duration of movements and *Ds*, and also the values of *Va* and *Vmax*. Since stillness of the animal is rarely absolute, for example animal can make rearing and grooming movements staying in same place of the arena, we involved speed threshold for movements called speed limit. This threshold provides choice if the movement of the part of body is to be assessed as moving or not. Every speed below this threshold is taken as stillness and above as movements.

Since the open-field procedure is most used for general assessment of animal basal locomotors activity and exploration, we can asses these parameters by analyzing results recorded in Fig. 1. It is shown that animal exhibits exploratory activity in the first 3 h of the control experiment while getting acquainted with the arena. After this, from 4^{th} to 9^{th} hour activity is significantly lower, and from 11^{th} hour it is rapidly increasing when light switch off and rat's nocturnal activity starts. After 19^{th} hour, activity is gradually decreasing, with the lowest average speed at 23^{rd} hour.

Further we tried to observe this exploratory activity closer and took only first 2-h segment from this experiment. The Fig. 2 shows that the activity corresponds to a higher level of *Va*, oscillating between 1.17 $m \cdot s^{-1}$ and 1.83 $m \cdot s^{-1}$. In this example the first 2 h of animal's exploratory activity is extruded, but we can extrude any time sequence from the entire experimental period. For instance, when the time period from 19^{th} to 23^{rd} hour is extruded (not shown) we found the activity within this period at very low level, oscillating between 0 and 0.33 $m \cdot s^{-1}$. By analyzing this sleeping period through the average speed calculated for every 5 (or less) min, we can exactly analyze the periods of absolute stillness (below the threshold of movements) and periods of the low activity. Sometimes the sleeping period can be the sole interest of investigation and in that case, the average speed (or distance) calculated for very short time durations (the limit is 0.02 s) can be analyzed. Practically this makes possible retrospective and sequential analyses for any amount of time.

To analyze animal's positioning and special component of movement we divided arena in virtual, software produced grid (see Fig. 3). This grid can be of any size or shape, because it is formatted by software as we input the certain request. The virtual grid is applicable to any kind of the arena, and most importantly, grid is determined after the experiment is done, so we can change grid format in the same experiment. So, except for just showing the special distribution of animal's motion this view enables exact and simple approach to investigate some external stimuli, such as smells, colors, electromagnetic field etc., applied to the specific section of the arena by simply assessing time that animal spent near or away from the source of those stimuli.

One of the ways to evaluate exploratory activity is to estimate the time that animal spent in the center of the field (Swiergiel 2007). If the animal spends more time in the center of the field (higher *Md*) we can assume that exploratory activity is higher and *vice versa*. Originally introduced parameters *Md* and *Am* are calculated by simply dividing of two known values. So, the question can be raised what their importance is. First of all, although these parameters are very easy to calculate they give us opportunity to observe animal's explorative potential (*Md*) and animal's activity potential (*Am*) in the function of time, observing in that way history of the whole event. For example we showed in the Fig. 7 that *Md* line has two peaks between 1^{st} and 5^{th} hour and between 19^{th} and 21^{st} hour indicating two phases (daily and nocturnal) of exploratory activity, but also nocturnal peak of the *Md* line can be explained as lower anxiety due to the fact that animal becomes more familiar with the arena. We also want to underline that *Md* can be calculated not only for center/periphery, but for any two sections of the arena that we want to. In this way we can estimate the influence of some stimuli on experimental animal (such as different smells, different colors etc.) applied to the specific sections of the arena. In similar way, Fig. 9 shows that *Am* line has two peaks between 1^{st} and 3^{rd} hour and between 20^{th} and 22^{nd} hour indicating two phases (daily and nocturnal) of locomotors activity. This enables us to quickly assess difference between animals in various tests.

We will give an example of that: in the Fig. 10, we displayed *Md* values for the first 30 min (calculated for each minute) in one of the control experiments and in one of the test drug experiments (with benzodiazepine), which can be another way of showing the obvious exploratory impairment

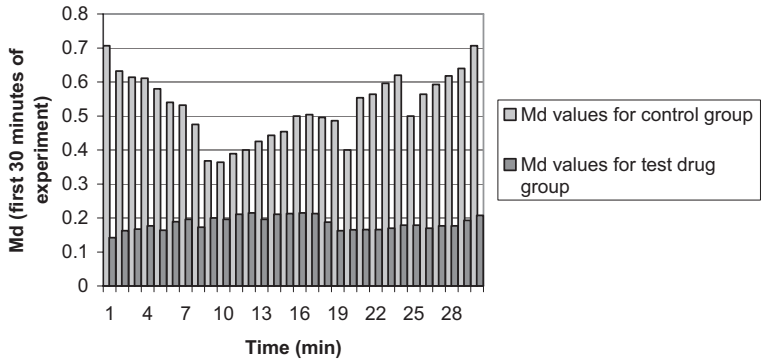

Figure 10. *Md* values for first 30 min of the control experiment and of the test drug experiment. Note that these results are obtained from one animal in each experimental group. The data given in this figure is calculated automatically by PostProc.

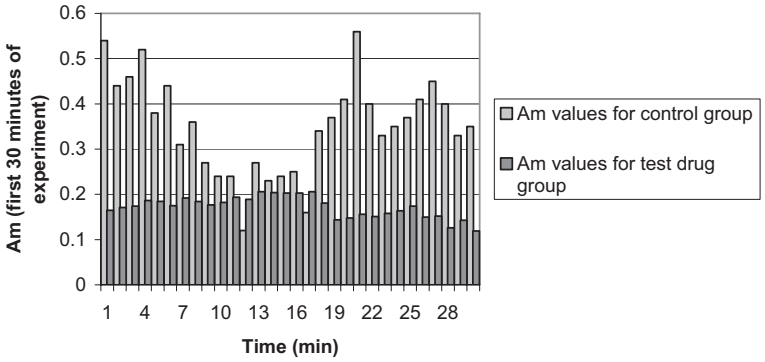

Figure 11. *Am* values for first 30 min of the control experiment and of the test drug experiments. Note that these results are obtained from one animal in each experimental group. The data given in this figure is calculated automatically by PostProc.

in tests with benzodiazepine. The difference between these two lines of *Md* undoubtedly shows the influence of the test drug on animal's exploratory activity. Furthermore, we can choose larger time window and then we can see, for example, in which particular time the experimental drug started to induce exploratory activity impairment. In the Fig. 11, we displayed *Am* values for the first 30 min (calculated for each minute) of the control experiment and for the test drug experiment (with benzodiazepine), for one animal from each group (control and test drug group), which is another way of showing the obvious locomotors impairment: here we can see actual drug influence on movement and locomotors activity in the function of time. This is not only important in quick assessment of the difference between tested and control animal, but also has great significance in recording the exact time of locomotors and motion impairment, when it started, when it ended or what events in time had influence on it.

To conclude we tried to present a new easy-to use and up-to date system for capturing, analyzing and processing data obtained from animal behavior experiments together with several new potentially useful parameters/tools for assessing the data. This method can be used by investigators who do not have any particular knowledge of computer science, but who do have advance demands in their behavioral experiments.

However, our method has its limitations. The first and most serious one is that we still have to improve the system to record and assess rearing and grooming movements. This we plan to solve by advancing our Animal Tracker to record changes in the surface that represents the animal in the arena, and as this surface shrinks it will record rearing or grooming movements depending on the amount of surface decreased. It can and will be improved to record and assess number of turns, and turn directions, although these data can be extruded from log file, but still it is not done automatically.

References

Ericson E., Samuelsson J., Ahlenius S. (1991): Photocell measurements of rat motor activity: a contribution to sensitivity

and variation in behavioral observations. J. Pharmacol. Methods **25**, 111–122

Giulian D., Silverman G. (1975): Solid-state animal detection system: its application to open field activity and freezing behavior. Physiol. Behav. **14**, 109–112

Godden D. H., Graham D. (1983): 'Instant' analysis of movement. J. Exp. Biol. **107**, 505–508

Hall C. S. (1934): Emotional behavior in the rat. I. Defecation and urination as measures of individual differences in emotionality. J. Comp. Psychol. **18**, 385– 403

Kooba A. O., Cirillob J., Babbsb C. F. (2006): A novel open field activity detector to determine spatial and temporal movement of laboratory animals after injury and disease. J. Neurosci. Methods **157,** 330–336

Lind N. M., Vinther M., Hemmingsen R. P., Hansen A. K. (2005): Validation of a digital video tracking system for recording pig locomotors behavior. J. Neurosci. Methods **143,** 123–132

Schwarting R. K., Goldenberg R., Steiner H., Fornaguera J., Huston J. P. (1993): A video image analyzing system for open-field behavior in the rat focusing on behavioral asymmetries. J. Neurosci. Methods **49,** 199–210

Swiergiel A. H., Dunn A. J. (2007): Effects of interleukin-1β and lipopolysaccharide on behavior of mice in the elevated plus-maze and open field tests. Pharmacol. Biochem. Behav. **86**, 651–659

Togasaki D. M., Hsu A., Samant M., Farzan B., DeLanney L. E., Langston J. W., De Monte D. A., Quik M. (2005): The webcam system: a simple, automated, computer-based video system for quantitative measurement of movement in nonhuman primates. J. Neurosci. Methods **145,** 159–166

Tort A. B. L., Neto W. P., Amaral O. B., Kazlauckas V., Souza D. O., Lara D. R. (2006): A simple webcam-based approach for the measurement of rodent locomotion and other behavioral parameters. J. Neurosci. Methods **57**, 91–97

Dynamic response of blood vessel in acute renal failure

Suzana Pantovic[1], Gvozden Rosic[1], Zdravko Obradovic[1], Goran Rankovic[3], Nenad Stojiljkovic[3] and Mirko Rosic[1,2]

[1] *Medical faculty, Department of Physiology, University of Kragujevac, Serbia*
[2] *Center for Sci. Res. Serbian Academy of Sci. Art and University of Kragujevac, Serbia*
[3] *Medical Faculty, Department of Physiology, University of Niš, Serbia*

Abstract. In this study we postulated that during acute renal failure induced by gentamicin the transient or dynamic response of blood vessels could be affected, and that antioxidants can prevent the changes in dynamic responses of blood vessels. The new approach to *ex vivo* blood vessel experiments in which not only the end points of vessels response within the time interval is considered, but also dynamics of this response, was used in this paper. Our results confirm the alteration in dynamic response of blood vessels during the change of pressure in gentamicin-treated animals. The beneficial effects of vitamin C administration to gentamicin-treated animals are also confirmed through: lower level of blood urea and creatinine and higher level of potassium. The pressure dynamic responses of isolated blood vessels show a faster pressure change in gentamicin-treated animals (8.07 ± 1.7 s vs. 5.64 ± 0.18 s). Vitamin C administration induced slowdown of pressure change back to the control values. The pressure dynamic properties, quantitatively defined by comparative pressure dynamic and total pressure dynamic, confirm the alteration in dynamic response of blood vessels during the change of pressure in gentamicin-treated animals and beneficial effects of vitamin C administration.

Key words: Blood vessel dynamic response — Gentamicin-nephrotoxicity — Vitamin C

Introduction

The aminoglykoside antibiotic, gentamicin, is well known to cause renal failure. Gentamicin-induced nephrotoxicity is a complex phenomenon leading to morphological and structural alterations of glomeruli and glomerular basement membrane as well as alterations of proximal tubules (Bennet 1986; Can et al. 2000; Stojiljkovic et al. 2008). The molecular mechanisms underlying gentamicin-induced renal failure have not been fully elucidated although superoxide production (Kays et al. 1991; Ben Ismail et al. 1994; Ata Secilmis et al. 2005), alteration in lysosomal enzymes (Olbricht et al. 1991) and inhibition of microsomal protein synthesis (Bennet et al. 1988) have been proposed to contribute to its deleterious effect.

The well known pattern of gentamicin-induced nephrotoxicity is characterized by reduction in glomerular filtration rate and consequent reduction in creatine clearance with increased serum creatinine. The plasma urea nitrogen is also increased as well as fractional excretion of Na^+ and Li^+. After 5 days of gentamicin administration to rats (100 $mg \cdot kg^{-1}$), unchanged blood pressure has been reported (Rivas-Cabanero et al. 1995; Can et al. 2000), but after 9 days of gentamicin administration to rats, significant increase in systolic blood pressure has been reported (Can et al. 2000). Recent investigations (Kingma et al. 2006) suggest that coronary vascular tone, reserve and vessel reactivity are markedly diminished in dogs with acute renal failure (ARF), suggesting impaired vascular function. It is also known that advanced oxidation protein products (AOPP) act as mediator of oxidative stress and monocyte respiratory burst, which points to monocytes as both target and actor in the immune dysregulation associated with uremia (Witko-Sarsat et al. 1998). Furthermore, it has been demonstrated that AOPP can induce the impairment of endothelium-dependent relaxation in isolated rat aorta rings, which may be partly due to decrease in NO production and/or release and increase in oxygen free radicals (Shuangxiu et al. 2005). Additionally, exposure to urea, which is elevated in renal failure, leads to the carbamilation

Correspondence to: Mirko Rosic, Department of Physiology, Medical Faculty, University of Kragujevac, Svetozara Markovića 69, 34 000 Kragujevac, Serbia
E-mail: mrosic@medf.kg.ac.yu

of proteins (Kraus and Kraus 2001). Recent investigations (Ok et al. 2005) demonstrated that carbamylated low-density lipoprotein (cLDL) induced dose-dependent vascular cell injuries which included the proliferation of vascular smooth muscle and endothelial cell death.

Impaired vascular function in ARF and possible molecular mechanisms underlying this impairment have been investigated by means of various experimental methods. Only the end points within the time interval of the blood vessels response, or so-called "alternate steady states" of the processes, were usually considered in these studies. By considering the end points only, we do not have an insight into the process variables between these alternate steady states. The behavior of a blood vessel between the alternate steady states is referred as the transient or dynamic response. In our previous work (Rosic et al. 2008) we developed the experimental model and adequate mathematical procedures, which can be used to describe dynamic response of isolated blood vessels to different stimuli.

In this study we postulated that the transient or dynamic response of blood vessels could be affected during ARF. We also postulated that antioxidants can prevent the changes in dynamic responses of blood vessels in ARF, because all mentioned molecular mechanisms underlying impaired vascular function in ARF (such as AOPP, cLDL, NO,…) are based on increase in oxygen free radicals production. In as much, the recent evidence suggests protective effects of vitamin C on gentamicin-induced nephrotoxicity (Kadkhodaee et al. 2005, 2007).

Materials and Methods

The total number of 35 animals was divided into 3 groups, one of which was used as a sham control. The control group of animals (C-group) received 1 ml/day saline intraperitoneally. The first experimental group (GM-group) of animals received gentamicin (Galenika AD, Belgrade, Serbia) intraperitoneally in a daily dose of 100 $mg \cdot kg^{-1}$. The second experimental group (GMC-group) of animals received gentamicin as the GM-group, and vitamin C in a daily dose of 50 mg. The experimental and control groups were treated over the period of 8 consecutive days. Following the last application, that is 9 days after the beginning of the experiment, all animals were sacrificed. Immediately, 2 ml blood was taken from the aorta for biochemical analysis. Plasma creatinine, blood urea, sodium and potassium concentrations were measured using an automatic biochemical analyzer (A25 biosystem, Barcelona, Spain).

Intraluminal pressure at the constant perfusion flow under different hydrostatic pressure conditions in the isolated perfused blood vessels segments were measured by means of the System for Biomechanical and Functional Tissue Investigations, described in details in our previous work (Rosic et al. 2008).

The pressure transducer is placed at the inlet of the blood vessel. The outlet of the vessel is connected to the two-way tap attached to two tubes filled with perfusion solution, allowing a change of hydrostatic pressure, from H_0 (0 mmHg) to H_1 (60 mmHg), as a step function. When an abrupt change of hydrostatic pressure from H_0 to H_1 occurs, the pressure wave propagates backward and is detected by the pressure transducer. The pressure change detected by transducer depends on elastic properties of the segment between the pressure transducer and two-way tap. Because the only elastic part of this segment is blood vessel (the rest of the segment are rigid tubes) we can assume that the dynamics of pressure change depends only on elastic properties of the blood vessel for an applied hydrostatic level.

Experimental procedure

All experiments were performed according to EU (86/609/EEC) and local ethical guidelines. Wistar rats of both sexes (200–250 g body weight) were killed by cervical dislocation. The segment of the abdominal aorta was rapidly isolated and transferred to the water bath. Glass cannulas with equally matched tip diameters are mounted at proximal (inflow) and distal (outflow) ends of the blood vessel. The proximal end of the artery is tied at the place on the proximal cannula with a silk thread, and the lumen is perfused with Krebs-Ringer physiological solution (KRS), using a peristaltic pump at 9 $ml \cdot min^{-1}$. The perfusate was continuously bubbled with a 95% O_2, and 5% CO_2, with the pH adjusted to 7.4 at 37°C. The distal end of the artery is then tied onto the distal cannula. The distal cannula was connected to the two-way tap attached to two tubes filled with perfusion solution, allowing a change of hydrostatic pressure from H_0 (0 mmHg) to H_1 (about 60 mmHg). The exterior of the vessel was also perfused with KRS from a reservoir using a peristaltic pump at 3 $ml \cdot min^{-1}$, on 37°C and aerated with the same gas mixture as the lumen of artery.

The artery was stretched to its approximate *in vivo* length using a micrometer (2–2.5 cm). The total time duration of our experiments was within the experimental time in the most frequently used procedures on the isolated blood vessels.

Experimental protocol

As described above, the blood vessels segment was dissected from the rat abdominal aorta and placed into the water bath. Following the equilibration period (20–30 min), the segment was treated by increasing hydrostatic pressure from H_0 to H_1. This protocol was repeated 3–5 times for each segment ($n = 5$) and a resting period of several minutes (usually 15

min) was allowed between two activities. The development of pressure was recorded on a computer, continuously using the system described above.

After this, we added acetylcholine (final molar concentrations in the perfusion fluid were 10 μmol l^{-1}) continuously into the perfusion system with micro infusion pump at 100 μl min^{-1}. The same protocol (in the presence of acetylcholine) from H_0 to H_1 hydrostatic pressure at constant perfusion flow was repeated 3–5 ($n = 5$).

Experimentally recorded dependence of pressure on time was fitted using an exponential mathematical function:

$$y = b_1\left(1 - e^{-b_2 x}\right) \tag{1}$$

where y is the pressure (in mmHg) and x is the time (in seconds). Also, b_1 and b_2 are the coefficients of this relationship: b_1 has units of pressure, and b_2 has units of T^{-1}.

This function is shown in Fig. 1A as the pressure vs. time curve. The constant b_1 represents the maximum developed pressure, i.e. the pressure corresponding to the alternate steady state.

We introduce a dominant time constant (T) as the time value corresponding to the cross section point between the asymptote of the exponential curve and the tangent of the exponential curve at the zero point. This constant follows from the Eq. (1):

$$T = 1/b_2 \tag{2}$$

We consider that the alternate steady state is reached for time $t = 5T$, because in this case, $e^{-t/T} = e^{-5} \approx 0$, and $y \approx b_1$.

Then, to define dynamic properties of the blood vessels, we introduced a parameter of the comparative pressure dynamics (P_d). This parameter is defined as the integral of the difference between two fitted curves, normalized with respect to the applied hydrostatic pressure (H):

$$P_d = \frac{1}{H}\int_0^{\infty}\left\{\left[b_1\left(1 - e^{-b_{2b}x}\right)\right] - \left[b_1\left(1 - e^{-b_{2a}x}\right)\right]\right\}dx \tag{3}$$

where b_{2a} is the coefficient of the first curve (control curve) and b_{2b} is the coefficient of the second curve (test curve). Control curve is the pressure-time relation in the absence of acetylcholine and test curve is the pressure-time relation in the presence of acetylcholine. Here b_1 is considered the same for both functions under the integral, which follows from the results (see below). The solution of the Eq. (3) is:

$$P_d = \frac{b_1}{H}\frac{b_{2b} - b_{2a}}{b_{2a} \times b_{2b}} \tag{4}$$

The calculated P_d is the area between the test and control curves and it is normalized to become a dimensionless quantity (Fig. 1B). Positive value of P_d indicates the shift of the test curve to the left and faster development of maximal pressure (alternate steady state). In contrary, negative value of the P_d indicates the shift of the test curve to the right and slower development of maximal pressure.

Further, we introduce the total P_d (TP_d) as the area under the test and/or control curves which can be calculated from the equation:

$$TP_d = b_1\left(x + \frac{e^{-b_2 x}}{b_2}\right) - \frac{b_1}{b_2} \tag{5}$$

where TP_d is total pressure dynamics and $x = 5T$.

Statistical analysis

Data are presented as means ± S.E.M. (standard error of the mean). Comparison between groups was analyzed by one-way analysis of variance followed by a Tukey's *post hoc* test

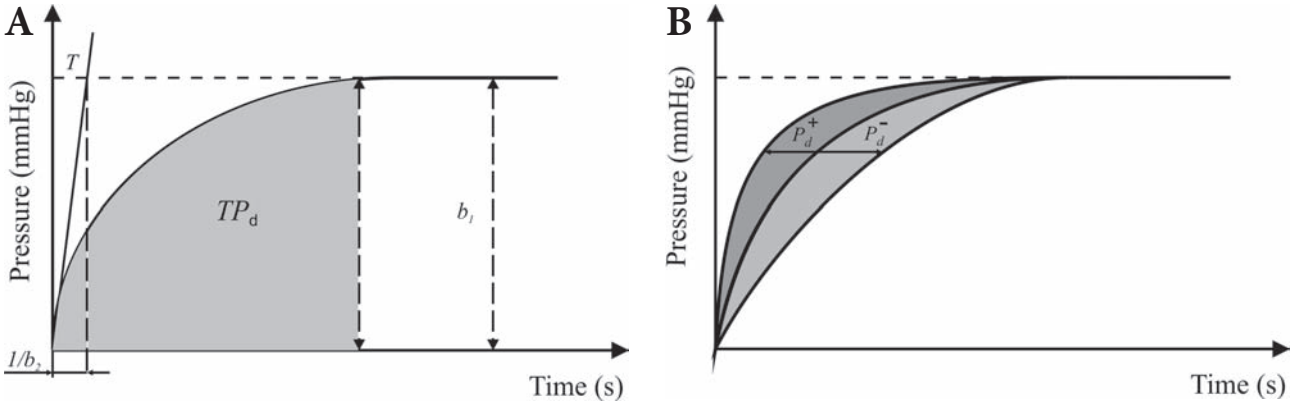

Figure 1. A. Exponential curve $y = b_1\ (1 - e^{-b2x})$ and the corresponding TP_d area. **B.** Three exponential curves and the corresponding positive (P_d^+) and negative (P_d^-) values of the parameter P_d (pressure dynamic).

Table 1. Concentrations of Na^+, K^+, urea and creatinine in control and experimental groups

Parameter	C-group	GM-group	GMC-group
Na^+ (mEq l^{-1})	149.33 ± 4.49	144.46 ± 6.07	147.71 ± 5.2
K^+ (mEq l^{-1})	5.9 ± 0.39	4.36 ± 0.88*	5.52 ± 0.76
Urea (μmol l^{-1})	6.86 ± 0.58	49.24 ± 8.79*	21.48 ± 3.36
Creatinine (μmol l^{-1})	64.2 ± 7.96	488.2 ± 62.85*	330.7 ± 38.5

Values are represented as mean ± S.E.M. * significantly different values.

(multiple comparison procedure). Also, data were analyzed using Student's t-test, where $p < 0.05$ was considered as statistically significant.

Results

In Table 1 we present serum levels of sodium, potassium, blood urea and creatinine in C-group, GM-group and GMC-group of animals.

Levels of blood urea and creatinine in GM-group were significantely elevated in comparison with the C-group and GMC-group. Serum potassium concentration in GM-group of animals was significantely decreased when compared to C-group and GMC-group. Concentration of sodium in serum of GM-group was lower than in C-group and GMC-group, but without statistical significance.

The experimental pressure-time curves were analyzed using a method described in the Materials and Methods section and the values of $5T$, b_1 and b_2 coefficients of the fitted experimental data (coefficient of correlation was 0.979 ± 0.0048) in the control and experimental groups are shown in Table 2. Our data indicate that coefficient b_2 in GM-group is significantly higher when compared to C-group and GMC-group. On the other hand, the $5T$ value in GM-group is significantly lower in comparison with the C-group and GMC-group.

To describe the pressure dynamic properties of the blood vessels, the parameters P_d and TP_d were calculated (see Eqs. (4) and (5)) as shown in Table 3. Our data indicate that the P_d as well as TP_d coefficient in GM-group is significantly lower when compared to C-group and GMC-group. There is no difference of these coefficients in GMC-group in comparison with C-group.

Table 2. Calculated mathematical parameters (b_1 and b_2) in the control and experimental groups, and time within which the maximal pressure is developed (taken as $5T$)

Parameter	C-group	GM-group	GMC-group
b_1	61.02 ± 0.9	61.89 ± 2.26	59.95 ± 1.3
b_2	0.71 ± 0.05	0.89 ± 0.03*	0.68 ± 0.04
$5T$	8.07 ± 1.7	5.64 ± 0.18*	7.45 ± 1.2

Values are represented as mean ± S.E.M. * significantly different values.

Table 3. Calculated values of P_d and TP_d in control and experimental groups

Parameter	C-group	GM-group	GMC-group
P_d	–0.11 ± 0.01	–0.08 ± 0.01*	–0.12 ± 0.02
TP_d	426.9 ± 95.5	284.28 ± 13.53*	618.59 ± 68.99

Values are represented as mean ± S.E.M. * significantly different values.

Discussion

In this paper we use a new approach (Rosic et al. 2008) to *ex vivo* blood vessel experiments in which not only the end points of vessels response within the time interval of dynamic loading is considered, but also dynamics of this response. The end points of blood vessel response to some drugs, for instance, could be the same but dynamic responses could be different. This will lead to different dynamic of shear stress and other biomechanical properties of the blood vessel, and the effects of these drugs will be different even they produce the same relaxation or constriction at alternate steady states. Although we may know the effects of some drug to blood vessel smooth muscle, manifested through constriction or relaxation, we cannot precisely predict the time history of relevant biomechanical variables in between alternate steady states. In order to elucidate the mentioned phenomena, we introduced a new experimental design. This design is created to measure the changes in pressure when an abrupt change of pressure occurs at the vessel outlet, by applying various hydrostatic levels, as step functions. We evaluate the time history of the pressure changes in-between alternate steady states, represented by the pressure-time curves. Further, we describe the dynamic behavior of the vessel, by proposing a mathematical relation in which the parameters are evaluated through the pressure-time curves relationships with the

experimental data. In the simple exponential mathematical function, the two coefficients have physical meaning: the first coefficient, in this function, b_1, numerically describes the maximal developed pressure, i.e. the pressure corresponding to the alternate steady state; while the second coefficient, b_2, is relevant for the description of the vessel transition response between alternate steady states. Also, in order to define dynamic behavior of the blood vessel in a quantitative manner, we introduced two parameters: P_d and TP_d (Eqs. (4) and (5)). In our previous work (Rosic et al. 2008) we demonstrated that these coefficients are very sensitive parameters to the conditions of the blood vessel dynamics.

Levels of blood urea, creatinine, potassium and sodium in GM-group, confirmed the well known pattern of gentamicin nephrotoxicity. Our results show that levels of blood urea and creatinine in GM-group were significantly elevated in comparison with the GMC-group. Also, serum potassium concentration in GM-group of animals was significantly decreased when compared to GMC-group. These findings are in accordance with previous reports (Kadkhodaee et al. 2005, 2007) confirming protective effects of antioxidants (including vitamin C) in gentamicin-induced nephrotoxicity.

Our results show that, in control and experimental groups of animals, there is no difference in b_1 coefficient. This means that the maximal pressure is the same in all groups of animals. The maximal pressure under the constant flow conditions only depends on the hydrostatic level in our experimental design, and thus the alternate steady state could not be affected. In the contrary, the b_2 coefficient in GM-group is significantly higher when compared to C-group and GMC-group, indicating alteration in dynamic response of blood vessels during the change of pressure in gentamicin-treated animals. The time interval within which the maximal pressure (alternate steady state) is developed decreases from 8.07 s in C-group to 5.64 s in GM-group, showing a faster pressure change in gentamicin-treated animals. The $5T$ value in GM-group is significantly lower in comparison with the GMC-group, indicating vitamin C-induced slowdown of pressure change, back to the control values. Calculated values of TP_d coefficients which quantitatively describe the pressure dynamic properties, confirm the alteration in dynamic response of blood vessels during the change of pressure in gentamicin-treated animal and beneficial effects of vitamin C administration.

P_d in all three groups of animals has a negative values indicating the shift of the exponential curves to the right in the presence of acetylcholine. This means that acetylcholine-induced vasodilatation leads to slower development of maximal pressure in all investigated animals. Our data indicate that the P_d coefficient in GM-group is significantly lower when compared to C-group suggesting reduced vasodilatatory response in gentamicin-treated animals. This findings are in acordance with recent investigation of coronary vessel reactivity in ARF (Kingma et al. 2006). The P_d value in GM-group is significantly lower in comparison with the GMC-group, indicating vitamin C-induced restoration of vasodilatatory response back to the control values.

As mentioned in Introduction section, the molecular mechanisms underlying gentamicin-induced renal failure include increased free radicals production (Kays et al. 1991; Ben Ismail et al. 1994; Ata Secilmis et al. 2005). On the other hand, free radicals are also, involved in impaired vascular function in ARF, partly by promoting AOPP as mediators of oxidative stress (Shuangxiu et al. 2005). From this point of view, antioxidants (including vitamin C) may have both, protective effects on gentamicin-induced nephrotoxicity (Kadkhodaee et al. 2005, 2007), as well as, direct protective effects on impaired vascular function in ARF. In addition, vitamin C-induced decreased level of blood urea in ARF may lead to lower production of cLDL and consequent prevention of vascular impairment.

References

Ata Secilmis M., Karatas Y., Yorulmaz O., Buyukafsar K., Singirik E., Doran F., Inal T. C., Dikmen A. (2005): Protective effect of L-arginine intake on the impaired renal vascular responses in the gentamicin-treated rats. Nephron Physiol. **100**, 13–20

Ben Ismail T. H., Ali B. H., Bashir A. A. (1994): Influence of iron, deferoxamine and ascorbic acid on gentamicin-induced nephrotoxicity in rats. Gen. Pharmacol. **25**, 1249–1252

Bennet W. M. (1986): Comparison of cyclosporine nephrotoxicity with aminoglycoside nephrotoxicity. Clin. Nephrol. **25**, 1515–1521

Bennet W. M., Mela-Riker L. M., Hougton D. C., Gilbert D. N., Buss W. C. (1988): Microsomal protein synthesis inhibition: an early manifestation of gentamicin nephrotoxicity. Am. J. Physiol. **255**, F265–269

Can C., Sen S., Boztok N., Tuglular I. (2000): Protective effect of oral L-arginine administration on gentamicin-induced renal failure in rats. Eur. J. Pharmacol. **390**, 327–334

Kadkhodaee M., Khastar H., Faghihi M., Ghaznavi R., Zahmatkesh M. (2005): Effects of co-supplementation of vitamins E and C on gentamicin-induced nephrotoxicity in rats. Exp. Physiol. **90**, 571–576

Kadkhodaee M., Khastar H., Arab H. A., Ghaznavi R., Zahmatkesh M., Mahdavi-Mazdeh M. (2007): Antioxidant vitamins preserve superoxide dismutase activities in gentamicin-induced nephrotoxicity. Transplant. Proc. **39**, 864–865

Kays S. E., Crowwell W. A., Johnson M. A. (1991): Iron supplementation increase gentamicin nephrotoxicity in rats. J. Nutr. **121**, 1869–1875

Kingma J. G. Jr., Vincent C., Rouleau J. R., Kingma I. (2006): Influence of acute renal failure on coronary vasoregulation in dogs. J. Am. Soc. Nephrol. **17**, 1316–1324

Kraus L. M., Kraus A. P. (2001): Carbamylation of amino acids and proteins in uremia. Kidney Int. **78**, S102–107

Ok E., Basnakian A., Apostolov E. O., Barri Y. M., Shah S. V. (2005): Carbamylated low-density lipoprotein induces death of endothelial cells: a link to atherosclerosis in patients with kidney disease. Kidney Int. **68**, 173–178

Olbricht C. J., Fink M., Gutjahr E. (1991): Alterations in lysosomal enzymes of the proximal tubule in gentamicin nephrotoxicity. Kidney Int. **39**, 639–646

Rivas-Cabanero L., Rodriguez-Barbero A., Arevalo M., Lopez-Novoa J. M. (1995): Effect of NG-nitro-L-arginine methyl ester on nephrotoxicity induced by gentamicin in rats. Nephron **71**, 203–207

Rosic M., Pantovic S., Rankovic V., Obradovic Z., Filipovic N., Kojic M. (2008): Evaluation of dynamic response and biomechanical properties of isolated blood vessels. J. Biochem. Biophys. Methods **70**, 966–972

Shuangxiu C., Liying L., Xueying S., Yuhui L., Tao S. (2005): Captopril restores endothelium-dependent relaxation induced by advanced oxidation protein products in rat aorta. J. Cardiovasc. Pharmacol. **46**, 803–809

Stojiljkovic N., Mihailovic D., Veljkovic S., Stojiljkovic M., Jovanovic I. (2008): Glomerular basement membrane alterations induced by gentamicin administration in rats. Exp. Toxicol. Pathol. **60**, 69–75

Witko-Sarsat V., Friedlander M., Khoa T. N., Capeilere-Blandin C., Nguyen A. T., Canteloup S., Dayer J.-M., Jungers P., Drueke T., Descamps-Latscha B. (1998): Advanced oxidation protein products as a novel mediators of inflammation and monocyte activation in chronic renal failure. J. Immunol. **161**, 2524–2532

Effects of hydroperoxides on contractile reactivity and free radical production of porcine brain arteries

Darco Stevanovic[1,2], Dayong Zhang[2], Anneke Blumenstein[2], Dragan Djuric[1] and Helmut Heinle[2]

[1] *Institute of Physiology, University of Belgrade, Serbia*
[2] *Institute of Physiology, University of Tübingen, Germany*

Abstract. Hydroperoxide-induced oxidative stress is assumed to be involved in vasospasm of cerebral arteries after subarachnoid hemorrhage. In order to study underlying mechanisms the effects of H_2O_2 and *tert* butylhydroperoxide on contractile functions as well as on free radical production of anterior cerebral artery from pig were investigated. The hydroperoxides increased in a similar dose-dependent arterial contraction, however, the underlying mechanisms involve impairment of endothelial-dependent relaxation as well as of smooth muscle contractile function as shown by experiments with inhibited endothelial NO-synthesis. Determination of lucigenine detectable O_2^--release showed rather low values with both hydroperoxides, whereas, in comparison, the unspecific luminol-dependent chemi-luminescence was increased up to 1000-fold, especially by H_2O_2. In conclusion it was shown that application of the hydroperoxides resulted in increased contraction of cerebral arteries, yet that the underlying mechanisms altering function of endothelial and smooth muscle cells need further exploration.

Key words: Brain arteries — Oxidative stress — Arterial contraction — Endothelium-dependent relaxation — Free radical production

Introduction

Cerebral vasospasm after subarachnoid hemorrhage (SAH) is a severe complication often responsible for death or strong impairment of brain function of the patients (Janjua and Mayer 2003). Its pathogenesis is still not completely understood, but evidence is provided that the underlying mechanisms are caused or at least accompanied by oxidative stress (Sonobe and Suzuki 1978; Gutteridge 1986; Braughler and Hall 1989; Gaetani et al. 1998; Janjua and Mayer 2003; Liu et al. 2007). Besides the activation of leukocytes producing reactive oxygen species (mainly O_2^-) *via* the NADPH-oxidase reaction, a dominant source of superoxide anion (O_2^-) is also found in the autoxidation of hemoglobin present in the subarachnoid space. Since by interaction with transition metals like Fe^{2+} the Fenton reaction will occur, different reactive species and degradation products like OH radical, H_2O_2, lipid peroxides, malondialdehyde will be generated in the extravasal compartment (Sano et al. 1980; Polodori et al. 1997; Kaynar et al. 2005). These reactive compounds were shown to induce contraction in different arteries of various species (Pelaez et al. 2000; Gao and Lee 2001; Zhang 2007).

Other explanations for vasospasm derive from the fact that O_2^- or ferrous hemoglobin can react with or bind to NO thus reducing the bioavailability of this endothelial relaxing factor (Pluta et al. 2001; Treggiari-Venzi et al. 2001; Janjua and Mayer 2003).

The importance of oxidative stress for cerebral vasospasm is supported also from the finding that pharmacological antioxidants or upregulation of antioxidative enzymes reduce the occurrence of peroxidative degradation products and vasospasm (Treggiari-Venzi et al. 2001; McGirt et al. 2002; Endo et al. 2007).

In order to characterize further mechanisms related to cerebral vasospasm we were interested to study the effects of oxidative stress induced by H_2O_2 and *tert* butylhydroperoxide (*tert* BHP) on serotonin (5HT)-stimulated contractions and free radical productions of anterior cerebral artery from pig brain.

Correspondence to: Helmut Heinle, Institute of Physiology, University of Tübingen, Gmelinstr. 5, 72076 Tübingen, Germany
E-mail: helmut.heinle@uni-tuebingen.de

Materials and Methods

Arterial samples

Pig brains were delivered from a local slaugther house within 3 h after death of the animals. The anterior part of the cerebral artery was excised under an operation microscope, and cleaned from blood and adhering tissue. Ring preparations (4 mm long) were dissected and used for contractions measurements and detection of free radicals, respectively.

Contraction measurement

The arterial rings were mounted in a thermostated (37°C) organ bath perfused by Tyrode solution, which allowed registration of contraction forces under isometric conditions as already described (Wagner et al. 2000). After prestretching the sample to 3 mN and equilibration for at least 30 min until a stable tone was achieved, contractions were evoked by application of 5HT (10 µmol/l) to the Tyrode solution.

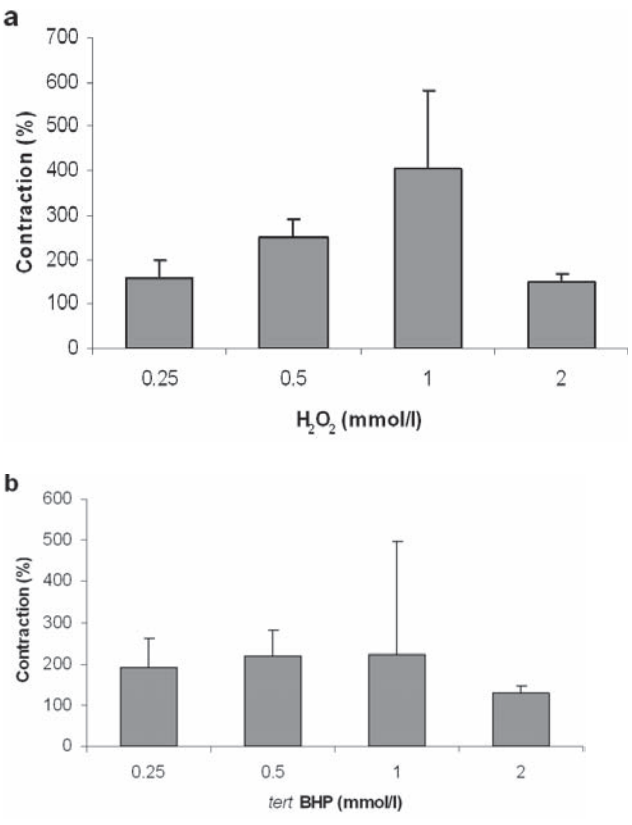

Figure 1. Effects of H_2O_2 (a) and *tert* butylhydroperoxide (*tert* BHP) (b) on serotonin (5HT)-induced contraction: dose response relation. The bars represent mean values ± SD, (n = 4–6). Absolute force of the control contraction induced by 10 µmol/l 5HT = 2.8 ±1.2 mN.

Generally, this type of vessels react under these conditions with a long lasting tonic contraction, the maximal force was evaluated. After wash out of the agonist, the stimulation with 5HT was repeated in the presence of H_2O_2 or *tert* BHP (final concentrations 0.25, 0.5, 1.0, 2.0 mmol/l). Each peroxide application was preceded by a control stimulation, a maximum of 3 applications were performed per arterial sample. The evaluated forces were related to the individual maximal 5HT-induced contraction of the corresponding specimen.

In order to estimate endothelial-dependent effects, in a second series of experiments 5HT was applied in the presence of 50 µmol/l nitroarginine (NA) (this antagonist was preperfused 10 min before 5HT-stimulation). Again, after wash out of 5HT, the stimulation was repeated with H_2O_2 or *tert* BHP (0.25 mmol/l) in the presence of NA (50 µmol/l). The effects on the contraction forces were evaluated and expressed in relation to the control contraction.

Measurement of free radical production

In order to characterize oxidative stress induced by the hydroperoxides, free radical generation was measured by chemiluminescence in a Biolumat 9600 (Berthold, Wildbad, Germany). Luminol and lucigenine were used as radical sensitive dyes and applied in separate incubation experiments. The arterial samples as prepared for the contraction experiments were incubated in 500 µl of Tyrode solution in the precence of the dye (0.1 mmol/l), and basal chemiluminescence was measured for 10 min. Thereafter H_2O_2 or *tert* BHP were added (final concentrations 0.05, 0.125, 0.25, 0.5, 1.0 mmol/l) and chemiluminescence was measured for another 10 min. Chemiluminescence, expressed as integrated counts per 10 min, was related to the dry weigth of the sample. The spontaneous chemiluminescence of the peroxide with the dyes was respectively considered.

Results

Effects of H_2O_2 and tert BHP in intact arteries

Fig. 1 shows that both hydroperoxides evoked similar dose-dependent effects on 5HT-induced contractions in the brain arteries: in concentrations below 1 mmol/l the standard contraction was increased up to 3–4-fold by H_2O_2 and up to 2-fold by *tert* BHP. At 2 mmol/l, inhibition was found with both peroxides. The further experiments were conducted with peroxide concentration of 0.25 mmol/l.

Effects of endothelium

When the preparations of anterior cerebral artery were stimulated by 5HT, no acetylcholine-induced, endothelium-

dependent vasorelaxation could be found (experiments were not described). However, effects of endothelium could be demonstrated when the stimulation occured in the precence of 50 µmol/l NA: under this condition a 3–4-fold increase in contraction force was found, showing that 5HT stimulates both smooth muscle contraction and endothelial NO production (Fig. 2, left panel).

In contrast, when the peroxides were applied in the presence of NA, 5HT induced a significantly decreased contraction force when compared with the NA effect without oxidative stress (Fig. 2, middle and right panel). Additionally, the figure shows again similar effects of both peroxides on arterial contractility under these conditions. These results suggest that peroxide-induced oxidative stress can modulate the contraction of brain arteries by inhibition of both smooth muscle contractility as well as endothelium-dependent relaxation.

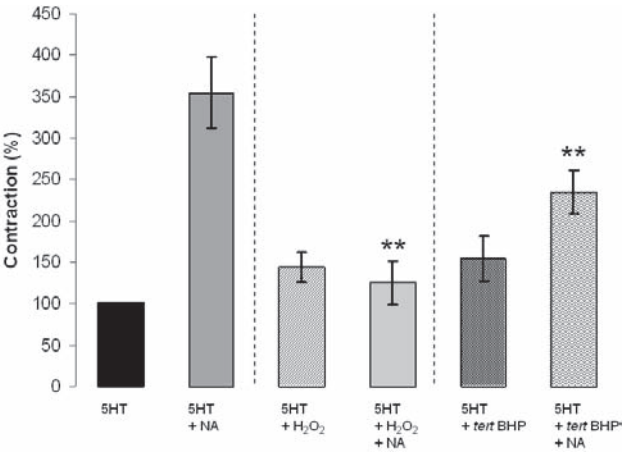

Figure 2. Effects of H_2O_2 and *tert* butylhydroperoxide (*tert* BHP) on serotonin (5HT)-induced contraction: importance of endothelium. Nitroarginine (NA) 50 µmol/l, H_2O_2 and *tert* BHP 250 µmol/l. The bars represent mean values ± SD, (n = 4–6), ** $p < 0.01$ compared with 5HT+NA, t-test.

Effects on free radical production

The consequences of hydroperoxide evoked oxidative stress on generation of free radicals were determined with the chemiluminescence dyes luminol and lucigenine. Table 1 shows that generally, the chemiluminescence is very much higher with H_2O_2, especially, when luminol is used as unspecific indicator of free radicals. However, the O_2^- specific dye lucigenine indicates similar chemiluminescence with H_2O_2 or *tert* BHP suggesting that O_2^- are formed with similar rates.

Discussion

Since 5HT is asssumed to be involved in vasospasm after SAH (Janjua and Mayer 2003) and since it evoked reproducible contractions in cerebral artery *in vitro,* we were interested in effects of oxidative stress induced by H_2O_2 and *tert* BHP on 5HT-induced contractions and free radical production.

Regarding the cellular metabolism of both peroxides, it is obvious that they induce different forms of oxidative stress: H_2O_2 is decomposed very effectively by catalase, but is a partner of the Fenton reaction to produce OH and different other radicals, *tert* BHP is mainly a substrate of glutathione peroxidase thus altering especially the sulfide-disulfide status of the cell.

Nevertheless, in the contraction experiments both peroxides revealed similar effects with similar dose response relations. The increase in contraction force, as seen in peroxide concentrations up to 1 mmol/l, could be a result of a direct stimulating effect on contractile apparatous of smooth muscle, e.g. by increasing cytoplasmic Ca^{2+}. Similar effects of H_2O_2 were also shown in other arterial preparations from various species and different parts of the arterial tree (Gao and Lee 2001; Blumenstein 2004; Gil-Longo and Gonzalez-Vazquez 2005; Zhang 2007). Another explanation

Table 1. Effects of H_2O_2 and *tert* BHP on reactive oxygen species production

	Luminol		Lucigenin	
Peroxide concentration (mmol/l)	H_2O_2 (counts per 10 min/mg)	*tert* BHP (counts per 10 min/mg)	H_2O_2 (counts per 10 min/mg)	*tert* BHP (counts per 10 min/mg)
0.05	300 ± 105	35 ± 20	220 ± 85	450 ± 75
0.125	19735 ± 6330	60 ± 40	780 ± 420	435 ± 185
0.25	164106 ± 42780	155 ± 95	1800 ± 190	930 ± 85
0.5	230900 ± 95320	1600 ± 1250	5825 ± 530	2890 ± 355
1.0	420870 ± 137680	8720 ± 5210	4260 ± 1590	3100 ± 1620

The values are mean values ± SD, n = 3–4.

for contraction stimulation could be that hydroperoxides inhibit endothelial-induced relaxation, thus increasing the resulting contraction force as also suggested for cerebral vasospams (Pluta et al 2001; Treggiari-Venzi et al. 2001; Janjua and Mayer 2003).

Yet, the results presented here show even more complex interactions: under blockade of endothelial NO synthesis by NA, the response to 5HT was 3–4-fold increased, indicating that the reaction of the intact vessel to this agonist was a moderate contraction as the sum of a strong stimulation of smooth muscle to contract and an additional stimulation of endothelial cells to produce the relaxing factor NO. When additionally oxidative stress was applied, the contraction stimulating effect of 5HT was significantly diminished. This means that in brain arteries rather low concentrations of hydroperoxides (0.25 mmol/l) can also lead to inhibited contractility, which is in contrast to all other samples of different arteries we investigated (Blumenstein 2004; Zhang 2007). Wether this mechanism is mediated by effects on ion channels, second messengers, or on the contractile proteins directly remains to be elucidated.

Under the pathological conditions of SAH, one can therefore assume that oxidative stress can induce different pathogenetic mechanisms, yet, maintenance or recovery of endothelial function is important in any case.

It is interesting to note that in coronary arterioles from pig and aorta from rat various signaling pathways were described to be effected by H_2O_2 (Thengchaisri and Kuo 2003; Gil-Longo and Gonzalez-Vazquez 2005). These include endothelium-dependent and -independent mechanisms which are related to the activation of cyclooxygenase as well as of potassium channels. Peroxide-induced hyperpolarisation of the membrane potential could be a direct relaxant effect in smooth muscle. In brain vessels these mechanisms have to be established by additional studies.

The different metabolism of the both hydroperoxides applied is clearly reflectd by the results of the free radical measurements. Using dye-enhanced chemiluminescence for their detection, the results showed that amount and nature of the generated free radicals are quite different using H_2O_2 and *tert* BHP, a phenomen also found e.g. in mouse aorta (Zhang 2007). Especially with H_2O_2 and the unspecific dye luminol, a high rate of free radical production was detectable, probably due to chain reactions of Fenton type. Using the O_2^- specific dye lucigenine, similar low rates were found with both peroxides. This could be due to a peroxide-dependent stimulation of NADPH oxidases present in the vascular wall generating O_2^- (Li et al. 2007). These results suggest that not the total rate of free radicals but perhaps the endogenous O_2^- production is responsible for hydroperoxide-induced effect on contractility of a. cerebri anterior.

In conclusion, the study shows that in 5HT-stimulated a. cerebri anterior there is an explicit oposing balance between smooth muscle contraction and endothelial-dependent relaxation.

Oxidative stress as induced by hydroperoxides can disturb this balance by inhibiting the endothelial function and also by impairment of smooth muscle contraction. Severe oxidative stress may induce smooth muscle relaxation probably by cellular damage of smooth muscle (Gil-Longo and Gonzalez-Vazquez 2005), however, under moderate conditions enhanced contractions will result. Therefore maintenance of endothelial function seems to be important to prevent or decrease vasospasm in cerebral arteries.

Acknowledgement. D. S. received a grant from Deutscher Akademischer Auslandsdienst) for contributing to this study.

References

Blumenstein A. (2004): Oxidative stress and vascular function: studies on the effect of hydroperoxides on contraction and endothelial function in arteries. (Thesis), Faculty of Chemistry and Pharmacy, Eberhardt-Karls University, Tuebingen (in Germany)

Braughler J. M., Hall E. D. (1989): Central nervous system trauma and stroke: I. Biochemical considerations for oxygen radical formation and lipid peroxidation. Free Radic. Biol. Med. **6,** 289–301

Endo H., Nito C., Kamada H., Yu F., Chan P. H. (2007): Reduction in oxidative stress by superoxide dismutase overexpression attenuates acute brain injury after subarachnoid hemorrhage via activation of Akt/glycogen synthase kinase-3beta survival signaling. J. Cereb. Blood Flow Metab. **27,** 975–982

Gaetani P., Pasqualin A., Rodriquez Y., Baena R., Borasio E., Marzatico F. (1998): Oxidative stress in the human brain after subarachnoid hemorrhage. J. Neurosurg. **89,** 748–754

Gao Y. J., Lee R. M. (2001): Hydrogen peroxide induces a greater contraction in mesenteric arteries of spontaneously hypertensive rats through thromboxane A(2) production. Br. J. Pharmacol. **134,** 1639–1646

Gil-Longo J., Gonzalez-Vazquez C. (2005): Characterization of four different effects elicited by H2O2 in rat aorta. Vascul. Pharmacol. **205,** 128–138

Gutteridge J. M. C. (1986): Iron promoters of the Fenton reaction and lipid peroxidation can be released from haemoglobin by peroxides. FEBS Lett. **201,** 291–295

Janjua N., Mayer S. A. (2003): Cerebral vasospasm after subarachnoid hemorrage. Curr. Opin. Crit. Care **9,** 113–119

Kaynar M. Y., Tanriverdi T., Kemerdere R., Atukeren P., Gumustas K. (2005): Cerebrospinal fluid superoxide dismutase and serum malondialdehyde levels in patients with aneurysmal subarachnoid hemorrhage:preliminary results. Neurol. Res. **27,** 562–567

Li W. G., Miller F. J. J, Zhang H. J., Spitz D. R., Oberley L. W., Weintraub N. L. (2001): H_2O_2-induced O_2^- production

by a non-phagocytic NAD(P)H oxidase causes oxidant injury. J. Biol. Chem. **276,** 29251–29256

Liu S., Tang J., Ostrowski R. P., Titova E., Monroe C., Chen W., Lo W., Martin R., Zhang J. H. (2007): Oxidative stress after subarachnoid hemorrhage in gp91phox knockout mice. Can. J. Neurol. Sci. **34,** 356–361

McGirt M. J., Parra A., Sheng H., Higuchi Y., Oury T. D., Laskowitz D. T., Pearlstein R. D., Warner D. S. (2002): Attenuation of cerebral vasospasm after subarachnoid hemorrhage in mice overexpressing extracellular superoxide dismutase. Stroke **33,** 2317–2323

Pelaez N. J., Braun T. R., Paul R. J., Meiss R. A., Packer C. S. (2000): H_2O_2 mediates Ca^{2+} and MLC(20) phosphorylation-independent contraction in intact and permeabilized vascular muscle. Am J. Physiol., Heart Circ. Physiol. **276,** H1185–1193

Pluta R. M., Thompson B. G., Afshar J. K., Boock R. J., Iuliano B., Oldfield E. H. (2001): Nitric oxide and vasospasm. Acta Neurochir. (Wien) **77,** 67–72

Polodori M. C., Frei B., Rordorf G., Ogilvy C. S., Koroshetz W., Beal M. F. (1997): Increased levels of plasma cholesteryl ester hydroperoxides in patients with subarachnoid hemorrhage. Free Radic. Biol. Med. **23,** 762–767

Sano K., Asano T., Tanishima T., Sasaki T. (1980): Lipid peroxidation as a cause of cerebral vasospasm. Neurol. Res. **2,** 253–272

Sonobe M., Suzuki J. (1978): Vasospasmogenic substance produced following subarachnoid hemorrhage, and its fate. Acta Neurochir. (Wien) **44,** 97–106

Thengchaisri N., Kuo L. (2003): Hydrogen peroxide induces endothelium-dependent and independent coronary arteriolar dilation: role of cyclooxygenase and potassium channels. Am. J. Physiol., Heart Circ. Physiol. **285,** H2255–2263

Treggiari-Venzi M. M., Suter P. M., Romand J.-A. (2001): Review of medical prevention of vasospam after aneurysmal subarachnoid hemorrhage: a problem of neurointensive care? Neurosurgery **48,** 249–262

Wagner C. A., Huber S. M., Wärntges S., Zempel G., Kaba N. K., Fux R., Orth N., Busch G. L., Waldegger S., Lambert I., Nilius B., Heinle H., Lang F. (2000): Effect of urea and osmotic cell shrinkage on Ca^{2+} entry and contraction of vascular smooth mucle cells. Pfügers. Arch. **440,** 295–301

Zhang D. (2007): Hydroperoxide-induced oxidative stress in the arterial wall: pharmacological characterization of the effects on arterial contractility. (Thesis), Faculty for Chemistry and Pharmacy, Eberhard-Karls University, Tuebingen

Human platelets perfusion through isolated guinea-pig heart: the effects on coronary flow and oxidative stress markers

Slobodan Novokmet[1], Vladimir Lj. Jakovljevic[2], Slobodan Jankovic[3], Goran Davidovic[4], Nebojsa Andjelkovic[4], Zvezdan Milanovic[5] and Dragan M. Djuric[6]

[1] *Department of Pharmacy, Faculty of Medicine, University of Kragujevac, Serbia*
[2] *Department of Physiology, Faculty of Medicine, University of Kragujevac, Serbia*
[3] *Department of Pharmacology, Faculty of Medicine, University of Kragujevac, Serbia*
[4] *Internal Clinic, CC Kragujevac, Faculty of Medicine, University of Kragujevac, Serbia*
[5] *Department of Physiology, Faculty of Medicine, Kosovska Mitrovica, Serbia*
[6] *Institute of Medical Physiology, School of Medicine, University of Belgrade, Serbia*

Abstract. Present study was designed to evaluate effect of perfusion with human platelets reach plasma (PRP) on coronary flow (CF) and oxidative stress markers in coronary vascular bed of the isolated guinea-pig heart. In coronary venous effluent the following oxidative stress markers were estimated: nitrite as a measure of nitric oxide (NO) production, superoxide anion (O_2^-), and index of lipid peroxidation (TBARS). Isolated guinea-pig hearts (n = 6, b.m. 250–300 g) were perfused according to a Langendorff's technique at different (30, 70, and 120 cmH_2O) coronary perfusion pressures (CPP). Samples were collected at control conditions and during perfusion with platelets rich plasma (PRP) obtained either from healthy volunteers or from patients with acute myocardial infarction (PRP (AMI)) with/or without previous inhibition of NO synthase (NOS) by Nω-nitro-L-arginine monomethyl ester (L-NAME, 30 μmol/l). PRP and PRP (AMI) perfusion induced reduction of CF and all evaluated oxidative stress parameters. The reduction of CF was more potentiated in PRP (AMI) as in PRP group, while oxidative stress parameters where significantly decreased only in PRP (AMI). In addition, previous blockade of NOS by L-NAME potentiated these effects only in PRP (AMI) group. It can be concluded that non-activated and activated platelets interact with coronary endothelium in similar way, with more significant influence of activated platelets on CF and oxidative stress markers.

Key words: Platelets reach plasma — Guinea-pig heart — Coronary flow — Oxidative stress

Introduction

Platelet-endothelium interaction represents a common mechanism in normal circulating blood, as well as mechanism of homeostasis regulation (Furie et al. 2008). Activation of platelets is tightly regulated, thus, oxidative stress can alter platelets responses and inhibit their function (Freedman 2008). The importance of platelet-vessel wall interactions in ischemic heart disease has been proved by certain studies demonstrating a protective effect of some antiplatelet drugs in patients with unstable angina and with myocardial infarction (Tantry et al. 2005; Scharf et al. 2008). Although there may be several distinct causes of myocardial ischemia, there is good evidence for platelet involvement in some of its main clinical manifestations (Takaya et al. 2005; Scharf 2008). Activated platelets in acute myocardial infarction provide specific reactions, including their role in coronary vasospasm and have very important effects on endothelium (Konidala et al. 2004). It is known that platelets contribute to ischemia- and reperfusion-induced injury of the heart (Seligmann et al. 2000), and in the coronary system can impair cardiac pump function and postischemic recovery of external heart work (Heindl et al. 1999). Nitric oxide (NO) provides protection effects on platelets and plays an important role as inhibitor of platelet activation in the coronary circulation (Pohl and

Correspondence to: Dragan M. Djuric, Institute of Medical Physiology, School of Medicine, University of Belgrade, Višegradska 26/II, 11000 Belgrade, Serbia
E-mail: drdjuric@eunet.rs

Busse 1989), without significant influence on platelet count in blood (Lowson et al. 1999).

The present study was designed to evaluate the effects of perfusion of human platelet rich plasma from healthy volunteers (PRP group) vs. PRP from patients with acute myocardial infarction (PRP (AMI) group) on coronary flow (CF) and oxidative stress markers during nitric oxide synthase (NOS) inhibition through coronary vascular bed of the isolated guinea-pig heart.

Materials and Methods

Isolated guinea-pig heart preparation

Guinea-pigs of either sex (body weight 250–300 g) were killed by cervical dislocation according to Schedule 1 of the Animals, Scientific procedures (Act 1986, UK), without use of any anticoagulants or anesthetics. After urgent thoracotomy and rapid arrest of the beating hearts by superfusion with ice-cold isotonic saline, the hearts were isolated and perfused according to the Langendorff's technique. The composition of the Krebs-Henseleit buffer (perfusion medium) was as follows (in mmol/l): NaCl 118; KCl 4.7; $CaCl_2 \times 2H_2O$ 2.5; $MgSO_4 \times 7H_2O$ 1.7; $NaHCO_3$ 25; KH_2PO_4 1.2; glucose 11; pyruvate 2. It was equilibrated with gas mixture (5% CO_2 – 95% O_2) at 37°C, (pH 7.4). All hearts were electrically paced (5 V) at constant rate of 320 bpm (beats/minute). Constant left ventricular draining through the dissected mitral valve was performed.

Physiological assay

Stabilization of preparation was performed at basal coronary perfusion pressure (CPP) of 70 cmH_2O for 30 min. During this period, the hearts were challenged by short-term occlusions (5–15 s). At the end of equilibration period, CPP was lowered to 30 cmH_2O (to mimic ischemia), then increased gradually in the reverse order to 70 cmH_2O (normal conditions), and further to 120 cmH_2O (to mimic shear stress). Myocardial perfusion was established at constant flow for all applied CPP. When flow was considered as stable at each value of perfusion pressure, samples of the coronary venous effluent were collected. At the end of this series of pressure changes (basic protocol), hearts were perfused with PRP, prepared from venous blood of healthy volunteers. In the second series of experiments, the basic protocol was followed by perfusion with PRP, prepared from venous blood of patients with acute myocardial infarction-early phase (PRP (AMI)). In the third series of experiments, hearts were perfused with Nω-nitro-L-arginine monomethyl ester (L-NAME, 30 μmol/l – final concentration), as an inhibitor of NOS (Emery 1995) from the beginning of the experiment and, after the first sequence of perfusion pressure changes protocol was repeated in the presence of PRP+L-NAME (30 μmol/l). The fourth series of experiments were the same as the third but PRP (AMI) was administered instead of PRP.

Preparation of PRP

Venous blood was obtained from healthy volunteers who had not received any medications as well as from the patients with acute myocardial infarction in early phase who had no received any anti-aggregating drugs; then it was collected into 3.8% sodium citrate (20% of final volume). PRP was obtained according to described method (Schrör et al. 1981) by centrifugation at 1000 g for 20 min, with previous incubation at room temperature for 15 min. The infusion of PRP and PRP (AMI) were performed, at constant rate of 1 ml/min for 5 min (each heart), as well as after administration of L-NAME (final concentration of 30 μmol/l; Merck, Darmstadt, Germany).

Biochemical assays

Samples of coronary venous effluent were collected after the stabilization of flow at each perfusion pressure value.

Nitrite determination

NO was assessed as nitrite and quantified by the spectrophometric method using the Griess-reagent. 0.5 ml of perfusate was precipitated with 200 μl of 30% sulfosalicylic acid, vortexed for 30 min and centrifuged at 3000 × *g*. Equal volumes of the supernatant and Griess reagent, containing 1% sulfanilamide in 5% phosphoric acid / 0.1% napthalene ethylenediamine-dihydrochloride was added and incubated for 10 min in the dark and read at 543 nmol/l. The nitrite levels were calculated by using sodium nitrite as a standard (Green et al. 1982).

Superoxide determination

The level of superoxide anion (O_2^-) was measured using NBT (nitro blue tetrazolium) reaction in Tris-buffer with coronary venous effluent and read at 530 nm. Krebs-Hensenleit solution was used as a blank probe (Auclair and Voisin 1985).

Index of lipid peroxidation (TBARS)

The degree of lipid peroxidation in coronary venous effluent was estimated by measuring of thiobarbituric acid reactive substances (TBARS) using 1% TBA in 0.05 NaOH incubated with coronary effluent at 100°C for 15 min and read at 530 nm. Krebs-Hensenleit solution was used as a blank probe (Ohkawa et al. 1979).

Statistical analysis

Values are expressed as means ± SEM. Statistical analysis was performed by using multifactorial analysis of variance for repeated measurements between subject factors as well as Bonferroni test. p values less than 0.05 were considered to be significant.

Results

PRP perfusion

PRP perfusion induced significant reduction of CF vs. control at all applied CPP (30, 70 and 120 cmH_2O): from 32% at 30 cmH_2O to 27% at 120 cmH_2O. On the other hand, only nitrite was significantly reduced under the influence of PRP: 46% at 70 cmH_2O and 28% at 120 cmH_2O. The level of oxidative stress markers was not significantly influenced by PRP (Figure 1A and Table 1).

PRP (AMI) perfusion

PRP (AMI) perfusion induced reduction of CF and oxidative stress markers vs. control at all applied CPP (30, 70 and 120 cmH_2O). The reduction increased at higher CPP values for CF and for oxidative stress markers: from 39% at 70 cmH_2O to 44% at 120 cmH_2O for CF, 42% at 70 cmH_2O to 35% at 120 cmH_2O for nitrite, 34% at 70 cmH_2O to 43% at 120 cmH_2O for O_2^-, and 90% at 70 cmH_2O to 74% at 120 cmH_2O for TBARS (Figure 1B and Table 2).

PRP perfusion plus L-NAME

PRP perfusion plus L-NAME (30 μmol/l), did not induced additional reduction of CF and oxidative stress markers

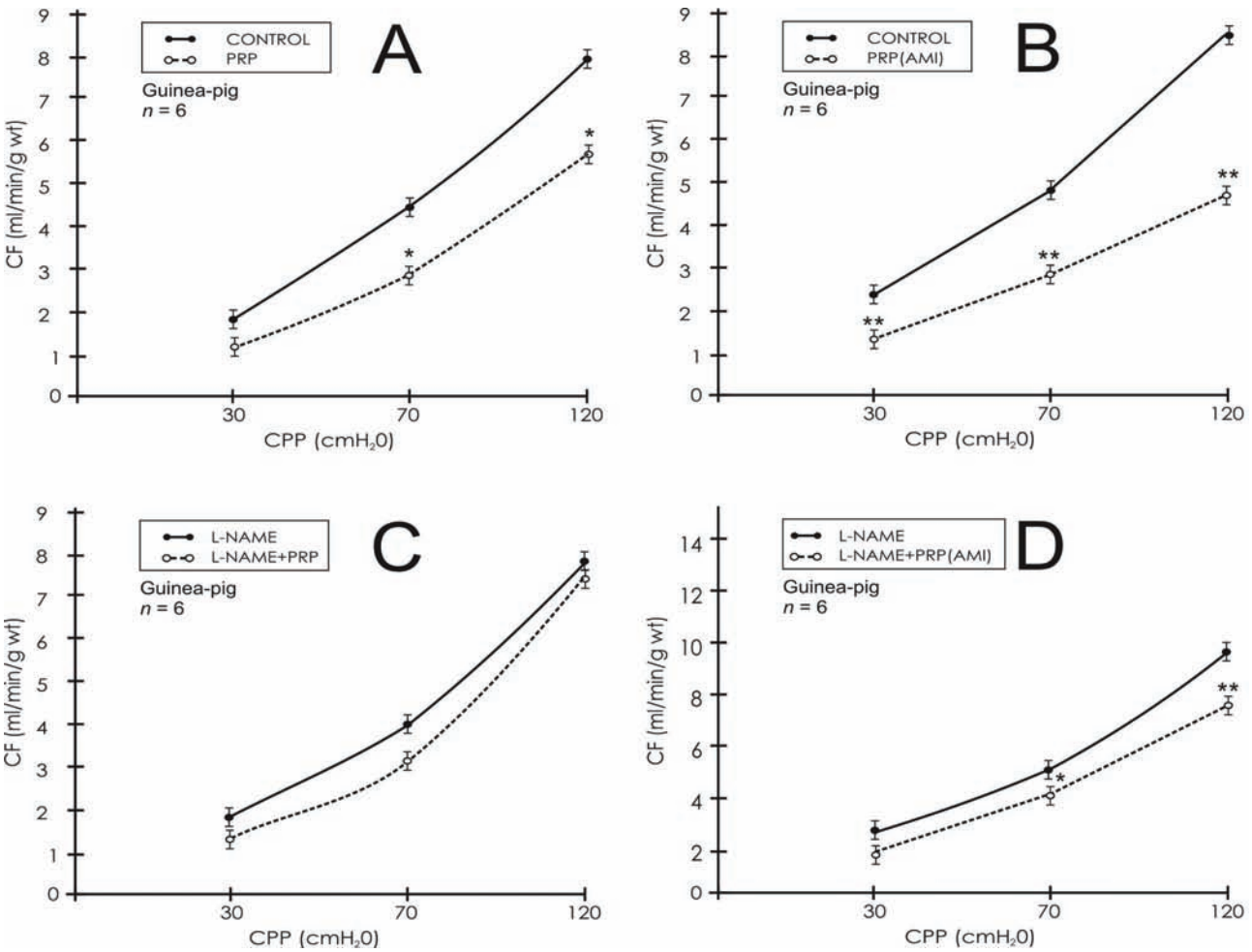

Figure 1. The effects of PRP or PRP (AMI) passage through isolated guinea-pig heart on CF alone (A, B) or in the presence of L-NAME (30 μmol/l) (C, D). *$p < 0.05$, **$p < 0.01$

Table 1. The effects of PRP perfusion through isolated guinea-pig heart on CF, nitrite, O_2^- and TBARS outflow

$n = 6$	CPP (cmH_2O)	CF (ml/min × g wt ± SE)	Nitrite (nmol/min × g wt ± SE)	O_2^- (nmol/min × g wt ± SE)	TBARS (nmol/min × g wt ± SE)
Control	30	1.960 ± 0.210	0.137 ± 0.041	5.296 ± 1.003	166.358 ± 16.117
	70	4.520 ± 0.351	0.664 ± 0.072	18.098 ± 5.023	323.552 ± 53.057
	120	7.960 ± 0.714	1.273 ± 0.061	27.854 ± 5.259	510.070 ± 138.971
PRP	30	1.340 ± 0.210*	0.102 ± 0.041	2.584 ± 1.003	70.316 ± 16.117
	70	3.000 ± 0.351*	0.355 ± 0.072**	13.248 ± 5.023	215.376 ± 53.057
	120	5.800 ± 0.714*	0.918 ± 0.061**	24.182 ± 5.259	319.982 ± 138.971

* $p < 0.05$, ** $p < 0.01$ – PRP vs. control.

Table 2. The effects of PRP (AMI) perfusion through isolated guinea-pig heart on CF, nitrite, O_2^- and TBARS outflow

$n = 6$	CPP (cmH_2O)	CF (ml/min × g wt ± SE)	Nitrite (mol/min × g wt ± SE)	O_2^- (nmol/min × g wt ± SE)	TBARS (nmol/min × g wt ± SE)
Control	30	2.475 ± 0.394	0.146 ± 0.030	2.613 ± 0.216	121.835 ± 16.715
	70	4.900 ± 0.509	0.350 ± 0.084	5.913 ± 0.530	371.580 ± 75.849
	120	8.500 ± 0.760	0.435 ± 0.070	8.795 ± 0.462	430.270 ± 42.575
PRP (AMI)	30	1.450 ± 0.394**	0.112 ± 0.030	1.500 ± 0.249	27.503 ± 16.715
	70	2.975 ± 0.509**	0.204 ± 0.084**	3.903 ± 0.612**	37.053 ± 75.849**
	120	4.800 ± 0.760**	0.284 ± 0.070**	5.057 ± 0.533**	109.257 ± 42.575**

* $p < 0.05$, ** $p < 0.01$ – PRP (AMI) vs. control.

Table 3. The effects of PRP perfusion through isolated guinea-pig heart with previous inhibiton of endothelial NOS (L-NAME 30 μmol/l) on CF, nitrite, O_2^- and TBARS outflow

$n = 6$	CPP (cmH_2O)	CF (ml/min × g wt ± SE)	Nitrite (nmol/min × g wt ± SE)	O_2^- (nmol/min × g wt ± SE)	TBARS (nmol/min × g wt ± SE)
L-NAME	30	1.860 ± 0.210	0.255 ± 0.032	4.490 ± 1.396	161.698 ± 39.300
	70	3.540 ± 0.314	0.494 ± 0.054	13.526 ± 3.930	326.762 ± 56.603
	120	6.580 ± 0.358	1.133 ± 0.084	21.822 ± 5.253	656.224 ± 130.485
L-NAME+PRP	30	1.475 ± 0.235	0.230 ± 0.036	3.185 ± 1.561	122.215 ± 43.939
	70	2.800 ± 0.351	0.453 ± 0.060	9.720 ± 4.394	220.498 ± 63.284
	120	6.250 ± 0.400	1.025 ± 0.094	21.908 ± 5.873	547.677 ± 145.887

Table 4. The effects of PRP (AMI) perfusion through isolated guinea-pig heart with previous inhibiton of endothelial NOS (L-NAME 30 μmol/l) on CF, nitrite, O_2^- and TBARS outflow

$n = 6$	CPP (cmH_2O)	CF (ml/min × g wt ± SE)	Nitrite (nmol/min × g wt ± SE)	O_2^- (nmol/min × g wt ± SE)	TBARS (nmol/min × g wt ± SE)
L-NAME	30	2.650 ± 0.195	0.07625 ± 0.005	4.852 ± 0.632	279.870 ± 20.223
	70	5.125 ± 0.272	0.179 ± 0.003	11.470 ± 1.459	413.298 ± 21.355
	120	9.675 ± 0.269	0.374 ± 0.006	21.235 ± 0.893	624.720 ± 30.779
L-NAME+PRP (AMI)	30	1.950 ± 0.195*	0.0492 ± 0.005	2.978 ± 0.632	217.035 ± 20.223
	70	4.225 ± 0.272*	0.147 ± 0.003*	9.393 ± 1.459	325.270 ± 21.355*
	120	7.550 ± 0.269**	0.292 ± 0.006*	16.548 ± 0.893*	487.415 ± 30.779*

* $p < 0.05$, ** $p < 0.01$ – L-NAME+PRP (AMI) vs. L-NAME.

compared to L-NAME alone at all applied CPP (Figure 1C and Table 3).

PRP (AMI) perfusion plus L-NAME

PRP (AMI) perfusion plus L-NAME (30 μmol/l) induced additional reduction of CF and oxidative stress markers vs. L-NAME alone at all applied CPP (30, 70 and 120 cmH_2O). The reduction was more pronounced at lower CPP values for CF and oxidative stress markers except for O_2^-: from 42% at 30 cmH_2O to 34% at 120 cmH_2O for CF, 50% at 30 cmH_2O to 34% at 120 cmH_2O for nitrite, 51% at 30 cmH_2O to 66% at 120 cmH_2O for O_2^-, and 40% at 30 cmH_2O to 34% at 120 cmH_2O for TBARS (Figure 1D and Table 4).

Discussion

Platelets-induced myocardial dysfunction in ischemic and reperfused guinea-pig hearts is mediated by reactive oxygen species (ROS) (Seligmann et al. 2002). Univalent reduction of molecular oxygen and univalent oxidation of hydrogen peroxide, in biological systems, provides formation of O_2^- (Fridovich 1998). The toxicity of O_2^- has been based on direct interaction with cells or its components which is the most common biochemical effect of O_2^- (Brüne et al. 1991). Lipid peroxidation is a degenerative process which is indicated by formation of TBARS (Dotan et al. 2004). Lipid peroxidation includes oxidative damage in cell membranes, lipoproteins, and other lipid-containing structures, and it has been linked to a variety of disorders, including atherogenesis and ischemia-reperfusion injury (Girotti 1998).

It is possible that response of endothelium to oxidative stress is dependent on platelet oxidant or antioxidant status (Freedman 2008). In addition to directly activating platelets or decreasing the threshold for platelet activation, O_2^- reacts with platelets or endothelium-derived NO forming $ONOO^-$, which is of particular importance for endothelial dysfunction and thrombosis (Krötz et al. 2004). This is primarily caused by the decreased bioavailability of NO as a potent inhibitor of platelet activation (de Belder et al. 1994). However, NO under physiological conditions prevents platelet activation by increasing cGMP levels (Moncada et al. 1991). It is not surprising, therefore, that the antithrombotic effect of NO is lost either when ROS are exogenously added to the system or when they are scavenged (Moncada et al. 1991).

Overall, there is accumulating evidence supporting a net prothrombotic effect of vascular-derived and platelet-derived ROS *in vitro* (Krötz et al. 2004). Taken together, these data point to an important role of platelet-derived ROS and the intraplatelet redox state in the regulation of physiological platelet activation (Krötz et al. 2004). In particular, the specific significance of the different types of ROS with respect to platelet activity has not definitely been determined (Ovechkin et al. 2007). Although it is clearly evident that ROS participate in platelet activation and subsequent thrombus formation, it is not fully understood whether ROS serve as indispensable signaling molecules for specific platelet activation pathways (Krötz et al. 2004).

Our results clearly show that during control conditions increased CF might be observed following increased CPP. It was probably a consequence of higher shear stress and increased NO production (Yan et al. 2007). PRP decreased CF at all applied perfusion pressures compared to the control, significantly (Figure 1A). Furthermore, perfusion with PRP (AMI) decreased CF at all CPP values more powerfull compared to PRP group (Figure 1B). The fact that CF drop was more pronounced in PRP (AMI) group was probably due to the endothelial stimulation by platelets (and/or plasma) enriched with more vasoconstrictor substances producing significant vasoconstriction (Cines et al. 1998). Also a relative insufficiency of coronary vasodilator mechanisms in contact with PRP (AMI) may not be exluded (Worthley et al. 2007). Thus, different substances like tromboxanes, prostaglandines, serotonin, ROS etc. which interact with endothelium might be released from platelets (Kleiman et al. 2008). In addition if NOS inhibitor (i.e. L-NAME) was administered to the medium, the curve of CF was shifted to the right indicating decreased CF and probably decreased NO synthesis/production (Jakovljevic et al. 2003). However, it has been proposed that perfusion of PRP or PRP (AMI) might elicit pressure-dependent NO release into coronary effluent which was less pronounced in PRP (AMI) group (Sun et al. 2004). Therefore, L-NAME blocked NO release in both experimental groups. When L-NAME was applied in concentration high enough to block NO synthesis, there was still some NO release persisting (Emery 1995). There are two posibilities: i) the concentration of L-NAME applied was not so sufficient to completely block NO synthesis; ii) NO could be probably produced from other cells than endothelium, i.e. vascular smooth muscle cells, platelets etc. (Vallance et al. 2002). In addition, when PRP (AMI) was administered in presence of L-NAME further decrease in CF suggests that the mechanisms other than decreased NO production may have been included in vasoconstriction (Just et al. 2005). Therefore, specific antagonists should be used in further experiments to evaluate these vasoconstrictor mechanisms and potential role in coronary vasospasm.

It can be concluded that PRP (AMI) which was obtained from the patients with acute myocardial infarction have more vasoconstrictor potential than platelets of healthy volunteers, similar like in recent studies (Brodov et al. 2008). There is significant PRP (AMI) ability to decrease CF and NO release. In our study blocking of NO synthesis

with L-NAME confirm this conclusion in paralell. However, there are some limitations of applied methodology. Activated platelets in acute myocardial infarction provided basic reactions and have important role for endothelium (Heindl et al. 1998a,b, 1999).

PRP administration induced reduction of CF, nitrite, superoxide, and TBARS outflow at all applied CPP values. This reduction was significant only for CF and nitrite, but not for oxidative stress markers. These data let us to conclude that estimated oxidative stress markers don't have role in platelet-endothelium interaction, considering platelets obtained from blood of healthy volunteers and not damaged vascular endothelium.

The administration of PRP (AMI) resulted in reduction of oxidative stress markers at 70 and 120 cmH_2O. Previous administration of L-NAME potentiated these reductions for CF and nitrite, considering PRP (AMI) administration, what was not a case with PRP administration. Although studies with washed platelets allow for "unaltered" information about the function of a specific ROS, this scenario is not necessarily representative of physiological conditions, because plasma or full blood possesses antioxidant capacities (Krötz et al. 2004). Thus, awareness of the assay conditions is of importance for the interpretation of data regarding the influence of ROS on platelets-endothelium interaction (Cominacini et al. 2003). If the influence of a specific ROS on platelets is investigated *in vitro*, then buffers that do not contain antioxidant substances may be appropriate (Krötz et al. 2004). If consequences of such signaling should be assessed with relevance for the *in vivo* situation, however, then the effects of addition of defined amounts of plasma or full blood should be tested (Krötz et al. 2004).

In summary, more significant decrease of oxidative stress markers in the presence of PRP (IAM) as in PRP group schould be the effect of increased plasma antioxidative capacities, induced by activated platelets. Additional influence of NOS blockade only in PRP (IAM), but not in PRP treated hearts suggested potential role of L-arginine/NO system on oxidative stress by previous activitation of circulating platelets.

Acknowledgement. This work was supported by grant No. 145014G of the Ministry of Science and Environmental Protection of Republic of Serbia.

References

Auclair C., Voisin E. (1985): Nitroblue tetrazolium reduction. In: Handbook of Methods for Oxygen Radical Research. (Ed. R. A. Greenwald), pp. 123–132, CRC Press, Boca Raton, Florida

Brodov Y., Sandach A., Boyko V., Matetzky S., Guetta V., Mandelzweig L., Behar S. (2008): Acute myocardial infarction preceded by potential triggering activities: angiographic and clinical characteristics. Int. J. Cardiol. **130**, 180–184

Brüne B., von Appen F., Ullrich V. (1991): Oxidative stress in platelets, in oxidants and antoxidants. In: Oxidative Stress. Oxidants and Antioxidants. (Ed. H. Siess), pp. 422–443, Academic Press, San Diego

Cominacini L., Pasini A. F., Garbin U., Pastorino A., Rigoni A., Nava C., Davoli A., Lo Cascio V., Sawamura T. (2003): The platelet-endothelium interaction mediated by lectin-like oxidized low-density lipoprotein receptor-1 reduces the intracellular concentration of nitric oxide in endothelial cells. J. Am. Coll. Cardiol. **41**, 499–507

Cines D. B., Pollak E. S., Buck C. A., Loscalzo J., Zimmerman G. A., McEver R. P, Pober J. S., Wick T. M., Konkle B. A., Schwartz B. S., Barnathan E. S., McCrae K. R., Hug B. A., Schmidt A.-M., Stern D. M. (1998): Endothelial cells in physiology and in the pathophysiology of vascular disorders. Blood **91**, 3527–3561

de Belder A. J., MacAllister R., Radomski M. W., Moncada S., Vallance P. J. T. (1994): Effects of S-nitroso-glutathione in the human forearm circulation: evidence for selective inhibition of platelet activation. Cardiovasc. Res. **28**, 691–694

Dotan Y., Lichtenberg D., Pinchuk I. (2004): Lipid peroxidation cannot be used as a universal criterion of oxidative stress. Prog. Lipid Res. **43**, 200–227

Emery C. J. (1995): Vasodilatator action of the S-nitrosothiol, SNAP, in rat isolated perfused lung. Physiol. Res. **44**, 19–24

Freedman J. E. (2008): Oxidative stress and platelets. Arterioscler. Thromb. Vasc. Biol. **28**, S11–16

Fridovich I. (1998): Oxygen toxicity: a radical explanation. J. Exp. Biol. **201**, 1203–1209

Furie B., Furie B. C. (2008): Mechanisms of thrombus formation. N. Engl. J. Med. **359**, 938–949

Girotti A. W. (1998): Lipid hydroperoxide generation, turnover, and effector action in biological systems. J. Lipid. Res. **39**, 1529–1542

Green L. C., Wagner D. A., Glogowski J., Skipper P. L., Wishnok J. S., Tannenbaum S. R. (1982): Analysis of nitrate, nitrite and [15N] nitrate in biological fluids. Anal. Biochem. **126**, 131–138

Heindl B., Becker B. F., Zahler S., Conzen P. F. (1998a): Volatile anaesthetics reduce adhesion of blood platelets under low-flow conditions in the coronary system of isolated guinea pig hearts. Acta Anaesthesiol. Scand. **42**, 995–1003

Heindl B., Zahler S., Welsch U., Becker B. F. (1998b): Disparate effects of adhesion and degranulation of platelets on myocardial and coronary function in postischaemic hearts. Cardiovasc. Res. **38**, 383–394

Heindl B., Conzen P. F., Becker B. F. (1999): The volatile anesthetic sevoflurane mitigates cardiodepressive effects of platelets in reperfused hearts. Basic Res. Cardiol. **94**, 102–111

Jakovljevic V. Lj., Ignjatovic V. S., Djurdjevic P. M., Tasic M. V., Jovovic D. M., Djuric D. M. (2003): The effects of nimodipine on coronary flow, nitrite outflow and superoxide anion release in isolated rat heart. Am. J. Hypertens. **16**, A74

Just A., Olson A. J. M., Falck J. R., Arendshorst J. R. (2005): NO and NO-independent mechanisms mediate ETB receptor buffering of ET-1-induced renal vasoconstriction in the rat. Am. J. Physiol., Regul. Integr. Comp. Physiol. **288**, R1168–1177

Kleiman N. S., Freedman J. E., Tracy P. B., Furie B. C., Bray P. F., Rao S. V., Phillips D. R., Storey R. F., Rusconi C. P., French P. A., Steinhubl S. R., Becker R. C. (2008): Platelets: developmental biology, physiology, and translatable platforms for preclinical investigation and drug development. Platelets **19**, 239–251

Konidala S., Gutterman D. D. (2004): Coronary vasospasm and the regulation of coronary blood flow. Prog. Cardiovasc. Dis. **46**, 349–373

Krötz F., Sohn H.-Y., Pohl U. (2004): Reactive oxygen species: players in the platelet game. Arterioscler. Thromb. Vasc. Biol. **24**, 1988–1996

Lowson S. M., Hassan H. M., Rich G. F. (1999): The effect of nitric oxide on platelets when delivered to the cardiopulmonary bypass circuit. Anesth. Analg. **89**, 1360–1365

Moncada S., Palmer R. M., Higgs E. A. (1991): Nitric oxide: physiology, pathophysiology, and pharmacology. Pharmacol. Rev. **43**, 109–142

Ohkawa H., Ohishi N., Yagi K. (1979): Assay for lipid peroxides in animal tissues by thiobarbituric acid reaction. Anal. Biochem. **95**, 351–358

Ovechkin A. V., Lominadze D., Sedoris K. C., Robinson T. W., Tyagi S. C., Roberts A. M. (2007): Lung ischemia-reperfusion injury: implications of oxidative stress and platelet-arteriolar wall interactions. Arch. Physiol. Biochem. **113**, 1–12

Pohl U., Busse R. (1989): EDRF increases cyclic GMP in platelets during passage through the coronary vascular bed. Circ. Res. **65**, 1798–1803

Scharf R. E. (2008): Acquired platelet function disorders – pathogenesis, classification, frequency, diagnosis, clinical management. Hämostaseologie **28**, 299–311 (in German)

Schrör K., Köhler P., Müller M. (1981): Prostacyclin-tromboxane interactions in the platelet-perfused *in vitro* heart. Am. J. Physiol., Heart Circ. Physiol. **241**, H18–25

Seligmann C., Schimmer M., Lietsch T., Bock A., Simsek C. (2000): A thrombocyte-induced myocardial dysfunction in the ischemic and reperfused guinea pig heart is mediated by reactive oxygen species. Free. Radic. Biol. Med. **29**, 1244–1251

Seligmann C., Simsek Y., Schimmer M., Leitsch T., Bock A., Schultheiss H. P. (2002): Human thrombocytes are able to induce a myocardial dysfunction in the ischemic and reperfused guinea pig heart mediated by free radicals – role of the GPIIb/IIIa-blocker tirofiban. Life Sci. **71**, 2319–2329

Sun D., Huang A., Kaley G. (2004): Mechanical compression elicits NO-dependent increases in coronary flow. Am. J. Physiol., Heart Circ. Physiol. **287**, H2454–2460

Takaya N., Katoh Y., Iwabuchi K., Hayashi I., Konishi H., Itoh S., Okumura K., Ra C., Nagaoka I., Daida H. (2005): Platelets activated by collagen through the immunoreceptor tyrosine-based activation motif in the Fc receptor γ-chain play a pivotal role in the development of myocardial ischemia-reperfusion injury. J. Mol. Cell. Cardiol. **39**, 856–864

Tantry U. S., Bliden K. P., Gurbel P. A. (2005): Resistance to antiplatelet drugs: current status and future research. Expert Opin. Pharmacother. **6**, 2027–2045

Vallance P., Leiper J. (2002): Blocking NO synthesis: how, where and why? Nat. Rev. Drug Discov. **1**, 939–950

Worthley M. I., Holmes A. S., Willoughby S. R., Kucia A. M., Heresztyn T., Stewart S., Chirkov Y. Y., Zeitz C. J., Horowitz J. D. (2007): The deleterious effects of hyperglycemia on platelet function in diabetic patients with acute coronary syndromes. Mediation by superoxide production, resolution with Intensive insulin administration. J. Am. Coll. Cardiol. **49**, 304–310

Yan C., Huang A., Kaley G., Sun D. (2007): Chronic high blood flow potentiates shear stress-induced release of NO in arteries of aged rats. Am. J. Physiol., Heart Circ. Physiol. **293**, H3105–3110

Comparative effects of L-arginine and vitamin C pretreatment in SHR with induced postischemic acute renal failure

Zoran Miloradović[1], Nevena Mihailović-Stanojević[1], Jelica Grujić Milanović[1], Milan Ivanov[1], Gordana Kuburović[2], Jasmina Marković-Lipkovski[3] and Đurđica Jovović[1]

[1] *Institute for Medical Research, University of Belgrade, Serbia*
[2] *Faculty of Dentistry, University of Belgrade, Serbia*
[3] *Medical School, University of Belgrade, Institute of Pathology, Serbia*

Abstract. Postischemic acute renal failure is worsened when occurs in a various conditions with impaired nitric oxide (NO) synthesis, such as arterial hypertension. Reoxygenation itself increases ischemic injury through the massive production of oxygen-free radicals. Therefore, we have directed our investigations to effects of both NO donor and antioxidant treatment on course of acute renal failure in experimental hypertension. Experiments were performed in anesthetized, adult male spontaneously hypertensive rats. In ARF groups the right kidney was removed, and rats were subjected to renal ischemia by clamping the left renal artery for 40 min. Experimental group received NO donor L-arginine (2 g/kg b.m.) (L-Arg group), or oxidant scavenger vitamin C (100 mg/kg b.m.) (Vit C group) during 3 days before the period of ischaemia. All parameters were measured 24 h after reperfusion. The mean arterial pressure was markedly reduced and renal vascular resistance significantly dropped in the ARF+L-Arg group vs. ARF group. Tubular injuries were similar between the ARF+L-Arg and ARF groups. Intensity of tubular necrosis and dilatation was markedly reduced in ARF+Vit C group in comparison to ARF. L-arginine failed to reduce tubular injury, despite its evident improvement of systemic and renal haemodynamic, thus NO seems to act as a double-egged sword, but reduction of tubular injury promotes vitamin C as an effective chemoprotectant against ishemia-reperfusion tubular injury in hypertension.

Key words: Acute renal ischemia — SHR — Nitric oxide — Vitamin C

Introduction

Postischaemic acute renal failure frequently occurring in clinical practice is associated with significant morbidity and mortality, despite advances in pharmacology and renal replacement therapy (Bonventre and Weinberg 2003).

There are several factors involved in the initiation and maintenance of the acute renal failure: decrease in glomerular capillary permeability, back-leak of glomerular filtrate, tubular obstruction and intrarenal vasoconstriction (Nissenson 1998), but their causality has never been selective and rarely preventable. On the other hand, long-lasting hypertension damages medium size and small-size renal blood vessels, disables adequate tubuloglomerular responses, and predisposes nephroangiosclerosis patients to acute renal failure (Welch et al. 2000). Also, patients with pre-existing hypertension are at a particular risk of fatal outcome (Rihal et al. 2002; Aronson and Blumenthal 1998). Recently, one of the most investigated mechanisms in the context of tone control is the nitric oxide (NO)-dependent vasodilatation. There is a decrease in the basal production of NO and expression of endothelial NO synthase in spontaneously hypertensive rats (SHR) (Crabos et al. 1997; Chou et al. 1998). NO participates in several vital processes in the kidney which encompass regulation of glomerular and medullar haemodynamic, tubuloglomerular feedback response, renin release, extracellular fluid volume (Kone 1997) and regulation of Na^+,K^+-ATPase, Na^+/H^+ exchangers, and paracellular permeability of proximal tubular cells (Liang and Knox 2000). Several studies have suggested that NO bioactivity is reduced in models of postischemic acute renal failure as assessed by a blunted response to endothelium-

Correspondence to: Zoran Miloradović, Institute for Medical Research, University of Belgrade, Dr. Subotića 4, 11129 Belgrade, P.O.Box 102, Serbia
E-mail: zokim@imi.bg.ac.yu

dependent vasodilators such as acetylcholine and bradykinin and increased constrictor responses to renal nerve stimulation and angiotensin II (Cherla and Jaimes 2004).

Oxidative stress appears to be the main mechanism causing tissue ischemia-reperfusion damage. Reperfusion injury generates significant amount of free oxygen radicals, the effect of which could not be „buffered"by endothelial cells exposed to ischemia (Radović 2006). Water-soluble vitamin C has frequently been used in experimental studies to interfere in mechanisms of oxidative injury. In addition, vitamin C has consistently proved to be a potent antioxidant in certain experimental and clinical conditions (Lloberas et al. 2002).

Therefore, we developed an experimental model that mimicked the clinical situation where kidneys which suffered from long-lasting hypertension have been subjected to ischemia-reperfusion injury. The main goal of this study was to compare the efficiency of an attempt to diminish reperfusion injury in SHR by NO donor or antioxidant pretreatment.

Materials and Methods

Materials

Male adult 3-month-old SHR, weighing about 300 g, were bred in the Institute for Medical Research, Belgrade and fed with a standard chow for laboratory rats (Veterinarski zavod, Subotica, Serbia) *ad libitum*. All animal experiments were conducted in accordance with local institutional guidelines for the care and use of laboratory animals. The investigation also conformed to the principles and guidelines of Conseil de l'Europe (published in the Official Daily N. L358/1-358/6, 18th December 1986), the U.S. National Institutes of Health (Guide for the Care and Use of Laboratory Animals, NIH publication No. 85-23), and the Canadian Council on Animal Care.

We used: i) L-arginine, substrate for NO (Sigma), ii) solubile vitamin C (Galenika a.d., Serbia), antioxidant molecule.

Experimental groups and model of acute renal failure

The animals were divided into two experimental groups: L-arginine treated animals with acute renal failure (ARF+L-Arg; $n = 10$) and vitamin C-treated animals with induced acute renal failure (ARF+Vit C; $n = 10$). There were two control groups, control sham operated rats (SHAM; $n = 9$) and control rats with acute renal failure (ARF; $n = 9$). In all ARF groups the right kidney was removed, and the rats were subjected to renal ischemia by clamping the left renal artery for 40 min. The SHAM group consisted of right nephrectomized rats and received vehicle *via* the same route as all other groups. All rats were placed in individual metabolic cages immediately after clamp removal and surgery procedures.

Experimental animals were pretreated by gavages with L-arginine (2 g/kg b.m.) or vitamin C (100 mg/kg b.m.) during 3 days before the period of ischaemia.

Haemodynamic measurements 24 h after reperfusion

Haemodynamic parameters were measured after the 24 h urine collection period. All animals were anaesthetized (35 mg/kg sodium pentobarbital; i.p.). Mean arterial pressure (MAP) was determined directly through a femoral artery catheter PE-50 (Clay-Adams, Parsippany, NY, USA), using a low-volume displacement transducer P23 Db (Statham, Oxnard, CA, USA), and recorded on a direct writing recorder.

For the blood flow measurement, the left renal artery was gently separated. An ultrasonic flow probe (1 RB, internal diameter = 1 mm) was placed around the artery for the measurement of renal blood flow, using a transonic small animal flowmeter T106 (Transonic System Inc., Ithaca, NY, USA). Renal vascular resistance (RVR) was calculated by dividing MAP by renal blood flow and expressed as mmHg·min·kg/ml.

Biochemical measurements 24 h after reperfusion

Urinary and plasma concentrations of creatinine and urine protein concentrations were determined using a COBAS INTEGRA® 400 plus (Hoffmann-La Roche, Germany) analyzer.

Urine volume was collected in a graduated tubes after the 24 h metabolic cage collection period.

Histological examination

Left kidney was examined morphologically, 24 h after the period of reperfusion. The renal tissue was fixed in 10% buffered formalin solution. Later, the kidney was dehydrated in alcohol, blocked in paraffin wax, and 5 μm thick sections were sliced and stained by periodic acid-Schiff (PAS) reaction. Using light microscopy, the following parameters were semi-quantitatively evaluated on the scale from 0 to 4 according to the degree of lesions: intensity and spread of tubular necrosis, number of intraluminal cast formations, swelling and vacuolization of cells, loss of luminal membrane or brush borders, tubular dilatation, interstitial oedema, separation of cells from tubular basal membrane. The severity of congestion, i.e. the accumulation of red blood cells in glomeruli, peritubular capillaries, and intrarenal veins, was graded on a scale from 1 to 3, as described by Mandal et al. (1977). The sum of these changes represented the histopathological score for comparison between groups.

Statistical analysis

The results are expressed as mean ± S.E.M. One-way analysis of variance (ANOVA) was applied. When the ANOVA results

were significant, Bonferroni's *t*-test was used to determine the level of significance and $p < 0.05$ was considered to be significant (Primer of Biostatistics, by Stanton A. Glanz).

Results

Hemodynamic parameters

The MAP was markedly, but not significantly, decreased in the both ARF+L-Arg group and ARF+Vit C group in comparison to ARF group (130.25 ± 3.75 mmHg and 128.60 ± 4.20 mmHg vs. 141.86 ± 12.04 mmHg). Also, in the both experimental groups, MAP was significantly decreased in comparison to SHAM (Figure 1).

The renal blood flow was not different between experimental groups, but markedly rose in ARF+L-Arg group in comparison to the controls (Figure 2). The RVR significantly dropped in the ARF+L-Arg group vs. ARF (67.81 ± 7.04 vs. 148.87 ± 26.85 mmHg·min·100 g/ml) (Figure 2).

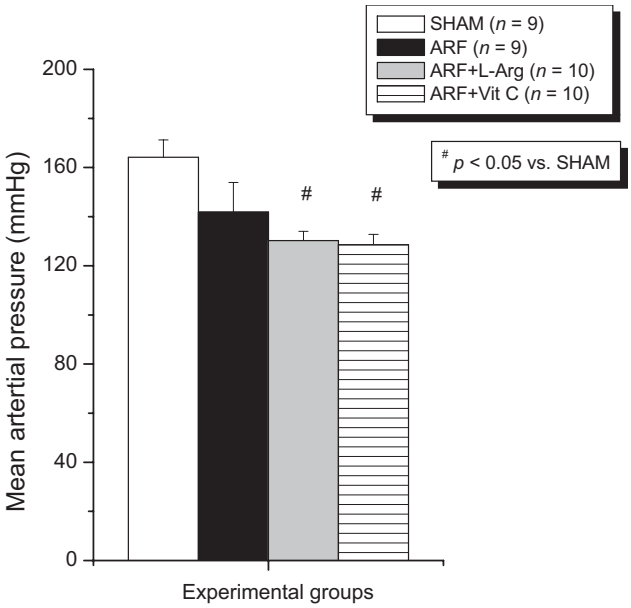

Figure 1. Mean arterial pressure in experimental groups.

Biochemical parameters

Glomerular filtration rate (GFR), presented as an endogenous creatinine clearance, significantly fell in all ARF groups 24 h after the period of ischemia. There were no significant differences between the ARF groups, but GFR was moderately increased in ARF+L-Arg group in comparison to ARF group (Table 1).

The value of the urine protein excretion showed no relevant differences between experimental groups (Table 1). The urine volume was significantly higher in ARF+L-Arg group in comparison to controls (Table 1).

Histological studies

Morphological examination of the renal tissue revealed significant differences between experimental groups of animals.

Glomeruli, tubulointerstitium and blood vessels of the sham-operated animals were without any changes on the light microscopy examination. In a few kidney specimens, only a small number of PAS positive casts were observed in the tubular lumen (Figure 3A).

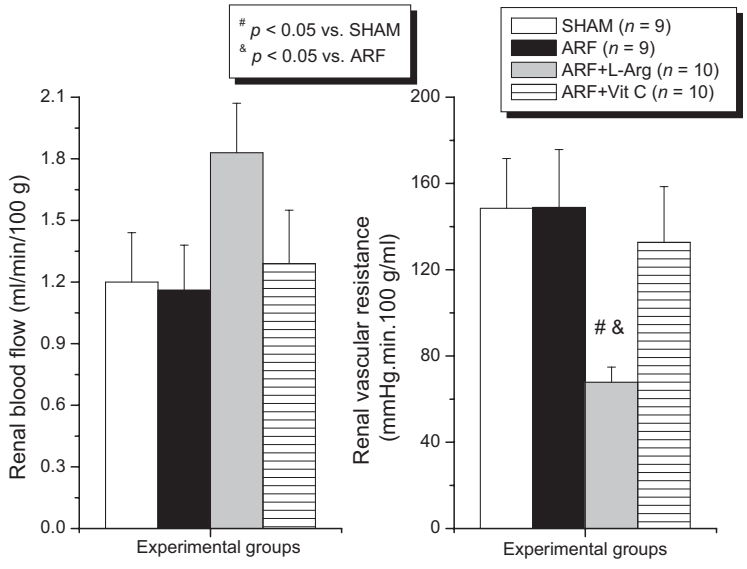

Figure 2. Renal blood flow and renal vascular resistance in experimental groups.

Kidneys in the ARF control group showed dilatation of some segments of proximal and distal tubules with or without loss of brush border of proximal tubular epithelium. Swelling of some proximal tubular epithelial cells was present. The most prominent lesions were widespread tubular necrosis in the corticomedullary zone and a huge number of PAS positive casts in the lumina of distal tubuli and collecting ducts. The intensity of interstitial oedema varied among specimens in this group. Glomeruli and blood vessels were the same as in the SHAM group (Figure 3B).

Table 1. Biochemical parameters and histopathological score

Groups	Creatinine clearance (ml/min/kg)	Plasma urea (mmol/l)	Urine protein excretion (mg/24 h/kg)	Urine volume (ml/24 h/kg)	Histopathological score
SHAM (n = 9)	5.44 ± 0.27	10.23 ± 0.29	468.55 ± 38.54	33.7 ± 3.8	0.58 ± 0.2
ARF (n = 9)	1.29 ± 0.38$^{\#}$	40,90 ± 3.75$^{\#}$	494.98 ± 113.30	40.00 ± 4.2	9.87 ± 0.66$^{\#}$
ARF+L-Arg (n = 10)	2.05 ± 0.81$^{\#}$	48.66 ± 5.28$^{\#}$	446.17 ± 53.40	67.3 ± 7.6	9.50 ± 0.43$^{\#}$
ARF+Vit C (n = 10)	0.95 ± 0.03$^{\#}$	47.62 ± 3.77$^{\#}$	353.53 ± 50.73	45.9 ± 7.1	6.71 ± 0.36$^{\# \&*}$

$^{\#}$ $p < 0.05$ compared to SHAM group; $^{\&}$ $p < 0.05$ compared to ARF control; * compared to ARF+L-Arg group; n, number of animals.

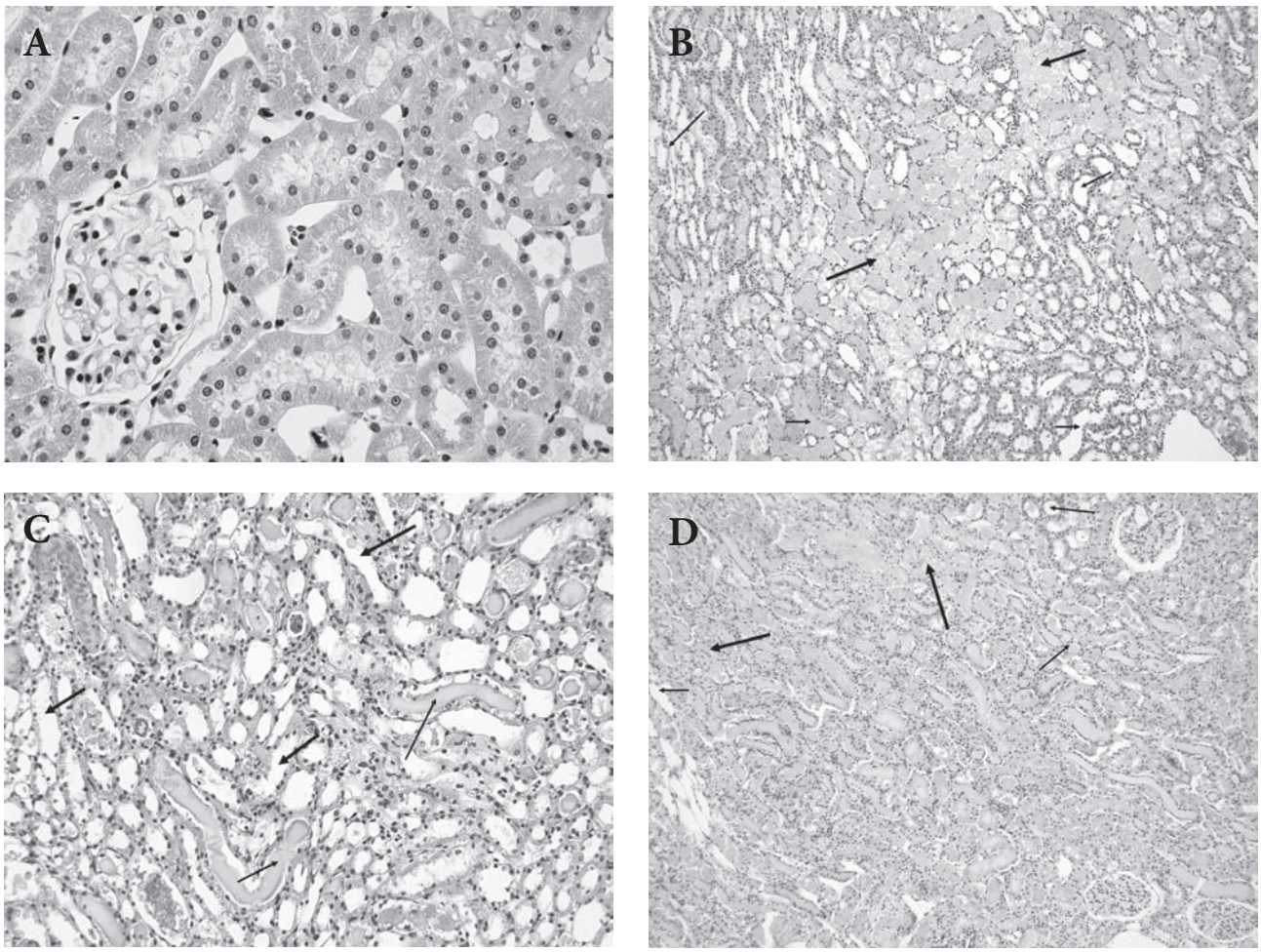

Figure 3. Histology of the kidney 24 h after reperfusion. **A.** A normal shape of the glomerulus and tubulointerstitium in the sham-operated animals (PASX320). **B.** Intensive corticomedullar tubular necrosis (bull arrow) and dilatation (thin arrow), PAS positive casts in the ARF group (PASX250). **C.** Intensive tubular dilatation and necrosis (bull arrow), PAS positive casts (thin arrow) and interstitial edema in ARF+L-Arg group (PASX250). **D.** Glomeruli, PAS positive casts, mild tubular necrosis (bull arrow) and slightly prominent proximal tubular dilatation (thin arrow) in ARF+Vit C group (PASX250).

Widespread tubular necrosis in the corticomedullary zone, huge number of PAS positive casts in distal tubuli and intensity of interstitial oedema, were similar in the ARF and ARF+L-Arg group (Figure 3C).

In some specimens of the ARF+Vit C group tubular necrosis in cortico medullary junction was less intense and less widespread in comparison to the control animals with acute renal failure. Also, intensity of tubular dilatation was markedly reduced in ARF+Vit C group in comparison to ARF group (Figure 3D).

Discussion

Recently, multiple strategies including L-arginine supplementation have been attempted to ameliorate course of acute renal failure. In several studies administration of exogenous L-arginine has been shown to protect the kidney against toxic or ischemic injury (Cherla and Jaimes 2004). Besides, decreased action or synthesis of NO has been implicated in diseases such as hypertension, hypercholesterolemia, diabetes or atherosclerosis (Moncada and Higgs 1995). In the present study, L-arginine markedly, but not significantly, decreased MAP, similarly to long-term L-arginine application in the study of Jerkić and co-workers, performed in Wistar rats (Jerkić et al. 1999). Our results indicate two possibilities, that NO synthesis is moderately decreased in SHR or that in models of ischemic acute renal failure changes in inducible NO synthase expression are accompanied by increased production of superoxide anion and peroxynitrite leading to nitrosative stress and vasoconstriction. By our opinion, second possibility seems realistically. In experimental models of hypertension, vitamin C, alone or in combination with vitamin E, accelerates degradation of *S*-nitrosoglutathione, increases synthesis of NO, and reduces blood pressure (Chen et al. 2001). In the present study, although MAP had tendency to decrease in the ARF+Vit C group in comparison with ARF group, this result is not statistically significant. Some other studies, investigating the importance of endogenously generated oxygen radicals in the regulation of blood pressure in SHR have shown modest or scant results also (Yoshioka et al. 1985; Nakazono et al. 1991).

This study has shown that renal haemodynamic was improved by L-arginine treatment and resulted in a significant decrease in RVR 24 h after ischemia. Chintala (Chintala et al. 1993) summarized that synthesis of endothelium-derived relaxing factor is probably turned on maximally by the ischemic insult, because treatment with L-arginine resulted in only a modest improvement of renal perfusion pressure and glomerular filtration rate in the ischemic kidney. However, beneficial effects of L-arginine treatment in the present study strongly suggest, that release of NO does not reach its maximum 24 h after reperfusion injury in SHR. This is similarly to study of Jerkić et al. (1999) performed in Wistar rats, and in accordance with Schramm (Schramm et al. 1996) who suggested that renal ischemia, which injures endothelial cells, reduced the production of NO in them also. In the present study, administration of vitamin C had no influence on renal haemodynamic parameters, leading us to conclude that free radical scavenging has no dominant influence on renal vasomotor control in SHR with induced postischemic acute renal failure.

Twenty four hours after acute renal failure induction, GFR was drastically reduced. It was not significantly different among groups with acute renal failure irrespective of their treatment, but had tendency to increase in L-arginine-treated animals. On the other hand, it's well known that creatinine clearance is not optimal indicator of glomerular filtration in rats treated with L-arginine (and only in them) since creatinine arises as a waste product in the decay of L-arginine. However, it seemed almost inconceivable to add a more appropriate method, e.g. determination of inulin clearance, to our procedure, which was already very difficult for the animals. Plasma urea rose due to ischemic injury and was not significantly different among groups with acute renal failure irrespective of their treatment, indicating irrelevant role of NO bioavailability and radical scavenging in reperfusion-induced uremia in SHR.

Increase in urine volume in animals treated with L-arginine could be a consequence of restoration of the pressure-dependent increases in renal medullar haemodynamic in association with restoration of pressure natriuresis in SHR (Larson and Lockhart 1995). Urine protein excretion was not different between groups, what is in accordance with findings of Basile et al. (2001) that during the first 14-week postinjury, protein excretion is low in both sham-operated and postischemic animals.

Our previous study (Jerkić et al. 1999) performed in Wistar rats has shown that treatment with L-arginine reduces tubular cell injury in acute post ischemic renal failure and that NO acts cytoprotectively in rat kidney. In the present study, our results show that widespread tubular necrosis in the corticomedullary zone, huge number of PAS positive casts in distal tubuli and intensity of interstitial oedema, were similar in the ARF and ARF+L-Arg group. The absence of tubular improvement could be explained by different rat strain and by production of other vasoconstrictors (such as endothelin 1 and angiotensin II) in post-ischemic condition in hypertension and particularly by pre-existing oxidative stress in SHR. On the other hand, long-lasting hypertension damages medium size and small-size renal blood vessels and disables adequate tubuloglomerular responses (Radović et al. 2006), leading to worsen reperfusion injuries.

Recently, it's well known that hypoxia, as a result of ischemia and subsequent reperfusion, is characterized by increased reactive oxygen species and decreased efficacy

of the antioxidant system, which lead to tubular cell injury and death (Mejı´a-Vilet et al. 2007). In many studies, antioxidant ascorbic acid has been shown to attenuate renal damage caused by a variety of insults, such as postischemic stress, cisplatin, aminoglycosides, and potassium bromate in animals and has an extensive safety record as a dietary supplement in humans (Spargias et al. 2004). Less intense and less widespread tubular necrosis in corticomedullary junction and reduced tubular dilatation in ARF+Vit C group in our study are in concordance with these findings. This effect suggests that free radical mediating vasoconstriction may represent an important pathophysiological mechanism of renal vasoconstriction and that vitamin C could be protective against acute ischemia-reperfusion injury in SHR.

In summary, our results suggest that short-term L-arginine supplementation improves sistemic and renal haemodynamic in combined model of experimental hypertension and acute renal failure, probably due to direct vasodilatatory action of NO on sistemic and renal vasculature and also, well known, natriuretic and diuretic effects of L-arginine. In opposite to previous, L-arginine supplementation failed to improve glomerular function and to reduce tubular injury. Thus, our results lead us to conclude that the deleterious effects abolish the beneficial during excess NO exposure in this model. This also implies other vasoconstrictors could be involved in post-ischemic condition in hypertension that impede NO donor to improve tubular injury. On the other hand, prior administration of natural antioxidant, vitamin C moderately improves renal hemodynamic, but reduction of tubular necrosis and dilatation promotes vitamin C as an effective chemoprotectant against ishemia-reperfusion tubular injury in the combined model of experimental hypertension and acute renal failure. Therefore, future studies in which vitamin C would be given after the induction of acute renal failure may mimic better clinical situation for possible promotion of antioxidants as therapeutic agents in ischemic acute renal failure with hypertension.

Acknowledgement. This work was supported by grant (project No. 145054) from the Ministry of Science and Technological Development of Serbia.

References

Aronson S., Blumenthal R. (1998): Perioperative renal dysfunction and cardiovascular anesthesia: concerns and controversies. J. Cardiothorac. Vasc. Anesth. **12**, 567–586

Basile D. P., Donohoe D., Roethe K., Osborn J. L. (2001): Renal ischemic injury results in permanent damage to peritubular capillaries and influences long-term function. Am. J. Physiol., Renal Physiol. **281**, F887–899

Bonventre J. V., Weinberg J. M. (2003): Recent advances in the pathophysiology of ischemic acute renal failure. J. Am. Soc. Nephrol. **14**, 2199–2210

Chen X., Touyz R. M., Park J. B., Schiffrin E. L. (2001): Antioxidant effects of vitamins C and E are associated with altered activation of vascular NADPH oxidase and superoxide dismutase in stroke-prone SHR. Hypertension **38**, 606–611

Cherla G., Jaimes E. A. (2004): Role of L-arginine in the pathogenesis and treatment of renal disease. J. Nutr. **134** (Suppl. 10), S2801–2806

Chintala M. S., Chiu P. J. S., Vemulapalli S., Watkins R. W., Sybertz E. J. (1993): Inhibition of endothelial derived relaxing factor (EDRF) aggravates ischemic acute renal failure in anesthetized rats. Naunyn-Schmiedeberg's Arch. Pharmacol. **348**, 305–310

Chou T. C., Yen M. H., Li C. Y., Ding Y. A. (1998): Alterations of nitric oxide synthase expression with aging and hypertension in rats. Hypertension **31,** 643–648

Crabos M., Coste P., Paccalin M., Tariosse L., Daret D., Besse P., Bonoron-Adèle S. (1997): Reduced basal NO-mediated dilatation and decreased endothelial NO-synthase expression in coronary vessels of spontaneously hypertensive rats. J. Mol. Cell. Cardiol. **29**, 55–65

Jerkić M., Varagić J., Jovović Đ., Radujković-Kuburović G., Nastić-Mirić D., Adanja-Grujić G., Marković-Lipkovski J., Dimitrijević J., Miloradović Z., Vojvodić S. B. (1999): L-arginine reduces tubular cell injury in acute postischemic renal failure. Nephrol. Dial. Transplant. **14**, 1398–1407

Kone B. C. (1997): Nitric oxide in renal health and disease. Am. J. Kidney Dis. **30**, 311–333

Larson T. S., Lockhart J. C. (1995): Restoration of vasa recta hemodynamics and pressure natriuresis in SHR by L-arginine. Am. J. Physiol., Renal Physiol. **268,** F907

Liang M., Knox F. G. (2000): Production and functional roles of nitric oxide in the proximal tubule. Am. J. Physiol., Regulatory Integrative Comp. Physiol. **278**, R1117–1124

Lloberas N., Torras J., Herrero-Fresneda I., Cruzado J. M., Riera M., Hurtado I., Grinyó J. M. (2002): Postischemic renal oxidative stress induces an inflammatory response through PAF and oxidized phospholipids: prevention by antioxidant treatment. FASEB J. **16**, 908–910

Mandal A. K., Bell R. D., Parker D., Nordquist J. A., Lindeman R. D. (1977): An analysis of the relationship of malignant lesions of the kidney to hypertension. Microvasc. Res. **14**, 279–292

Mejía-Vilet J. M., Ramírez V., Cruz C., Uribe N., Gamba G., Bobadilla N. A. (2007): Renal ischemia-reperfusion injury is prevented by the mineralocorticoid receptor blocker spironolactone. Am. J. Physiol., Renal Physiol. **293**, F78–86

Moncada S., Higgs E. A. (1995) Nitric oxide in the cardiovascular system. In: Pharmacological Sciences: Perspectives for Research and Therapy in the Late 1990s. (Eds. Cuello A. C. and Collier B.), pp. 347–353, Birkhauser Verlag, Basel

Nakazono K., Watanabe N., Matsuno K., Sasaki J., Sato T., Inque M. (1991): Does superoxide underlie the patho-

genesis of hypertension? Proc. Natl. Acad. Sci. U.S.A. **88**, 10045–10048

Nissenson A. R (1998): Acute renal failure: definition and pathogenesis. Kidney Int. Suppl. **66**, 7–10

Radović M., Miloradović Z., Popović T., Mihailović-Stanojević N., Jovović Dj., Tomović M., Čolak E., Simić-Ogrizović S., Djukanović L. (2006): Allopurinol and enalapril failed to conserve urinary NOx and sodium in ischemic acute renal failure in spontaneously hypertensive rats. Am. J. Nephrol. **26**, 388–399

Rihal C. S., Textor S. C., Grill D. E., Berger P. B., Ting H. H., Best P. J., Singh M., Bell M. R., Barsness G. W., Mathew V., Garrat K. N., Holmes D. R. Jr. (2002): Incidence and prognostic importance of acute renal failure after percutaneous coronary intervention. Circulation **105**, 2259–2264

Schramm L., Heidbreder E., Lopau K., Schaar J., Zimmermann J., Harlos J., Teschner M., Ling H., Heidland A. (1996): Influence of nitric oxide on renal function in toxic acute renal failure in the rat. Miner. Electrol. Metab. **22**, 168–177

Spargias K., Alexopoulos E., Kyrzopoulos S., Iacovis P., Greenwood D. C., Manginas A., Voudris V., Pavlides G., Buller C. E., Kremastinos D., Cokkinos D. V. (2004): Ascorbic acid prevents contrast-mediated nephropathy in patients with renal dysfunction undergoing coronary angiography or intervention. Circulation **110**, 2837–2842

Welch W. J., Tojo A., Wilcox C. S. (2000): Roles of NO and oxygen radicals in tubuloglomerular feedback in SHR. Am. J. Physiol., Renal Physiol. **278**, F769–776

Yoshioka M., Aoyama K., Matsushita T. (1985): Effects of ascorbic acid on blood pressure and ascorbic acid metabolism in spontaneously hypertensive rats. Int. J. Vitam. Nutr. Res. **55**, 301–307

Effects of angiotensin II type-1 receptor blocker losartan on age-related cardiovascular risk in spontaneously hypertensive rats

Nevena Mihailović-Stanojević, Zoran Miloradović, Jelica Grujić-Milanović, Milan Ivanov and Djurdjica Jovović

Institute for Medical Research, University of Belgrade, Belgrade, Serbia

Abstract. Ageing and hypertension are the major risk factors for the development of cardiovascular and renal diseases, and the renin-angiotensin system has been shown responsible for these pathologies. Thus, the aim of this study was to compare the effects of losartan, angiotensin II type-1 receptor blocker, on systolic (SBP), diastolic (DBP), and mean (MBP) blood pressure, pulse pressure (PP) and heart rate as well as regional haemodynamics, cardiac hypertrophy and biochemical parameters in adult (L_9: 9-month-old) and aged (L_{18}: 18-month-old) spontaneously hypertensive rats (SHRs). Aged match untreated SHRs served as controls (U_9: 9-month-old and U_{18}: 18-month-old). Aortal blood flow and resistance were significantly improved by losartan treatment in L_9 vs. U_9 ($p < 0.05$). In aged SHRs, losartan significantly reduced SBP, MBP, PP, right ventricle weight index, and improved age-related impairment of left ventricular weight index (U_{18}: 4.21 ± 0.09 mg/g vs. U_9: 3.54 ± 0.34 mg/g, $p < 0.05$ and vs. L_{18}: 3.65 ± 0.07 mg/g, $p < 0.001$), carotid, renal, and aortal vascular resistance, and glomerular filtration rate (U_{18}: 2.75 ± 0.27 ml/min/kg vs. U_9: 4.84 ± 0.85 ml/min/kg, $p < 0.05$ and vs. L_{18}: 3.65 ± 0.07 ml/min/kg, $p < 0.05$). These results demonstrate significantly impaired systemic and regional haemodynamics and left ventricular hypertrophy in old SHRs. Losartan decreased age and hypertension associated cardiovascular risk by decreasing vascular resistance and pressure overload, ventricular hypertrophy, and preserving kidney function.

Key words: Hypertension — Ageing — Cardiovascular risk — Losartan

Introduction

Cardiovascular complications, associated with ageing and/or hypertension, are caused by alterations in vascular structure and function (Taddei et al. 1997). High blood pressure (BP) is a powerful cardiovascular (CV) risk factor that acts on the arterial wall and is responsible in part for various CV events, such as cerebrovascular accidents and ischemic heart disease (Safar et al. 2003). Systolic and diastolic dysfunctions are independent CV risk factors in the elderly patients, while pulse pressure (PP) is a powerful predictor of CV events in this population (Van Bortel et al. 2001; Fyhrquist et al. 2005). In essential hypertension haemodynamic alterations characterized by increased resistance in peripheral circulation are a consequence of structural, mechanical and functional changes in peripheral vasculature. Advanced age is associated with many CV pathophysiological states, including arteriosclerosis (Iwamoto et al. 2000), stroke (Arboix et al. 2006), heart failure and coronary artery disease (Susic et al. 1999b), and progressive renal damage (Mihailovic-Stanojevic et al. 2003). Age-associated remodeling of the walls of large arteries of rodents, nonhuman primates and humans includes luminal dilation, intimal and medial thickening, vascular stiffening, and endothelial dysfunction (Lakatta 2003). In addition, increase in intima-media thickness of the common carotid artery that occurred with ageing are associated with a number of CV complications and therefore can be predictive and independent factor of CV risk (Ariff et al. 2002). Left ventricular hypertrophy (LVH), ventricular fibrosis and impaired ventricular performances are cardiac manifestations of both hypertension and ageing, and components of the ventricle are affected in hyperten-

Correspondence to: Nevena Mihailović-Stanojević, Department of Cardiovascular Physiology, Institute for Medical Research, University of Belgrade, Dr. Subotića 4, P.O.Box 102, 11129 Belgrade, Serbia
E-mail: nevena@imi.bg.ac.rs

sive heart disease as well as in ageing heart (Varagic et al. 2001a). The spontaneously hypertensive rats (SHRs) have been extensively studied as a model of cardiac hypertrophy that results from genetically-induced pressure overload and leads to the development of failure in advanced age (Brooks et al. 1997).

On the other hand, Komatsu (Komatsu et al. 1995) has demonstrated that the 73-week-old SHR naturally developed all pathophysiological and clinical alterations that are associated with end stage renal disease (ESRD) in patients with essential hypertension. Decrease in total renal blood flow (RBF) along with structural and functional changes of the kidney of this rat strain further induces the progression of renal failure to ESRD (Mihailovic-Stanojevic et al. 2003).

Numerous studies confirmed the important role of the renin-angiotensin system in the domain of cardiovascular and renal physiology and pathophysiology. Angiotensin II (Ang II), the effector peptide of the renin-angiotensin system, exerts a variety of actions in physiological BP and body fluid regulation, and has also been implicated as a pathogenic factor, *via* angiotensin type-1 (AT1) receptor, in the development of cardiovascular (Pratt 1999; Unger 2001) and renal diseases (Hall et al. 1999). In ageing endothelial cells, production of vasoconstricting growth factors such as Ang II and endothelin-1 (ET-1) are increased, and that of vasodilatory factors (e.g. nitric oxide, prostacyclin, and endothelium-derived hyperpolarizing factor) are reduced (Najjar et al. 2005). Previously we showed that losartan successfully protect kidney vessels against ageing and hypertension-induced dysfunction and remodeling by reducing hypertrophy and hyperplasia of vascular smooth muscle cells and by attenuating abnormal expressions α-SMA (an indicator of mesangial activation and renal fibrosis) (Mihailovic-Stanojevic et al. 2004).

Previous studies from others in young and adult animals have shown that hypertensive CV changes are reversible, while only a few studies with antihypertensive agents were processed in aged SHR (Susic et al. 1999a), being more or less effective in improving heart, renal, and vascular changes, depending on drags that were used and/or duration of treatment in those studies (Oddie et al.1993; Brilla et al.1996; Linz et al.1999; Cerbai et al.2000; Linz et al. 2000; Tsotetsi et al. 2001).

In this study we compared the effects of Ang II AT1 receptor antagonist, losartan on hypertension/ageing-related changes of systemic (systolic, diastolic, mean, pulse pressure and heart rate) and regional (carotid, aortal, and renal) haemodynamics, cardiac hypertrophy and biochemical parameters in adult and aged SHRs. We have now investigated whether 4-week losartan treatment could reduce hypertension and ageing-induced heart, renal and vascular changes, and thus decrease age-related CV risk in SHR.

Materials and Methods

Animals

Male SHRs, 9- and 18-months-old, obtained in this study were bred at the Institute for Medical Research (Belgrade, Serbia) and were descendants of breeders originally obtained through Taconic Farms (Germantown, NY, USA). They were maintained in temperature and humidity controlled rooms on a 12 : 12 h light/dark cycle. Animals were fed with standard laboratory chow (Veterinary Center Subotica) and water *ad libitum*. All experiments were done according to our Institutional guidelines for animal research and principals of the European Convention for the Protection of Vertebrate Animals Used for Experimental and Other (Official Daily N. L. 358/1-358/6, December 18, 1986).

Experimental protocol

Animals were divided into four groups: untreated groups (9- and 18-month-old) received tap water, while treated SHR (9- and 18-month-old) received losartan dissolved in tap water (DUP 153, Du Pont, Wilmington, DE, USA; 10 mg/kg b.w./day) by gavage during four weeks of experiment.

Before haemodynamic measurements all animals were weight and placed in metabolic cages during 24 h for collection of urine for biochemical analysis and measurement of urine flow.

All procedures were done under general anesthesia (i.p. sodium-pentobarbital 35 mg/kg b.w.). Left femoral artery was cannulated by polyethylene catheter (P-50, Clay-Adams, Parsippany, NJ, USA) and connected to physiograph by low-volume displacement transducer (P23 Db; Statham, Oxnard, CA, USA) and a direct writing recorder (Physiograph Four; Nacro Bio System, Inc.) for continuous BP measurement. Systolic (SBP) and diastolic (DBP) blood pressure were measured directly, and mean blood pressure (MBP) was obtained by electronic integration, while heart rate was recorded at the same time. PP was displayed as the difference between SBP and DBP. For regional blood flow measurements left carotid artery was gently separated from the surrounding tissue. An ultrasonic flowprobe, 1RB (internal diameter = 1 mm) was placed around the artery and total carotid blood flow (CBF) was recorded using a Transonic T106 small animal flowmeter (Transonic System Inc., Ithaca, NY, USA). After abdominal incision renal artery preparation was utilized and RBF was recorded. Vascular resistance in these two vascular beds (carotid vascular resistance (CVR) and renal vascular resistance (RVR)) were calculated by dividing mean arterial pressure with total blood flow through

respective blood vessel, normalized for the body weight and expressed as mmHg·min·kg/ml. The segment of the abdominal aorta under the bifurcation of the renal artery was carefully prepared and aortal blood flow (ABF) was measured at the same procedure as for CBF and RBF, but with ultrasonic flowprobe, 2RB (internal diameter = 2 mm) and the aortal vascular resistance (AVR) was calculated as described above.

At the end of the study, blood samples were collected for the biochemical analysis. Urinary and plasma total protein and creatinine concentrations, and total plasma cholesterol and triglyceride levels were determined using Cobas Mira, Rosh analyzer and Cobas Integra 400 Plus (Elitech Diagnostic). Standard formula was used to calculate protein excretion, urine protein/creatinine ratio and creatinine clearance as estimation of renal function.

After that, animals were sacrificed and the heart was removed immediately. The atria were dissected free from the ventricles and discarded. The free wall of the right ventricle (RV) was separated carefully from the left ventricle (LV). Wet weight (g) of the both ventricles was measured, and corrected for the body weight and expressed as ventricular weight indexes (mg/g).

Statistical analysis

Results are expressed as mean ± S.E.M. One way analysis of variance (ANOVA) and unpaired Student's *t*- test was applied as appropriate. The differences between examined groups were considered being significant if $p < 0.05$.

Results

Haemodynamic parameters

Chronic losartan treatment significantly reduced SBP, MBP, and PP in the aged SHR. On the other hand, in the adult SHR, given losartan during four weeks resulted in slight, but not significant decrease in SBP, DBP and MBP without effects on heart rate and PP (Table 1).

CBF and CVR (Figure 1) were unaltered in adult SHR after losartan treatment. However, CBF was significantly lower and thus CVR was markedly higher in aged compared to adult untreated SHR. In the aged SHR, losartan has induced increased CBF and decreased CVR. Although, RBF was significantly lower in both untreated and losartan-treated aged, compared to adult SHR, but only in aged untreated SHR, RVR was significantly higher than in adult untreated group (Figure 2). Aortal blood flow was significantly increased and AVR (Figure 3) was significantly decreased in adult losartan-treated group compared to age match untreated SHR. At the same time, in the aged SHR, treatment with losartan slightly affects ABF, but resulted in the significant decrease in AVR. However, ABF was significantly lower and AVR higher in the aged losartan group then in adult SHR that received losartan.

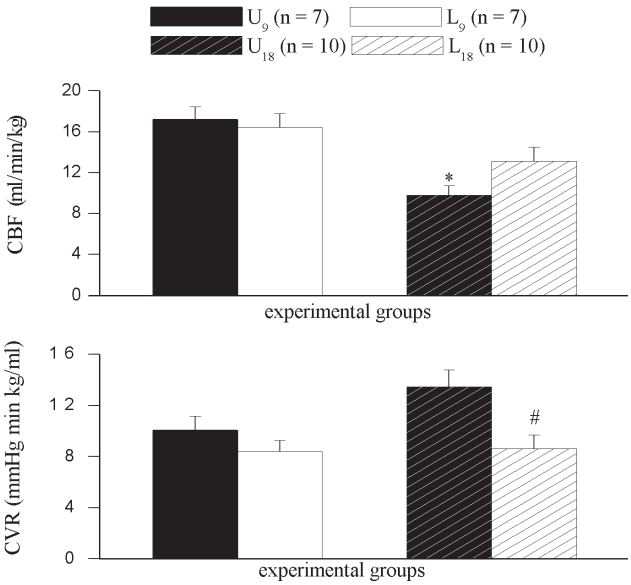

Figure 1. Carotid blood flow (CBF) and carotid vascular resistance (CVR) in SHRs. U_9 and U_{18}, untreated SHRs 9 and 18 months of age; L_9 and L_{18}, 9 and 18 months aged SHRs treated with losartan during four weeks of experiment; $^{\#}$ $p < 0.05$ vs. the age match untreated SHRs; * $p < 0.05$ vs. the adult SHRs.

Table 1. Systolic (SBP), diastolic (DBP), and mean (MBP) blood pressure, pulse pressure (PP), and heart rate (HR) in SHRs

	U_9 ($n = 6$)	L_9 ($n = 7$)	U_{18} ($n = 10$)	L_{18} ($n = 13$)
SBP (mmHg)	194.00 ± 10.91	174.43 ± 6.89	197.80 ± 8.84	147.85 ± 12.45 $^{\#}$
DBP (mmHg)	129.17 ± 13.15	110.86 ± 6.45	136.90 ± 8.94	98.46 ± 11.16
MBP (mmHg)	163.36 ± 17.07	133.32 ± 7.35	157.90 ± 9.14	114.15 ± 12.39 $^{\#}$
PP (mmHg)	64.83 ± 3.89	63.57 ± 5.53	60.90 ± 6.61	49.38 ± 3.76 *
HR (bpm)	388.33 ± 10.46	364.29 ± 7.82	347.40 ± 12.16 *	345.92 ± 8.81

U_9 and U_{18}, untreated SHRs 9 and 18 months of age; L_9 and L_{18}, 9 and 18 months aged SHRs treated with losartan during four weeks of experiment; $^{\#}$ $p < 0.05$ vs. the age match untreated SHRs; * $p < 0.05$ vs. the adult SHRs.

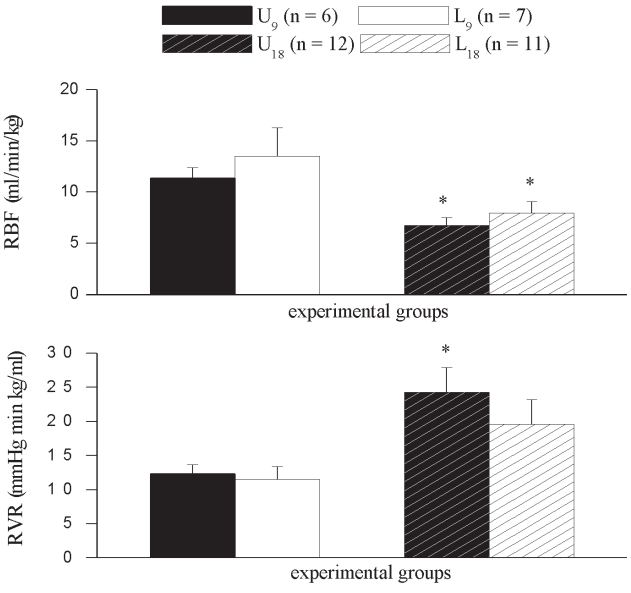

Figure 2. Renal blood flow (RBF) and renal vascular resistance (RVR) in SHRs. U_9 and U_{18}, untreated SHRs 9 and 18 months of age; L_9 and L_{18}, 9 and 18 months aged SHRs treated with losartan during four weeks of experiment; * $p < 0.05$ vs. the adult SHRs.

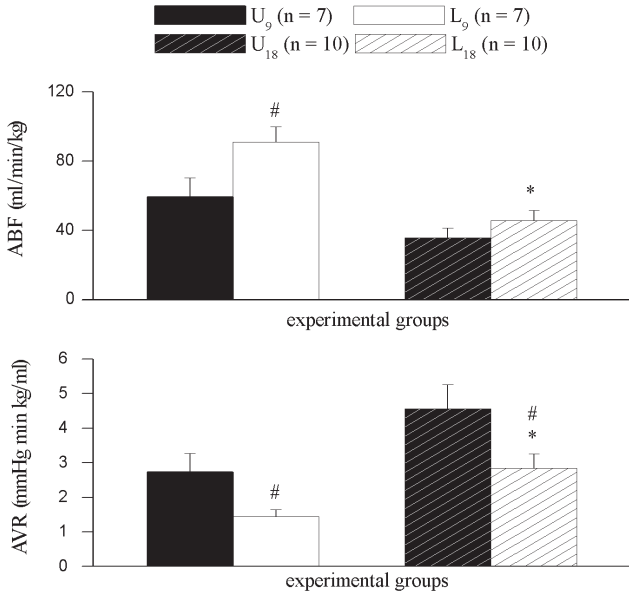

Figure 3. Aortal blood flow (ABF) and aortal vascular resistance (AVR) in SHR. U_9 and U_{18}, untreated SHRs 9 and 18 months of age; L_9 and L_{18}, 9 and 18 months aged SHRs treated with losartan during four weeks of experiment; $^{\#}$ $p < 0.05$ vs. the age match untreated SHRs; * $p < 0.05$ vs. the adult SHRs.

Body and LV and RV weight

No difference in body weight was found among the experimental groups (Table 2). Left and right ventricular weight and ventricular weight indexes were significantly (LV: $p < 0.01$; LVI: $p < 0.001$; RV: $p < 0.05$; RVI: $p < 0.05$) lower in losartan-treated aged SHR than in untreated controls (Table 3). There were no differences in LV and RV weight and ventricular weight indexes between adult losartan-treated and untreated SHR (Table 3).

Biochemical parameters

Biochemical parameters are shown in (Table 2). The total plasma cholesterol and triglyceride levels were significantly increased in aged versus adult SHR, and losartan did not affect either of these parameters. Plasma creatinine level was significantly elevated, while urine creatinine concentration was significantly reduced in untreated aged, compared to adult SHR, thus creatinine clearance dropped significantly

Table 2. Body weight (b.w.), triglyceride (Trg), cholesterol (Chol), plasma creatinine (PCr) and urine creatinine (UCr) concentrations, total plasma protein (TP), urine flow (Uf), protein excretion (Pexc), creatinine clearance (CCr) and urine protein/creatinine ratio (UP/Cr) in SHRs

	U_9 ($n = 7$)	L_9 ($n = 7$)	U_{18} ($n = 10$)	L_{18} ($n = 13$)
b.w. (g)	302.86 ± 9.93	291.43 ± 13.17	308.50 ± 10.11	307.50 ± 9.26
Trg (mmol/l)	0.35 ± 0.04	0.38 ± 0.08	1.33 ± 0.2 ***	1.32 ± 0.27 *
Chol (mmol/l)	0.70 ± 0.04	0.65 ± 0.05	1.28 ± 0.07 ***	1.25 ± 0.09 ***
PCr (μmol/l)	48.71 ± 1.34	51.57 ± 1.13	54.71 ± 1.99 *	54.40 ± 2.73
TP (g/l)	66.77 ± 0.99	73.47 ± 2.67 $^{\#}$	61.03 ± 4.06	55.66 ± 1.66 ***
UCr (mmol/l)	10.56 ± 1.82	10.59 ± 1.64	3.22 ± 0.34 ***	4.84 ± 0.55 $^{\#\,**}$
Uf (μl/min/kg)	23.36 ± 2.58	20.78 ± 2.47	47.07 ± 2.21 ***	43.86 ± 2.56 ***
Pexc (mg/min/kg)	0.18 ± 0.02	0.15 ± 0.02	0.39 ± 0.05 **	0.41 ± 0.08 **
CCr (ml/min/kg)	4.84 ± 0.85	4.01 ± 1.25	2.75 ± 0.27 *	3.84 ± 0.26 $^{\#}$
UP/Cr (mg/mg)	7.43 ± 0.77	6.55 ± 0.53	24.22 ± 2.85 ***	17.69 ± 2.63 **

U_9 and U_{18}, untreated SHRs 9 and 18 months of age; L_9 and L_{18}, 9 and 18 months aged SHRs treated with losartan during four weeks of experiment; $^{\#}$ $p < 0.05$ vs. the age match untreated SHRs; * $p < 0.05$, ** $p < 0.01$, *** $p < 0.001$ vs. the adult SHRs.

Table 3. Left and right ventricular (LV and RV) weight and weight indexes (LVI and RVI) in SHRs

	U_9 (n = 6)	L_9 (n = 7)	U_{18} (n = 16)	L_{18} (n = 14)
LV (g)	1.06 ± 0.10	1.09 ± 0.08	1.29 ± 0.04 *	1.14 ± 0.04 $^{\#\#}$
RV (g)	0.26 ± 0.06	0.24 ± 0.04	0.27 ± 2.02	0.22 ± 0.01 $^{\#}$
LVI (mg/g)	3.54 ± 0.34	3.74 ± 0.25	4.21 ± 0.09 *	3.65 ± 0.07 $^{\#\#\#}$
RVI (mg/g)	0.87 ± 0.18	0.82 ± 0.15	0.88 ± 0.06	0.71 ± 0.03 $^{\#}$

U_9 and U_{18}, untreated SHRs 9 and 18 months of age; L_9 and L_{18}, 9 and 18 months aged SHRs treated with losartan during four weeks of experiment; $^{\#}$ $p < 0.05$, $^{\#\#}$ $p < 0.01$, $^{\#\#\#}$ $p < 0.001$ vs. the age match untreated SHRs; * $p < 0.05$, vs. the adult SHRs.

($p < 0.05$) in this group versus values in untreated adults. Chronic losartan treatment significantly increased urine creatinine concentration ($p < 0.05$), without changes in plasma creatinine, and therefore significantly increase glomerular filtration rate (GFR) measured by creatinine clearance ($p < 0.05$) in aged SHR. Urine flow, protein excretion and urine protein/creatinine ratio were also increased significantly with aging, and losartan decreased urine protein/creatinine ratio in aged SHR, but the difference was not significant.

Discussion

The data from the present study demonstrated that 4-week AT1 receptor blockade with losartan (10 mg/kg/day) improved BP, LVH carotid and aortic haemodynamics and preserved renal function and therefore decreased age-related CV risk in hypertensive rats. We also showed that Ang II is involved in RV remodeling in old SHR, because losartan treatment significantly reduced RV weight and RVI. Likewise, we demonstrated that in adult SHRs, when age-related cardiac and renal failure have not been completely developed yet, prolonged treatment with losartan resulted in marked but not significant reduction of SBP and MBP and improved haemodynamics in aorta.

Systolic hypertension and increased PP are independent risk factors for the development of cardiac hypertrophy (Zannad 1996; Izzo 2004). In the present study SBP, MBP and PP were significantly decreased after chronic losartan administration in aged SHRs. In addition to these beneficial effects on pressure overload, losartan reduced LVH that has been developed as a consequence of sustained hypertension and ageing. Susic and coauthors showed that angiotensin-converting enzyme inhibitor, enalapril, could reduce arterial pressure, total peripheral resistance, LV mass and ventricular fibrosis, without effect on RV mass in 65-week-old SHRs (Susic et al. 1999b). In the present study, however, we did not measure hydroxyproline content, as a marker of ventricular fibrosis, but our previous study confirmed the ability of losartan to improve cardiac performances by normalizing arterial BP, decreasing total peripheral vascular resistance and preventing LVH without significant reduction in myocardial and perivascular fibrosis in old SHRs (Mihailović-Stanojević et al. 2002). Thus, the reduction in pressure overload (afterload) could be, at last partly, sufficient to improve cardiac performances in aged SHR, suggesting that other mechanisms could account for myocardial fibrosis. Contrary to aged, in adult SHR LVH as an adaptive response to increased pressure overload, remain unchanged after losartan treatment, even marked but non-significant decrease in BP. In recent years, a large body of evidence demonstrated that Ang II acts not only through AT1 but also through Ang II type-2 (AT2) receptors that modulate the opposing effects of AT1 receptors on cardiac and vascular myocytic and fibrocytic mitogenesis as well as in cellular differentiation and arterial pressure regulation (Varagic et al. 2001b). This different response between adult and aged SHR could be explained due to enhanced AT2 receptor-mediated bradykinin and nitric oxide cascade during the AT1 receptor blockade (Siragy et al. 2000), Namely, there is an evidence that AT2 receptor mRNA is not expressed in detectable quantities in the adult heart, kidney, and vasculature, while its expression is increased in experimental heart failure, myocardial infarction, and vascular injury (Carey et al. 2000). Another explanation could involve the mechanisms that not include Ang II pathways, but is also responsible for pressure overload hypertrophy, such as endothelins or mechanical stretch (Harada et al. 1998).

The transition from hypertensive hypertrophy to heart failure in aged SHR is accompanied with marked changes of extracellular matrix composition, partly through transforming growth factor-$ß_1$ regulating mechanisms and the mRNA for this growth factor was found to be enhanced in both ventricles of SHR with failing heart (Boluyt and Bing 2000). It is of interest that 4 week of AT1 receptor blockade reduces the right, as well LV weight to body weight ratio in advanced age, thus providing the evidence for losartan non-haemodynamic action in ventricular remodeling.

Decreased regional blood flow (CBF, RBF, and ABF) and increased vascular resistance of the respective vascular beds in the present experiment suggest the important role of ageing and hypertension in relation to the progression of vascular dysfunction. Vascular remodeling as a response to alterations in blood flow, pressure and atherosclerosis involves changes

in vascular smooth muscle cell growth, migration and vessel matrix alteration, and include mechanisms that increase production of vasoactive molecules such as Ang II and ET-1 (Berk 2001). Results obtained from our study agree that Ang II plays an important role in hypertension and age dependent vascular remodeling *via* type-1 receptors, thus the blockade of Ang II AT1 receptors with losartan significantly improved haemodynamics in aorta of adult as well aged SHR, however, AVR was still higher in aged than in adult SHRs, while haemodynamics in carotid artery was improved only in aged SHRs. Thus the beneficial effects of Ang II AT1 receptor antagonist on structure and function of the conductive arteries could account for the decline of CV risk in old rats.

Age-induced increase in total cholesterol and triglyceride levels, were not changed after 4 weeks of antihypertensive treatment with losartan. These results are in agreement with results obtained from study of Andrzejczak et al. (2007) who found non-significant difference in total cholesterol and high density lipoprotein level after enalapril, quinapril and losartan treatment in SHR.

We evaluated age-related kidney function through GFR and urinary protein/creatinine ratio as a marker of proteinuria (Krishna et al. 1987). Our results show that aging markedly reduced GFR in hypertensive rats. Chronic administration of Ang II receptor blocker, losartan, induced the significant increase in GFR in aged, without any effect in adult SHR. Tank et al. (1994) has obtained greater reduction in GFR and renal plasma flow in 15-month-old than in 3-month-old SHRs. They also found that responses to systemic vasoconstrictor stimuli, such as Ang II and ET-1, were exaggerated in the aging kidney, whereas responsiveness to losartan was preserved but not enhanced. Urinary protein/creatinine ratio was markedly elevated in both untreated and losartan-treated aged SHRs, as a consequence of renal disease progression, and losartan slightly attenuate age and hypertension-induced proteinuria. Taking all together, we conclude that protective effects of AT1 receptor blockade on renal function could be in part due to dilatory effects of Ang II blocker on efferent and afferent arterioles and augmentation of glomerular membrane permeability.

In summary, these results demonstrated that regional haemodynamics and LVH, as well GFR were significantly impaired in SHRs with advanced age. Moreover, presented data indicates that losartan within 4 weeks, beside its beneficial effects on haemodynamics, LVH and kidney function, also regresses RV weight, and therefore further decreases CV risk in aged hypertensive rats. This could contribute to better outcomes in elderly humans with hypertensive cardiac and renal complications.

Acknowledgments. This work was supported by a grant from the Ministry of Science and Technological Development, Serbia (project No. OI-145054).

References

Andrzejczak D., Gorska D., Czarnecka E. (2007): Influence of enalapril, quinapril and losartan on lipopolysaccharide (LPS)-induced serum concentrations of TNF-α, IL-1β, IL-6 in spontaneously hypertensive rats (SHR). Pharmacol. Rep. **59**, 437–446

Arboix A., Miguel M., Ciscar E., Garcia-Eroles L., Massons J., Balcells M. (2006): Cardiovascular risk factors in patients aged 85 or older with ischemic stroke. Clin. Neurol. Neurosurg. **108**, 638–643

Ariff B., Stanton A., Barratt D., Augst A., Glor F., Poulter N., Sever P., Xu Y., Hughes A., Thom S. A. (2002): Comparison of the effects of antihypertensive treatment with angiotensin II blockade and beta-blockade on carotid wall structure and haemodynamics: protocol and baseline demographics. J. Renin Angiotensin Aldosterone Syst. **3**, 116–122

Berk B. C. (2001): Vascular smooth muscle growth: autocrine growth mechanisms. Physiol. Rev. **81**, 999–1030

Boluyt M. O., Bing O. H. L. (2000): Matrix gene expression and decompensated heart failure: the aged SHR model. Cardiovasc. Res. **46**, 239–249

Brilla C. G., Matsubara L., Weber K. T. (1996): Advanced hypertensive heart disease in spontaneously hypertensive rats. Lisinopril-mediated regression of myocardial fibrosis. Hypertension **28**, 269–275

Brooks W. W., Bing O. H., Conrad C. H., O'Neill L., Crow M. T., Lakatta E. G., Dostal D. E., Baker K. M., Boluyt M. O. (1997): Captopril modifies gene expression in hypertrophied and failing hearts of aged spontaneously hypertensive rats. Hypertension **30**, 1362–1368

Carey R. M., Wang Z. Q., Siragy H. M. (2000): Role of the angiotensin type 2 receptor in the regulation of blood pressure and renal function. Hypertension **35**, 155–163

Cerbai E., Crucitti A., Sartiani L., De Paoli P., Pino R., Rodriguez M. L., Gensini G., Mugelli A. (2000): Long-term treatment of spontaneously hypertensive rats with losartan and electrophysiological remodeling of cardiac myocytes. Cardiovasc. Res. **45**, 388–396

Fyhrquist F., Dahlof B., Devereux R. B., Kjeldsen S. E., Julius S., Beevers G., de Faire U., Ibsen H., Kristianson K., Lederballe-Pedersen O., Lindholm L. H., Nieminen M. S., Omvik P., Oparil S., Hille D. A., Lyle P. A., Edelman J. M., Snapinn S. M., Wedel H. (2005): Pulse pressure and effects of losartan or atenolol in patients with hypertension and left ventricular hypertrophy. Hypertension **45**, 580–585

Hall J. E., Brands M. W., Henegar J. R. (1999): Angiotensin II and long-term arterial pressure regulation: the overriding dominance of the kidney. J. Am. Soc. Nephrol. **10** (Suppl. 12), S258–265

Harada K., Komuro I., Shiojima I., Hayashi D., Kudoh S., Mizuno T., Kijima K., Matsubara H., Sugaya T., Murakami K., Yazaki Y. (1998): Pressure overload induces cardiac hypertrophy in angiotensin II type 1A receptor knockout mice. Circulation **97**, 1952–1959

Iwamoto T., Ami M., Shimizu T., Tanaka Y., Nishimura T., Takasaki M. (2000): Clinical findings of arteriosclerosis and serum

lipoprotein(a) concentration in elderly patients. Nippon Ronen Igakkai Zasshi **37**, 811–818 (in Japanese)

Izzo J. L. Jr. (2004): Arterial stiffness and the systolic hypertension syndrome. Curr. Opin. Cardiol. **19**, 341–352

Komatsu K., Frohlich E. D., Ono H., Ono Y., Numabe A., Willis G. W. (1995): Glomerular dynamics and morphology of aged spontaneously hypertensive rats. Effects of angiotensin-converting enzyme inhibition. Hypertension **25**, 207–213

Krishna K. S., Pandey A. P., Kirubakaran M. G., Kanagasabapathy A. S. (1987): Urinary protein/creatinine ratio as an indicator of allograft function following live related donor renal transplantation. Clin. Chim. Acta **163**, 51–61

Lakatta E. G. (2003): Arterial and cardiac aging: major shareholders in cardiovascular disease enterprises: Part III: cellular and molecular clues to heart and arterial aging. Circulation **107**, 490–497

Linz W., Heitsch H., Scholkens B. A., Wiemer G. (2000): Long-term angiotensin II type 1 receptor blockade with fonsartan doubles lifespan of hypertensive rats. Hypertension **35**, 908–913

Linz W., Wohlfart P., Schoelkens B. A., Becker R. H., Malinski T., Wiemer G. (1999): Late treatment with ramipril increases survival in old spontaneously hypertensive rats. Hypertension **34**, 291–295

Mihailović-Stanojević N., Jovović D., Miloradović Z., Lastić-Maletić S., Jerkić M. (2002): Haemodynamics and cardiac morphological effects of endothelin and angiotensin II type I receptor blockade in aged spontaneously hypertensive rats. Acta Biol. Med. Exp. **27**, 11–16

Mihailovic-Stanojevic N., Varagic J., Jovovic D., Miloradovic Z., Markovic-Lipkovski J., Jerkic M. (2003): Aging and hypertension as factors of progressive renal failure. Med. Pregl. **56** (Suppl. 1), 59–64 (in Serbian)

Mihailovic-Stanojevic N., Jovovic D., Miloradovic Z., Drndarevic N., Markovic-Lipkovski J., Jerkic M. (2004): Long-term losartan but not bosentan treatment revert vascular injury in the kidney of aged spontaneously hypertensive rats. In: Besondere Aspekte der Cerebrovaskularen und Peripheren Ateriosklerose. (Eds. H. Heinle, H. Schulte and H. Hahmann), pp. 175–184, Tübingen

Najjar S. S., Scuteri A., Lakatta E. G. (2005): Arterial aging: is it an immutable cardiovascular risk factor? Hypertension **46**, 454–462

Oddie C. J., Dilley R. J., Kanellakis P., Bobik A. (1993): Chronic angiotensin II type 1 receptor antagonism in genetic hypertension: effects on vascular structure and reactivity. J. Hypertens. **11**, 717–724

Pratt R. E. (1999): Angiotensin II and the control of cardiovascular structure. J. Am. Soc. Nephrol. **10** (Suppl. 11), S120–128

Safar M. E., Levy B. I., Struijker-Boudier H. (2003): Current perspectives on arterial stiffness and pulse pressure in hypertension and cardiovascular diseases. Circulation **107**, 2864–2869

Siragy H. M., de Gasparo M., Carey R. M. (2000): Angiotensin type 2 receptor mediates valsartan-induced hypotension in conscious rats. Hypertension **35,** 1074–1077

Susic D., Francischetti A., Frohlich E. D. (1999a): Prolonged L-arginine on cardiovascular mass and myocardial hemodynamics and collagen in aged spontaneously hypertensive rats and normal rats. Hypertension **33**, 451–455

Susic D., Varagic J., Frohlich E. D. (1999b): Pharmacologic agents on cardiovascular mass, coronary dynamics and collagen in aged spontaneously hypertensive rats. J. Hypertens. **17**, 1209–1215

Taddei S., Virdis A., Mattei P., Ghiadoni L., Fasolo C. B., Sudano I., Salvetti A. (1997): Hypertension causes premature aging of endothelial function in humans. Hypertension **29**, 736–743

Tank J. E., Vora J. P., Houghton D. C., Anderson S. (1994): Altered renal vascular responses in the aging rat kidney. Am. J. Physiol. **266**, F942–948

Tsotetsi O. J., Woodiwiss A. J., Netjhardt M., Qubu D., Brooksbank R., Norton G. R. (2001): Attenuation of cardiac failure, dilatation, damage, and detrimental interstitial remodeling without regression of hypertrophy in hypertensive rats. Hypertension **38**, 846–851

Unger T. (2001): Pharmacological properties of angiotensin II antagonists: examining all the therapeutic implications. J. Renin Angiotensin Aldosterone Syst. **2** (Suppl. 2), S4–7

Van Bortel L. M., Struijker-Boudier H. A., Safar M. E. (2001): Pulse pressure, arterial stiffness, and drug treatment of hypertension. Hypertension **38**, 914–921

Varagic J., Susic D., Frohlich E. (2001a): Heart, aging, and hypertension. Curr. Opin. Cardiol. **16**, 336–341

Varagic J., Susic D., Frohlich E. D. (2001b): Coronary hemodynamic and ventricular responses to angiotensin type 1 receptor inhibition in SHR – interaction with angiotensin type 2 receptors. Hypertension **37**, 1399–1403

Zannad F. (1996): Concomitant diseases in elderly hypertensives: the position of nicardipine. J. Hypertens. Suppl. **14**, 37–40

Effect of simvastatin on proinflammatory cytokines production during lipopolysaccharide-induced inflammation in rats

Lana Nežić[1], Ranko Škrbić[1], Silva Dobrić[2], Miloš P. Stojiljković[3], Svjetlana S. Šatara[1], Zoran A. Milovanović[2] and Nataša Stojaković[1]

[1] *Department of Pharmacology, Toxicology and Clinical Pharmacology, Medical Faculty, University of Banja Luka, Save Mrkalja 14, 78000 Banja Luka, Republic of Srpska, Bosnia and Herzegovina*
[2] *National Poison Control Centre, Medical Military Academy, Crnotravska 11, 11000 Belgrade, Serbia*
[3] *Department of Pharmacology, Medical Faculty, University of East Sarajevo, 51000 Foča, Republic of Srpska, Bosnia and Herzegovina*

Abstract. The effect of simvastatin applied in a short-term pretreatment on proinflammatory cytokines production in acute systemic inflammation induced by endotoxin – lipopolysaccharide (LPS) in rats was investigated. Both LPS and simvastatin doses were established in separate experiments in which increasing doses of both compounds were given to obtain the LD_{50} LPS and the maximally protective dose of simvastatin against LD_{50} LPS. To determine the anti-inflammatory effect, simvastatin was given orally for 5 days, followed by a single intraperitoneal non-lethal dose of LPS (0.25 LD_{50}). Plasma concentrations of tumor necrosis factor alpha (TNF-α), interleukin (IL)-1β and IL-6 were measured by enzyme-linked immunosorbent assay. The acute i.p. LD_{50} LPS amounted to 22.15 mg/kg. Simvastatin of 20 mg/kg p.o. was maximally protective against LD_{50} LPS, and this dose was used for studying its effects on LPS-induced cytokines production. Cytokines concentrations were significantly increased upon challenge of non-lethal dose of LPS. The peak levels of TNF-α and IL-1β were significantly suppressed by simvastatin, compared to control rats only treated with dimethylsulfoxide before LPS. In contrast, simvastatin did not affect IL-6 levels at all timepoints. Simvastatin pretreatment given orally produced acute anti-inflammatory effects by inhibiting TNF-α and IL-1β, but no IL-6 production.

Key words: Simvastatin — Endotoxin — Inflammation — Cytokines — Rat

Introduction

Several clinical trials showed that statins reduce the risk of cardiovascular events even in the absence of a significant drop of blood cholesterol levels (Ridker et al. 1998; Davignon 2004), suggesting that the benefits of statin therapy may also be ascribed to their action on nonlipid factors involved in inflammation-fibroproliferation, an important feature of atherosclerosis (Marz and Wieland 2000; Bonetti et al. 2003). There is growing evidence that statins have additional anti-inflammatory properties by reducing inflammatory parameters such as C-reactive protein (Albert et al. 2001; Joukhadar et al. 2001), tumor necrosis factor α (TNF-α) and interleukin (IL)-1β in patients with hypercholesterolemia and heart transplant recipients (Holm et al. 2001; Koh et al. 2004), unrelated to their lipid-lowering activity. Moreover, recent studies have shown that prior statins therapy prevented vascular hyporeactivity during acute systemic inflammation in humans (Pleiner et al. 2004) and was associated with a reduction of severe sepsis development (Almog et al. 2004).

Statins are 3-hydroxy-3-methylglutaryl-coenzyme A (HMG-CoA) reductase inhibitors, which reduce low-density lipoprotein (LDL) cholesterol levels by blocking the mevalonate pathway and increase LDL cholesterol receptor expression in the liver. By inhibiting HMG-CoA reductase, statins might directly influence the cellular events other than cholesterol synthesis, because mevalonate, the product of HMG-CoA reductase, is the precursor of not only cholesterol, but also of

Correspondence to: Lana Nežić, Department of Pharmacology, Toxicology and Clinical Pharmacology, Medical Faculty, Save Mrkalja 14, 78000 Banja Luka, Republic of Srpska, Bosnia and Herzegovina
E-mail: lanne@doctor.com

many non-steroidal isoprenoid compounds. The isoprenoids farnesyl pyrophosphate and geranylgeranyl pyrophosphate are known to play an important role in signal transduction pathways by their attachment to signalling proteins, such as Ras and Rho (Kwak et al. 2000; Cordle et al. 2005).

Inhibition of HMG-CoA reductase activity in monocytes (Terkeltaub et al. 1994) and rat mesangial cells (Kim et al. 1995) treated with lipopolysaccharide (LPS) and granulocyte-macrophage-colony stimulating factor reduced the production of IL-8, IL-6, and MCP-1, (monocyte chemotactic protein-1) responsible for leukocyte recruitment at the infection site. Statins have been shown as effective endothelium-protective agents that reduced leukocyte-endothelial cell interactions and improved endothelial function *via* increasing endothelial nitric oxide synthase (eNOS) (Laufs et al. 2002; Pruefer et al. 2002). Recently, using a common model of acute local inflammation (carrageenan-induced rat paw oedema), we also showed that simvastatin administered orally in the single dose produced significant anti-inflammatory activity (footpad swelling inhibition and reduction of polymorphonuclear leukocytes infiltration) comparable to that of indomethacin (Nežić et al. 2009). Study by Wagner et al. (2002) showed that acute pretreatment with atorvastatin inhibits TNF-α plus interferon-γ stimulated transcription factor activation in native endothelial cells *in situ* and the subsequent expression of inducible nitric oxide synthase (iNOS) involved in vascular inflammation and atherosclerosis. Also, cerivastatin administered intraperitoneally (i.p.) significantly improved the survival of mice with LPS-induced sepsis and reduced TNF-α, IL-1β and IL-6 overproduction (Ando et al. 2000; Chaudhry et al. 2008).

In the present study, we investigated if simvastatin, a widely used statin, when given orally to imitate the regular route of statins use in humans, may attenuate systematic inflammation by inhibition of proinflammatory cytokines production. The first part of this study consisted of an experiment examining both lethal and protective doses of LPS and simvastatin, respectively. The second part of the study presented *in vivo* experiments examining anti-inflammatory effects of simvastatin administered in short-term pretreatment prior to non-lethal, but inflammatory dose of LPS, on the pro-inflammatory cytokines (TNF-α, IL-1β and IL-6) production.

Endotoxin or LPS is a component of the outer cell wall of Gram-negative bacteria. Systemic injection of LPS to experimental animals is a widely used *in vivo* model for the study of endotoxic shock and acute systemic inflammation. LPS activates the immune system leading to release of endogenous proinflammatory cytokines such as TNF-α, IL-1β and IL-6 (Ando et al. 2000; Dogan et al. 2002). The important feature of this model is that simvastatin given in short-term treatment does not affect plasma lipid levels (cholesterol-lowering activities takes at least two weeks of therapy), and therefore the results may be interpreted without this confounding variable (Rosenson 1999).

Materials and Methods

Animals

Adult male Wistar rats were obtained from Military Medical Academy Research Laboratories (Belgrade, Serbia) and kept in the animal unit 7 days before the experiment. Animals were given standard laboratory diet and tap water *ad libitum* and housed in an air-conditioned room with an ambient temperature of 22–24°C and a 12 h light/dark cycle (light on at 07:00 a. m.). At the start of the experiment, rats weighing 200–220 g were placed in individual cages. All experimental procedures on animals were conducted in accordance with the Guidelines on human care of experimental animals adopted by the Ethical Committee and other corresponding national legal codes.

Experimental design

Endotoxin-induced lethality in rats

The animals were divided into three groups (n = 6 per group), given saline orally (p.o.) and challenged with one of the three various doses of LPS (10, 20, 30 mg/kg b.w.) given i.p. The lethality was then monitored over the next 7 days. The number of dead rats resulting from LPS was recorded and the median lethal dose (LD_{50}) of LPS (i.p.) was calculated (Litchfield and Wilcoxon 1949).

Protective effect of simvastatin on lethality induced by endotoxin

To determine the effect of short-term pretreatment of simvastatin on the survival of rats injected with LD_{50} of LPS, the animals were divided into three groups (n = 6 per group); simvastatin was given to rats p.o. in one of the three various doses (5, 10, and 20 mg/kg b.w.) per day for 5 days, and 1.5 h after the last dose of simvastatin the single LD_{50} of LPS was injected i.p. The survival of animals was monitored for a period of the next 7 days. Simvastatin alone had no effect on the survival of the animals. The doses of simvastatin used were comparable to those that had previously been used in rat/murine studies *in vivo* (typically 10–100 mg/kg/day) and were higher than those used in humans because of a significant up-regulation (3- to 8-fold) of HMG-CoA reductase induced by statin treatment in rodents (Kita et al. 1980; Sparrow et al. 2001; Leung et al. 2003).

Effect of simvastatin on proinflammatory cytokines production

In this experiment, simvastatin was used in a dose of 20 m/kg p.o. (the maximally protective dose of simvastatin against the single LD_{50} of LPS in rats). To induce acute systemic

inflammation and proinflammatory cytokines production, the animals were challenged with a non-lethal dose of endotoxin i.p. (0.25 LD_{50} of LPS).

The rats were randomized into the control and simvastatin-treated experimental groups ($n = 8$ per group). Simvastatin (20 mg/kg) was given p.o. *via* oral gavage for 5 days, and 1.5 h after the last dose of simvastatin, LPS (*Escherichia coli* serotype 0127:B8; Sigma Aldrich, Munich, Germany) at a non-lethal single dose (5.5 mg/kg b.w.) was i.p. administered. The control animals received the same volume of 0.1% dimethylsulfoxide (DMSO) for 5 days, as a vehicle, before LPS injection. The rats were restrained using a restraint tube and blood was collected by tail vein puncture at various time points (0, 60, 90, 120, 180, 240 min) after LPS injection. Blood samples were collected into Eppendorff tubes containing EDTA (ethylenediamine tetraacetic acid) solution and centrifuged (1000 × *g*, 20 min, 4°C). The plasma was stored at –70°C until assay. Plasma levels of TNF-α, IL-1β and IL-6 were determined using rat ELISA (enzyme-linked immunoassay) kits in accordance with to the manufacturer's recommended protocols (R&D Systems, UK). Sensitivity of detection was 20 pg/ml for cytokines.

Drugs

Simvastatin (donated by Krka, Novo Mesto, Slovenia) was dissolved in 0.1% DMSO as a 10 mg/ml stock. LPS from *E. coli* serotype 0127:B8 (Sigma Aldrich) was injected i.p. after dilution with sterile pyrogen-free physiologic saline solution, at an injection volume of 1 ml/kg.

Statistical analysis

The median lethal dose of endotoxin that was lethal to 50% of the rats (LD_{50} of LPS) was calculated by the Lichfield and Wilcoxon procedure (Lichfield and Wilcoxon 1949).

Differences in plasma TNF-α, IL-1β and IL-6 level between the simvastatin treated and the control animals were determined with nonparametric Mann-Whitney U-test and Kruscal-Wallis test. Results were expressed as mean ± SE (standard errors), $p < 0.05$ was considered significant.

Results

Determination of LD_{50} of LPS and protective dose of simvastatin

In Table 1, LPS dose-dependently increased lethality of rats during 7 days after injection is shown. The LD_{50} of LPS administered i.p. was calculated to be 22.15 mg/kg b.w.

The efficacy of various doses of simvastatin administered p.o. in the short-term treatment prior to LD_{50} of LPS challenge resulted in a dose-dependent increase in survival. As shown in Table 1, complete lethality protection was observed at dose of 20 mg/kg b.w. (p.o.) of simvastatin.

Effect of simvastatin on proinflammatory cytokines production

For the purpose of this part of the experiment we used a single dose of LPS (5.5 mg/kg b.w., i.p.) as a non-lethal dose (0.25 LD_{50} of LPS) to induce acute systemic inflammation. The dose of 20 mg/kg b.w. (p.o.) of simvastatin that protected the animals from LPS LD_{50} induced lethality was used to determine the effect of the drug on proinflammatory cytokines production induced by LPS.

All the animals survived this experiment. In addition, simvastatin itself neither increased serum levels of cytokines nor affected the clinical status and the behavior of rats, such as their dietary intake or body weight gain (data not shown).

TNF-α response

The time course of plasma TNF-α level

Intraperitoneal injection of LPS induced a marked increase in plasma TNF-α level. The plasma level increased at 60 min and peaked at 90 min after injection ($p < 0.002$) compared to baseline, with no significant difference in plasma TNF-α levels between these timepoints ($p = 0.52$), and thereafter

Table 1. The effect of simvastatin pretreatment on LPS-induced lethality in rats

Simvastatin pretreatment (mg/kg/day p.o)[b]	LPS (mg/kg i.p)[a]	No. of rats (dead/total)
none	10	0/6
	20	3/6
	30	4/6
5	LD_{50}	3/6
10		1/6
20		0/6

[a] Adult male Wistar rats were divided into three groups ($n = 6$ per group), challenged with one of the various doses of LPS (10, 20, 30 mg/kg b.w.) i.p. Lethality was monitored over the 7 days. The dose of LPS that was lethal to 50% of the rats, i.e. LD_{50} of LPS administered i.p. was calculated to be 22.15 mg/kg b.w. by the Litchfield and Wilcoxon procedure (Litchfield and Wilcoxon 1949). [b] Rats were divided into three groups ($n = 6$) and were given simvastatin p.o. in doses of 5, 10, and 20 mg/kg/day for 5 days, after which the single LD_{50} of LPS was administered i.p. Survival of animals was monitored for a period of the 7 days.

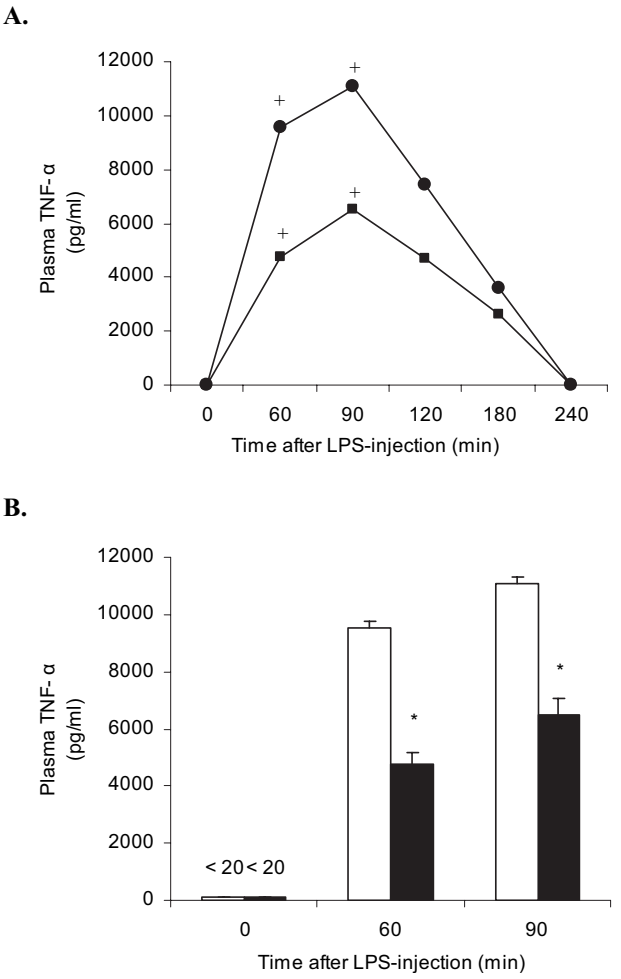

Figure 1. Time course of plasma TNF-α level in control (closed circle, vehicle + LPS) and simvastatin + LPS (closed quadrate)-treated rats. Animals (n = 8 per group) were given simvastatin (20 mg/kg/day p.o) 5 days prior to single dose of LPS (5.5 mg/kg i.p.). Plasma TNF-α was determined at 0, 60, 90, 120, 180 and 240 min after LPS. $^{+}$ $p < 0.002$ compared to baseline (panel A). Maximal inhibitory effect of simvastatin (20 mg/kg, p.o. given 5 days prior to a single dose of LPS of 5.5 mg/kg, i.p.) (black column) was shown at the peak plasma values of TNF-α at 60 and 90 min post LPS injection (values are mean ± S.E.M.). * $p < 0.05$ compared to the control group (white column; vehicle + LPS). The amounts of TNF-α in plasma (baseline) were bellow detection limit (<20 pg/ml) (panel B).

gradually decreased to near basal levels by 240 min (Figure 1, panel A).

The effects of simvastatin on LPS-induced plasma TNF-α elevation

As shown in Figure 1A, in rats pretreated with simvastatin prior to LPS injection, the plasma TNF-α levels significantly increased at 60 min and 90 min, post LPS injection ($p < 0.002$) compared to baseline, with no significant difference in TNF-α plasma levels between these timepoints ($p > 0.05$). *Post hoc* analysis revealed that simvastatin significantly reduced the plasma TNF-α levels compared to the control group, with maximal effects at 60 and 90 min ($p < 0.05$) (Figure 1, panel B).

IL-1β response

The time course of plasma IL-1β level

Plasma IL-1β levels increased significantly with peak value at 120 min after LPS injection ($p < 0.002$), remained elevated at 180 min ($p < 0.002$) and slightly decreased thereafter, but still present after 240 min timepoint (Figure 2, panel A).

The effects of simvastatin on LPS-induced plasma IL-1β elevation

As shown in Figure 2A, in rats pretreated with simvastatin prior to LPS injection, the plasma IL-1β levels significantly increased at 120 min and 180 min post LPS ($p < 0.002$), compared to baseline, with no significant differences in IL-1β levels after 120 min ($p > 0.05$). *Post hoc* analysis revealed that simvastatin significantly reduced the plasma IL-1β levels compared to the control group, with maximal effects at 120 min ($p < 0.01$) and 180 min ($p < 0.05$) (Figure 2, panel B).

IL-6 response

The time course of plasma IL-6 level

Plasma IL-6 levels increased significantly at 120 min ($p < 0.002$), peaked at 180 min and 240 min, after LPS injection ($p < 0.002$), with no significant difference in IL-6 levels between these timepoints, and remained elevated after 240 min (Figure 3, panel A).

The effects of simvastatin on LPS-induced plasma IL-6 elevation

As shown in Figure 3A, in rats pretreated with simvastatin prior to LPS injection, the kinetics of plasma IL-6 levels was similar to that of the control group, and significantly increased compared to baseline ($p < 0.05$). *Post hoc* analysis revealed that simvastatin had no significant effect on the plasma IL-6 levels compared to the control group at all timepoints (Figure 3, panel B).

Discussion

In the present study, we have shown that short-term pretreatment with simvastatin effectively prevented endo-

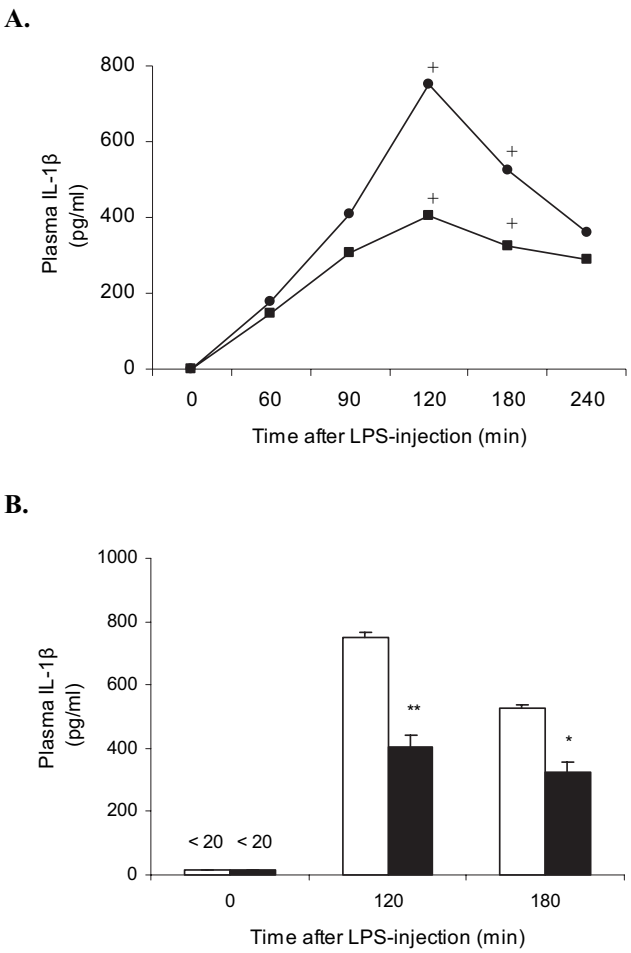

Figure. 2. Time course of plasma IL-1β level in control (closed circle, vehicle + LPS) and simvastatin + LPS (closed quadrate)-treated rats. Animals ($n = 8$ per group) were given simvastatin (20 mg/kg/day p.o) 5 days prior to single dose of LPS (5.5 mg/kg i.p.). Plasma IL-1β was determined at 0, 60, 90, 120, 180 and 240 min after LPS. $^{+}p < 0.002$ compared to baseline (panel A). Maximal inhibitory effect of simvastatin (20 mg/kg p.o. given 5 days prior to a single dose of LPS of 5.5 mg/kg i.p.) (black column) was shown at the peak plasma values of IL-1β at 120 and 180 min post LPS injection (values are mean ± S.E.M.). ** $p < 0.01$; * $p < 0.05$ compared to the control group (white column; vehicle + LPS). The amounts of IL-1β in plasma (baseline) were bellow detection limit (<20 pg/ml) (panel B).

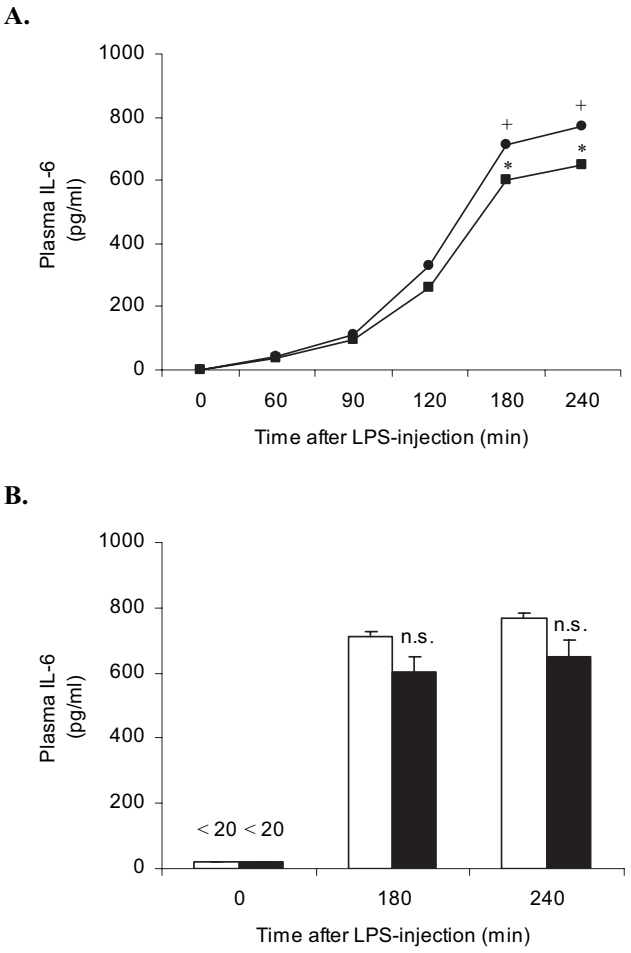

Figure. 3. Time course of plasma IL-6 level in control (closed circle, vehicle + LPS) and simvastatin + LPS (closed quadrate) treated rats. Animals ($n = 8$ per group) were given simvastatin (20 mg/kg/day p.o) 5 days prior to a single dose of LPS (5.5 mg/kg i.p.). Plasma IL-6 was determined at 0, 60, 90, 120, 180 and 240 min after LPS. $^{+}p < 0.002$; * $p < 0.05$ compared to baseline (panel A). Maximal inhibitory effect of simvastatin (20 mg/kg, p.o. given 5 days prior to a single dose of LPS of 5.5 mg/kg i.p.) (black column) was shown at the peak plasma values of IL-6 at 180 and 240 min post LPS injection (values are mean ± S.E.M.). n.s, non significant compared to the control group (white column; vehicle + LPS). The amounts of IL-6 in plasma (baseline) were bellow detection limit (<20 pg/ml) (panel B).

toxin-induced lethality in a dose dependent manner. This is consistent with the results from previous animal studies (Ando et al. 2000; Merx et al. 2004). Also, several clinical studies showed that statin usage was associated with reduced mortality from sepsis and/or bacterial infection in patients with atherosclerosis and present comorbities including diabetes mellitus, chronic renal failure, or a history of infections (Liappis et al. 2001; Almog et al. 2004; Hackam et al. 2006). However, mechanisms by which statins could prevent development of severe sepsis are not completely known yet. Gram negative sepsis is initiated by exposure to the LPS which induces overproduction of proinflammatory cytokines, which in turn up-regulate the expression of iNOS. Large amount of cytokines and nitric oxide contribute to LPS-induced hypotension, multiple organ failure and lethality. Recent study by Yasuda et al. (2006), revealed that short-term pretreatment with simvastatin improved sepsis-induced lethality and acute renal injury,

reversed microvascular perfusion defect with corresponding improvement in tissue oxygenation and also reduced a serum TNF-α. Cerivastatin also acutely protected mice against sepsis related death *via* reduced proinflammatory cytokines production and enhanced bacterial clearance (Chaudhry et al. 2008).

The results of our study demonstrated that a non-lethal dose of LPS challenge results in increased circulating concentrations and similar time courses of proinflammatory cytokines TNF-α, IL-1β and IL-6 as previously described (Ando et al. 2000; Dogan et al. 2002). In this *in vivo* model of acute systemic inflammation, we observed that short-term pretreatment with simvastatin administered orally inhibited LPS-induced secretion of TNF-α and IL-1β, both at their peaked time points following LPS administration. In contrast, simvastatin pretreatment failed to alter LPS-stimulated IL-6 secretion at any of the time points examined. Similar results have been shown in two experimental studies, where simvastatin given orally in lower dose (10 mg/kg) in short-time pretreatment significantly inhibited proinflammatory cytokines production in acute local and systemic inflammation (Diomede et al. 2001; Souza et al. 2006).

In several clinical trials, statins have shown anti-inflammatory effects; also on a short-time scale similar to ours (Holm et al. 2001; Plenge et al. 2002; Steiner et al. 2005). However, our results do not confirm that simvastatin completely modulate proinflammatory cytokines production, as IL-6 levels only tended to be nonsignificantly lower in the simvastatin group. This finding is in line with a previous clinical study that reported slight lowering effect of simvastatin on IL-6 and IL-1β production during endotoxemia (Pleiner et al. 2004). In addition, in a recent study Erikstrup et al. (2006) observed that in *in vivo* model of low-grade inflammation short-term treatment of simvastatin failed to inhibit endotoxin-induced increase in plasma levels of TNF-α, IL-6, IL-1β receptor antagonist, C-reactive protein or leucocytes count. There is a debate regarding the IL-6 response to statin therapy in the literature. Although some studies report a decrease (Rezaie-Majd et al. 2002), others report little (Kinlay et al. 2003) or no effect on IL-6 levels (Jialal et al. 2001). This is probably due to a great circadian variation in IL-6 levels and a high interindividual variability in IL-6 levels, which was also observed after LPS administration (Endler et al. 2004). The molecular mechanisms are unclear and this reflects some of the divergent results reported for statins effects on IL-6 production.

There are several potential mechanisms of acute anti-inflammatory actions of statins in this and similar models of inflammation. Statins, *via i*nhibition of mevalonate pathway, block the synthesis of isoprenoids, geranylgeranyl pyrophosphate and farnesyl pyrophosphate and facilitate accumulation of inactive Rho and Ras in the cytoplasm. Furthermore, statins have also been reported to inhibit nuclear factor kappa B (NF-κB) activation, a transcription factor of a signal transduction pathways that is activated in response to inflammatory stimuli, such as LPS, cytokines (e.g. IL-1β, TNF-α) or trough activated GTP binding proteins (Ras-Rho). In fact, upon stimulation NF-κB enters the nucleus where it can induce the transcription of inflammatory genes and numerous proinflammatory cytokines production (Beutler 2004; Seasholtz and Brown 2004; Abeles and Pillinger 2006). Also, it has been shown that anti-inflammatory effects of statins involves up-regulation of an inhibitor of NF-κB (I κBα), which traps NF-κB in the cytosol (Kleemann et al. 2004). The most frequently proposed model is that statins interrupt the proinflammatory signalling by down-regulation of Rho-related protein activation**,** that, in turn, requires posttranslational modification involving nonsterol mevalonate-derived compounds to be active (Seasholtz and Brown 2004; Abeles and Pillinger 2006). Increasing evidence suggests that statins modulate macrophage functions by inhibiting the activation of inflammatory response genes, such as IL-1β, IL-6, and TNF-α, metalloproteinase (MMP)-2, and MMP-9, and iNOS as a consequence of interference with the sGTP binding proteins/NF-κB transduction pathway (Takemoto and Liao 2001). Recent *in vivo* and *in vitro* studies have also revealed that statins could act in an inflammation *via* mechanisms involving peroxisome proliferator-activated receptor (PPAR) pathway. PPAR is a nuclear receptor, with three isoforms PPAR-α, PPAR-γ and PPAR-δ, which regulate lipid metabolism but also exert pronounced anti-inflammatory activities. It exerts anti-inflammatory activities by negatively interfering with proinflammatory signaling pathways including NF-κB. (Marx et al. 2004; Paumelle et al. 2006). It has been shown that statins, simvastatin and atorvastatin, reduce activity of iNOS, as well as IL-6 and TNF-α levels by increasing PPAR-α and PPAR-γ activities, respectively (Grip et al. 2002; Paumelle et al. 2006).

There are several limitations to our experimental design. We chose endotoxin as an inductor of endotoxic shock and inflammation, but this is just one of many ways to activate the immune system. Clinical endotoxic shock is more complex than can be modeled in these experiments. Patients may be subjected to a large bolus of endotoxin release from an infected site or even a continual release of endotoxin depending on the patient. Also it must be emphasized that we induced only an acute, short-lived activation and not an extended inflammatory state where proinflammatory cytokines circulating levels exist longer. The animal species, the dose of endotoxin, as well as the dose and duration of simvastatin treatment, could also affect the results. Although we have assessed potential effects on survival and only circulating parameters, we cannot exclude that statins might possess anti-inflammatory properties at the tissue or endothelial level.

It is important to emphasize that simvastatin, as shown in our study, could have protective and anti-inflammatory effects when administered orally, which is the route of administration of the drug in clinical practice.

In conclusion, we showed that simvastatin might be useful in prevention of LPS relating severe conditions providing preliminary evidence that circulating levels of proinflammatory cytokines were partly attenuated by simvastatin in an animal *in vivo* model of acute systemic inflammation. However, mechanisms behind the protective and anti-inflammatory properties afforded by short-term treatment of simvastatin and its implications in a clinical setting are not clear enough and warrant further investigation.

References

Abeles A. M., Pillinger M. H. (2006): Statins as antiinflammatory and immunomodulatory agents: a future in rheumatologic therapy? Arthritis Rheum. **54**, 393–407

Albert M. A., Danielson E., Rifai N., Ridker P. M. (2001): Effect of statin therapy on C-reactive protein levels. The pravastatin inflammation/CRP evaluation (PRINCE): a randomized trial and cohort study. JAMA **286**, 64–70

Almog Y., Shefer A., Novack V., Maimon N., Barski L., Eizinger M., Friger M., Zeller L., Danon A. (2004): Prior statin therapy is associated with decreased rate of severe sepsis. Circulation **110**, 880–885

Ando H., Takamura T., Ota T., Nagai Y., Kobayashi K. (2000): Cerivastatin improves survival of mice with lipopolysaccharide induced sepsis. J. Pharmacol. Exp. Ther. **294**, 1043–1046

Beutler B. (2004): Inferences, questions and possibilities in Toll-like receptor signaling. Nature **430**, 257–263

Bonetti P. O., Lerman L. O., Napoli C., Lerman A. (2003): Statin effects beyond lipid lowering are they clinically relevant. Eur. Heart J. **24**, 225–248

Chaudhry M. Z., Wang J. H., Blankson S., Redmond H. P. (2008): Statin (cerivastatin) protects mice against sepsis-related death *via* reduced proinflammatory cytokines and enhanced bacterial clearance. Surg. Infect. (Larchmt.) **9**, 183–194

Cordle A., Koenigsknecht-Talboo J., Wilkinson B., Limpert A., Landreth G. (2005): Mechanisms of statin-mediated inhibition of small G-protein function. J. Biol. Chem. **280**, 34202–34209

Davignon J. (2004): Beneficial cardiovascular pleiotropic effects of statins. Circulation **109** (Suppl. 1), III39–43

Diomede L., Albani D., Sottocorno M., Polentarutti N., Donati M. B., Bianchi M., Fruscella P., Salmona M. (2001): The *in vivo* anti-inflammatory effect of statins is mediated by nonsterol mevalonate products. Arterioscler. Thromb. Vasc. Biol. **21**, 1327–1332

Dogan M. D., Ataoglu H., Akarsu E. S. (2002): Characterization of the hypothermic component of LPS-induced dual thermoregulatory response in rats. Pharmacol. Biochem. Behav. **72**, 143–150

Endler G., Marsik C., Joukhadar C., Marculescu R., Mayr F., Mannhalter C., Wagner O. F., Jilma B. (2004): The interleukin-6 G(-174)C promoter polymorphism does not determine plasma interleukin-6 concentrations in experimental endotoxemia in humans. Clin. Chem. **50**, 195–200

Erikstrup C., Ullum H., Pedersen B. K. (2006): Short-term simvastatin treatment has no effect on plasma cytokine response in a human in vivo model of low-grade inflammation. Clin. Exp. Immunol. **144**, 94–100

Grip O., Janciauskiene S., Lindgren S. (2002): Atorvastatin activates PPAR-γ and attenuates the inflammatory response in human monocytes. Inflamm. Res. **51**, 58–62

Hackam G. D., Mamdani M., Li P., Redelmeiweer A. D. (2006): Statins and sepsis in patients with cardiovascular disease: a population-based cohort analysis. Lancet **367**, 413–418

Holm T., Andreassen A. K., Ueland T., Kjekshus J., Froland S. S., Kjekshus E., Simonsen S., Aukrust P., Gullestad L. (2001): Effects of pravastatin on plasma markers of inflammation and peripheral endothelial function in male heart transplant recipients. Am. J. Cardiol. **87**, 815–818

Jialal I., Stein D., Balis D., Grundy S. M., Adams-Huet B., Devaraj S. (2001): Effect of hydroxymethyl glutaryl coenzyme A reductase inhibitor therapy on high sensitive C-reactive protein levels. Circulation **103**, 1933–1935

Joukhadar C., Klein N., Prinz M., Schrolnberger C., Vukovich T., Wolzt M., Schmetterer L., Dorner G. T. (2001): Similar effects of atorvastatin, simvastatin and pravastatin on thrombogenic and inflammatory parameters in patients with hypercholesterolemia. Thromb. Haemost. **85**, 47–51

Kim S. Y., Guijarro C., O'Donnell M. P., Kasiske B. L., Kim Y., Keane W. F. (1995): Human mesangial cell production of monocyte chemoattractant protein-1: modulation by lovastatin. Kidney Int. **48**, 363–371

Kinlay S., Schwartz G. G., Olsson A. G., Rifai N., Leslie S. J., Sasiela W. J., Szarek M., Libby P., Ganz P. (2003): High-dose atorvastatin enhances the decline in inflammatory markers in patients with acute coronary syndromes in the MIRACL study. Circulation **108**, 1560–1566

Kita T., Brown M. S., Goldstein J. L. (1980): Feedback regulation of 3-hydroxy-3-methylglutaryl coenzyme A reductase in livers of mice treated with mevinolin, a competitive inhibitor of the reductase. J. Clin. Invest. **66**, 1094–1100

Kleemann R., Verschuren L., de Rooij B. J., Linderman J., de Maat M. M., Szalai A. J., Princen H. M., Kooistra T. (2004): Evidence for anti-inflammatory activity of statins and PPARalpha activators in human C-reactive protein transgenic mice *in vivo* and in cultured human hepatocytes *in vitro*. Blood **103**, 4188–4194

Koh K. K., Son J. W., Ahn J. Y., Jin D. K., Kim H. S., Choi Y. M., Ahn T. H., Kim D. S., Shin E. K. (2004): Vascular effects of diet and statin in hypercholestrolemic patients. Int. J. Cardiol. **95**, 185–191

Kwak B., Mulhaupt F., Myit S., Mach F. (2000): Statins as a newly recognized type of immunomodulator. Nat. Med. **6**, 1399–1402

Laufs U., Gertz K., Dirnagl U., Böhm M., Nickenig G., Endres M. (2002): Rosuvastatin, a new HMG-CoA reductase inhibitor, upregulates endothelial nitric oxide synthase and protects from ischemic stroke in mice. Brain Res. **942**, 23–30

Leung B. P., Sattar N., Crilly A., Prach M., McCarey D. W., Payne H., Madhok R., Campbell C., Gracie J. A., Liew F. Y., McInnes I. B. (2003): A novel anti-inflammatory role for simvastatin in inflammatory arthritis. J. Immunol. **170**, 1524–1530

Liappis A. P., Kan V. L., Rochester C. G., Simon G. L. (2001): The effect of statins on mortality in patients with bacteremia. Clin. Infect. Dis. **33,** 1352–1357

Litchfield J. T., Wilcoxon F. (1949): A simplified method of evaluating dose effective experiments. J. Pharmacol. Exp. Ther. **96,** 99–113

Marx N., Duez H., Fruchart J. C., Staels B. (2004): Peroxisome proliferator-activated receptors and atherogenesis: regulators of gene expression in vascular cells. Circ. Res. **94**, 1168–1178

Marz W., Wieland H. (2000): HMG-CoA reductase inhibition: anti-inflammatory effects beyond lipid lowering? Herz **25**, 117–125

Merx M. W., Liehn E. A., Janssens U., Lütticken R., Schrader J., Hanrath P., Weber C. (2004): HMG-CoA reductase inhibitor simvastatin profoundly improves survival in a murine model of sepsis. Circulation **109**, 2560–2565

Nežić L., Škrbić R., Dobrić S., Stojiljković M. P., Jaćević V., Stoisavljević Š. S., Milovanović Z., Stojaković N. (2009): Simvastatin and indomethacin have similar anti-inflammatory activity in a rat model of acute local inflammation. Basic Clin. Pharmacol. Toxicol. **104**, 185–191

Paumelle R., Blanquart C., Briand O., Barbier O., Duhem C., Woerly G., Percevault F., Fruchart J. C., Dombrowicz D., Glineur C., Staels B. (2006): Acute antiinflammatory properties of statins involve peroxisome proliferator-activated receptor-alpha *via* inhibition of the protein kinase C signaling pathway. Circ. Res. **98**, 361–369

Pleiner J., Schaller G., Mittermayer F., Zorn S., Marsik C., Polterauer S., Kapiotis S., Wolzt M. (2004): Simvastatin prevents vascular hyporeactivity during inflammation. Circulation **110**, 3349–3354

Plenge J. K., Hernandez T. L., Weil K. M., Poirier P., Grunwald G. K., Marcovina S. M., Eckel R. H. (2002): Simvastatin lowers C reactive protein within 14 days: an effect independent of low density lipoprotein cholesterol reduction. Circulation **106**, 1447–1452

Pruefer D., Makowski J., Schnell M., Buerke U., Dahm M., Oelert H., Sibelius U., Grandel U., Grimminger F., Seeqer W., Meyer J., Darius H., Buerke M. (2002): Simvastatin inhibits inflammatory properties of *Staphylococcus aureus* α-toxin. Circulation **106**, 2104–2110

Rezaie-Majd A., Maca T., Bucek R. A., Valent P., Müller M. R., Husslein P., Kashanipour A., Minar E., Baghestanian M. (2002): Simvastatin reduces expression of cytokines interleukin-6, interleukin-8, and monocyte chemoattractant protein-1 in circulating monocytes from hypercholesterolemic patients. Arterioscler. Thromb. Vasc. Biol. **22**, 1194–1199

Ridker P. M., Rifai N., Pfeffer M. A., Sacks F. M., Moye L. A., Goldman S., Flaker G. C., Braunwald E. (1998): Inflammation, pravastatin and risk of coronary events after myocardial infarction in patients with average cholesterol levels. Circulation **98**, 839–844

Rosenson R. S. (1999): Non-lipid-lowering effects of statins on atherosclerosis. Curr. Cardiol. Rep. **1**, 225–232

Seasholtz T. M., Brown J. H. (2004): RHO signaling in vascular diseases. Mol. Interv. **4**, 348–357

Souza Neto J. L., Araújo Filho I., Rego A. C., Dominici V. A., Azevedo I. M., Egito E. S., Brandao-Neto J., Medeiros A. C. (2006): Effects of simvastatin in abdominal sepsis in rats**.** Acta Cir. Bras. **21**, 8–12 (Portuguese)

Sparrow C. P., Burton C. A., Hernandez M., Mundt S., Hassing H., Patel S., Rosa R., Hermanowski-Vosatka A., Wang P. R., Zhang D., Peterson L., Detmers P. A., Chao Y. S., Wright S. D. (2001): Simvastatin has anti-inflammatory and antiatherosclerotic activities independent of plasma cholesterol lowering. Arterioscler. Thromb. Vasc. Biol. **21**, 115–121

Steiner S., Speidl W. S., Pleiner J., Seidinger D., Zorn G., Kaun C., Wojta J., Huber K., Minar E., Wolzt M., Kopp C. W. (2005): Simvastatin blunts endotoxin induced tissue factor *in vivo*. Circulation **111**, 1841–1846

Takemoto M., Liao J. K. (2001): Pleiotropic effects of 3-hydroxy-3-methylglutaryl coenzyme A reductase inhibitors. Arterioscler. Thromb. Vasc. Biol. **21**, 1712–1719

Terkeltaub R., Solan J., Barry M., Santoro D., Bokoch G. M. (1994): Role of the mevalonate pathway of isoprenoid synthesis in IL-8 generation by activated monocytic cells. J. Leukoc. Biol. **55**, 749–755

Wagner A. H., Schwabe O., Hecker M. (2002): Atorvastatin inhibition of cytokine-inducible nitric oxide synthase expression in native endothelial cells in situ. Br. J. Pharmacol. **136,** 143–149

Yasuda H., Yuen P. S., Hu X., Zhou H., Star R. A. (2006): Simvastatin improves sepsis-induced mortality and acute kidney injury *via* renal vascular effects. Kidney Int. **69**, 1535–1542

Early detection of myocardial viability by hyperbaric oxygenation in patients with acute myocardial infarction treated with thrombolysis

Milica Dekleva[1], Miodrag Ostojic[2], Aleksandar Neskovic[3], Sanja Mazic[4], Alja Vlahovic[3], Jelena Suzic Lazic[1] and Nikola Dekleva[†]

[1] *University Clinical Centre "Dr. Dragiša Mišović-Dedinje", Belgrade, Serbia*
[2] *Institute for Cardiovascular Diseases, Clinical Center of Serbia, Serbia*
[3] *Clinical-Hospital Center Zemun, Belgrade, Serbia*
[4] *Institute of Medical Physiology, Faculty of Medicine, University of Belgrade, Serbia*

Abstract. Hyperbaric oxygen treatment (HBO) could transiently reverse hypoxia during acute myocardial infarction (AMI). In order to evaluate whether early HBO can identify viable segments after AMI, improvement of wall motion score index (WMSI) after HBO was compared to dobutamine stress echocardiography (DSE). Thirty-one patients with first AMI treated with thrombolysis received 100% oxygen at 2 technical atmospheres for 1 h within 24 h of the onset of chest pain. All patients underwent echocardiography before and after HBO and during DSE. Improvements in WMSI after HBO, as well as during DSE were considered as proof of viability. Total of 186 akinetic segments were detected before HBO. Functional recovery was defined at 73 after HBO and 113 segments were fixed. Eighty-one segments improved contraction with DSE. WMSI improved before HBO compared to the one after HBO (1.79 vs. 1.65, $p = 0.024$) and DSE (1.79 vs. 1.60, $p < 0.001$). Close relationship between WMSI after HBO and DSE was found ($r = 0.417$, $p = 0.022$). Sensitivity and specificity of HBO for viability were 73% and 85%, respectively. HBO may identify viable myocardium as early as day one after AMI. The highest number of responding segments was detected in patients who received HBO within shortest intervals following the onset of chest pain.

Key words: Myocardial viability — Hyperbaric oxygenation — Acute myocardial infarction

Introduction

In the setting of myocardial infarction treated with thrombolysis loss of myocardial contractile function may be due to myocardial necrosis, stunning or hibernation. Whereas myocardial necrosis usually suggests irreversible myocardial dysfunction, stunning and hibernation reflect reversibility of myocardial function (Braunwald and Rutherford 1986; Rahimtoola 1989). In the case of hibernating myocardium, coronary revascularization may reduce heart failure symptoms and improve left ventricular (LV) function and survival (Rahimtoola 1998; Bax et al. 1999; Schinkel et al. 2002). The improvement is directly related to the number of dysfunctional, but viable segments (Bax et al. 1997; Wijns et al. 1998). It has been hypothesized that acute, as well as chronic hypoperfusion may result in down regulation of myocardial contractile function to preserve myocardial integrity and this process may be reversed after adequate restoration of myocardial perfusion.

The hibernating myocardium has been demonstrated to have several characteristics: cell membrane integrity, preserved glucose metabolism and inotropic reserve. Various techniques that are currently available for assessment of myocardial viability are based on the evaluation of these characteristics (Wijns et al. 1998). Currently, most frequently used are scintigraphic imaging with either positron emission tomography (PET) for intact metabolism, thalium, contrast or single photon emission computer tomography (SPECT) for intact microvascular circulation

Correspondence to: Jelena Suzic Lazic, Department of Echocardiography, University Clinical Centre "Dr. Dragiša Mišović-Dedinje", Milana Tepića 1, 11000 Belgrade, Serbia
E-mail: jsuzic@eunet.rs; mildek@sbb.rs

and echocardiography during stepwise infusion of dobutamine for intact inotropic reserve. None of the available techniques for the identification of myocardial viability can be considered unequivocally superior to the others. By far most widely used is one with low dose dobutamine stress echocardiography (LDSE) as the preferred stressor for assessing myocardial viability.

The hallmark for viability using LDSE (5–20 μg/kg/m) is the improvement of contractility of asynergic segment after adrenergic stimulation. Enhanced inotropic state, heart rate and blood pressure require increased myocardial oxygen consumption (VO_2). In the absence of myocardial ischemia, myocardial contractility in akinetic, but viable segments will enhance resulting in improvement of myocardial thickening during LDSE. The most specific indicator of myocardial viability in setting of hibernation is deterioration of this zone showing initial augmentation in response to increasing dose of dobutamine referred to as the biphasic response. Hibernating myocardium may be identified by DSE with highest specificity (81%) and with an accuracy of 80% in prediction functional recovery (Geleijnse et al. 1997; Wijns et al. 1998; Sicari et al. 2008).

Hyperbaric oxygen improves ventricular function and reduces tissue injury when administrated during evolving myocardial infarction (Jain 1990). Experimental and clinical data suggest that this effect is mediated by decreasing tissue edema, reducing formation of lipid peroxide radicals, altering nitric oxide syntheses, expression and inhibition of leukocyte adherence and plugging in the microcirculation. (Cameron et al. 1966; Thomas et al. 1990; Stavitsky et al. 1998; Dekleva et al. 2004; Sharifi et al. 2004; Vlahovic et al. 2004). Hyperbaric oxygenation can produce hyperoxia in ischemic tissue and reveal hibernating myocardium in the setting of recent myocardial infarction (Swift et al. 1992).

The aim of this study was to evaluate by two-dimensional echocardiography whether hyperbaric oxygen treatment (HBO) early after acute myocardial infarction (AMI) can identify viable segments and compare these finding to changes in segmental wall motion to myocardial viability determined by dobutamine stress echocardiography (DSE) as a clinically relevant method for viability detection.

Materials and Methods

Study population

The study population was selected from 37 consecutive patients admitted to our coronary care unit who satisfied the following criteria: first AMI diagnosed on the basis of typical ischemic chest pain >20 min in duration, acute ST segment elevation >2 mm in two contiguous electrocardiographic (ECG) leads, a significant rise and fall in serum troponin and creatine kinaze and MB isoenzyme levels and demonstrable wall motion abnormality on routine TTE. Exclusion criteria were: presence of uncontrolled heart failure, arrhythmias or significant postinfarction angina and presence of serious non-coronary disease that might preclude dobutamine echocardiography. Further exclusions to HBO were the inability to equilibrate pressure in the middle ear space secondary to thinitis or otitis, severe claustrophobia and chronic obstructive pulmonary disease. Study patients were treated with 1.5 million IU of streptokinase by rapid infusion (over 30 to 60 min) followed by infusion of heparin after six hours (25,000 IU) and aspirin (300 mg). All patients were treated with HBO after thrombolysis. After one week they underwent DSE. However, 5 patients with serious ventricular arrhythmia and one with severe hypertension at rest were contraindicated for DSE.

HBO

After thrombolytic therapy, within first 24 h, patients were treated in monoplace hyperbaric chamber. Under medical supervision, each patient was treated with 100% oxygen pressurized at 2 AT for 45 min followed by 15 min of decompression breathing the same gas mixture. Inside the chamber 3-lead ECG were recorded before hyperbaric exposure, during bottom time and during decompression.

Coronary angiography

Coronary angiography was performed after hospital discharge. Perfusion of the infarct-related artery was assessed by using criteria from the Thrombolysis in Myocardial Infarction (TIMI) trial (TIMI Study Group 1985, see References). Successful reperfusion was coded as TIMI grade 3.

Echocardiography

Two-dimensional echocardiography was obtained with commercially available imaging system using Acuson 128 XP system (Acuson Corp., Mountain View, California USA) with a 2.5 MHz transducer and images acquired in parasternal long and short axis and apical 4 and 2 chamber views. The complete echocardiographic studies were recorded for subsequent playback analysis performed on day one of AMI before and after HBO and during LDSE. Left ventricular ejection fraction (LVEF) was determined from apical two and four chamber views by using Simpson's biplane formula according to the recommendations of American Society of Echocardiography (Schiller et al. 1989; Cheitlin et al. 2003). Tracing of endocardial borders in the endsystole and enddiastole was performed in the technically best cardiac cycle.

Two independent, well-trained experienced observers performed blind analysis of regional wall motion thickening after the patients had received HBO. Interobserver agreement was 96%. Presence of viability has been defined by improvement at least one grade in two or more LV segments after HBO or DSE. Segments with unchanged wall motion were considered non viable (Pellikka et al. 2007).

DSE

Two dimensional (2D) echocardiograms and 12-lead ECG monitoring were performed during LDSE. The protocol used dobutamine infusion at two low dose stages (5 and 10 μg/kg/min) with each stage lasting 3 min. The benefit of proceeding to higher doses (20, 30, 40 μg/kg/min) of dobutamine even if contractile reserve is demonstrated at lower doses is to observe a "biphasic response" (Geleijnse et al. 1997; Sicari et al. 2008). In present study we obtained high DSE according to the 3 min increment protocol in all patients who did not have contraindications. DSE was scheduled within one week of the hyperbaric study and all study procedures were performed between one and ten days after AMI. All antianginal medications were withheld before DSE (nitrates 24 h and B blockers and calcium antagonists 48 h before the test). Non echocardiographic end points requiring test interruption were the following: severe chest pain or significant ST segment changes, symptoms of intolerance, blood pressure > 240/120 mmHg, decrease in blood pressure >30 mmHg, and significant arrhythmia.

Regional wall motion was assessed according to the recommendation of the American Society of Echocardiography with 16 segment model (Schiller et al. 1989). In all studies segmental wall motion was semi quantitatively graded from 1 to 4 as follows: 1 – normal motion at rest with normal wall motion after HBO or increased wall motion during dobutamine infusion, 2 – hypokinetic (marked reduction in endocardial motion and thickening), 3 – akinetic (absence of inward motion and thickening), 4 – dyskinetic (paradoxical wall motion away from the center of the left ventricle in systole). The wall motion score index (WMSI) was derived by dividing the sum of individual segment scores with the number of interpretable segments calculated for baseline, after HBO and during DSE. Myocardial segments were considered normal in cases when regional wall motion was normal or mild hypokinetic. Only dysfunctional segments (segments with severe hypokinesia, akinesia or dyskinesia at resting echocardiography) were evaluated for myocardial viability.

Statistical analysis

All continuous data are expressed as mean ± SD; percentages are rounded. Continuous variables were compared by means of the Student's *t*-test for paired samples. Relationships between examined variables included echocardiographic parameters before and after HBO and during DSE were compared using Pearson's correlation test. Sensitivity, specificity and accuracy were evaluated using standard definitions and expressed as percentage points. Statistical significance was defined as $p < 0.05$.

Results

Demographic, clinical and angiographic data

Patient's demographic, clinical and angiographic data are listed in Table 1. The study population was predominantly male (29/8) aged 55 ± 7 years. There were more patients with acute inferior (23 patients, 62%) than with anterior (14 patients, 38%) myocardial infarction. As shown in Table 2,

Table 1. Patient's demographic, clinical and angiographic characteristics

Characteristic	Patients
Mean age (years)	55 ± 7
Female/male	8/29
Hypertension (%)	14 (38)
Diabetes mellitus (%)	8 (22)
Cigarette smoking (%)	30 (81)
Killip class > 2 (%)	2 (5)
Time to STK (h)	2.4 ± 1.6
Localization, anterior (%)	14 (38)
Peak value CK (U/l)	989 ± 643
Multivessel CAD (%)	19 (51)
TIMI 3 flow (%)	22 (59)
Collaterals (%)	9 (24)
Cardiac mortality (%)	0 (0)

Table 2. Pharmacological therapies during hospital stay and at discharge

Medications	Patients (%)
Heparin	37 (100)
Aspirin	36 (97)
Oral anticoagulation	5 (14)
Nitroglycerin IV	7 (19)
Long-acting nitrates	30 (81)
Calcium channel blockers	1 (3)
β-blockers	26 (70)
Digitalis	1 (3)
Diuretics	3 (8)
ACE inhibitors	8 (22)

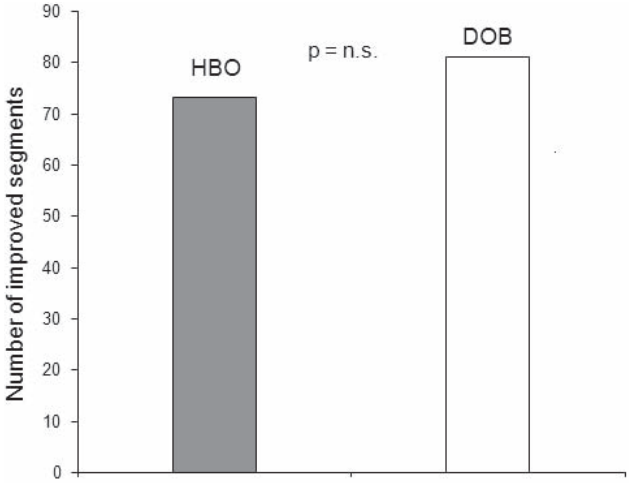

Figure 1. Contractile response of LV segments during DSE and after hyperbaric oxygen treatment (HBO). DOB, dobutamine; n.s., non-significant.

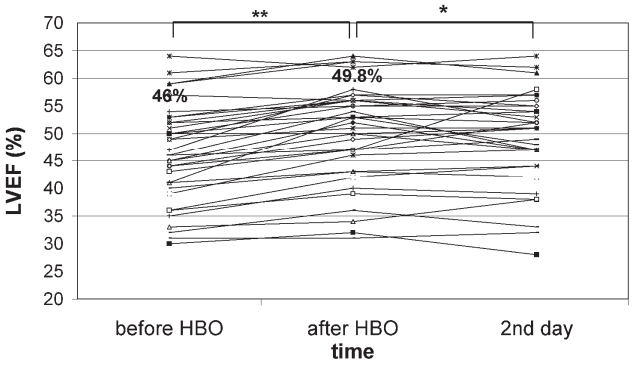

Figure 2. Global LV systolic function before and after hyperbaric oxygen treatment (HBO). LVEF, left ventricular ejection fraction;* $p < 0.001$, * p = non-significant.

all patients received similar therapy during their hospital stay and at discharge including β blockers, ACE inhibitors, long acting nitrates, calcium channel inhibitors, digitalis and diuretics.

From 419 detectible segments, 186 segments were defined as akinetic or severe hypokinetic in 31 patients by rest echocardiograms after cessation of thrombolytic therapy and before HBO, during day one of AMI. There were no dyskinetic segments.

Functional recovery was defined at 73 segments after HBO (38.9%) and other 113 segments remained unchanged, there were no deteriorated segments. In 6 patients no changes were found compared to rest echocardiogram. During DSE there were only 6 patients with biphasic response and other wall motion improvements were detected by LDSE. Patients with biphasic response obtained DSE with dobutamine infusion 20–30 μg/kg/min. Eighty-one segments (43.5%) of resting wall motion abnormality showed improved contraction with DSE. Thus, positive predictive value for improvement of WMSI by HBO compared to DSE was 90%. Resting asynergy was associated with no improvement in contraction with HBO in 113 segments of which 105 during DSE were also unchanged (negative predictive value 92%). Wall motion response during DSE and after HBO was without significant difference ($t = 1.56$, $p = 0.32$; Fig. 1). Score indices significantly improved from rest echocardiogram before HBO to echocardiogram after HBO exposure (1.79 ± 0.32 vs. 1.65 ± 0.21, $p = 0.024$) and from rest echocardiogram to DSE (1.79 ± 0.32 vs. 1.60 ± 0.22, $p < 0.001$). The level of functional regional systolic LV function, measured by score indices improvement, calculated after HBO and during LDSE was similar (1.65 vs. 1.60, $t = 1.30$, $p = 0.22$). There was close relationship between the number of improved segments calculated by 2D echocardiography immediately after HBO and during DSE ($r = 0.417$, $p = 0.022$). Sensitivity and specificity of HBO for detection of viability were 73% and 85 %, respectively. Global systolic function obtained from LVEF after HBO significantly increased compared to basal values of LVEF after thrombolysis (46.0 ± 8.8 vs. 49.78 ± 8.7%, $t = 7.47$; $p < 0.001$; Fig. 2).

The number of improved LV segments in the infarction zone after HBO or during DSE was not closely related to TIMI flow of the infraction related artery ($r = 0.74$, p = non-significant). Therefore, in our study, the number of viable segments was not predictable for its patency.

The interval at which patients received HBO within the 24 h of AMI ranged from 3 to 20 h, averaging 13 h. There was significant negative correlation between the level of functional recovery or contractile improvement of LV wall segments and time from the onset of chest pain to HBO exposure ($r = -0.557$, $p = 0.002$), and also between the time from thrombolysis to HBO ($r = -0.499$, $p = 0.007$; Fig. 3). The response of viable segments was optimal in cases when the HBO was performed during the first 10 h from the onset of the chest pain ($r = 0.498$, $p = 0.003$).

Discussion

The ability to distinguish myocardial hibernation from necrosis in early phase of AMI may be important in the selection of patients for mechanical or surgical intervention (Smart et al. 1997). Furthermore, following thrombolytic therapy for AMI, viable myocardium in reperfused zone may remains ischemic and can be at risk of progression to necrosis if not salvaged by early mechanical intervention (Lew et al. 1990).

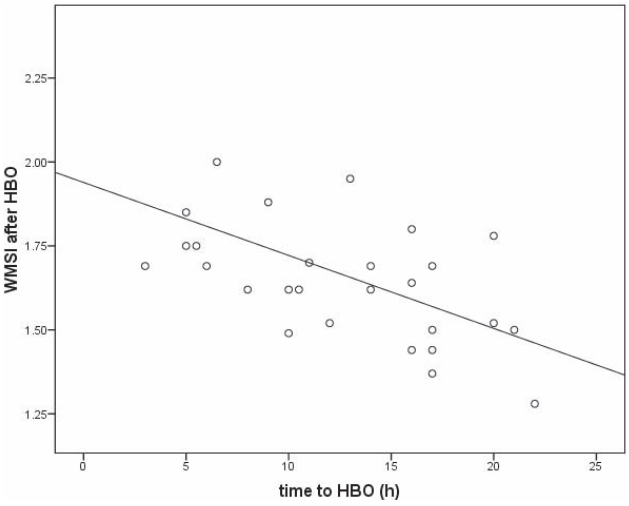

Figure 3. Relationship between time to hyperbaric oxygen treatment (HBO) and wall motion score index (WMSI) after oxygen exposure.

Mechanism of functional recovery of hibernating myocardium with HBO

Administrating of 100% oxygen at 2 AT increases the amount of oxygen dissolved in the blood and tissue by 10-fold and is more than enough to meet the resting cellular requirements without any contribution from hemoglobin-bound oxygen (Jain 1990). At least three different mechanisms are responsible for favorable changes in myocardial oxygen supply and demand during HBO: increase in total barometric pressure, direct increase in oxygen partial pressure in arterial blood, significant increase in oxygen content of arterial blood, interstitial fluids and tissues especially plasma dissolved fraction. All mechanisms produce different oxygen transport regimens in specific conditions and increase effective cellular oxygenation at very low rates of blood flow by achieving high arterial O_2 pressure. The net effect is an approximately 25% enhanced oxygen blood content and consumption with 3 to 4 times increased tissue oxygen diffusion distance. In case of critical coronary stenosis, the difference in high oxygen tension pressure between ischemic and non-ischemic tissue, improves penetration of oxygen into hypoxic tissue (Jain 1990; Rochitte et al. 1998; Dekleva et al. 2004).

During AMI there are structural changes in coronary microcirculation followed by decreased density and disturbed perfusion in capillary bed (Rochitte et al. 1998; Wu et al. 1998). In ischemic and hypoxic tissues, the capillaries are often partially occluded by microthrombi, and the transport of red blood cells along the capillary may be compromised or halted. In certain circumstances only plasma with large amount of dissolved oxygen under hyperbaric condition can flow through the suffering blood vessel. This phenomenon is known as "plasma skimming" and can be of vital importance as the only vehicle to assure adequate oxygen transport to the areas beyond the capillary subobstruction and also may represent the way to discover hibernating myocardium (Wu et al. 1998). Oxygenation occurs in "local blood flow" in "supply" dependent tissues, in which oxygen transport in normobaric condition falls below 8–10 ml/O_2/kg/min. Regional myocardial function may remain abnormal unless transmural ischemia is almost completely reversed by reperfusion (Yogaratnam et al. 2008). Therefore wall motion analysis after HBO may indicate a more relevant improvement of wall contraction without functional-perfusion mismatch.

Recent studies have shown that treatment with HBO postischemia and reperfusion ameliorated myocardial ischemia-reperfusion injury by stimulating the endogenous production of nitric oxide (Cabigas et al. 2006; Yogaratnam et al. 2008). Favorable circumstances of hyperoxic and hyperbaric actions of HBO induced cardio-protection and functional recovery by activation of nitric oxide synthetase, which is directly dependent of oxygen availability (Cabigas et al. 2006).

In condition of recent myocardial infarction the capacity of transporting hemoglobin-bind oxygen to the sites of utilization is severely decreased. During DSE, adrenergic stimulation enhances oxygen demand, provoking the tense contractile reserve to detect the viable myocardium. Contrary to this, hyperbaric oxygen enables favorable oxygen tension and functional recovery of hibernating myocardium.

Previous studies

According to previous studies the role of HBO in patients with AMI was controversial ranging from not beneficial to a favorable effect (Cameron et al. 1966; Thomas et al. 1990). Recent studies suggested that adjunctive HBO in patients with AMI treated with thrombolysis or with percutaneous coronary interventions is a safe and beneficial therapy. These studies, in addition to showed feasibility of use HBO, demonstrated that HBO, as an adjunct to the management of AMI, pharmacologically limits myocardial damage and improves myocardial function (Stavitsky et al. 1998; Dekleva et al. 2004; Sharifi et al. 2004; O'Neil et al. 2007). Similar to present results, improved myocardial salvage after adjunctive use of HBO after thrombolysis was documented by improving of global systolic function measured by higher value of LVEF after HBO (Stavitsky et al. 1998; Dekleva et al. 2004).

The hypothesis that transitory hyperoxia in dysfunctional myocardium would be followed by transitory improvement in contraction of viable segments has been proved by Swift et al (1992). These authors tried to detect viable myocardium in postinfarction patients by immediate transthoracic (TTE) and transesophageal echocardiography (TEE) after

HBO and compared results with thallium-201 SPECT exercise scintigraphy. They demonstrated that TTE and TEE are complementary in their ability to define improvement in myocardial contraction after HBO. Swift et al. (1992) showed that there was no improvement of wall motion abnormality in patients receiving hyperbaric room air after AMI. According to their results, from the non contracting segments at rest (62), 20 segments (32%) improved with HBO and 29 segments (47%) had evidence of viability on thallium SPECT. From the 20 segments with improvement of contraction after HBO, 18 segments were viable by SPECT. In our study also close relationships between improved segments with HBO and DSE was established. Similar to our results, positive predictive value of improvement by HBO for viability on thallium scintigraphy was 90%. Swift et al. (1992) reported that fixed contraction abnormalities were obtained in 42 segments after HBO, of which 30 segments showed a fixed defect in SPECT (negative predictive value 71%). To describe myocardium with reversible thallium defects with no improvement of contractility after HBO, those authors proposed term "covert hibernation". Because rapid improvement in O_2 delivery to myocardium is not always followed by an immediate improvement of contractile function, even though, tissue oxygen tension remained elevated for several hours after cessation of HBO and tissue remained oxygenated.

The study conducted by Veselka et al. (1999) examined the possibility of using echocardiography after HBO to detect viable myocardium. Results from 17 patients were compared with DSE. Patients enrolled in that study had LV dysfunction and heart failure. This study suggested that the number of segments with improved contraction after HBO (36–17.6%) was lower than in DSE at 10 μg/kg/min (82–40.2%) but higher than DSE at an infusion rate of 5 μg/kg/min (31–15.2%). Thus HBO echocardiography was statistically equivalent to low dose, but inferior to higher dose during DSE, so authors presumed that sensitivity of HBO for detection of myocardial viability might be about 70% which is similar to our results. According to the present study, Veselka et al. (1999) showed that there was no significant difference between improved segments detected by HBO and low rate of dobutamin during DSE (5 μg/kg/min). This study suggested that HBO is capable of detecting viable myocardium in patients with LV dysfunction, but authors proposed that a combination of DSE and HBO could have greater accuracy than just DSE or HBO.

Limitation of the study

This study is limited by the small number of patients. There is no follow up of patients with viable myocardium. Confirmation of myocardial viability in stress echocardiography remains the eyeballing interpretation of regional wall motion in black and white cine-loops. New echocardiographic technologies proposed to establish the viability on a more quantitative basis, but are not completely validated in their clinical meaning. In the present study we didn't used the new technologies applied to DSE.

Tissue characteristics in setting of the acute infarction are dynamic, but there was no possibility to obtain HBO and DSE at the same time. All coronary angiograms were obtained more than one month after AMI.

Because HBO requires additional logistic support, we excluded from the study patients with severely impaired left ventricle and severe heart failure who may, in fact, have benefited the most from detection of viable segments by HBO for further treatment and survival.

Conclusions

Different forms of radionuclide myocardial perfusion imaging for detection of myocardial viability, utilizing thallium rest or stress-redistribution SPECT, FDG-PET scanning or technetium-sestamibi SPECT take time exposure for active uptake or passive diffusion of the agent. Interpretation of radionuclide myocardial distribution takes high quality of gamma camera imaging characteristics, making these techniques less accessible and more expensive. There are several side effects of radionuclide techniques such as long lasting physical half life, presence of gamma and mercury rays, high proton energy or transient hepatic uptake. Prolongation and repetition of the perfusion procedures are not proper for the early phase of AMI.

Our data indicate that HBO and echocardiography can identify hibernating myocardium as early as day one after AMI. Oxygen supply under hyperbaric condition could detect viability within one hour, by functional recovery of the infarcted segments without adrenergic or any other harmful stimulation, producing only ameliorate effects Therefore, clinical application of HBO as a test of myocardial viability after AMI is rational and can further expand therapeutic application of HBO. On the other hand, DSE provides in viable segments prospective improvement of contractility. The combination of these two methods possibly reflects more completely the functional properties of viable segments following myocardial infarction.

Acknowledgement. Dr. Nešković was supported in part by the research grant No. 14538 from the Ministry of Science of the Republic of Serbia for 2006–2010.

References

Bax J. J., Wijns W., Cornel J. H., Visser F. C., Boersma E., Fioretti P. M. (1997): Accuracy of currently available

techniques for prediction of functional recovery after revascularization in patients with left ventricular dysfunction due to chronic coronary artery disease: comparison of pooled data. J. Am. Coll. Cardiol. **30**, 1451–1460

Bax J. J., Poldermans D., Elhendy A., Cornel J. H., Boersma E., Rambaldi R., Roelandt J. R., Fioretti P. M. (1999): Improvement of left ventricular ejection fraction, heart failure symptoms and prognosis after revascularization in patient with chronic coronary artery disease and viable myocardium detected by dobutamine stress echocardiography. J. Am. Coll. Cardiol. **34**, 163–169

Braunwald E., Rutherford J. D. (1986): Reversible ischemic left ventricular dysfunction: evidence for the "hibernating myocardium". J. Am. Coll. Cardiol. **8**, 1467–1470

Cabigas B. P., Su J., Hutchins W., Shi Y., Schaefer R. B., Recinos R. F., Nilakantan V., Kindwall E., Niezgoda J. A., Baker J. E. (2006): Hyperoxic and hyperbaric-induced cardioprotection: role of nitric oxide syntetase 3. Cardiovasc. Res. **72**, 143–151

Cameron A. J. V., Hutton I., Kenmure A. C. F., Murdoch W. R. (1966): Hemodynamic and metabolic effect of hyperbaric oxygen in myocardial infarction. Lancet **3**, 833–837

Cheitlin M. D., Armstrong W. F., Aurigemma G. P., Beller G. A., Bierman F. Z., Davis J. L., Douglas P. S., Faxon D. P., Gillam L. D., Kimball T. R., Kussmaul W. G., Pearlman A. S., Philbrick J. T., Rakowski H., Thys D. M., Antman E. M., Smith S. C. Jr., Alpert J. S., Gregoratos G., Anderson J. L., Hiratzka L. F., Faxon D. P., Hunt S. A., Fuster V., Jacobs A. K., Gibbons R. J., Russell R. O. (2003): ACC, AHA, ASE, ACC/AHA/ASE 2003 guideline update for the clinical application of echocardiography: summary article. A report of the American College of Cardiology/American Heart Association Task Force on Practice Guidelines (ACC/AHA/ASE Committee to Update the 1997 Guidelines for Clinical Application of Echocardiography). J. Am. Soc. Echocardiogr. **16**, 1091–1110

Dekleva M., Neskovic A. N., Vlahovic A., Putnikovic B., Beleslin B., Ostojic M. (2004): Adjunctive effect of hyperbaric oxygen treatment after thrombolysis on left ventricular function in patients with acute myocardial infarction. Am. Heart J. **148**, 1–17

Geleijnse M. L., Fioretti P. M., Roelandt J. R. (1997): Methodology, feasibility, safety and diagnostic accuracy of dobutamine stress echocardiography. J. Am. Coll. Cardiol. **30**, 595–606

Jain K. K. (1990): Hyperbaric oxygen therapy in cardiovascular diseases. In: Textbook of Hyperbaric Medicine. pp. 283–307, Hagrefe and Huber, Seatle

Lew A. S., Maddahi J., Shah P. K., Cercek B., Ganz W., Berman D. S. (1990): Critically ischemic myocardium in clinically stable patients following thrombolytic therapy for acute myocardial infarction: potential implications for early coronary angioplasty in selected patients. Am. Heart J. **120**, 1015–1025

O'Neil W. W., Martin J. L., Dixon S. R., Bartorelli A. L., Trabattoni D., Oemrawsingh P. V., Atsma D. E., Chang M., Marquardt W., Oh J. K., Krucoff M. W., Gibbons R. J., Spears J. R. (2007): Acute myocardial infarction with hyperoxemic therapy (AMIHOT). J. Am. Coll. Cardiol. **50**, 397–405

Pellikka P. A., Nagueh S. F., Elhendy A. A., Kuehl C. A., Sawada S. G. (2007): American Society of Echocardiography recommendations and performance, interpretation and application of stress echocardiography. J. Am. Soc. Echocardiogr. **20**, 1021–1041

Rahimtoola S. H. (1998): From coronary artery disease to heart failure: role of hibernating myocardium. N. Engl. J. Med. **339**, 173–181

Rahimtoola S. H. (1989): The hibernating myocardium. Am. Heart J. **117**, 211–221

Rochitte C. E., Lima J. A., Bluemke D. A., Reeder S. B., McVeigh E. R., Furuta T., Becker L. C., Melin J. A. (1998): Magnitude and time course of microvascular obstruction and tissue injury after acute myocardial infarction. Circulation **98**, 1006–1014

Schiller N. B., Shah P. M., Crawford M., DeMaria A., Devereux R., Feigenbaum H., Gutgesell H., Reichek N., Sahn D., Schnittger I., Silverman N. H., Tajik A. J. (1989): Recommendations for quantification of the left ventricle by two dimensional echocardiography: American Society of Echocardiography Committee on Standards, subcommittee on quantisation of two dimensional echocardiograms. J. Am. Soc. Echocardiogr. **2**, 358–367

Schinkel A. F., Bax J. J., Boersma E., Elhendy A., Vourvouri E. C., Roelandt J. R., Poldermans D. (2002): Assessment of residual myocardial viability in regions with chronic electrocardiographic Q-wave infarction. Am. Heart J. **144**, 865–869

Sharifi M., Fares W., Abdel-Karin I., Koch J. M., Sopko J., Adler D. (2004): Usefulness of hyperbaric oxygen therapy to inhibit restenosis after percutaneous coronary intervention for acute myocardial infarction or unstable angina pectoris. Am. J. Cardiol. **93**, 1533–1535

Sicari R., Nihoyannopoulos P., Evangelista A., Kasprzak J. (2008): Stress echocardiography expert consensus statement. Eur. J. Echocardiogr. **9**, 415–437

Smart S. C., Kinkelbine T., Stoiber T. R., Carlos M., Wynsen J. C., Sagar K. B. (1997): Safety and efficiency of dobutamine – atropine stress echocardiography for the detection of residual stenosis of the infarct–related artery and multivessel disease during the first week after myocardial infarction. Circulation **95**, 1394–1939

Stavitsky Y., Shandling A. H., Ellestad M. H., Hart G. B., Van Natta B., Messenger J. C., Strauss M., Dekleva M. N., Alexander J. M., Mattice M., Clarke D. (1998): Hyperbaric oxygen and thrombolysis in myocardial infarction: the "HOTMI" randomized multicenter study. Cardiology **90**, 131–135

Swift P. C., Turner J. H., Oxer H. F., O'Shea J. P., Lane G. K., Woollard K. V. (1992): Myocardial hibernation identified by hyperbaric oxygen treatment and echocardiography in postinfarction patients: comparison with exercise thallium scintigraphy. Am. Heart J. **124**, 1151–1157

Thomas M. P., Brown L. A., Sponseller D. R., Williamson S. E., Diaz J. A., Guyton D. P. (1990): Myocardial infarction size reduction by synergic effect of hyperbaric oxygen

and recombinant tissue plasminogen activator. Am. Heart J. **120**, 791–800

TIMI Study Group (1985): The thrombolysis in myocardial infarction (TIMI) trial. Phase I findings. N. Engl. J. Med. **312**, 932–936

Veselka J., Mates M., Dolezal V. (1999): Detection of viable myocardium: comparison of dobutamine echocardiography and echocardiography after hyperbaric oxygenation. Undersea Hyperb. Med. **26**, 9–13

Vlahovic A., Neskovic A. N., Dekleva M., Putniković B., Popović Z. B., Otasević P., Ostojić M. (2004): Hyperbaric oxygen treatment does not affect left ventricular chamber stiffness after myocardial infarction treated with thrombolysis. Am. Heart J. **148**, E1

Wijns W., Vatner S. F., Camaci P. G. (1998): Hibernating myocardium. N. Engl. J. Med. **339**, 173–181

Wu K. C., Kim R. J., Bluemke D. A., Rochitte C. E., Zerhouni E. A., Becker L. C., Lima J. A. (1998): Quantification and time course of microvascular obstruction by contrast enhanced echocardiography and magnetic resonance imaging following acute myocardial infarction and reperfusion. J. Am. Coll. Cardiol. **32**, 1756–1764

Yogaratnam J. Z., Laden G., Guvendik L., Cowen M., Cale A., Griffin S. (2008): Pharmacological preconditioning with hyperbaric oxygen: can this therapy attenuate myocardial ischemic reperfusion injury and induce myocardial protection *via* nitric oxide? J. Surg. Res. **149**, 155–164

Attenuation of cold restraint stress-induced gastric lesions by an olive leaf extract

Dragana Dekanski[1], Snežana Janićijević-Hudomal[2], Slavica Ristić[2], Nevena V. Radonjić[3], Nataša D. Petronijević[3], Vesna Piperski[4] and Dušan M. Mitrović[5]

[1] *R&D Institute, Galenika a.d. Belgrade, Serbia*
[2] *Institute of Pharmacology, School of Medicine, University of Prishtine, Kosovska Mitrovica, Serbia*
[3] *Institute of Medical and Clinical Biochemistry, School of Medicine, University of Belgrade, Serbia*
[4] *Medical Academy, US Medical School, Belgrade, Serbia*
[5] *Institute of Medical Physiology, School of Medicine, University of Belgrade, Serbia*

Abstract. Olive leaf extract (OLE) possesses, among other, antioxidative properties, but whether it influences gastroprotection against stress-induced gastric lesions remains unknown. In this study we investigated the protective effect of OLE, a natural antioxidant, on gastric mucosal damage induced by cold restraint stress (CRS) in rats. Three different doses of commercial OLE EFLA® 943 were applied intragastrically (i.g.) 30 min prior to stress induction. Macroscopic gastric lesions were evaluated and ulcer index (UI) was calculated. Histological evidence of gastric mucosal lesions was also obtained. Concentration of malondialdehyde (MDA) as an index of lipid peroxidation, and catalase (CAT) and superoxide dismutase (SOD) activities were determined in gastric mucosa. The effects of applied OLE on gastric mucosal lesions, lipid peroxidation and antioxidative enzymes activity were compared with effects of i.g. pretreatment of reference drug, ranitidine. CRS caused severe gastric lesions in all non-pretreated animals, and this finding was confirmed histologicaly. Pretreatment with OLE (40, 80 and 120 $mg \cdot kg^{-1}$), as well as with ranitidine (50 $mg \cdot kg^{-1}$), significantly ($p < 0.001$) attenuated stress-induced gastric lesions. Treatment with 80 $mg \cdot kg^{-1}$ of OLE was the most effective in prevention of rise in gastric MDA level and decrease in CAT and SOD activity. The results obtained indicate that OLE possesses gastroprotective activity against CRS-induced gastric lesions in rats, possibly related to its antioxidative properties.

Key words: Olive leaf — Gastroprotection — Cold restraint stress — Rats

Introduction

Olive (*Olea europaea* L.) leaf has been traditionally used for centuries to prevent and treat different diseases. It is used to enhance the immune system, in heart disease and as an antimicrobial agent. Folk medicine uses also include hypertonia, arteriosclerosis, rheumatism, gout, diabetes mellitus, and fever (PDR for Herbal Medicine 2000), and the most known feature of olive leaf is cardioprotection. Experimental animal studies on different total olive leaf extract (OLE) or their constituents have demonstrated hypoglycemic (Gonzales et al. 1992; Al-Azzawie and Alhamdani 2006), hypotensive (Khayyal et al. 2002; Scheffler et al. 2008), antiarrhythmic (Somova et al. 2004), anti-atherosclerotic (Wang et al. 2008), and vasodilator effects (Zarzuelo et al. 1991). Antimicrobial (Bisignano et al. 1999; Furneri et al. 2002; Markin et al. 2003; Pereira et al. 2007), antiviral (Lee-Huang et al. 2003; Micol et al. 2005), anti-tumor (Hamdi and Castellon 2005; Abaza et al. 2007) and anti-inflammatory activity (Pieroni et al. 1996) were also reported. Moreover, antihypertensive and cholesterol-lowering actions of OLE EFLA®943 were confirmed in a clinical study (Perrinjaquet-Moccetti et al. 2008).

The beneficial properties of olive leaf are further enhanced by the good bioavailability of its polyphenolic constituents, the same as in olive oil, which are readily absorbed through

Correspondence to: Dragana Dekanski, Biomedical Research, R&D Institute, Galenika a.d., Pasterova 2, 11000 Beograd, Serbia
E-mail: ddekan@sezampro.rs

the gastrointestinal tract, resulting in significant levels in the circulation (Visioli et al. 2000; Vissers et al. 2002).

Despite a number of papers published on different effects of olive leaf and its constituents, none of them has focused on influence on gastric defense mechanisms and gastroprotective activity of total OLE. However, our recent results indicated that it has beneficial effect on ethanol-induced gastric lesions in rats (Dekanski et al. 2009). Furthermore, it was reported that olive oil, thanks to its minor components, improved antioxidant defense systems in rat stomach (Odabasoglu et al. 2008).

The main constituent of the olive leaves is oleuropeine, one of iridoide monoterpenes, which is thought to be responsible for pharmacological effects. Furthermore, the olive leaves contain triterpenes (oleanolic and maslinic acid), flavonoides (luteolin, apigenine, rutin, ...), and chalcones (olivin, olivin-diglucoside) (PDR for Herbal Medicines 2000; Meirinhos et al. 2005; Pereira et al. 2007). It is its chemical content that makes olive leaf one of the most potent natural antioxidants. Oleuropein has high antioxidant activity *in vitro*, comparable to a hydrosoluble analog of tocopherol (Speroni et al. 1998), as do other constituents of olive leaf (Briante et al. 2002). It was shown that total OLE had antioxidant activity higher than vitamin C and vitamin E, due to the synergy between flavonoids, oleuropeosides and substituted phenols (Benavente-Garcia et al. 2000).

Stress has been shown to be associated with altered homeostasis that may lead to oxidant-antioxidant imbalance. It is well known that the pathogenesis of stress-induced gastric lesions includes the generation of reactive oxygen species (ROS) that seem to play an important role, namely due to generation of lipid peroxides, accompanied by impairment of antioxidative enzyme activity of cells (Das et al. 1997; Kwiecien et al. 2002). Administration of antioxidants such as reduced glutathione or sodium benzoate prior to stress, causes significant decrease in ulcer index (UI) and lipid peroxidation, suggesting the involvement of ROS in cold restraint stress (CRS)-induced gastric ulceration (Das and Banerjee 1993). Therefore, treatment with a potent antioxidant, as total OLE is, could decrease stress-induced gastric mucosal damage. To test this hypothesis, we investigated the protective antioxidative effect of OLE on gastric mucosal damage induced by CRS in rats.

Materials and Methods

Materials

Standardized dry OLE EFLA®943 was purchased from Frutarom Switzerland Ltd. (Wädenswil, Switzerland). The extract was manufactured from the dried leaves of *Olea europaea* L., applying an ethanol (80% m/m) extraction procedure. After a patented filtration process (EFLA®HyperPure) the crude extract was dried. Previously reported quantitative analysis of total phenols, flavonoids and tannins content of OLE (Dekanski et al. 2009) revealed that extract used had high oleuropein content (19.8%), total flavonoids (0.29%), including caffeic acid, luteolin-7-O-glycoside, apigenine-7-O-glycoside and quercetin, as well as tannins (0.52%). Ranitidine tablets were obtained from Galenika a.d. (Belgrade, Serbia). Hydrogen peroxide and thiobarbituric acid (TBA) were purchased from Sigma-Aldrich (Schnelldorf, Germany). All other reagents used in biochemical analysis were obtained from Merck (Darmstadt, Germany).

Animals

Male Wistar rats ($n = 36$) from Biomedical Research Center, R&D Institute, Galenika a.d. (Belgrade, Serbia), weighing 180–220 g were used in this study. Rats were housed 3 in a cage under constant environmental conditions (20–24°C; 12 h light-dark cycle), and were given *ad libitum* access to standard pelleted food and water. This study was approved by the Ethical Committee, Medical School, University of Belgrade, and run in accordance to the statements of European Union regarding handling of experimental animals (86/609/EEC).

Gastric lesions induction and evaluation

Before the experiment, the animals were randomly divided into 6 groups (6 rats in each group), they were placed in individual metabolic cages, and they were fasted for 24 h, but had free access to water. The first, control, non-ulcerated group received distilled water intragastricaly (i.g.) using metal tube for gavage and it was the group of normal, healthy animals without any pretreatment or stress induction. The second group received distilled water i.g. 30 min prior to stress induction. We applied three different doses of OLE on the next three groups, and finally, the last group (positive control) received i.g. 50 $mg \cdot kg^{-1}$ of ranitidine, H_2 receptor antagonist, as a reference drug. The dose used in this *in vivo* experiments was based on the average consumption of olive drupes and olive oil (Quaranta and Rotundo 2000) in the Mediterranean area. We expressed total polyphenol consumption from olive drupes or olive oil in Mediterranean diet as the molecular equivalent of oleuropein and its metabolites, calculated to be approximately 100 mg daily. For the extrapolation of the dosage from humans to rats, we used the metabolic body size or food intake rather than body weight as a criterion (Rucker and Storms 2002; Rucker 2007). The estimated quantity of oleuropein expressed per unit of human diet was 0.2 $mg \cdot kg^{-1}$ of dry food (Andreadou et al. 2006). For rats, this consumption corresponded to a dose of 8 mg/kg of oleuropein. It was reported that in

OLE investigated, oleuropein content was 20%. Hence, 40 $mg \cdot kg^{-1}$ of OLE was administered. Higher doses of 80 and 120 $mg \cdot kg^{-1}$ were also given to test for a dose response. Both OLE and ranitidine were suspended in distilled water before administration. To induce cold-restraint stress, the rats were immobilized in individual restraint boxes without possibility of visual contact (Popović et al. 1997) and subjected to cold (4 ± 1°C) stress for 3.5 h. This regimen of cold-restraint stress has been reported to produce gastric ulcers reliably in food-deprived rats (Senay and Levine 1967; Das et al. 1993).

At the end of this period, animals were sacrificed under the ether anesthesia, abdomen was opened by the midline incision, the stomach was removed, opened along the greater curvature, rinsed gently with water and pinned open for macroscopic examination and for photo-documentation by digital camera (Hewlett Packard PhotoSmart R507). The number and severity of gastric lesions were evaluated according to the following rating scale (Buyukcoskun et al. 2007): 0 – no lesion, 1 – mucosal edema and petechiae, 2 – from 1 to 5 small lesions (1–2 mm), 3 – more than 5 small lesions or 1 intermediate lesion (3–4 mm), 4 – 2 or more intermediate lesions or 1 gross lesion (greater than 4 mm) and 5 – perforated ulcers. The sum of the total scores divided by the number of animals in group was expressed as the UI ± SD (standard deviation). Percent of inhibition in UI in relation to the non-pretreated CRS group were estimated from formula:

$$\% \text{ inhibition} = [1 - (\text{UI pretreatment} / \text{UI non-pretreatment})] \times 100$$

Histopathological evaluation

Histological evidence of gastric mucosal lesions in all experimental groups was also obtained. Gastric tissue samples were fixed in 10% buffered formalin, dehydrated in graded alcohols, cleared in xylene, and embedded in paraffin. Sections of 5 μm thicknesses were cut by rotatory microtome, stained with haematoxylin and eosin, and examined microscopically for histopathological changes using microscope with digital camera (Olympus BX41, Japan) and Olympus DP-SOFT 5.0 programme for photo-documentation.

Biochemical examination of gastric mucosa

The mucosal tissue from each animal was scraped from the stomach with a blunt knife and the tissue was weighed, transferred to the ice-cooled test tube and homogenized by Ultra-Turrax T25, (Janke & Kunkel Gmbh& Co., IKA®-Labortechnik, Staufen, Germany) in 20 mmol/l Tris buffer, pH 7.4, containing 5 mmol butylated hydroxytoluene to prevent new lipid peroxidation that can occur during the homogenization. The homogenate was then centrifuged at 12,000 rpm at 4°C, (Megafuge 2.0.R, Heraeus, Germany) for 10 min. Supernatant was aliquoted and stored at –70°C until determination of total protein, catalase (CAT), superoxide dismutase (SOD) and malondialdehyde (MDA).

The protein content of the tissue samples was estimated by the method of Lowry et al. (1951) using bovine serum albumin as a standard.

Lipid peroxidation of gastric mucosa was determined spectrophotometrically (UV-Vis spectrophotometer HP 8453, Agilent Technologies, Santa Clara, CA) at 533 nm and MDA concentration was quantified by using the molar extinction coefficient, 1.56×10^5 $mol^{-1} \cdot cm^{-1}$ (Buege and Aust 1978).

Activity of CAT in gastric mucosa was determined according to the procedure of Goth (1991) by following the absorbance of hydrogen peroxide at 230 nm and pH 7.0.

SOD activity in the gastric mucosa was determined by measuring the inhibition of autooxidation of epinephrine at pH 10.2 at 30°C by the method of Misra and Fridovich (1972). One unit of SOD activity represents the amount of SOD necessary to cause 50% inhibition of adrenaline autooxidation.

Statistical analysis

All results are expressed as means ± SD. Statistical analysis was done using *t*-test, and *p* values less than 0.05 were considered as significant.

Results

Effect of OLE suspension on gastric lesions induced by CRS

Cold restraint stress produced visible gastric lesions in all non-pretreated animals. They were located mostly in the corpus. No visible lesions developed in the nonsecretory part of the rat stomach which is well known response to CRS. Moreover, after opening, haemorrhagical content was found in stomach lumens. Following 3.5 h of cold-restraint stress, the average ulcer score in non pretreated group was very high (4.3 ± 0.8). All administered doses of OLE (40, 80 and 120 $mg \cdot kg^{-1}$) significantly prevented the gastric mucosal lesions induced by cold-restraint stress. Percent of inhibition in UI was 49%, 70%, and 63%, respectively. The gastroprotective effect of OLE was similar to that achieved by the pretreatment with H_2 receptor antagonist, ranitidine (50 $mg \cdot kg^{-1}$), which caused 70% inhibition of UI (Fig. 1). No visible sign of ulceration was observed in animals in non-ulcerated group.

Effect of OLE pretreatment on histopathological changes

Histological examination of gastric mucosa showed stress induced extensive damage of the surface epithelium and

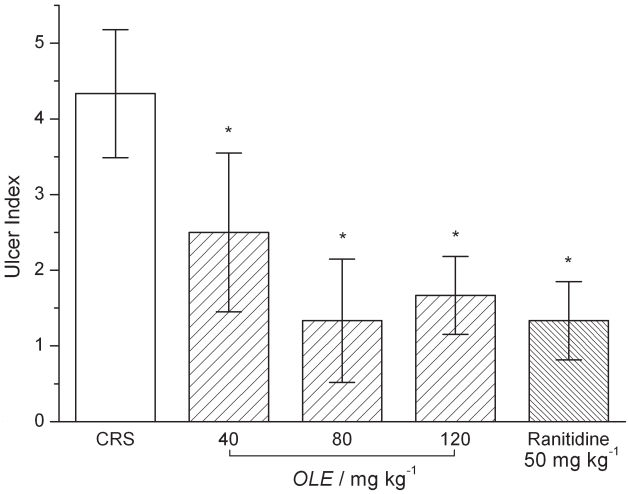

Figure 1. Effect of intragastric pretreatment with olive leaf extract (OLE) applied in graded doses ranging from 40 mg·kg^{-1} up to 120 mg·kg^{-1} and ranitidine (50 mg·kg^{-1}) on the ulcer index induced by CRS. Asterisk indicates statistical significance in ulcer index ($p < 0.001$), as compared to the control value.

lamina propria, with lesions extending up to submucosa in some cases. Various histopathological changes including congestion, haemorrhage, submucosal edema, necrosis, inflammatory changes, erosions and ulcers were seen (Fig. 2A). All these changes were significantly less expressed in rats pretreated with both OLE (Fig. 2B) and ranitidine. Fig. 2C shows normal gastric mucosa.

Effect of OLE pretreatment on lipid peroxidation and antioxidative enzymes activity

Cold restraint stress significantly increased lipid peroxidation in gastric mucosa, evaluated as MDA formation (445.4 ± 43.6 vs. 287.1 ± 15.6 in control; ($p < 0.05$)). MDA was reduced significantly by pretreatment with 80 and 120 mg·kg^{-1} of OLE (23% and 16%, respectively). Administration of 50 mg·kg^{-1} and ranitidine prior to CRS exposure also restricted rise in MDA concentration, but these effects were not statistically significant. Fig. 3 shows MDA concentration in normal gastric mucosa and in gastric mucosa of non-pretreated rats and rats pretreated with OLE and ranitidine.

As shown in Fig. 4, SOD activity averaged 35.5 ± 2.3 U (mg prot)$^{-1}$ in intact gastric mucosa. Following exposure of rats to CRS, a significant decrease of SOD activity to the value of 30.3 ± 0.9 U (mg prot)$^{-1}$ was observed. Both OLE and ranitidine administration reduced the fall in SOD activity, but only effects of 80 and 120 mg·kg^{-1} of OLE were statistically significant.

Catalase activity in gastric mucosa, also, significantly decreased after CRS (17.7 ± 5.2 U (mg prot)$^{-1}$ in control group vs. 9.2 ± 3.5 U (mg prot)$^{-1}$ in CRS group). Pretreatment of

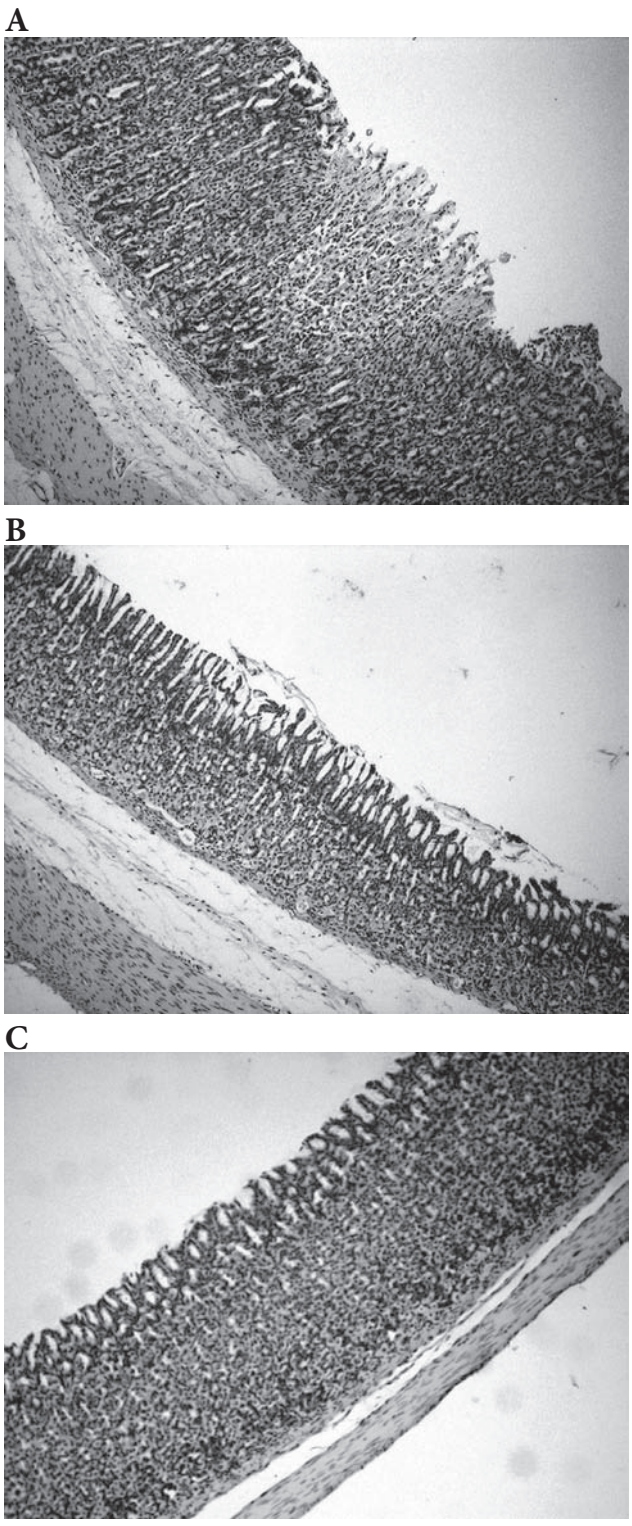

Figure 2. Examples of histopathological changes in stomach of CRS exposed rats. **A.** Deep erosion and massive extravasation of erytrocytes, submucosal edema and cell infiltration in non-pretreated rat. **B.** Surface epithelium damage and submucosal edema without deep erosions and bleeding, in olive leaf extract pretreated rat. **C.** Stomach from control, non-ulcerated rat.

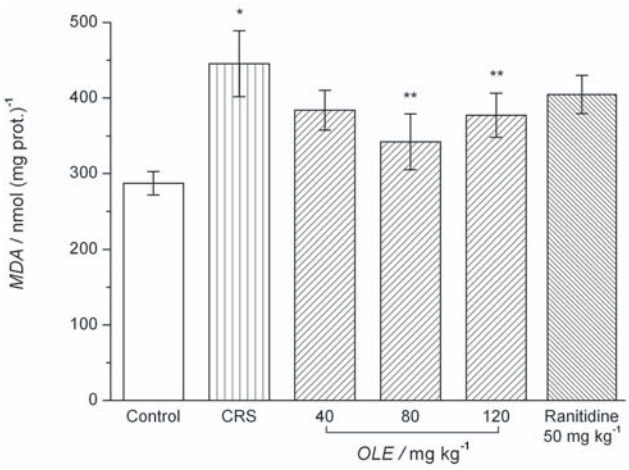

Figure 3. Effect of intragastric pretreatment with olive leaf extract (OLE) applied in graded doses ranging from 40 mg·kg^{-1} up to120 mg·kg^{-1} and ranitidine (50 mg·kg^{-1}) on the malondyaldehyde (MDA) concentration (nmol·mg prot^{-1}) in gastric mucosa. * indicates statistical significance ($p < 0.05$) of difference in MDA concentrations in non-pretreated rats exposed to CRS as compared to the control animals. ** indicates statistical significance ($p < 0.05$) of difference in MDA concentrations in pretreated rats as compared to the CRS exposed rats without pretreatment.

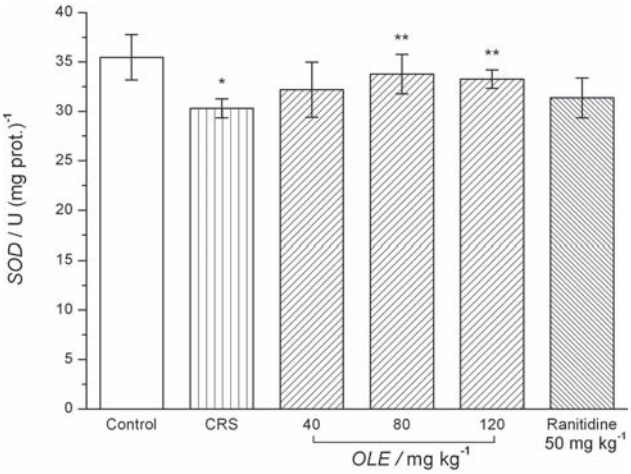

Figure 4. Effect of intragastric pretreatment with olive leaf extract (OLE) applied in graded doses ranging from 40 mg·kg^{-1} up to120 mg·kg^{-1} and ranitidine (50 mg·kg^{-1}) on the SOD activity (U (mg prot)$^{-1}$) in gastric mucosa. * indicates statistical significance ($p < 0.05$) of difference in SOD activity in non-pretreated rats exposed to CRS as compared to the control animals. ** indicates statistical significance ($p < 0.05$) of difference in superoxide dismutase (SOD) activity in pretreated rats as compared to the CRS exposed rats without pretreatment.

all three doses of OLE significantly reduced the fall of CAT activity, while the effect of ranitidine was not statistically significant (Fig. 5).

Discussion

There is an increasing interest in medicinal plant extracts, the greatest value of which may be due to constituents that contribute to the modulation of the oxidative balance *in vivo*. Various plant originated gastroprotectors have been used in clinical and folk medicine due to their beneficial effects on the gastric mucosa. Literature has centered primarily on their pharmacological action in experimental animals using different models of gastric lesions induction (Borelli and Izzo 2000; Zayachkivska et al. 2005; Olaleye and Farombi 2006). It was shown previously that stress with cold exposure and restraint for 3.5 h induces severe gastric mucosal damage in rats.

In this study we used CRS experimental model to investigate the protective effect of OLE, a natural antioxidant, on gastric mucosal damage, since in this model the pathogenesis of the lesions has been related with production of ROS. Hence, the aim of the study was to evaluate the effect of an OLE on stress-induced histological changes, as well as biochemical perturbations, in this animal model.

Pretreatment with all three doses of OLE significantly ($p < 0.01$) reduced gastric lesions induced by CRS. CRS caused minimum of gastric lesions and the best inhibition

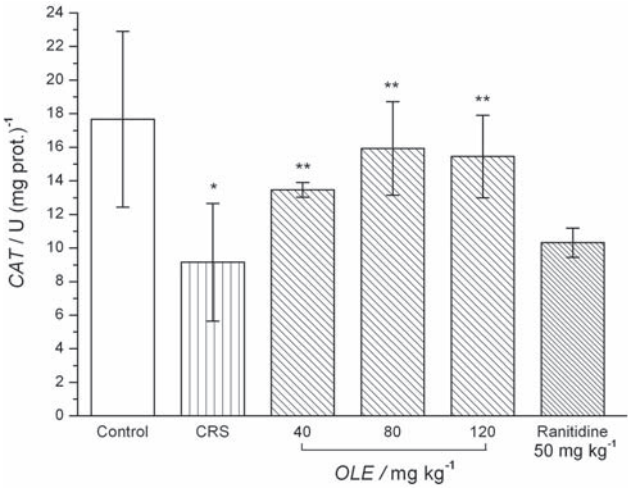

Figure 5. Effect of intragastric pretreatment with olive leaf extract (OLE) applied in graded doses ranging from 40 mg·kg^{-1} up to120 mg·kg^{-1} and ranitidine (50 mg·kg^{-1}) on the catalase (CAT) activity (U (mg prot)$^{-1}$) in gastric mucosa. * indicates statistical significance ($p < 0.05$) of difference in CAT activity in non-pretreated rats exposed to CRS as compared to the control animals. ** indicates statistical significance ($p < 0.05$) of difference in CAT activity in pretreated rats as compared to the CRS exposed rats without pretreatment.

of UI, related to the non-pretreated group, was obtained in animals pretreated with 80 mg·kg^{-1} of OLE (70%). Only gastric mucosal edema and petechiae were seen in almost

all (5 of 6) animals in this experimental group. The higher dose (120 mg·kg^{-1}) did not show the greatest effect, so the dose-response of three investigated doses of OLE was not obtained. We can only assume that dose-response could be obtained in experiments where the lowest dose investigated is 10 or 20 mg·kg^{-1}. Moreover, on the basis of our results we suppose that doses of 160 or 200 mg·kg^{-1} or higher, could cause pro-oxidative effects and consequently worse results, because it is happened in experimental studies of natural antioxidants (Lankin et al. 1999; Park and Lee 2008).

Macroscopic results were confirmed histologically. CRS exposed non-pretreated animals displayed a loss of superficial epithelium and necrosis of the upper mucosal layer, deep erosions and submucosal edema. In addition, a dense acute inflammatory cell infiltrate, consisting mainly of neutrophils, was noted. In striking contrast, gastric specimens from the OLE pretreated animals displayed minimal or no pathohistological changes. Only superficial erosions and vasodilatation were seen.

Since lipid peroxidation is a well-established mechanism of cellular injury (Kwiecien et al. 2002), we measured the changes in the MDA concentrations as an indicator of lipid peroxidation in gastric mucosa. Pretreatment with OLE (80 mg·kg^{-1} and 120 mg·kg^{-1}) significantly restricted rise in gastric MDA concentration caused by CRS. The results obtained in our study are in agreement with previously reported results. Thus, status of the antioxidant enzymes along with lipid peroxidation was studied in CRS-induced ulcers by Govindarajan et al. (2006), and increase in MDA concentration was noticed. A study conducted by Brzozowski et al. (2005) documented that MDA concentration is significantly increased in gastric mucosa exposed to ethanol or water immersion and restraint stress (WRS).

Antioxidant enzymes SOD and CAT, important cellular antioxidants, contribute to the gastric oxidative-antioxidative balance. Decrease of both SOD and CAT activity in gastric mucosa of immobilized rats leads to the accumulation of ROS and consequently to MDA concentration rise. In our investigation, CRS induced inhibition of SOD and CAT activity, suggesting important role of these enzymes in pathogenesis of stress ulcer disease. Other published results support this finding: SOD and CAT activity in rat stomach tissue was decreased by indomethacin- and HCl/ethanol-induced oxidative gastric mucosal damage (Olaleye and Farombi 2006), CAT activity decreased in CRS (Govindarajan et al. 2006); SOD activity is significantly decreased in 3.5 h of WRS (Brzozowski et al. 2005). In the present study, OLE administered to rats prior to stress induction attenuated inhibition of SOD and CAT activity, and thus implicated its role in modulation of the oxidative balance in gastric mucosal defense.

The antioxidative effect of total OLE most probably results from the ability of its constituents to scavenge ROS, produced in CRS, which initiate lipid peroxidation. Phytochemical analysis of OLE EFLA®943 performed by our laboratory shown high oleuropein content (almost 20%) and other constituents important for gastroprotection (apigenine-7-*O*-glycoside, luteolin-7-*O*-glycoside, quercetin, and caffeic acid), as well as, low concentration of tannins (Dekanski et al. 2009).

Previous studies shown that membrane lipid peroxidation was prevented by oleuropein, which exhibited strong antioxidant protection in oxidative stress during ischemia-reperfusion in experimental model of myocardial injury (Manna et al. 2004; Andreadou et al 2006).

Luteolin-7-*O*-glycoside is widespread in plant species, its anti-radical activity is well known, and its anti-ulcer activity was previously confirmed (Borelli and Izzo 2000).

Also, it has been reported that quercetin prevent gastric mucosal lesions induced by ethanol. Possible mechanisms include inhibition of lipid peroxidation (Alarcon de la Lastra et al. 1994), inhibition of the gastric proton pump (Di Carlo et al. 1999), and scavenging of free radicals associated with a significant enhancement in glutathione peroxidase activity (Martin et al. 1998).

Radical scavenging abilities for apigenine-7-*O*-glycoside and for caffeic acid were also reported (Benavente-Garcia et al. 2000).

Furthermore, recent study demonstrated gastroprotective effect of oleanolic acid (OA) derivatives (Sanches et al. 2006). A single oral administration of OA derivatives at the selected concentrations inhibited the appearance of gastric lesions induced by ethanol, aspirin and pylorus ligature. The effect of OA, which is important constituent of olive leaf and olive oil, was comparable with that of ranitidine at 50 mg·kg^{-1} and with that of omeprazole at 20 mg·kg^{-1} (Astudillo et al. 2002).

It is known that low concentration of tannins has role to „tan" the gastric mucosa and to render it less permeable and more resistant to chemical and mechanical injury or irritation (Asuzu and Onu 1990). Gastroprotective effect of tannins is experimentally confirmed when administration of tannins showed significantly lower stomach free radical concentrations in rats (Ramirez and Roa 2003). All of above mentioned effects of OLE constituents are of great importance in their possible synergistic effects in gastroprotection.

The results obtained indicate that the gastroprotective potential of OLE is probably related to its ability to maintain the cell membrane integrity, by its antilipid peroxidative activity that protects the gastric mucosa against oxidative damage, and by its ability to strengthen the mucosal barrier, the first line of defense against exogenous and endogenous ulcerogenic agents. The gastroprotective effect of OLE in fasted rats was similar to that obtained with antisecretory drug, ranitidine. Hence, we could not exclude the useful

role of antisecretory medications in the prevention of stress-related gastric mucosal damage, as acid and pepsin also contributed to the development of this condition. We infer that a combination regimen, including both antioxidants and antisecretory drugs, may be beneficial in preventing mucosal cell damage. In order to further elucidate the OLE mechanism of gastroprotective effect, our future investigation will be focused on other experimental models of mucosal injury and additional gastric mucosal defense mechanisms.

References

Abaza L., Talorete T. P. N., Yamada P., Kurita Y., Zarrouk M., Isoda H. (2007): Induction of growth inhibition and diferentiation of human leukemia HL-60 cells by tunisian gerboui olive leaf extract. Biosci. Biotechnol. Biochem. **71**, 1306–1312

Alarcon de la Lastra C., Martin M. J., Motilva V. (1994): Antiulcer and gastroprotective effects of quercetin: a gross and histologic study. Pharmacology **48**, 56–62

Al-Azzawie H. F., Alhamdani M. S. (2006): Hypoglycemic and antioxidant effect of oleuropein in alloxan-diabetic rabbits. Life Sci. **78**, 1371–1377

Andreadou I., Iliodromitis E. K., Mikros E., Constantinou M., Agalias A., Magiatis P., Skaltsounis A. L., Kamber E., Tsantili-Kakoulidou A., Kremastinos D. Th. (2006): The olive constituent oleuropein exhibits anti-ischemic, antioxidative, and hypolipidemic effects in anesthetized rabbits. J. Nutr. **136**, 2213–2219

Astudillo L., Rodriguez J. A., Schmeda-Hirschmann G. (2002): Gastroprotective activity of oleanolic acid derivatives on experimentally induced gastric lesions in rats and mice. J. Pharm. Pharmacol. **54**, 583–588

Asuzu I. U., Onu O. U. (1990): Anti-ulcer activity of the ethanolic extract of Combretum dolichopetalum root. Int. J. Crude Drug. Res. **28**, 27–32

Benavente-Garcia O., Castillo J., Lorente J., Ortuno A., Del Rio J. A. (2000): Antioxidant activity of phenolics extracted from *Olea europea* L. leaves. Food Chem. **68**, 457–462

Bisignano G., Tomaino A., Lo Cascio R., Crisafi G., Uccella N., Saija A. (1999): On the *in vitro* antimicrobial activity of oleuropein and hydroxytyrosol. J. Pharm. Pharmacol. **51**, 971–974

Borelli F., Izzo A. A. (2000): The plant kingdom as a source of anti-ulcer remedies. Phytother. Res. **14**, 581–591

Briante R., Paturni M., Terenziani S., Bismuto E., Febbraio F., Nucci R. (2002): *Olea europaea* L. leaf extract and derivatives: antioxidant properties. J. Agric. Food Chem. **50**, 4934–4940

Brzozowski T., Konturek P. C., Drozdowicz D., Konturek S. J., Zayachivska O., Pajdo R., Kwiecien S., Pawlik W. W., Hahn E. G. (2005): Grapefruit-seed extract attenuates ethanol-and stress-induced gastric lesions *via* activation of prostaglandin, nitric oxide and sensory nerve pathways. World J. Gastroenterol. **11**, 6450–6458

Buege J. A., Aust S. D. (1978): Microsomal lipid peroxidation. Methods Enzymol. **52**, 302–310

Büyükcoşkun N. I., Güleç G., Etöz B. C., Ozlük K. (2007): Central effects of glucagon-like peptide-1 on coldrestraint stress-induced gastric mucosal lesions. Turk. J. Gastroenterol. **18**, 150–156

Das D., Bandyopadhyay D., Bhattacharjee M., Banerjee R. K. (1997): Hydroxyl radical is the major causative factor in stress-induced gastric ulceration. Free Radic. Biol. Med. **23**, 8–18

Das D., Banerjee R. K. (1993): Effect of stress on the antioxidant enzymes and gastric ulceration. Mol. Cell. Biochem. **125**, 115–125

Dekanski D., Janicijevic-Hudomal S., Tadic V., Markovic G., Arsic I., Mitrovic D. M. (2009): Phytochemical analysis and gastroprotective activity of an olive leaf extract. J. Serb. Chem. Soc. **74**, 367–377

Di Carlo G., Mascolo N., Izzo A. A., Capasso F. (1999): Flavonoids: old and new aspects of a class of natural therapeutic drugs. Life Sci. **65**, 337–353

Furneri P. M., Marino A., Saija A., Ucella N., Bisignano G. (2002): *In vitro* antimycoplasmal activity of oleuropein. Int. J. Antimicrob. Agents **20**, 293–296

Gonzalez M., Zarzuelo A., Gamez M. J., Utrilla M. P., Jimenez J., Osuna I. (1992): Hypoglycemic activity of olive leaf. Planta Med. **58**, 513–515

Goth L. (1991): A simple method for determination of serum catalase activity and revision of reference range. Clin. Chim. Acta **196**, 143–151

Govindarajan R., Vijayakumar M., Singh M., Rao C. V., Shirwaikar A., Rawat A. K., Pushpangadan P. (2006): Antiulcer and antimicrobial activity of *Anogeissus latifolia*. J. Ethnopharmacol. **106**, 57–61

Hamdi H. K., Castellon R. (2005): Oleuropein, a non-toxic olive iridoid, is an anti-tumor agent and cytoskeleton disruptor. Biochem. Biophys. Res. Commun. **334**, 769–778

Khayyal M. T., el-Ghazaly M. A., Abdallah D. M., Nassar N. N., Okpanyi S. N., Kreuter M. H. (2002): Blood pressure lowering effect of an olive leaf extract (*Olea europaea*) in L-NAME induced hypertension in rats. Arzneimittelforschung **52**, 797–802

Kwiecien S., Brzozowski T., Konturek S. J. (2002): Effects of reactive oxygen species action on gastric mucosa in various models of mucosal injury. J. Physiol. Pharmacol. **53**, 39–50

Lankin V. Z., Tikhaze A. K., Konovalova G. G., Kozachenko A. I. (1999): Concentration inversion of the antioxidant and pro-oxidant effects of beta-carotene in tissues *in vivo*. Biull. Eksp. Biol. Med. **128**, 314–316 (in Russian)

Lee-Huang S., Zhang L., Huang P. L., Chang Y. T. (2003): Anti-HIV activity of olive leaf extract (OLE) and modulation of host cell gene expression by HIV-1 infection and OLE treatment. Biochem. Biophys. Res. Commun. **307**, 1029–1037

Lowry O. H., Rosenbrough N. J., Farr A. L., Randall R. J. (1951): Protein measurement with the Folin phenol reagent. J. Biol. Chem. **193**, 265–275

Manna C., Migliardi V., Golino P., Scognamiglio A., Galletti P., Chiariello M., Zappia V. (2004): Oleuropein prevents oxidative myocardial injury induced by ischemia and reperfusion. J. Nutr. Biochem. **15**, 461–466

Markin D., Duek L., Berdicevsky I. (2003): *In vitro* antimicrobial activity of olive leaves. Mycoses **46**, 132–136

Martin M. J., La Casa C., Alarcon de la Lastra C., Cabezza J., Villegas I., Motilva V. (1998): Anti-oxidant mechanisms involved in gastroprotective effects of quercetin. Z. Naturforsch., B: Biosci. **53,** 82–88

Meirinhos J., Silva B. M., Valentao P., Seabra R. M., Pereira J. A., Dias A., Andrade P. B., Ferreres F. (2005): Analysis and quantification of flavonoidic compounds from Portuguese olive (*Olea europea* L.) leaf cultivars. Nat. Prod. Res. **68**, 189–195

Micol V., Caturla N., Perez-Fons L., Estepa A., Mas V., Perez L. (2005): The olive leaf extract exhibits antiviral activity against viral haemorrhagic septicaemia rhabdovirus (VHSV). Antiviral Res. **66**, 129–136

Misra H. P., Fridovich I. (1972): The role of superoxide anion in the autoxidation of epinephrine and a simple assay for superoxide dismutase. J. Biol. Chem. **247**, 3170–3175

Odabasoglu F., Halici Z., Cakir A., Halici M., Aygun H., Suleyman H., Cadirci E., Atalay F. (2008): Beneficial effects of vegetable oils (corn, olive and sunflower oils) and alpha-tocopherol on anti-inflammatory and gastrointestinal profiles of indomethacin in rats. Eur. J. Pharmacol. **591**, 300–306

Olaleye S. B., Farombi E. O. (2006): Attenuation of indomethacin- and HCl/ethanol-induced oxidative gastric mucosa damage in rats by kolaviron, a natural biflavonoid of Garcinia kola seed. Phytother. Res. **20**, 14–20

Park S. W., Lee S. M. (2008): Antioxidant and prooxidant properties of ascorbic acid on hepatic dysfunction induced by cold ischemia/reperfusion. Eur. J. Pharmacol. **580**, 401–406

Pereira A. P., Ferreira I. C., Marcelino F., Valentao P., Andrade P. B., Seabra R., Estevinho L., Bento A., Pereira J. A. (2007): Phenolic compounds and antimicrobial activity of olive (*Olea europaea* L. *Cv*. Cobrançosa) leaves. Molecules **12**, 1153–1162

Perrinjaquet-Moccetti T., Busjahn A., Schmidlin C., Schmidt A., Bradl B., Aydogan C. (2008): Food supplementation with an olive (*Olea europaea* L.) leaf extract reduces blood pressure in borderline hypertensive monozygotic twins. Phytother. Res. **22**, 1239–1242

PDR for Herbal Medicines (Physician's Desk References for Herbal Medicines.) (2000), (Ed. T. Fleming), pp. 556–557, Medical Economics Company, Montvale, New Jersey

Pieroni A., Heimler D., Pieters L., van Poel B., Vlietinck A. J. (1996): *In vitro* anti-complementary activity of flavonoids from olive (*Olea europaea* L.) leaves. Pharmazie **51**, 765–768

Popović M., Popović N., Bokonjić D., Dobrić S. (1997): Cold restraint-induced gastric lesions in individual- and group-stressed rats. Int. J. Neurosci. **91**, 1–10

Quaranta G., Rotundo V. (2000): Economic and commercial prospects for olive oil in view of the changes in the common market organisation (CMO) (part one). Olivae **91**, 20–24

Ramirez R. O., Roa C. C. Jr. (2003): The gastroprotective effect of tannins extracted from duhat (*Syzygium cumini* Skeels) bark on HCl/ethanol induced gastric mucosal injury in Sprague-Dawley rats. Clin. Hemorheol. Microcirc. **29**, 253–261

Rucker R., Storms D. (2002): Interspecies comparison of micronutrient requirements: metabolic vs. absolute body size. J. Nutr. **132**, 2999–3000

Rucker R. B. (2007): Allometric scaling, metabolic body size and interspecies comparisons of basal nutritional requirements. J. Anim. Physiol. Anim. Nutr. **91**, 148–156

Sanchez M., Theoduloz C., Schmeda-Hirschmann G., Razmilic I., Yanez T., Rodriguez J. A. (2006): Gastroprotective and ulcer-healing activity of oleanolic acid derivatives: *in vitro-in vivo* relationships. Life Sci. **79**, 1349–1356

Scheffler A., Rauwald H. W., Kampa B., Mann U., Mohr F. W., Dhein S. (2008): *Olea europaea* leaf extract exerts L-type Ca^{2+} channel antagonistic effects. J. Ethnopharmacol. **120**, 233–240

Senay E. C., Levine R. J. (1967): Synergism between cold and restraint for rapid production of stress ulcer in rats. Proc. Soc. Exp. Biol. Med. **124**, 1221–1223

Somova L. I., Shode F. O., Mipando M. (2004): Cardiotonic and antidysrhythmic effects of oleanolic and ursolic acids, methyl maslinate and uvaol. Phytomedicine **11**, 121–129

Speroni E., Guerra M. C., Minghetti A., Crespi-Perellino N., Pasini P., Piazza F. (1998): Oleuropein evaluated *in vitro* and *in vivo* as an antioxidant. Phytother. Res. **12**, 98–100

Visioli F., Galli C., Bornet F., Mattei A., Patelli R., Galli G., Caruso D. (2000): Olive oil phenolics are dose-dependently absorbed in humans. FEBS Lett. **468**, 159–160

Vissers M. N., Zock P. L., Roodenburg A. J. C., Leenen R., Katan M. B. (2002): Olive oil phenols are absorbed in humans. J. Nutr. **132**, 409–417

Wang L., Geng C., Jiang L., Gong G., Liu D., Yoshimura H., Zhong L. (2008): The anti-atherosclerotic effect of olive leaf extract is related to suppressed inflammatory response in rabbits with experimental atherosclerosis. Eur. J. Nutr. **47**, 235–243

Zarzuelo A., Duarte J., Jimenez J., Gonzales M., Utrilla M. P. (1991): Vasodilator effect of olive leaf. Planta Med. **57**, 417–419

Zayachkivska O. S., Konturek S. J., Drozdowicz D., Konturek P. C., Brzozowski T., Ghegotsky M. R. (2005): Gastroprotective effects of flavonoids in plant extracts. J. Physiol. Pharmacol. **56**, 219–231

Effects of protamine sulphate on spontaneous and calcium-induced contractile activity in the rat uterus are potassium channels-mediated

Zorana Oreščanin-Dušić[1], Slobodan Milovanović[2], Ratko Radojičić[1,3], Aleksandra Nikolić-Kokić[1], Isabella Appiah[1], Marija Slavić[1], Neđo Čutura[4], Stevan Trbojević[2], Mihajlo Spasić[1] and Duško Blagojević[1]

[1] *Department of Physiology, Institute for Biological Research "Siniša Stanković", Belgrade, Serbia*
[2] *Faculty of Medicine, University of Eastern Sarajevo, Foča, Bosnia and Herzegovina*
[3] *Faculty of Biology, University of Belgrade, Belgrade, Serbia*
[4] *Gynaecology and Obstetrics Clinic "Narodni Front", Belgrade, Serbia*

Abstract. Protamine sulphate (PS) effect on spontaneous and calcium-induced rhythmic contractions of isolated virgin rat uteri was studied. PS caused dose-dependent relaxation of both types of contractions (two-way ANOVA, significant dose effects). Pretreatment with NG-nitro-L-arginine methyl ester (L-NAME; 10^{-5} mol/l), methylene blue (MB; 0.9×10^{-6} mol/l) or propranolol (1.7×10^{-5} mol/l) enhanced PS-mediated uterine muscle relaxation of spontaneous contractions. Dose-dependent relaxation of spontaneous active isolated rat uterus with PS was lower in uteri pretreated with single dose of tetraethylammonium (TEA; 6×10^{-3} mol/l), glibenclamide (2×10^{-6} mol/l) and 4-aminopyridine (4-AP; 10^{-3} mol/l). Calcium-induced activity of the isolated rat uterus pretreated with the same concentration of L-NAME, MB, or propranolol modified the kinetic of PS-induced relaxation without changes in EC_{50} values. Pre-treatment with glibenclamide, TEA and 4-AP significantly reduce PS relaxing effect of calcium-induced activity and according to EC_{50} values the order of magnitude was glibenclamide > TEA > 4-AP.

PS is mixture of polyamines and may activate different signal-transduction pathways. Our results cleary demonstrate that in uterine smooth muscle PS act dominantly through potassium chanels and marginaly through β-adrenergic receptos or nitric oxide-dependent pathways.

Key words: Nitric oxide — Protamine sulphate — Potassium channels — Rat uterus

Abbreviations: PS, protamine sulphate; EDRF, endothelium-derived relaxing factor; BK_{Ca} channel, large conductance calcium-activated potassium channel; K_{ATP} channel, ATP-activated potassium channel; L-NAME, NG-nitro-L-arginine methyl ester; MB, methylene blue; TEA, tetraethylammonium; 4-AP, 4-aminopyridine; NOS, nitric oxide synthase; cAMP, cyclic adenosine monophosphate; cGMP, cyclic guanosine monophosphate; PMCA, plasma membrane Ca^{2+} ATPase.

Introduction

Protamine sulphate (PS) is a mixture of polycationic amines used clinically to reverse heparin overdose. However, PS administration causes vasodilatation which leads to systemic hypotension. It was shown that PS-caused vasodilatation is mediated by endothelium-derived relaxing factor (EDRF) nitric oxide (NO) (Viaro et al. 2002). PS is rich in the amino acid L-arginine, a precursor of EDRF/NO, but there is little evidence to support PS-inducing EDRF/NO release by enhancing supply of its substrate L-arginine (Pearson et al. 1992). The endothelium-dependent relaxation induced by PS was inhibited by NG-monomethyl-L-arginine acetate demonstrating that PS stimulates the release of EDRF. Our recent results showed concentration-dependent PS-mediated

Correspondence to: Duško Blagojević, Department of Physiology, Institute for Biological Research "Siniša Stanković", Bul. Despota Stefana 142, 11000 Belgrade, Serbia
E-mail: dblagoje@ibiss.bg.ac.rs

relaxation of isolated mesenteric arteries without endothelium indicating that vascular smooth muscle plays a significant role in PS-mediated relaxation (Oreščanin-Dušić et al. 2008). There are several possible mechanisms that could cause the relaxation of smooth muscle *via* the action of different types of receptors or signalling processes: NO-mediated signalling, K^+ channels, Ca^{2+}-mediated effect, but to date there are no data of this kind available.

Uterus is rich in different kind of receptors, but the regulation of uterine relaxation is poorly understood as well as the contribution of different types of receptors and channels to the regulation of myometrial contractility. Research in myometrial tissue and other types of smooth muscle has defined a number of receptors, ion channels and regulatory proteins that are likely to be involved (Lopez-Bernal 2007). Myometrial ion channels are targets for a plethora of biological signals including hormones, peptides, pH fluctuations and stretch tension which have important consequences for myometrial function (Khan et al. 2001; Novaković et al. 2007). Large conductance calcium-activated potassium (BK_{Ca}) channel, β-2 adrenoceptor, and long-lasting type calcium channel are the main channels and receptor that are involved in the uterine contraction/relaxation process (Chanrachakul 2006). To date, several types of potassium channels have been identified in the myometrium. These include BK_{Ca} channels (Anwer et al. 1993) and three types of voltage-gated potassium currents (Knock et al. 1999). In addition, pharmacological and biochemical evidence for myometrial ATP-activated potassium (K_{ATP}) channels has also been presented (Morrison et al. 1993; Curley et al. 2002).

The aim of the study was to identify the main pathway of PS action on isolated rat uterus as model system.

Materials and Methods

Drugs and solutions

PS was supplied by Galenika a.d. (Belgrade, Serbia). Propranolol, methylene blue (MB), NG-nitro-L-arginine methyl ester (L-NAME), tetraethylammonium, glibenclamide and 4-aminopyridine (4-AP) were purchased from Sigma-Aldrich (St. Louis, MO, USA). All drugs were dissolved in distilled water except for glibenclamide which was dissolved in polyethylene glycol. Salts for De Jalon's solution (g/l: NaCl 9.0, KCl 0.42, $NaHCO_3$ 0.5, $CaCl_2$ 0.06, glucose 0.5) were obtained from ZORKA Pharma (Sabac, Serbia), Merck (Darmstadt, Germany) and Centrohem d.o.o. (Stara Pazova, Serbia).

Tissue preparation and contractility recording

All protocols for handling the rats were approved by the Local Ethical Committee for Animal Experimentation that strictly follows international guidelines (the Institute for Biological Research, Belgrade, Serbia, approval No. 3/06). Isolated uteri of virgin Wistar rats (200–250 g) in oestrus state determined by examination of daily vaginal lavage were used in this study. Uterus was suspended in an isolated organ bath chamber (Experimetria, Budapest, Hungary) containing De Jalon's solution and aerated with 95% O_2 and 5% CO_2. The temperature was maintained at 37°C. Isometric contractions were recorded using an isometric force transducer (Experimetria, Budapest, Hungary). The preload of the preparation was about 1 g.

Experimental procedures

After an equilibration period (about 30 min), when uteri achieved stable contractions (spontaneous or calcium-induced), the tissues were exposed to increasing concentrations of PS until total cessation of contractions took place. To explore the mechanism of PS action different antagonists were used as the pre-treatment of PS (L-NAME (10^{-5} mol/l), a NOS inhibitor; MB (0.9×10^{-6} mol/l), a cyclic guanosine monophosphate (cGMP) signalling pathway inhibitor; propranolol (1.7×10^{-5} mol/l), a non-selective β-adrenergic blocker; glibenclamide (2×10^{-6} mol/l), a selective ATP-sensitive potassium channel blocker; tetraethylammonium (TEA) (6×10^{-3} mol/l), non-specific inhibitor of BK_{Ca} and voltage-sensitive potassium channels; 4-AP (10^{-3} mol/l), a voltage-sensitive potassium channel blocker). Each substance was added to the De Jalon's solution 10 min before PS. PS-induced relaxation is expressed as the percent of maximal tension observed in the presence of L-NAME, MB, propranolol, glibenclamide, TEA or 4-AP.

Statistical analysis

Statistical analyses (descriptive statistics, analysis of variance – ANOVA, F-test) were performed according to protocols described by Manley (1986) using Statistical analysis software, version 9.1.3 (SAS Institute Inc., NC, USA). Effects of treatments on uterine contractions were calculated as the percentage of control, untreated, contractions. All data are expressed as the mean ± SEM. Differences between groups were tested by two-way ANOVA with treatment and dose as factors and were considered statistically significant when $p < 0.05$. Dose-response curves were fit sigmoid to a Boltzmann functions (the concentration axis was set linear) and PS concentration required for half-maximal effect (EC_{50}) was calculated. Sigmoid curves were compared using F-test. EC_{50} values were compared using one way-ANOVA followed by post hoc Newman-Keuls test for multiple comparisons (significance $p < 0.05$).

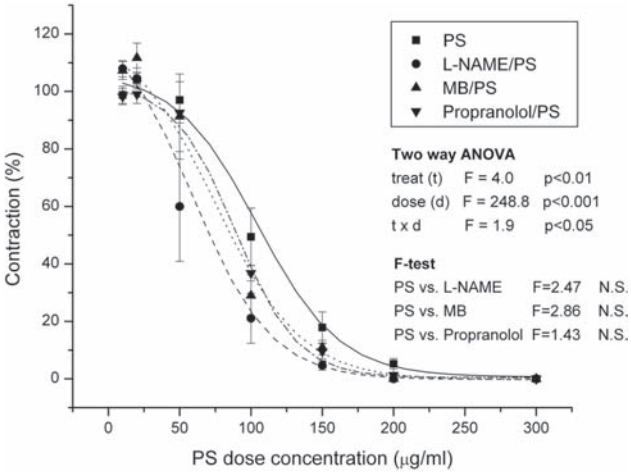

Figure 1. Dose-response sigmoid fit curves for PS-induced relaxation of spontaneous rhythmic activity of the isolated rat uterus pre-treated with L-NAME (10^{-5} mol/l), MB (0.9×10^{-6} mol/l), and propranolol (1.7×10^{-5} mol/l). Data are expressed as mean ± SE (the number of observations $n = 7$). Sigmoid fit was performed according to Boltzmann equation. Results of statistical analyses both two-way ANOVA (treatment – treat (t) and dose (d) as factors) and F-test are given (F factors and p values).

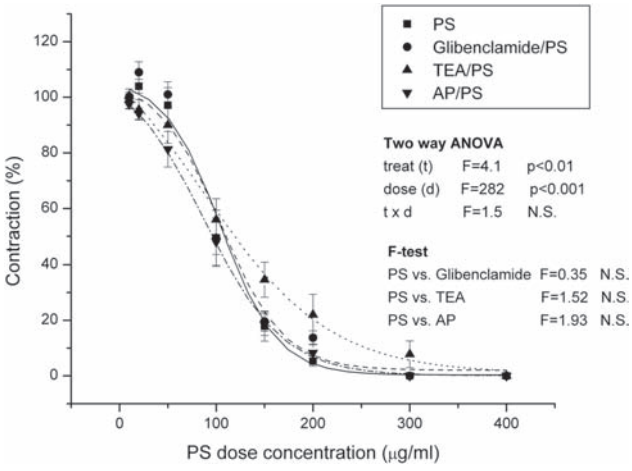

Figure 2. Dose-response sigmoid fit curves for PS-induced relaxation of spontaneous rhythmic activity of the isolated rat uterus pre-treated with TEA (6×10^{-3} mol/l), 4-AP (10^{-3} mol/l), and glibenclamide (2×10^{-6} mol/l). Data are expressed as mean ± SE (the number of observations $n = 7$). Sigmoid fit was performed according to Boltzmann equation. Results of statistical analyses both two-way ANOVA (treatment – treat (t) and dose (d) as factors) and F-test are given (F factors and p values).

Results

PS (μg/ml: 10, 20, 50, 100, 150, 200, 300, 400, 500, 600) relaxes both spontaneous active and calcium-induced rat uteri in a dose-dependant manner (two-way ANOVA, significant dose effects, Figs. 1–4). Pre-treatment of spontaneous active uteri with L-NAME (10^{-5} mol/l), MB (0.9×10^{-6} mol/l) or propranolol (1.7×10^{-5} mol/l) enhanced PS-mediated uterine muscle relaxation (two-way ANOVA, significant treatment t, and interaction treatment t × dose d effects, Fig. 1), without statistically significant effects on sigmoid fit shapes (non-significant F-test, Fig. 1). Dose-dependent relaxation of spontaneous active isolated rat uterus by PS was lower in uteri pre-treated with single dose of glibenclamide (2×10^{-6} mol/l), TEA (6×10^{-3} mol/l) and 4-AP (10^{-3} mol/l) (two-way ANOVA, significant dose d effect and treatment t effects without significant interaction effect, Fig. 2), without significant effect on sigmoid fit shapes (non-significant F-test, Fig. 2). EC_{50} values were similar in all analysed groups (one-way ANOVA, Table 1).

PS (μg/ml: 10, 20, 50, 100, 150, 200, 300, 400, 500, 600) caused dose-dependent relaxation of calcium-induced activity of the isolated rat uterus despite the presence of L-NAME, MB and propranolol (two-way ANOVA, significant dose effect, Fig. 3). The presence of used antagonists modified the kinetics of PS induced relaxation (significant differences obtained by F-test, Fig. 3), without changes in EC_{50} values (one-way ANOVA, Table 1). However, treatment with glibenclamide, TEA and 4-AP significantly reduced PS relaxing effects (two-way ANOVA, significant treatment t effect, $p < 0.001$, Fig. 4) and the kinetics of PS relaxation (significant F-test, Fig. 4). The extent of the reduction was treatment dependent (two-way ANOVA, interaction treatment t × dose d effect, $p < 0.001$). According to the EC_{50} values, the order of magnitude was glibenclamide > TEA > AP (one-way

Table 1. EC50 values for protamine sulphate doses calculated from sigmoid fit curves for different treatments

Treatment	Ca^{2+}-induced EC_{50}	Spontaneous EC_{50}
PS	149 ± 13	98 ± 1
L-NAME/PS	168 ± 20	58 ± 14
MB/PS	133 ± 10	76 ± 9
Propranolol/PS	141 ± 5	94 ± 3
Glibenclamide/PS	241 ± 15*	94 ± 4
TEA/PS	211 ± 10*	96 ± 16
AP/PS	187 ± 15	93 ± 12
ANOVA	$p < 0.001$	N.S.

Results are presented as mean ± SE, number of examinations $n = 7$. Results were tested by one-way ANOVA. $p < 0.05$ was considered as significant) and post hoc compared by Newman-Keuls test. * statistical significant difference comparing to PS; N.S., non significant.

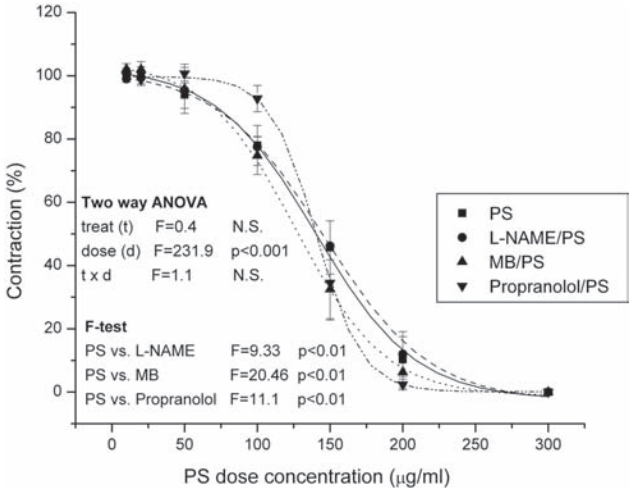

Figure 3. Dose-response sigmoid fit curves for PS-induced relaxation of calcium-induced rhythmic activity of the isolated rat uterus pre-treated with L-NAME (10^{-5} mol/l), MB (0.9×10^{-6} mol/l), and propranolol (1.7×10^{-5} mol/l). Data are expressed as mean ± SE (the number of observations $n = 7$). Sigmoid fit was performed according to Boltzmann equation. Results of statistical analyses both two-way ANOVA (treatment – treat (t) and dose (d) as factors) and F-test are given (F factors and p values).

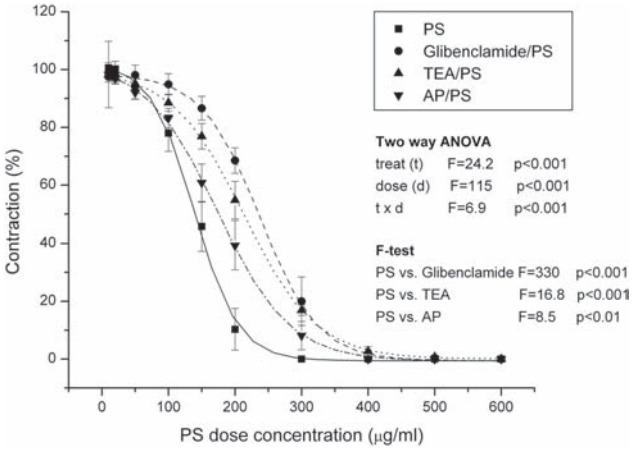

Figure 4. Dose-response sigmoid fit curves for PS-induced relaxation of calcium-induced rhythmic activity of the isolated rat uterus pre-treated with TEA (6×10^{-3} mol/l), 4-AP (10^{-3} mol/l), and glibenclamide (2×10^{-6} mol/l). Data are expressed as mean ± SE (the number of observations $n = 7$). Sigmoid fit was performed according to Boltzmann equation. Results of statistical analyses both two-way ANOVA (treatment – treat (t) and dose (d) as factors) and F-test are given (F factors and p values).

ANOVA, $p < 0.01$, post hoc comparison by Newman-Keuls test, Table 1).

Discussion

PS is a mixture of polyamines and it may have action through different pathways. Our results clearly demonstrate (according to EC_{50} values and maximum relaxation dose) that its action on uterine smooth muscle is dominantly through potassium channels. Processes through β-adrenergic receptor and by NO dependent pathway play a role in PS-mediated relaxation (treatment with L-NAME, MB and propranolol had effect on PS-mediated relaxation, Fig. 1), but its significance is far less than through potassium channels according to maximum relaxation dose (up to 300 μg/ml vs. up to 600 μg/ml in uteri pretreated with potassium channel antagonists: TEA, glibenclamide and 4-AP). Although basic mechanisms of PS-mediated relaxation of spontaneous and calcium-induced contractile activity seem to be similar, their extent is different.

TEA is widely used as an inhibitor of BK_{Ca} channels (Gil-Longo et al. 2005; Rogers et al. 2007; Rosenfeld et al. 2008; Chen et al. 2009; Lloyd et al. 2009) but it is also known that suppress some types of voltage-gated potassium channel currents (Aaronson et al. 2006). In rat myometrium smooth muscle cells BK_{Ca} current coexists with three types of voltage-gated K^+ currents. These include 4-AP-sensitive, rapidly inactivating A-type current and two delayed rectifier K^+ currents that could be suppressed by TEA and 4-AP (Knock et al. 1999). Although there are indications that BK_{Ca} channels play little or no part in controlling basal rhythmicity in rat myometrium (Aaronson et al. 2006) and that voltage-gated potassium channels play a crucial role in this regard, human myometrial contractility was affected by TEA suggesting that the large conductance BK_{Ca} channels may actively participate in control of human myometrial cell membrane potential (Anwer et al. 1993). That may suggest that TEA inhibition of PS effects on spontaneous contractile activity indicate important role of BK_{Ca} and two delayed rectifier K^+ currents in control of spontaneous contractile activity in our experimental conditions.

A large number of previously conducted studies support NO's involvement in PS-mediated relaxation of blood vessels (Pearson et al. 1992; Raikar et al. 1996; Cable et al. 1999; Milovanović et al. 2004; Oreščanin et al. 2007) and other smooth muscles (Li et al. 1999; Chuang et al. 2003). That mechanism by which PS mediates its effects and the effects of free haemoglobin on PS-induced responses in endothelium-denuded and intact human internal thoracic artery rings pre-contracted with phenylephrine or high KCl suggests that PS-induced relaxation responses is not NO- or endothelium-dependent but appears to depend on interactions between PS and calcium ion influxes and/or calcium

ion release from intracellular stores (Golbasi et al. 2003). Our current study showed that L-NAME (a NOS inhibitor), propranolol (a non-selective β-adrenergic blocker) and MB (a cGMP inhibitor), enhanced PS's relaxing effect on spontaneous activity. These results indicate that PS's relaxation capacity is downstream of adrenoceptors. Castresana and colleagues (1995) showed that PS does not alter the levels of cGMP and cAMP in response to the sodium nitroprusside, atrial natriuretic peptide, isoproterenol and forskolin (all vasodilators). David et al. (2001) found that although PS may act at several sites downstream of the adrenoceptor, one of its main sites of action is situated downstream from cAMP-mediated protein phosphorylation. Since PS is a mixture of different amines the other metabolic pathways and subsequent resulting relaxation (or changes in relaxing signalling) can not be excluded.

When contractile activity is extracellular calcium-induced, TEA, glibenclamide and 4-AP decreased PS-mediated uterine muscle relaxation and increased PS dose (EC_{50}) that relax calcium-dependant uterine activity. This implies potassium channels as important mediators of PS induced uterine relaxation. On the other hand, there were no effects of pre-treatment with L-NAME, MB or propranolol on PS dose response (Fig. 3, no dose effect). However, pre-treatment changed the shape of sigmoid curves, according to inherent receptors characteristics and signalling kinetics.

The calcium-mediated initiation spike of the tissue level action potential in myometrium is terminated relatively quickly by a partial repolarization driven by both voltage-sensitive (IK1, IK2 and IK, A) (Knock et al. 1999; Parkington et al. 1999) and calcium-sensitive (BK_{Ca} [Maxi K] and SK3) (Khan et al. 2001) potassium currents. The main function of potassium channels is to dampen cellular excitability by maintaining the cell membrane potential close to the reversal potential of potassium ions. Therefore, depolarizing stimuli are blocked by the generation of outward potassium current which causes hyperpolarization or repolarization thereby terminating action potential generation and ultimately rendering contraction less likely (Khan et al. 2001). The predominant source of calcium for a contraction triggered by an action potential is voltage-gated calcium entry from the extracellular space. The relaxation of uterine smooth muscle is initiated by the intracellular Ca^{2+} decrease following the removal of contractile stimuli (agonists or depolarization). For a Ca^{2+} efflux, the two plasma membrane routes of calcium extrusion, Na-Ca exchange and plasma membrane Ca^{2+} ATPase (PMCA) are required, with PMCA playing the major role in uterine preparations (Taggart et al. 1997; Shmigol et al. 1998; Matthew et al. 2004).

In conclusion, our results demonstrated that PS relaxation effect on the smooth muscle of isolated rat uteri is dominantly potassium channel-dependent. In spontaneous contractile activity BK_{Ca} and two delayed rectifier K^+ currents play significant role in PS-induced relaxation. When contractions are calcium-induced we found that all three types of potassium channels play a crucial role in PS-induced relaxation on this type of smooth muscle and according to EC_{50} values the order of magnitude was glibenclamide > TEA > 4-AP (far less significant). Models of spontaneous and calcium-induced contractile activity are significant for elucidation mechanisms of PS action, indicating PS interactions with all types of potassium channels.

Acknowledgement. This work was supported by the grant from the Ministry of Science of the Republic of Serbia, project No. 143034B.

References

Aaronson P. I., Sarwar U., Gin S., Rockenbauch U., Connolly M., Tillet A., Watson S., Liu B., Tribe R. M. (2006): A role for voltage-gated, but not Ca^{2+}-activated, K^+ channels in regulating spontaneous contractile activity in myometrium from virgin and pregnant rats. Br. J. Pharmacol. **147**, 815–824

Anwer K., Oberti C., Perez G. J., Perez-Reyes N., McDougall J. K., Monga M., Sanborn B. M., Stefani E., Toro L. (1993): Calcium-activated K^+ channels as modulators of human myometrial contractile activity. Am. J. Physiol., Cell Physiol. **265**, C976–985

Cable D. G., Sorajja P., Oeltjen M. R., Schaff H. F. (1999): Different effects of protamine on canine coronary microvessel and conductance arteries: evidence of hyperpolarizing factor release. Surgery **126**, 835–841

Castresana M. R., Zhang L. M., Newman W. H. (1995): Protamine does not affect the formation of cGMP or cAMP in pig vascular smooth muscle cells in response to vasodilators. Crit. Care Med. **23**, 939–943

Chanrachakul N. (2006): Ion channels: new targets for the next generation of tocolytics agents. J. Med. Assoc. Thai. **4**, 178–183

Chen J., Liu J., Wang T., Xiao H., Yin C., Yang J., Chen X., Ye Z. (2009): The relaxation mechanisms of tetrandrine on the rabbit corpus cavernosum tissue *in vitro*. Nat. Prod. Res. **23**, 112–121

Chuang Y. C., Chancellor M. B., Seki S., Yoshimura N., Tyagi P., Huang L., Lavelle J. P., De Groat W. C., Fraser M. O. (2003): Intravesical protamine sulfate and potassium chloride as a model for bladder hyperactivity. Urology **61**, 664–670

Curley M., Cairns M. T., Friel A. M., McMeel O. M., Morrison J. J., Smith T. J. (2002): Expression of mRNA transcripts for ATP-sensitive potassium channels in human myometrium. Mol. Hum. Reprod. **8**, 941–945

David J. S., Vivien B., Lecarpentier Y., Coriat P., Riou B. (2001): Interaction of protamine with alpha- and beta-adrenoceptor stimulations in rat myocardium. Anesthesiology **95**, 1226–1233

Gil-Longo J., González-Vázquez C. (2005): Characterization of four different effects elicited by H2O2 in rat aorta. Vascul. Pharmacol. **43**, 128–138

Golbasi I., Nacitarhan C., Ozdem S., Turkay C., Karakaya H., Sadan G., Bayezid O. (2003): The inhibitory action of protamine on human internal thoracic artery contractions: the effect of free hemoglobin. Eur. J. Cardiothorac. Surg. **23**, 962–968

Khan R. N., Matharoo-Ball B., Arulkumaran S., Ashford M. L. J. (2001): Potassium channela in the human myometrium. Exp. Physiol. **86**, 255–264

Knock G. A., Smirnov S. V., Aaronson P. I. (1999): Voltage-gated K^+ currents in freshly isolated myocytes of the pregnant human myometrium. J. Physiol. **518**, 769–781

Li Y., Cho C. H. (1999): The ulcer healing effect of protamine sulphate in rat stomach. Aliment. Pharmacol. Ther. **13**, 1351–1362

Lloyd E. E., Marrelli S. P., Bryan R. M. Jr. (2009): Cyclic GMP does not activate two-pore domain K^+ channels in cerebrovascular smooth muscle. Am. J. Physiol., Heart Circ. Physiol. **296**, H1774–1180

Lopez-Bernal A. (2007): The regulation of uterine relaxation. Semin. Cell Dev. Biol. **18**, 340–347

Manley B. F. J. (1986): Multivariate Statistical Methods. Chapman & Hall, London

Matthew A., Shmygol A., Wray S. (2004): Ca entry, efflux and release in smooth muscle. Biol. Res. **37**, 617–624

Milovanović S. R., Oreščanin Z., Spasić S., Miletić S., Prostran M., Spasić M. B. (2004): Effect of MnSOD (*E. coli*) on the relaxation caused by sodium nitroprusside on isolated rat renal artery. J. Serb. Chem. Soc. **69**, 973–980

Morrison J. J., Ashford M. L., Khan R. N., Smith S. K. (1993): The effects of potassium channel openers on isolated pregnant human myometrium before and after the onset of labor: potential for tocolysis. Am. J. Obstet. Gynecol. **169**, 1277–1285

Novaković R., Milovanović S., Protić D., Đokić J., Heinle H., Gojković-Bukarica Lj. (2007): The effect of potassium channel opener pinacidil on the non-pregnant rat uterus. Basic Clin. Pharmacol. Toxicol. **101**, 181–186

Oreščanin Z., Milovanović S. R., Spasić S. D., Jones D. R., Spasić M. B. (2007): Different responses of mesenteric artery from normotensive and spontaneously hypertensive rats to nitric oxide and its redox congeners. Pharmacol. Rep. **59**, 325–332

Oreščanin-Dušić Z., Milovanović S., Spasić M., Radojičić R., Blagojević D. (2008): Effect of protamine sulfate on the isolated mesenteric arteries of normotensive and spontaneously hypertensive rats. Arch. Biol. Sci. **60**, 163–168

Parkington H. C., Tonta M. A., Davies N. K., Brennecke S. P., Coleman H. A. (1999): Hyperpolarization and slowing of the rate of contraction in human uterus in pregnancy by prostaglandins E2 and F2α: involvement of the Na^+ pump. J. Physiol. **514**, 229–243

Pearson P. J., Evora P. R., Ayrancioglu K., Schaff H. V. (1992): Protamine releases endothelium-derived relaxing factor from systemic arteries: a possible mechanism of hypotension during heparin neutralization. Circulation **86**, 289–294

Raikar G. V., Hisamochi K., Raikar B. L. (1996): Nitric oxide inhibition attenuates systemic hypotension produced by protamine. J. Thorac. Cardiovasc. Surg. **111**, 1240–1246

Rogers P. A., Chilian W. M., Bratz I. N., Bryan R. M., Dick G. M. (2007): H_2O_2 activates redox- and 4-aminopyridine-sensitive Kv channels in coronary vascular smooth muscle. Am. J. Physiol., Heart Circ. Physiol. **292**, H1404–411

Rosenfeld C. R., Word R. A., DeSpain K., Liu X. T. (2008): Large conductance Ca^{2+}-activated K^+ channels contribute to vascular function in nonpregnant human uterine arteries. Reprod. Sci. **15**, 651–660

Shmigol A., Eisner D. A., Wray S. (1998): Carboxyeosin decreases the rate of decay of the [Ca]i transient in uterine smooth muscle cells isolated from pregnant rats. Pflügers. Arch. **437**, 158–160

Taggart M. J., Wray S. (1997): Agonist mobilization of sarcoplasmic reticular calcium in smooth muscle: functional coupling to the plasmalemmal Na^+/Ca^{2+} exchanger. Cell Calcium **22**, 333–341

Viaro F., Marcelo B. D., Evora P. R. B. (2002): Catastrophic cardiovascular adverse reactions to protamine are nitric oxide/cyclic guanosine monophosphate dependent and endothelium mediated. Should methylene blue be the treatment of choice? Chest **122**, 1061–1066

Diltiazem prevention of toxic effects of monosodium glutamate on ovaries in rats

Vladimila Bojanić[1], Zoran Bojanić[2], Stevo Najman[3], Todorka Savić[1], Vladimir Jakovljević[4], Staša Najman[1] and Snežana Jančić[5]

[1] *Institute for Pathophysiology, Faculty of Medicine, Niš, Serbia*
[2] *Institute for Pharmacology, Faculty of Medicine, Niš, Serbia*
[3] *Institute for Biology and Human Genetics, Faculty of Medicine, Niš, Serbia*
[4] *Institute for Physiology, Faculty of Medicine, Kragujevac, Serbia*
[5] *Institute for Pathology, Faculty of Medicine, Kragujevac, Serbia*

Abstract. The female reproductive system is very sensitive to different harmful environmental factors. A great danger is hidden in an increased use of food additives like monosodium glutamate (MSG). Numerous studies have shown that application of high doses of MSG to different kinds of animals during the neonatal period may cause lesions of neural structures and the retina. Later in adulthood animals exhibit a series of neuroendocrine disorders: a stunted growth, obesity and infertility. The mechanism of MSG action is not well explained yet. We hypothesized that high concentration of MSG could alter permeability of neural membrane for calcium. We studied whether pretreatment with diltiazem prevented the effects of MSG on ovaries in rats. Female rat pups were treated with: 0.9% NaCl, MSG, diltiazem or diltiazem with MSG. MSG treatment resulted in a cystic degeneration of ovaries and irregular and prolonged estrus phase of estrus cycle. The other treated groups of rats had normal ovarian histology and estrus cycle. The pretreatment with diltiazem prevented development of morphological and functional disorders of ovaries. Our results suggest that calcium overloading play an important role in mechanisms of MSG toxicity.

Key words: Monosodium glutamate — Rat — Ovary — Estrus cycle — Diltiazem

Introduction

Female infertility is a very real medical problem in developed countries. The female reproductive system is very sensitive to different harmful environmental factors. Modern lifestyle with an increased number of women who decide to have babies later in life and the negative influence of alcohol, smoking habit, and excessive overweight or underweight and contraception are factors which should not be underestimated. A great advance in technology is followed by an increased use of chemicals which can seriously harm female fertility. Some chemicals are counteractive with estrogen. A great danger is hidden in an increased use of different food additives like monosodium glutamate (MSG). MSG is the salt of nonessential glutamic acid. It has a property to enhance the perception that flavours are well blended and full-bodied. MSG also compensates for the absence of superior ingredients in food and disguise unwelcome tastes. This popular taste enhancer is widely used not only in the food industry, but also in homes and restaurants.

This taste enhancer is present in: flavoured chips and snacks, soups or sauces (canned, packed), prepared meals, frozen foods and meals, fresh sausages, marinated meats, and stuffed or seasoned chicken, bottled soy or oriental sauces, manufactured meats, some hams, luncheon chicken and turkey, flavoured tuna, vegetarian burgers and sausages.

Numerous studies have shown that parenteral application of high doses of MSG (1–4 mg/g b.w.) to animals dur-

Correspondence to: Vladmnila Bojanić, Institute for Pathophysiology, Faculty of Medicine, Bul. Dr. Z. Djindjića 81, 18000 Niš, Serbia
E-mail: vladmilab@gmail.com

ing the neonatal period may cause lesions of the preoptic nuclei, arcuate nuclei, the circumventricular organs and the retina (Lukas and Newhouse 1957; Potts et al. 1960; Cohen 1967; Olney 1969, 1971; Olney and Ho 1970; Lemkey-Johnston and Reynolds 1972, 1974; Olney et al. 1972; Sasaki and Sano 1986; Gao et al. 1994). Animals treated with injections of MSG during the first 10 neonatal days, exhibit a series of neuroendocrine disorders during their adult lives. The most prominent disorders are: stunted growth, obesity and decreased fertility. Studies were carried out in different kinds of animals: mice, rats, rabbits, hamsters, dogs, chickens and monkeys. Many studies have shown that MSG can harm when given orally, too (Olney and Ho 1970; Burde et al. 1971, 1972; Olney 1971; Lemkey-Johnston and Reynolds 1972; Olney et al. 1972; Takasaki 1979, 1980).

The results of some studies indicate that MSG could exhibit harmful effect on human body including: obesity, urticaria (Botey et al. 1988; Roberts 1996), asthma (Schaumburg et al. 1969; Rosenblum et al. 1971; Kenney and Tidball 1972; Reif-Lehrer and Stemmermann 1975; Andermann et al. 1976; Diamond et al. 1986; Allen et al. 1987; Sands et al. 1991; Scopp 1991; Ehlers et al. 1998). The way of MSG action is not well explained yet. It is well known that MSG has high excitotoxic potential, which is mediated at the level of second messenger by calcium anions (Gao et al. 1994; Lin et al. 1995). We therefore hypothesised that high concentration of MSG could alter permeability of neural membrane for calcium which could be involved in the mechanisms of MSG toxicity. The purpose of this investigation was to study if pretreatment with diltiazem (L-calcium channel blocker) could alter the effects of MSG on ovaries and estrus cycle in rats.

Materials and Methods

The study was carried out in neonatal female Wistar rats. The animals were injected subcutaneously interscapularly with the same volume of: 0.9% NaCl solution (C group), 4 mg/g b.w. of MSG (M group), 5 mg/g b.w. of diltiazem (D group) and 5 mg/g b.w. of diltiazem and 60 min later with 4 mg/g b.w. of MSG (DM group). The injections were administered at 2^{nd}, 4^{th}, 6^{th}, 8^{th} and 10^{th} day of life. The animals were housed under controlled conditions. The room temperature was 23 ± 2°C and air humidity 50 ± 5%.The rhythm of light and darkness was established (light phase from 6:00 a.m. to 6:00 p.m.). The rats were weaned at age of 28 days. Females were housed in standard cages. They had free access to tap water and to standard laboratory chow pellets ("Veterinarski zavod" Zemun). Females were marked with a non-toxic pencil.

Vaginal smears were collected from three months old females during 25 days. There were six females in each group. The cages with rats were carried to the experimental room by the same order at 8:00 a.m. every morning. Vaginal secretion was taken with a clean plastic pipette filled with 0.1 ml of normal saline (0.9% NaCl) by inserting into rat vagina not too deep. Vagina was washed out and one drop of vaginal fluid was placed on a clean glass microscope slide. A different slide was used for each animal. Vaginal fluid drop was pushed with the clean spreader to the end of slide with smooth movement. The slide was left to dry in the air.

Vaginal smears were fixed with methanol for 5 min. Methanol was rinsed with distilled water for 5 min and after that slides were gently totally covered with 10% Giemsa stain for 10 min. The stain was rinsed with clean distilled water and slides were dried. Stained slides were observed under light microscope. Three types of cells could be recognized: epithelial cells, cornified cells and leukocytes. The proportion among these cells was used for determination of the estrous cycle phase.

The animals were sacrificed at age of four months under pentobarbital sodium anesthesia (40 mg/kg b.w. intraperitoneally). The ovaries were carefully removed and prepared according to appropriate procedures with HE methods for micromorphological examinations. All procedures on animals followed Guideline for work on experimental animals approved by Ethic Committee of Faculty of Medicine in Niš.

Results of statistical analysis are expressed as means ± standard deviation. Statistical significance was determined with analysis of variance (ANOVA) test. The differences were considered significant at $p < 0.05$ level. All statistical analyses were performed using the SPSS statistical software (version 15).

Results

Determination of estrus cycle length and duration of its phases is performed. Average estrus cycle in rats neonatally treated with MSG was 5.2 days and it was significantly prolonged, compared to duration of average estrus cycle in rats in C group (4.1 days) (Fig. 1). There were no significant differences between control and the other groups – D (4.3 days) and DM (4.6 days).

In females of M group estrus phase was more often registered than in females from the other groups (Fig. 2). The difference was statistically significant between M and C groups (9.67 ± 2.42 vs. 6.67 ± 1.21; $p < 0.05$), as well as between M and D groups (9.67 ± 2.42 vs. 6.67 ± 0.82; $p < 0.01$). Metaestrus was recorded more often in animals of groups C and D, than in females from DM and M groups. In females of DM group and M group diestrus phase was more often recorded than in rats of C and D groups, but this was

not statistically significant. In rats of M group proestrus was registered statistically significant more rarely than in C group (4.00 ± 0.63 vs. 6.00 ± 0.00; $p < 0.001$), D group (4.00 ± 0.63 vs. 6.17 ± 0.98; $p < 0.001$), as well as in DM group (4.00 ± 0.63 vs. 5.50 ± 0.55; $p < 0.01$).

The ovaries in rats from C, D, and DM groups showed normal morphology (Fig. 3). Their ovaries had wide cortex with numerous primary, secondary and Graafian follicles, as well as newly formed and degenerated *corpora lutea*. Histology of ovaries of MSG-treated rats showed cystic degeneration. Fibrotically changed stroma and arteriolar hyalinosis were found. Ovaries contained many atretic follicles and no *corpora lutea*.

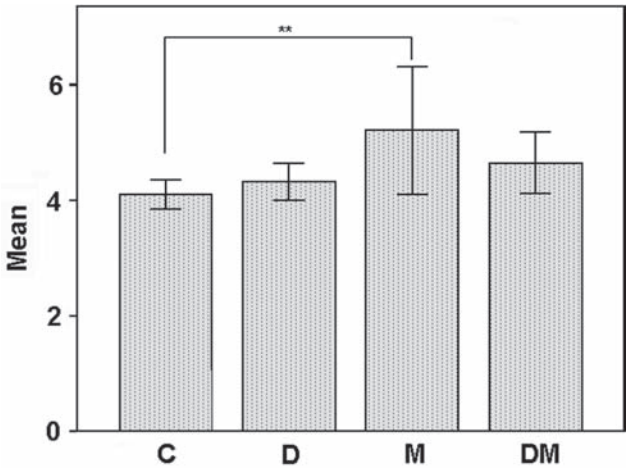

Figure 1. The average duration of estrus cycle of Wistar rats from different groups. C, control; D, diltiazem-treated; M, MSG-treated; DM, diltiazem- and MSG-treated; ** $p < 0.01$, error bars: 95% CI (ANOVA).

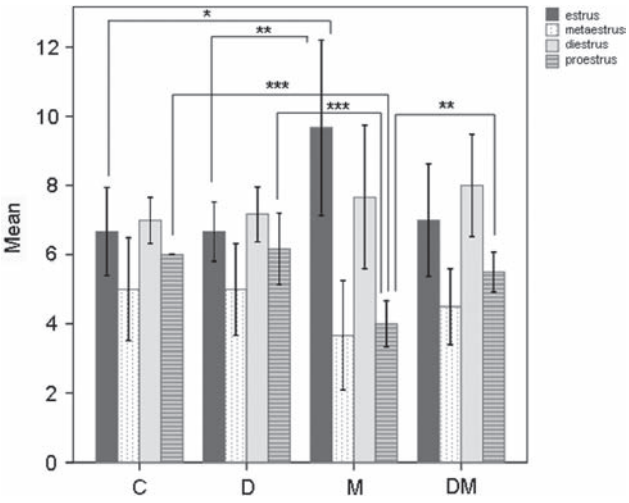

Figure 2. The summ of days with registered estrus phasis of estrus cycle within period of cycle determination and statistical significance of diferences between groups. C, control; D, diltiazem-treated; M, MSG-treated; DM, diltiazem- and MSG-treated; * $p < 0.05$; ** $p < 0.01$; *** $p < 0.001$, error bars: 95% CI (ANOVA).

Discussion

There are conflicting reports concerning the effect of neonatal treatment with MSG on female neuroendocrine system. Olney (1969) registered sterility in female mice, which were treated with MSG during first ten days of their neonatal life. There were twice as more atretic follicules in their ovaries than in animals of the control group. The wall of their uterus was very tiny. Adamo and Ratner (1970) reported that female Wistar rats after administration of a single dose of MSG (4 mg/g b.w.) in neonatal period, later cycled normally and were capable of mating and producing normal litters. Although their relative ovarian weights were significantly less then in control animals, ovarian histological findings were normal.

In this paper the histology of ovaries of MSG-treated rats showed cystic degeneration. Ovaries contained many atretic follicles with no *corpora lutea* and fibrotically changed stroma. Arteriolar hyalinosis was found too. Ovaries of rats from C, D and DM groups showed normal morphology. They had primary, secondary and Graafian follicles, as well as newly formed and the degenerated *corpora lutea* in ovary cortex depending on phase of cycle.

Nagasawa et al. (1974) found that estrus cycle of the MSG-treated mice had longer periods of estrus and shorter periods of diestrus than in controls. Clemens et al. (1978) reported the weight reduction of ovaries and uteri and irregular prolonged estrus cycle in MSG-treated Sprague-Dawley rats. Lorden and Caudle (1986) found decreased ovary weight and delayed puberty in mice neonatally treated with MSG. MacDonald and Wilkinson (1990) had quite opposite findings. They found that neonatal treatment with MSG accelerated sexual maturation of rats. Sasaki and Sano (1986) reported that ovaries in MSG-treated mice contained many atretic follicles but no *corpora lutea*. Shapiro et al. (1986) recorded prolongation of estrus in rats neonatally treated with MSG.

The results of this study showed that estrus cycles of rats neonatally treated with MSG were prolonged significantly compared to the duration of estrus cycles in rats neonatally treated with normal saline, diltiazem and diltiazem with MSG.

Estrus cycle is prolonged due to extension of estrus phase and diestrus phase in MSG-treated rats compared to the other experimental groups. Changed permeability of neural membrane for calcium due to effect of MSG is involved in the mechanisms of MSG toxicity.

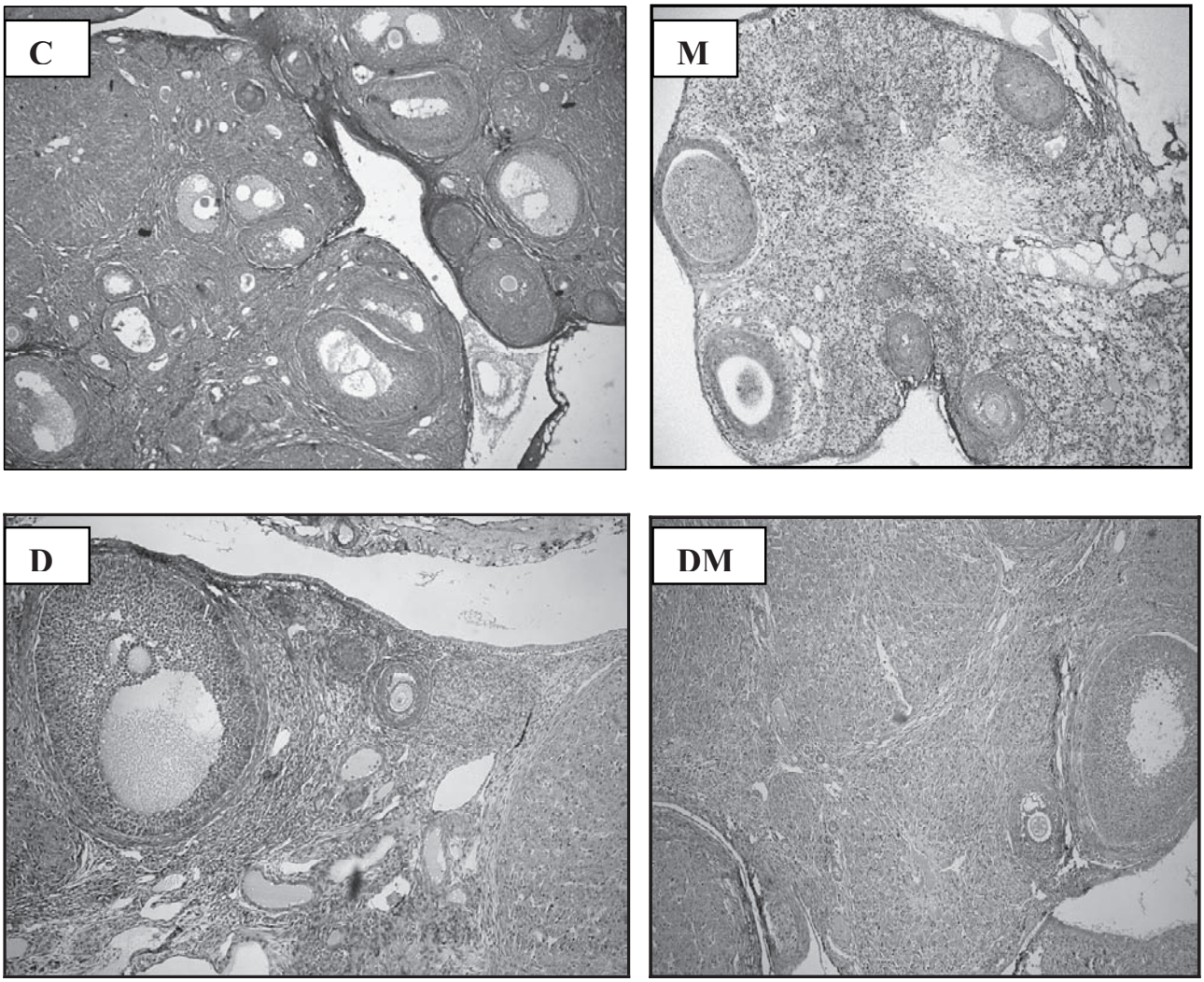

Figure 3. Sections of ovaries of female rats from: group C (control), group D (neonatally treated with diltiazem), group M (neonatally treated with MSG) and group DM (neonatally treated with diltiazem and MSG); HE stained. Magnification ×100.

The toxic effect of MSG on female reproductive system has been atributed to its direct effect on nuclei of hypothalamus for years. Central effect of MSG is proven (Lamperti and Blaha 1979).

Recent studies have shown that glutamate receptors play very important role in pathogenesis of disorders induced by MSG. Glutamate is predominant excitatory neurotransmitter in the mammalians central nervous system (Robinson 2006; Schlett 2006; Greenwood and Connolly 2007; Liguz-Lecznar and Skangiel-Kramska 2007). There are two basic types of glutamate receptors: ionotropic (NMDA, kainate and AMPA) and metabotropic (mGluR) (Smith et al. 2001; Weston et al. 2006; Gerber et al. 2007). Neurotoxicity of MSG is related with glutamate receptors activation (Gao et al. 1994; Beas-Zarate et al. 2001). Sustained high concentration of MSG could alter ionic permeability of neural membrane and induce persistent depolarisation. Such excessive activation of glutamate receptors and overloading with intracellular calcium can induce neural death (Gil-Loyzaga et al. 1993; Bojanic 1997). Glutamate receptors are present in different tissues: hypothalamus, heart, lungs, liver, kidneys, endocrine system, ovaries, uterus, etc. (Gill et al. 2008). Eweka and Om'Iniabohs (2007) referred that prolonged administration of high doses of MSG induced degenerative and atrophic changes in rat ovaries.

The results of our study showed that the pretreatment with diltiazem was efficient in prevention of MSG toxicity on ovaries histology and estrus cycle in Wistar rats.

We consider that excessive activation of glutamate receptors could be responsible for neurotoxic potencial of

MSG. Our subsequent studies should be done to elucidate if chronic low MSG doses activation of glutamate receptors in peripheral tissues could induce damage of ovaries in adult animals.

Acknowledgement. This work was sponsored by Ministry of Science Republic of Serbia (project No. 145072).

References

Adamo N. J., Ratner A. (1970): Monosodium glutamate: lack of effects on brain and reproductive function in rats. Science **169**, 673–674

Allen D. H., Delohery J., Baker G. (1987): Monosodium L-glutamate-induced asthma. J. Allergy Clin. Immunol. **80**, 530–537

Andermann F., Vanasse M., Wolfe L. S. (1976): Letter: Shuddering attacks in children: essential tremor and monosodium glutamate. N. Eng. J. Med. **295,** 174

Beas-Zárate C., Rivera-Huizar S. V., Martinez-Contreras A., Feria-Velasco A., Armendariz-Borunda J. (2001): Changes in NMDA-receptor gene expression are associated with neurotoxicity induced neonatally by glutamate in the rat brain. Neurochem. Int. **39**, 1–10

Bojanic V. (1998): Experimental Study of Pathogenesis of Monosodium Glutamate Induced Obesity. (PhD thesis). Faculty of Medicine, University of Nis, Serbia

Botey J., Cozzo M., Marin A., Eseverri J. L. (1988): Monosodium glutamate and skin pathology in pediatric allergology. Allergol. Immunopathol. (Madr.) **16**, 425–428 (in Spanish)

Burde R. M., Schainker B., Kayes J. (1971): Acute effect of oral and subcutaneous administration of monosodium glutamate on the arcuate nucleus of the hypothalamus in mice and rats. Nature **233**, 58–60

Burde R. M., Schainker B., Kayes J. (1972): Monosodium glutamate: necrosis of hypothalamic neurons in infant rats and mice following either oral or subcutaneous administration. J. Neuropathol. Exp. Neurol. **31**, 181

Clemens J. A., Roush M. E., Fuller R. W., Shaar C. J. (1978): Changes in luteinizing hormone and prolactin control mechanisms produced by glutamate lesions of the arcuate nucleus. Endocrinology **103**, 1304–1312

Cohen A. I. (1967): An electron microscopic study of the modification by monosodium glutamate of the retinas of normal and "rod-less" mice. J. Anat. **120**, 319–356

Diamond S., Prager J., Freitag F. G. (1986): Diet and headache. Is there link? Postgrad. Med. **79**, 279–286

Ehlers I., Niggemann B., Binder C., Zuberbier T. (1998): Role of nonalergic hypersensitivity reaction in children with chronic urticaria. Allergy **53**, 1074–1077

Eweka A. O., Om'Iniabohs F. A. E. (2007): Histological studies of the effects of monosodium glutamate on the ovaries of adult Wistar rats. The Internet Journal of Gynecology and Obstetrics **8**

Gao J., Wu J., Zhao X. N., Zhang W. N., Zhang Y. Y., Zhang Z. X. (1994): Transplacental neurotoxic effects of monosodium glutamate on structures and functions of specific brain areas of filial mice. Sheng Li Xue Bao **46**, 44–51 (in Chinese)

Gerber U., Gee C. E., Benquet P. (2007): Metabotropic glutamate receptors: intracellular signaling pathways. Curr. Opin. Pharmacol. **7**, 56–61

Gil-Loyzaga P., Hernandez-Ortiz M. J., Rodriguez-Benito T., Lasso de la Vega M. (1993): Diltiazem protects against neurotoxicity induced by excitotoxic amino acids on cochlear afferent fibers. ORL; J. Otorhinolaryngol. Relat. Spec. **55**, 211–215

Gill S., Barker M., Pulido O. (2008): Neuroexcitatory targets in the female reproductive system of the nonhuman primate (Macaca fascicularis). Toxicol. Pathol. **36**, 478–484

Greenwood S. M., Connolly C. N. (2007): Dendritic and mitochondrial changes during glutamate excitotoxicity. Neuropharmacology **53**, 891–898

Kenney R. A., Tidball C. S. (1972): Human susceptibility to oral monosodium L-glutamate. Am. J. Clin. Nutr. **25**, 140–146

Kwok H. M. R. (1968): Chinese-restaurant syndrome. N. Eng. J. Med. **278**, 796–802

Lamperti A., Blaha G. (1979): Ovarian function in hamsters treated with monosodium glutamate. Biol. Reprod. **21**, 923–928

Lemkey-Johnston N., Reynolds W. A. (1972): Incidence and extent of brain lesions in mice following ingestion of monosodium glutamate (MSG). Anat. Rec. **172**, 354

Lemkey-Johnston N., Reynolds W. A. (1974): Nature and extent of brain lesions in mice related to ingestion of monosodium glutamate. A light and electron microscope study. J. Neuropathol. Exp. Neurol. **33**, 74–97

Liguz-Lecznar M., Skangiel-Kramska J. (2007): Vesicular glutamate transporters (VGLUTs): the three musketeers of glutamatergic system. Acta Neurobiol. Exp. (Wars.) **67**, 207–218

Lin L., Gu H. M., Zhang W. N., Zhao X. N., Zhang H. Y., Tang G. Z., Li M. Y., Zhang Z. X. (1995): Effects of morphine on monosodium glutamate neurotoxicity and its mechanism. Yao Xue Xue Bao **30**, 806–811 (in Chinese)

Lorden J. F., Caudle A. (1986): Behavioral and endocrinological effects of single injections of monosodium glutamate in the mouse. Neurobehav. Toxicol. Teratol. **8**, 509–519

Lucas D. R., Newhouse J. P. (1957): The toxic effect of sodium-L-glutamate on the inner layers of the retina. AMA Arch. Ophthalmol. **58**, 193–201

MacDonald M. C., Wilkinson M. (1990): Peripubertal treatment with N-methyl-D-aspartic acid or neonatally with monosodium glutamate accelerates sexual maturation in female rats, an effect reversed by MK-801. Neuroendocrinology **52**, 143–149

Nagasawa H., Yarai R., Kikuyama S. (1974): Irreversible inhibition of pituitary prolactin and growth hormone secretion and of mammary gland development in mice by monosodium glutamate administered neonatally. Acta Endocrinol. **75**, 249–259

Olney J. W. (1969): Brain lesions, obesity, and other disturbances in mice treated with monosodium glutamate. Science **164**, 719–721

Olney J. W., Ho O. L. (1970): Brain damage in infant mice following oral intake of glutamate, aspartate, or cysteine. Nature **227**, 609–611

Olney J. W. (1971): Glutamate-induced neuronal necrosis in the infant mouse hypothalamus. J. Neuropathol. Exp. Neurol. **30**, 75–90

Olney J. W., Ho O. L., Rhee V. (1971): Cytotoxic effects of acidic and sulphur containing amino acids on the infant mouse central nervous system. Exp. Brain. Res. **14**, 61–76

Olney J. W., Sharpe L. G., Feigin R. D. (1972): Glutamate-induced brain damage in infant primates. J. Neuropathol. Exp. Neurol. **31**, 464–488

Potts A. M., Modrell K. W., Kingsbury C. (1960): Permanent fractionation of the electroretinogram by the sodium glutamate. Am. J. Ophtalmol. **59**, 900–907

Reif-Lehrer L., Stemmermann M. G. (1975): Letter: Monosodium glutamate intolerance in children. N. Engl. J. Med. **293**, 1204–1205

Roberts H. J. (1996): Aspartame as a cause of allergic reactions, including anaphylaxis. Arch. Intern. Med. **156**, 1027–1028

Robinson M. B. (2006): Acute regulation of sodium-dependent glutamate transporters: a focus on constitutive and regulated trafficking. Handb. Exp. Pharmacol. **175**, 251–275

Rosenblum I., Bradley J. D., Coulston F. (1971): Single and double blind studies with oral monosodium glutamate in man. Toxicol. Appl. Pharmacol. **18**, 367–373

Sasaki F., Sano M. (1986): Roles of the arcuate nucleus and ovary in the maturation of growth hormone, prolactin, and nongranulated cells in the mouse adenohypophysis during postnatal development: a stereological morphometric study by electron microscopy. Endocrinology **119**, 1682–1689

Schaumburg H. H., Byck R., Gerstl R., Mashman J. H. (1969): Monosodium L-glutamate: its pharmacology and role in the Chinese restaurant syndrome. Science **163**, 826–828

Schlett K. (2006): Glutamate as a modulator of embryonic and adult neurogenesis. Curr. Top. Med. Chem. **6**, 949–960

Scopp A. L. (1991): MSG and hydrolyzed vegetable protein induced headache: review and case studies. Headache **31**, 107–110

Shapiro B. H., Albucher R. C., MacLeod J. N., Bitar M. S. (1986): Normal levels of hepatic drug-metabolizing enzymes in neonatally induced, growth hormone-deficient adult male and female rats. Endocrinology **125**, 2935–2944

Smith Y., Charara A., Paquet M., Kieval J. Z., Paré J. F., Hanson J. E., Hubert G. W., Kuwajima M., Levey A. I. (2001): Ionotropic and metabotropic GABA and glutamate receptors in primate basal ganglia. J. Chem. Neuroanat. **22**, 13–42

Takasaki Y. (1979): Protective effect of mono- and disaccharides on glutamate-induced brain damage in mice. Toxicol. Lett. **4**, 205–210

Takasaki Y. (1980): Protective effect of arginine, leucine, and preinjection of insulin on glutamate neurotoxicity in mice. Toxicol. Lett. **5**, 39–44

Weston M. C., Gertler C., Mayer M. L., Rosenmund C. (2006): Interdomain interactions in AMPA and kainate receptors regulate affinity for glutamate. J. Neurosci. **26**, 7650–7658

Neonatal influence of monosodium glutamate on the somatometric parameters of rats

Milan Ćirić[1], Stevo Najman[2], Vladmila Bojanić[3], Snežana Cekić[1], Milkica Nešić[1] and Nela Puškaš[4]

[1] *Institute of Physiology, Faculty of Medicine, Niš, Serbia*
[2] *Institute of Biology and Human Genetics, Faculty of Medicine, Niš, Serbia*
[3] *Institute of Pathophysiology, Faculty of Medicine, Niš, Serbia*
[4] *Institute of Histology, Faculty of Medicine, Belgrade, Serbia*

Abstract. The glutamate receptors are expressed in various cell types including bone and adipose cells. The effects of neonatal administration of monosodium glutamate (MSG) on the "programming" of somatometric parameters in Wistar rats during the period up to 14th week of life were estimated. The rats were treated subcutaneously with five doses of 4 mg/g MSG (10 μl/g body mass) during the first 10 postnatal days (group M). The control (group C) was treated in the same manner with normal saline solution. During three months, body mass, naso-anal length and tail length were measured in 14 days intervals, while femoral and tibial masses and lengths, and testicular mass were measured following sacrificing. The body mass at the end of this period in the M group of males was higher than the body mass in the group C. Reduction in relative bone length, body and tail lengths and the relative as well as absolute testicular mass were registered in MSG-treated rats. A significant reduction in somatometric parameters was registered only in female MSG-treated rats during period of sexual maturation compared to controls.

Key words: Monosodium glutamate — Obesity — Bones — Rat — Somatometry

Introduction

Monosodium glutamate (MSG) (EU food additive code-E 621) is a substance that has toxic effects on numerous animal species. It is widely used as a food and pharmaceutical additive. Experimental models have revealed various harmful effects of MSG. The main toxicity affected loci are the hypothalamic nuclei and the median eminence. The consecutive changes in central nervous system (CNS) and hypothalamo-pituitary axis are the cause of generalized effects. The most prominent manifestations of the neuroendocrine-metabolic disorders caused by these lesions are: growth retardation, obesity and infertility (Olney 1969; Nemeroff et al. 1977; Klingberg et al. 1987). MSG-treatment in rats during the neonatal period causes morphologic and functional changes in the endocrine glands (Terry et al. 1981; Shapiro et al. 1989; Miskowiak et al. 1993). Today, increasing evidence demonstrates that adipose tissue is an endocrine organ secreting a large number of signaling proteins (adipokines) such as leptin and adiponectin, also nerve growth factor and brain-derived neurotrophic factor (this issue), which affect bone and cardiovascular system (Hamerman 2002; Chaldakov et al. 2004). *Via* the intracerebroventricular pathway, leptin enhances the bone loss and causes sympathetic hyperactivity and hypertension in rats (Ducy et al. 2000; Ren 2004). Large adipose content is associated with high leptin levels. The high level of leptin is found in MSG-treated rats, also (Camihort et al. 2005). Adipose tissue is also linked to adiponectin release (Chandran et al. 2003), which has important implications to atherosclerosis and bone mineral density.

Glutamate signal system was discovered in the CNS first. It is now clear that this system is also functional in the non-neural tissues such as the bones, liver, pancreas and skin (Skerry and Genever 2001). Both the metabotropic and ionotropic glutamate receptors and transporters are expressed in osteoblasts (Laketic-Ljubojevic et al. 1999; Gu et al. 2002) and osteoclasts (Epsinosa et al. 1999; Peet et al. 1999).

Correspondence to: Stevo Najman, Institute of Biology and Human Genetics, Faculty of Medicine, University of Niš; Bulevar Dr. Zorana Djindjića 81, 18 000 Niš, Serbia
E-mail: snajman@Eunet.yu

The aim of our work was to study the effects of neonatal administration of MSG on somatometric parameters in Wistar rats during their growth up to 14th week of life and to estimate the effects on morphometric parameters of long bones (femur and tibia).

Materials and Methods

The research was carried out on 40 neonatal Wistar rats of both sexes. The animals were housed in the Institute for Biomedical research vivarium and all procedures on animals followed Guideline for work on experimental animals approved by Ethic Committee of School of Medicine in Niš. The animals were housed in standard plastic cages under controlled conditions (room temperature 23 ± 2°C; air humidity 50 ± 5%; photoperiod of 12 h of light from 6:00 a.m. to 6:00 p.m.). The animals were divided into two groups. In each group of rats: the experimental (group M) and control (group C) was 10 males and 10 females. The pups were injected with either 4 mg/g body mass of MSG or an equal volume of normal saline solution subcutaneously to the interscapular region on alternate days for the first 10 days of life. The pups were weaned at age of 28 days. They had free access to tap water and to standard laboratory rat food ("Veterinarski zavod" Zemun). Morphometric parameters (body mass, naso-anal and tail length) of the animals were measured in 14 days intervals. The animals were sacrificed following an intraperitoneal application of ketamine at age of 14 weeks. The last measurements were performed before anesthetized animals were sacrificed. After the sacrificing of the animals, the rear extremities were separated in the hip joint level. The bone surrounding tissues of the femurs and tibiae were carefully removed and bone mass and bone lengths were measured. The testes were carefully removed, cleaned of the surrounding tissue and mass was measured.

Results of statistical analysis are expressed as means ± SD (standard deviation) and statistical significance was determined with Independent samples Student's *t*-test. Differences were considered significant at $p < 0.05$ level. All statistical analyses were performed using the SPSS statistical software (version 15).

Results

Somatometric parameters were measured periodically in Wistar rats of both sexes.

Body mass

The body masses in MSG-treated and control Wistar rats are shown in Table 1. There were no statistically significant differences in body mass of the male rats between C and M groups. Significantly lower body mass was registered in MSG-treated females then in C group, both at the age of six weeks (132.0 ± 15.3 g vs. 158.2 ± 15.0 g; $p < 0.001$) and at the age of eight weeks (153.0 ± 20.2 g vs. 188.6 ± 15.1 g; $p < 0.001$). Both MSG-treated females at age of six weeks and at age of eight weeks had significantly lower body mass then MSG-treated males (132.0 ± 15.3 g *vs.* 156.0 ± 23.7 g; $p < 0.01$; 153.0 ± 20.2 g vs. 180.3 ± 27.4 g; $p < 0.01$). MSG-treated females had significantly lower body mass than MSG-treated males at age of twelve and fourteen weeks (272.3 ± 26.1 g vs. 318.3 ± 31.2 g; $p < 0.05$). The females from C group had significantly lower body mass then males from C group both at age of ten weeks (199.2 ± 23.5 g vs. 225.0 ± 13.4 g; $p < 0.05$) and twelve weeks (219.2 ± 26.3 g vs. 250.8 ± 13.2 g; $p < 0.05$).

Naso-anal body length

The naso-anal body length values are shown in the Table 2. Lower values of naso-anal lengths were recorded both in males and females of the M groups compared to the C groups. Statistically significant differences were found in the females at the ages of: four weeks (15.1 ± 0.80 cm *vs.* 16.0 ± 0.72 cm; $p < 0.05$), six weeks (16.8 ± 0.67 cm vs. 17.7 ± 0.75 cm; $p < 0.01$), and eight weeks (18.1 ± 0.84 cm vs. 19.2 ± 0.46 cm; $p < 0.01$). Related to sex, significantly shorter naso-anal

Table 1. Body mass in MSG-treated and control Wistar rats of both sexes measured at different age

Groups		Age (weeks)						
		2	4	6	8	10	12	14
♂	C	52.4 ± 10.7	126.9 ± 9.5	167.9 ± 13.5	196.9 ± 16.4	225.0 ± 13.4	250.8 ± 13.2	311.6 ± 20.7
	M	48.6 ± 8.3	117.4 ±2 1.9	156.0 ± 23.7	180.3 ± 27.4	217.0 ± 28.5	252.5 ± 29.9	318.3 ± 31.2
♀	C	48.8 ± 10.8	123.9 ± 25.9	158.2 ± 15.0	188.6 ± 15.1	199.2 ± 23.5[a]	219.2 ± 26.3[a]	288.4 ± 22.3
	M	45.6 ± 8.6	105.2 ± 13.5	132.0 ± 15.3[b,c]	153.0 ± 20.2[b,c]	185.0 ± 31.6	211.0 ± 28.6[d]	272.3 ± 26.1[d]

The values are expressed as mean ± SD in grams; ♂, males; ♀, females; M, rats treated with monosodium glutamate; C, rats treated with normal saline. Statistically significant difference between: [a] C♀ and C♂ for the level of $p < 0.05$; [b] M♀ and C♀ for the level of $p < 0.001$; [c] M♀ and M♂ for the level of $p < 0.01$; [d] M♀ and M♂ for the level of $p < 0.05$.

Table 2. Naso-anal length in MSG-treated and control Wistar rats of both sexes measured at different age

Groups		Age (weeks)			
		4	6	8	14
♂	C	16.0 ± 0.37	18.2 ± 0.33	20.0 ± 0.53	22.8 ± 0.82
	M	16.0 ± 0.93	17.7 ± 0.85	19.7 ± 0.71	22.2 ± 0.75
♀	C	16.0 ± 0.72	17.7 ± 0.74	19.2 ± 0.46[c]	21.5 ± 0.89[a]
	M	15.1 ± 0.79[e,b]	16.8 ± 0.67[f, b]	18.1 ± 0.83[f,d]	21.2 ± 1.30

The values are expressed as mean ± SD in centimeters; ♂, males; ♀, females; M, rats treated with monosodium glutamate; C, rats treated with normal saline. Statistically significant difference between: [a] C♀ and C♂ for the level of $p < 0.05$; [b] M♀ and M♂ for the level of $p < 0.01$; [c] C♀ and C♂ for the level of $p < 0.01$; [d] M♀ and M♂ for the level of $p < 0.001$; [e] M♀ and C♀ for the level of $p < 0.05$; [f] M♀ and C♀ for the level of $p < 0.01$.

Table 3. Tail length in MSG-treated and control Wistar rats of both sexes measured at different age

Groups		Age (weeks)			
		4	6	8	14
♂	C	13.0 ± 0.71	15.8 ± 1.02	17.1 ± 0.82	18.4 ± 0.37
	M	12.7 ± 1.32	15.5 ± 0.98	17.1 ± 0.73	18.3 ± 1.32
♀	C	13.4 ± 0.84	16.0 ± 0.81	17.0 ± 0.47	18.9 ± 0.73
	M	12.8 ± 0.90	14.9 ± 1.08[a]	15.7 ± 0.93[b,c]	17.9 ± 2.26

The values are expressed as mean ± SD in centimeters; ♂, males; ♀, females; M, rats treated with monosodium glutamate; C, rats treated with normal saline. Statistically significant difference between: [a] M♀ and C♀ for the level of $p < 0.05$; [b] M♀ and M♂ for the level of $p < 0.05$; [c] M♀ and C♀ for the level of $p < 0.001$.

body lengths were measured in MSG-treated females then in MSG-treated males at the ages of: four weeks (15.1 ± 0.79 cm vs. 16.0 ± 0.93 cm; $p < 0.01$), six weeks (16.8 ± 0.67 cm vs. 17.7 ± 0.85 cm; $p < 0.01$) and eight weeks (18.1 ± 0.83 cm vs. 19.7 ± 0.71 cm; $p < 0.001$). Also, significantly shorter naso-anal body lengths were recorded in females then in males of C groups: in the eighth (19.2 ± 0.46 cm vs. 20.0 ± 0.53 cm; $p < 0.01$) and fourteenth week of age (21.5 ± 0.89 cm vs. 22.8 ± 0.82 cm; $p < 0.05$).

Tail length

Tail length values are shown in Table 3. There were no significant differences in tail length in the males between C and M group. The mean tail length of the females treated with MSG was significantly shorter compared to the females of C groups both at the age of six weeks (14.9 ± 1.08 cm vs. 16.0 ± 0.82 cm; $p < 0.05$) and at the age of eight weeks (15.7 ± 0.93 cm vs. 17.0 ± 0.47 cm; $p < 0.05$). MSG-treated females had significantly shorter tails than MSG-treated males at the age of eight weeks (15.7 ± 0.93 cm vs. 17.1 ± 0.73 cm; $p < 0.05$).

Although, the differences in some somatometric parameters were not significant between MSG-treated and control groups the most of animals, especially females from M group had increased content of abdominal fat tissue (Fig. 1).

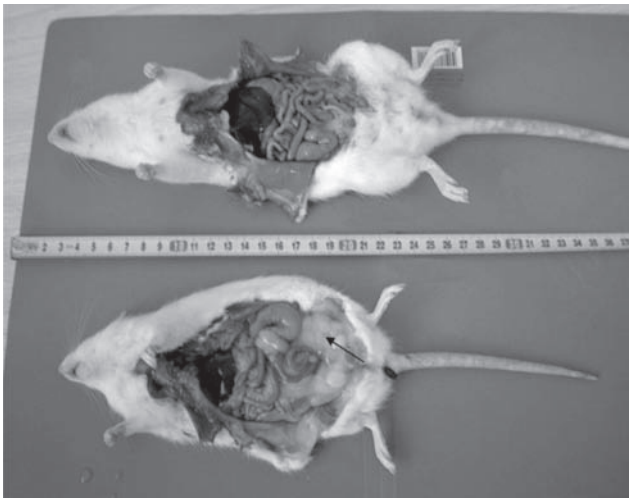

Figure 1. Differences in both naso-anal and tail lengths and fat tissue (arrow) content between normal saline-treated females (up) and MSG- treated females (down).

Bone lengths

Mean femoral and tibial lengths in both the females and males are shown in Table 4. The differences in mean absolute and relative femoral and tibial lengths were not significant between

Table 4. Absolute and relative femoral and tibial lengths in MSG-treated and control Wistar rats of both sexes

Groups		Femoral length		Tibial length	
		Absolute	Relative	Absolute	Relative
♂	C	34.0 ± 0.89	10.92	37.8 ± 0.95	12.13
	M	33.9 ± 1.47	10.64	37.2 ± 1.47	11.67
♀	C	33.0 ± 1.57	11.44	36.8 ± 1.72	12.70
	M	32.0 ± 0.45[a]	11.75	36.1 ± 1.11	13.27

Absolute lengths are expressed as mean ± SD in millimeters; ratios are expressed in percents related to body mass; ♂, males; ♀, females; M, rats treated with monosodium glutamate; C, rats treated with normal saline; [a] statistically significant difference between M♀ and M♂ for the level of $p < 0.05$.

Table 5. Absolute and relative femoral and tibial masses in MSG-treated and control Wistar rats of both sexes

Groups		Femoral mass		Tibial mass	
		Absolute	Relative	Absolute	Relative
♂	C	0.65 ± 0.06	0.21 ± 0.03	0.54 ± 0.06	0.18 ± 0.03
	M	0.59 ± 0.11	0.18 ± 0.02	0.46 ± 0.06	0.15 ± 0.09
♀	C	0.63 ± 0.05	0.22 ± 0.02	0.51 ± 0.04	0.18 ± 0.01
	M	0.51 ± 0.02[b]	0.18 ± 0.01[b]	0.41 ± 0.02[a]	0.14 ± 0.01[a]

Absolute masses are expressed as mean ± SD in grams; relative masses are expressed as mean ± SD in %; ♂, Males; ♀, Females; M, rats treated with monosodium glutamate; C, rats treated with normal saline; statistically significant difference between: [a] M♀ and C♀ group for the level of $p < 0.01$; [b] M♀ and C♀ group for the level of $p < 0.05$

Table 6. Absolute and relative testicular mass in MSG-treated and normal saline-treated Wistar rats

Groups	Absolute mass	Relative mass
C	3.32 ± 0.18	1.06 ± 0.09
M	2.93 ± 0.35[a]	0.92 ± 0.09[a]

Absolute masses are expressed as mean ± SD in grams; relative masses are expressed as mean ± SD in %; M, rats treated with monosodium glutamate; C, rats treated with normal saline; [a] statistically significant difference between M and C group for the level of $p < 0.05$.

MSG-treated and normal saline-treated males and females. The femurs in MSG-treated females were significantly shorter than in MSG-treated males (32.0 ± 0.45 mm vs. 33.9 ± 1.47 mm; $p < 0.05$). Tibial length differences between groups were not statistically significant. Females had shorter tibias compared to males, but those differences were not significant too.

Bone mass

Mean absolute and relative femoral and tibial masses for both males and females are shown in Table 5. The differences in absolute femoral mass between M and C group of females were not significant. MSG-treated females had significantly lowered absolute and relative femoral mass compared to normal saline-treated females (0.18 ± 0.01 vs. 0.22 ± 0.02; $p < 0.05$). Absolute and relative tibial masses were significantly lower in MSG-treated females than in normal saline-treated females (0.41 ± 0.02 vs. 0.51 ± 0.04; $p < 0.01$ and 0.14 ± 0.01 vs. 0.18 ± 0.01; of $p < 0.01$) respectively. The differences between both MSG-treated males and females and normal saline-treated males and females were not significant.

Testicular mass

Mean values of absolute and relative testicular masses in MSG-treated and normal saline-treated Wistar rats at age of 100 days are shown in Table 6. Absolute and relative masses of MSG treated rats were significantly lower than in normal saline-treated rats.

Discussion

Neonatal MSG-treatment causes morphometric changes in rats. The majority of previous studies recorded a body mass reduction in the rats (Terry et al. 1981; Millard et al. 1982; Shapiro et al. 1989; Waxman et al.1990). The reduction in body mass in MSG-treated males was not registered by Miskowiak et al. (1993) and Bojanić (1998). Significantly lower body mass was registered in MSG-treated than in normal

saline-treated female Wistar rats (Bojanić 1998). The results of our study showed that MSG-treated males had lower body mass during the first ten weeks of life. MSG-treated rats overgrew normal saline-treated rats in the twelfth week of life.

At the other hand, retardation in mass gain of MSG-treated females compared to controls was especially expressed and statistically highly significant at the age of 6 and 8 weeks ($p < 0.001$). The differences in body mass between M and C groups decreased, or disappeared, or even the rats of M group overgrew the rats from C group in later period.

In peripubertal period the differences between sexes within identically treated groups of males and females were also recorded. Differences between sexes are especially emphasized in group M. Body mass of MSG-treated females was significantly lower than in MSG-treated males.

Numerous studies showed stunted growth in rats. Both female and male MSG-treated rats had significantly shorter both naso-anal and tail length than normal saline-treated rats (Terry et al. 1981; Shapiro et al. 1989; Waxman et al.1990; Miskowiak et al. 1993; Bojanic 1998). In our study, the most prominent changes in body mass and naso-anal and tail lengths of MSG-treated rats compared to normal saline-treated rats were at the age of six and eight weeks. As well, MSG-treated females compared to males showed the most prominent differences in mentioned parameters in the same period.

We can conclude that neonatal exposition to MSG affected rat growth and development, especially during period of sex maturation and that the females are more sensitive to MSG treatment than males. This means that pubertal period is characterized with pronounced vulnerability and sensitivity for expression of external influences, particularly in females.

Animal linear growth decrease can be attributed to depressed activity of growth and sexual hormones. Because, MSG application in the neonatal period reduces growth in males and females, the therapy with growth hormone (GH) was used in attempt to make correction of this disorder (Rol de Lama et al. 1998a). GH substitution therapy is effective for growth acceleration after the age of 30 days, with a partial recovery in males and a complete recovery in females (Rol de Lama et al. 1998a). MSG treatment reduced GH and insulin-like growth factor-1 (IGF-1) levels in rats of both sexes, causing a less pronounced reduction in tibial growth and body mass gain in females compared to males (Rol de Lama et al. 1998b). In MSG-treated males reduction of pituitary LH content was found what was different than in females. This dimorphic action of MSG on the gonadal axis could be explanation for the observed differences in growth rate (Rol de Lama et al. 1998b).

Bones of MSG-treated rats in our research were shorter and had lower mass in animals of both sexes. Kovács et al. (1996) summarized that neonatal MSG -treatment had a negative effect on bone growth and was associated with reduced levels of pituitary and serum GH, serum IGF-1 and pituitary GH receptors concentration. GH administration increased leg length in the animals of both sexes treated with MSG, but more effectively in females, in spite of a similar IGF-1 levels in both sexes (Rol de Lama et al. 1998b). Decreased femoral strength following MSG- treatment is addressed to reduced activity of the hypothalamo-pituitary-GH-IGF-1 system (Stevenson et al. 2009). The crucial effect of GH decreased level on the body growth is due to MSG- dependent anatomic and functional hypothalamic and adenohypophyseal reorganization. In this way neonatal treatment with MSG made programming of further animal development.

Increased fat content in MSG-treated rats (Fig 1.) should be reconsidered in attempt to explain possible effects on bones. It's well known that obese animals have high leptin level which has effect on bones. Leptin expression in bone basic cellular system, which is primarily involved in bone formation and/or bone resorption, indicates the possibility that leptin is involved in modulating of the initial phases of bone modeling and remodeling processes (Morroni et al. 2004). Mainly, leptin has reputation of antiosteogenic mediator (Cock and Auwerx 2003). Guidobono et al. (2006) found that leptin reduced the accretion of total femoral bone mineral content and bone mineral density of both femur and tibia in growing rats after long-term continuous intracerebroventricular infusion. One of the ways of leptin's action is over alpha-Melanocyte-stimulating hormone. This hormone regulates appetite and body mass, and it can decrease the bone volume directly affecting the skeleton (Cornish et al. 2003).

The studies in leptin receptor-deficient Zucker (fa/fa) rats indicate that leptin could have positive effect on bones (Tamasi 2003). Anyway, the obesity could influence bone tissue by leptin independent mechanisms. Cornish et al. (2002) offered the explanation for diversity of findings about action of leptin on bone tissue indicating on the differences between its central and peripheral effects. Obviously, the effect of leptin on bones is determined by kind of experimental model, doze and route of application. It should be mentioned, that in our experimental model, there was a relatively short period for development of obesity, because the full effect of MSG-treatment should be expected later.

There is much controversy about the effect of MSG on testis. Olney (1969) found no difference in testis hystology between mice neonatally treated with MSG and mice of control group. His findings were supported by reports of some other authors (Adamo and Ratner 1970; Nikoletseas 1977). Waxman et al. (1990) emphasized that rats neonatally treated with MSG were fertile with normal secretion of gonadotropines and sex steroids. Redding et al. (1971) reported significantly reduced gonadal weights in MSG-treated rats at 40 and 110 days of age and a marked decrease in GH and

luteinizing hormone content in the anterior pituitaries of male MSG-treated rats at 40 days. Reproductive dysfunction was seen by Pizzi et al. (1977) in male mice. Males treated with MSG showed reduced fertility and decreased testis weights. Miskowiak et al. (1993) registered desquamation of spermatosoal cells in seminal tubules of four months old rats neonatally treated with MSG. Testicular atrophy in Wistar rats neonatally treated with MSG was reported by Bojanić (1998). França et al. (2006) revealed a significant ($p < 0.05$) reduction in testis weight and the number of Sertoli (SC) and Leydig cells (LC) per testis in prepubertal MSG rats. They concluded that testis development as well as SC and LC proliferation was disturbed. In adult MSG-treated rats no apparent alterations were observed in testis structure. But, the number of SCs per testis was significantly ($p < 0.05$) reduced in the adult males. Decreased gland mass is indirect indicator of decreased function of the gland. So, neonatal "castration" with MSG, *via* the hypothalamus and the hypophysis, significantly modifies the somatic status. Any way MSG-induced somatometric alterations could be addressed to neonatal reprogramming of developmental and maturation processes due to changed hypothalamo-pituitary-gonadal secretory functions.

Acknowledgement. This work was supported by Ministry of Science of Serbia (grant No. 145072).

References

Adamo N. J., Ratner A. (1970): Monosodium glutamate: lack of effects on brain and reproductive function in rats. Science **169**, 673–674

Bojanić V. (1998): Study of pathogenesis of obesity induced with monosodium glutamate. (PhD thesis), University of Niš, Serbia

Camihort G., Gómez D. C., Luna G., Ferese C., Jurado S., Moreno G., Spinedi E., Cónsole G. (2005): Relationship between pituitary and adipose tissue after hypothalamic denervation in the female rat. A morphometric immunohistochemical study. Cells Tissues Organs **179**, 192–201

Chaldakov G. N., Fiore M., Stankulov I. S., Manni L., Hristova M. G., Antonelli A., Ghenev P. I., Aloe L. (2004): Neurotrophin presence in human coronary atherosclerosis and metabolic syndrome: a role for NGF and BDNF in cardiovascular disease? Prog. Brain Res. **146**, 279–289

Chandran M., Phillips S. A., Ciaraldi T., Henry R. R. (2003): Adiponectin: More than just another fat cell hormone? Diabetes Care **26**, 2442–2450

Cock T. A., Auwerx J. (2003): Leptin: cutting the fat off the bone. Lancet **362**, 1572–1574

Cornish J., Callon K. E., Bava U., Lin C., Naot D., Hill B. L., Grey A. B., Broom N., Myers D. E., Nicholson G. C., Reid I. R. (2002): Leptin directly regulates bone cell function *in vitro* and reduces bone fragility *in vivo*. J. Endocrinol. **175**, 405–415

Cornish J., Callon K. E., Mountjoy K. G., Bava U., Lin J. M., Myers D. E., Naot D., Reid I. R. (2003): Alpha-melanocyte-stimulating hormone is a novel regulator of bone. Am. J. Physiol., Endocrinol. Metab. **284**, E1181–1190

Ducy P., Amling M., Takeda S. (2000): Leptin inhibits bone formation through a hypothalamic relay: a central control of bone mass. Cell **100**, 197–207

Epsinosa L., Itzstein C., Cheynel H., Delmas P., Chenu C. (1999): Active NMDA glutamate receptors are expressed by mammalian osteoclasts. J. Physiol. **518**, 47–53

França L. R., Suescun M. O., Miranda J. R., Giovambattista A., Perello M., Spinedi E., Calandra R. S. (2006): Testis structure and function in a nongenetic hyperadipose rat model at prepubertal and adult ages. Endocrinology **147**, 1556–1563

Guidobono F., Pagani F., Sibilia V., Netti C., Lattuada N., Rapetti D., Mrak E., Villa I., Cavani F., Bertoni L., Palumbo C., Ferretti M., Marotti G., Rubinacci A. (2006): Different skeletal regional response to continuous brain infusion of leptin in the rat. Peptides **27**, 1426–1433

Gu Y., Genever P. G., Skerry T. M., Publicover S. J. (2002): The NMDA type glutamate receptors expressed in primary rat osteoblasts have the same electrophysiological characteristics as neuronal receptors. Calcif. Tissue Int. **70**, 194–203

Hamerman D. (2002): Molecular-based therapeutic approaches in treatment of anorexia of aging and cancer cachexia. J. Gerontol. Med. Sci. **57**, M511–518

Klingberg H., Brankački J., Klingberg F. (1987): Long-term effects on behaviour after postnatal treatment with monosodium-L-glutamate. Biomed. Biochem. Acta **46**, 705–711

Kovács M., Halmos G., Groot K., Izdebski J., Schally A. V. (1996): Chronic administration of a new potent agonist of growth hormone-releasing hormone induces compensatory linear growth in growth hormone-deficient rats: mechanism of action. Neuroendocrinology **64**, 169–176

Laketic-Ljubojevic I., Suva L. J, Maathuis F. J, Sanders D., Skerry T. M. (1999): Functional characterization of N-methyl-D-aspartic acid-gated channels in bone cells. Bone **25**, 631–637

Millard W. J., Martin J. B. Jr., Audet J., Sagar S. M., Martin J. B. (1982): Evidence that reduced growth hormone secretion observed in monosodium glutamate-treated rats is the result of a deficiency in growth hormone-releasing factor. Endocrinology **110**, 540–550

Miskowiak B., Limanowski A., Partyka M. (1993): Effect of perinatal administration of monosodium glutamate (MSG) on the reproductive system of the male rat. Endokrynol. Pol. **44**, 497–505

Morroni M., De Matteis R., Palumbo C., Ferretti M., Villa I., Rubinacci A., Cinti S., Marotti G. (2004): *In vivo* leptin expression in cartilage and bone cells of growing rats and adult humans. J. Anat. **205**, 291–296

Nemeroff C. B., Konkol R. J., Bissette G., Youngblood W., Martin J. B., Brazeau P., Rone M. S., Prange A. J. Jr., Breese G. R., Kizer J. S. (1977): Analysis of the disruption in

hypothalamic-pituitary regulation in rats treated neonatally with monosodium glutamate (MSG): Evidence for the involvement of tuberoinfundibular cholinergic and dopaminergic systems in neuroendocrine regulation. Endocrinology **101**, 613–622

Nikoletseas M. M. (1977): Obesity in exercising, hypophagic rats treated with monosodium glutamate. Physiol. Behav. **19**, 767–773

Olney J. W. (1969): Brain lesions, obesity and other disturbances in mice treated with monosodium glutamate. Science **164**, 719–721

Peet N. M., Grabowski P. S., Laketic-Ljubojevic I., Skerry T. M. (1999): The glutamate receptor antagonist MK801 modulates bone resorption by a mechanism predominantly involving osteoclast differentiation. FASEB J. **13**, 2179–2185

Pizzi W. J., Barnhart J. E., Fanslow D. J. (1977): Monosodium glutamate administration to the newborn reduces reproductive ability in female and male mice. Science **196**, 452–454

Redding T. W., Schally A. V., Arimura A., Wakabayashi I. (1971): Effect of monosodium glutamate on some endocrine functions. Neuroendocrinology **8**, 245–255

Ren J. (2004): Leptin and hyperleptinemia – from friend to foe for cardiovascular function. J. Endocrinol. **181**, 1–10

Rol de Lama M. A., Perez-Romero A., Ariznavarreta M. C., Hermanussen M., Tresguerres J. A. (1998a): Periodic growth in rats. Ann. Hum. Biol. **25**, 441–541

Rol de Lama M. A., Pérez-Romero A., Hermanussen M., Ariznavarreta C., Tresguerres J. A. (1998b): Sexual dimorphism in growth as measured by microknemometry: different responses to GH deficiency and exogenous GH administration. Neuroendocrinology **68**, 210–219

Shapiro B. H., MacLeod J. N., Pampori N. A., Morrissey J. J. (1989): Signaling elements in the ultradian rhythm of circulating growth hormone regulating expression of sex-dependent forms of hepatic cytochrome P450. Endocrinology **125**, 2935–2944

Skerry T. M., Genever P. G. (2001): Glutamate signalling in non-neuronal tissues. Trends Pharmacol. Sci. **22**, 174–181

Stevenson A. E., Evans B. A., Gevers E. F., Elford C., McLeod R. W., Perry M. J., El-Kasti M. M., Coschigano K. T., Kopchick J. J., Evans S. L., Wells T. (2009): Does adiposity status influence femoral cortical strength in rodent models of growth hormone deficiency? Am. J. Physiol., Endocrinol. Metab. **296**, E147–156

Terry L. S., Epelbaum J., Martin J. B. (1981): Monosodium glutamate: acute and chronic effects on rhytmic growth hormone and prolactin secretion and somatostatin in the undisturbed male rat. Brain Res. **217**, 129–142

Tamasi J. A., Arey B. J., Bertolini D. R., Feyen J. H. (2003): Characterization of bone structure in leptin receptor-deficient Zucker (fa/fa) rats. J. Bone Miner. Res. **18**, 1605–1611

Waxman D. J., Morrissey J. J., MacLeod J. N., Shapiro B. H. (1990): Depletion of serum growth hormone in adult female rats by neonatal monosodium glutamate treatment without loss of female-specific hepatic enzymes P450 2d (IIC12) and steroid 5 alpha-reductase. Endocrinology **126**, 712–720

Precancerous morphologic and functional aberrations in the rat mammary glands carcinogenesis

Ivana Joksimović[1], Vladmila Bojanić[2], Slaviša Janćić[3], Zoran Bojanić[2], Jelena Živanov-Čurlis[2], Sanja Perić[1] and Snežana Janćić[4]

[1] *Health Center of Niš, Serbia*
[2] *Institute for Pathophysiology, Pharmacology and Biology, Faculty of Medicine Niš, Serbia*
[3] *Department of Oncology, Clinical Center, Niš, Serbia*
[4] *Institute for Pathology, Faculty of Medicine, Kragujevac, Serbia*

Abstract. The precancerous changes of mammary glands in 7,12-dimethylbenz(α)anthracene (DMBA) induced carcinogenesis in Wistar rats were examined. Carcinogen was inserted into the left fifth mammary gland of the anesthetised rats. After 35 days all the animals were sacrificed and mammary glands were extirpated. Macroscopic examination of mammary glands was performed and the tissue was processed for a pathohistological analysis. H&E, VanGieson's and Toluidine-blue methods were applied, as well as ABC immunohistochemical method with anti-cytokeratin antibodies.The identified precancerous changes resembled to aberrations of fibrocystic disease in women. The fibrosclerosis, lobular hyperplasia, cystic ductal dilatation and apocrine metaplasia of ductal epithelium were found. Micropapillomatoid hyperplasia was another frequent finding, but the presence of the real papilloma was not registered. The keratocysts with the squamous epithelial metaplasia were present in three of the animals. Dysplastic changes were found in the skin, above the treated glands. The difference in expression of cytokeratins, between normal and preneoplastic epithelium, makes cytokeratin useful for verification of early precancerous lesions. The epithelial ductus and ductulus cells of the mammary glands of animals belonging to the control group showed neither CK 19 nor CK 14 expression.

Key words: Rat — Mammary gland — Carcinogenesis — Precancerous lesions — Cytokeratins

Introduction

Mammary gland is one of the most complex "target" organs. The growth, secretion, differentiation, lactogenesis and galactogenesis are under the constant influence of "interplay" of ovarian and adrenal steroids, as well as of pituitary and thyroid hormones (Macejova et al. 2005; Nilsson and Dabrosin 2006; Rajkumar et al. 2006; Applanat et al. 2008). Various morphologic units out of which a breast is made, are the base for a numerous and heterogeneous group of diseases. These diseases have high incidence and are the precursors of cancer frequently, in both the reproductive and postmenopausal period (Jmor et al. 2002; Applanat et al. 2008; Bertelsen et al. 2008).

Correspondence to: Snežana Jančić, Institute of Pathology, Medical Faculty, 34000 Kragujevac, Serbia
E-mail: sjancic@medf.kg.ac.yu

According to epidemiological data the breast carcinoma represents the most frequent malignant neoplasm. One of eight women bears the risk to develop this kind of tumour (Abeloff et al. 2004). The various experimental models for the examination of breast tumorogenesis (Thompson and Singh 2000) are made, with the main aim to improve the disease prevention.

Having in mind that the five year survival is up to 97% if the cancer is diagnosed at an early stage (Rosen 2001), the key goal of our work is to identify precancerous lesions and to perform an immunohistochemical examination of cytoskeletal polypeptides in them.

For the purposes of our research we used the well known and successful model of mammary gland cancer induction with 7,12-dimethylbenz(α)anthracene (DMBA) (Huggins et al. 1961; Russo and Russo 1987, 2000; Russo et al. 1990; Padmavathi et al. 2006).

Materials and Methods

Animals

The study was carried out on 27 female, virgin albino Wistar rats (weighting 120 ± 10 g), 35–37 day of age. The animals were raised in controlled laboratory conditions (in an animal room with a 12 h light/12 h dark cycle, at 22 ± 2°C). The animals had free access to the laboratory chow and tap water *ad libitum*. All procedures on animals followed Guideline for work on experimental animals approved by Ethic Committee of Faculty of Medicine in Kragujevac.

Experimental protocol

The rats were divided in two groups: the control group and the experimental group. Nine animals of control group did not undergo the treatment.

In the experimental group were 18 animals. The mixture DMBA carcinogen (Wako Pure Chemical Industries, Ltd., Osaka, Japan) and cholesterol-buffer (serving as a vehicle) was implanted by incision in the fifth left mammary gland of the anesthetised rats. The amount of the implanted mixture for each rat was 2 mg (1 mg of DMBA and 1 mg of cholesterol-buffer). After the implantation, the incision was closed with the surgery stitch.

After 35 days all the animals were sacrificed and their left fifth mammary glands were extirpated. Macroscopic examinations and a diameter measurement of extirpated mammary glands were performed. The mammary glands were fixed in a Bouin solution for 24 h.

Micromorphologic examination

The complete material underwent routine preparations and was embedded in paraffin. The 4 μm cuttings then went through the classic H&E methods for lesion verification, histochemical VanGieson's and Gommori methods for the presentation of collagen and reticuline fibres, Toluidine-blue method for mastocyte detection and ABC immunohistochemical technique with specific antibody to Cytokeratin 14 (CK 14) (Cymbus, 1 : 200) and Cytokeratin 19 (CK 19) (ABCAM, 1 : 400).

Results

Macroscopic analysis

The animals of control group had mammary glands of the equal dimensions, 0.3–0.5 cm in diameter. Mammary glands were white-yellow colour, with a glassy look of sections and solid consistence.

The mammary glands of animals from experimental group were enlarged, 0.7–1 cm in diameter, clearly separated from the surrounding tissue and very solid consistency. They were covered with macroscopically intact skin.

Micromorphologic analysis

The microscopic examination of the mammary glands of the animals from the control group showed no pathologic changes.

The micromorphologic examination of the mammary glands from the experimental group verified a spectra of hyperplastic-dysplastic changes on the level of ductulus, ductus and acinus, frequently giving the picture of adenomatosis. A malignant process was not found.

Severe hyperplasia of smaller ductuses and ductules was followed by nuclear hyperchromasia. Hyperplastic acini are present as epitheliosis very often. In some animals, lobulus and ductulus hyperplasia is more expressed and gives the picture of microadenoma.

Larger ductuses are dilated, lengthened and curved with frequently present micropapillomatosis. Along with the papillomatosis, a cystic ductus dilatation with flattened epithelium was found. In nine animals was found cystic ductus hyperplasia with apocrine metaplasia, as well as dysplastic epitheliosis and micropapillomatosis (Fig. 1). These animals had an impressive "grape-like" hyperplasia of the myoepithelial cells in larger dilated ductuses.

Keratocysts were found in three animals. They were characterized by cystic ducts with non-structural content, small keratin bodies in lumen and the squamous epithelial metaplasia (Fig. 2).

Fibroplasia was present not only in stroma around ductuses, but also interlobulary and intralobulary (Fig. 3).

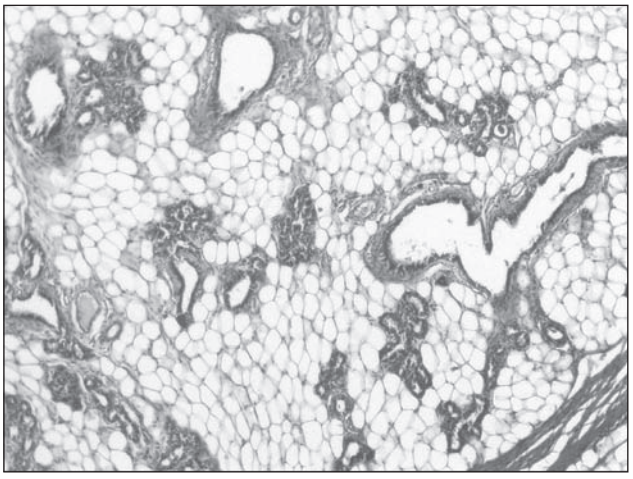

Figure 1. Dysplastic epitheliosis and micropapillomatosis (HEX150).

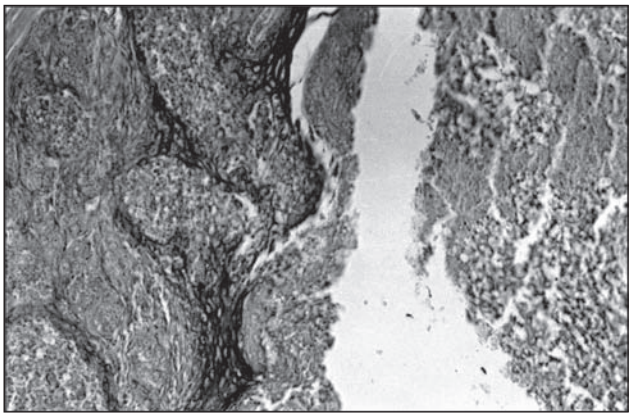

Figure 2. Cystic ductus with squamous methaplastic epithelium and necrotic content in the lumen (ABCX250).

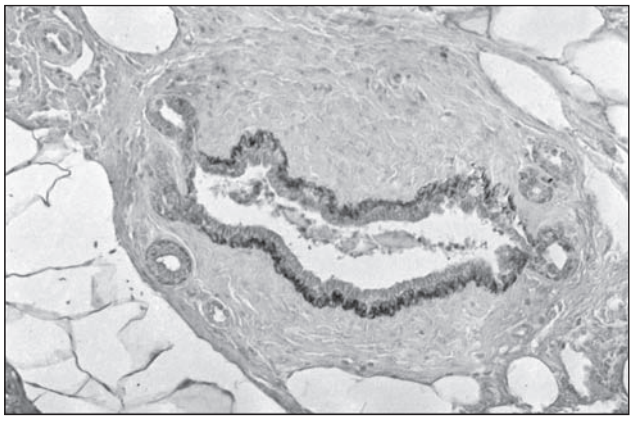

Figure 3. Strong immunoreactivity to cytokeratins of myoepithelial cells in cystic ductus (ABCX250).

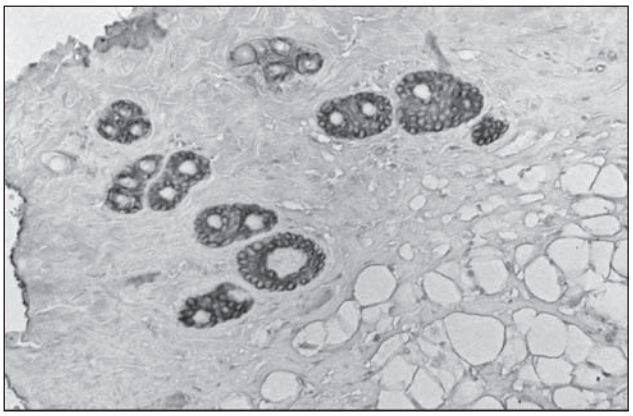

Figure 4. Strong immunoreactivity of displastic cells of ductal and ductular epithelium to cytokeratins (ABCX200).

Rich lymphoplasmocytic infiltrate had no germinative centres. Hyperplastic ductules and acini were surrounded with numerous hypergranulated polymorph mastocytes in lipomatous stroma.

Dysplastic changes accompanied by dyskeratosis, hyperkeratosis, parakeratosis and the hyperplasia of granular layer were found in stratified squamoid skin epithelium.

Immunohistochemical analysis

In the mammary glands of animals of the control group, more than 95% of myoepithelial cells of acinus showed a strong CK 14 expression (++). In epithelial ductus cells neither CK 14 nor CK 19 (–) expression was verified.

In the animals of the experimental group, in hyperplastic acini and ductules are found rare cells with heterogeneous CK 19 expression (+ to ++). In numerous dysplastic cells of ductus and ductulus a strong CK 19 (+++) expression was also present (Fig. 4). In cystic ductuses, more than 95% of myoepithelial cells showed homogenous and clearly expressed immunoreactivity to CK 14 antibodies (++ to +++) (Fig. 3). In the foci of intraductal papillomatosis the cells had predominant perinuclear content of CK 19 (+ to ++). In the foci of squamous metaplasia was present moderately strong immunoreactivity to CK 19 (++) (Fig. 2).

Discussion

In 1961, Huggins and his associates described rat mammary gland carcinoma induced by DMBA and N-methyl-N-nitrosourea chemical carcinogens. Having in mind that this method of chemical carcinogenesis of mammary glands has proven to be very efficient and, with small modifications, used by many researchers for years (Russo and Russo 1987; Korkola and Archer 1999; Leung et al. 2003), we decided to employ it for our experiment.

The examinations related to the animal age showed that the receptiveness of rat mammary gland for carcinogen is the highest in the young rats. In the older animals spontaneous mammary gland tumours are found more frequently.

Autohistoradiographic examination revealed that the terminal duct buds have the most intensive proliferation activity and that they bind the biggest amount of DMBA for the nuclear DNA. The differentiation of the terminal duct buds in 35–46 day of age rats was the most active. With the usage of DMBA, the frequency of cancer is the highest if it is implanted in this period of the animal's life (Russo and Russo 1978; Chandra et al. 1992; Haseman et al. 1998). The mentioned statements lead us towards using 35–37 day of age rats in our experiment.

Sprague-Dawley rats are the most often used for similar experiments, F344 Wistar rats and mice are used seldom, and in very rare cases rabbits and dogs (Russo and Russo 2000; Thompson and Singh 2000). In our experiment, DMBA and its vehicle are directly inserted into the fifth mammary gland of the animals. Although it is emphasized that Sprague-Dawley rats have an extraordinary receptiveness for DMBA carcinogen, we used Wistar rats and in all animals on 35th day we verified proliferative precancerous lesions.

Hyperplastic, dysplastic, cystic and metaplastic-squamous ductuses and acini changes present in animals treated with DMBA are known as "fibrocystic breast disease" in human pathology. The earliest descriptions of the fibrocystic disease included fibrosis, cyst genesis and epithelial proliferation (Bertelsen et al. 2008).

Today, the fibrocystic disease is considered as one of the precancerous breast diseases (Abeloff et al. 2004). In the literature is used a set of terminology issues connected to this disease. In England, in the past, the term ANDI (Aberration of normal development and involution) was used for fibrocystic disease (Hughes and Bundred 1989). The acceptance of such a term is based on the fact that the largest number of benign breast conditions represents the relatively small aberrations of the normal development process, cyclic hormone response and involution, which overlap throughout the whole life. The term "aberration" is used because it describes a spectra of changes which range from the smallest to the biggest ones.

The most frequent aberrations in fibrocystic disease are cysts, which can be microcysts and macrocysts. They are the consequence of the normal lobular involution joined by the active secretion of apocrine epithelium which is under hormonal stimulation. There is the opinion that multiple and recurrent cysts joined by a small cysts, have significantly increased risk for the breast carcinoma development (Tran and Lawson 2002).

Other aberrations adenosis, lobular hyperplasia, fibrosclerosis and sclerotic adenosis belong to the group of higher risk for breast carcinoma development. This is the case with sclerotic adenosis, which is sometimes hardly differentiated from carcinoma (Page et al. 2000; Salarieh and Sneige 2007). Abeloff et al. (2004) reported that the proliferation changes, first of all ductal and lobular hyperplasia, have a relative risk graded from 1.5 to 2. Atypical hyperplasia is connected with a much greater relative risk graded from 3 to 5. In women with the hereditary anamnesis of breast cancer atypical proliferation changes have a relative risk graded 11. These data suggest a recognizable process of a malignant transformation, starting from normal, turning into hyperplastic and then atypical epithelium, which is followed by a progression into ductal carcinoma *in situ* and ending in invasive breast carcinoma.

The precancerous changes found in our experimental animals are very similar to aberrations of fibrocystic disease found in women. Fibrosclerosis, lobular hyperplasia, cystic ductus dilatation, apocrine metaplasia of ductal epithelium are found almost in all animals. The micropapillomatosal hyperplasia of ductal epithelium was present but there were no real papilloma. None of the animals in our experiment developed sclerotic adenosis, which is also very rare in women (Rosen 2001).

In our material, keratocysts are verified with security after a positive immunohistochemical staining to keratin. In the identification of the comedo type of adenocarcinoma, noted in the literature (Russo and Russo 2000), one should be very careful having, in mind that keratocysts in lumen can contain necrotic detritus. The epithelium may be flattened at the same time, so that it could be very difficult with use of the classic H&E staining to identify it as a squamoid-cellular epithelial type. We have no data that this aberration is described in human breasts.

In the animal skin, above the region of the mammary gland into which the carcinogen has been inserted, dysplastic changes were noticed. In women with precancerous lesions this changes are not reported.

Recently, many researchers have dedicated their studies to investigation of functional activity of cytoskeletal polypeptides in various phases of neoplastic cell transformation. It is now well known that the cytokeratin expression is characteristic of a specific epithelium cell type, which can be used for the purpose of the identification of phenotype cell properties. Knowledge about clear difference between keratin expression of myoepithelial or base cells and glandular or luminal cells in breast, induced the formation of the new functional classification of breast carcinoma (Gusterson et al. 2005; Fulford et al. 2006; Laakso et al. 2006).

Examining the cytokeratin expression in our experiment, we found that the base cells did not show the CK 19 expression, while the luminal cells in all the preneoplastic lesions reacted to CK 19 with a specific antibody. The CK 19 expression in hyperplastic acinus and ductulus cells was heterogeneous both in terms of distribution and of reaction intensity. Heterogeneous reaction with CK 8, 18 and 19 antibodies was also described in case of the fibrocystic disease of human breasts. The same authors noted that the luminal epithelium of fibroadenoma was not reactive for CK 19 antibody and suggested that its value as a diagnostic discriminator is limited (Heatley et al. 1995).

The epithelial cells of ductus and ductulus of the mammary glands of animals of the control group did not show either CK 19 or CK 14 expression. In the literature, a subunit of luminal epithelial cells which do not react with CK 19 antibodies was identified. It is believed that negative luminal CK 19 cells of normal breast tissue have a good proliferation potential *in vitro*. This cell type was found in benign

proliferative diseases *in vivo* in a much larger number than in the normal breast tissue (Boecker and Büerger 2003). These discoveries contribute to the realization of the existence of various cellular compartments within a normal breast, which includes the progenitor compartment. In other words, it is assumed that the CK 19 negative cells can create a proliferation compartment with the possibility to contain stem cells. This supports the "early carcinogenesis" concept (Büerger et al. 2006).

We verified a homogenous CK 14 expression in myoepithelial cells of the mammary glands of all animals (both control and experimental). This mode of expression of cytokeratin is noticed in human breasts. With the help of different molecules (which along with the cytokeratin filament protein contain actin, myosin, S100 and p63) was differentiated "basal-like" breast carcinoma or tumours with myoepithelial phenotype (Clarke et al. 2005). At the same time, it is stated that the "basal-like" phenotype of breast carcinoma is joined with poor prognosis (Potemski et al. 2005).

In conclusion, we can emphasize that the preneoplastic aberrations in the rat mammary glands resembled the known changes in fibrocystic disease in women. However, the keratocysts and dysplastic changes in the squamous epithelium of skin above the preneoplastic lesions have not been described in human breast pathology. The difference between the secretory activity of normal and preneoplastic epithelium makes that cytokeratin is useful for identification of early precancerous lesions because the epithelial ductus and ductulus cells of the mammary glands in animals belonging to the control group showed neither CK 19 nor CK 14 expression.

Acknowledgement. This work was supported by Ministry of Science Republic of Serbia (project NO. 145072).

References

Abeloff M. D., Wolff A. C., Wood W. C., Weber B. L. (2004): Cancer of the breast. In: Clinical Oncology (Eds. M. D. Abeloff, J. O. Armitage, J. E. Niederhuber and M. B. Kastan), pp. 2369–2397, Churchill Livingstone, Philadelphia

Applanat M. P., Buteau-Lozano H., Herve M. A., Corpet A. (2008): Vascular endothelial growth factor is a target gene for estrogen receptor and contributes to breast cancer progression. Adv. Exp. Med. Biol. **617**, 437–444

Bertelsen L., Mellemkjaer L., Balslev E., Olsen J. H. (2008): Benign breast disease among first-degree relatives of young breast cancer. Am. J. Epidemiol. **168,** 261–267

Boecker W., Büerger H. (2003): Evidence of progenitor cells of glandular and myoepithelial cell lineages in the human adult female breast epithelium: a new progenitor (adult stem) cell concept. Cell Prolif. **36**, 73–84

Büerger H., Kersting C., Hungermann D., Decker T., Böcker W. (2006): The significance of "normal tissue" in the development of breast cancer: new concepts of early carcinogenesis. Pathologe **27,** 319–325 (in German)

Chandra M., Riley M. G., Johnson D. E. (1992): Spontaneous neoplasms in aged Sprague-Dawley rats. Arch. Toxicol. **66**, 496–502

Clarke C., Sandle J., Lakhani S. R. (2005): Myoepithelial cells: pathology, cell separation and markers of myoepithelial differentiation. J. Mammary Gland Biol. Neoplasia **10,** 273–280

Fulford L. G., Easton D. F., Reis-Filho J. S., Sofronis A., Gillett C. E., Lakhani S. R., Hanby A. (2006): Specific morpholohical features predictive for the basal phenotype in grade 3 invasive ductal carcinoma of breast. Histopathology **49**, 22–34

Gusterson B. A., Ross D. T., Heath V. J., Stein T. (2005): Basal cytokeratins and their relationship to the cellular origin and functional classification of breast cancer. Breast Cancer Res. **7**, 143–148

Haseman J. K., Hailey J. R., Morris R. W. (1998): Spontaneous neoplasm incidences in Fischer 344 rats and B6C3F1 mice in two-year carcinogenicity studies: a National Toxicology Program update. Toxicol. Pathol. **26**, 428–441

Heatley M., Maxwell P., Whiteside C., Toner P. (1995): Cytokeratin intermediate filament expression in benign and malignant breast disease. J. Clin. Pathol. **48**, 26–32

Huggins C., Grand L. C., Brillantes F. P. (1961): Mammary cancer induced by a single feeding of polymucular hydrocarbons, and its suppression. Nature **189**, 204–207

Hughes L. E., Bundred N. J. (1989): Breast macrocysts. World J. Surg. **13**, 711–714

Jmor S., Al-Sayer H., Heys S., Payne S., Miller I., Ah-See A. Hutcheon A., Evemin O. (2002): Breast cancer in women aged 35 and under: prognosis and survival. J. R. Coll. Surg. Edinb. **47**, 693–699

Korkola J. E., Archer M. C. (1999): Resistance to mammary tumorigenesis in Copenhagen rats is associated with the loss preneoplasic lesions. Carcinogenesis **20**, 221–227

Laakso M., Tanner M., Nilsson J., Wiklund T., Erikstein B., Malmstrom P., Kellokumpu P., Wilking N., Bergh J., Isola J. (2006): Basoluminal carcinoma: a new biologically and prognostically distinct entity between basal and luminal breast cancer. Clin. Cancer Res. **12**, 4185–4191

Leung G., Tsao S. W., Wong Y. C. (2003): Sex hormone-induced mammary carcinogenesis in female Noble rats: detection of differentially expressed genes. Breast Cancer Res. Treat. **77**, 49–63

Macejova D., Radikova Z., Macho L., Liska J., Brtko J. (2005): MNU-induced carcinogenesis of rat mammary gland: effect of thyroid hormone on expression of retinoic acid receptors in tumours of mammary gland. Mol. Cell. Endocrinol**. 244**, 47–56

Nilsson U. W., Dabrosin C. (2006): Estradiol and tamoxifen regulate endostatin generation via matrix metalloproteinase activity in breast cancer. Cancer Res. **66**, 4789–4794

Padmavathi R., Senthilnathan P., Chodon D., Sakthisekaran D. (2006): Therapeutic effect of paclitaxel and propolis on lipid peroxidation and antioxidant system in 7,12 dimethyl benz(a)anthracene-induced breast cancer in female Sprague Dawley rats. Life Sci.**78**, 2820–2825

Page D. L., Jensen R. A., Simpson J. F., Dupont W. E. (2000): Historical and epidemiologic background of human premalignant breast disease. J. Mammary Gland Biol. Neoplasia **5**, 341–349

Potemski P., Kusinska R., Watala C., Pluciennik E., Bednarek A. K., Kordek R. (2005): Prognostic relevance of basal cytokeratin expression in operabile breast cancer. Oncology **69**, 478–485

Rajkumar L., Balasubramanian K., Arunakaran J., Govindarajulu P., Srinivasan N. (2006): Influence of estradiol on mammary tumor collagen solubility in DMBA-induced rat mammary tumors. Cell Biol. Int. **30**, 164–169

Rosen P. P. (2001): Rosen's breast pathology. Lippincott Williams and Wilkins, Philadelphia

Russo I. H., Russo J. (1978): Developmental stage of the rat mammary gland as determinant of its susceptibility to 7,12-dimethylbenz(a)anthracene. J. Natl. Cancer Inst. **59**, 435–444

Russo J., Russo I. H. (1987): Biological and molecular bases of mammary carcinogenesis. Lab. Invest. **57**, 112–137

Russo J., Gusterson B. A., Rogers A. E., Russo I. H., Wellings S. R., van Zwieten M. J. (1990): Comparative study of human and rat mammary tumorigenesis. Lab. Invest. **62,** 244–273

Russo J., Russo I. H. (2000): Atlas and histologic classification of tumours of the rat mammary gland. J. Mammary Gland Biol. Neoplasia **5**, 187–198

Salarieh A., Sneige N. (2007): Breast carcinoma arising in microglandular adenosis. Arch. Pathol. Lab. Med. **131**, 1397–1399

Thompson H. J., Singh M. (2000): Rat models of premalignat breast disease. J. Mammary Gland Biol. Neoplasia **5**, 409–420

Tran D. D., Lawson J. S. (2002): Microcysts and breast cancer: a study of biological markers in archival biopsy material. Breast Cancer Res. Treat. **75**, 213–220

The irritative property of α-tricalcium phosphate to the rabbit skin

Zvezdana Kojic[1], Dobrica Stojanovic[2], Svetlana Popadic[3], Milan Jokanovic[4] and Djordje Janackovic[2]

[1] *Institute of Medical Physiology, School of Medicine, University of Belgrade, Serbia*
[2] *Faculty of Technology and Metallurgy, University of Belgrade, Serbia*
[3] *Department of Dermatology, School of Medicine, University of Belgrade, Serbia*
[4] *Department of Toxicology, Faculty of Pharmacy, University of Niš, Serbia*

Abstract. The aim of this study was to assess the irritant properties of a new developed calcium phosphate ceramic, α-tricalcium phosphate (α-TCP) after single application to intact skin of the rabbit. The test substance, α-TCP was produced by modified hydrothermal method and prepared in two different forms, as a solid material (disc 5 × 2 mm) and paste. Both, solid material and paste of α-TCP were evaluated for primary skin irritation to the ISO 10993-10:2002/Amd 1:2006 Biological Evaluation of Medical Devices – Part 10. At the end of the study macroscopic examination of the skin was performed. In this model, general and local tolerances were good. Score of primary irritation (SPI) and primary irritation index (PII) of α-TCP for both, solid material and paste, revealed that there was no significant toxicity/irritability (PII = 0.0) as compared to the negative control (PII = 0.0). Positive control did cause significant skin irritation in acute irritation test using Draize technique in rabbit model (PII = 2.11). Based on present results, it can be concluded that the the irritation potential of the tested material is negligible. However, other procedures for preclinical safety assessments of the α-TCP material are needed in order to completely elucidate its toxic potential.

Key words: Biocompatibility — Calcium phosphate ceramics — Skin irritation test

Introduction

A biomaterial is any material, natural or man-made, that comprises whole or part of a living structure, or biomedical device which performs, augments, or replaces a natural function (Williams 1986). Biomaterials are used in heart valves, blood vessel prostheses, joint replacements, bone plates, bone cement, artificial ligaments and tendons, dental implants for tooth fixation, skin repair devices, cochlear replacements, contact lenses etc. The clinical application of a biomaterial should not cause any adverse reaction in the organism and should not endanger the life of the patient (Bollen 2005). Any material to be used as part of a biomaterial device has to be biocompatible (Barile 2008).

The definition of biocompatibility includes that the material has to be nontoxic, nonallergenic, noncarcinogenic and nonmutagenic, and that it does not influence the fertility of a given patient (Williams 1986). Preclinical safety assessments of the toxic potential of the materials are needed in order to minimize the potential hazard to the patients. At present, safety assessments of medical devices are guided by the studies recommended in the International Organization for Standardization (ISO) 10993 standard. Since physiological responses of the body to foreign material are complex, it would seem odd that one can make one test to determine the biocompatibility of any given material. At present, tests that may be used in an evaluation of medical device biocompatibility include procedures for cytotoxicity, skin sensitization, dermal irritation and intracutaneous reactivity, acute systemic toxicity, subchronic toxicity, mutagenicity, implantation, hemocompatibility, chronic toxicity, and carcinogenicity (ISO 10993; Bollen 2000).

Having a chemical composition very close to the mineral phase of natural bone, calcium phosphate compounds have long been the subject of intensive investigation as bone substitutes. Several materials consisting of hydroxyapatite

Correspondence to: Zvezdana Kojic, Institute of Medical Physiology, School of Medicine, Višegradska 26/II, 11000 Belgrade, Serbia
E-mail: zvezdanak@med.bg.ac.rs

(HAP), α-tricalcium phosphate (α-TCP), or β-TCP have been clinically applied in orthopedic, reconstructive and maxillofacial surgery (Bohner 2000). α-TCP is known to be biocompatible, osteoconductive, osteoinductive and highly soluble at physiological pH (resorbable ceramic) and is expected to yield a porous structure capable of osseointegration i.e. promoting bone ingrowth (Durucan and Brown 2000). A number of animal studies indicated that application of α-TCP to bone defects was effective in promoting new bone formation (Kurashina et al. 1997; Wiltfang et al. 2002). However, some problems with these ceramics have been reported (Lu 2004; Fellah 2007). A major problem is that devices implanted within living tissue must interact with the physiological functions of the host with no development of the foreign body reaction around implant material (Williams 1986; Barile 2008). However, with many orthopedic devices, failure commonly occurs within 5–10 years of implantation. Better understanding of the interaction between ceramics and the adverse environment of the human body is important in improving and devising effective ceramic implants used in various treatment applications (Bollen and Harling 2002; Barile 2008).

Recently, in our laboratory it has been developed calcium phosphate cement – α-TCP (Janackovic et al. 2001, 2003). The cement obtained by our, modified hydrothermal method, beside α-TCP, contains a small quantity of calcium-HAP as residual phase, which could act as a centre for nucleation of newly formed HAP (Jokic et al. 2007). As a consequence, faster transformation into the HAP phase is observed during the setting of cement paste in simulated body fluid. Further, the HAP obtained by the hydrolysis of this cement has a more compact and denser microstructure with the finer nanostructure and crystal size of newly formed calcium deficient hydroxyapatite (CDHAP) below 100 nm, and compressive strength up to 80 MPa after 3 days of immersion in simulated body fluid (Jokic et al. 2006). A precise and detailed physical and chemical characterization of developed α-TCP has already been done (Janackovic et al. 2001, 2003; Jokic et al. 2006, 2007), but its biological evaluation was not examined.

The purpose of the present investigation was to determine the irritant properties of this newly developed α-TCP material after single application to intact skin of the rabbit.

Materials and Methods

Synthesis of α-TCP

α-TCP cement was obtained by heating of CDHAP particles synthesized by the modification of our method described earlier (Janackovic et al. 2001, 2003; Jokic et al. 2006, 2007). The various amounts of $Ca(NO_3)_2$, $Na_2H_2EDTA{\cdot}2H_2O$, NaH_2PO_4 and urea (reagents were Merck p.a. grade) were dissolved in 2000 ml of distilled water (Table 1).

The solution was heated at 160°C during 3 h in a sealed tube. The precipitated CDHAP particles were further washed with distilled water and dried at 105°C for 2 h. Afterward the particles are heated at 1500°C during 120 min, with the heating rate of 10°C/min. The heated samples were milled planetary mill during 30 min. Obtained cement powder was further mixed with phosphate solution (2.5 wt.% solution of Na_2HPO_4) at a liquid to powder ratio of 0.32 ml/g in order to obtain the cement paste. These pastes were molded in cylindrical shaped in cylindrical pills (diameter 5 mm, height 1 mm) by pressing at 22 and 45 MPa.

Experimental Animals

A test material α-TCP was evaluated for primary skin irritation to the international standard for testing biocompatibility (ISO 10993-10:2002/Amd 1:2006 – see in References).

Experiments were performed on twelve rabbits of either sex (New Zealand White, weight 4.2 ± 0.4 kg) bred in the Institute of Physiology, and raised under controlled environmental conditions (temperature 22 ± 2°C; 14 h light/10 h dark). Animals were provided *ad libitum* access to a commercial rabbit-diet and drinking water was supplied to each cage. Experiments were approved by the Local Animal Ethical Committee of the School of Medicine, the University of Belgrade and were conducted in accordance with the principles and procedures of the NIH Guide for Care and Use of Laboratory Animals and ISO 10993-2: 2006 – see in References).

Table 1. Synthesis of α-tricalcium phosphate cement

Sample	$Ca(NO_3)_2{\cdot}4H_2O$ (g)	EDTA (g)	$NaH_2PO_4{\cdot}2H_2O$ (g)	$CO(NH_2)_2$ (g)
HAP (Ca/P = 1.50)	13.73	7.4	6.08	12.0

HAP, hydroxyapatite; Ca/P, calcium/phosphor ratio; $Ca(NO_3)_2{\cdot}4H_2O$, calcium nitrate; EDTA, ethylenediaminetetraacetic acid; $NaH_2PO_4{\cdot}2H_2O$, monosodium phosphate dehydrate; $CO(NH_2)_2$, urea (carbamide).

Experimental protocol

The area on the back of each rabbits was clipped free of fur with an electric clipper 24 h before the application of the sample. For the experiment, the clipped areas of skin of each rabbit were divided into four sites with the same area (20 × 20 mm). At each rabbit the test material α-TCP, either as a solid material (disc 5 × 2 mm) or as paste was applied to only two sites; the other two were used as negative controls (no material present, hypoallergic adhesive strip only). The positive control of this experiment was 98% lactic acid. The special control–blank liquid was the patch with H_2PO_4 (2.5%) (blank liquid: solvent portion treated in the same manner as the identical solvent used for the preparation of test samples-pasta, but without test material, and which is intended for the determination of background response of the solvent). Three rabbits were used per group; each rabbit had two patches with the same test material.

All the sites were covered by gauze and the back of the rabbit was wrapped with a non-occlusive bandage. After 4 h, the bandage and the test material were removed; 1 h later the sites were macro-pathologically examined for skin irritation and the observation was repeated after 24, 48 and 72 h (Draize et al. 1944). Skin reactions are graded separately for erythema and edema, each on a 0–4 grading scale. For erythema: 0 – no erythema; 1 – very slight erythema, barely perceptible; 2 – well-defined erythema; 3 – moderate to severe erythema; 4 – severe erythema (beet redness) to slight eschar formation (injuries in depth). For edema: 0 – no edema; 1 – very slight edema, barely perceptible; 2 – slight edema (edges of area well defined by raising); 3 – moderate edema (raised approximately 1 mm); 4 – severe edema (raised more than 1 mm and extending beyond the area of exposure).

The score of primary irritation (SPI) was calculated for each rabbit as the difference between the sum of the scores for erythema and edema at 24, 48 and 72 h divided by the number of the observations for the treated sites and the sum of the scores for erythema and edema at 24, 48 and 72 h divided by the number of the observations for the control sites (see formula below). The primary irritation index (PII) was calculated as the arithmetical mean of the SPI values of the three animals, e.g. of the six patches with the same test-material.

Formula used to calculate the SPI:

$$SPI = \left[\frac{\sum (Er+Ed)_{t1} + (Er+Ed)_{t2} + (Er+Ed)_{t3}}{n}\right]_T - \left[\frac{\sum (Er+Ed)_{t1} + (Er+Ed)_{t2} + (Er+Ed)_{t3}}{n}\right]_C$$

Er, erythema; Ed, edema, t1, 24 h; t2, 48 h; t3, 72 h; *n*, number of experiments; T, treated; C, control.

Test materials producing PII values 0 are considered no irritation, less than 2 are mildly irritating, 2 to 5 are moderately irritating, and greater than 5 are severely irritating.

Statistical analysis

Comparison between the mean values of SPI of the experimental groups was made by *t*-test. Statistical significance was considered at a probability $p < 0.05$.

Results

General tolerance

All rabbits recovered well and showed no signs of illness within the following 72 h.

Local tolerance

The effect of α-TCP, solid material

In all test animals, erythema or edema was not present after 24, 48 and 72 h in treated and control sites. Individual results of skin SPI for α-TCP solid material are reported in Table 2. There was no difference between treated and control sides ($p > 0.05$). The PII of the test material was 0 on a scale of 0.00 to 8.00.The PII of 0 is evaluated as no irritation.

Table 2. Score of erythema and edema after application of α-TCP solid phase

Animal (rabbit)		24 h		48 h		72 h		SPI	PII
		T	C	T	C	T	C		
1	Erythema	0–0	0–0	0–0	0–0	0–0	0–0	0/6 – 0/6 = 0	0
	Edema	0–0	0–0	0–0	0–0	0–0	0–0		
2	Erythema	0–0	0–0	0–0	0–0	0–0	0–0	0/6 – 0/6 = 0	0
	Edema	0–0	0–0	0–0	0–0	0–0	0–0		
3	Erythema	0–0	0–0	0–0	0–0	0–0	0–0	0/6 – 0/6 = 0	0
	Edema	0–0	0–0	0–0	0–0	0–0	0–0		

T, treated site; C, control site; SPI, score of primary irritation; PII, primary irritation index.

The effect of α-TCP paste

In all test animals, erythema or edema was not present after 24, 48 and 72 h in treated and control sites. Individual results of skin SPI for α-TCP paste are reported in Table 3. There was no difference between treated and control sides ($p > 0.05$). The PII of the test material was 0 on a scale of 0.00 to 8.00. The PII of 0 is evaluated as no irritation.

The effect of solvent Na_2HPO_4 (2.5%) – blank liquid

In all test animals, erythema or edema was not present after 24, 48 and 72 h in treated and control sites. Individual results of skin SPI for blank liquid, solvent Na_2HPO_4 (2.5%) used for preparation of α-TCP paste are reported in Table 4. There was no difference between treated and control sides ($p > 0.05$). The PII of the solvent–blank liquid was 0 on a scale of 0.00 to 8.00. The PII of 0 is evaluated as no irritation.

The effect of lactic acid (98%) – positive control

At the 24-h observation point, well defined erythema (score 2) was observed in one of the three test animals. In the other two animals moderate erythema (score 3) was observed. At the 48 h, moderate erythema remained on one of the three test animals (score 3); on the other two test animals there were well-defined (score 2) and very slight erythema (score 1). At 72-h observation points, the irrita-

Table 3. Score of erythema and edema after application of α-TCP paste

Animal (rabbit)		24 h		48 h		72 h		SPI	PII
		T	C	T	C	T	C		
1	Erythema	0–0	0–0	0–0	0–0	0–0	0–0	0/6 – 0/6 = 0	0
	Edema	0–0	0–0	0–0	0–0	0–0	0–0		
2	Erythema	0–0	0–0	0–0	0–0	0–0	0–0	0/6 – 0/6 = 0	0
	Edema	0–0	0–0	0–0	0–0	0–0	0–0		
3	Erythema	0–0	0–0	0–0	0–0	0–0	0–0	0/6 – 0/6 = 0	0
	Edema	0–0	0–0	0–0	0–0	0–0	0–0		

T, treated site; C, control site; SPI, score of primary irritation; PII, primary irritation index.

Table 4. Score of erythema and edema after application of blank liquid, Na_2HPO_4 (2.5%)

Animal (rabbit)		24 h		48 h		72 h		SPI	PII
		T	C	T	C	T	C		
1	Erythema	0–0	0–0	0–0	0–0	0–0	0–0	0/6 – 0/6 = 0	0
	Edema	0–0	0–0	0–0	0–0	0–0	0–0		
2	Erythema	0–0	0–0	0–0	0–0	0–0	0–0	0/6 – 0/6 = 0	0
	Edema	0–0	0–0	0–0	0–0	0–0	0–0		
3	Erythema	0–0	0–0	0–0	0–0	0–0	0–0	0/6 – 0/6 = 0	0
	Edema	0–0	0–0	0–0	0–0	0–0	0–0		

T, treated site; C, control site; SPI, score of primary irritation; PII, primary irritation index.

Table 5. Score of erythema and edema after application of lactic acid 98% (positive control)

Animal (rabbit)		24 h		48 h		72 h		SPI	PII
		T	C	T	C	T	C		
1	Erythema	3–3	0–0	2–2	0–0	2–2	0–0	14/6 – 0/6 = 2.33	2.1
	Edema	0–0	0–0	0–0	0–0	0–0	0–0		
2	Erythema	2–2	0–0	1–1	0–0	1–1	0–0	8/6 – 0/6 = 1.33	
	Edema	0–0	0–0	0–0	0–0	0–0	0–0		
3	Erythema	3–3	0–0	3–3	0–0	2–2	0–0	16/6 – 0/6 = 2.67	
	Edema	0–0	0–0	0–0	0–0	0–0	0–0		

T, treated site; C, control site; SPI, score of primary irritation; PII, primary irritation index.

tion was reversed, and well-defined erythema remained on two test animals and very slight erythema, barely perceptible remained on only one test animal. Edema was not observed at any time. Individual results of skin SPI for lactic acid (98%) are reported in Table 5. There was difference between SPI for treated and control sides ($p < 0.05$). The PII of the test material was 2.11 on a scale of 0.00 to 8.00. The PII of 2.11 is evaluated as moderately irritating.

Discussion

In this work we have reported the irritant properties of new developed α-TCP material. This *in vivo* investigation of the irritant properties of α-TCP paste and α-TCP solid material, tested after direct contact to rabbit skin, did not determine any cutaneous reaction such as erythema, edema, and necrosis. Moreover, the material did not give rise to allergic reactions.

A comprehensive, general guideline on the testing of biocompatibility of materials for medical applications is specified in the ISO 10993. Local skin compatibility is one of the crucial parameters for their possible clinical application. The irritation test is one of the estimates the local irritation potential of devices, materials or extracts, using sites such as skin or mucous membranes, usually in an animal model (ISO 10993-10:2002/Amd 1:2006).

The ISO 10993-10:2002/Amd 1:2006 standard describes skin-irritation tests for both single and cumulative exposure to a device. The preferred animal species is the albino rabbit, whose highly sensitive, light skin makes it possible to detect even very slight skin irritation caused by a substance.

The *in vivo* skin irritation/corrosion test in rabbits was introduced by Draize in the 1940s to predict hazardous effects of substances coming into contact with human skin (Draize 1944). This method gradually became the world standard, although several aspects of the test have been criticized. These include: the subjectivity of the method; the overestimation of human responses and the method's cruelty (McDouglas 1998; Patil et al. 1998). The European Centre for the Validation of Alternative Methods and the Interagency Coordinating Committee on the Validation of Alternative Methods were created in Europe and the United States respectively, in order to develop alternative methods. In Japan, the Japanese Society of Alternatives to Animals Experiments is responsible for carrying out validation assays. In recent years, different studies have been developed to validate alternatives to the skin irritation *in vivo* test (Human skin keratinocyte cytotoxicity/neutral red assay, Skin Squared^{TM} and Episkin^{TM}, Skintex assay). The application of tissue culture techniques, cellular and molecular biology, and analytic cytometric techniques can lead us closer to our goal of eliminating the need for animals in eye and skin irritation testing (Vinardell and Mitjans 2008). However, at present, despite the quantity and quality of the work carried out, with the exception of corrosion and phototoxicity, no alternative *in vitro* tests for skin irritation are available for regulatory purposes (reviewed in Vinardell and Mitjans, 2008). The *in vivo*, or Draize method has been the method of choice for determining the irritation/corrosion potential of chemicals (ISO 10993-10:2002/Amd 1:2006).

Since we tested a new developed material, no information was found in the available literature relative to the PII of this material. For this reason it is not possible to relate this investigation to similar relevant studies.

Previous biological evaluations of α-TCP material have been performed only in cell cultures using cytotoxicity tests. Our *in vitro* studies have suggested that there were significant differences ($p < 0.05$) between the tested concentrations of α-TCP. In the first experiment (qualitative and quantitative assay) α-TCP, in concentrations 200 mg/ml and 20 mg/ml, was clearly cytotoxic, while in concentration 2 mg/ml was mild cytotoxic. In experiment two (qualitative assay) α-TCP in concentration 100 mg/ml, 50 mg/ml and 10 mg/ml, showed clearly cytotoxic effect, in concentrations 10 mg/ml, 5 mg/ml and 1 mg/ml moderate cytotoxic effect, in concentration 0.5 mg/ml and 0.1 mg/ml mild cytotoxic effect while in concentrations 0.05 mg/ml and 0.01 mg/ml showed no cytotoxic effect. In experiment three, extract of α-TCP (50%, 75% and 100%) showed mild cytotoxic effect while in lower concentration (<50%) did not show any cytotoxic effect. We concluded that, in mouse fibroblast L929 cell culture system α-TCP showed concentration dependent cytototoxic effect which, predominantly, resulted from its inhibitory effect on cell growth (Jokanovic et al. 2008; Medovic et al. 2008; Stojanovic et al. 2008a,b).

Dos Santos et al. (2002) demonstrated that after 7 days of incubation the α-TCP-based cement has some degree of toxicity in cell cultures. The level of the α-TCP cement's cytotoxicity was determined, from which IC_{50} values ranging from 30% to 78%.

Otherwise, Ehara et al. (2003) showed that α-TCP is nontoxic even when tested in exaggerated culture conditions (i.e. prolonged exposure of cells to the materials). α-TCP showed no significant influence on cell proliferation, but the number of cells attached to the culture plates after incubation with/without α-TCP is the same at concentrations.

Any direct comparison or ranking between different biocompatibility tests would be inappropriate; therefore caution is warranted in attempting to correlate cell culture tests with animal experiments.

The similar materials to this that was tested in this investigation are already in clinical use. According to our data, PII of new developed α-TCP material (as a paste and solid material) is zero. The irritation potential of the testet material is negligible and cannot be considered as primary irritant to the skin, but further investigations are necessary to

demonstrate if in a range of physiological concentration, new developed calcium phosphate ceramic, α-TCP, demonstrates any health hazard potential.

Acknowledgements. Supported by grants: EUREKA project E3033 "Hydroxyapatite nanocomposite ceramics – new implant material for bone substitutes" (Bionanocomposit), Ministry of Science and Technological Development, Serbia.

References

Barile F. A. (2008): Principles of toxicology testing. CRC Press, Boca Raton, London, New York

Bollen L. S. (2005): New trends in biological evaluation of medical devices. Med. Device Technol. **16**, 10–15

Bollen L. S., Harling R. J. (2002): Biological evaluation as part of risk assessment. Med. Device Technol. **13**, 10–13

Bollen L. S. (2000): Preclinical evaluation of medical devices. Med. Device Technol. **11**, 8–11

Bohner M. (2000): Calcium phosphates in medicine: from ceramics to calcium phosphate cements. Injury **31**, 37–47

Draize J. H., Woodard G., Calvery H. O. (1944): Methods for the study of irritation and toxicity of substances applied topically to the skin and the mucous membranes. J. Pharmacol. Exp. Ther. **82**, 377–390

Durucan C., Brown P. W. (2000): Alpha-tricalcium phosphate hydrolysis to hydroxyapatite at and near physiological temperature. J. Mater. Sci. Mater. Med. **11**, 365–371

Ehara A., Ogata A., Imazato S., Ebisu S., Nakano T., Umakoshi Y. (2003): Effects of a-TCP and TetCP on MC3T3-E1 proliferation, differentiation and mineralization. Biomaterials **24**, 831–836

Fellah B. H, Josselin N., Chappard D., Weiss P., Layrolle P. (2007): Inflammatory reaction in rat muscle after implantation of biphasic calcium phosphate micro particles. J. Mater. Sci. Mater. Med. **18**, 287–294

ISO 10993-1:2003: Biological Evaluation of Medical Devices – Part 1: Evaluation and Testing

ISO 10993-2:2006: Biological Evaluation of Medical Devices – Part 2: Animal Welfare Requirements

ISO 10993-10:2002/Amd 1:2006: Biological Evaluation of Medical Devices – Part 10: Tests for Irritation and Delayed-Type Hypersensitivity

Janackovic Dj., Petrovic-Prelevic I., Kostic-Gvozdenovic Lj., Petrovic R., Jokanovic V., Uskokovic D. (2001): Influence of Synthesis Parameters on the Particle Sizes of Nanostructured Calcium-Hydroxyapatite. Key Engin. Mater. **192–195**, 203–206

Janackovic Dj., Jankovic I., Petrovic R., Kostic-Gvozdenovic Lj., Milonjic S., Uskokovic D. (2003): Surface properties of HAP particles obtained by hydrothermal decomposition of urea and calcium-EDTA chelates. Key Engin. Mater. **240-242**, 437–440

Jokanovic M., Markov J., Ristic S., Kojic Z. (2008): Nonclinical testing of biocompatibility of new materials. In: Contemporary Materials, book XIV (Ed. R. Kuzmanovic), pp. 637–645, Academy of Science and Art, Banjaluka

Jokic B., Jankovic-Castvar I., Veljovic Dj., Petrovic R., Drmanic S., Janacković Dj. (2006): Preparation of α-TCP cements from calcium deficient hydroxiapatite obtained by hydrothermal method. Key Engin. Mater. **309–311**, 821–824

Jokic B., Jankovic-Castvan I., Veljovic Dj., Bucevac D., Obradovic-Djuricic K., Petrovic R., Janackovic Dj. (2007): Synthesis and settings behavior of α-TCP from calcium deficient hyroxyapatite obtained by hydrothermal method. J. Optoelectron. Adv. M. **9**, 1904–1910

Kurashina K., Kurita H., Kotani A., Takeuchi H., Hirano M. (1997): In vivo study of a calcium phosphate cement consisting of α-tricalcium phosphate/dicalcium phosphate dibasic/tetracalcium phosphate monoxide. Biomaterials **18**, 147–151

Lu B., Lu X., Zhang Z., Li S., Pei F., Li Y., Cheng J. (2004): Application of enzyme histochemistry in evaluation of in vitro and in vivo biocompatibility of HA/TCP. Sheng Wu Yi Xue Gong Cheng Xue Za Zhi **21**, 631–635 (in Chinese)

McDouglas J. N. (1998): Physiologically based pharmacokinetic modeling. In: Dermatotoxicology Methods. (Chapter 6.), (Eds. F. N. Marzulli and H. I. Mailbach), pp. 51–66, Bristol

Medovic A., Kojic Z., Tasic G., Milakovic B., Kostic M., Skundric P. (2008): Toxicity and kinetic of insulin release from hormoneactive polysaharide fibres. Med. Investig. **42**, 17–22

Patil S. M., Patrick E., Maibach H. I. (1998): Animal, human, and *in vitro* test methods for predicting skin irritation. In: Dermatotoxicology Methods. (Chapter 9), (Eds. F. N. Marzulli and H. I. Mailbach), pp. 89–108, Bristol

dos Santos L. A., Carrodeguas R. G., Rogero S. O., Higa O. Z., Boschi A. O., Arruda A. C. (2002): α-tricalcium phosphate cement: "in vitro" cytotoxicity. Biomaterials **23**, 2035–2042

Stojanovic D., Janackovic Dj., Kojic Z., Colic M., Jokanovic M. (2008): α-Tricalcium Phosphate Cement: "*In Vitro*" Cytotoxicity. (Abstract book). 10th Congress of the Romanian Society of Physiological Science. Cluj, 5–7 June 2008, 80

Stojanovic D., Janackovic Dj., Markovic D., Tasic G., Aleksandric B., Kojic Z. (2008): A tissue-implant reaction associated with subcutan implantation of alpha-tricalcium phosphate, dental ceramic, and hydroxyapatite bioceramics in rats. Acta Veterinaria **58**, 381–393

Vinardell M. P., Mitjans M. (2008): Alternative Methods for Eye and Skin Irritation Tests: An Overview. J. Pharm. Sci. **97**, 46–59

Wiltfang J., Merten H. A., Schlegel K. A., Schultze-Mosgau S., Kloss F. R., Rupprecht S., Kessler P. (2002): Degradation characteristics of α and β tri-calcium-phosphate (TCP) in minipigs. J. Biomed. Mater. Res. **63**, 115–121

Williams D. F. (1986): Definitions in biomaterials. In: Progress in Biomedical Engineering. Proceedings of a Consensus Conference of the European Society for Biomaterials. (Ed. D. F. Williams), pp. 20–29, Chester, England

Calcium blocking activity as a mechanism of the spasmolytic effect of the essential oil of *Calamintha glandulosa* Silic on the isolated rat ileum

Suzana V. Brankovic[1], Dusanka V. Kitic[2], Mirjana M. Radenkovic[1], Slavimir M. Veljkovic[1] and Tatjana D. Golubovic[3]

[1] *Department of Physiology, Faculty of Medicine, University of Niš, Serbia*
[2] *Department of Pharmacology, Faculty of Medicine, University of Niš, Serbia*
[3] *Faculty of Occupational Safety, University of Niš, Serbia*

Abstract. In this paper we present the results of studying the effects of the essential oil of *Calamintha glandulosa* Silic (EOCG) on the isolated rat ileum. *C. glandulosa* Silic has been used in folk medicine as an antispasmodic. EOCG (0.003–1 mg/ml) inhibited spontaneous contraction of the ileum (EC50 of 210.48 ± 9.12 μg/ml). The calcium channel blocking activity was confirmed by inhibition of K^+ (80 mmol/l) induced contractions with EOCG (EC50 of 88.81 ± 6.01 μg/ml). EOCG shifted cumulative calcium curves in depolarizing medium downward (EC50 of 18.18 ± 1.87 mmol/l), similar to the effects of verapamil. Our results confirm that the EOCG shows spasmolytic action in rat ileum. The spasmolytic effect of the EOCG was due to blockade of calcium influx. One of the main components of the EOCG is monoterpenoide pulegone. Namely, pulegone (0.15–50 μmol/l) inhibited the spontaneous (EC50 of 9.02 ± 0.08 μg/ml), and K^+ induced contractions of the ileum (EC50 of 4.05 ± 0.14 μg/ml), and run rightward the dose response curve of calcium. Pulegone may have a main role in spasmolytic activities of the plant.

Key words: *Calamintha glandulosa* Silic — Spasmolytic — Calcium antagonism — Pulegone

Introduction

Family Labiatae (Lamiaceae), or Minth family, consists of perennial or annual aromatic herbs and shrubs (rarely trees) widely distributed around Mediterranean coast. The family comprises about 200 genera and 3500 species commonly utilized worldwide in folk remedies against a variety of complaints. The widespread use of infusions of dry peppermint leaves (*Mentha piperita* L., Lamiaceae) for their known antispasmodic, carminative and sedative effects is well established and documented (Della Logia et al. 1990). The species that have similar scent as peppermint are often used as folk remedies for the same purposes, even though they belong to a different genus. *Calamintha glandulosa* Silic is a perennial aromatic plant belonging to the family of Lamiaceae, with the purple flowers and a strong, refreshing odor of the mint (name is derivate from Greek, "*cala*" meaning "good" and "*minth*" meaning "smell"). Some species of the *Calamintha* Miller genus have been traditionally used as a substitute for the mints, in infusion as a stomach tonic, an antiseptic and an expectorant (Mimica-Dukic et al. 2004). Due to its pleasant odor and a distinctive taste the aerial part of the plants can be added to meat stuffing as a seasoning. The leaves, flowers and stems of *Calamintha* species are used as herbal teas and in the production of traditional remedies, mainly as stimulants, antiseptics and antispasmodics (Kokkalou and Stefanou 1990; Baldovini et al. 2000). The extracts and essential oils exhibit hypoglycaemic (Lemhadri et al. 2004), sedating and antipyretic effects in rats (Ortiz et al. 1989), and antimicrobial activity (Kitic et al. 2002). In the last 15–20 years, there has been intensive phytochemical research of *Calamintha* species conducted on antimicrobial agent of herbs *in vitro,* which was mostly focused on their essential oils.

Generally, the essential (or volatile) oil composition is a mixture of various volatile secondary metabolites, mainly

Correspondence to: Suzana V. Brankovic, Department of Physiology, Faculty of Medicine, University of Niš, Bul. Zorana Djindjića 81, 18000 Niš, Serbia
E-mail: brankovic.suzana@yahoo.com

monoterpenes, sesquiterpenes, and their oxygenated derivatives (alcohols, aldehydes, esters, ethers, ketones, phenols and oxides). Other volatile compounds may include phenylpropenes and specific sulphur- or nitrogen-containing substances. In the last decades, the interest has been focused on the essential oils and various other extracts of plants, as they demonstrate a wide range of pharmacological effects, such as anti-inflammatory, antioxidant, cytotoxic. They have been screened for their potential uses as alternative remedies for the treatment of many diseases. The composition of the essential oil from the aerial part of plants of *C. glandulosa* has been recently described (Kitic et al. 2002). In the oils one constituent may prevail over all others. The analysis of the essential oil composition indicates that the main component in the oil was pulegone. The herbs with high pulegone content have been used as components of herbal teas for stomach disorders in Turkey (Özek 1990).

To the best of our knowledge, there has not yet been published any investigation of spasmolytic activity of the oil of *Calamintha* species. Guided by ethnobotanical literature and availability from natural sources, our main object was to assess the effects of the essential oil of *Calamintha glandulosa* Silic (EOCG) and pulegone, the principal component in the oil, on the contractility of isolated rat ileum.

Materials and Methods

Animals

In this study, Wistar albino rats (n = 18), were used age 12 weeks, body weight 200–250 g, obtained from the Animal Research Center of Medical Faculty, University of Niš, Serbia. The rats were housed in stainless steel cages under standard laboratory conditions. These animals were maintained at 20–24°C with a 12 h light-dark cycle (light on 08:00 to 20:00 h) at least 1 week before the experiment. All animals were fed with standard pellet and they had free access to food and water. All experimental procedures with animals were in compliance with the European Council Directive of November 24, 1986 (86/609/EEC).

The experiments in rat ileum were carried out as previously described (Radenkovic et al. 2006). The ileum portions were isolated out and cleaned off mesenteries. Preparations of 2 cm long parts of the ileum were mounted in 20 ml tissue baths containing Tyrode`s solution maintained at 37°C and aerated with a mixture of 5% carbon dioxide in oxygen. The composition of Tyrode`s solution was (in mmol/l): NaCl 136.89, KCl 2.68, $MgCl_2$ 1.05, $CaCl_2$ 1.80, NaH_2PO_4 0.42, $NaHCO_3$ 11.90 and glucose 5.5. The fragment were stretched to a sufficient tension and equilibrated for at least 30 min before starting experiments. The change of intestinal contractility was recorded using myograph transducer F-50 (Narco Bio-Systems, Inc., Houston). After each assay, tissue was washed with fresh Tyrode and equilibrated for about 10 min.

Plant material

The aerial parts of flowering plant were collected in August 2006 from the population growing wild in Igalo-Sutorina River. A voucher specimen has been deposited in the Institute of Botany Herbarium (BEOU No. 16014), Botanical Garden, Faculty of Biology, University of Belgrade.

Drugs and chemicals

The following drugs were used: verapamil hydrochloride (Sigma Chemicals Company, St. Louis, MO, USA), pulegone (Sigma-Aldrich Chemie GmbH, Diesenhofen, Germany) and EOCG. Pulegone was dissolved in distilled water.

Preparation of EOCG

Dried and pulverized aerial parts of the plant (100 g) were hydrodistilled for 3 h using a Clevenger type apparatus (Pharmacopeia Jugoslavica). The oil was extracted from the distillate with Et_2O and then dried with anhydrous Na_2SO_4. After filtration, the solvent was removed by distillation under the atmospheric pressure and pure yellow oil, 0.6 ml, was kept at 4°C until analysis (Kitic 2003).

Experimental design

After stabilization period EOCG (0.003–1 mg/ml), verapamil (0.01–3 μmol/l) and pulegone (0.15–50 μmol/l) were added to the bath. Effects of different EOCG, verapamil and pulegone concentrations on ileal basal tonus are expressed as percent of changes in baseline values of basal tonus.

Ileal preparations were contracted with depolarizing solution KCl (80 mmol/l). A high concentration of K^+ ions produced a tonic contraction. Then EOCG (0.003–1 mg/ml) was cumulatively added to the organ bath. The same protocol was carried out with verapamil (0.01–3 μmol/l) and pulegone (0.15–50 μmol/l). The relaxation of the intestinal preparations, precontracted with K^+, was expressed as the percentage of the control response mediated by K^+.

After the stabilization during 45 min in Tyrode, the external calcium was eliminated with Tyrode (Ca^{2+}-free) and then muscle depolarized with Tyrode (Ca^{2+}-free, 80 mmol/l K^+ isoosmotic) (Karamenderes and Apaydin 2003). A cumulative concentration-response curves of Ca^{2+} were obtained by cumulatively adding $CaCl_2$ to reach concentrations from 0.01 to 10 mmol/l in the absence and presence of EOCG (0.1–0.3 mg/ml), verapamil (0.03–0.3 μmol/l) and pulegone (5–15 μmol/l), which were added to the bath 15 min before addition of Ca^{2+}. This curve was compared with

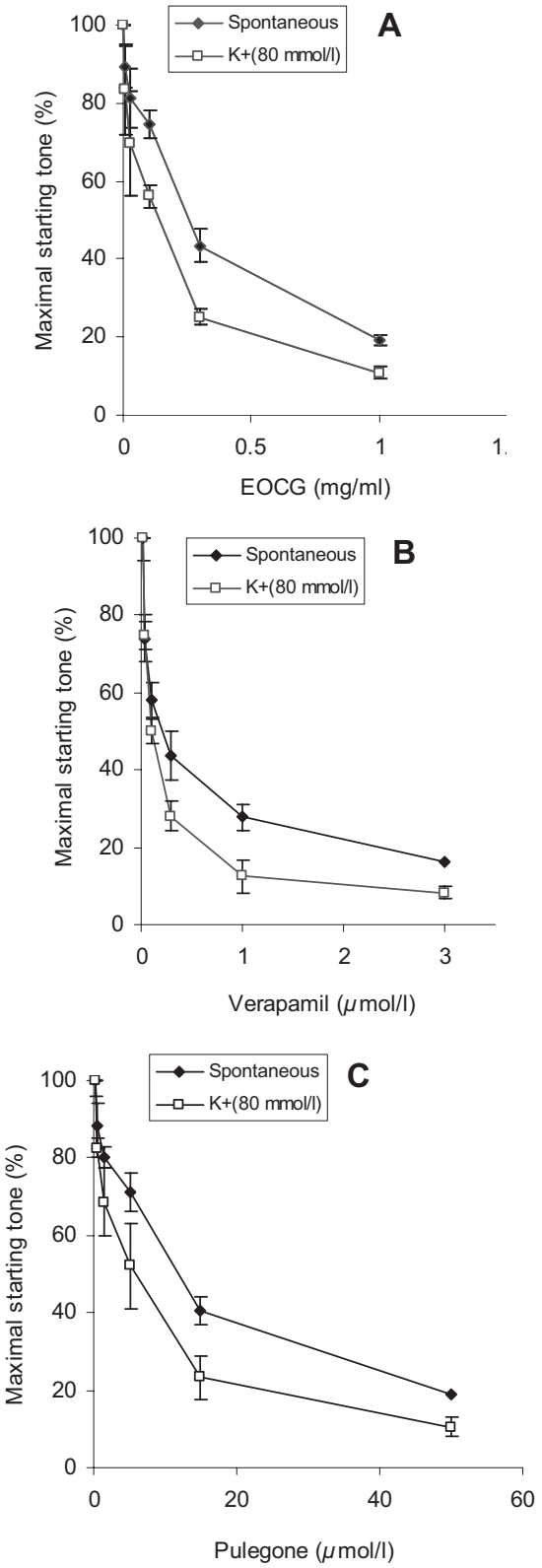

Figure 1. Relaxant effect of EOCG (A), verapamil (B) and pulegone (C) on spontaneous and K^+ (80 mmol/l)-induced contraction in isolated rat ileum (n = 6). The values are expressed as mean ± SEM.

that obtained in the presence of $CaCl_2$ alone and expressed as percentages of the maximal response to $CaCl_2$.

Statistical analysis

The results were expressed as mean ± SD of six determinations. Statistical evaluation was performed using the Student's t-test or one-way analysis of variance (ANOVA). A probability value of $p < 0.05$ was considered to be significant. The mean effective concentration EC50, that is the concentration which elicited 50% of maximal response, was established by regression analysis.

Results

Relaxant effects of EOCG, verapamil and pulegone on basal tonus of the ileum

A concentration dependent decreasing effect of the EOCG on the basal tonus of the rat ileum reaches its maximum effect at 1 mg/ml (Fig. 1A). The EC50 values for the EOCG induced relaxation was 210.48 ± 9.12 μg/ml. The relaxant effect of EOCG was reversible after washing the preparation. Verapamil (0.01–3 μmol/l, Fig. 1B) and pulegone (0.15–50 μmol/l, Fig. 1C) also relaxed the basal tonus of intestine in a concentration-dependent manner.

When concentrations of EOCG, verapamil and pulegone are expressed as μg/ml (Table 1), pulegone was twenty three times as potent as EOCG in relaxing spontaneous contraction. Verapamil was ninety times as potent as pulegone in inhibiting spontaneous contraction of rat ileum. These results suggest that pulegone can be responsible for EOCG-induced relaxation.

Relaxant effects of EOCG, verapamil and pulegone on contraction induced by KCl

Solution of KCl (80 mmol/l) induced depolarization and tonic contraction of the ileum. EOCG (0.003–1 mg/ml) relaxed contraction with EC50 values of 88.81 ± 6.01 μg/ml. Verapamil (0.01–3 μmol/l) and pulegone (0.15–50 μmol/l) also relaxed contraction induced by K^+ (80 mmol/l), and they

Table 1. EC50 values (μg/ml) for the inhibition spontaneous and K^+-induced contraction of isolated rat ileum

	EOCG	Verapamil	Pulegone
Spontaneous contraction	210.48 ± 9.12	0.10 ± 0.009	9.02 ± 0.08
K^+-induced contraction	88.81 ± 6.01	0.059 ± 0.006	4.05 ± 0.14

were more potent than the oil with an EC50 value of 0.059 ± 0.006 μg/ml and 4.05 ± 0.14 μg/ml, respectively (Fig. 1).

Effect of EOCG, verapamil and pulegone on concentration response curves to $CaCl_2$ in Ca^{2+}-free medium

Fig. 2 shows the effect of EOCG (A), verapamil (B) and pulegone (C) on cumulative $CaCl_2$-induced contractions in Ca^{2+}-free and high K^+ depolarizing medium. EOCG in concentration (0.1–0.3 mg/ml) inhibited the contractions induced by $CaCl_2$, in a concentration dependent manner. The concentration response curves of $CaCl_2$, in presence of EOCG were significantly shifted downward ($p < 0.01$). Verapamil (0.03–0.3 μmol/l) and pulegone (5–15 μmol/l) also significantly shifted the $CaCl_2$ response curves to the right and down ($p < 0.01$). The EC50 values of calcium ions (0.66 ± 0.03 mmol/l) were affected by EOCG (EC50 of 18.18 ± 1.87 mmol/l), verapamil (EC50 of 73.88 ± 7.94 mmol/l) and pulegone (EC50 of 22.79 ± 1.02 mmol/l).

Discussion

EOCG exhibited relaxant activity in isolated rat ileum. The effect was reversible after washing, suggesting that the inhibition was not due to the damage of the intestine by the oil.

Depending on EOCG concentration, contraction induced by high concentration of potassium, were relaxed. Calcium is the regulator of tension in smooth muscles, and their contraction depends on Ca^{2+} influx from extracellular space through calcium channels. It is well known that the increase in external K^+ concentration (KCl 80 mmol/l) induces smooth muscle contraction through the activation the voltage operated calcium channels and subsequent calcium release from the sarcoplasmic reticulum (Bolton 1979; Santos et al. 2007). Therefore, agents that inhibit contraction induced by KCl should somehow inhibit the entry of Ca^{2+} ions or otherwise inhibit the intercellular contraction mechanism (Sandraei et al. 2003).

Essential oil decreased the Ca^{2+} dose-response curves, constructed in the Ca^{2+}-free medium, similar to that caused by verapamil. The common characteristic of verapamil is dose-dependent inhibition of the slow entry of calcium. The observed effect of the plant extract to inhibit Ca^{2+} contraction, similar to that of verapamil, suggests the presence of calcium antagonist in the extract (Godfrain et al. 1986; Gilani et al. 2005).

The antagonistic effect produced by extract on spontaneous activity of rat ileum or on contraction induced by KCl and $CaCl_2$ suggests spasmolytic action *via* the modulation of calcium entry through calcium channels. There is a report about antispasmodic effect of another species of *Satureja* L. (Cruz et al. 1990), and other plants of Lamiaceae family (Hajhashemi et al. 2000). Effect of this species is consistent with our results.

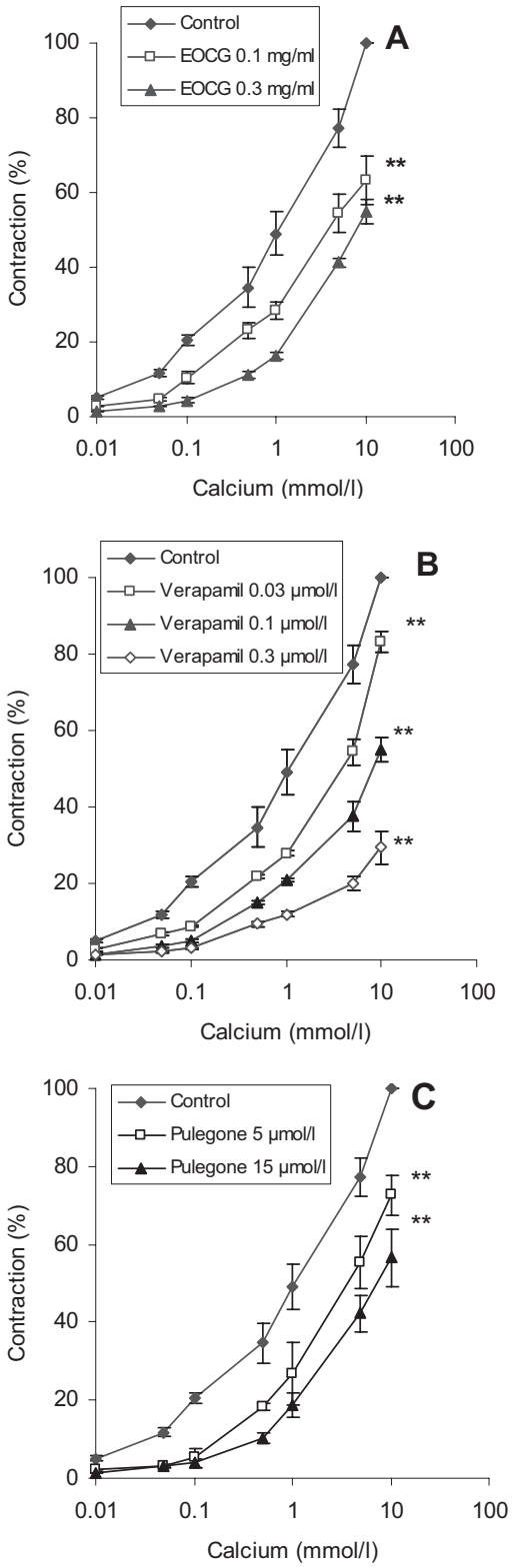

Figure 2. Relaxant effect of EOCG (A), verapamil (B) and pulegone (C) on Ca^{2+} induced contraction in isolated rat ileum ($n = 6$). Data are expressed as the mean ± SEM. ** $p < 0.01$ vs. contractions induced in the presence of stimulator alone.

It is well known that some terpenoides can act as spasmolytic agents by involving calcium antagonism (Shabana et al. 2005). Terpenoid pulegone is the principal component of the essential oil of *Mentha pulegium* and induced an inhibitory effect on the contractile activity of the isolated rat myometrium (Soares et al. 2005).

The results of oil analysis of *C. glandulosa* shown that pulegone was the main component (37.5%) (Kitic et al. 2002). Pulegone exerts concentration dependent inhibition of spontaneous contraction of the ileum and effect was twenty three times as potent as EOCG in inhibiting contractions.

Conclusion

The results obtained in this work showed that EOCG exerts significant spasmolytic effect, which may underline the therapeutic action of the plant. Antispasmodic activity on rat ileum is probably caused by inhibition of calcium influx through voltage-operated Ca^{2+} channels. Pulegone, the principal constituent of EOCG, is most probably responsible for EOCG-induced relaxation.

Acknowledgements. The authors thank Bojan Zlatković, Department of Chemistry, Faculty of Science and Mathematics University of Niš, Serbia, for the identification of the plant material. We are also grateful for the financial support of the Ministry of Sciences and Environmental Protection of the Republic of Serbia, grant No. 145081B and the project Training and Research in Environmental Health in the Balkans D43 TW00641 supported by the NIH/Fogarty International Center, USA.

References

Bolton T. B. (1979): Mechanisms of action of transmitters and other substances on vascular smooth muscle. Physiol. Rev. **59**, 606–718

Baldovini N., Ristorcelli D., Tomi F., Casanova J. (2000): Infraspecific variability of the essential oil of *Calamintha nepeta* from Corsica (France). Flav. Fragr. J. **15**, 50–54

Cruz T., Cabo M., Jimenez J. (1990): Composition and pharmacological activity of the essential oil of *Satureja obavata* spasmolytic activity. Fitoterapia **61**, 247–251

Della Logia R., Tubaro A., Lunder T. L. (1990): Evaluation of some pharmacological activities of a peppermint extract. Fitoterapia **61**, 215–221

Gilani A. H., Jabeen Q., Ghayur M. N., Janbaz K. H., Akhtar M. S. (2005): Studies on the antihypertensive, antispasmodic, bronchodilator and hepatoprotective activities of the *Carum copticum* seed extract. J. Ethnopharmacol. **98**, 127–135

Godfraind T., Miller R., Wibo M. (1986): Calcium antagonism and calcium entry blockade. Pharmacol. Rev. **38**, 321–416

Hajhashemi V., Sadraei H., Ghannadi A. R., Mohseni M. (2000): Antispasmodic and anti-diarrhoeal effect of *Satureja hortensis* L. essential oil. J. Ethnopharmacol. **71**, 187–192

Karamenderes C., Apaydin S. (2003): Antispasmodic effect of *Achillea nobilis* L. subsp. *Sipylea* (O. Schwarz) Bässler on the rat isolated duodenum. J. Ethnopharmacol. **84**, 175–179

Kitic D., Palic R., Stojanovic G., Ristic M., Jovanovic T. (2002): Chemical composition and antimicrobial activity of the essential oil of *Calamintha nepeta* (L.) Savi subsp. *glandulosa* (Req.) P. W. Ball from Montenegro. J. Essent. Oil Res. **14**, 150–152

Kitic D. (2003): Chemical and microbial investigation plant species of genus *Calamintha Miller*. (PhD thesis), Department of Chemistry, Faculty of Science and Mathematics, University of Niš, Serbia

Kokkalou E., Stefanou E. (1990): The volatile oil of *Calamintha nepeta* (L.) Savi subsp. *glandulosa* (Req.). Ball endemic to Greece. Flav. Fragr. J. **5**, 23–26

Lemhadri A., Zegqwaqh A., Maghrani M., Jouad H., Eddouks M. (2004): Hypoglicaemic effect of *Calamintha officinalis* Moench in normal and streptozotocin-induced diabetic rats. J. Pharm. Pharmacol. **56**, 795–799

Mimica-Dukic N., Couladis M., Tzakou O., Jancic R., Slavkovska V. (2004): Essential Oils of *Calamintha sylvstica* Bromf. and *Calamintha vardarensis* Silic. J. Essent. Oil Res. **16**, 219–222

Ortiz U., Martin M., Montero M., Moran A., San Roman L. (1989): Sedating and antipyretic activity of the essential oil of *Calamintha sylvatica* subsp. *Ascedens*. J. Ethnopharmacol. **25**, 165–171

Özek T. (1990): Composition of the Essential Oils of *Micromeria congesta. (*MSc dissertation), Anadolu University, Eskisehir, Turkey

Radenkovic M., Ivetic V., Popovic M., Mimica-Dukic N., Veljkovic S. (2006): Neurophysiological effects of Mistletoe (*Viscum album* L.) on isolated rat intestines. Phytother. Res. **20**, 374–377

Sandraei H., Ghannadi A., Malekshahi K. (2003): Relaxant effect of essential oil of *Melissa officinalis* and citral on rat ileum contractions. Fitoterapia **74**, 445–452

Santos M., Carvalho A., Medeiros I., Alves P., Marchioro M., Antoniolli A. (2007): Cardiovascular effects of *Hyptis fruticosa* essential oil in rats. Fitoterapia **78,** 186–191

Shabana C., Ahsana D., Shakeel A., Atta-ur-Ralman (2005): Evaluation of *Alstonia scholaris* leaves for broncho-vasodilatatory activity. J. Ethnopharmacol. **97**, 469–476

Soares P. M., Assreuy A. M., Souza E. P., Lima R. F., Silva T. O., Fontenele S. R., Criddle D. N. (2005): Inhibitory effects of the essential oil of *Mentha pulegium* on the isolated rat myometrium. Planta Med. **71**, 214–218

Adipose tissue-derived nerve growth factor and brain-derived neurotrophic factor: results from experimental stress and diabetes

Federica Sornelli[1], Marco Fiore[1], George N. Chaldakov[2] and Luigi Aloe[1]

[1] *Institute of Neurobiology and Molecular Medicine, CNR, Rome, Italy*
[2] *Division of Cell Biology, Medical University, Varna, Bulgaria*

Abstract. Recently, adipobiology (adiposcience) became a focus of numerous studies showing that the adipose tissue is the body's largest endocrine and paracrine organ producing multiple signaling proteins collectively designated adipokines; at present these include more than hundred proteins. However, studies on adipobiology of neurotrophins have recently emerged, nerve growth factor (NGF) and brain-derived neurotrophic factor (BDNF) being examples of adipose-derived neurotrophins. Here we present data showing that NGF and BDNF are expressed in both white and brown adipose tissue following experimental stress (in mice) and in type 1 diabetes (in rats). We suggest that both neurotrophic and metabotrophic potentials of NGF and BDNF may be involved in the molecular mechanism of stress and diabetes and consequently, in the pathogenesis of cardiometabolic diseases.

Key words: Adipose tissue — Adipokines — Neurotrophins — Diabetes — Stress

Introduction

There is a growing awareness that adipose tissue is an endocrine and paracrine organ producing multiple signaling proteins designated adipokines (Chaldakov et al. 2003; Bulcão et al. 2006; Sacks and Fain 2007; Töre et al. 2007; Chaldakov 2008; Trayhurn et al. 2008). There is evidence indicating that the neurotrophin nerve growth factor (NGF) is also produced by adipose tissue (Chaldakov et al. 2004; Ryan et al. 2008), whereas only two available publications exist about adipose tissue-derived brain-derived neurotrophic factor (BDNF) (Hausman et al. 2006; Sornelli et al. 2007), another important member of the protein family of neurotrophins. In addition to their stimulatory action on neuronal growth and survival, the neurotrophins also act on a number of other cell types including immune cells (Aloe et al. 2001) and pancreatic β cells (Yamanaka et al. 2006). Noteworthy, NGF and BDNF were recently designated metabokines (Sornelli et al. 2007), because i) exert metabotrophic effects on glucose, lipid and energy homeostasis (Töre et al. 2007; Unger et al. 2007), and ii) the levels of NGF and BDNF in coronary atherosclerosis (Chaldakov et al. 2004), acute coronary syndromes (Manni et al. 2005), metabolic syndrome (Chaldakov et al. 2004; Geroldi et al. 2006; Bulló et al. 2007) and obesity/diabetes (El-Gharbawy et al. 2006; Larrieta et al. 2006; Yamanaka et al. 2006; Bulló et al. 2007; Sposato et al. 2007; Unger et al. 2007) are significantly altered, also in stress condition (Aloe et al. 1986; Manni et al. 2007; Fiore et al. 2009).

Hence the question was asked whether the presence of NGF and BDNF might also be altered in both white and brown adipose tissues (WAT and BAT, respectively), in experimental stress and diabetes.

Materials and Methods

Stress was produced in adult male mice of Swiss CD-1 strain (n = 10; 90-day-old, body weight 35.03 ± 0.88 g) by social isolation for 8 weeks followed by housing with a fellow male mice of the same strain and age for 60 min, isolated for the same time period. This profile leads to aggressive behavior and fighting. Intact non-isolated male subjects (n = 10; body weight 34.08 ± 1.34 g) of the same strain and age were used as control group (see Aloe et al. 1986; Fiore et al. 2005). All

Part of this study was presented at The First International Symposium on Adipobiology and Adipopharmacology, October 20th, 2007, Varna, Bulgaria.
Correspondence to: Luigi Aloe, Institute of Neurobiology and Molecular Medicine, CNR-NGF Section, Via del Fosso di Fiorano 64/65, I-00143 Rome, Italy
E-mail: aloe@inmm.cnr.it

experimental procedures have been carried out in accordance with the European Communities Council Directive of 24 November 1986 (86/609/EEC), the Italian legislation (Decreto L.vo 116/92) and following the guidelines indicated by Intramural Committee and Institutional Guidelines in accordance with National and International law (EEC council directive 86/609, OJ L 358, 1, 12 December, 1987). All efforts were taken to prevent or reduce animal suffering and for limiting the number of experimental subjects.

Diabetes (type 1) was induced in adult Sprague Dawley male rats ($n = 10$; 120-day-old, body weight 358.76 ± 12.24 g) by a single intravenous injection of streptozotocin at a dose of 60 mg/kg dissolved in PBS (Larrieta et al. 2006; Sposato et al. 2007). Rats were considered diabetic and included in the study if they had a fasting plasma glucose level >350 mg/dl 8 weeks after administration of streptozotocin. Ketoacidosis was not observed following this experimental procedure. An equal number of adult male rats of the same age ($n = 10$; body weight 365.12 ± 18.44 g) received a physiological solution and served as controls. During the treatments, rats were housed three per cages.

Stressed and diabetic animals and their respective controls were sacrificed with an overdose of Nembutal, and WAT of the epicardial region, and BAT of the interscapular region were isolated and used for NGF and BDNF immunoenzymatic assay. As heart-associated adipose tissue plays a role in cardiovascular pathology (Chaldakov et al. 2003; Sacks and Fain 2007; Chaldakov 2008), we used epicardial WAT for our studies.

For NGF and BDNF determination, WAT and BAT samples were homogenated with ultrasonication in extraction buffer (in mmol/l: 20 Tris-acetate, pH 7.5, 150 NaCl, 1 EDTA, 1 EGTA, 2.5 sodium-pyrophosphate, 1 orthovanadate, 1 ß-glycerolphosphate, 100 NaF, 1 PMFS, and 1 µg/ml leupeptin) and centrifuged at 4°C for 20 min at 10,000 rpm. The resultant supernatants were recovered and used for analysis of NGF by an enzyme-linked immunosorbent assay (ELISA) kit, "NGF Emax immunoassay system number G7631" by Promega (Madison, WI, USA), following the manufacturer's instructions. BDNF was measured by an ELISA kit, "BDNF Emax immunoassay system number G7611" by Promega (Madison), following the manufacturer's instructions. The concentration of NGF and BDNF was expressed as pg/g of protein. ANOVA was performed by using the StatView software (Mac version). Data were expressed as mean ± SEM.

Results

NGF and BDNF were detected in both WAT and BAT. As shown in Fig. 1 the concentration of NGF in BAT is significantly increased in stressed mice as compared to control tissue ($p < 0.05$). In WAT the elevation was not fully significant

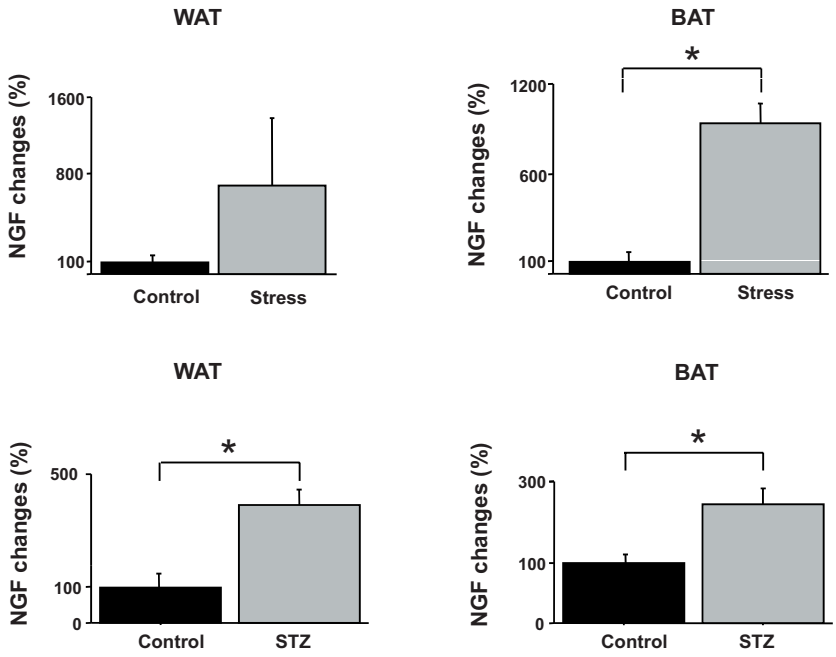

Figure 1. Changes in the amount of nerve growth factor (NGF) in white adipose tissue (WAT) and brown adipose tissue (BAT) of controls compared to the concentration of NGF in stressed mice (Stress) and streptozotocin-induced diabetic rats (STZ), expressed as percentage of controls. Note the enhanced presence of NGF in WAT and BAT in stressed mice as well as diabetic rats. The vertical lines in the figure indicate pooled S.E.M. derived from appropriate error mean square in the ANOVA. * significant differences between groups ($p < 0.05$).

($p < 0.075$). Likewise the presence of NGF in WAT and BAT is significantly enhanced in diabetic rats ($ps < 0.05$). Together these findings indicate that adipo-derived NGF is affected by stressful and diabetic conditions.

Changes were also found in the concentration of BDNF (Fig. 2). Diabetic rats displayed enhanced levels of BDNF in the adipose tissues analyzed ($p < 0.05$). Specifically, ANOVA revealed a mild increase in both WAT and BAT ($p = 0.08$ in post-hocs). However, BDNF presence was not altered in stressed mice.

The cellular source of NGF (see Ryan et al. 2008 for adipocytes) and BDNF in WAT and BAT is not known. Since the adipose tissue contains mast cells (Chaldakov et al. 2000), and these cells are known to be both source of and target for NGF and BDNF (Aloe et al. 1977; Aloe and Levi-Montalcini 2001), we investigated the number of mast cells in WAT and BAT. Our results demonstrate that these cells undergo numerical and degranulation changes under stress or diabetic conditions as previously shown (De Simone et al. 1990; Cirulli et al. 1998; Hristova et al. 2001), suggestive of NGF and/or BDNF secretion by adipose mast cells (data not shown).

Discussion

Since a number of emerging findings indicated that certain obese-related disorders are characterized by altered expression of systemic and/or local NGF and BDNF (Chaldakov et al. 2004; Manni et al. 2005; El-Gharbawy et al. 2006; Geroldi et al. 2006; Larrieta et al. 2006; Yamanaka et al. 2006; Bullò et al. 2007; Manni et al. 2007; Sposato et al. 2007; Unger et al. 2007), the aim of the present study was to evaluate the presence of these neurotrophins in both WAT and BAT of rodents in experimentally-induced stress and diabetic conditions.

We found that NGF and BDNF are present in the adipose tissues and that NGF levels are more significantly altered than BDNF levels in the experimental conditions studied. Further studies are required to prove the secretory activity of adipose tissue cells, as related to NGF and BDNF. Intriguingly, NGF exerts healing effect in diabetic skin ulcers (Generini et al. 2004), and BDNF is known to be a potent metabokine having antidiabetic and anorexigenic effects (Geroldi et al. 2006; Lebrun et al. 2006; Yamanaka et al. 2006; Unger et al. 2007). Further, our data for the first time reveal the presence of both NGF and BDNF in epicardial adipose tissue, which role in the pathogenesis of cardiovascular disease is increasingly studied recently (reviewed in Sacks and Fain 2007; Chaldakov 2008). Note that in addition to NGF and BDNF, other neurotrophic factors as well as various neuropeptides and their receptors are also expressed in adipose tissue (Kos et al. 2007 and references therein; Sacks and Fain 2007; Wang et al. 2008). This might be suggestive of a neuroendocrine potential

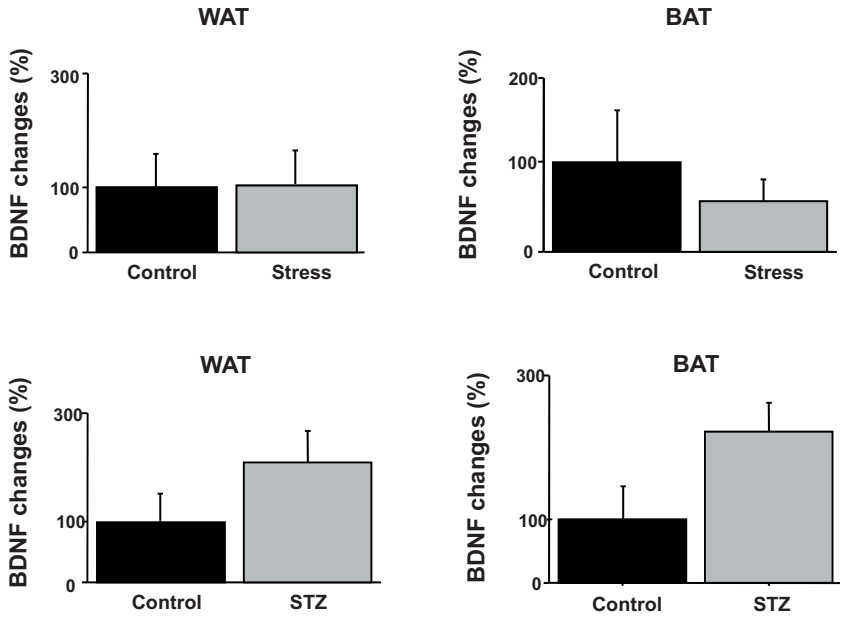

Figure 2. Changes in the amount of brain-derived neurotrophic factor (BDNF) in epicardial white adipose tissue (WAT) and brown adipose tissue (BAT) of controls compared to the concentration of BDNF in stressed mice (Stress) and streptozotocin-induced diabetic rats (STZ), expressed as percentage of controls. The vertical lines in the figure indicate pooled S.E.M. derived from appropriate error mean square in the ANOVA.

of adipose tissue. In line with Levi-Montalcini's general paradigm (Levi-Montalcini 1987), NGF produced and released by adipocytes and/or mast cells (see De Simone et al. 1990; Cirulli et al. 1998; Chaldakov et al. 2000, 2004; Hristova et al. 2001) may serve to regulate the sympathetic innervation of adipose tissue. Such an activity together with NGF/BDNF's effects on extraneuronal functions (Aloe et al. 2001; Chaldakov et al. 2003, 2004; Lebrun et al. 2006; Yamanaka et al. 2006; Unger et al. 2007; Ryan et al. 2008) may implicate adipose-derived neurotrophins to the pathogenesis of cardiometabolic diseases.

Acknowledgements. This study was supported by Italian National Research Council. F. Sornelli was supported by a fellowship from Associazione-Levi-Montalcini.

References

Aloe L., Levi-Montalcini R. (1977): Mast cells increase in tissues of neonatal rats injected with the nerve growth factor. Brain Res. **133**, 358–366

Aloe L., Alleva E., Böhm A., Levi-Montalcini R. (1986): Aggressive behaviour induces release of nerve growth factor from mouse salivary gland into blood stream. Proc. Natl. Acad. Sci. U.S.A. **83**, 6184–6187

Aloe L., Tirassa P., Bracci-Laudiero L. (2001): Nerve growth factor in neurological and non-neurological diseases: basic findings and emerging pharmacological prospectives. Curr. Pharm. Des. **7**, 113–123

Bulcão C., Ferreira S. R., Giuffrida F. M., Ribeiro-Filho F. F. (2006): The new adipose tissue and adipocytokines. Curr. Diabetes Rev. **2**, 19–28

Bulló M., Peeraully M. R., Trayhurn P., Folch J., Salas-Salvadó J. (2007): Circulating nerve growth factor levels in relation to obesity and the metabolic syndrome in women. Eur. J. Endocrinol. **157**, 303–310

Chaldakov G. N., Tonchev A. B., Tuncel N., Atanassova P., Aloe L. (2000): Adipose tissue and mast cells. Adipokines as yin-yang modulators of inflammation. In: Nutrition and Health: Adipose Tissue and Adipokines in Health and Disease. (Eds. G. Fantuzzi and T. Mazzone), pp. 147–154, Humana Press, Totowa, New Jersey

Chaldakov G. N., Stankulov I. S., Hristova M., Ghenev P. I. (2003): Adipobiology of disease: adipokines and adipokine-targeted pharmacology. Curr. Pharm. Des. **9**, 1023–1031

Chaldakov G. N., Fiore M., Stankulov I. S., Manni L., Hristova M. G., Antonelli A., Ghenev P. I., Aloe L. (2004): Neurotrophin presence in human coronary atherosclerosis and metabolic syndrome: a role for NGF and BDNF in cardiovascular disease? Prog. Brain Res. **146**, 279–289

Chaldakov G. N. (2008): Cardiovascular adipobiology: a novel. Heart-associated adipose tissue in cardiovascular disease. Ser. J. Exp. Clin. Res. **9**, 81–88

Cirulli F., Pistillo L., de Acetis L., Alleva E., Aloe L. (1998): Increased number of mast cells in the central nervous system of adult male mice following chronic subordination stress. Brain, Behav., Immun. **12**, 123–133

De Simone R., Alleva E., Tirassa P., Aloe L. (1990): Nerve growth factor released into the bloodstream following intraspecific fighting induces mast cell degranulation in adult male mice. Brain, Behav., Immun. **4**, 74–81

El-Gharbawy A. H., Adler-Wailes D. C., Mirch M. C., Theim K. R., Ranzenhofer L., Tanofsky-Kraff M., Yanovski J. A. (2006): Serum brain-derived neurotrophic factor concentrations in lean and overweight children and adolescents. J. Clin. Endocrinol. Metab. **91**, 3548–3552

Fiore M., Amendola T., Triaca V., Alleva E., Aloe L. (2005): Fighting in the aged male mouse increases the expression of TrkA and TrkB in the subventricular zone and in the hippocampus: implication for neurogenesis. Behav. Brain Res. **157,** 351–362

Fiore M., Laviola G., Aloe L., Di Fausto V., Mancinelli R., Ceccanti M. (2009): Early exposure to ethanol but not red wine at the same alcohol concentration induces behavioral and brain neurotrophin alterations in young and adult mice. Neurotoxicology **30,** 59–71

Generini S., Tuveri M. A., Matucci Cerinic M., Mastinu F., Manni L., Aloe L. (2004): Topical application of nerve growth factor in human diabetic foot ulcers. A study of three cases. Exp. Clin. Endocrinol. Diabetes **112**, 542–544

Geroldi D., Minoretti P., Emanuele E. (2006): Brain-derived neurotrophic factor and the metabolic syndrome: more than just hypothesis. Med. Hypotheses **67**, 195–196

Hausman G. J., Poulos S. P., Richardson R. L., Barb C. R., Andacht T., Kirk H. C., Mynatt R. L., Crandall D., Hreha A. (2006): Secreted proteins and genes in fetal and neonatal pig adipose tissue and stromal-vascular cells. J. Anim. Sci. **84**, 1666–1681

Hristova M., Aloe L., Ghenev P. I., Fiore M., Chaldakov G. N. (2001): Leptin and mast cells: a novel adipoimmune link. Turk. J. Med. Sci. **31**, 581–583

Kos K., Harte A. L., James S., Snead D. R., O'Hare J. P., McTrenan P. G., Kumar S. (2007): Secretion of neuropeptide Y in human adipose tissue and its role in maintenance of adipose tissue mass. Am. J. Physiol., Endocrinol. Metab. **293**, E1335–1340

Larrieta M. E., Vital P., Mendoza-Rodríguez A., Cerbon M., Hiriart M. (2006): Nerve growth factor increases in pancreatic beta cells after streptozotocin-induced damage in rats. Exp. Biol. Med. **231**, 396–402

Lebrun B., Bariohay B., Moyse E., Jean A. (2006): Brain-derived neurotrophic factor (BDNF) and food intake regulation: a minireview. Auton. Neurosci. **126**, 30–38

Levi-Montalcini R. (1987): The nerve growth factor 35 years later. Science **217**, 1154–1162

Manni L., Nikolova V., Vyagova D., Chaldakov G. N., Aloe L. (2005): Reduced plasma levels of NGF and BDNF in patients with acute coronary syndromes. Int. J. Cardiol. **102**, 169–171

Manni L., Di Fausto V., Chaldakov G. N., Aloe L. (2007): Brain leptin and nerve growth factor are differently affected by stress in male and female mice: possible neuroendocrine and cardio-metabolic implications. Neurosci. Lett. **426**, 39–44

Ryan V. H., German A. J., Wood I. S., Morris P., Trayhurn P. (2008): NGF gene expression and secretion by canine adipocytes in primary culture: upregulation by the inflammatory mediators LPS and TNF-α. Horm. Metab. Res. **40**, 1–8

Sacks H. S., Fain J. N. (2007): Human epicardial adipose tissue: a review. Am. Heart. J. **153**, 907–917

Sornelli F., Fiore M., Chaldakov G. N., Aloe L. (2007): Brain-derived neurotrophic factor: a new adipokine. Biomed. Rev. **18**, 85–88

Sposato V., Manni L., Chaldakov G. N., Aloe L. (2007): Streptozotocin-induced diabetes is associated with cahnges in NGF levels in pancreas and brain. Arch. Ital. Biol. **145**, 87–97

Töre F., Tonchev A. B., Fiore M., Tuncel N., Atanassova P., Aloe L., Chaldakov G. N. (2007): From adipose tissue protein secretion to adipopharmacology of disease. Immunol. Endocr. Metab. Agents. Med. Chem. **7,** 149–155

Trayhurn P., Wang B., Wood I. S. (2008): Hypoxia in adipose tissue: a basis for the dysregulation of tissue function in obesity? Br. J. Nutr. **100**, 227–235

Unger T. J., Calderon G. A., Bradley L. C., Sena-Esteves M., Rios M. (2007): Selective deletion of BDNF in the ventromedial and dorsomedial hypothalamus of adult mice results in hyperphagic behavior and obesity. J. Neurosci. **27**, 14265–1474

Wang B., Wood I. S., Trayhurn P. (2008): PCR arrays identify metallothionein-3 as a highly hypoxia-inducible gene in human adipocytes. Biochem. Biophys. Res. Commun. **368**, 88–93

Yamanaka M., Itakura Y., Inoue T., Tsuchida A., Nakagawa T., Noguchi H., Taiji M. (2006): Protective effect of brain-derived neurotrophic factor on pancreatic islets in obese diabetic mice. Metabolism **55**, 1286–1292

Insulin resistance and chronic inflammation are associated with muscle wasting in end-stage renal disease patients on hemodialysis

Zorica Rašić-Milutinović[1], Gordana Peruničić-Peković[2], Danijela Ristić-Medić[3], Tamara Popović[3], Maria Glibetić[3] and Dragan M. Djurić[4]

[1] *Department of Endocrinology, Diabetes and Metabolism, University Hospital Zemun, Belgrade, Serbia*
[2] *Department of Hemodialysis, University hospital Zemun, Belgrade, Serbia*
[3] *Institute for Medical Research, Laboratory for Nutrition and Metabolism, Belgrade, Serbia*
[4] *Institute for Medical Physiology, Medical Faculty, University of Belgrade, Serbia*

Abstract. Muscle wasting is independent predictor of mortality in end-stage renal disease (ESRD) patients on maintenance hemodialysis (MHD). We investigated the effect of insulin resistance on lean body mass (LBM), and association between insulin resistance, chronic inflammation, and body composition in these patients. We analyzed cross-sectionally body composition, nutritional status and biochemical parameters in 35 non-diabetic ESRD patients who were on MHD. Bioelectrical impedance analysis was performed to quantify body fat, lean body mass and total body water (FAT (%), FAT (kg), LBM (%), LBM (kg) and TBW(%)). The association between LBM (kg) and gender, FAT (kg), high sensitivity C-reactive protein (hs-CRP), and homeostatic model assessment score (HOMA-IR) was recorded. Multiple linear regression analysis using LBM (kg) as dependent variable showed that FAT (kg) ($\beta = 0.563$, $p = 0.05$), HOMA-IR ($\beta = 0.619$, $p = 0.03$), and hs-CRP ($\beta = 0.488$, $p = 0.04$) were independently associated with LBM in males. In females, only FAT (kg) ($\beta = 0.648$, $p = 0.001$) significantly predicted LBM. Those variables explained 37% of variance of LBM (kg) in males, and 44% in females. It seems that insulin resistance participates independently in the pathogenesis of muscle wasting in both sexes, particularly in males. The effect of chronic inflammation was not so strong in females, and this point out that regulation of muscle wasting in female patients probably differs from that in males.

Key words: Insulin resistance — Muscle wasting — Chronic inflammation — End-stage renal disease

Introduction

Insulin plays a pivotal role in regulating body protein metabolism. Insulin deficiency, as seen in untreated type 1 diabetes mellitus (T1DM) is associated with increased skeletal muscle catabolism (Felig et al. 1977) and urinary nitrogen loss. In humans, systemic insulin administration inhibits muscle protein breakdown in patients with T1DM (Pacy et al. 1991) and in healthy subjects (Toffolo et al. 2003). Chow et al. (2006) confirmed that normal physiological levels of insulin inhibit muscle protein breakdown as well as exert stimulatory effect on muscle protein synthesis. Ikizler et al. (1994) demonstrated that hemodialysis (HD) is a catabolic event, decreasing circulating amino acids, accelerating rates of whole body and muscle proteolysis, stimulating muscle release of amino acids, elevating net whole body and muscle protein loss, and increasing energy expenditure.

It is known that complex syndrome of uremia can trigger muscle protein breakdown including metabolic acidosis, decreased insulin action, increased glucocorticoid production, high levels of angiotensin II, and inflammation (Pupim et al. 2005; Song et al. 2005). A common cellular signaling pathway is a decrease in phosphatidylinositol 3-kinase (PI3K) activity. Reduced PI3K-Akt signaling enhances protein breakdown in muscle (Du and Mitch 2005).

In the present study we examined the relationship between insulin resistance, as measured by HOMA-IR, inflam-

Correspondence to: Zorica Rasic-Milutinovic, Department of Endocrinology, Diabetes and Metabolism, University hospital Zemun, Vukova 9, 11080 Belgrade, Serbia
E-mail: zoricar@eunet.yu

matory marker, as measured by high sensitivity C-reactive protein (hs-CRP), and lean body mass (LBM) of maintenance hemodialysis (MHD) patients.

Materials and Methods

Subjects

The study group included 35 (20 male and 15 female), sex and age-matched, stable (their body weight had been stable for at least 6 months before the study) end-stage renal disease (ESRD) patients on MHD, with median dialysis duration of 48 months (inter quartiles range (IQR) 24.0–82.0). Exclusion criteria were: diabetes mellitus, cardiac failure (NYHA III or IV), acute myocardial infarction and acute infective disorders during 3 months before the inclusion. They were not obese and without severe malnutrition (BMI was between 20 and 30 kg/m^2). Patients were dialyzed with synthetic membranes and a bicarbonate dialysate with 1.25, 1.5 or 1.75 mmol/l calcium according to the serum calcium-phosphate equilibrium and with obligatory use of 1,25-dihydroxy vitamin D3 to control the parathyroid hormone (PTH) levels. The duration of HD was individually tailored (thrice weekly) to control body fluids and blood chemistries and with aim to achieve an adequate dose of dialysis Kt/v > 1.2 (1.46 ± 0.13). Patients regularly did not receive erythropoietin therapy at that time, because health insurance didn't pay it. Antihypertensive drugs were prescribed when necessary to obtain pre-dialysis blood pressure <160/90 mmHg. None of the patients received lipid lowering drugs, β-blockers, L-carnitine or vitamin B_{12} during 3 months before the inclusion. Calcium carbonate ($CaCO_3$) was used to try to obtain pre-dialysis serum phosphate level <2.0 mmol/l. All patients were sedentary (<1 h/week of physical activity), free of alcohol abuse and non-smokers. They maintained their habitual diets (35 kcal/kg b.w., protein intake 1.01–2 g/kg b.w., fats <35% caloric intake) with sodium and potassium restriction. Each patient gave informed written consent to participate in the study, which was approved by the Institutional Ethic Committee.

Methods

The study was cross-sectionally designated. To determine the nutritional status, body composition and the presence of inflammation of HD patients, the following methods were used: subjective global assessment (SGA); anthropometric measurements, including BMI and waist circumference, which were recorded by a standardized protocol (dry weight or post dialysis weight was used for calculating BMI); bioelectrical impedance analysis was performed to quantify body fat (FAT (%), FAT (kg)), LBM (%), LBM (kg), total body water (TBW (%)) using a body fat analyser TBF-110 (Tanita, Japan); biochemical parameters measurements (levels of serum albumin, hemoglobin, ferritin, i-PTH, TNF-α, IL-6, hs-CRP, glucose and insulin). The blood samples were also taken for the determination of the red blood cell phospholipids fatty acids composition. SGA is a clinical method for evaluating nutritional status, including history, symptoms, and physical parameters. The history used in the SGA focuses on 5 areas: body weight, dietary intake, gastrointestinal symptoms, functional capacity, and disease state. The percentage of body weight lost in the previous 6 months is characterized as mild (<5%), moderate (5–10%), or severe (>10%). Dietary intake is classified as normal or abnormal as judged by a change in intake and whether the current diet is nutritionally adequate. The presence of persistent gastrointestinal symptoms such as anorexia, nausea, vomiting, diarrhea, and abdominal pain for at least 2 weeks is recorded. In addition to the medical history, there is also a physical examination, which is noted as normal, mild, moderate, or severe alterations. The loss of subcutaneous fat is evaluated in the triceps region and the midaxillary line at the level of the lower ribs. These measurements are not precise but are merely a subjective impression of the degree of subcutaneous tissue loss. The second feature is muscle wasting in the temporal areas and in the deltoids and quadriceps, as determined by loss of bulk and tone detectable by palpation. A neurologic deficit will interfere with this assessment. The presence of edema in the ankle and sacral regions and the presence of ascites are noted. Coexisting disease such as heart failure will modify the weight placed on the finding of edema. The findings of the history and physical examination are used to categorize patients as having very mild malnutrition to being well nourished (SGA-A score), having moderate or suspected malnutrition (SGA-B score) , or having severe malnutrition (SGA-C score). Fluid shifts or ascites must be considered when interpreting changes in body weight. Laboratory measurements, the level of glucose, albumin, hemoglobin and iron were assessed with a convential autoanalyzer, using blood samples obtained midweek, after overnight fasting and immediately prior to dialysis. Serum ferritin was measured using an imunoradiometric assay. The levels of i-PTH were assessed using immunoradiometric assay (CIS-Bio) and plasma insulin levels were measured using a radioimmunoassay method (INEP Zemun, Belgrade). IL-6 and TNF-α concentrations were measured in duplicate by Immunotech IL-6 immunoassays and Immunotech TNF-α immunoassays (Beckman Counter^{TM}). hs-CRP was measured by the Olympus (Latex) assay on the Olympus AU 400 analyzer. Insulin resistance index was calculated from fasting insulin and glucose concentration using HOMA-IR (Matthews et al. 1985).

Statistical analysis

Before statistical analysis, normal distribution of the variances was evaluated using the Kolmogorov-Smirnov test. Descriptive results are expressed as mean ± SD or as median and IQR, depending on whether the distribution was normal or skewed. The values of insulin, HOMA-IR, hs-CRP, and i-PTH were log transformed to achieve a normal distribution. The Pearson's correlation and simple regression analysis were used to evaluate the association between measured variables and LBM (kg). Demographic characteristics (age and sex), serum albumin and creatinine concentrations were considered as potential confounders of the relation between LBM (kg) measures and markers of insulin resistance, inflammation and body composition. All p values were based on a two-sided test of statistical significance. Significance was accepted at the level of $p < 0.05$. Statistical analyses were performed with the SSPS statistical package, version 15 (SPSS, Chicago, IL).

Table 1. Baseline demographic, nutritional characteristics and body composition

Variable	Male	Female	p
Sex	20 (57.14%)	15 (38.86%)	0.40
Age (years)	55.74 ± 13.11	54.11 ± 10.76	0.54
Duration of HD (years)	60 (34–28)	39 (23.50–67)	0.21
Kt/v	1.26 ± 0.18	1.38 ± 0.23	0.62
Body weight (kg)	67.08 ± 8.43	58.93 ± 9.10	0.60
BMI (kg/m^2)	21.40 ± 2.92	23.35 ± 2.91	0.58
Waist (cm)	87.30 ± 8.51	85.7 ± 11.52	0.16
FAT (kg)	8.99 ± 5.81	17.6 ± 8.47	0.01
LBM (kg)	39.08 ± 18.92	24.51 ± 5.49	0.04
SGA-A (%)	9 (39)	11 (75)	0.03

Values are presented as mean ± SD for normally distributed data, median and IQR for non-normally distributed data, and percentages as appropriate. HD, hemodialysis; Kt/v, number used to quantify hemodialysis adequacy; BMI, body mass index; FAT, fat mass; LBM, lean body mass; SGA-A (%), subjective global assassement-A group.

Results

The baseline characteristics of the 35 patients, 20 men and 15 women, on MHD, who completed the study, are presented in Table 1. The two groups (men and women) were with similar age and BMI, but women, as expected, had more FAT (kg), and smaller amount of LBM (kg), than men (Table 1). On the opposite, according to SGA assessment the majority of men were mild to moderate malnourished (69%), then women (25%). Biochemical parameters, as albumin, creatinine, glucose, insulin and inflammatory markers: hs-CRP, TNF-α, IL-6 and fibrinogen, did not differ between groups. Despite exclusion of patients with diabetes mellitus and obesity, the median (interquartile range) HOMA-IR score was 9.25 (6.45–12.32) and 12.11 (6.45–17.05), respectively (Table 2). We recorded strong association between IL6 and FAT (kg) ($r = 0.462$, $p = 0.04$), only in women, and association between TNF-α and FAT (kg) ($r = 0.331$, $p = 0.08$) was with borderline significance, for these patients. By linear regression analysis we evaluated the correlation between measured variables and LBM (kg) in the both groups. LBM (kg) correlated significantly with sex, age, BMI, FAT (kg), hs-CRP, fibrinogen, albumin, creatinine and HOMA-IR (data are not showed).

To determine the independent factors responsible for LBM (kg), for both sexes, respectively, we performed multivariate analysis, including the abovementioned variables in a model. After adjustment for age, Kt/v, fibrinogen, serum albumin and creatinine, the association between the LBM

Table 2. Basaline biochemical analysis of study patients

Variable	Male	Female	p
Serum albumin (g/l)	32.21 ± 13.63	32.56 ± 2.58	0.25
Serum hs-CRP (mg/l)	3.53 (1.42–12.8)	3.62 (0.84–7.14)	0.65
Serum TNF-α (pg/ml)	2.30 (1.24–2.82)	2.04(0.37–2.80)	0.24
Serum IL-6 (pg/ml)	3.23 (1.06–9.60)	1.60 (1.15–5.04)	0.37
Serum fibrinogen (g/l)	3.40 ± 0.60	3.02 ± 0.69	0.65
i-PTH (pg/ml)	454.40 (96.92–905.25)	172.55 (7.95–423.22)	0.17
Serum creatinine (μmol/l)	328.34 ± 38.60	253.20 ± 41.32	0.09
Serum glucose (mmol/l)	5.58 ± 11.21	5.54 ± 1.03	0.35
Serum insulin (mU/l)	34.20 (26.80–43.00)	55.10 (28.10–69.90)	0.25
HOMA-IR	9.25 (6.45–12.32)	12.11 (6.45–17.05)	0.30

Values are presented as mean ± SD for normally distributed data, median and IQR for non-normally distributed data.

(kg) and independent variables (FAT (kg), HOMA-IR and hs-CRP) explained 37% of variation of LBM in men (Table 3). The similar association was established in women, where the same independent predictors (FAT (kg), HOMA IR and hs-CRP) predicting LBM (kg) (hs-CRP with borderline significance), indicating an even stronger association, and explained 44% of variation of LBM (Table 4).

Table 3. Association between LBM and FAT, insulin resistance and hs-CRP in males

Variable	β	*p*
FAT (kg)	0.563	0.05
HOMA-IR	–0.619	0.03
hs-CRP	–0.488	0.04

Adjusted $R^2 = 0.37$, $p = 0.04$.

Table 4. Association between LMB and FAT, insulin resistance and hs-CRP in females

Variable	β	*p*
FAT (kg)	0.648	0.001
HOMA-IR	–0.496	0.05
hs-CRP	–0.341	0.06

Adjusted $R^2 = 0.44$, $p = 0.01$.

Discussion

The current study demonstrated that insulin resistance, together with total fat mass and chronic inflammation measured by hs-CRP could be independent predictor for LBM in non-diabetic chronic dialysis patients. Chevalier et al. (2005) has demonstrated the presence of insulin resistance and enhanced whole-body protein catabolism in young healthy obese women compared to lean women during the post-absorptive state. Although, our patients were not obese, men and women, separately, have many reasons for the presence of insulin resistance including acidosis, chronic inflammation, anemia, higher level of serum iron and iron stores (Rašić-Milutinović et al. 2000, 2007a,b, 2008). We studied non-obese middle-aged and older ESRD patients where many factors including acidosis, inflammation, and dialysis itself are known to influence visceral protein stores. Our results indicate that in the absence of diabetes, or obesity (BMI < 30), insulin resistance is evident in the HD patients and inversely correlates with LBM, a relationship that persists even after adjustment for fat mass and chronic inflammation. That association is stronger in male patients.

Many studies have attempted to explain the loss of protein stores, and especially the loss of muscle mass in ESRD patients. Siew et al. (2007) concluded that insulin resistance significantly contributes to the enhanced muscle protein catabolism observed in MHD patients. Investigations by tracer kinetic models and insulin clamp techniques in healthy individuals have detailed that it remains the blunting of proteolysis rather than enhanced protein synthesis is net protein anabolic effect of insulin in the post-absorptive state (Gelfand and Barrett 1987; Chow et al. 2006). The increase in muscle protein degradation in uremia and most other catabolic disease states is mostly due to programmed activation of the ubiquitin-proteasome system (UPS) (Rajan and Mitch 2008). The underlying mechanism demonstrated by Du and Mitch (2005) appears to be suppression of insulin receptor substrate-1-associated phosphatidylinositol 3-kinase activity resulting in stimulation of the UPS *via* caspase-3. The present results underline an independent role of insulin resistance in muscle protein metabolism, and in agreement with the findings of other authors, that have shown the contribution of insulin resistance to muscle atrophy in HD patients, through defects in insulin receptor signaling (Lee et al. 2007) independently of total fat mass.

It is generally accepted that obesity produces insulin resistance, through the induction of peripheral disruption of insulin signaling pathways by increasing the level of circulating free fatty acids (FFA) and inflammatory mediators. As the largest endocrine organ, adipose tissue is able to regulate various biological processes through adipose-derived signaling proteins termed adipokines (Chaldakov et al. 2003), insulin sensitivity, feeding behavior and the sequestration of FFA as triglycerides also being targeted (Guilherme et al. 2008). Evidence based from humans as well as animal models shows that increased concentrations of inflammatory markers are associated with insulin resistance and reduction in lean mass (Garcia-Martinez et al. 1993; Mayer-Davis et al. 1998). We showed that plasma concentrations of hs-CRP were inversely associated with muscle mass, significantly only in men on HD. Our results confirm data from previous studies demonstrating a relation between BMI and total fat mass and markers of inflammation in ESRD patients (Stenvinkel et al. 1999). Based on these observations, we hypothesized that insulin resistance significantly contributes to the enhanced muscle protein catabolism observed in MHD patients, particularly men. Male patients were significantly mild to moderate malnourished (61%), with lower total fat mass and LBM, but without any differences for peripheral insulin resistance compared to women. That emphasize that the association between insulin resistance and LBM remained significant, independently of fat mass, in male group. In female group, the association between insulin resistance and LBM is weaker, and total fat mass is strongest independent predictors for LBM. Inflammatory cytokines of female patients, particularly IL-6, correlated with insulin resistance, and total

fat and we could explain its effect more as those of adipokines. Obviously, some of cytokines appear negative effect on LBM indirectly, by potentiating insulin resistance. Wang et al. (2006) have recently demonstrated in an animal model that the enhanced muscle proteolysis associated with insulin resistance appears to be reversible with the administration of the peroxisome proliferator-activated receptor-gama agonist Rosiglitazone. These results need to be extended to human studies. However, the reduction of insulin resistance by supplemented n-3 PUFAs in ESRD patients (Rasic-Milutinovic et al. 2007) may contribute to muscle wasting. Kato et al. (2003) found significantly higher prevalence of cardiovascular (63 vs. 25%) and pulmonary deaths (30 vs. 0%) in men on regular HD, with lower limb/trunk lean mass (LTLM) ratio, and he revealed that reduced LTLM ratios were significant determinants of 5 year mortality in men. Kalantar-Zadeh et al. (2004) examined the predictability of markers of the malnutrition-inflammation complex syndrome (MIS) in HD patients and concluded that MIS score and CRP were the only variables to have statistically significant associations with mortality and hospitalization.

Our results should be interpreted with some limitations. At first, the cross-sectional design of the study did not allow us to investigate the cause-effect relation between markers of insulin resistance, inflammation and body-composition measures.

In conclusion, it has been observed that ESRD patients on MHD are at risk for a progressive loss in LBM not entirely accounted for by inadequate nutrient intake alone. The results of this study indicate that insulin resistance and inflammation in ESRD may be an important contributor to protein wasting that represents a novel target for intervention.

References

Chaldakov G. N., Stankulov I. S., Hristova M., Ghenev P. I. (2003): Adipobiology of disease: adipokines and adipokine-targeted pharmacology. Curr. Pharm. Des. **9**, 1023–1031

Chevalier S., Marliss B. E., Morais J. A., Lamarche M., Gougeon R. (2005): Whole-body protein anabolic response is resistant to the action of insulin in obese women. Am. J. Clin. Nutr. **82**, 355–365

Chow L. S., Albright R. C., Bigelow M. L., Toffolo G., Cobelli C., Nair K. S. (2006): Mechanism of insulin's anabolic effect on muscle – measurements of muscle protein synthesis and breakdown using aminoacyl tRNA and other surrogate measures. Am. J. Physiol., Endocrinol. Metab. **291,** E729–736

Du J., Mitch W. E. (2005): Identification of pathways controlling muscle protein metabolism in uremia and other catabolic conditions. Curr. Opin. Nephrol. Hypertens. **14,** 378–382

Felig P., Wahren J., Sherwin R., Palaiologos G. (1977): Amino acid and protein metabolism in diabetes mellitus. Arch. Intern. Med. **137,** 507–513

Garcia-Martinez C., Lopez-Soriano F. J., Argiles J. M. (1993): Acute treatment with tumor necrosis factor-alpha induces changes in protein metabolism in rat skeletal muscle. Mol. Cell. Biochem. **125,** 11–18

Gelfand R. A., Barrett E. J. (1987): Effect of physiologic hyperinsulinemia on skeletal muscle protein synthesis and breakdown in man. J. Clin. Invest. **80**, 1–6

Guilherme A., Virbasius J. V., Puri V., Czech M. P. (2008): Adipocyte dysfunctions linking obesity to insulin resistance and type 2 diabetes. Nat. Rev. Mol. Cell Biol. **9,** 367–377

Ikizler T. A., Flakoll P. J., Parker R. A., Hakim R. M. (1994): Amino acid and albumin losses during hemodialysis. Kidney Int. **46,** 830–837

Kalantar-Zadeh K., Kopple J. D., Humphreys M. H., Block G. (2004): Comparingoutcome predictability of markers of malnutrition-inflammation complex syndrome in haemodialysis patients. Nephrol. Dial. Transplant. **19,** 1507–1519

Kato A., Odamaki M., Yamamoto T., Yonemura K., Maruyama Y., Kumagai H., Hishida A. (2003): Influence of body composition on 5 year mortality in patients on regular haemodialysis. Nephrol. Dial. Transplant. **18**, 333–340

Lee S. W., Park G. H., Lee S. W., Song J. H., Hong K. C., Kim M. J. (2007): Insulin resistance and muscle wasting in non-diabetic end-stage renal disease patients. Nephrol. Dial. Transplant. **22,** 2554–2562

Matthews D. R., Hosker J. P., Rudenski A. S., Naylor B. A., Treacher D. F., Turner R. C. (1985): Homeostasis model assessment: insulin resistance and B-cell function from fasting plasma glucose and insulin concentrations in man. Diabetologia **28**, 412–419

Mayer-Davis E. J., D'Agostino R. J., Karter A., Haffner S. M., Rewers M. J., Saad M., Bergman R. N. (1998): Intensity and amount of physical activity in relation to insulin sensitivity: the insulin resistance atherosclerosis study. JAMA **279**, 669–674

Pacy P. J., Bannister P. A., Halliday D. (1991): Influence of insulin on leucine kinetics in the whole body and across the forearm in post-absorptive insulin dependent diabetic (type 1) patients. Diabetes Res. **18,** 155–162

Pupim L. B., Heimburger O., Qureshi A. R., Ikizler T. A., Stenvinkel P. (2005): Accelerated lean body mass loss in incident chronic dialysis patients with diabetes mellitus. Kidney Int. **68**, 2368–2374

Rajan V. R., Mitch W. E. (2008): Muscle wasting in chronic kidney disease: the role of the ubiquitin proteasome system and its clinical impact. Pediatr. Nephrol. **23,** 527–535

Rašić-Milutinović Z., Peruničić G., Plješa S. (2000): Clinical significance and pathogenetic mechanisms of insulin resistance in chronic renal insufficiency (part two): pathogenetic factors of insulin resistance in chronic renal insufficiency. Med. Pregl. **53**, 159–163 (in Serbian)

Rašić-Milutinović Z., Peruničić-Peković G., Plješa S., Gluvić Z., Ilić M., Stokić E. (2007a): Metabolic syndrome in HD patients: association with body composition, nutritional status, inflammation and serum iron. Intern. Med. **46,** 945–951

Rašić-Milutinović Z., Peruničić-Peković G., Plješa S., Gluvić Z., Sobajić S., Djurić I., Ristić D. (2007b): Effects of N-3 PUFAs supplementation on insulin resistance and inflammatory biomarkers in hemodialysis patients. Ren. Fail. **29**, 321–329

Rašić-Milutinović Z., Peruničić-Peković G., Plješa S., Čavala A., Gluvić Z., Bokan Lj., Stanković S. (2008): The effect of recombinant human erythropoietin treatment on insulin resistance and inflammatory markers in non-diabetic patients on maintenance hemodialysis. Hippokratia **12,** 157–161

Siew E. D., Pupim L. B., Majchrzak K. M., Shintani A., Flakoll P. J., Ikizler T. A. (2007): Insulin resistance is associated with skeletal muscle protein breakdown in non-diabetic chronic hemodialysis patients. Kidney Int. **71**, 146–152

Song Y. H., Li Y., Du J., Mitch W. E., Rosenthal N., Delafontaine P. (2005): Muscle-specific expression of insulin-like growth factor-1 blocks angiotensin II-induced skeletal muscle wasting. J. Clin. Invest. **115**, 451–458

Stenvinkel P., Heimburger O., Paultre F., Diczfalusy U., Wang T., Berglund L., Jogestrand T. (1999): Strong association between malnutrition, inflammation and atherosclerosis in chronic kidney failure. Kidney Int. **55,** 1899–1911

Toffolo G., Albright R., Joyner M., Dietz N., Cobelli C., Nair K. S. (2003): Model to assess muscle protein turnover: domain of validity using amino acyl-tRNA vs. surrogate measures of precursor pool. Am. J. Physiol., Endocrinol. Metab. **285,** E1142–1149

Wang X., Hu Z., Hu J., Du J., Mitch W. E. (2006): Insulin resistance accelerates muscle protein degradation: activation of the ubiquitin-proteasome pathway by defects in muscle cell signaling. Endocrinology **147,** 4160–4165

Serum and erythrocyte membrane phospholipids fatty acid composition in hyperlipidemia: effects of dietary intervention and combined diet and fibrate therapy

Danijela Ristic-Medic[1], Slavica Suzic[2], Vesna Vucic[1], Marija Takic[1], Jasna Tepsic[1] and Marija Glibetic[1]

[1] *Institute for Medical Research, Laboratory for Nutrition and Metabolism, University of Belgrade, Serbia*
[2] *Institute for Physiology, School of Medicine, Belgrade, Serbia*

Abstract. Hyperlipidemia is found to be associated with changes in fatty acid (FA) profiles. The aim of this study was to investigate the effects of AHA-Step-1 dietary treatment and combination of fibrates (gemfibrozil) with dietary intervention on serum and erythrocyte phospholipid FA composition in human hyperlipidemia. 78 study participants with hyperlipidemia were divided in two groups. In D group (n = 41) subjects followed AHA-Step-1 diet (<30% of total from fat, <10% of energy from saturated fat, and <300 mg cholesterol per day). D+F group (n = 37) followed Step-1 diet and were receiving gemfibrozil (300 mg/twice per day). Serum lipid levels and phospholipid serum and erythrocyte FA compositions were analyzed at the beginning and after 12 weeks of treatment. Alteration in serum and erythrocyte phospholipid FA profile were found in both groups. After both treatments we found significantly higher serum phospholipid percentages of n-3, n-6 and total polyunsaturated FA. Linoleic (LA, n-6) and docosahexaenoic acid (DHA, n-3) were higher in D group, but arachidonic (AA, n-6) and linolenic acid (LNA, n-3) in D+F group. In erythrocyte phospholipid levels of stearic, palmitoleic (16 : 1, n-7) and LA were significantly higher in D group, but palmitic acid, AA and eicosapentaenoic acid (EPA, n-3) in D+F group. Stronger correlation between serum triglycerides with EPA and DHA in erythrocyte membrane phospholipid was found in D+F group. Markedly increased percentage of AA in serum and erythrocyte membrane phospholipid in hyperlipidemic patients receiving gemfibrozil on Step-1 diet is especially important for physiological functions (inflammation, vascular tone, hemostasis etc.) in relation to cardiometabolic risk.

Key words: AHA-Step-1 diet — Gemfibrozil — Fatty acids — Phospholipids — Erythrocyte

Introduction

Dietary fat intake is a risk factor for coronary heart disease and the modification of dietary habits is important for the prevention of cardiovascular disease (CVD) (Grundy and Denke 1990; Lichtenstein et al. 2002). The assessment of dietary fat intake is a critically important first step in clinical decision-making regarding dietary and pharmacotherapeutic advice on coronary risk reduction. Large intakes of saturated fatty acids (SFA) and cholesterol together with low dietary levels of polyunsaturated fatty acid (PUFA), particularly long-chain n-3 PUFA, appear to have a great impact on the development of CVD (Hodson et al. 2001; Lichtenstein et al. 2002). A high dietary n-6/n-3 PUFA ratio is also considered as a marker of elevated risk of CVD, though little data on dietary intake is available (de Lorgeril and Salen 2003).

Biomarkers of essential fatty acid (FA) are among the best available biomarkers of previous dietary FA intakes (Sarkkinen et al. 1994; Bingham 2002). They offer an objective alternative to dietary assessment because they reflect actual, rather than reported intake, thus avoiding, for example, the particular problems in dietary assessment of under or over reporting food consumption or quantifying "hidden fats" in the diet (Bingham 2002; Arab 2003). Under homeostatic weight conditions and if

Correspondence to: Danijela Ristic-Medic, Institute for Medical Research, Laboratory for Nutrition and Metabolism, University of Belgrade, 11 129 Belgrade, Serbia
E-mail: dristicmedic@gmail.com
danijelar@imi.bg.ac.yu

properly sampled, collected and analyzed, the biomarkers can represent long-term intakes of individual fats, what appears to be a more objective marker for dietary intake than dietary questionnaire assessment (Rivellese et al. 2002). Concentration of essential n-6 and n-3 PUFA in cell membrane or in serum phospholipids are highly correlated with dietary intake (Ma et al. 1995; Arab 2003). Erythrocytes are a better long-term marker of dietary FA intake than platelet or plasma lipids because the turnover of erythrocytes (120-day lifespan) is much slower than that of platelets (10 days) (Arab 2003).

In addition, high serum cholesterol is a well-known primary risk factor for coronary heart disease (Wood et al. 1998; Yu-Poth et al. 1999). For this reason the US National Cholesterol Education Program recommendations for general population are as follows: total dietary fat should be reduced to 30% or less, saturated fat intake to 10% or less of total calories and daily dietary cholesterol intake has to be limited to 300 mg (Yu-Poth et al. 1999; NCEP Panel III 2001). These guidelines are consistent with the World Health Organization dietary recommendations for prevention of chronic diseases (see References:WHO 2003).

The attention of pharmacologists and clinicians to fibrates has been renewed in recent years in light of their multifaceted action on plasma lipids. Cardioprotective effects of fibrates such as gemfibrozil in the HHS and VA-HIT studies were substantially greater than those found with other fibrates in WHO, BIP and FIELD studies (Barter and Rye 2006; Asztalos et al. 2008). Fibrates are lipid lowering drugs that act as peroxisome proliferator-activated receptor-α (PPAR-α) agonist and are currently used in clinical settings to improve atherogenic lipid profiles (Formann et al. 1997; Schindler 2007). PPAR-α serves as a FA sensor (clear preference for PUFA) and as an important regulator of FA metabolism and energy homeostasis (see review article Krey et al. 1997; Kersten 2008). Strong evidence suggests that FA are major dietary constituents in the regulation of gene expression in response to food intake and qualitative nutritional changes (Kliewer et al. 1997; Kersten 2008). Only limited information exists on interaction between diet, fibrates and FA profile in human hyperlipidemia (Agheli and Jacotot 1991; Tavella et al. 1993; Nyuala et al. 2008).

The aim of this study was to investigate the effects of American Heart Association (AHA)-Step-1 dietary treatment and combined effects of fibrates (gemfibrozil) with dietary intervention on serum and erythrocyte phospholipid composition, as well as their interrelationship with plasma lipid concentration.

Materials and Methods

Study population

A total of 379 individuals were screened for enrolment in the study at the Department of Nutrition and Metabolism of the Institute for Medical Research in Belgrade. All participants received a full medical examination and standard laboratory blood tests were performed before enrolment. The participants were eligible for the study on the basis of the following criteria: 1. being between 45 and 65 years of age; 2. a body mass index (BMI) <32 and weight stable (±2 kg) for 6 months prior to the beginning of the study; 3. normal fasting glucose levels according to WHO criteria (fasting glucose <6.1 mmol/l); 4. mild hyperlipidemia as defined by total serum cholesterol 5.2–7.8 mmol/l, serum LDL-cholesterol 3.39–4.91 mmol/l and/or triglycerides levels 1.7–3.5 mmol/l. Fulfillment of these criteria was based on data obtained from two fasting serum lipid profiles taken one week apart.

Participants were not adhering to any special diet, were not on prescribed medication known to affect lipid metabolism (lipid lowering drugs, β-blockers, diuretics or hormones) nor did they take vitamin and/or mineral supplements in 12 weeks prior to the start of the study. Subjects that had evidence of any chronic disease, including hepatic, renal, cardiovascular and thyroid dysfunction, diabetes mellitus, uncontrolled hypertension, and known family lipid disorders (familiar combined hyperlipidemia or familiar hypercholesterolemia) were excluded. Individuals who smoked and those with an alcohol intake of more than 30 g per day were also excluded from the study.

78 free-living adults (25 man and 53 women) were selected fulfilling the criteria of the study design. The women were postmenopausal and were not taking hormone replacement therapy. All subjects consumed their habitual diet, typical for Serbian population, characterized by: low consumption of foods containing soy, fish intake once in two weeks and high animal fat intake (pork meat, eggs and whole milk products were consumed everyday) (Pavlovic et al. 2005). Study subjects did not take dietary supplementation of oils rich in long-chain FA (fish oil, sesame oil or linseed oil) at the time of recruitment, as it was determined by dietary assessment. Participants were either sedentary or moderately active as observed in a physical activity questionnaire.

All study participants signed an informed consent document and the whole study was approved by the Medical Ethics Committee (Institute for Medical Research, Belgrade) and conducted according to principles of the Declaration of Helsinki.

Study design

The participants were divided into two groups. In one group (D+F) were allocated subjects who agreed to take the prescribed lipid lowering drugs (fibrate gemfibrozil) from their cardiologist, in other group (D) were those who decided to try only the diet first. Participants were instructed to follow AHA-Step-1 diet (Yu-Poth et al. 1999).

Subjects in D group (n = 41) were on Step-1 diet for 12 weeks with no change in energy intake compared to their previous energy intake. In D+F group (n = 37) subjects were on Step-1 diet and additionally were taking gemfibrozil (300 mg/twice per day) for 12 weeks. Target intakes in NCEP AHA-Step-1 diet were less than 30% of energy gained from fat, 50–60% gained from carbohydrates and 20% from protein. Less than 10% of energy should come from saturated FA, 10% from PUFA and 12% of energy from monounsaturated FA (MUFA). Dietary cholesterol intake did not exceed 300 mg/day.

Information concerning dietary intake was obtained at the beginning of the study (the habitual diet) and at the end of the dietary intervention period using a semi-quantified food frequency questionnaire (FFQ). The FFQ contained 142 food items and beverages commonly consumed in Serbia. Dietary intake was prescribed individually according to data obtained from dietary questionnaires to maintain the initial caloric intake and nutrient proportions constant throughout the study. The main goal of the diet was to restrict both dietary total fat and daily cholesterol intake. The recommended food during the low-lipid diet included lean meat, fat-free or skimmed milk and low-fat dairy products, whole grain/high-fiber food, fruit and vegetables. Fish was suggested as a main meal twice a week. Restricted food included high-fat meat and dairy products, eggs, fried food, cream sauces, high-fat pastries and sweets. A registered dietitian provided assistance in adhering to the AHA-Step-1. Nutrient calculations were performed using US Department of Agriculture food composition tables (see References: USDA 2005) or Serbian food composition tables (Jokic et al. 1999) for certain local foodstuffs.

Body weight was measured weekly to determine whether subjects' weight remained stable, using a Tanita body composition analyzer (model TBF-300, Japan). Standing height was measured, while subjects were barefoot, to the nearest 0.5 cm using a wall-mounted statiometer. BMI was calculated by dividing the body mass in kg by the square of height in meters (kg/m^2). The subjects were encouraged to maintain their habitual level of physical activity through the intervention period. Two participants from group D left the study, for reasons unrelated to the study.

Biochemical Determination

Laboratory assays were determined on the day of the screening visit, on the day of randomization and after 12 weeks of treatment. Serum samples were prepared from venous blood collected after a 12–14 h fast. Blood was centrifuged on 4°C and serum was collected. Total cholesterol and triglyceride levels were measured in triplicate using a commercial colorimetric enzymatic reaction kits (EliTech Diagnostic, Sées, France). HDL-cholesterol was determined in supernatant liquid after precipitation with phosphotungstic acid and magnesium chloride (Lopes-Virela et al. 1977). LDL-cholesterol was estimated using Friedewald formula (Friedewald at al. 1972). Non-HDL cholesterol was calculated by subtracting HDL-cholesterol from total cholesterol. Serum lipids were extracted according to method of Sperry and Brand (Matusik et al. 1984), which uses chloroform-methanol mixture (2 : 1 v/v) with 10 mg/100 ml 2,6-di-tert-buthyl-4-methylphenol (BHT) added as an antioxidant. Red blood-cell lipids were extracted by the method of Harth (Harth et al. 1978). The phospholipids fraction was isolated from the lipid extract using one-dimensional thin-layer chromatography (TLC) in a neutral lipid solvent system hexane-diethyl ether-acetic acid (87:12:1, v/v/v) using Silica Gel GF plates (C. Merck, Darmstadt, Germany).

FA determination

Methyl esters of phospholipids FA were prepared by methods that have already been reported (Ristić Medić et al. 2003). Methyl esters derivatives were analyzed by gas chromatography using Varian GC (model 3400, Varian Associates) equipped with DB-23 (30 m × 0.53 mm i.d., film thickness 0.5 μm; J&W Scientific Inc. Bellefonte, Folsona, CA, USA) fused silica capillary column. The flame ionization detector was set at 250°C, the injection port at 220°C and the oven temperature programmed from 130 to 190°C, at a heating rate of 3°C/min. Analysis was performed in duplicate for each sample. Individual FA methyl esters were identified by comparing peak retention times with authentic standards (Sigma Aldrich, Germany) and/or the PUFA-2 standard mixtures (Supelco Inc., Bellefonte). The results were expressed as the relative percentage of total identified FA.

Statistical analysis

All results were expressed as means ± SD. The differences between formed groups at the beginning of the study, as well as the differences before and after the treatment were analyzed using an unpaired Student's t-test, accepting an alpha level of significance, $p \leq 0.05$. The Pearson correlation coefficients were computed for examination of the relation between serum lipids and between serum and erythrocyte FA percentages. The SPSS 10.0 program for Windows (Chicago IL, USA) was used for statistical analysis.

Results

The mean clinical and metabolic parameters are shown in Table 1. No differences for lipid parameters, dietary intake and FA composition in serum and erythrocyte phospholipids

were found between groups at baseline (Tables 1–3). Both diet alone and diet combined with gemfibrozil induced significant decrease in serum triglyceride (TG), total cholesterol (TC), LDL and non-HDL cholesterol concentrations ($p < 0.001$) and also induced a slight, but significant increase in HDL cholesterol level (Table 2). Consequently, TC/HDL, LDL/HDL and non-HDL/HDL cholesterol ratios were significantly decreased in both groups. In Group D+F we found higher reduction in concentrations of all lipid parameters (but increased HDL) than in Group D, but only changes in TC level showed a significant difference ($p < 0.05$) between two groups.

Combination of gemfibrozil and diet and dietary intervention alone induced significant alteration in serum phospholipids FA profile (Table 3). Saturated 16 : 0, 18 : 0 and total SFA significantly decreased and total MUFA increased in serum phospholipids after both treatments. The differences in SFA and MUFA between D and D+F groups after treatments were not significant. Percentages of linoleic (LA; 18 : 2 n-6), dihomo-γ-linoleic (DGLA; 20 : 3 n-6), arachidonic (AA; 20 : 4 n-6), docosapentaenoic (22 : 5 n-3), alfa-linolenic (LNA; 18 : 3 n-3), eicosapentaenoic (EPA; n-3) and docosahexaenoic acids (DHA; 22 : 6 n-3) in serum phospholipids were significantly higher after 12 weeks of dietary intervention. Consistent with the previous were the increases in n-6 PUFA, n-3 PUFA, total PUFA and PUFA/SFA ratios as well.

Combined gemfibrozil-diet treatment also led to a significant increase in DGLA, AA, LNA, EPA and DHA, but percentages of docosapentaenoic and docosatetraenoic acids were not changed, while LA was even decreased after the intervention (Table 3). Comparing the two groups of patients, which were similar at the baseline, we found significantly higher LA and DHA in D group, but AA and LNA in D+F group. The n-6/n-3 ratio was significantly lower after the diet, while gemfibrozil-diet combination did not significantly affect this ratio. AA/DGLA ratio, as a measure of Δ-5-desaturase activity was significantly lower in D group, but higher levels were found in D+F group. Although DGLA/LA ratio, as a measure of Δ-6-desaturase activity, was significantly higher in both groups after 12 weeks of treatment, it was higher in gemfibrozil-diet combination than in diet alone.

Combined effects of gemfibrozil-diet treatment and dietary intervention alone induced significant alteration in erythrocyte membrane phospholipids FA profile (Table 4). Both treatments significantly decreased SFA, and increased MUFA, n-6 PUFA, n-3 PUFA, total PUFA and PUFA/SFA ratio. Comparing the two groups after treatments, we found significantly higher stearic acid (18 : 0), palmitoleic acid (16 : 1 n-7) and LA in D group and higher palmitic acid (16 : 0), AA, EPA, AA/DGLA, 18 : 1/18 : 0 and DGLA/LA ratios in D+F group.

Table 1. Baseline anthropometric and dietary characteristics of study participants

	D group	D+F group
Age (years)	56 ± 6	55 ± 5
Male/female	13/28	12/25
Weight (kg)	72 ± 14	71 ± 12
BMI (kg/m^2)	24.47 ± 3.07	24.57 ± 2.84
Energy (kcal/day)	2273 ± 102	2253 ± 91
Protein (% of energy)	17.30 ± 2.25	17.03 ± 3.67
Carbohydrates (% of energy)	47.84 ± 1.54	47.69 ± 2.86
Total fat (% of energy)	34.83 ± 1.58	35.28 ± 2.18
Saturated fat (% of energy)	15.15 ± 1.03	15.80 ± 1.16
Monounsaturated fat (% of energy)	11.05 ± 2.84	10.95 ± 2.47
Polyunsaturated fat (% of energy)	8.23 ± 0.96	7.98 ± 0.96
PUFA/SFA	0.55 ± 0.08	0.51 ± 0.03
Cholesterol (mg/day)	498 ± 76	507 ± 84

Table 2. Serum lipids at baseline and changes induced by dietary intervention alone (D group) or diet and fibrate combination treatments (D+F group)

Serum (mmol/l)	D group baseline	D group after 12 wk	D+F group baseline	D+F group after 12 wk
Triglycerides	2.10 ± 0.45	1.49 ± 0.43***	2.15 ± 0.44	1.35 ± 0.43***
Total cholesterol (TC)	6.82 ± 0.61	5.85 ± 0.65***	6.72 ± 0.57	5.57 ± 0.60***[a]
LDL cholesterol	4.62 ± 0.67	3.83 ± 0.66***	4.44 ± 0.70	3.72 ± 0.79***
HDL cholesterol	1.25 ± 0.09	1.35 ± 0.13**	1.30 ± 0.18	1.37 ± 0.12*
non HDL cholesterol	5.57 ± 0.64	4.51 ± 0.70***	5.42 ± 0.59	4.18 ± 0.80***
TC/HDL cholesterol	5.50 ± 0.71	4.51 ± 0.70***	5.25 ± 0.88	4.12 ± 0.56***
LDL/HDL cholesterol	3.37 ± 0.69	2.85 ± 0.68***	3.52 ± 0.86	2.76 ± 0.64***
non HDL/HDL cholesterol	4.50 ± 0.71	3.40 ± 0.75***	4.28 ± 0.88	3.09 ± 0.69***

All data represented as mean ± SE. * $p < 0.05$, ** $p < 0.01$, *** $p < 0.001$ – intergroups compared baseline to after 12 weeks (wk) treatment; [a] $p < 0.05$ – compared groups after 12 wk treatment.

Table 3. Serum phospholipids fatty acid composition at baseline and changes induced by dietary intervention alone (D group) or diet and fibrate combination treatments (D+F group)

	D group baseline	D group after 12 wk	D+F group baseline	D+F group after 12 wk
16 : 0	30.30 ± 1.39	27.03 ± 0.68***	30.20 ± 1.27	27.29 ± 1.33***
18 : 0	15.74 ± 0.85	14.96 ± 0.85***	15.38 ± 1.30	14.84 ± 1.07*
SFA	46.03 ± 1.47	41.99 ± 0.34***	45.58 ± 1.51	42.12 ± 1.60***
16 : 1 n-7	0.39 ± 0.06	0.34 ± 0.08***	0.36 ± 0.09	0.32 ± 0.06*
18 : 1 n-9	11.24 ± 0.87	12.17 ± 0.96*	11.17 ± 1.08	12.36 ± 0.98***
MUFA	11.63 ± 0.86	12.56 ± 0.92***	11.53 ± 1.09	12.76 ± 0.85***
18 : 2 n-6 LA	23.13 ± 1.35	24.74 ± 0.96***	23.08 ± 1.52	22.27 ± 1.60*^{c}
20 : 3 n-6	3.01 ± 0.36	3.52 ± 0.26***	3.15 ± 0.66	3.60 ± 0.67**
20 : 4 n-6	11.37 ± 1.04	11.90 ± 0.89**	11.64 ± 1.16	14.01 ± 1.5***^{c}
22 : 4 n-6	0.44 ± 0.06	0.40 ± 0.06*	0.41 ± 0.10	0.41 ± 0.08
n-6	37.96 ± 1.73	40.56 ± 1.23***	38.27 ± 1.65	40.29 ± 1.46***
18 : 3 n-3 LNA	0.10 ± 0.02	0.12 ± 0.02***	0.10 ± 0.02	0.19 ± 0.13***^{b}
20 : 5 n-3 EPA	0.29 ± 0.05	0.38 ± 0.06***	0.30 ± 0.04	0.38 ± 0.06***
22 : 5 n-3	0.55 ± 0.08	0.60 ± 0.06**	0.57 ± 0.08	0.61 ± 0.32
22 : 6 n-3 DHA	3.10 ± 0.32	3.73 ± 0.33***	3.09 ± 0.38	3.39 ± 0.69*^{c}
n-3	4.05 ± 0.31	4.84 ± 0.34***	4.06 ± 0.42	4.57 ± 0.81**
PUFA	42.01 ± 1.69	45.40 ± 1.32***	42.33 ± 1.57	44.87 ± 1.63***
n-6/n-3	9.43 ± 0.94	8.43 ± 0.66***	9.55 ± 1.26	9.26 ± 2.98^{c}
20 : 4/20 : 3	3.81 ± 0.45	3.40 ± 0.36***	3.82 ± 0.72	4.02 ± 0.85
22 : 6/22 : 5	5.77 ± 1.22	6.27 ± 0.83*	5.47 ± 0.81	6.24 ± 1.00***
18 : 1/18 : 0	0.72 ± 0.07	0.82 ± 0.07***	0.73 ± 0.12	0.84 ± 0.08***
20 : 3/18 : 2	0.13 ± 0.02	0.14 ± 0.01***	0.14 ± 0.03	0.16 ± 0.04**^{b}
PUFA/SFA	0.91 ± 0.06	1.08 ± 0.05***	0.93 ± 0.06	1.07 ± 0.07***

All data are presented as a mean ± SE. Fatty acids concentrations are expressed in % of totally detected fatty acids. SFA, saturated fatty acids; MUFA, monounsaturated fatty acids; PUFA, polyunsaturated fatty acids; * $p < 0.05$, ** $p < 0.01$, *** $p < 0.001$ – intergroups compared baseline to after 12 wk treatment; ^{b} $p < 0.01$, ^{c} $p < 0.001$ – compared groups after 12 wk treatment.

A negative correlation between serum lipids (TC, TG, LDL and non-HDL) and LA, LNA, EPA and DHA percentage in serum phospholipids were found in D group, while HDL-cholesterol was in positive correlation with LNA, EPA and DHA (Table 5). Also, serum lipids (TC, TG, and non-HDL) in gemfibrozil-diet treatment inversely correlated with AA, LNA and EPA percentages in serum phospholipids. TC and non-HDL negatively correlated with DHA, while LDL cholesterol negatively correlated with LNA, EPA and DHA serum phospholipids contents. HDL cholesterol was in a positive correlation only with EPA level (Table 6).

An inverse correlation between serum lipids (TC, TG, LDL and non-HDL) with LA and LNA percentage in erythrocyte membrane phospholipids was found in diet intervention group. TG was also in negative correlation with EPA, while HDL-cholesterol showed positive correlation with LA, AA and LNA (Table 7). Serum TC, TG, LDL and non-HDL in gemfibrozil-diet treatment negatively correlated with AA and LNA in erythrocyte membrane phospholipids. TC and non-HDL were also in inverse correlation with EPA, and TG with EPA and DHA (Table 8).

Discussion

In the present study we evaluated dietary AHA-Step-1 intervention alone and combined effects of fibrate (gemfibrozil) and dietary treatment on serum and erythrocyte membrane phospholipids FA composition in patients with hyperlipidemia. However, it is important to notice that Group D was allocated from patients who preferred not to take drugs at the beginning, and rather try to improve their lipid profile by the diet alone. Regarding different compliance of study participants to follow medical advice in term of lipid lowering drugs, the obtained differences between D and D+F groups might not originated only from fibrate therapy, but also from other factors related to the decision of patients to take no drugs. Although, there were a number of important features of this study. First, the effects of dietary treatment on

Table 4. Erythrocyte phospholipids fatty acid composition at baseline and changes induced by dietary intervention alone (D group) or diet and fibrate combination treatments (D+F group)

	D group baseline	D group after 12 wk	D+F group baseline	D+F group after 12 wk
16 : 0	23.64 ± 0.90	20.59 ± 0.70***	24.00 ± 0.95	21.30 ± 0.59***^{c}
18 : 0	17.58 ± 0.94	16.88 ± 0.70***	17.20 ± 0.90	16.35 ± 0.55***^{c}
SFA	41.23 ± 1.29	37.47 ± 0.70***	41.20 ± 1.33	37.64 ± 0.55***
16 : 1 n-7	0.25 ± 0.05	0.23 ± 0.05***	0.24 ± 0.06	0.20 ± 0.02***^{b}
18 : 1 n-9	17.00 ± 1.47	18.20 ± 0.52***	17.09 ± 1.13	18.10 ± 0.80***
MUFA	17.26 ± 1.48	18.43 ± 0.53***	17.33 ± 1.13	18.31 ± 0.80***
18 : 2 n-6 LA	13.55 ± 1.11	15.27 ± 0.89***	13.43 ± 0.92	13.21 ± 1.36^{c}
20 : 3 n-6	1.49 ± 0.20	1.59 ± 0.26*	1.49 ± 0.18	1.56 ± 0.11*
20 : 4 n-6	16.53 ± 1.47	17.07 ± 0.77*	16.65 ± 1.29	19.03 ± 1.04***^{c}
22 : 4 n-6	3.65 ± 0.55	3.83 ± 0.56*	3.65 ± 0.47	3.87 ± 0.41*
n-6	35.23 ± 2.15	37.75 ± 0.95***	35.20 ± 1.16	37.68 ± 0.77***
18 : 3 n-3 LNA	0.10 ± 0.02	0.17 ± 0.03***	0.12 ± 0.02	0.18 ± 0.04***
20 : 5 n-3 EPA	0.33 ± 0.08	0.37 ± 0.05***	0.35 ± 0.07	0.40 ± 0.03***^{a}
22 : 5 n-3	1.57 ± 0.30	1.57 ± 0.32	1.54 ± 0.24	1.55 ± 0.20
22 : 6 n-3 DHA	3.83 ± 0.56	4.12 ± 0.45	3.89 ± 0.51	4.06 ± 0.50
n-3	5.89 ± 0.63	6.22 ± 0.67*	5.89 ± 0.53	6.19 ± 0.54**
PUFA	41.12 ± 2.31	43.96 ± 0.88***	41.10 ± 1.08	43.86 ± 0.73***
n-6/n-3	6.05 ± 0.73	6.15 ± 0.77	6.03 ± 0.66	6.14 ± 0.60*
20 : 4/20 : 3	11.28 ± 1.90	11.02 ± 1.81*	11.42 ± 1.99	12.25 ± 1.04*^{c}
22 : 6/22 : 5	2.52 ± 0.59	2.70 ± 0.46	2.58 ± 0.53	2.65 ± 0.44
18 : 1/18 : 0	0.97 ± 0.090	1.08 ± 0.06***	1.00 ± 0.10	1.11 ± 0.07***^{b}
20 : 3/18 : 2	0.11 ± 0.02	0.10 ± 0.02	0.11 ± 0.01	0.12 ± 0.02^{b}
PUFA/SFA	1.00 ± 0.08	1.17 ± 0.05***	1.0 ± 0.05	1.17 ± 0.04***

All data are presented as a mean ± SE. Fatty acids concentrations are expressed in % of totally detected fatty acids. SFA, saturated fatty acids; MUFA, monounsaturated fatty acids; PUFA, polyunsaturated fatty acids; * $p < 0.05$, ** $p < 0.01$, *** $p < 0.001$ – intergroups compared baseline to after 12 wk treatment; ^{a} $p < 0.05$, ^{b} $p < 0.01$, ^{c} $p < 0.001$ – compared groups after 12 wk treatment.

Table 5. Pearson correlation coefficients between serum lipids and serum phospholipids fatty acids percentage in dietary intervention treatment

	TG		TC		HDL		LDL		non HDL	
	r	*p*	*r*	*p*	*r*	*p*	*r*	*p*	*r*	*p*
LA	–0.364	0.001	–0.377	0.001	0.201	0.073	–0.305	0.006	–0.375	0.001
AA	–0.292	0.008	–0.206	0.066	0.185	0.101	–0.150	0.185	–0.225	0.045
LNA	–0.252	0.024	–0.245	0.028	0.299	0.007	–0.220	0.050	–0.268	0.016
EPA	–0.464	<0.001	–0.468	<0.001	0.285	0.01	–0.381	<0.001	–0.477	<0.001
DHA	–0.515	<0.001	–0.417	<0.001	0.325	0.003	–0.319	0.004	–0.436	<0.001

Table 6. Pearson correlation coefficients between serum lipid and serum phospholipids fatty acids percentage in diet and fibrate combination treatment

	TG		TC		HDL		LDL		non HDL	
	r	*p*	*r*	*p*	*r*	*p*	*r*	*p*	*r*	*p*
LA	-0.222	0.054	–0.189	0.101	0.109	0.348	–0.186	0.109	–0.174	0.132
AA	–0.414	<0.001	–0.319	0.005	0.113	0.330	–0.188	0.103	–0.280	0.014
LNA	–0.254	0.027	–0.291	0.011	0.168	0.148	–0.255	0.026	–0.288	0.012
EPA	–0.512	<0.001	–0.374	0.001	0.291	0.011	–0.235	0.041	–0.404	<0.001
DHA	–0.031	0.793	–0.322	0.005	0.140	0.227	–0.248	0.031	–0.304	0.008

Table 7. Pearson correlation coefficients between serum lipids and erythrocyte membrane phospholipids fatty acids percentage in dietary intervention treatment

	TG		TC		HDL		LDL		non HDL	
	r	*p*	*r*	*p*	*r*	*p*	*r*	*p*	*r*	*p*
LA	–0.316	0.004	–0.466	<0.001	0.277	0.013	–0.423	0.001	–0.472	<0.001
AA	–0.151	0.182	–0.090	0.429	0.052	0.047	–0.037	0.743	–0.075	0.511
LNA	–0.408	<0.001	–0.304	<0.001	0.187	0.096	–0.214	0.056	–0.308	0.005
EPA	-0.273	0.014	-0.170	0.131	0.158	0.161	-0.151	0.310	-0.185	0.100
DHA	-0.193	0.087	-0.146	0.196	0.100	0.375	-0.107	0.346	-0.154	0.173

Table 8. Pearson correlation coefficients between serum lipid and erythrocyte phospholipid fatty acids percentage in diet and fibrate treatment

	TG		TC		HDL		LDL		non HDL	
	r	*p*	*r*	*p*	*r*	*p*	*r*	*p*	*r*	*p*
LA	0.131	0.266	–0.024	0.839	0.182	0.121	–0,068	0.566	–0.042	0.725
AA	–0.494	<0.001	–0.444	<0.001	0.013	0.912	–0.231	0,048	–0.376	0.001
LNA	–0.507	<0.001	–0.556	<0.001	0.134	0.254	–0,316	0.006	–0.490	0.001
EPA	–0.371	<0.001	–0.286	<0.014	0.066	0.578	–0.131	0.267	–0,247	0.034
DHA	–0.272	0.019	0.007	0.954	0.015	0.897	–0.100	0.399	–0.040	0.735

serum and erythrocyte membrane phospholipids FA profile were consistent with published data and reflected changes in the FA composition of the diet (Kobayashi et al. 2001; King et al. 2006; Skeaff et al. 2006). Our results showed that dietary-induced changes in erythrocyte phospholipids FA composition were similar to plasma phospholipids. These results provide convincing, although indirect evidence, that the input of FA from plasma to erythrocytes is a major determinant of their membrane FA composition (King et al. 2006). Small but significant changes in PUFA/SFA ratio were recorded in erythrocyte membrane phospholipids after Step-1 diet, from 1.00 to 1.17. Therefore, it appears that red cell membrane changes parallel dietary intervention and hence are a potential marker for effects of dietary changes.

Higher proportions of LA and LNA, that form a potentially less atherogenic FA profile, were found in subjects after the Step-1 diet only, suggesting an additional benefit of the dietary intervention (Hodson et al. 2001; Lichtenstein et al. 2002). Increased formation of long-chain PUFA was important for membrane functions in several tissues, such as endothelium and thrombocytes. These functions may partly be mediated through eicosanoid metabolites of the membrane-bound 20-carbon FA: AA (the precursor of 2-series prostaglandins and thromboxanes and 4-series leukotrienes), DGLA (the precursor of 1-series prostaglandins), and EPA (the precursor of 3-series prostaglandins and thromboxanes and 5-series leukotrienes). A number of eicosanoids has been shown to activate PPAR. The strong preference of the PUFA for PPAR-α suggests that this receptor may play a specific role in situations of nutritional lipid overload (Kersten et al 2008). Recently, Calkin et al. (2007) have shown that both PPAR-α agonists – gemfibrozil and fenofibrate confer anti-atherosclerotic effects, partly independent of their metabolic effects.

Gemfibrozil is extremely effective in reducing cardiovascular risk in people with components of metabolic syndrome. Insulin sensitivity can be modulated by different lifestyle factors and the quality of dietary fat seems to be an important factor (Warensjö et al. 2006). Clifton et al. (1998) found an inverse relationship for fasting plasma insulin with erythrocyte membrane percentage of AA, total n-6 PUFA and a positive relationship with percentage of SFA in healthy men. Thus, the strong positive correlation between AA and the indexes of insulin sensitivity in previously reported studies may represent an effect on insulin action of eicosanoids specifically derived from this parent FA. In human obesity palmitoleic acid is reported to correlate with index of adiposity and insulin concentration (Okada et al. 2005). After combination of gemfibrozil and the dietary therapy decreased levels of palmitoleic acid were observed in our study. Our data showed a strong evidence of increasing levels of AA in serum and erythrocyte phospholipid after gemfibrozil-diet treatment in hyperlipidemic patients. Previous studies of coronary circulation suggested that endothelium-derived hyperpolarizing factor (EDHF), an important mediator of vasodilatation, especially in small arteries, may be a product of the non-cyclo-oxygenase-mediated metabolism of AA (Oltman et al. 2001). These observations lead one to

speculate that AA induced vasodilatation without the tonic inhibition. In this case a predominant regulatory pathway in arteriosclerosis could become the EDHF pathway (De Caterina et al. 2000).

An increased formation of DGLA, as observed here during the dietary intervention and in gemfibrozil-diet combination, may increase the formation of vasodilatory, anti-inflammatory and antiproliferative prostaglandin E1 (Mikhailidis et al. 1986). DGLA and its 15-OH derivate block the transformation of AA to proinflammatory 4-series leukotrienes (Iversen et al. 1992) and also increase the conversion of EPA to PGI-3, a vasodilatator and platelet anti-aggregator (Holman 1977). EPA inhibits the activity of the enzyme Δ-5-desaturase, disabling DGLA conversion to AA and increasing the tissue levels of DGLA (Das 1995). In previous cross-sectional studies in humans, reduced Δ-5-desaturase activity (AA/DGLA ratio) in membranes has been associated with insulin resistance (Borkman et al. 1993). According to animal studies, a high-cholesterol diet decreased the Δ-5- and Δ-6-desaturase steps, whereas a low-cholesterol diet had opposite effects (Garg et al. 1986; Leikin et al. 1988). These data show that AHA-Step-1 diet decreased levels of Δ-5-desaturase activity in serum and membrane phospholipid. The mode of action of fibrate on FA cascade remains speculative. In theory, fibrate may have direct or indirect stimulatory effects on FA desaturase and elongase enzyme activities. Thus, an increased Δ-5-desaturase activity, observed in our study after gemfibrozil-diet combination in serum and membrane phospholipid, may be at least partly influenced by gemfibrozil.

Nyalala et al. (2008) recently showed that gemfibrozil produced major modifications in FA composition of plasma lipids and red cell membrane in patients with hypertriglyceridemia. These changes were FA and lipid class specific, with generally decreased SFA and increased PUFA (mainly AA n-6). Results of this study are consistent with effect of gemfibrozil-diet combination from our data in patients with hyperlipidemia. Recently published article reported that the proportion of serum LA was inversely related, whereas serum FAs, associated with saturated fat intake (palmitic, palmitoleic, and DGLA), were directly related to total and cardiovascular mortality (Warensjö et al. 2008).

High proportion of n-3 FA in red blood cell membranes has been associated with a reduced risk of primary cardiac arrest (Siscovick et al. 1995). The cardioprotective action of n-3 PUFA can be attributed to their effect on lipids, hemostatic system and endothelial cell proliferation and function (Das 2000; De Caterina et al. 2000; Crowe et al. 2006). In agreement with Grimsgard et al. (2000), the present study shows strong correlation of decreased serum triglycerides with higher levels of EPA n-3. Lower levels of LDL-cholesterol after both treatments correlated with LNA, EPA and DHA n-3 in serum phospholipids.

We have demonstrated that both the dietary intervention, and combination of gemfibrozil and the diet resulted in significantly better serum lipid profile as well as serum and erythrocyte membrane phospholipid FA composition. This study also provides valuable data on the interrelationship of FA composition of lipids and plasma lipid concentration. Although the present study is unable to comment on the potential additional benefit of gemfibrozil over diet alone, due to a lack of random allocation of the subjects, it is evident that the combination of the diet and fibrate led to a more favorable lipid and FA profile in hyperlipidemic patients.

Acknowledgement. This work was supported by the Ministry of Science and Environmental Protection of the Republic of Serbia, project No. 145071.

References

Agheli N., Jacotot B. (1991): Effect of simvastatin and fenofibrate on the fatty acid composition of hypercholesterolaemic patients. Br. J. Clin. Pharmacol. **32**, 423–428

Arab L. (2003): Biomarkers of fat and fatty acid intake. J. Nutr. **133**, 925–932

Asztalos B. F, Collins D., Horvath K. V., Bloomfield H. E., Robins S. J., Schaefer E. J. (2008): Relation of gemfibrozil treatment and high-density lipoprotein subpopulation profile with cardiovascular events in the veterans affairs high-density lipoprotein intervention trial. Met. Clin. Exp. **57**, 77–83

Barter P. H. J., Rye K. A. (2006): Cardioprotective Properties of Fibrates which Fibrate, which patients, what mechanism? Circulation **113**, 1553–1555

Bingham S. (2002): Biomarkers in nutritional epidemiology. Public Health Nutr. **5**, 821–827

Borkman M., Storlien L. H., Pan D. A,. Jenkins A. B., Chrisholm D. J., Campbell L. V. (1993): The relation between insulin sensitivity and the fatty-acid composition of skeletal-muscle phospholipids. N. Engl. J. Med. **328**, 238–244

Clifton P. M., Nestel P. J. (1998): Relationship between plasma insulin and erythrocyte fatty acid composition. Prostaglandins Leukot. Essent. Fatty Acids **59**, 191–194

Calkin A. C., Jandeleit-Dahm K. A., Sebekova E., Allen T. J., Mizrahi J., Cooper M. E., Tikellis C. (2007): PPARs and diabetes-associated atherosclerosis. Curr. Pharm. Des. **13**, 2736–2741

Crowe F. L., Skeaff C. M., Green T. J., Gray A. R. (2006): Serum fatty acids as biomarkers of fat intake predict serum cholesterol concentrations in a population-based survey of New Zealand adolescents and adults. Am. J. Clin. Nutr. **83**, 887–894

Das U. N. (1995): Essential fatty acid metabolism in patients with essential hypertension, diabetes mellitus and coronary heart disease. Prostaglandins Leukot. Essent. Fatty Acids **52**, 387–391

Das U. N. (2000): Beneficial effect(s) of n-3 fatty acids in cardiovascular diseases: but, why and how? Prostaglandins Leukot. Essen. Fatty Acids **63**, 351–362

De Caterina R., Liao J. K., Libby P. (2000): Fatty acid modulation of endothelial activation. Am. J. Clin. Nutr. **71**, S213–223

de Lorgeril M., Salen P. (2003): Dietary prevention of coronary heart disease: focus on omega-6/omega-3 essential fatty acid balance. World Rev. Nutr. Diet. **92**, 57–73

Iversen L., Fogh K., Kragballe K. (1992): Effect of dihomogammalinolenic acid and its 15-lipoxygenase metabolite on eicosanoid metabolism by human mononuclear leukocytes in vitro: selective inhibition of the 5-lipoxygenase pathway. Arch. Dermatol. Res. **284**, 222–226

Forman B. M., Chen J., Evans R. M. (1997): Hypolipidemic drugs, polyunsaturated fatty acids, and eicosanoids are ligands for peoxisome proliferator-activated receptors alpha and delta. Proc. Natl. Acad. Sci. USA **94**, 4312–4317

Friedewald W. T., Levy R. I., Friedrickson D. S. (1972): Estimination of the concentration of low density lipoprotein cholesterol in plasma without use of the ultracentrifuge. Clin. Chem. **18**, 449–502

Garg M. L., Snoswell A. M., Sabine J. R. (1986): Influence of dietary cholesterol on desaturase enzymes of rat liver microsomes. Prog. Lipid Res. **25**, 639–644

Grimsgaard S., Bonaa K. H., Bjerve K. S. (2000): Fatty acid chain length and degree of unsaturation are inversely associated with serum triglycerides. Lipids **35**, 1185–1193

Grundy S. M., Denke M. A. (1990): Dietary influences on serum lipids and lipoproteins. J. Lipid Res. **31**, 1149–1172

Harth S., Dreyfus H., Urban P. F., Mandel P. (1978): Direct thin-layer chomatography of gangliosides of total lipid extracts. Anal. Biochem. **86**, 543–551

Hodson L., Skeaff C., Chisholm W. A. (2001): The effect of replacing dietary saturated fat with polyunsaturated or monounsaturated fat on plasma lipids in free-living young adults. Eur. J. Clin. Nutr. **55**, 908–915

Holman R. T. (1977): Esential fatty acids in human nutrition. In: Function and biosynthesis of lipids. (Eds. N. G. Bazán, R. R. Brenner and M. N. Giusto), pp. 515–534, Plenum Press, New York

Jokic N., Dimic M., Pavlica M. (1999): Chemical composition tables of nutrition products. Kulin Art, Zavod za ekonomiku domacinstva Srbije, Belgrade (in Serbian)

Kersten S. (2008): Peroxisome proliferator activated receptors and lipoprotein metabolism. PPAR Res. **2008**, 132960

Kliewer S. A., Sundseth S. S., Jones S. A., Brown P. J., Wisely G. B., Koble C. S., Devchand P., Wahli W., Wilson T. M., Lenhard J. M., Lehmann J. M. (1997): Fatty acids and eicosanoids regulate gene expression through direct interactions with peroxisome proliferator-activated receptors α and β. Proc. Natl. Acad. Sci. U.S.A. **94**, 4318–4323

Krey G., Braissant O., L'Horset F., Kalkhoven E., Perroud M., Parker M. G., Wahli W. (1997): Fatty acids, eicosanoids, and hypolipidemic agents identified as ligands of peroxisome proliferator-activated receptors by coactivator-dependent receptor ligand assay. Mol. Endocrinol. **11**, 779–791

King I. B., Lemaitre R. N., Kestin M. (2006): Effect of a low-fat diet on fatty acid composition in red cells, plasma phospholipids, and cholesterol esters: investigation of a biomarker of total fat intake. Am. J. Clin. Nutr. **83**, 227–236

Kobayashi M., Sasaki S., Kawabata T., Hasegawa K., Akabane M., Tsugane S. (2001): Single measurement of serum phospholipid fatty acid as a biomarker of specific fatty acid intake in middle-aged Japanese men. Eur. J. Clin. Nutr. **55**, 643–645

Leikin A. I., Brenner R. R. (1988): *In vivo* cholesterol removal from liver microsomes induces changes in fatty acid desaturase activities. Biochim. Biophys. Acta **963**, 311–319

Lichtenstein A. H., Ausman L. M., Jalbert S. M., Vilella-Bach M., Jauhiainen M., McGladdery S., Erkkilä A. T., Ehnholm C., Frohlich J., Schaefer E. J. (2002): Efficacy of a therapeutic lifestyle change/step 2 diet in moderately hypercholesterolemic middle-aged elderly female and male subjects. J. Lipid Res. **43**, 264–273

Lopes-Virela M. F., Stone P., Ellis S., Colwell J. A. (1977): Cholesterol determination in high-density lipoproteins separated by three different methods. Clin. Chem. **23**, 882–884

Ma J., Folsom A. R., Sharar E., Eckfeldt J. H. (1995): Plasma fatty acid composition as an indicator of habitual dietary fat intake in middle-aged adults. Am. J. Clin. Nutr. **62**, 564–571

Matusik E. J., Reeves V. B., Flanagan V. P. (1984): Determination of fatty acid methyl esters. Anal. Chim. Acta. **166**, 179–188

Mikhailidis D. P., Kirtland S. J., Barradas M. A., Mahadeviah S., Dandona P. (1986): The effect of dihomogammalinolenic acid on platelet aggregation and prostaglandin release, erythrocyte membrane fatty acids and serum lipids: evidence for defects in PGE1 synthesis and delta 5-desaturase activity in insulin-dependent diabetics. Diabetes Res. **3**, 7–12

National Cholesterol Education Program (2001): Third report of the expert panel on detection, evaluation, and treatment of high blood cholesterol in adults (Adult Treatment Panel III). NIH Pub. No. 01-3670. Bethesda, MD: National Heart, Lung and Blood Institute

Nyalala J. O., Wang J., Dang A., Faas F. H., Smith W. G. (2008): Hypertriglyceridemia and hypercholesterolemia: effects of drug treatment on fatty acid composition of plasma lipids and membranes**.** Prostaglandins Leukot. Essent. Fatty Acids **78**, 271–280

Oltman C. L., Kane N. L., Fudge J. L, Weintraub N. L., Dellsperger K. C. (2001): Endothelium-derived hyperpolarizing factor in coronary microcirculation: responses to arachidonic acid. Am. J. Physiol. Heart Circ. Physiol. **281**, H1553–1560

Okada T., Furuhashi N., Kuromori Y., Miyashita M., Iwata F., Harada K. (2005): Plasma palmitoleic acid content and obesity in children. Am. J. Clin. Nutr. **82**, 747–750

Pavlovic M., Grujic V., Oshaug A. (2005): Nutrition and physical activity of the population in Serbia. World Rev. Nutr. Diet. **94**, 51–59

Ristić Medić D., Ristić V., Tepšić V., Ranić M., Ristić G., Vrbaški S., Estelecki I. (2003): Effect of soybean leci-vita product on serum lipids and fatty acids composition in patients with elevated serum cholesterol and triglyceride levels. Nutr. Res. **23**, 465–477

Rivellese A., de Natale C., Lilli S. (2002): Type of dietary fat and insulin resistance. Ann. N. Y. Acad. Sci. **967**, 329–335

Sarkkinen E., Agren J., Ahola I., Ovaskainen M., Uusitupa M. (1994): Fatty acid composition of serum cholesterol esters, and erythrocyte and platelet membranes as indicators of long-term adherence to fat-modified diets. Am. J. Clin. Nutr. **59**, 364–370

Schindler C. (2007): The metabolic syndrome as an endocrine disease: is there an effective pharmacotherapeutic strategy optimally targeting the pathogenesis? Ther. Adv. Cardiovasc. Dis. **1**, 7–26

Skeaff C. M., Hodson L., McKenzie J. E. (2006): Dietary-induced changes in fatty acid composition of human plasma, platelet, and erythrocyte lipids follow a similar time course. J. Nutr. **136,** 565–569

Siscovick D. S, Raghunathan T. E, King I., Weinmann S., Wicklund K. G. (1995). Dietary intake and cell membrane levels of long-chain n-3 polyunsaturated fatty acids and the risk of primary cardiac arrest. JAMA **27,** 1363–1367

Tavella M., Corder C. N., McConathy W. (1993): Effect of gemfibrozil on fatty acids in lipid fractions of plasma from patients with hypertriglyceridemia. J. Clin. Pharmacol. **33**, 35–39

USDA (2005): US Department of Agriculture, Agricultural Research Service. USDA National Nutrient Database for Standard Reference, Release 18. Nutrient Data Laboratory Home Page, http://www.nal.usda.gov/fnic/foodcomp

WHO Technical Report Series 916 (2003): Diet, nutrition and the prevention of chronic disease. Report of the Joint WHO, FAO Expert Consultation, Geneva, Switzerland

Wood D., De Backer G., Faergeman O., Graham I., Mancia G., Pyorala K. (1998): Prevention of coronary heart disease in clinical practice: recommendations of the Second joint task force of European and other societies on coronary prevention. Atherosclerosis **140**, 199–270

Yu-Poth S., Zhao G., Etherton T., Naglak M., Jonnalagadda S., Kris-Etherton P. M. (1999): Effects of the National Cholesterol Education Program s Step I and Step II dietary intervention programs on cardiovascular disease risk factors: a meta-analysis. Am. J. Clin. Nutr. **69**, 632–646

Warensjö E., Sundström J., Lind L., Vessby B. (2006): Factor analysis of fatty acids in serum lipids as a measure of dietary fat quality in relation to the metabolic syndrome in men. Am. J. Clin. Nutr. **84,** 442–448

Warensjö E., Sundström J., Vessby B., Cederholm T., Risérus U. (2008): Markers of dietary fat quality and fatty acid desaturation as predictors of total and cardiovascular mortality: a population-based prospective study. Am. J. Clin. Nutr. **88**, 203–209

Overweight in trained subjects – are we looking at wrong numbers? (Body mass index compared with body fat percentage in estimating overweight in athletes.)

Sanja Mazic[1], Marina Djelic[1], Jelena Suzic[2], Slavica Suzic[1], Milica Dekleva[2], Dragan Radovanovic[2], Ljiljana Scepanovic[1] and Vesna Starcevic[1]

[1] *Institute of Medical Physiology, School of Medicine, University of Belgrade, Serbia*
[2] *University Clinical Center "Dr. Dragiša Mišović-Dedinje", Belgrade, Serbia*

Abstract. Body mass index (BMI) is widely used as an index of obesity in adults. In trained population, individual with low body fat could be classified as overweight by BMI. To evaluate this problem, the purposes of this study were to determine the BMI and body fat percentage (BF%) of trained and untrained subjects and to evaluate the accuracy of BMI classification (≥25 kg·m^{-2}) as a prediction of overweight/obesity in trained subjects. The total number of 299 trained (basketball players) and 179 untrained male subjects participated in this study. Body height and body mass were measured; BMI was calculated for all subjects. BF% was determined *via* Tanita bioimpedance body composition analyzer. BMI ≥ 25 kg·m^{-2} and BF% > 20% were used to define overweight. There was no significant age differences. Body mass, height ($p < 0.01$) and BMI ($p < 0.05$) were significantly higher, although BF% was significantly lower ($p < 0.01$) in trained group when compared to untrained. Eighty-five trained subjects had a BMI of 25 or higher, indicating overweight. Of these, only three individuls had excess BF%. The results of the present study suggest that a BMI ≥ 25 kg·m^{-2} is not an accurate predictor of overweight in trained subjects.

Key words: Body mass index — Body fat percentage — Overweight/obesity — Trained subjects (athletes)

Introduction

The prevalence of adolescent and adult obesity is increasing at an alarming rate. Obesity is a serious health concern and is associated with many chronic diseases, including cardiovascular disease, diabetes, arthritis, gall bladder disease, certain cancers, and respiratory diseases (Pi-Sunyer 1993).

Body mass index (BMI) is widely used as an indicator expressing the level of obesity. According to the Expert Panel on the Identification, Evaluation and Treatment of Overweight and Obesity in Adults (see References: NHLBI 2000), BMI of 25–29.9 kg·m^{-2} is considered overweight and BMI ≥ 30 kg·m^{-2} is considered obese.

Correspondence to: Sanja Mazic, Institute of Physiology, School of Medicine, University of Belgrade, Višegradska 26/II, 11000 Belgrade, Serbia
E-mail: sagabgyu@yahoo.com

In the recent study, Harp and Hecht (2005) used high BMI (≥25 kg·m^{-2}) as a synonym for obesity in professional football players. They reported overweight in 85% of athletes. This study was point of much of scientific debate.

Since BMI is obtained from numerical values of body height and mass, it obviously does not take into account body fat. However, BMI is thought to have a correlation with amount of body fat (Garrow and Webster 1985; Prentice and Jebb 2001) and is shown to be simple and stable indicator of obesity. It is not supported by some authors, who found low correlations between BMI and body fat percentage (BF%) in a large group of subjects aged 7–83 years (Deurenberg et al. 1991).

It is well known that the BMI classification system is valid for the general adult population, but it does have some limitations. One of these limitations involves the accuracy of using BMI for physically active, trained subjects. Using BMI for trained subjects can overestimate their level of body fat because muscle is denser than fat

and it weighs more. It is especially true for trained subjects whose body fat can be normal or even low, but individual BMI is high.

Therefore, the use of BF% is more accurate than BMI in assessing obesity in physically active subjects (Deurenberg et al. 1991; Jonnalagadda et al. 2004; Ode et al. 2007). Despite potential limitations of BMI, it is still used to assess obesity not only in adults (Ogden et al. 2006) but in trained subjects and professional athletes, too (Ode et al. 2007). Therefore, it is critical to evaluate relationship between BMI and BF% in physically active population.

The purposes of this study were i) to determine the BMI and BF% of trained and untrained subjects and ii) to determine and evaluate the accuracy of the BMI classification of overweight (≥25 kg·m^{-2}) as a prediction of overweight/obesity in trained subjects according to measurement of BF%.

Materials and Methods

Subjects

Two hundred and ninety nine male basketball players aged 18 or over (mean ± SD; age, 21.57 ± 3.58 years, trained group) and 179 untrained men (21.05 ± 3.11 years, untrained group) participated in this study. All trained individuals were included in the Basketball league of Serbia. All basketball players had at least five years of training and during the current season trained 15–20 h per week. In order to standardize the effect of physical activity on body composition, we selected the sample of trained subjects participated in one sport and components of training were similar for all trained subjects. Control subjects were healthy, untrained adult men. They were randomly selected from students of Belgrade University who applied to participate in the study. The control subjects had not engaged in any formal exercise during the previous 2 years, had less than 8 h of physical activity per week and had never engaged in any athletic competition involving endurance activities. All subjects gave their written informed consent to the procedures approved by the Ethics Committee of the School of Medicine, University of Belgrade.

Anthropometric data

Body mass was assessed to the nearest 0.1 kg using a beam balance scale while individuals wear minimal clothing. Body height was assessed to the nearest 0.1 cm using a portable stadiometer fixed to the wall. The stadiometer and scale were calibrated periodically during the study.

BMI was calculated for all the participants as the ratio of mass (kilograms) divided by height (meters) squared.

For all individuals, BMI was classified using the National Institutes of Health standards for adults (<18.5, underweight; 18.5 to 24.9, normal; 25 to 29.9, overweight; >30, obesity).

BF% was measured using the Tanita bioimpedance segmental body composition analyzer (model BC 418). Subjects followed recommendations for body composition assessment by method of bioimpedance (Sigal 1996). They were asked to stand barefoot on the metal sole plates of the machine, and gender and height details were entered manually into the system *via* a keyboard. BF% was displayed and printed out.

Statistical analysis

All values are given as mean ± standard deviation (SD). Statistical analyses were carried out using the statistical package SPSS 10.0 for Windows (Chicago, IL, USA). The tests included *t* tests for testing differences between the two groups. Where appropriate, Chi square test was used for assess the significance of differences between variables. Statistical significance was set at $p < 0.05$.

Results

Anthropometric characteristics of the trained and untrained subjects are presented in Table 1. There was no significant differences for age between trained and untrained subjects. Body mass and height were significantly higher ($p < 0.01$) in the group of trained subjects when compared to untrained group. BMI was also significantly higher ($p < 0.05$) in trained group than in untrained (Table 1).

According to BMI classification system, subjects were distributed in the overweight categorie (BMI > 25 kg·m^{-2})

Table 1. Anthropometric characteristics of the trained and untrained subjects

	Group	Mean	SD	*p* (a vs. b)
Age (years)	a	21.57	4.58	>0.05
	b	21.05	3.11	
BM (kg)	a	94.45	12.44	<0.01
	b	77.97	9.84	
BH (cm)	a	199.11	8.54	<0.01
	b	183.37	8.97	
BMI (kg·m^{-2})	a	23.76	2.09	<0.05
	b	23.15	2.11	
BF% (%)	a	10.41	3.98	<0.01
	b	14.56	4.69	

BM, body mass; BH, body height; BMI, body mass index; BF%, body fat percentage; a, trained group ($n = 299$); b, untrained group ($n = 179$). The values are the means ± SD.

(Table 2). The maximal value of BMI in the group of trained subjects was 29.20 kg·m^{-2}, although in the untrained group was 30.04 kg·m^{-2} (BMI of 25–29. 9 kg·m^{-2} is considered overweight, or class-I obesity). In the group of trained subjects, 85 subjects (28%) have BMI in the overweight category, although in the untrained group, there were 37 subjects in this category (21%) (Table 2). This difference between trained and untrained subjects was statistically significant ($p < 0.01$).

BF% of the subjects is presented in Table 1. The average BF% of the subjects in the group of trained subjects was 10.41 ± 3.98%, and in the untrained group it was 14.56 ± 4.69%. The difference in BF% between trained and untrained subjects was statistically significant ($p < 0.01$). According to BF% recommendation for general population, the subjects were distributed in the overweight categorie if BF% is over 20 (Table 3).

According to World Health Organization (WHO) recommendation for general population optimal BF% is from 8 to 20% for male individulas, aged from 18 to 39 (Gallaghar et al. 2000). BF% from 20–25% is considered overweight, and above 25% – obese. In the group of trained, among 299 subjects, only three subjects (1%) had BF% higher than 20%. In the untrained group 17 subjects (9.5%) had BF% higher 20%. In this group 7 individulas were in overweight group, 10 in obese group. Nevertheless, 76 subjects in trained group had BF% less than 8%.

We found statistically significant correlation between values of BMI and BF% within group of trained and untrained subjects ($r = 0.535$; $p < 0.01$ and $r = 0.596$; $p < 0.01$, respectively). In the group of trained individuals with BMI over 25, there is nonlinear relationship between the two variables (BMI and BF%) in the assessment of obesity of trained subjects, accordingly correlation coefficient ($r = 0.161$, $p = 0.142$).

Table 2. Prevalence of body mass index (BMI) higher than 25, in the group of trained and untrained subjects

BMI > 25	Trained		Untrained	
	n	%	*n*	%
yes	85	28	37	21
no	214	72	142	79

Table 3. Ranges of body fat percentage (BF%) in the group of trained and untrained subjects

BF%	Trained		Untrained	
	n	%	*n*	%
<8%	76	25	3	2
8–20%	220	74	159	89
>20%	3	1	17	9

Chi-quadrate test showed statistically significant difference in prevalence of BF% > 20 in groups of trained ($n = 3$, 1.38%) and untrained ($n = 17$, 45.9%) subjects with BMI > 25 ($p < 0.01$).

Discussion

BMI has been used as a standard to define obesity. It is well known that BMI is an attractive anthropometric index because it meets the four requirements for an ideal method (Garrow and Webster 1985). The two instruments that are required (scale and tape measure) are inexpensive, require minimal training to use and are virtually maintenance-free, and repeated values can be obtained with good precision. Prentice and Jebb assessed the validity of BMI as a measure of obesity (Prentice and Jebb 2001). They have shown that the accuracy of BMI to detect overweight vary across trained subjects because of differences in body composition. BF% in trained subjects is attributable to greater muscle mass at a given body mass. It is well known that muscle is denser than fat, it weighs more. Therefore, the accuracy of BMI in assessing overweight in trained subjects is remaining question.

In the present study body mass, body height and BMI were significantly higher in trained group than in untrained. The mean BMI values in both groups were in the range of 18.5 to 24.9 kg·m^{-2} which is considered to be desirable for adults (Lee and Nieman 1993). Also, mean BF% in both groups were in the range 8–20% which is considered to be optimal for adults (Gallagher et al. 2000). All trained subjects had lower BF% compared with the untrained group.

In several studies the general BMI classification system has been used to assess obesity in athletes (Deurenberg et al. 1991; Jonnalagadda et al. 2004; Ode et al. 2007). Harp and Hecht (2005) used BMI ≥ 25 kg·m^{-2} to define overweight in professional football players. They showed that 97, 56, 26, and 3% of the NFL (National Football League) players had a BMI of 25 or higher, 30 or higher, 35 or higher, 40% or higher, respectively (Harp and Hecht 2005). This data are highly contradictory. More than sixty years before, in the same journal, Welham et al. (1942) reported that during World War II, many professional football players were deemed overweight by military service criteria and rejected for military service. However, using densitometry, Behnke showed that football players actually had smaller BF% (Behnke et al. 1995).

In our study, BMI in trained subjects was significantly higher than in untrained group. More than 28% of trained subjects had BMI in the overweight class (25–29.9 kg·m^{-2}). Regarding BMI, these data could suggest higher prevalence of obesity in trained subjects. Meanwhile, our study also indicates that only 1% of trained subjects had BF% over 20, compared with untrained where more than 9% had BF% over

20%. Similar to our results, the recent studies illustrated that higher BMI does not necessarily represent overfatness across athletic populations (Witt and Bush 2005; Nevill et al. 2006; Ode et al. 2007). However, we found strong correlation of BMI and BF% within both groups which may suggest that both parameters could be used in trained population but in ranges specifically derived concerning age, gender and physical activity level. Fact that in the group of untrained subjects with BMI over 25 $kg \cdot m^{-2}$ only 45.9% had elevated BF% showed that BMI could be also poor predictor of overweight in untrained persons. However, those results should be taken with caution, after taking in consideration that in our control group were only young individuals.

Influence of physical activity on BF% is not surprising. Study of large populations of men has shown that physical performance is negatively related to body fat and positively related to skeletal muscle mass (Mateigka 1921). Other investigators also examined the effect of exercise on anthropometric characteristics of trained subjects (Curtin et al. 1997; Harris et al 2003; Watts et al. 2003; Goh et al. 2004; Witt and Bush 2005).

Several methods have been used for measuring BF%, including dual-energy X-ray absorptiometry (Mateigka 1921; Curtin et al. 1997), skinfolds (Goh 2004), and hydrodensitometry (Hortobagyi et al. 1994; Kraemer et al. 2005). These methods of measuring BF% are more accurate than BMI, especially in trained subjects. In the present study, the BF% was measured using bioimpedance analyzer. Wang et al. (2000) reported that anthropometry and bioelectrical impendance are the most widely used methods for large studies, when no economic resource is available or when a quick measure is required. On the other hand, Segal (1996) illustrate that bioelectric impedance is another promising method for screening trained subjects, but it is difficult for trained subjects to follow the exercise, hydration and eating guidelines needed for reliable measurements.

Compared with the current recommendation BF%, in our study the BF% below 8% had 76 subjects (25%) in trained group and only 3 subjects (2%) in untrained group. The results suggest that recommendation for general population in assessing body fat could be underestimated. Despite the inherit recommendation 25% of basketball players are considered underweight. This illustrates the limitations in the current general recommendation for adult population. Consequently, a different, specific classification system should be used to assess BF% in trained subjects.

Previous studies recommended specific values for BF% in male trained subjects for different sports activities (Sinning 1974; Rusko et al. 1978; Siders et al. 1991; Hortobagyi et al. 1994). In Siders study, for basketball players, BF% at 12.4% was used as cut point (Siders et al. 1991). According to this finding, in our study 97 basketball players (32%) had BF% values higher than recommended.

Conclusion

In conclusion, the results of our study suggest that BMI ≥ 25 $kg \cdot m^{-2}$ is not an accurate predictor of overweight in trained subjects. Because of a larger muscle mass, BMI incorrectly classifies trained subjects as overweight. Our results suggest that in assessing overweight apart age and gender we have to consider the type and level of physical activity. On the other side, strong relationship of BMI and BF% within trained and untrained, showed that both methods could be used but with specifically derived cut-off points.

References

Behnke A. R. Jr., Feen B. G., Welham W. C. (1995): The specific gravity of healthy men. Body mass divided by volume as an index of obesity. Obes. Res. **3,** 295–300

Curtin F., Morabia A., Pichard C., Slosman D. O. (1997): Body mass index compared to dual-energy X-ray absorptiometry: evidence for a spectrum bias. J. Clin. Epidemiol. **50**, 837–843Deurenberg P., Weststrate J. A., Seidell J. C. (1991): Body mass index as a measure of body fatness: age and sex specific prediction formulas. Br. J. Nutr. **65,** 105–114

Gallagher D., Heymsfield S. B., Heo M., Jebb S., Murgatroyd P. R., Sakamato Y. (2000): Health percentage fat ranges: an approach for developing guidelines based on body mass index. Am. J. Clin. Nutr. **72**, 694–701

Garrow J. S., Webster J. (1985): Quetelet's index (W/H2) as a measure of fatness. Int. J. Obes. **9**, 147–153

Goh V. H. H., Tain C. F., Tong T. Y. Y., Mook H. P. P., Wong M. T. (2004): Are BMI and other anthropometric measures appropriate as indices for obesity? A study in an Asian population. J. Lipid Res. **45**, 1892-1898

Harp J. B., Hecht L. (2005): Obesity in the National Football League. JAMA **293**, 1061–1062

Harris N., Rosenberg A., Jangda S., O'Brien K., Gallagher M. L. (2003): Prevalence of obesity in International Special Olympic athletes as determined by body mass index. J. Am. Diet. Assoc. **103,** 235–237

Hortobágyi T., Israel R. G., O'Brien K. F. (1994): Sensitivity and specificity of the Quetelet index to assess obesity in men and women. Eur. J. Clin. Nutr. **48**, 369–375

Jonnalagadda S. S., Skinner R., Moore L. (2004): Overweight athlete: fact or fiction? Curr. Sports Med. Rep. **3**, 198–205

Kraemer W. J., Torine J. C., Silvestre R. (2005): Body size and composition of National Football League Players. J. Strength Cond. Res. **19**, 485–489

Lee R., Nieman D. (1993): Anthropometry. In: Nutritional Assessment. (Ed. J. Wheatly), pp. 121–163, McGraw Hill Higher Education, Madison

Mateigka J. (1921): The testing of physical efficiency. Am. J. Phys. Anthropol. **4,** 223–225

Nevill A., Stewart A., Olds T., Holder R. (2006): Relationship between adiposity and body size reveals limitations of BMI. Am. J. Phys. Anthropol. **129**, 151–156

NHLBI (2000): National Heart, Lung and Blood Institute Obesity Education Initiative Expert Panel on the Identification, Evaluation, and Treatment of Overweight and Obesity in Adults. The Practical Guide. Bethesda, MD

Ode J. J., Pivarnik M. J., Reeves J. M., Knous L. J. (2007): Body mass index as a predictor of percent fat in college athletes and nonathletes. Med. Sci. Sports Exerc. **39**, 403–409

Ogden C., Carroll M., Curtin L., McDowell M., Tabak C., Flegal K. (2006): Prevalence of overweight and obesity in the United States, 1999–2004. JAMA **295,** 1549–1555

Pi-Sunyer F. X. (1993): Medical hazards of obesity. Ann. Intern. Med. **119**, 655–660

Prentice A. M., Jebb S. A. (2001): Beyond body mass index. Obes. Rev. **2,** 141–147

Rusko H., Havu M., Karivien E. (1978): Aerobic performance capacity in athletes. Eur. J. Appl. Physiol. **38,** 151–159

Segal K. R. (1996): Use of bioelectrical impedance analysis measurements as an evaluation for participating in sports. Am. J. Clin. Nutr. **64**, S469–471

Siders W. A., Bolonchuk W. W., Lukaski H. C. (1991): Effects of participation in a collegiate sport season on body composition. J. Sports Med. Phys. Fitness **31**, 571–576

Sinning W. E. (1974): Body composition assessment of college wrestlers. Med. Sci. Sports Exerc. **6**, 139–145

Wang J., Thornton J. C., Kolesnik S., Pierson R. N. Jr. (2000): Anthropometry in body composition. An overview. Ann. N. Y. Acad. Sci. **904**, 317–326

Watts P. B., Joubert L. M., Lish A. K., Mast J. D., Wilkins B. (2003): Anthropometry of young competitive sport rock climbers. Br. J. Sports Med. **37,** 420–424

Welham W. C., Behnke A. R. Jr. (1942): The specific gravity of healthy men: body weight-volume and other physical characteristics of exceptional athletes and of naval personnel. JAMA **118**, 498–501

Witt K. A., Bush E. A. (2005): College athletes with an elevated body mass index often have a high upper arm muscle area, but not elevated triceps and subscapular skinfolds. J. Am. Diet. Assoc. **105,** 599–602

Oxidative stress biomarker response to concurrent strength and endurance training

Dragan Radovanovic[1], Milovan Bratic[1], Mirsad Nurkic[1], Tatjana Cvetkovic[2], Aleksandar Ignjatovic[1] and Marko Aleksandrovic[1]

[1] *Faculty of Sport and Physical Education University of Niš, Serbia*
[2] *Institute for Biochemistry, Faculty of Medicine, University of Niš, Serbia*

Abstract. The purpose of this study was to investigate the effects of concurrent training on oxidative stress biomarkers in judokas, as well as to compare the effects of such training on performance characteristics in relation to usual training programs. A total number of 14 male judokas were divided into two groups: experimental (E) and control (C). Over 12 weeks, subjects from E group were included into specially designed training composed of concurrent strength and endurance training and perfecting of specific judo techniques. Subjects from C group were included into the same strength training and perfecting of specific judo techniques, but did not have any endurance training. The investigation protocol consisted of Wingate test for the upper extremities, estimation of maximum oxygen uptake, the assessment of body composition, special judo fitness test and determination of selected markers of oxidative stress. The results obtained suggest that usual training program pattern had no effects on oxidative stress levels in C group subjects, while concurrently performed training for strength and endurance induces the increases in anaerobic power and maximal oxygen uptake, but also affects oxidative stress biomarkers. A significant increase in erythrocyte malondialdehyde and plasma catalase can be considered negative effects of this training program.

Key words: Oxidative stress — Concurrent training — Judo — Power

Abbreviations: ROS, reactive oxygen species; MDA, malondialdehyde; CAT, catalase; VO_{2peak}, maximal aerobic uptake; SJFT, special judo fitness test.

Introduction

Free radicals, chemical species containing one or more unpaired electrons that are capable of independent existence, are produced in all living cells. The majority of free radicals produced *in vivo* are oxidants, which are capable of oxidizing a range of biological molecules, including carbohydrates, amino acids, fatty acids and nucleotides. Generation of reactive oxygen species (ROS) is a normal process in the life of aerobic organisms. Under physiological conditions, these deleterious species are mostly removed by the cellular antioxidant systems, which include antioxidant vitamins, protein and non-protein thiols, and antioxidant enzymes. Muscular exercise increases the production of free radicals and other forms of ROS (Alessio et al. 2000). The risk of oxidative stress with exercise depends on exercise intensity and the participant's state of training (Radovanovic and Rankovic 2004). It is widely assumed that oxidative stress is detrimental to exercise performance, but there is little experimental evidence to support this (Sachdev and Davies 2008).

Judo is characterized by short duration, high-intensity, intermittent exercise followed by a period of constant pulling, pushing, lifting, grappling and gripping movements in preparation for the next explosive effort. As a result, judo is often considered to be an explosive sport which demands great anaerobic strength and capacity, accom-

Correspodence to: Dragan Radovanović, Faculty of Sport and Physical Education, University of Niš, Čarnojevića 10A, 18000 Niš, Serbia
E-mail: drdr@bankerinter.net

panied by a well developed aerobic system. A high level of physical fitness and strength, with good fatigue tolerance, are necessary preconditions for competitive success (Pulkkinen 2001). From the aspect of exercise physiology, competitive success depends significantly on the ability of the judokas to, within their own weight category, achieve higher levels of anaerobic capacity and manifest great muscle strength with quick recovery between successive matches (Borkowski et al. 2001).

In the past decade, concurrent strength and endurance training has received much attention as a form of training. Many of previous investigations have examined similar variables including maximal aerobic uptake (VO_{2peak}), anaerobic power, isotonic and isokinetic strength, and body composition during concurrent training (Dolezal and Potteiger 1998; Leveritt et al. 1999). Moreover, they have demonstrated that the impact of concurrent training appears to be more determinable to potential strength gains and not to aerobic power (Rahnama et al. 2007). Additionally, after concurrent strength and endurance training, investigators have noted positive changes in body composition (decreases in fat mass and body fat percentage) (Garcia-Lopez et al. 2007; Rahnama et al. 2007).

The purpose of this study was to investigate the effects of concurrent training on oxidative stress biomarkers in judokas, as well as to compare the effects of such training on performance characteristics in relation to usual training programs during the preparatory period in judokas.

Materials and Methods

Subjects

A total number of 14 male judokas, with several-year-lasting sport experience, participated in the investigation. They were divided into two groups: experimental (E, $n = 7$) and control (C, $n = 7$). Over 12 weeks, subjects from E group were included into specially designed training program composed of concurrent strength and endurance training and perfecting of specific judo techniques. Subjects from C group were included into the same strength training and perfecting of specific judo techniques, but did not have any endurance training. The whole investigation was carried out during preparatory period, before the start of competition period.

The purpose of the study was explained to the subjects and all gave their informed consent. None of the participants suffered any illness for at least two weeks before the study. They were not taking any medication known to affect hormonal or metabolic responses to exercise. In the present study, however, we did not assess the dietary intake of the subjects.

Experimental design

Strength training

The 12-week whole-body strength training was carried out, under supervision, three times per week. The program included three to five exercises for the main muscle groups of the body. Mainly, machine exercises were used throughout the training period. All exercises were performed using concentric muscle action, followed by eccentric action. The loads were determinate according to the one-repetition maximum (1RM) method. The intensity ranged from 60 to 85% of the 1RM. The number of sets in each exercise increased and the number of repetitions decreased during the training program.

Endurance training

Endurance training consisted of running twice a week. All the training sessions were supervised and a heart rate monitor was used. Subjects were engaged in a 30 min training session divided into four loading intervals: 10 min under aerobic threshold, 5 min between aerobic-anaerobic thresholds, 5 min above the anaerobic threshold and again 10 min under aerobic threshold. The focus of training was to improve maximal endurance in a 30-min session.

Laboratory testing

The anaerobic capacity parameters (peak power and mean power) were determined by the "all-out" 30-s anaerobic Wingate test (Inbar et al. 1996). This test is known to be a highly reliable and valid test of anaerobic power. For the purpose of this test, an arm cycle ergometer (Monark, Sweden) equipped with an electronic measuring device with a display was used. The setting up of the equipment and the subjects' warm-up was carried out according to standard protocols. Data registration was carried out with the help of a specially designed computer program on the basis of the standards devised by the author of the test and the published technical description of a system for registering data by means of a computer (Inesta et al. 1995).

VO_{2peak} was estimated by a method of extrapolation (American College of Sports Medicine 2006) after a standardized submaximal test on the leg cycle ergometer (Kettler, Germany) and arm cycle ergometer (Monark, Sweden) along with telemetric monitoring of heart function (Polar, Finland). The testing was carried out at least 24 h prior the execution of the "all-out" Wingate test. All laboratory testing were carried out in the morning hours; in a room where the temperature was 21–23°C, and the humidity was 55–60%, so that the microclimatic conditions conformed to the standards for functional laboratory testing (Winter et al. 2007).

The percentage of fat mass was measured by bioelectrical impedance analysis (see in References: National Institute of Health Technology 1996) and the device BF300 (Omron, Japan) was used. Data regarding percentage of fatty tissue were read off the display with an accuracy of 0.1%.

Field test

The special judo fitness test (SJFT) (Franchini et al. 1998) was performed in a training gym, at least 6 h after Wingate test, in the following sequence: two *Uke* judokas in the same weight category and of similar height were positioned at a distance of 6 m from each other, while the tested subject, *Tori*, stood in the middle between them. When the command *Hajime* was given, the *Tori* was required to run up to one of the *Ukes* and perform an *Ippon-seoi-nage* throw, followed by the same type of throw on the second *Uke*. This procedure was repeated for 15 s (series A), after which the *Matte* command was given, followed by a 10-s break. Series B and series C followed on after procedures was repeated for 15 s (series A), after which the *Matte* command was given, followed by a 10-s break. Series B and series C followed on after a second and third 10-s break. The heart rate was measured after 1 min rest, which followed immediately on the series A, B and C throws. The SJFT index was calculated according to the following equation: $(HReff + HRres)\cdot(A + B + C)^{-1}$ where HReff and HRres are the heart rate following the effort, and 1 min after the test, respectively, and A + B + C is the total number of throws effected in series A, B and C. A lower index indicated better results.

Blood sample preparation and analysis

Venous blood samples were taken using ethylenediaminetetraacetic acid as an anticoagulant. Blood samples obtained from brachiocephalic vein at rest at the beginning of investigation, and after 12 weeks were analyzed for the determination of selected markers of oxidative stress – malondialdehyde (MDA), catalase (CAT), carbonyl and sulphydryl group assay for determination of modified proteins and total antioxidant status. Blood markers of oxidative stress were determined by standardized spectrophotometry techniques (Goth 1991; Levine et al. 1994; Koracevic et al. 2001).

Statistical analysis

Depending on a statistical marker, measurement scale, type of distribution, and number and size of samples, the following tests were used: Student's *t*-test, Mann-Whitney U test, the Wilcoxon rank sum test, and the Wilcoxon test for paired samples. In order to process the results of the study, the SPSS statistical program for Windows (Release 10.0; Chicago, IL, USA) was used. Statistical significance was set at $p = 0.05$ for all statistical analyses.

Results

The results of study are presented in Tables 1, 2 and 3.

Table 1. Subject physical characteristics along 12-week experimental training period

	E ($n = 7$)	C ($n = 7$)
Age (years)	23 ± 1.5	22 ± 1.8
Sport experience (years)	13 ± 4.2	12 ± 3.7
Body height (cm)	178.4 ± 6.18	176.9 ± 7.44
Body weight (kg)		
Pre-training	75.3 ± 11.2	74.1 ± 10.5
Post-training	72.6 ± 9.9 *	72.8 ± 9.7
Body fat content (%)		
Pre-training	9.08 ± 3.86	8.82 ± 4.08
Post-training	7.86 ± 4.04 *	8.4 ± 3.64

Values are means ± SD; * significant difference ($p < 0.05$) from corresponding pre-training value; E, experimental group; C, control group.

Table 2. Subjects performance characteristics along 12-week experimental training period

	E ($n = 7$)	C ($n = 7$)
Peak power ($W\cdot kg^{-1}$) on arm ergometer		
Pre-training	9.82 ± 1.66	9.44 ± 1.82
Post-training	11.78 ± 1.8 *	12.34 ± 1.94 *
Mean power ($W\cdot kg^{-1}$) on arm ergometer		
Pre-training	7.16 ± 0.96	7.31 ± 1.08
Post-training	8.54 ± 1.1 *	8.98± 1.22 *
VO_{2peak} ($ml\cdot kg^{-1}\cdot min^{-1}$) on arm ergometer		
Pre-training	46.52 ± 6.67	48.32 ± 6.22
Post-training	50.86 ± 5.92 *	47.66 ± 5.84
VO_{2peak} ($ml\cdot kg^{-1}\cdot min^{-1}$) on leg ergometer		
Pre-training	51.24 ± 7.38	50.28 ± 6.6
Post-training	54.58 ± 6.96 *	51.98 ± 7.08
SJFT index		
Pre-training	15.86 ± 2.32	15.41 ± 2.08
Post-training	13.24 ± 1.75 *	13.58 ±1.91 *

Values are means ± SD; * significant difference ($p < 0.05$) from corresponding pre-training value. E, experimental group; C, control group.

Table 3. Oxidative stress biomarkers along the study period

	E ($n = 7$)	C ($n = 7$)
Erythrocyte MDA ($\mu mol \cdot l^{-1}$)		
Pre-training	14.74 (10.69–16.81)	13.86 (9.56–16.12)
Post-training	19.18 (15.17–27.21)*	15.62 (10.06–21.88)
Plasma CAT ($IU \cdot l^{-1}$)		
Pre-training	8.57 (4.08–14.72)	7.21 (3.65–13.24)
Post-training	25.66 (10.38–44.20)*	9.44 (5.56–18.28)
Sulphydryl group ($\mu mol \cdot l^{-1}$)		
Pre-training	211.10 (183.80–258.01)	191.06 (170.12–216.46)
Post-training	246.28 (235.97–353.64)	205.73 (186.49–217.31)
Carbonyl group ($\mu mol \cdot g^{-1}$)		
Pre-training	0.60 (0.53–1.18)	0.71 (0.6–0.98)
Post-training	0.89 (0.55–1.11)	0.82 (0.66–1.06)
Total antioxidant status (%)		
Pre-training	74.65 (47.08–94.53)	59.91 (37.66–82.29)
Post-training	84.55 (83.80–86.43)	62.67 (40.02–88.26)

Values are Me (25–75. percentil); * significant difference ($p < 0.05$) from corresponding pre-training value (Wilcoxon test); E, experimental group; C, control group.

Discussion

Strenuous exercise is characterized by an increased oxygen consumption and disturbance of intracellular prooxidant-antioxidant homeostasis. Under physiological conditions, these deleterious species are mostly removed by the cellular antioxidant systems, which include antioxidant vitamins, protein and non-protein thiols, and antioxidant enzymes. Some conditions associated with intense exercise, such as local tissue hypoxia or elevated tissue temperatures, could also contribute to reactive oxygen production (Alessio et al. 2000). The evidence that muscle conditioning results in upregulation of antioxidant defenses (Gomez-Cabrera et al. 2008) also suggests a close relationship between reactive oxygen and contractile activity. Therefore, there appears to be a significant role for reactive oxygen in normal muscle physiology. However, a number of conditions may lead to an imbalance of oxidant production and antioxidant defense, and these, presumably, do create conditions of oxidant stress (Bloomer et al. 2005). To defend against ROS, muscle cells contain complex cellular defense mechanisms to reduce the risk of oxidative injury. Two major classes of endogenous protective mechanisms (enzymic and non-enzymic) work together to reduce the harmful effects of oxidants in the cell (Sachdev and Davies 2008). The mechanisms of exercise-induced oxidative stress are not well understood. There is no evidence that this affects sporting performance in the short term, although it may have longer term, not necessarily detrimental, health consequences.

Strength and endurance training, when performed independently, induces different functional and structural adaptations with little overlap between them. Strength training typically results in the increase in muscle mass and muscle power. In contrast, endurance training induces increases in maximal oxygen uptake and metabolic adaptation that lead to an increased exercise capacity (Hennessy and Watson 1994). In many sports, a combination of strength and endurance trainings is performed simultaneously which may lead to a potential interference in strength development making such a combination seemingly incompatible. It is now clear that, at molecular level, different forms of exercise induce antagonistic intracellular signaling mechanism that, in turn, could have a negative impact on muscle's adaptive responses to this particular form of training (McCarthy et al. 1995).

The effects of long-term exercise on steady-state dynamics of enzymatic antioxidant defense system are not clear, and there is an evident lack of studies focused on combat sports. The magnitude of oxidative damage may be related to the power of the pro-oxidant attack (intensity and duration of physical exercise) and capacity of the individual exerciser's antioxidant system (Bloomer et al. 2005; Degoutte et al. 2006).

The results of the conducted investigation showed that in the C group subjects there was a significant increase in the examined values of anaerobic capacity parameters, peak and mean power, after 12 weeks' strength training (Figures 1 and 2). In this group of subjects, VO_{2peak} value did not change significantly after 12 weeks (Figures 3 and 4). A methodical plan aimed to improve the performance of specific judo techniques, performed under the supervision of experienced trainers, resulted in a greater number of throws made during SJFT. With a somewhat lower value of

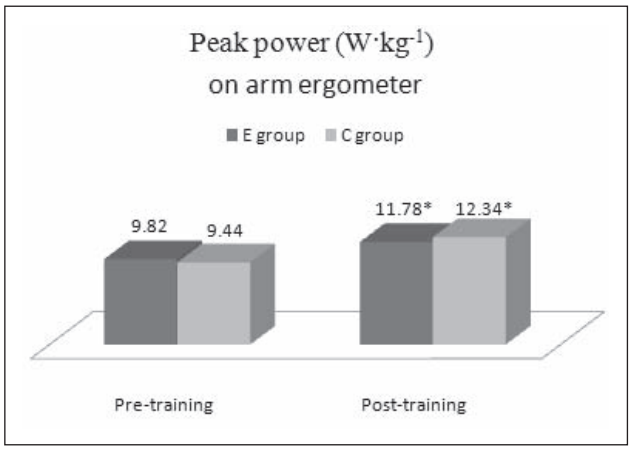

Figure 1. The anaerobic capacity parameter peak power in experimental (E group) and control (C group) subjects. The levels of peak power were determined as described in Materials and Methods. Values are means ± SD; * significant difference ($p < 0.05$) from corresponding pre-training value.

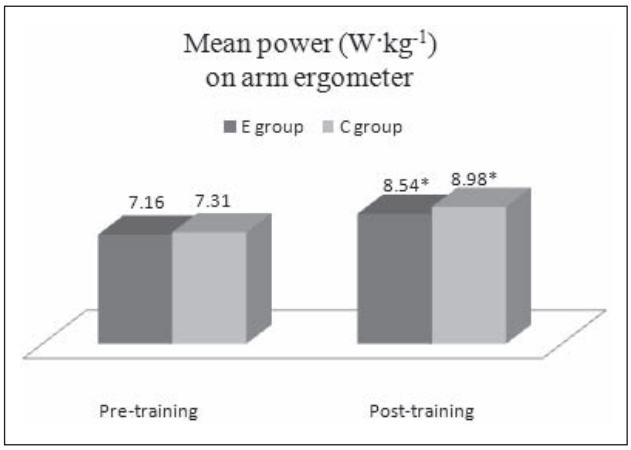

Figure 2. The anaerobic capacity parameter mean power in E group and C group. The levels of mean power were determined as described in Materials and Methods. Values are means ± SD; * significant difference ($p < 0.05$) from corresponding pre-training value.

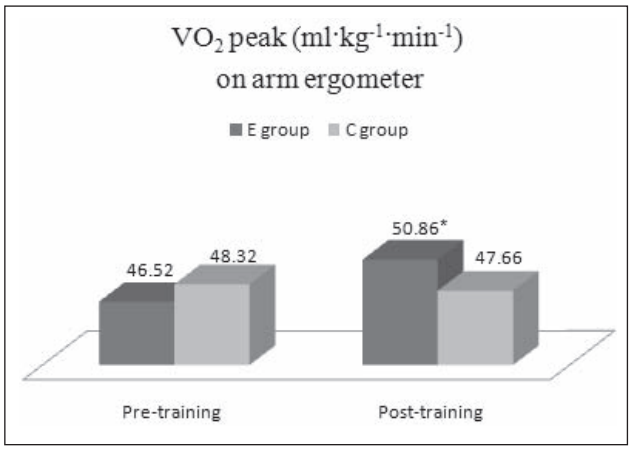

Figure 3. Maximal aerobic uptake (VO_{2peak}) estimated after a standardized test on the arm cycle ergometer in E group and C group. The levels of VO_{2peak} were determined as described in Materials and Methods. Values are means ± SD; * significant difference ($p < 0.05$) from corresponding pre-training value.

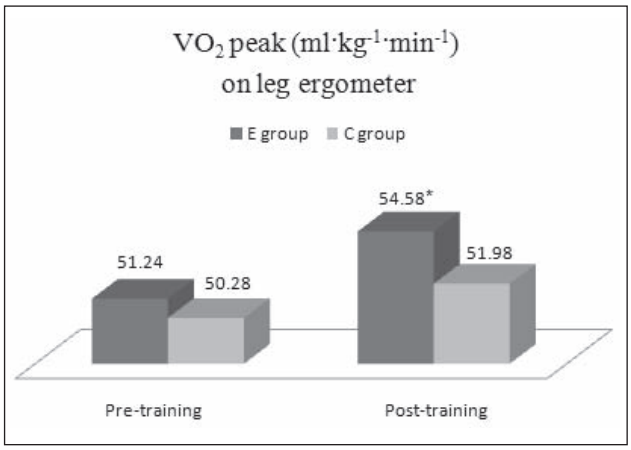

Figure 4. Maximal aerobic uptake (VO_{2peak}) estimated after a standardized test on the leg cycle ergometer in E group and C group. The levels of VO_{2peak} were determined as described in Materials and Methods. Values are means ± SD; * significant difference ($p < 0.05$) from corresponding pre-training value.

the heart frequency, the overall SJFT index was lower, and the achievement was better. The comparison of values of the mentioned index in the C group subjects showed that the increase was above the threshold for statistical significance (Figure 5). The changes in all examined oxidative stress markers showed no statistical significance (Table 3). The explanation for this finding can be found in the fact that the subjects, although chronologically young, had a long experience with the similar pre-competitive preparation programs. The applied program differed by its higher intensity and duration of strength training as well as longer overall duration of daily trainings from common trainings conducted throughout the year. It can be concluded that this training program pattern had no effects on oxidative stress levels in well-trained young judokas, and that the body's natural antioxidant defenses responded adequately to increases in 12-weeks training program.

In the E group subjects, 12-weeks' concurrent training resulted in a statistically significant increase in the values of anaerobic capacity parameters (Figures 1 and 2). The

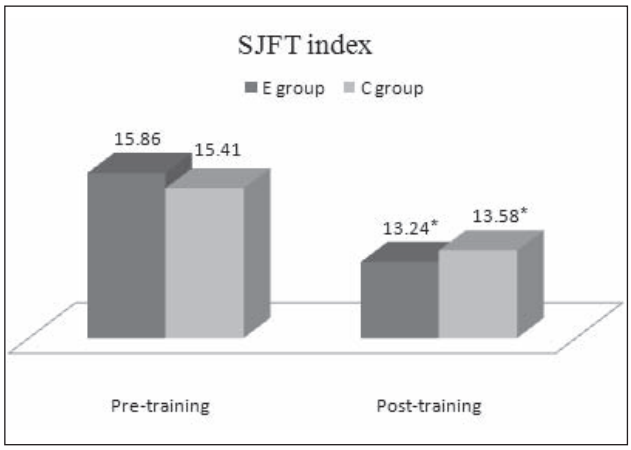

Figure 5. The special judo fitness test (SJFT) index in E group and C group. SJFT index was calculated as described in Materials and Methods. Values are means ± SD; * significant difference ($p < 0.05$) from corresponding pre-training value.

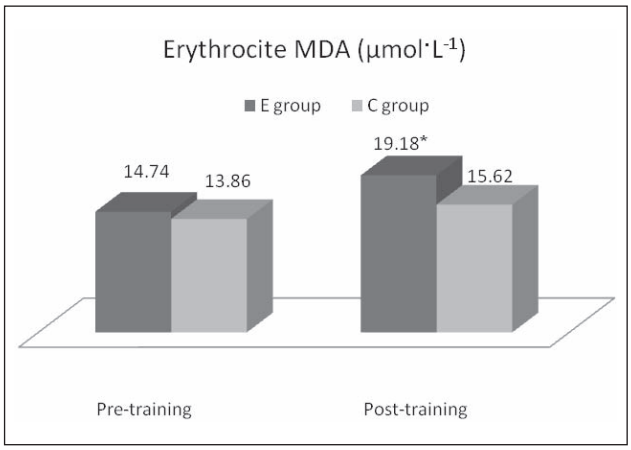

Figure 6. Marker of oxidative stress erytrocite malondialdehyde (MDA) in E group and C group. The levels of different oxidative stress biomarkers were determined as described in Materials and Methods. Values are Me (25–75. percentil). * significant difference ($p < 0.05$) from corresponding pre-training value (Wilcoxon test).

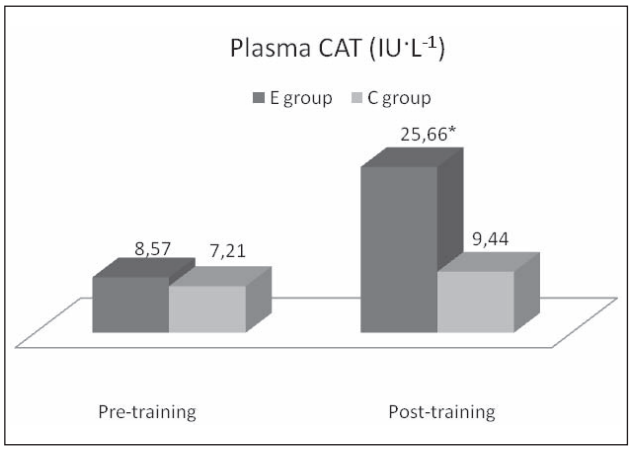

Figure 7. Marker of oxidative stress plasma catalase (CAT) in E group and C group. The levels of different oxidative stress biomarkers were determined as described in Materials and Methods. Values are Me (25–75. percentil). * significant difference ($p < 0.05$) from corresponding pre-training value (Wilcoxon test).

comparison of results obtained between groups showed that at the beginning and end of the investigation there were no statistically significant differences in the examined parameters. However, the values of anaerobic capacity parameters were higher in the C group subjects after 12 weeks. The above mentioned points out that the concurrent training resulted in somewhat smaller effects of strength training in the E group subjects. VO_{2peak} values were statistically significantly higher after 12-weeks' training (Figures 3 and 4), pointing out to the effectiveness of concurrent training on the development of endurance. SJFT index values were statistically significantly lower after 12-weeks' preparatory period (Figure 5). Such a result is attributed to the improvement in performances of specific judo techniques, the same as in the C group subjects, as well as to a significantly lower heart frequency during the test which is considered to be another effect of endurance training. After both 12 weeks' training programs we noticed statistically significant changes in body composition of subjects involved in study, decreased of body weight and body fat content (Table 1). A smaller percentage of fatty tissue in elite judokas is thought to enable better metabolic adaptation to different technical-tactical demands during the match (Kim et al. 1996). The comparison of the examined markers of oxidative stress showed that the values of erythrocyte MDA (Figure 6) and plasma CAT (Figure 7) were statistically significantly increased after 12-weeks' training. We consider the results obtained, especially if compared to the results in the C group, a consequence of simultaneously applied strength and endurance training.

The findings of similar investigation (Bloomer et al. 2005; Rahnama et al. 2007; Garcia-Lopez et al. 2007) of the application of concurrent training in other sports may indirectly confirm our conclusions. Other investigations that studied simultaneous training for the development of endurance and muscle power in a long-time period (Hennessy and Watson 1994; McCarthy et al. 1995) indicated the possibility of a decrease in physical abilities in athletes with a several-year-lasting training experience. The abilities that require demonstration of power, i.e. large muscle power and speed, are the most susceptible to the "incompatibility" with the above-mentioned programs for large-extent and high-

intensity trainings to which elite athletes are subjected to. The successful combination of training depends on many factors such as the athlete's genetic potential, length of training experience, current physical preparation form, intensity and extent of training, optimal periodization, nutrition and supplementation etc.

The results obtained suggest that concurrently performed training for strength and endurance induces the increase in anaerobic power and maximal oxygen uptake, but also affects oxidative stress biomarkers. A significant increase in erythrocyte MDA and plasma CAT can be considered negative effects of this training program. Since certain biomarkers of oxidative stress are increased after functionally effective specially designed judo training, future research may investigate the methods of reducing macromolecule oxidation, possibly through the use of antioxidant supplementation.

References

Alessio H. M., Hagerman A. E., Fulkerson B. K. (2000): Generation of reactive oxygen species after exhaustive aerobic and isometric exercise. Med. Sci. Sports Exerc. **32**, 1576–1581

American College of Sports Medicine (2006): ACSM's Guidelines for Exercise Testing and Prescription. (7th edition), Lippincott Williams & Wilkins, Baltimore

Bloomer R. J., Goldfarb A. H., Wideman L., McKenzie M. J., Consitt L. A. (2005): Effects of acute aerobic and anaerobic exercise on blood markers of oxidative stress. J. Strength Cond. Res. **19**, 276–285

Borkowski L., Faff J., Straczewska-Czapowska J. (2001): Evaluation of the aerobic and anaerobic fitness in judoists from the Polish national team. Biol. Sport **18**, 107–117

Degoutte F., Jouanel P., Bègue R. J., Colombier M., Lac G., Pequignot J. M., Filaire E. (2006): Food restriction, performance, biochemical, psychological, and endocrine changes in judo athletes. Int. J. Sports Med. **27**, 9–18

Dolezal B. A., Potteiger J. A. (1998): Concurrent resistance and endurance training influence basal metabolic rate in nondieting individuals. J. Appl. Physiol. **85**, 695–700

Franchini E., Nakamura F. Y., Takito M. Y., Kiss M., Sterkowicz S. (1998): Special judo fitness test in judo athletes. Biol. Sport **3**, 135–140

Garcia-Lopez D., Hakkinen K., Cuevas M. J., Lima E., Kauhanen A., Mattila M., Sillanpää E., Ahtiainen J. P., Karavirta L., Almar M., González-Gallego J. (2007): Effects of strength and endurance training on antioxidant enzyme gene expression and activity in middle-aged men. Scand. J. Med. Sci. Sports **17**, 595–604

Gomez-Cabrera M. C., Domenech E., Viña J. (2008): Moderate exercise is an antioxidant: upregulation of antioxidant genes by training. Free Radic. Biol. Med. **44**, 126–131

Goth L. (1991): Serum catalase: reversibly formed charge isoform of erythrocyte catalase. Clin. Chem. **37**, 2043–2047

Hennessy L. C., Watson A. S. (1994): The interference effect of training for strength and endurance simultaneously. J. Strength Cond. Res. **8**, 12–19

Inbar O., Bar-Or O., Skinner J. S. (1996): The Wingate Anaerobic Test. Human Kinetics Europe Ltd.

Inesta J. M., Izquierdo E., Angeles Sarti M. (1995): Software tools for using a personal computer as a timer device to assess human kinetic performance: a case study. Comput. Methods Prog. Biomed. **47**, 257–265

Kim K. J., Kim E. H., Han M. W. (1996): A comparation of physiological and performance responses for analysis of the degree of judo training intensity. Kor. J. Sport. Sci. **8**, 52–64

Koracevic D., Koracevic G., Djordjevic V. (2001): Method for the measurement of antioxidant activity in human fluids. J. Clin. Pathol. **54**, 356–361

Leveritt M., Abernethy P. J., Barry B. K., Logan P. A. (1999): Concurrent strength and endurance. Sports. Med. **28**, 413–427

Levine R. L., Wiliams J. A., Stadtman E. R. (1994): Carbonil assay for determination of oxidative modified proteins. Methods Enzymol. **233**, 346–357

McCarthy M. J., Agre J. C., Graf B. K., Poziniak M. A., Vailas A. C. (1995): Compatability of adaptive responses with combining strength and endurance training. Med. Sci. Sport Exercise **27**, 429–436

National Institute of Health Tehnology (1996): Bioelectrical impedance analysis in body composition measurement. Assement conference statement. Am. J. Clin. Nutr. **64**, 524–536

Pulkkinen W. J. (2001): The Sport Science of Elite Judo Athletes: a Review and Application for Training. Pulkinetics Inc., Guelph, Ontario, Canada

Radovanovic D., Rankovic G. (2004): Oxidative stress, stress proteins and antioxidants in exercise. Acta Med. Medianae. **43**, 45–48

Rahnama N., Gaeini A. A., Hamedinia M. R. (2007): Oxidative stress responses in physical education students during 8 weeks aerobic training. J. Sports Med. Phys. Fitness **47**, 119–123

Sachdev S., Davies K. J. (2008): Production, detection, and adaptive responses to free radicals in exercise. Free Radic. Biol. Med. **44**, 215–223

Winter E. M., Andrew M. J., Richard Davison R. C., Bromley P. D., Mercer T. H. (2007): Sport and Exercise Physiological Testing. Guidelines of British Association of Sport and Exercise Sciences. Routledge, London

Live monitoring of brain damage in the rat model of amyotrophic lateral sclerosis

Danijela Bataveljić[1], Nevena Djogo[1], Ljubica Župunski[1], Aleksandar Bajić[1], Charles Nicaise[2], Roland Pochet[2], Goran Bačić[3] and Pavle R. Andjus[1]

[1] *Department of Physiology and Biochemistry, School of Biology, University of Belgrade, Serbia*
[2] *Laboratory for Histology, Neuroanatomy and Neuropathology, School of Medicine, ULB, Brussels, Belgium*
[3] *Faculty of Physical Chemistry, University of Belgrade, Serbia*

Abstract. Amyotrophic lateral sclerosis (ALS) is a devastating neurological disorder affecting upper and lower motoneurons. The transgenic ALS rat model (hSOD-1^{G93A}) was used for magnetic resonance imaging (MRI) study using a low field wide bore magnet. T2-weighted hyperintensities were observed in the brainstem, rubrospinal tract and vagus motor nuclei with prominent lateral ventricle and cerebral aqueduct enlargements. These changes could be observed already in presymptomatic animals. T2*-weighted MRI with magnetically labeled antibodies (against CD4) revealed lymphocyte infiltration in the brainstem-midbrain region corresponding to the areas of dilated lateral ventricles. Confocal imaging revealed reactive astroglia in these areas. Thus, with the use of wide bore MRI new sites of neurodegeneration and inflammation were revealed in the hSOD-1^{G93A} rat model.

Key words: Amyotrophic lateral sclerosis — Magnetic resonance imaging — Ultra small particles of iron oxide — hSOD-1^{G93A} rat model — CD4 cells — Astrogliosis

Introduction

Amyotrophic lateral sclerosis (ALS) is the most frequently encountered primary form of progressive motoneuron disease. It is a devastating neurological disorder affecting upper and lower motoneurons. It is characterized by progressive muscle weakness and atrophy. It is almost invariably fatal, usually within 3 to 6 years after the beginning of the symptoms.

ALS tissue studies reveal microglial activation as well as other markers of inflammatory processes in both human and transgenic mouse models (Alexianu et al. 2001; Appel and Simpson 2001; McGeer and McGeer 2002; Henkel et al. 2004). Moreover, neuroimmunologic evidence also exists for the systemic immunologic activation in sporadic ALS patients (Zhang et al. 2005). Flow cytometry of immune cell markers has thus revealed activated monocyte/macrophages, the degree of activation being directly correlated to the rate of disease progression. In addition, disease associated changes were also observed for parameters of T-cell activation and immune globulin levels. In a recent study of the role of individual cell types in the murine superoxide dismutase 1 (SOD-1)-based ALS the mutant gene SOD-1^{G37R} was selectively "turned down" in motor neurons or in microglia (Boillee et al. 2006). In addition to a substantial delay of onset and progression of the disease in motor neurons with suppressed mutant SOD-1, selective diminution of the mutant enzyme in microglia greatly delayed the progression of the later disease stage. Thus, the initiation role of microglia in the final stage leading to the demise of motor neurons in ALS was underlined. However, it could not be excluded that the slowing of the later disease phase may have also been caused in part by gene inactivation in peripheral macrophages or their progenitors and/or from the migration of those cells into the central nervous system after initial motor neuron damage.

Magnetic resonance imaging (MRI) as a non-invasive technique is becoming a preferred neuroimaging technique for the diagnosis of ALS since this is the only technique that can access the degenerative processes inside the upper motor cortex. ALS as "multi-focal system syndrome" is character-

Correspondence to: Pavle R. Andjus, School of Biology, Department of Physiology and Biochemistry, University of Belgrade, Studentski trg 12, 11001 Belgrade, Serbia
E-mail: pandjus@bf.bio.bg.ac.yu

ized by the degeneration of motor neurons followed by the loss of myelinated fibers which are clearly manifested as hyperintense areas in T2-weighted MRI (Ellis et al. 1999; Basak et al. 2002). However, a number of other neurological diseases can produce similar MRI findings. Numerous standard and advanced MRI techniques including diffusion imaging and magnetic resonance spectroscopy have been used to improve diagnostic capabilities and enhance specificity of the MRI examination (Hecht et al. 2002, Suhy et al. 2002; Sach et al. 2004), but it became clear that no further progress can be achieved without the reliable animal model where MRI findings can be compared to the pathological findings and putative therapeutic approaches can be tested in longitudinal studies. Transgenic mice overexpressing mutated human SOD-1 (hSOD-1) provided the first and still widely used animal model of familial ALS (Gurney 1997). In this model the foci of degeneration in brainstem and lumbar spinal cord have been shown to be similar to the findings in human pathology (Lowry et al. 2001). An MRI study of the transgenic mouse model (Zang et al. 2004) also revealed degenerative changes in the brain and cerebellum resembling findings in human MRI studies, but their findings were not very informative in terms of revealing underlying mechanisms.

Recently a transgenic rat model of ALS that expresses multiple copies of hSOD-1 carrying the G93A missense mutation (hSOD-1^{G93A}) has been developed (Howland et al. 2002) and it has been observed that this model of ALS exhibits electrophysiological and morphological features also manifested in human ALS (Philippeau et al. 2005). Due to the larger size as compared to the mouse model the hSOD-1^{G93A} transgenic rat allows for better phenotypic characterization, in particular more reliable use of physiological and biochemical techniques. Larger size of animals is also advantageous for MRI studies but no MRI study has been performed so far on this rat model presumably because of the common belief that specialized MRI machines are required. In line with the advantages of the rat model we have undertaken an MRI study of its brain in symptomatic and presymptomatic animals as compared to wild-type (WT) using clinical MRI and matching these findings with confocal microscopy of immunostained brain slices. In order to enhance the specificity of MRI evaluation and to demonstrate that an infiltration of inflammatory cells occurs in the neurodegenerative foci *in vivo* we also used CD4 antibodies commercially available as magnetically labeled with ultra small particles of iron oxide (USPIO). These paramagnetic nanoparticles are detectable through their property of generating strong susceptibility effects. Recently, several groups have reported success with immune cell-specific imaging, using superparamagnetic contrast materials that are either internalized by cells after *ex vivo* incubation, or bound to the cells by specific antibodies (Anderson et al. 2004; Bulte and Kraitchman 2004). Applying this approach for the first time in the ALS rat model we aimed to open doors for a better understanding of inflammatory infiltration through live tissue monitoring in this neurodegenerative disease.

Materials and Methods

Animals

Experiments were performed on Sprague-Dawley rats: genetically modified, expressing multiple copies of mutated (G93A) human SOD-1 gene (hSOD-1^{G93A}; Taconic Farms Inc. NY) and WT (standard Sprague-Dawley rats; kind gift from Dr. J. Borota). The disease was expressed 7 to 8 months upon birth and 20 ± 1 day (n = 7) was the period from the onset to the disease end-stage (mean age at end-stage was 254 ± 11 days, n = 8). The disease process was followed by visually checking the movement of the animal on a flat surface and by testing the regaining of stature after turning to the side and if the latter was not possible the end-stage of the disease was indicated and the animal was sacrificed for histology.

MRI

Animals were imaged in different stages of the disease – presymptomatic, symptomatic and end-stage. Rats were anaesthetized by intraperitoneal (i. p.) injection of 0.045 g/ml Nembutal (45 mg per kg body weight) and placed in the prone position for brain and brainstem imaging. Animals were treated in strict accordance with the European Communities Council Directive (86/609/EEC) and with approval of the Ethical Committee of the Faculty of Biology University of Belgrade. Accordingly all efforts were made to minimize animal suffering and to reduce the number of animals used. Standard T1-weighted (T1W) and T2W images of rats were obtained using the clinical 1.5 T Avanto MRI imager (Siemens) with a 3 cm mini surface radio frequence (RF) coil placed over the skull. Images were obtained using the Turbo Spin Echo T2W sequence with repetition time TR = 5800 ms; echo time TE = 200 ms, and the slice thickness of 1.5 mm (voxel dimensions 1.5 × 0.2 × 0.3 mm) and T1W imaging with TR = 400 ms, TE = 23 ms. The total scanning time including preparation of animal for imaging was about 45 min. Such relatively short scanning time allowed for work without supplemental body heating. Following MRI scans, rats were warmed and monitored until they recovered fully.

In order to check for the infiltration of inflammatory cells in the brain tissue antibodies against CD4 cells (mostly T cells and some macrophages and monocytes (Jefferies et al. 1985)), magnetically labeled with USPIO (MACS®, Miltenyi Biotec) were i.p. injected into rats (200 µl of original solu-

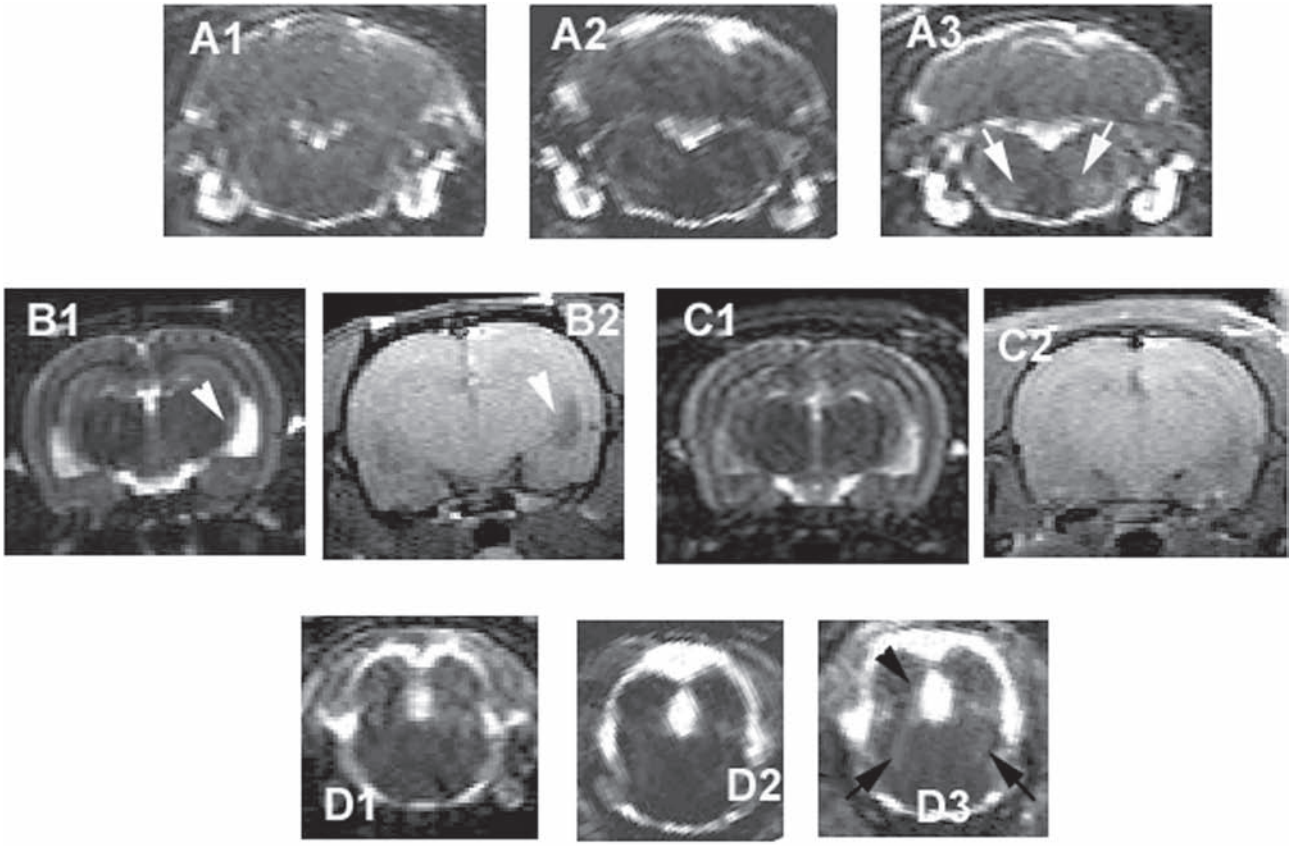

Figure 1. Coronal MRI of the brainstem of WT and presymptomatic and symptomatic hSOD-1^{G93A} rats at different levels. Hyperintensity can be observed in two cranial nerve nuclei: nucleus ambiguous and motor trigeminal nucleus, as well as in the paragigantocellular nucleus in the presymptomatic (243-days-old; A2) and in the disease end-stage (same animal 272-days-old; A3 – arrowheads), but not in WT of comparable age (A1). T2W and T1W MRI showed significant enlargement of the lateral ventricles at the end-stage in hSOD-1^{G93A} rats (B1 and B2, respectively, another animal, note arrowheads) as compared to WT (C1 and C2). Also note at the level of pons hyperintensity in the area of the rubrospinal tract – presymptomatic (D2) and symptomatic (D3), and an enlarged aqueduct (same animal as in A) as compared to WT (D1).

tion in 1 ml of physiological saline). Animals were injected 24 h prior to imaging, estimated as optimal incubation time for such studies (Floris et al 2004; Pirko et al. 2004). The anaesthetized animals were then scanned using the clinical 3.0 T MRI magnet (Intera, Phillips) with two small surface RF coils placed laterally at each side of the animal head (slice thickness – 2 mm, number of averages – 6, phase encoding number – 256, field of view – 100 mm, acquisition matrix – 256). Images were taken using the Gradient Echo T2*-weighted sequences (TR = 50 ms) and two different TE (20 ms and 30 ms) were used to confirm that the observed artifacts (signal voids) originate from uptaken USPIO-labeled antibodies. The specific small size and optimal filling factor of the excitation RF coils (Pirko et al. 2004) used in both MRI setups as well as the larger rat model as compared to the mouse allowed for obtaining good resolution even with a wide bore magnet.

Immunofluorescence

Brains were dissected from animals deeply anaesthetized with i. p. injection of Nembutal and fixed in 4% paraformaldehyde in 0.1 mol/l phosphate buffer pH 7.4 overnight at 4°C. Cryoprotection was achieved by immersion in 30% sucrose in 0.1 mol/l phosphate buffer. The brains were cut on a cryostat in 50 μm-thick coronal slices that were mounted on gelatinised microscope slides and dried overnight at room temperature. Slices were treated with 10% goat serum in PBS for 30 min and then incubated overnight at 4°C with primary antibodies in 2% goat serum in 0.01 mol/l PBS. Cell antigens were labelled for astrocytes with mouse monoclonal anti-glial fibrilary acidic protein (GFAP; 1 : 100, Molecular Probes Eugene). After wash in 0.01 mol/l PBS slices were incubated 2 h with secondary antibodies diluted in PBS. Visualization of primary labelling was done with Alexa Fluor 555-conjugated goat anti-mouse

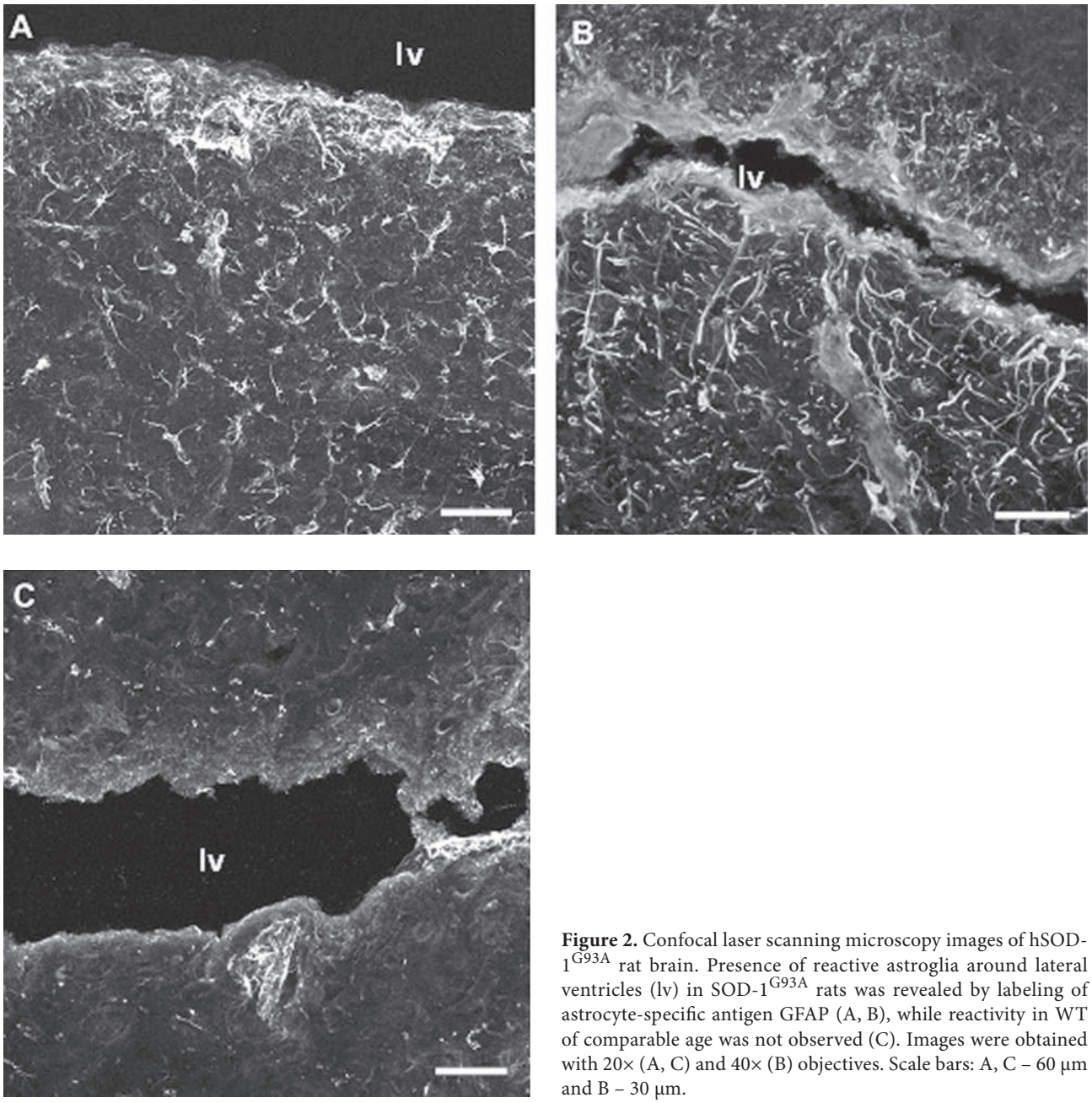

Figure 2. Confocal laser scanning microscopy images of hSOD-1^{G93A} rat brain. Presence of reactive astroglia around lateral ventricles (lv) in SOD-1^{G93A} rats was revealed by labeling of astrocyte-specific antigen GFAP (A, B), while reactivity in WT of comparable age was not observed (C). Images were obtained with 20× (A, C) and 40× (B) objectives. Scale bars: A, C – 60 μm and B – 30 μm.

antibodies (1 : 200, polyclonal, Molecular Probes). The stained sections were embedded with glycerol in PBS, glass covered and finally examined using LSM 510 confocal laser scanning microscope (Carl Zeiss, Jena, Germany).

Results and Discussion

In eight transgenic animals and two WT rats of comparable age MRI coronal images were obtained from the frontal cortex towards the brainstem medulla. As compared to age matched WT animals, hyperintensive areas in the tissue indicative of foci of neurodegeneration, were found in the brainstem of the G93A rats (Fig. 1). This was most apparent on T2-weighted images in the areas corresponding to the trigeminal and vagus motor nuclei, trigeminal spinal tract, parvicellular and paragigantocellular reticular nucleus, and nucleus ambiguus (see example in Fig. 1A3). These findings were congruent with the MRI study on the murine model (Zang et al. 2004). In the present study, however, hyperin-

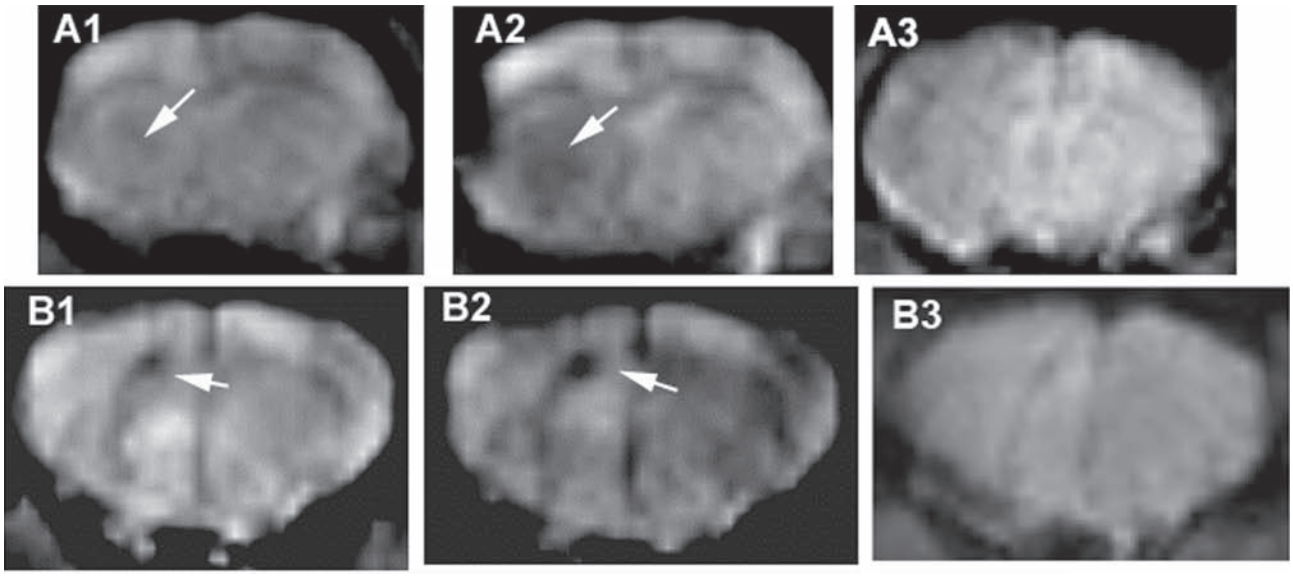

Figure 3. MRI of the brain of SOD-1^{G93A} rat at two disease stages (A – 222 and B – 215 days) injected with USPIO-tagged antibodies against CD4. For the midbrain region T2W images with TE = 20 ms revealed dark areas in the vicinity of the lateral ventricle (A1 – arrow) that became more apparent with TE = 30 ms (A2 – arrow). The latter protocol does not reveal a similar signal void in WT of comparable age (A3). Rostrally to the midbrain region in the vicinity of the lateral ventricle an apparent USPIO signal artefact was also observed with TE = 20 ms (B1 – arrow) and became more apparent with TE = 30 ms (B2 – arrow) with no similar effect of the latter protocol in the WT (B3).

tensive foci not observed in WT animals (Fig. 1A1) were already observable in presymptomatic animals (Fig. 1A2 – 243-days-old animal). Specifically for the rat model MRI also revealed neurodegeneration in the rubrospinal tract and vagus motor nuclei (presymptomatic vs. symptomatic – Fig. 1D2 vs. D3 – 29 days apart). However, the most apparent features of brain tissue atrophy observed in this model were the widespread enlargements of the lateral ventricles, clearly noted on T2W (Fig. 1B1, hyperintense regions) as well as on T1W images (Fig. 1B2, hypointense regions), not observed in WT (Fig. 1C), and a dilated cerebral aqueduct (Fig. 1D3). The latter phenomenon has previously been observed in the murine model (Zang et al. 2004) but was revealed here also in presymptomatic cases (see Fig. 1D2) as compared to the lack of such appearances in age related WT cases (Fig. 1D1).

Regardless of the pulse sequences employed it is difficult to detect inflammatory and neurodegenerative foci near ventricles since those tissues would appear hyperintense in T2W and hypointensive in T1W images and may be mixed with the signal from the cerebro-spinal fluid. In order to check for the changes in the brain tissue close to the dilated lateral ventricles brain slices from end-stage animal models were immuno-labelled for the astroglial marker – GFAP. By means of laser scanning confocal microscopy this immunocytochemical approach revealed reactive astrogliosis in the vicinity of lateral ventricles (Fig. 2). Namely, in ALS preparations an intense GFAP signal was observed revealing astrocytes with enlarged cell bodies and extended thick processes. Such reactive astrocytes became much denser in close proximity of the lateral ventricles.

It would greatly enhance the progress of ALS research if inflammatory processes associated with ALS could be more specifically imaged by MRI. In fact, among different immune system alterations in ALS patients it was observed that the percentage of CD4 expressing lymphocytes was increased (Zhang et al. 2005). Thus, in order to follow the inflammatory cells in ALS brain tissue we chose to use commercially available antibodies against CD4 receptors tagged with USPIO nanoparticles. These were i.p. injected to G93A animals in the symptomatic, late phase of the disease and compared to age matched WT animals treated with the same dose of CD4 USPIOs. A similar procedure has been used in studies on experimental allergic encephalomyelitis, the animal correlate of multiple sclerosis (Floris et al. 2004; Pirko et al. 2004). However the latter experimental procedures of identifying the location of uptaken USPIO particles were rather elaborate and questionable in terms of specificity. Here we used the MRI protocol that employs the fact that accumulated superparamagnetic nanoparticles, USPIOs induce susceptibility artefacts that are manifested as a signal void (dark spots) in MR images. The area of the signal void is larger than the actual size of the tissue that accumulates USPIOs and this effect depends on the particular MRI pulse sequence. To

make sure that the signal void in MR images arises from accumulated nanoparticles – USPIOs, we performed two consecutive gradient echo T2* images with different values of echo times (20 or 30 ms). Prolonging the echo time in the gradient echo sequence augments the signal artefact generated by the magnetic particles, thus comparison of images obtained using different echo times becomes a reasonably good sign of USPIO presence in the tissue. We also used a 3.0 T MRI instrument since the susceptibility-induced artefacts increase with the magnetic field strength. In addition to the T2* imaging, the obtained signal artefact could also be double-checked with T1W imaging that would usually give a hyperintensity in the congruent region (not shown). The USPIO-generated T2* signal void was studied mainly in the midbrain region in the vicinity of lateral ventricles (Fig. 3). This USPIO-generated effect was also recorded for the tissue around the lateral ventricle more rostrally to the midbrain region (Fig. 3B). These images point to a general phenomenon in the ALS model – infiltration of inflammatory cells (lymphocytes) into the brain tissue in the vicinity of the lateral ventricles. A direct live monitoring of immune cell markers is thus demonstrated allowing for further studies with additional magnetically labelled antibodies that should address the topology of specific cells. It is likely that the lymphocyte infiltration is a consequence of a compromised blood brain barrier as recently indicated for the mouse model (Garbuzova-Davis et al. 2007). The latter can be assessed by using contrasting agents such as Gd-DTPA (Floris et al. 2004) in conjunction with MRI protocols used here.

In conclusion, using clinical MRI we managed to assess neurodegenerative processes in the hSOD-1^{G93A} transgenic ALS rat model comparable to the images obtained for the mouse model at 4.7 T (Zang et al. 2004). Additional foci of neurodegeneration were also observed with the lateral ventricle dilation as the most apparent feature of brain tissue atrophy. Degenerative processes in these areas were also confirmed by confocal images of reactive astroglia. By means of a wide bore 3.0 T MRI and anti-CD4 antibodies tagged with magnetic nanoparticles it was also demonstrated that in the vicinity of the dilated ventricles an accumulation of inflammatory cells occurs. Thus, in the hSOD-1^{G93A} transgenic rat model of ALS neuroinflammatory markers were revealed also justifying future studies on specific cell populations with different magnetically labeled antibodies and on the role of blood brain barrier with MRI contrasting agents.

Acknowledgements. The authors would like to thank Drs. Istvan Pirko and Slobodan Macura for their help in designing the experiments. Wyeth Research and ALSA are acknowledged for making the laboratory animals available through Taconic. This work was supported by grants MSTD RS 143054, EC FP6-INCO-SSA 026400, FNRS-FRSM 3.4545.05 and ESF-COST B30.

References

Alexianu M. E., Kozovska M., Appel S. H. (2001): Immune reactivity in a mouse model of familial ALS correlates with disease progression. Neurology **57**, 1282–1289

Anderson S. A., Shukaliak-Quandt J., Jordan E. K., Arbab A. S., Martin R., McFarland H., Frank J. A. (2004): Magnetic resonance imaging of labeled T-cells in a mouse model of multiple sclerosis. Ann. Neurol. **55**, 654–659

Appel S. H., Simpson E. P. (2001): Activated microglia: the silent executioner in neurodegenerative disease? Curr. Neurol. Neurosci. Rep. **1**, 303–305

Basak M., Erturk M., Oflazoglu B., Ozel A., Yildiz G. B., Forta H. (2002): Magnetic resonance imaging in amyotrophic lateral sclerosis. Acta Neurol. Scand. **105**, 395–399

Boillee S., Yamanaka K., Lobsiger C. S., Copeland N. G., Jenkins N. A., Kassiotis G., Kollias G., Cleveland D. W. (2006): Onset and progression in inherited ALS determined by motor neurons and microglia. Science **312**, 1389–1392

Bulte J. W., Kraitchman D. L. (2004): Iron oxide MR contrast agents for molecular and cellular imaging. NMR Biomed. **17**, 484–499

Ellis C. M., Simmons A., Dawson J. M., Williams S. C., Leigh P. N. (1999): Distinct hyperintense MRI signal changes in the corticospinal tracts of a patient with motor neuron disease. Amyotroph. Lateral Scler. Other Motor Neuron Disord. **1**, 41–44

Floris S., Blezer E. L., Schreibelt G., Dopp E., van der Pol S. M., Schadee-Eestermans I. L., Nicolay K., Dijkstra C. D., de Vries H. E. (2004): Blood-brain barrier permeability and monocyte infiltration in experimental allergic encephalomyelitis: a quantitative MRI study. Brain **127**, 616–627

Garbuzova-Davis S., Haller E., Saporta S., Kolomey I., Nicosia S. V., Sanberg P. R. (2007): Ultrastructure of blood-brain barrier and blood-spinal cord barrier in SOD1 mice modeling ALS. Brain Res. **1157**, 126–137

Gurney M. E. (1997): Transgenic animal models of familial amyotrophic lateral sclerosis. J. Neurol. **244,** S15–20

Hecht M. J., Fellner F., Fellner C., Hilz M. J., Neundorfer B., Heuss D. (2002): Hyperintense and hypointense MRI signals of the precentral gyrus and corticospinal tract in ALS: a follow-up examination including FLAIR images. J. Neurol. Sci. **199**, 59–65

Henkel J. S., Engelhardt J. I., Siklos L., Simpson E. P., Kim S. H., Pan T., Goodman J. C., Siddique T., Beers D. R., Appel S. H. (2004): Presence of dendritic cells, MCP-1, and activated microglia/macrophages in amyotrophic lateral sclerosis spinal cord tissue. Ann. Neurol. **55**, 221–235

Howland D. S., Liu J., She Y., Goad B., Maragakis N. J., Kim B., Erickson J., Kulik J., DeVito L., Psaltis G., DeGennaro L. J., Cleveland D. W., Rothstein J. D. (2002): Focal loss of the glutamate transporter EAAT2 in a transgenic rat model of SOD1 mutant-mediated amyotrophic lateral sclerosis (ALS). Proc. Natl. Acad. Sci. U.S.A. **99**, 1604–1609

Jefferies W. A., Green J. R., Williams A. F. (1985): Authentic T helper CD4 (W3/25) antigen on rat peritoneal macrophages. J. Exp. Med. **162**, 117–127

Lowry K. S., Murray S. S., McLean C. A., Talman P., Mathers S., Lopes E. C., Cheema S. S. (2001): A potential role for the p75 low-affinity neurotrophin receptor in spinal motor neuron degeneration in murine and human amyotrophic lateral sclerosis. Amyotroph. Lateral Scler. Other Motor Neuron Disord. **2**, 127–134

McGeer P. L., McGeer E. G. (2002): Inflammatory processes in amyotrophic lateral sclerosis. Muscle Nerve **26**, 459–470

Sach M., Winkler G., Glauche V., Liepert J., Heimbach B., Koch M. A., Buchel C., Weiller C. (2004): Diffusion tensor MRI of early upper motor neuron involvement in amyotrophic lateral sclerosis. Brain **127**, 340–350

Suhy J., Miller R. G., Rule R., Schuff N., Licht J., Dronsky V., Gelinas D., Maudsley A. A., Weiner M. W. (2002): Early detection and longitudinal changes in amyotrophic lateral sclerosis by ^{1}H MRSI. Neurology **58**, 773–779

Philippeau M., Manto M., Sokolow S., Laute M. A., Brion J. P., Pandolfo M., Pochet R. (2005): Recent advances in transgenic models of ALS – electrophysiological, morphological and neurochemical characterization of hSOD-1 G93A transgenic rats. Recent Research Development in Physiology **3**, 13–31

Pirko I., Johnson A., Ciric B., Gamez J., Macura S. I., Pease L. R., Rodriguez M. (2004): *In vivo* magnetic resonance imaging of immune cells in the central nervous system with superparamagnetic antibodies. FASEB J. **18**, 179–182

Zang D. W., Yang Q., Wang H. X., Egan G., Lopes E. C., Cheema S. S. (2004): Magnetic resonance imaging reveals neuronal degeneration in the brainstem of the superoxide dismutase 1 transgenic mouse model of amyotrophic lateral sclerosis. Eur. J. Neurosci. **20**, 1745–1751

Zhang R., Gascon R., Miller R. G., Gelinas D. F., Mass J., Hadlock K., Jin X., Reis J., Narvaez A., McGrath M. S. (2005): Evidence for systemic immune system alterations in sporadic amyotrophic lateral sclerosis (sALS). J. Neuroimmunol. **159**, 215–224

Cranial irradiation modulates hypothalamic-pituitary-adrenal axis activity and corticosteroid receptor expression in the hippocampus of juvenile rat

Natasa Velickovic[1], Ana Djordjevic[1], Dunja Drakulic[1], Ivana Stanojevic[1], Bojana Secerov[2] and Anica Horvat[1]

[1] *Laboratory for Molecular Biology and Endocrinology, Institute of Nuclear Sciences "Vinča", P.O.Box 522, 11001 Belgrade, Serbia*
[2] *Laboratory for Radiation Chemistry and Physics, Institute of Nuclear Sciences "Vinča", P.O.Box 522, 11001 Belgrade, Serbia*

Abstract. Glucocorticoids, essential for normal hypothalamic-pituitary-adrenal (HPA) axis activity, exert their action on the hippocampus through two types of corticosteroid receptors: the glucocorticoid receptor (GR) and the mineralocorticoid receptor (MR). Recent studies report that exposure of juvenile rats to cranial irradiation adversely affects HPA axis stability leading to its activation along with radiation-induced inflammation. This study was aimed to examine the acute effects of radiation on HPA axis activity and hippocampal corticosteroid receptor expression in 18-day-old rats. Since immobilization was part of irradiation procedure, both irradiated and sham-irradiated animals were exposed to this unavoidable stress. Our results demonstrate that the irradiated rats exhibited different pattern of corticosteroid receptor expression and hormone levels compared to respective controls. These differences included upregulation of GR protein in the hippocampus with a concomitant elevation of GR mRNA and an increase in circulating level of corticosterone. In addition, the expression of MR, both at the level of protein and gene expression, was not altered. Taken together, this study demonstrates that cranial irradiation in juvenile rats leads to enhanced HPA axis activity and increased relative GR/MR ratio in hippocampus. The present paper intends to show that neuroendocrine response of normal brain tissue to localized irradiation comprise both activation of HPA axis and altered corticosteroid receptor balance, probably as consequence of innate immune activation.

Key words: HPA axis — Corticosteroid receptor — Irradiation — Hippocampus

Introduction

Cranial radiotherapy (CRT) is widely used not only to treat patients with primary and secondary brain tumors, but also as prophylaxis, to prevent brain metastases development and central nervous system (CNS) involvement in hematological malignancies (Gibbs et al. 2006). However, damage to surrounding normal tissue constitutes a major problem, and CRT is associated with both acute and long-lasting severe side effects. Children treated for brain tumors with radiotherapy are at risk of developing endocrine deficits when the hypothalamus-pituitary axis falls within the fields of radiation, which may resul in growth hormone deficiency and adrenal dysfunction (Schmiegelow et al. 2003; Spoudeas et al. 2003; Darzy and Shalet 2005). Animal models may therefore be useful in assessing the neuroendocrine response following CNS irradiation, in a more controlled and reproducible way than is possible in the clinic.

The initial response of the brain to irradiation involves expression of inflammatory mediators (tumor necrosis factor-α (TNF-α), interleukin-1β (IL-1β), inter-cellular adhesion molecule 1 (ICAM-1)), which are probably responsible for clinically observed early symptoms of CRT (Hong et al. 1995; Van de Meeren et al. 2001). Concomitantly with the radiation-induced inflammation, hypothalamic-pituitary-adrenal (HPA) axis is activated in early response phase, as reported by a number of studies. In these studies, HPA axis hyperactivity has been documented by increased level of plasma cortisol in patients (Girinsky et al. 1994), increased

Correspondence to: Natasa Velickovic, Laboratory for Molecular Biology and Endocrinology, Institute of Nuclear Sciences "Vinča", P.O.Box 522, 11001 Belgrade, Serbia
E-mail: natasaxx@vinca.rs

corticosterone (CORT) level in mice (Van de Meeren et al. 2001) and rats (Lebaron-Jacobs et al. 2004) and enlargement of adrenal glands after irradiation (Lebaron-Jacobs et al. 2004). This acute activation of HPA axis most likely contributes to the neuroprotection against oxidative stress and inflammatory reaction caused by irradiation.

One of the prime neuronal targets for glucocorticoid action is the hippocampus (De Kloet et al. 1998), which comprises two types of corticosteroid receptors: the glucocorticoid receptor (GR) and the mineralocorticoid receptor (MR). GR and MR are two closely-related members of the steroid receptor family of transcription factors that bind common ligands (CORT and cortisol) with different affinity in the brain. High-affinity MR in the hippocampus mediates non-stress circadian fluctuation of glucocorticoids and is primarily activational. The low-affinity GR can be activated additionally to MR only when CORT levels are high, such as the circadian peak or during stress (De Kloet et al. 1998). Thus, CORT action *via* MR exerts a tonic, permissive influence on hippocampus-associated functions, whereas activation of GR in this brain region mediates feedback actions aimed to terminate stress-induced HPA activation (De Kloet et al. 1998). An imbalance in GR/MR-mediated actions underlies behavioral deficits and neuroendocrine disturbances, increasing vulnerability for stress-related brain disorders (De Kloet 2000).

Recently, we showed in juvenile rats that radiation-induced late response is characterized by hyposuppressive state of the HPA axis that is associated with a decrease in GR/MR ratio (Velickovic et al. 2008). Therefore, we designed the present studies to determine i) whether cranial irradiation modulates the HPA axis activity in acute response phase and ii) whether cranial irradiation could modify the efficiency of glucocorticoid feedback on the HPA axis through changes in the expression of GR and MR. For this purpose, main product of HPA axis activity, CORT, was measured in serum of irradiated rats and appropriate sham-irradiated controls using ELISA assay. In addition, GR and MR mRNA and protein in the hippocampus were determined at various time intervals after radiation treatment. The experiments were performed on previously established animal model for CNS prophylactic therapy in children with acute lymphoblastic leukemia (ALL) (Mullenix et al. 1990).

Materials and Methods

Animals

Experiments were conducted on 18-days-old male Wistar rats, weighing 32.45 ± 0.71 g, bred at the Institute of Nuclear Sciences "Vinča". The animals were maintained in the animal room on a 12 : 12 h light/dark cycle (lights on: 7:00 a.m.– 7:00 p.m.), under constant temperature (22°C) and humidity (55 ± 5%). The animals had free access to food-commercial rat pellets (provided by Veterinary Institute Subotica, Serbia), and water. All procedures were approved by the Ethics Committee of the Serbian Association for the Use of Animals in Research and Education.

Irradiation procedure

Previously established animal model for CNS prophylactic therapy of childhood ALL (Mullenix et al. 1990) was used in this study. At the age of 18 days (the day of birth taken as day 0), animals were divided into two groups: sham-irradiated (sham-IR) controls and irradiated (IR) animals. Since irradiated animals were immobilized for 1 h during irradiation procedure (Bayer and Peters 1977), the sham-irradiated controls were treated equally, except for being exposed to the source of radiation. Immobilization was performed by placing the animal on the 2.5-cm thick polystyrene bar and fixation with medical plaster tape so that the animal was unable to move. The heads of the IR rats were exposed to a single 10 Gy dose of γ-rays using ^{60}Co-source (Laboratory for Radiation Chemistry and Physics, Institute of Nuclear Sciences "Vinča"). This dose approximated a biological equivalent to the clinical dose of 24 Gy given in 12–14 fractions in CNS prophylactic therapy of childhood ALL (Schunior et al. 1990). In order to minimize radiation exposure of the abdomen or adrenals, the bodies of the animals were protected by a 5-cm lead blocks with a 2.5-cm thick polystyrene bar. Scattered radiation to the shielded parts of the body was measured using Fricke dosimeter. Radiation was administered in the morning (9:00 to 10:00 a.m.), with a source-skin distance of 31 cm and dose rate 0.32 Gy/min. The entire procedure was completed within 32 min, four animals being irradiated at a time. After completing irradiation procedure, the irradiated and appropriate sham-irradiated animals were sacrificed by decapitation in the following time intervals: 1, 2, 4, 8 and 24 h (in 11:00, 12:00, 14:00, 18:00 h and next day in 11:00 h). In order to evaluate the effects of immobilization stress on activity of HPA axis, in an additional experiment we included as third group: non-immobilized (control) animals. They were sacrified by decapitation in following time points: in 11:00, 12:00 and 14:00 (correspond to 1 h, 2 h and 4 h post-irradiation intervals). Each group was consisting of 8–9 animals.

CORT assay

After decapitation, trunk blood was rapidly collected and the sera, obtained by centrifugation for 15 min at 2500 × *g*, were kept at –20°C until assayed. Serum obtained from each

individual animal was used for CORT measurement and the results are presented as mean ± SEM (n = 7–8 animals). The level of serum CORT was measured in group of non-immobilized (control), sham-irrradiated and irradiated animals.

CORT levels were measured by ELISA assay (REF AC-14F1; Immunodiagnostics Systems, UK). The standards and samples were measured in duplicate, all in one assay. The difference between the pairs was less than 6%. The ELISA plates were read at 450 and 650 nm on the WALLAC 1420-Victor2 Multilabel Counter (LKB, UK).

Tissue collection

After blood collections, brains were quickly removed and placed on ice for immediate dissection of the hippocampus. For each group, 3–5 hippocampi were pooled, and either placed in cold buffer (4°C) and homogenized within 10 min after collection, or rapidly frozen in liquid nitrogen and stored at –70°C for subsequent processing.

RNA extraction and reverse transcription

RNA was isolated by a modified single step method based on acid guanidinium thiocyanate-phenol-chloroform extraction (Chomczynski and Sacchi 1987). Hippocampi were homogenized in 1 ml of denaturing solution per 100 mg of tissue (4 mol/l guanidinium thiocyanate, 0.5% sarcosyl, 25 mol/l sodium citrate, pH 7.0 and 0.1 mol/l 2-mercaptoethanol) in glass-teflon homogenizer. Sequentially, 0.05 ml 2 mol/l sodium acetate, pH 4.0, 0.5 ml phenol (water saturated) and 0.1 ml of chloroform-isoamyl alcohol mixture (49 : 1) were added to the homogenate, with thorough mixing after the addition of each reagent. Samples were centrifuged at 10,000 × g for 20 min at 4°C. The aqueous phase was mixed with 1 ml of isopropanol and kept at –20°C overnight to precipitate RNA. Pelleted (10,000 × g, 20 min, 4°C) RNA was dissolved in 0.3 ml denaturing solution, and precipitated once more with 1 vol. of isopropanol at –20°C for 1 h. After centrifugation (10,000 × g, 10 min, 4°C), the RNA pellet was resuspended in 75% ethanol, centrifuged (7500 × g, 5 min, 4°C), dried on air and dissolved in 50–100 µl 0.1% diethyl pyrocarbonate water.

For the synthesis of cDNAs, First Strand cDNA Synthesis Kit (#K1612; Fermentas, Lithuania) was used by manufacturer's instructions.

Semi-quantitative PCR

cDNAs were amplified using primers designed for the amplification of MR and GR together with a housekeeping gene glyceraldehyde-3-phosphate dehydrogenase (GAPDH) (Table 1). For polymerase chain reaction (PCR), appropriate dilutions of cDNA samples representing 200 ng total RNA were mixed with PCR buffer containing 10 mmol/l deoxyribonucleotide triphosphate, 2.1 mmol/l $MgCl_2$, 0.25 µmol/l primers for GR or MR, 0.125 µmol/l primers for GAPDH, and 2U Taq polymerase in a total volume of 25 µl. cDNAs were amplified in a Techne thermocycler (UK) for 30 cycles (GR) or 28 cycles (MR) using the following conditions: denaturation 94°C/1 min; annealing 57°C/45 s (GR) or 59°C/45 s (MR), extension 72°C/45 s; final extension 72°C/5 min. PCR products were electrophoresed on 2% agarose gels together with a DNA Molecular Weight Marker X, 0.07–12.2 kbp, (Boehringer Mannheim, Germany) and visualized under UV light using ethidium bromide. The intensity of PCR products were measured with an image analysis system GelDoc 1000 (BioRad, CA, USA) and expressed in arbitrary units (count). The arbitrary units related to the MR or GR amplification products were divided by that corresponding to the GAPDH product obtained in same PCR reaction. All the experiments were replicated three times, each time with the new groups of sham-irradiated and irradiated animals, each group consisting of 3–5 animals.

Preparation of cytosols

Cytosols were prepared from the pools of 3–5 hippocampi. Briefly, the tissue was homogenized with a glass-teflon homogenizer in 2 vol. (w/v) of ice-cold buffer A (0.25 mol/l sucrose, 15 mmol/l Tris-HCl, pH 7.9, 16 mmol/l KCl, 15 mmol/l NaCl, 5 mmol/l EDTA, 1 mmol/l EGTA, 0.15 mmol/l spermine and 0.15 mmol/l spermidine) and supplemented with 1 mmol/l DTT and the following protease inhibitors: 0.1 mmol/l phenylmethanesulphonyl fluoride, 2 µg/ml leupeptin, 5 µg/ml aprotinin, 5 µg/ml antipain. After centrifugation (10 min, 2000 × g, 4°C), the resulting supernatants were further processed to generate cytosol extracts. Supernatant was centrifuged 60 min, at 105,000 × g, at 4°C and the final supernatant was aliquotted and stored at –70°C. Protein

Table 1. Primer sequences used in RT-PCR analysis

Product size	Primer sequence[a]	Gene position[b]
GR	TGCAAACCTCAATAGGTCGACCG	509–532
(522 bp)	TAAACTGGGCCCAGTTTCTCTTGC	1007–1030
MR	AGCTCTTCTGTTAGCAGCCCGCTG	1044–1067
(472 bp)	CTGAAGTGGCATAGCTGAAGGCT	1492–1515
GAPDH	AAGGTGAAGGTCGGAGTCAACG	8–29
(332 bp)	GGCAGAGATGATGACCCTTTTGGC	362–339

[a] the upper and lower primers of each amplification pair represent the 5'- and 3'-primers, respectively (the 3'-primers are antisense); [b] nucleotides corresponding to the amplified sequences.

concentration was determined by the modified method of Lowry (Markwell et al. 1978) using bovine serum albumin as a standard.

Western blot analysis

Samples containing 20 μg protein were mixed with Laemmli's sample buffer, boiled for 5 min and loaded on 8% polyacrylamide gels. For Western blot analysis, the samples intended to be directly compared were always run on the same gel and GR and MR proteins were simultaneously detected on same membranes, however, the samples for 24 h time point, both irradiated and respective sham-irradiated control, were analyzed on another gel due to limited number of wells. Cruz Marker™ Molecular Weight Standards (Santa Cruz Biotechnology, USA), consisting of 6 bands (132, 90, 55, 43, 34 and 23 kDa), were used as molecular mass references. Separated proteins were transferred to polyvinylidene fluoride membranes (Amersham Biosciences, USA). The blots were blocked in 5% (w/v) nonfat dry milk in TBST (Tris-buffered saline, 0.1% Tween-20) (50 mmol/l Tris-HCl, pH 7.4, 150 mmol/l NaCl, 0.1% Tween-20) for 2 h. After extensive washing, membranes were incubated overnight (4°C) with primary antibodies (rabbit polyclonal anti-GR, PA1-511A, 1 : 1000, Affinity Bioreagents (USA); mouse monoclonal anti-MR, MA1-620, 1 : 1000, Affinity Bioreagents; goat polyclonal anti-β-actin, C-11, 1 : 2500, Santa Cruz Biotechnology). Membranes were subsequently washed in TBST and incubated for 2 h with peroxidase-conjugated anti-rabbit or anti-mouse immunoglobuline antibodies (Santa Cruz Biotechnology, 1 : 5000), and subsequently with anti-goat immunoglobuline antibodies (Santa Cruz Biotechnology, 1 : 10,000). Immunopositive bands were visualized by enhanced chemiluminiscent method (Cell Signaling, USA). β-actin was used as an equal load control. The optical density (OD) of bands visible on light-sensitive films (Fuji, Japan) was measured using image analysis system (ImageJ). Background OD levels were subtracted from the OD of each individual immunoreactive band. All the experiments were replicated three times, each time with the new groups of sham-irradiated and irradiated animals, each group consisting of 3–5 animals.

Statistics

Data were expressed as means ± SEM. One-way ANOVA followed by Tukey *post hoc* test was used to determine statistical significance of measured parameters with respect to the control. All interactions between factors were assesed using two-way ANOVA test followed by Tukey *post hoc* test. Differences were considered as significant at $p < 0.05$.

Results

HPA axis activity after cranial irradiation

In order to assess the acute effects of irradiation on responsiveness of the juvenile HPA axis, serum CORT levels were measured in the sera of 18-day-old animals, both irradiated (IR) and sham-irradiated (sham-IR). Since immobilization was unavoidable part of irradiation procedure, and both irradiated and sham-irradiated animals were exposed to immobilization stress in duration of 1 h, in an additional experiment we included non-immobilized (control) animals and measured the level of CORT in the serum. We found major effects of immobilization stress 1 h after treatment (Fig. 1, control (1 h) vs. sham-irradiated (1 h), $p < 0.001$), while 2 h and 4 h after treatment there was no difference between control (non-immobilized) and sham-irradiated (immobilized) animals (Fig. 1). Two way ANOVA, followed by Tukey *post hoc* test, showed that interaction between immobilization and irradiation was significant in 1 h time point (Fig. 2, $F = 40.288$, $p < 0.001$). However, no interaction between immobilization and irradiation was observed in 2 h and 4 h time points (Fig. 2, $F = 0.185$, p = n.s. (not significant)).

Cranial irradiation led to increased activity of juvenile HPA axis, as CORT level was raised by 60% 2 h after irradiation, compared to sham-irradiated control (Fig. 2, IR_{2h} vs. sham-IR_{2h}, $p < 0.05$). It is important to remark that the observed enhancement of serum CORT is foremost the effect of cranial irradiation than result of additive effect

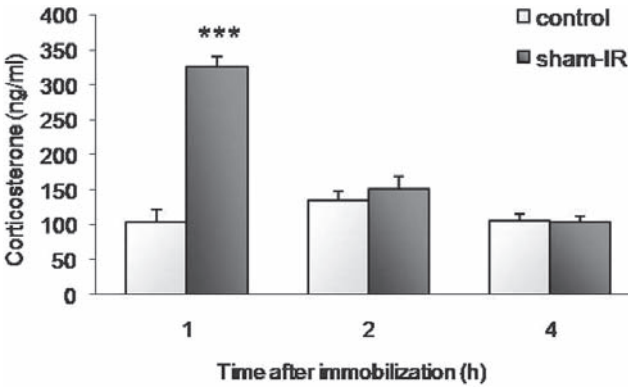

Figure 1. Effect of unavoidable immobilization stress on HPA axis activity in sham-irradiated animals. Serum corticosterone levels were determined in the blood of 18-day-old animals, which were untreated (control) or immobilized for 1 h during irradiation procedure, but not exposed to source of radiation (sham-IR) and sacrificed in different time intervals following treatment (1, 2 and 4 h). The results are expressed as the mean ± SEM ($n = 7–8$ animals per experimental group). Statistical analysis was done by comparing sham-IR group to the corresponding control group using one way ANOVA. * $p < 0.001$, sham-IR_{1h} vs. control (1 h).

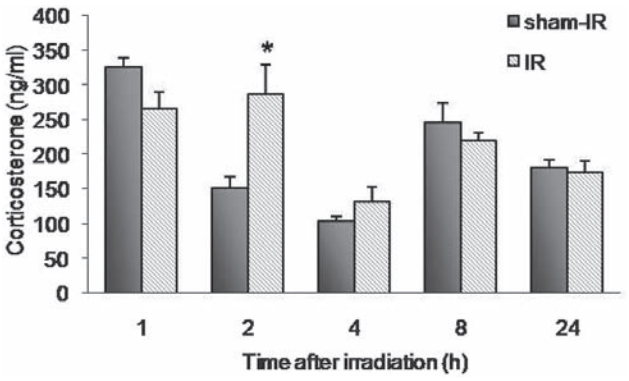

Figure 2. Activity of the HPA axis after cranial irradiation. Serum corticosterone levels were determined in the blood of 18-day-old animals, which were irradiated (IR) or sham-irradiated (sham-IR) and sacrificed in different time intervals following treatment (1, 2, 4, 8 and 24 h). The results are expressed as the mean ± SEM (n = 7–8 animals per experimental group). Statistical analysis was done by comparing IR to the corresponding sham-IR group using one way ANOVA. * $p < 0.05$, IR_{2h} vs. sham-IR_{2h}.

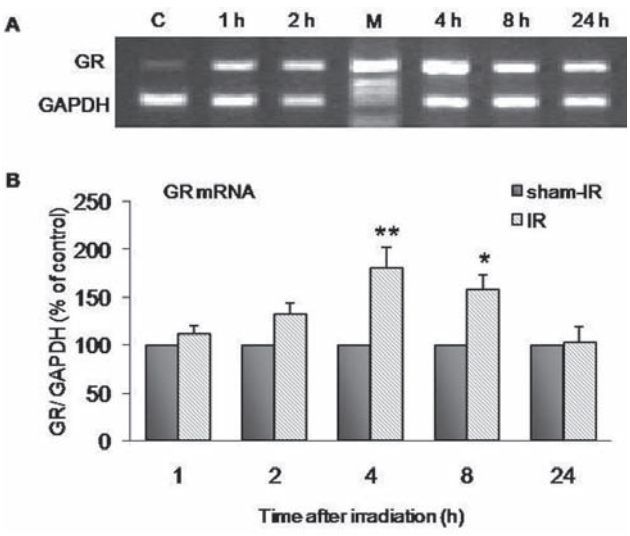

Figure 3. The effect of cranial irradiation on GR mRNA levels in the rat hippocampus. Panel A: The level of GR mRNA was examined by RT-PCR in the hippocampi of sham-irradiated (sham-IR) and irradiated (IR) rats in different time intervals after treatment (1, 2, 4, 8 and 24 h). C, appropriate sham-irradiated animals; M, DNA molecular weight marker. Panel B: Relative mRNA levels of GR were normalized to GAPDH (glyceraldehyde-3-phosphate dehydrogenase) mRNA level in the same samples. Each sample is a pool of 3–5 animals belonging to the same experimental group. The relative GR mRNA levels are expressed as percent of control (sham-IR rats). Data represent the means ± SEM from 3 independent experiments. Statistical analysis was done by comparing IR group to the corresponding sham-IR group using one way ANOVA. * $p < 0.05$, significantly different from sham-irradiated rats; ** $p < 0.01$, significantly different from sham-IR rats.

of immobilization and irradiation, given that there is no interaction between immobilization and irradiation in 2 h post-irradiation interval. This radiation-mediated inducement is time-limited and CORT returns to basal level within 4 h (Fig. 2).

GR and MR mRNA expression in the hippocampus

The acute effects of irradiation on the GR and MR mRNA levels were examined in the rat hippocampus of 18-day-old animals (Fig. 3 and Fig. 4). Cranial irradiation of 10 Gy led to time-dependent increase in GR mRNA level, compared to sham-irradiated control, with maximum achieved 4 h after radiation treatment (Fig. 3B, F = 4.655, $p < 0.01$). On the other hand, MR mRNA level was not significantly different between the two groups of animals (Fig. 4B, F = 0.668, p = n.s.).

GR and MR protein expression in the hippocampus

To examine possible influence of cranial irradiation on level of GR and MR proteins, the two receptors were detected by semi-quantitative Western blotting in cytosolic extracts of the rat hippocampus. As seen in Fig. 5, cytosolic GR steady-

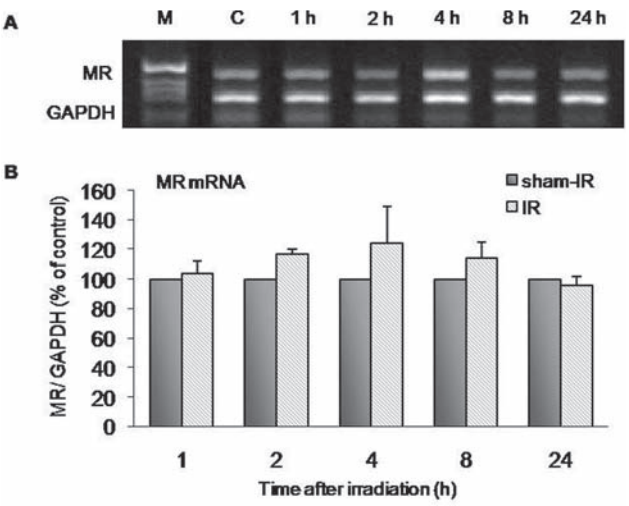

Figure 4. The effect of cranial irradiation on MR mRNA levels in the rat hippocampus. Panel A: The level of MR mRNAs was examined by RT-PCR in the hippocampi of sham-irradiated (sham-IR) and irradiated (IR) rats in different time intervals after treatment (1, 2, 4, 8 and 24 h). C, appropriate sham-irradiated animals; M, DNA molecular weight marker. Panel B: Relative mRNA levels of MR were normalized to GAPDH mRNA level in the same samples. Each sample is a pool of 3–5 animals belonging to the same experimental group. The relative MR mRNA levels are expressed as percent of control. Data represent the means ± SEM from 3 independent experiments.

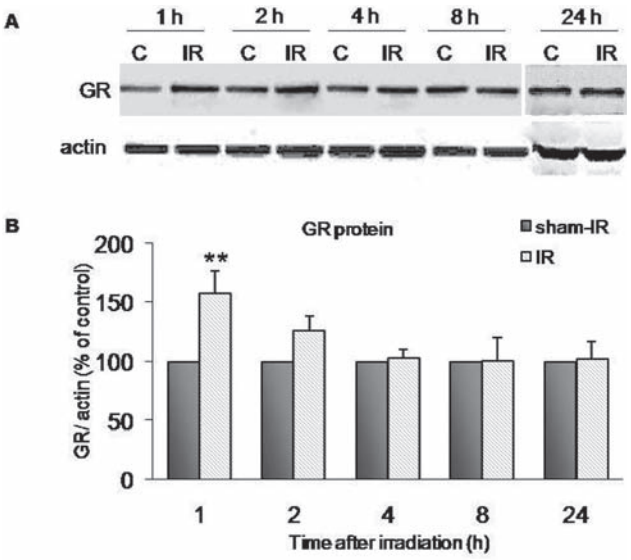

Figure 5. GR protein level in the cytosolic extract of rat hippocampus after cranial irradiation. Panel A: Western blot analysis of cytosolic GR protein in hippocampi of sham-irradiated (sham-IR) and irradiated (IR) rats in different time intervals after treatment (1, 2, 4, 8 and 24 h). C, appropriate sham-irradiated animals. Panel B: The relative abundance of GR protein is quantified by densitometry and normalized against the level of β-actin in the same sample. Each sample is a pool of 3–5 animals belonging to the same experimental group. The relative GR protein levels are expressed as percent of control (sham-IR rats). The values represent the mean ± SEM. from three independent experiments. Statistical analysis was done by comparing IR group to the corresponding sham-IR group using one way ANOVA. ** $p < 0.01$, significantly different from sham-IR rats.

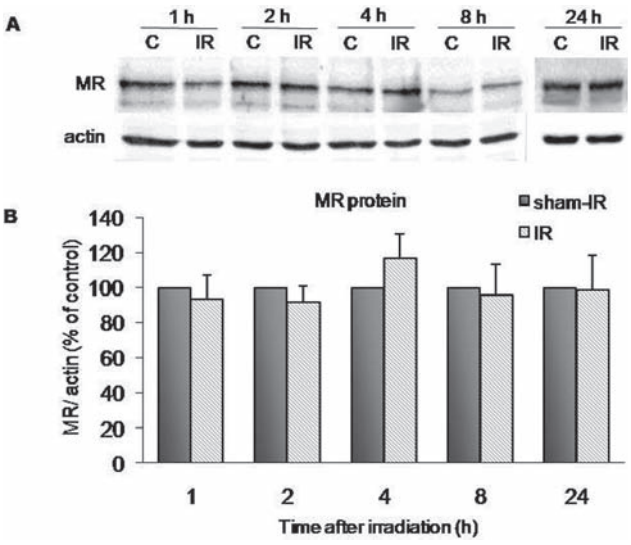

Figure 6. MR protein level in the cytosolic extract of rat hippocampus after cranial irradiation. Panel A: Western blot analysis of cytosolic MR protein in hippocampi of sham-irradiated (sham-IR) and irradiated (IR) rats in different time intervals after treatment (1, 2, 4, 8 and 24 h). C, appropriate sham-irradiated animals. Panel B: The relative abundance of MR protein is quantified by densitometry and normalized against the level of β-actin in the same sample. Each sample is a pool of 3–5 animals belonging to the same experimental group. The relative MR protein levels are expressed as percent of control. The values represent the mean ± SEM from three independent experiments.

state level was significantly increased in irradiated rats compared to sham-irradiated animals (Fig. 5B, F = 3.360, $p < 0.05$); increment observed in 1 h post-irradiation time declined to basal level after 4 h. In contrast to GR protein level, cytosolic MR protein level remained unchanged in the rat hippocampus after irradiation (Fig. 6B, F = 0.642, p = n.s.).

Deregulation of GR/MR balance in hippocampal neurons appears critical for neuronal excitability, stress responsiveness and behavioral adaptability (De Kloet et al. 1998). Direct comparison between the GR and MR mRNA and protein levels in the hippocampus revealed radiation-induced increase in GR/MR ratio (Fig. 7), suggesting that cranial irradiation is accompanied by a shift in GR/MR balance. Increment of GR protein above MR protein was observed in 1 h and 2 h post-irradiation time (Fig. 7, $GR_{1h\ WB}$ vs. $MR_{1h\ WB}$, $p < 0.05$), due to upregulation of GR while expression of MR was unaltered. At the level of gene expression, increase in relative GR/MR mRNA ratio was significant only in 8 h post-irradiation time, although GR mRNA is maintained at high level in comparisons to MR mRNA all through examined time interval (Fig. 7, $GR_{8h\ PCR}$ vs. $MR_{8h\ PCR}$, $p < 0.05$).

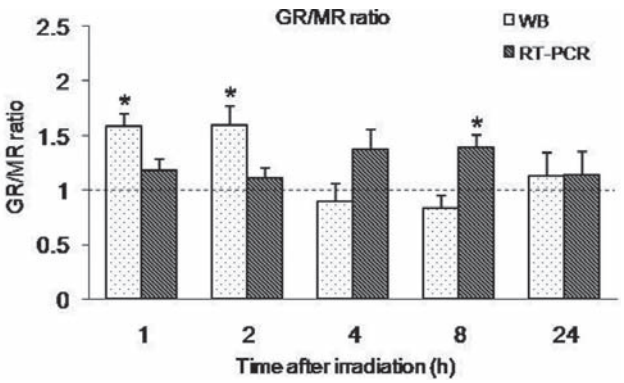

Figure 7. The GR/MR mRNA and protein ratio in the hippocampus after cranial irradiation. The levels of GR and MR mRNAs and proteins in the hippocampus of sham irradiated (sham-IR) and irradiated (IR) rats were determined by RT-PCR (Figs. 3 and 4) and Western blot (Figs. 5 and 6), respectively, and presented as their relative ratio. If GR/MR relative ratio is above or under 1 (marked as a dash line) the GR/MR balance are shifted to one direction or the other. The values are the means ± SEM from three independent experiments. * $p < 0.05$, significantly different from sham-IR rats; WB, Western blot.

Discussion

The goal of the present study was to examine, *in vivo*, the acute effects of cranial irradiation on HPA axis activity and corticosteroid receptors (GR and MR) expression in hippocampus of 18-day-old Wistar rats under unavoidable stress. We analyzed the radiation-response effects after a single dose of 10 Gy, a dose equivalent to those used for CNS prophylactic therapy in children with ALL (Schunior et al. 1990). In this study cranial irradiation led to acute activation of HPA axis, characterized by an enhancement of serum CORT level 2 h after radiation treatment, compared to sham-irradiated control (Fig. 2). This inducement is time-limited and CORT returns to normal level within 4 h (Fig. 2). Observed increase in serum CORT is consistent with a previous report of acute response of HPA axis 30 min to 6 h after radiation exposure (Van de Meeren et al. 2001; Lebaron-Jacobs et al. 2004). In patients, single dose (10 Gy) of total body irradiation also induced the activation of HPA axis, manifested as concomitant increase in cortisol and adrenocorticotropic hormone (ACTH) (Girinsky et al. 1994). Although we can generally conclude that an activation of HPA axis is a consequence of radiation, this response has not been fully characterized. Many studies have provided evidence that acute effects of ionizing irradiation involve release of inflammatory mediators, associated with changes in microvasculature, activation of microglia and neurogenesis (Girinsky et al. 1994; Hong et al. 1995; Van de Meeren et al. 2001; Monje et al. 2003). Cranial irradiation induces significant increases in TNF-α, IL-1β and IL-1α mRNA in the brain (Hong et al. 1995), increase in IL-6 in plasma or increase in IL-1β protein in whole brain (Van de Meeren et al. 2001). Increasing data indicate that activation of innate immune responses in brain after cranial irradiation may contribute to altered regulation of neuroendocrine system, especially activity of HPA axis (Miller et al. 2008). This hypothesis is plausible because several studies have demonstrated the potent action of cytokines (IL-1, IL-6, TNF-α) directly on the HPA axis activity, and consequently release of glucocorticoids (Turnbull and Rivier 1999; Dunn 2000). Prostaglandins are also involved in the increase in plasma ACTH and CORT levels induced by radiation, as shown by study of Kandasamy et al. (1995). More recently, chronic oxidative stress has been suggested to contribute to the progression of radiation-induced inflammatory reactions (Raju et al. 1999; Tofilon and Russell 2002), thus leading to further activation of HPA axis trough negative action of glucocorticoids on nuclear factor-kappa B activity (Ramdas and Harmon 1998). Systemically, by activation of the HPA axis, an excessive release of glucocorticoids stimulates an important negative feedback mechanism, which protects the organism from an overshoot of proinflammatory cytokines and other tissue-damaging products after irradiation (Turnbull and Rivier 1999; De Bosscher et al. 2003).

Hippocampus plays the major inhibitory role on HPA axis activity and the sensitivity of the HPA axis to glucocorticoid feedback suppression depends on activation of two corticosteroid receptors: GR and MR (Feldman and Weidenfeld 1999). Whereas MRs maintain neuronal homeostasis and limit the disturbance by stress, GRs insure an efficient negative feedback action on the HPA axis. If the MR/GR activation ratio is shifted, the control of glucocorticoids on neuronal excitability, neuroendocrine reactivity and behavior will change (De Kloet et al. 1998). Therefore, we examined the effects of irradiation on the hippocampal glucocorticoid and mineralocorticoid receptors, both at the level of protein and mRNA. Western blot revealed that GR protein is significantly increased in the cytosolic fraction 1 h after irradiation (Fig. 5), although it returns to normal level within an 4 h postirradiation time. Accumulation of GR protein in cytosol after irradiation could be result of action of proinflammatory cytokine such as interleukin-1α (IL-1α), which interfere with GR shuttling from the cytoplasm to the nucleus, thus leading to cytoplasmic retention of activated GR (Pariante et al. 1999). The observed rise of circulating CORT level 2 h after irradiation probably restore the nucleo-cytoplasmic shuttling (Nishi and Kawata 2006), hence decreasing its level in cytosolic fraction. Parallel to GR protein, GR mRNA in hippocampus was increased with time following irradiation (Fig. 3). However, effects at the mRNA level with time have been more pronounced, implying that transcriptional changes are not readily translated into increases in protein expression. The change in GR expression is a cumulative result of a number of distinct steps, including receptor assembly, phosphorylation, interactions with heat shock proteins, and regulation by transcription factors (Pariante et al. 1999).

Contrary to GR, neither MR protein (Fig. 6) nor MR mRNA (Fig. 4) were affected by irradiation, since these high-affinity receptors are responsible for maintenance of basal circadian HPA axis activity and are principally activated under basal level of CORT (De Kloet et al. 1998).

Overall, these data emphasizes that expression profile of corticosteroid receptors in juvenile rat hippocampus is specifically regulated in acute radiation-response phase. The relative GR/MR ratio is disturbed in hippocampus following CRT, showing the selective enhancement in GR relative to MR (Fig. 7), which leads to enhanced HPA axis activation after irradiation. These results are in accordance with "MR/GR balance hypothesis" (De Kloet et al. 1994), which states that IL-1 secretion, which is generally associated with radiation treatment, appears to change the MR/GR balance. The change in receptor balance induced by IL-1 leads to a condition characterized by deficient MRs and increased stimulation of GRs. Since hippocampus conveys inhibitory influences over the HPA axis, increase in the amount of GR versus MR is thought to produce limbic disinhibition

and enhanced HPA activation (De Kloet et al. 1994). This hypothesis was confirmed by other authors, reporting radiation-induced raise of proinflamatory cytokines IL-1β in brain altogether with increase in plasma CORT (Van de Meeren et al. 2001).

Our previous study analyzed late response of neuroendocrine system of juvenile rats after cranial irradiation, characterized by hyposuppressive state of the HPA axis, decreased relative GR/MR ratio and reduced functioning of glucocorticoid negative feedback (Velickovic et al. 2008). On the other side, early radiation response phase is distinguished by acute activation of HPA axis and increased relative GR/MR ratio. Therefore, this study suggest that early neuroendocrine response after cranial irradiation comprise an alteration of both HPA axis activity and corticosteroid receptor expression, probably as adaptive mechanism which protects the organism from an overshoot of proinflammatory cytokines and other tissue-damaging products after irradiation.

Acknowledgments. We gratefuly acknowledge Dr. Miroslav Demajo and Dr. Goran Korićanac for helpful advices on the present study. This work was supported by Ministry of Science of the Republic of Serbia, grant No. 143044B.

References

Bayer S. A., Peters P. J. (1977): A method for x-irradiating selected brain regions in infant rats. Brain Res. Bull. **2**, 153–156

Chomczynski P., Sacchi N. (1987): Single-step method of RNA isolation by acid guanidinium thiocyanate-phenol-chloroform extraction. Anal. Biochem. **162**, 156–159

Darzy K. H., Shalet S. M. (2005): Absence of adrenocorticotropin (ACTH) neurosecretory dysfunction but increased cortisol concentrations and production rates in ACTH-replete adult cancer survivors after cranial irradiation for nonpituitary brain tumors. J. Clin. Endocrinol. Metab. **90**, 5217–5225

De Bosscher K., Berghe W. V., Haegeman G. (2003): The interplay between the glucocorticoid receptor and nuclear factor-κB or activator protein-1: molecular mechanisms for gene repression. Endocr. Rev. **24**, 488–522

De Kloet E. R., Oitzl M. S., Schobitz B. (1994): Cytokines and the brain corticosteroid receptor balance: relevance to pathophysiology of neuroendocrine-immune communication. Psychoneuroendocrinology **19,** 121–134

De Kloet E. R., Vreugdenhil E., Oitzl M. S., Joëls M. (1998): Brain corticosteroid receptor balance in health and disease. Endocr. Rev. **19,** 269–301

De Kloet E. R. (2000): Stress in the brain. Eur. J. Pharmacol. **405**, 187–198

Dunn A. J. (2000): Cytokine activation of the HPA axis. Ann. N. Y. Acad. Sci. **917,** 608–617

Feldman S., Weidenfeld J. (1999): Glucocorticoid receptor antagonists in the hippocampus modify the negative feedback following neural stimuli. Brain Res. **821**, 33–37

Gibbs I. C., Tuamokumo N., Yock T. I. (2006): Role of radiation therapy in pediatric cancer. Hematol. Oncol. Clin. North Am. **20**, 455–470

Girinsky T. A., Pallardy M., Comoy E., Benassi T., Roger R., Ganem G., Cosset J. M., Socie G., Magdelenat H. (1994): Peripheral blood corticotropin-releasing factor, adrenocorticotropic hormone and cytokine (interleukin beta, interleukin 6, tumor necrosis factor alpha) levels after high- and low-dose total-body irradiation in humans. Radiat. Res. **139**, 360–363

Hong J. H., Chiang C. S., Campbell I. L., Sun J. R., Withers H. R., McBride W. H. (1995): Induction of acute phase gene expression by brain irradiation. Int. J. Radiat. Oncol., Biol., Phys. **33**, 619–626

Kandasamy S. B., Thiagarajan A. B., Harris A. H. (1995): Possible involvement of prostaglandins in increases in rat plasma adrenocorticotropic hormone and corticosterone levels induced by radiation and interleukin-1α alone or combined. Toxicol. Sci. **25**, 196–200

Lebaron-Jacobs L., Wysocki J., Griffiths N. M. (2004): Differential qualitative and temporal changes in the response of the hypothalamus-pituitary-adrenal axis in rats after localized or total-body irradiation. Radiat. Res. **161**, 712–722

Markwell M. A., Haas S. M., Bieber L. L., Tolbert N. E. (1978): A modification of the Lowry procedure to simplify protein determination in membrane and lipoprotein samples. Anal. Biochem. **87,** 206–210

Miller A. H., Ancoli-Israel S., Bower J. E., Capuron L., Irwin M. R (2008): Neuroendocrine-immune mechanisms of behavioral comorbidities in patients with cancer. J. Clin. Oncol. **26**, 971–982

Monje M. L., Palmer T. D., Toda H. (2003): Inflammatory blockade restores adult hippocampal neurogenesis. Science **302**, 1760–1765

Mullenix P. J., Kernan W. J., Tassinari M. S., Schunior A., Waber D. P., Howes A., Tarbell N. J. (1990): An animal model to study toxicity of central nervous system therapy for childhood acute lymphoblastic leukemia: effects on behaviour. Cancer Res. **50**, 6461–6465

Nishi M., Kawata M. (2006): Brain corticosteroid receptor dynamics and trafficking: implications from live cell imaging. Neuroscientist **12**, 119–133

Pariante C. M., Pearce B. D., Pisell T. L., Sanchez C. I., Po C., Su C., Miller A. H. (1999): The proinflammatory cytokine, interleukin-1α, reduces glucocorticoid receptor translocation and function. Endocrinology **140**, 4359–4366

Raju U., Gumin G. J., Tofilon P. J. (1999): NF kappa B activity and target gene expression in the rat brain after one and two exposures to ionizing radiation. Radiat. Oncol. Investig. **7**, 145–152

Ramdas J., Harmon J. M. (1998): Glucocorticoid-induced apoptosis and regulation of NF-κB activity in human leukemic T cells. Endocrinology **139**, 3813–3821

Schmiegelow M., Feldt-Rasmussen U., Rasmussen A. K., Lange M., Poulsen H. S., Müller J. (2003): Assessment of the hypothalamo-pituitary-adrenal axis in patients treated with radiotherapy and chemotherapy for childhood brain tumor. J. Clin. Endocrinol. Metab. **88**, 3149–3154

Schunior A., Zengel A. E., Mullenix P. J., Tarbell N. J., Howes A., Tassinari M. S. (1990): An animal model to study toxicity of central nervous system therapy for childhood acute lymphoblastic leukemia: effects on growth and craniofacial proportion. Cancer Res. **50**, 6455–6460

Spoudeas H. A., Charmandari E., Brook C. G. (2003): Hypothalamo-pituitary-adrenal axis integrity after cranial irradiation for childhood posterior fossa tumours. Med. Pediatr. Oncol. **40,** 224–229

Tofilon P. J., Russell J. S. (2002): Radiation-induced activation of nuclear factor-κB involves selective degradation of plasma membrane-associated IκBα. Mol. Biol. Cell **13**, 3431

Turnbull A. V., Rivier C. L. (1999): Regulation of the hypothalamic-pituitary-adrenal axis by cytokines: actions and mechanisms of action. Physiol. Rev. **79**, 1–71

Van de Meeren A., Monti P., Lebaron-Jacobs L., Marquette C., Gourmelon P. (2001): Characterization of the acute inflammatory response after irradiation in mice and its regulation by interleukin 4 (Il4). Radiat. Res. **155**, 858–865

Velickovic N., Djordjevic A., Matic G., Horvat A. (2008): Radiation-induced hyposuppression of the hypothalamic-pituitary-adrenal axis is associated with alterations of hippocampal corticosteroid receptor expression. Radiat Res. **169**, 397–407

The efficacy of two protocols for inducing motor cortex plasticity in healthy humans – TMS study

Nela V. Ilić[1], Jelena Sajić[2], Melanija Mišković[2], Jelena Krstić[2,3], Sladjan Milanović[4], Vladislava Vesović-Potić[1], Miloš Ljubisavljević[4] and Tihomir V. Ilić[4,5]

[1] *Clinic of Rehabilitation Clinical Center of Serbia*
[2] *Faculty of Biology, University of Belgrade, Serbia*
[3] *Department of Psychiatry Clinical Center "Dr. Dragiša Mišović", Belgrade, Serbia*
[4] *Institute for Medical Research, Belgrade, Serbia*
[5] *Department of Clinical Neurophysiology, Military Medical Academy, Belgrade, Serbia*

Abstract. Stimulation-induced plasticity represents an experimental model of motor cortex reorganization. It can be produced in awaked humans by combining the non-invasive electrical stimulation of somatosensory afferents *via* mixed peripheral nerves with the transcranial magnetic stimulation (TMS) of the motor cortex. Animal experiments indicate that an application of two converging inputs from various sources in a tightly coupled manner, following the so called Hebbian rule of learning, leads to an increase in motor cortical excitability.

The aim of our study was to compare the effects of two plasticity-inducing protocols by quantifying the motor cortex changes using TMS. Plasticity was induced by combining peripheral nerve stimulation with TMS (paired associative stimulation – PAS) and by peripheral motor point stimulation of two adjacent hand muscles (dual associative stimulation – DAS). The protocols were randomly applied in 12 right-handed healthy volunteers. The amplitudes of TMS-induced motor-evoked potentials (MEPs) in the right abductor pollicis brevis muscle were recorded before, immediately after PAS or DAS stimulation, and 10, 20 and 30 min later.

Both protocols led to significant and lasting changes in MEP amplitudes, however, a significantly larger increase in MEPs was observed after PAS than DAS. The results indicate that afferent input can differently affect cortical motor circuits and produce variable motor output. Thus, the efficacy of LTP-like mechanisms, presumably involved in Hebbian-like plasticity in humans, varies with the types/origin of the converging inputs. Our findings may be relevant when designing therapeutic interventions for improving motor function after neurological injury or disease.

Key words: Transcranial magnetic stimulation — Paired associative stimulation — Motor cortex plasticity — Humans

Introduction

In humans, plastic changes in the primary motor cortex (M1) have been explored in numerous studies by means of the non-invasive, safe, and painless technique of transcranial magnetic stimulation (TMS). Thus, TMS is well suited for transfering experimental concepts from the level of cellular physiology to the regional network level in humans. A magnetic coil placed on the scalp stimulates the motor cortex by electromagnetic induction, producing multiple descending potentials in the human cortico-spinal tract that can be recorded as short-latency motor-evoked potentials (MEPs) in the contralateral limb muscles. Since TMS induces electrical current flow parallel to the surface of the brain, horizontally oriented interneurones are preferentially excitated, causing transsynaptic activation of corticospinal tract neurones, at least at the threshold intensity (Hallett 2007).

Correspondence to: Tihomir V. Ilić, Department of Clinical Neurophysiology, Military Medical Academy, Crnotravska 17, 11000 Belgrade, Serbia
E-mail: tihoilic@eunet.rs

Early applications of TMS were primarily aimed at monitoring and detecting changes in motor cortex excitability and corticospinal tract integrity. It was subsequently found that the technique has a potential to interfere with an ongoing neuronal activity (Siebner and Rothwell 2003). This led to a series of studies aimed to detemine how to purposefully modulate motor cortex excitability in order to induce plastic changes. Low-frequency repetitive TMS (≤1 Hz) causes a consistent and lasting decrease in motor cortical excitability in healthy individuals in contrast to the "facilitatory" effects induced by a high-frequency repetitive TMS (5–20 Hz) (Pascual-Leone et al. 1994; Chen et al. 1997). Thus, TMS can induce a long-term reorganization of M1 since the effects outlast the period of stimulation.

Aside from the TMS, a long-term reorganization of M1 has also been reported after prolonged (~2 h) electrical stimulation of peripheral mixed nerve (Ridding et al. 2000) or motor point stimulation of adjacent small hand muscles (Ridding et al. 2003). The converging evidence led to combining central with peripheral stimulation to induce motor cortex plasticity in humans. This approach is analogous to the procedure used in neurophysiological model of associative stimulation in cortical slices. The concept is based on the principle of associative or Hebbian plasticity, which states that temporally correlated and convergent inputs from different sources result in increased synaptic strength of neurons that fire together. At a higher level of neuronal organization, Hebbian-based learning rules are related to responses of cortical neuronal networks, in a more temporally coherent manner, following behaviorally important inputs (Hebb 1949).

Hebbian-like principle may be employed in humans by pairing electric stimuli delivered to the median nerve with a single pulse TMS over the contralateral M1 at a precisely defined inter-stimulus interval (ISI; ~25 ms) to ensure a repetitive synchronous arrival of both inputs to M1 (Stefan et al. 2000). Plastic changes induced by this paired associative stimulation (PAS) protocol persist for at least 30–60 min, are topographically specific and critically time-dependent (Wolters et al. 2003).

The present study was designed to evaluate to what extent different stimulation-induced protocols can modulate motor cortex plasticity. Thus, we compared the effects of two frequently used protocols, namely PAS, that employs paired associative central and peripheral stimulation, and dual associative stimulation (DAS; Ridding et al. 2003) based on peripheral motor point stimulation of two adjacent hand muscles.

Materials and Methods

Experiments were performed on 12 right-handed healthy volunteers (4 women and 8 men) between 32 and 41 years of age (mean 34.1 ± 5.8 years). None had a history of neurological disease or was on CNS-active drugs at the time of the experiments. All subjects gave their written informed consent for participation in the study. The study was approved by the local Ethical Committee of the Military Medical Academy, Belgrade. The experiments conformed to the Declaration of Helsinki.

Timeline of experiment

Each subject participated in two experiments carried out in a pseudo-randomized order at least one week apart (Fig. 1).

EMG recording

During the experiment, subjects were comfortably seated in an armchair with their hands supported by armrests. Surface electromyographic (EMG) recordings in a belly-tendon montage were made from the right abductor pollicis brevis (APB) muscle using Ag-AgCl electrodes (diameter 9 mm). The raw EMG signal was amplified and filtered with a bandpass filter range of 20 Hz to 1 kHz (MS91; Medelec, UK). Signals were digitized at 5 kHz (CED 1401 plus; Cambridge Electronic Design, UK) and stored on a computer for subsequent off-line analysis.

Somatosensory evoked potentials

Median-nerve somatosensory-evoked potentials were recorded according to international guidelines (Cruccu et al. 2008) using surface electrodes. The active electrode was placed over the skull region overlying the primary somatosensory cortex (C3' using the international 10-20 system) while the reference electrode was placed over Fz. For each of a minimum of three reproductions, 1024 electrical stimuli (pulse width 300 μs, 3 Hz, 10–20 mA) were applied to the contralateral median nerve.

TMS

TMS was performed using a Magstim 200 stimulator with a monophasic current waveform (Magstim Co., Dyfed, UK) connected to a figure-of-eight-shape coil. The coil was held with a handle pointing backwards and laterally approximately 45 degrees to the inter-hemispheric line to induce an anteriorly directed current in the brain. This is the optimal orientation for activating the corticospinal system transsynaptically *via* horizontal cortical connections (Sakai et al. 1997). The coil was optimally positioned to evoke MEPs in the right APB muscle.

The resting motor threshold (RMT) was defined as a minimal stimulator output intensity that evoked a MEP

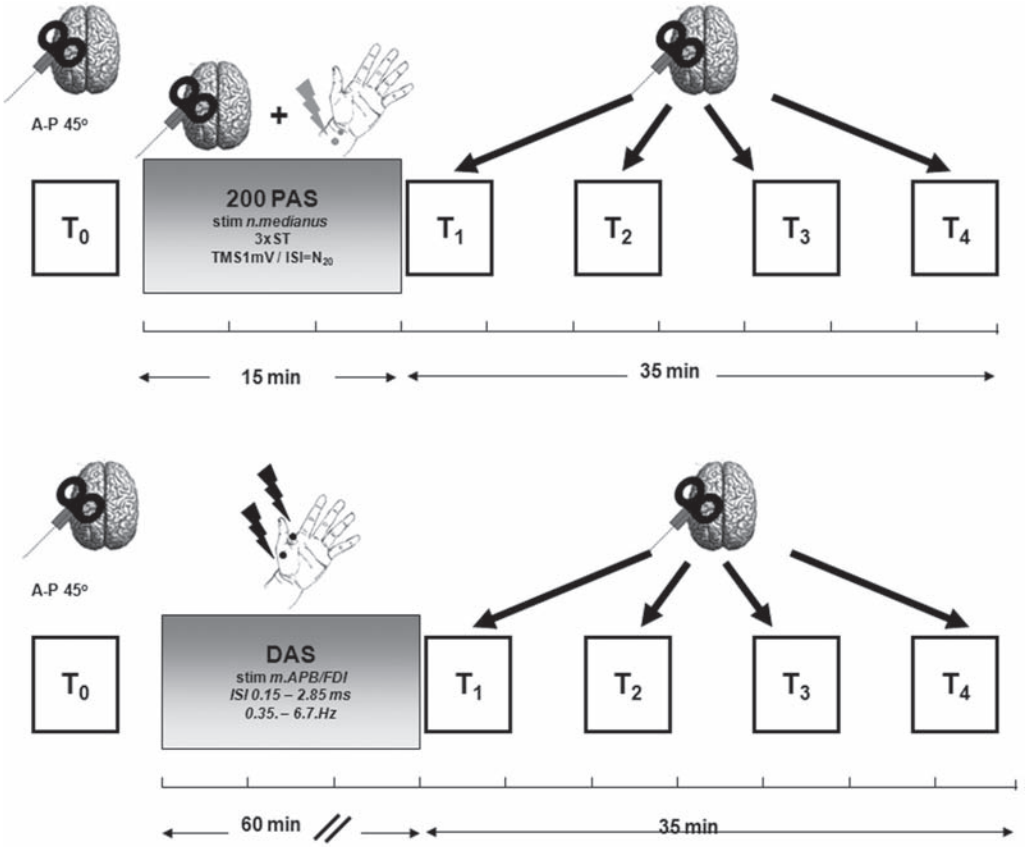

Figure 1. Time line of experiments (for details, see Materials and Methods). MEP amplitudes were measured before paired associative stimulation (PAS) or dual associative stimulation (DAS) (time point T_0), immediately after (T_1), and 10 min (T_2), 20 min (T3) and 30 min (T_4) later.

of ≥50 μV in five out of ten consecutive trials (Rossini et al. 1994). The intensity of magnetic stimulation was then adjusted to induce approximate peak-to-peak amplitude of 1 mV in the resting APB, when given without the preceding median nerve stimulus.

PAS

PAS consisted of 200 electrical stimuli of the right median nerve at the wrist, each paired with consecutive TMS over of the hand area of the left M1, at fixed ISI. The rate of paired stimulation was 0.25 Hz thus taking about 15 min to complete. Electrical stimulation was applied through a bipolar electrode (cathode proximal) using a constant current square wave pulse (duration 1 ms) at an intensity of 3 times perceptual threshold (range 0.9–3.6 mA). ISI between the median nerve stimulus and TMS were individually adjusted based on the N20 cortical component of the median nerve somatosensory evoked potential (Ziemann et al. 2004). Hence, ISIs for each subjects were equalling to the individual N20 cortical component of the median nerve somatosensory evoked potential (paired associative stimulation at ISI of individual N20 latency – PASN20) to induce a long-term potentiation-like increase in MEP amplitude in the APB. The values of N20 cortical latencies were in range 18.1–20.9 ms.

DAS

DAS paradigm was based on Ridding et al. (2003). Square-wave electrical stimuli of 1 ms duration (MS91; Medelec, UK) were applied to the motor points of the first dorsal interosseous and APB muscles simultaneously using surface electrodes (intensity of stimulation was in range from 12–28 mA). The timing between successive pairs of stimuli was randomised between 0.15 and 2.85 s in 8 steps (range 0.35–6.7 Hz). The timing of the inter-pulse intervals was controlled by Signal software (Cambridge Electronic Design Ltd., UK). The intensity of stimulation was adjusted for each muscle separately and set at a level just sufficient to evoke a minimal visible motor response. This intensity of stimulation was not painful. DAS paradigm was applied for a period of 1 h.

During the PAS and DAS procedures, the subjects were instructed to perform a task that demanded attention to the stimulated hand, because attention accentuates the LTP-like effect maximally (Stefan et al. 2004).

Quantification of PAS and DAS effects

MEP amplitudes were measured before PAS or DAS (time point T_0), immediately after (T_1), and 10 min (T_2), 20 min (T3) and 30 min (T_4) later (Fig. 1) in order to assess changes in left M1. The MEP amplitude reflects synaptic excitability in M1, which is regulated through various inhibitory and excitatory neurotransmitter systems (Boroojerdi et al. 2001).

RMT was measured immediately before T_0 and T_1 to check if PAS or DAS protocol induced changes in MEP amplitude that may confound their direct comparison. At each time point, 20 MEP were obtained at a mean inter-trial interval of 10 s and a random inter-trial interval variation of 25%. For each subject and time point, the single-trial peak-to-peak MEP amplitudes were averaged and normalized to the MEP amplitude measured at T_0.

Data analysis

Relaxation of the APB was monitored audio-visually with high gain EMG (50 μV/div.). Trials contaminated with voluntary EMG activity were discarded from analysis. Changes in MEPs induced by PAS and DAS were averaged over time points T_1 and T_4 and compared to MEPs before the intervention (T_0) using a two-tailed paired *t*-test. To test for the effect group, a two-way ANOVA was employed with time (T_1–T_4) as the within-subject factors and the induction protocol (PAS/DAS) as the between-subject factor. Paired two-tailed *t*-test was applied for post-hoc analyses (*p* value was adjusted for the number of comparisons during post-hoc analyses). Effects were considered significant, if $p < 0.05$. Results are given as means ± SD.

Results

Effects of stimulation protocols on RMT

RMTs were not affected by PAS or DAS, registered immediately after interventional procedure ($F_{2,12} = 0.97$, $p = 0.42$ and $F_{2,12} = 1.06$, $p = 0.41$, respectively). However, possible RMT changes later in the time course, could not be excluded totaly, although less probable. The results are shown in Fig. 2.

Effects of PAS and DAS on MEP amplitude

PAS resulted in an expected increase in MEP amplitude in the APB from 1.25 ± 0.33 mV at T_0 to an average of 1.97 ± 0.61 mV for time points T_1 to T_4 (T = 6.022, $p = 0.001$). The effect lasted for at least 30 min (Fig. 3, filled squares).

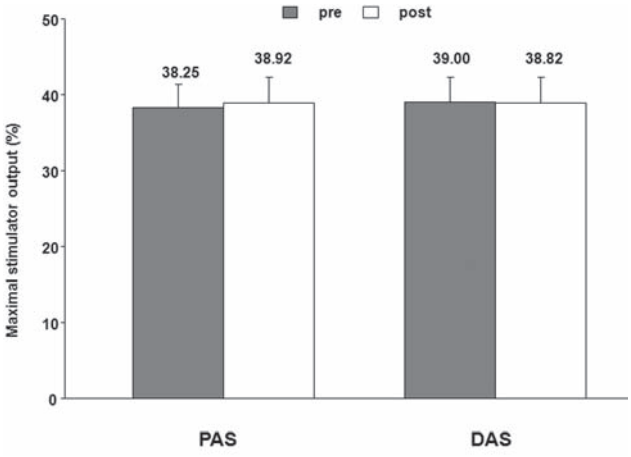

Figure 2. Effects of paired associative stimulation (PAS) and dual associative stimulation (DAS) on RMT ($n = 12$).

DAS also resulted in an expected increase in MEP amplitude in the APB (1.18 ± 0.22 mV at T_0 to 1.49 ± 0.43 mV at T_1–T_4, T = 5.02, $p = 0.01$) that lasted for at least 20 min (Fig. 3, empty circles).

The difference in MEP modulation between the PAS and DAS group was highly significant ($F_{1,11} = 43.2$, $p < 0.001$). The peak increase relative to baseline was 42 ± 13 % for PAS and 23 ± 6 % for DAS and occurred at 20 and 10 min after the stimulation period, respectively.

In summary, both protocols lead to significant and lasting changes of MEP amplitudes, however, the magnitude and duration of MEP increase was significantly greater after PAS than DAS protocol.

Correlations between motor cortex excitability and after-effects of two protocols for inducing motor cortex plasticity

To test whether the the RMT might be related to peak change after PAS and DAS, we examined the relationship between RMT and magnitude of peak amplitude changes for each protocol, separately. Simple regression analysis between the resting MEP threshold measured expressed in percentages of maximal magnetic stimulator output (with the peak MEP amplitudes changes (normalized data) has shown weak positive associations for PAS and no association for DAS (Pearson's rho $\rho = 0.368$ PAS and $\rho = 0.042$ DAS, $p < 0.05$; Fig. 4).

Correlation between peak changes in PAS and DAS across subjects has revealed weak positive association, too ($\rho = 0.51$, $p < 0.05$), but without possibility to establish relevant corela-

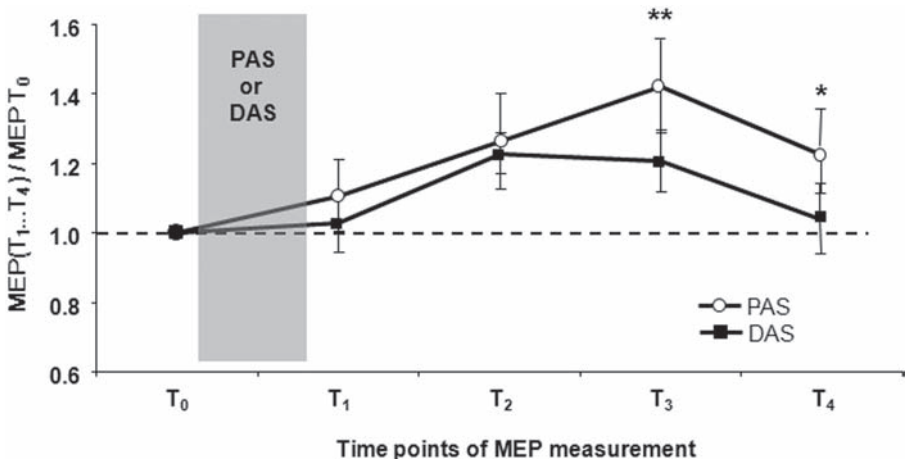

Figure 3. Lasting increase in motor-evoked potential (MEP) amplitude in the resting APB muscle induced by paired associative stimulation (PAS, empty circles) and dual associative stimulation (DAS, filled squares). Times of MEP testing are denoted on the x-axis (see Fig. 1). MEPs at different time points (MEP $T_1 \ldots T_4$) are normalized to MEP amplitude measured at T_0 (MEP T_0). Each subject was tested twice. All data are means ± SEM from 12 subjects.

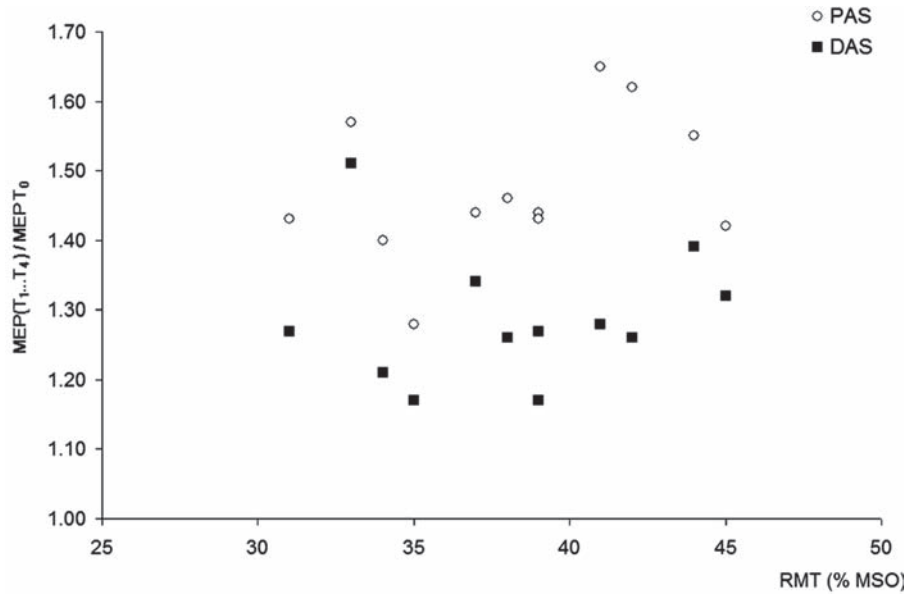

Figure 4. Individual peak changes of motor-evoked potential (MEP) amplitudes (y-axis) are plotted against the resting motor threshold (RMT, x-axis) for induced by paired associative stimulation (PAS, empty circles) and dual associative stimulation (DAS, filled squares) across subjects. MEPs at different time points (MEP $T_1 \ldots T_4$) are normalized to MEP amplitude measured at T_0 (MEP T_0). MSO, maximal stimulator output.

tion between after-effect magnitude for different protocols at same subjects.

Discussion

The most relevant finding of our study is the induction of significant and lasting MEP changes with both interventional procedures, with a maximal increase in motor cortex excitability at 20 min thereafter. However, an increase in motor excitability was significantly larger after PAS compared to DAS protocol.

A number of studies have shown that different experimental manipulations, such as application of repetitive TMS over M1, somatosensory afferent input modulation, or administration of CNS-active pharmacological agents lead to

a modulation of M1 output (for review see Ilić and Ziemann 2005). Hence, it is generally accepted that by changing the level of motor cortex excitability it is possible to open key permissive mechanisms of plasticity (Sanes and Donoghue 2000). In particular, experimental animal models have shown that reducing motor cortex inhibitory tone, such as after the cortical lesions, promotes functional plasticity of representational maps in the cerebral cortex (Nudo 1997). According to this concept, reduction of GABA-ergic inhibitory tone could be efficacious in promoting motor recovery in persons with chronic motor deficits (Hallett 2002).

This view is in keeping with the well-established analogy between the LTP, as shown in animal models of learning-induced cortical plasticity (Rioult-Pedotti et al. 2000) and the LTP-like plasticity in humans (Ziemann et al. 2004) that is considered a basic mechanism for acquisition of new motor skills.

To the best of our knowledge, this is the first report comparing the effects of two non-invasive inductive protocols on motor cortex plasticity in the same group of healthy subjects. Similar concept was applied previously in an attempt to compare three plasticity inducing protocols on the excitability of motor cortex as well as sensorimotor organization (Rosenkranz and Rothwell 2006). Their findings have shown that different protocols have been tested shown a different distribution of effects on various neurophysiological parameters. Several reasons have been discussed to explain changes that have been described. It is suggested that different protocols can have effects on different subsets of cortical neurones, that is high probable. However, the main difference between this study and our approach is that we have used two models of convergent impulses to sensori-motor cortex. Although, there are several differences between applied protocols that are not balanced, like shorter duration of PAS comparing to DAS. However, in spite the fact that each associative stimulation protocols were claimed highly effective to induce prolonged after-effect MEP changes, there was no head-to-head comparision.

The non-invasive plasticity inducing TMS protocols applied in our study reflect different mechanisms of M1 modulation. PAS is based on the original concept of Hebbian rule of learning, wherein employing two stimuli originating from different sources in a strict temporally coherent manner increases the synaptic strength of the two related inputs. On the other hand, DAS relies on synergistic effects on the M1 of paired afferent inputs from similar peripheral afferents (Ridding et al. 2003).

Correlation analyses that have been performed showed no significant associations between resting MEP threshold and peak MEP changes after PAS and DAS across subjects. As a matter of fact, that finding was not surprising because original papers had not reported any threshold modulation in spite of robust effects on induced MEP amplitude arround or above 1 mV (Stefan et al. 2000; Ridding et al. 2003). Following to widely accepted hypothesis of motor cortex excitability, RMT assesses excitation of the first few neurons recruited by the lowest intensity of cortical stimulation (so called "core motor neurons"), which have the highest excitability (Ridding and Rothwel 1997). Further to magnetic stimulation intensity increase, additional neural elements are excitated as reveals the recruitment curve. Obviously, effects of plastic modulation of motor cortex, at least by the way as we estimate, are prominent at sigmoid part of input-output curve.

Finally, we have performed an additional correlation analysis between peak MEP changes in PAS and DAS across subjects, that have shown only weak positive association without acceptable statistical significance. Nevertheless, similar mode of afferent stimulation still opens a possibility that PAS and DAS, at least partially could share some common mechanisms (e.g. cortical neuronal subsets) through which observed effects are realized.

In summary, the present findings show that PAS compared to DAS induces a greater and longer lasting MEP facilitation in a shorter period of time. Our results favour the use of PAS when the goal is to increase motor cortex excitability, as it may be advantageous when combining various rehabilitation interventions aimed at improving motor recovery. Further experiments in neurologic population are necessary for refining plasticity inducing TMS protocols and for testing the potential of PAS protocol in combination therapies.

Acknowledgement. This work was supported by the Ministry of Science and Technological Development of the Republic of Serbia, project No. 145083.

References

Boroojerdi B., Battaglia F., Muellbacher W., Cohen L. G. (2001): Mechanisms influencing stimulus-response properties of the human corticospinal system. Clin. Neurophysiol. **112**, 931–937

Chen R., Classen J., Gerloff C., Celnik P., Wassermann E. M., Hallett M., Cohen L. G. (1997): Depression of motor cortex excitability by low-frequency transcranial magnetic stimulation. Neurology **48**, 1398–1403

Cruccu G., Aminoff M. J., Curio G., Guerit J. M., Kakigi R., Mauguiere F., Rossini P. M., Treede R. D., Garcia-Larrea L. (2008): Recommendations for the clinical use of somatosensory-evoked potentials. Clin. Neurophysiol. **119**, 1705–1719

Hallett M. (2002): Recent advances in stroke rehabilitation. Neurorehabil. Neural Repair **16**, 211–217

Hallett M. (2007): Transcranial magnetic stimulation: a primer. Neuron **55**, 1871–1899

Hebb D. O. (1949): The Organization of Behavior: A Neuropsychological Theory. Lawrence Erlbaum, London

Ilić T. V., Ziemann U. (2005): Exploring motor cortical plasticity using transcranial magnetic stimulation in humans. Ann. N. Y. Acad. Sci. **1048**, 175–184

Nudo R. J. (1997): Remodeling of cortical motor representations after stroke: implications for recovery from brain damage. Mol. Psychiatry **2**, 188–191

Pascual-Leone A., Valls-Solé J., Wassermann E. M., Hallett M. (1994): Responses to rapid-rate transcranial magnetic stimulation of the human motor cortex. Brain. **117**, 847–858

Ridding M. C., Brouwer B., Miles T. S., Pitcher J. B., Thompson P. D. (2000): Changes in muscle responses to stimulation of the motor cortex induced by peripheral nerve stimulation in human subjects. Exp. Brain Res. **131**, 135–143

Ridding M. C., Rothwell J. C. (1997): Stimulus/response curves as a method of measuring motor cortical excitability in man. Electroencephalogr. Clin. Neurophysiol. **105**, 340–344

Ridding M. C., Uy J. (2003): Changes in motor cortical excitability induced by paired associative stimulation. Clin. Neurophysiol. **114**, 1437–1444

Rioult-Pedotti M. S., Friedman D., Donoghue J. P. (2000): Learning-induced LTP in neocortex. Science **290**, 533–536

Rosenkranz K., Rothwell J. C. (2006): Differences between the effects of three plasticity inducing protocols on the organization of the human motor cortex. Eur. J. Neurosci. **23**, 822–829

Rossini P. M., Barker A. T., Berardelli A., Caramia M. D., Caruso G., Cracco R. Q., Dimitrijevic M. R., Hallett M., Katayama Y., Lucking C. H. (1994): Non-invasive electrical and magnetic stimulation of the brain, spinal cord and roots: basic principles and procedures for routine clinical application. Report of an IFCN committee. Electroencephalogr. Clin. Neurophysiol. **91**, 79–92

Sakai K., Ugawa Y., Terao Y., Hanajima R., Furubayashi T., Kanazawa I. (1997): Preferential activation of different I waves by transcranial magnetic stimulation with a figure eight-shaped coil. Exp. Brain Res. **113**, 24–32

Sanes J. N., Donoghue J. P. (2000): Plasticity and primary motor cortex. Annu Rev. Neurosci. **23**, 393–415

Siebner H. R., Rothwell J. (2003): Transcranial magnetic stimulation: new insights into representational cortical plasticity. Exp. Brain Res. **148**, 1–16

Stefan K., Kunesch E., Cohen L. G., Benecke R., Classen J. (2000): Induction of plasticity in the human motor cortex by paired associative stimulation. Brain **123**, 572–584

Stefan K., Wycislo M., Classen J. (2004): Modulation of associative human motor cortical plasticity by attention. J. Neurophysiol. **92**, 66–72

Wolters A., Sandbrink F., Schlottmann A., Kunesch E., Stefan K., Cohen L. G., Benecke R., Classen J. (2003): A temporally asymmetric Hebbian rule governing plasticity in the human motor cortex. J. Neurophysiol. **89**, 2339–2345

Ziemann U., Ilić T. V., Pauli C., Meintzschel F., Ruge D. (2004): Learning modifies subsequent induction of long-term potentiation-like and long-term depression-like plasticity in human motor cortex. J. Neurosci. **24**, 1666–1672

The effect of inhibition of nitric oxide synthase on aluminium-induced toxicity in the rat brain

Ivana D. Stevanović[1], Marina D. Jovanović[1], Ankica Jelenković[2], Milica Ninković[1], Mirjana Đukić[3], Ivana Stojanović[4] and Miodrag Čolić[1]

[1] *Institute of Medical Research, Military Medical Academy, Belgrade, Serbia*
[2] *Institute of Biological Research, Belgrade, Serbia*
[3] *Department of Toxicology, Faculty of Pharmacy, University of Belgrade, Serbia*
[4] *Department of Biochemistry, Faculty of Medicine, University of Niš, Serbia*

Abstract. The goal of the present study was to examine the effectiveness of a non-specific nitric oxide synthase (NOS) inhibitor N-nitro-L-arginine methyl ester (L-NAME) to modulate the toxicity of aluminium chloride ($AlCl_3$). Rats were killed at 3 h and at 30 days after treatments and the striatum was removed. Nitrite, superoxide, superoxide dismutase activity, malondialdehyde and reduced glutathione were determined. $AlCl_3$ exposure promoted oxidative stress in the striatum. The biochemical changes observed in neuronal tissues show that aluminium acts as pro-oxidant, while the NOS inhibitor exerts antioxidant action in $AlCl_3$-treated rats. We conclude that L-NAME can efficiently protect neuronal tissue from $AlCl_3$-induced toxicity.

Key words: Aluminium — L-NAME — Nitric oxide — Oxidative stress — Striatum

Introduction

Aluminium (Al) is a neurotoxic metal that contributes to the progression of several neurodegenerative diseases (Ferreira et al. 2008). Al influx into brain tissues involves transferrin receptor-mediated endocytosis and a more rapid process which transports low molecular weight Al species. Reports have documented ghost-like neurons with Al deposition within their cytoplasmic and nuclear vacuoles (Platt et al. 2001; Miu et al. 2003). The hippocampus contains extracellular accumulations of Al and amyloid surrounded by nuclei of degenerating cells which are termed neuritic plaques (Drago et al. 2008). Al promotes the formation and accumulation of insoluble β amyloid (Aβ) and hyperphosphorylated tau. In addition, Al mimics the deficit of cortical cholinergic neurotransmission seen in several neurodegenerative diseases (Exley 2007).

Excessive microglial activation contributes to the neurodegenerative process by releasing potent cytotoxic substances including the free radical nitric oxide ($NO^{\bullet}$) (Hara et al. 2007). Chronic exposure to Al impairs glutamate-induced activation of NO synthase (NOS) and $NO^{\bullet}$-induced activation of guanylate cyclase (Cucarella et al. 1998). Cortical nitroxidergic neurons and granule cells are specific targets of Al-dependent neurotoxicity (Rodella et al. 2001).

NOS is present in the mammalian brain as three different isoforms, two constitutively-active (neuronal – nNOS, and endothelial – eNOS) and one inducible (iNOS). All three isoforms are aberrantly expressed during Al intoxication resulting in elevated NO levels. Elevated NO levels contribute to neurodegenerative process *via* different mechanisms including oxidative stress and the activation of intracellular signalling mechanisms (Luth et al. 2001).

Under physiological and pathological conditions and in the presence of molecular oxygen, reactive oxygen species (ROS) production such as the superoxide anion radical ($O_2^{\bullet -}$), hydrogen peroxide (H_2O_2) and the hydroxyl radical ($HO^{\bullet}$) occurs (Scandalios 2005). Elevated iron concentration in the brain promotes $HO^{\bullet}$ formation through the Fenton reaction, while $O_2^{\bullet -}$ reacts with $NO^{\bullet}$ to form the harmful peroxynitrite anion ($ONOO^-$). All together, the above-mentioned processes contribute to oxidative stress within the brain (Johnson 2001).

Correspondence to: Ivana Stevanović, Institute for Medical Research, Military Medical Academy, Crnotravska 17, 11 000 Belgrade, Serbia
E-mail: ivanav13@yahoo.ca

Pro-oxidants attack lipids within cell membranes *via* the process termed lipid peroxidation. The concentration of malondialdehyde (MDA) has been used as an index of lipid peroxidation in situations of Al exposure (Tanino et al. 2000).

Oxygen derivatives are eliminated *via* a coordinated antioxidant defence system comprising enzymes (glutathione (GSH) peroxidase, superoxide dismutase (SOD) and catalase) and water- or fat-soluble non-enzymatic antioxidants (vitamins C and E, GSH and selenium) (Stanczyk et al. 2005).

Changes in neurite morphology and cell death are partly reduced by attenuation of the effects of $NO^{\bullet}$ (Yang et al. 1998). Our previous results demonstrated positive effects of NOS inhibitors on the development of neurotoxicity (Vasiljević et al. 2002; Stevanović et al. 2008). In view of the above, the present study was undertaken to examine whether one or more oxidative stress status parameters (nitrite, $O_2^{\bullet -}$, SOD activity, MDA and GSH) change after intracerebral injections of aluminium chloride ($AlCl_3$) into rats and if they are modulated by pre-treatment of the rats with N-nitro-L-arginine methyl ester (L-NAME), a non-specific NOS inhibitor.

Materials and Methods

Animals

Adult male Wistar rats, weighing 500 ± 50 g, were used for the experiments. Two or three animals were housed per cage in an air-conditioned room at a temperature of 23 ± 2°C with 55 ± 10% humidity and with light intervals of 12 h/day (07.00–19.00 h). The animals were given a commercial rat diet and tap water *ad libitum*.

Animals used for all experimental procedures were handled in strict accordance with the NIH Guide for Care and Use of Laboratory Animals, 1985.

Reagents

All chemicals were of analytical grade or better. $AlCl_3$, L-NAME, EDTA, epinephrine and bovine serum albumin were purchased from Sigma (St. Louis, MO, USA), thiobarbituric acid reagent (TBAR) and 15% trichloroacetic acid were from Merck (Darmstadt, Germany), carbonate buffer was from Serva (Feinbiochemica, Germany) and saline solution (0.9% sodium chloride) was provided by the hospital pharmacy (Military Medical Academy, Belgrade). All solutions of drugs were prepared on the day of experiment.

Experimental procedures

The rats were intraperitoneally anesthetised with sodium pentobarbital (45 mg/kg body weight – b.w.) before intrahippocampal administration of the following: the control group ($n = 8$) was treated with 10 µl of saline solution; the $AlCl_3$ group ($n = 15$) was treated with $AlCl_3$ in one single dose (3.7×10^{-4} g/kg b.w. in 0.01 ml of deionised water); the L-NAME+$AlCl_3$ group ($n = 10$) was pre-treated with L-NAME in one single dose (1×10^{-4} g dissolved in saline solution) before $AlCl_3$ administration; the L-NAME group ($n = 10$) was treated with L-NAME in one single dose (1×10^{-4} g dissolved in saline solution) before saline solution administration. L-NAME was administered immediately before the $AlCl_3$/saline solution. L-NAME's half life varies from 7.5 min up to 222 min (Mitsube et al. 2002).

Using a stereotaxic instrument for small animals, the drugs were administered *via* a Hamilton microsyringe and injected into the CA1 sector of the hippocampus (coordinates: 2.5 A; 4.2 L; 2.4 V) (König and Klippel 1963). In all the treated animals the injected intracerebral volume was 10 µl and it was always injected into the same left side.

Each of the four experimental groups (defined above according to drug treatment) were divided into two subgroups. At 3 h and 30 days after treatment the rats were decapitated. The heads were immediately frozen in liquid nitrogen and stored at –70°C until use. A crude mitochondrial fraction from the striatum was used for the biochemical analyses (Gurd et al. 1974).

Biochemical analyses

After deproteinisation $NO^{\bullet}$ was quantitated by measuring nitrite and nitrate concentrations. Nitrites were directly assayed spectrophotometrically at 492 nm using the colourimetric method described by Griess (Griess reagent: 1.5% sulphanilamide in 1 mol/l HCl containing 0.15% N-(1-naphthyl)ethylendiamine dihydrochloride). Nitrates had to be converted into nitrites by cadmium reduction (Navarro-Gonzalvez et al. 1998).

Superoxide anion was determined *via* the reduction of nitroblue-tetrazolium (Merck, Darmstadt, Germany) in alkaline buffer (oxygen-free), with kinetic analysis performed at 550 nm (Auclair and Voisin 1985).

SOD activity was measured spectrophotometrically as inhibition of spontaneous epinephrine auto-oxidation at 480 nm. Enzyme activity in samples was monitored in a bicarbonate buffer (50 mmol/l, pH 10.2) containing 0.1 mmol/l EDTA after the addition of 10 mmol/l epinephrine (Sun and Zigman 1978).

The lipid peroxidation index was determined according to the quantity of MDA produced. TBAR (15% trichloroacetic acid + 0.375% TBA + 0.25% mol HCl) reacts with MDA originating from polysaturated fatty acid peroxidation. The product of the reaction, MDA, was measured spectrophotometrically at 533 nm (Villacara et al. 1989).

Reduced GSH was determined using 5,5-dithiobis-2-nitrobenzoic acid (36.9 mg in 10 ml of methanol) which reacts

with aliphatic thiol compounds in Tris-HCl buffer (0.4 mol/l, pH 8.9) generating a yellow coloured p-nitrophenol anion. Colour intensity was spectrophotometrically determined at 412 nm. Brain tissue was prepared in 10% sulphosalicylic acid for GSH determination (Anderson 1986).

The protein content in the rat brain homogenates (striatum, ipsilateral and contralateral) was measured by the method of Lowry using bovine serum albumin as a standard (Lowry et al. 1951).

Data presentation and analysis

Data are expressed as means ± S.D. Differences were deemed statistically significant if $p < 0.05$ *via* either the Student's *t*-test or ANOVA, the latter followed by Tukey's test.

Results

Nitrite concentration in the rat striatum

Three hours after $AlCl_3$ injection the nitrite concentration increased bilaterally in the striatum, compared to control-injected rats (Fig. 1A). In the L-NAME+$AlCl_3$ group, the bilateral nitrite concentration was lower in the striatum, compared to the $AlCl_3$-treated group (Fig. 1A). Thirty days after L-NAME+$AlCl_3$ injection, the bilateral nitrite concentration was lower compared to both control- and $AlCl_3$-injected rats (Fig. 1B). Three hours after L-NAME injection, the nitrite concentration increased bilaterally in the striatum, compared to both control- and L-NAME+$AlCl_3$-injected rats (Fig. 1A). However, after 30 days L-NAME injection resulted in lower nitrite concentrations in both the ipsi- and contralateral striatum compared to control- and $AlCl_3$-injected rats.

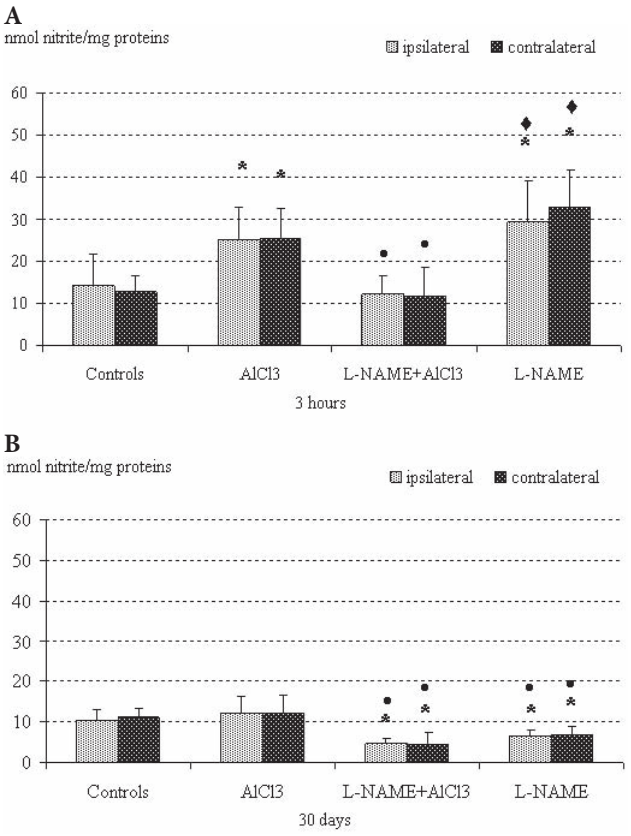

Figure 1. The effect of intrahippocampal drug administration on the concentration of nitrite (nmol/l nitrite/mg protein) in the rat ipsilateral and contralateral striatum at different times post injection: 3 h (A) and 30 days (B). Data are means ± S.D. of 10 animals. ✶ statistically significant difference between treated ($AlCl_3$-, L-NAME+$AlCl_3$- and L-NAME-treated) and control (sham-operated) animals ($p < 0.05$); ● statistically significant difference between treated (L-NAME+$AlCl_3$- and L-NAME-treated) and $AlCl_3$-treated animals ($p < 0.05$); ♦ statistically significant difference between L-NAME-treated and L-NAME+$AlCl_3$-treated animals ($p < 0.05$).

Superoxide production in the rat striatum

$AlCl_3$ injection resulted in higher $O_2^{\bullet-}$ production both after 3 h and after 30 days in both the ipsi- and contralateral striatum, compared to control rats ($p < 0.05$). In the L-NAME+$AlCl_3$ group $O_2^{\bullet-}$ production after 3 h decreased bilaterally in the striatum compared to the $AlCl_3$-treated group (Fig. 2A). Furthermore, after 30 days in the L-NAME+$AlCl_3$ group $O_2^{\bullet-}$ production decreased bilaterally in the same brain structure compared to both the control group as well as to the $AlCl_3$-injected group (Fig. 2B). Three hours after L-NAME injection, $O_2^{\bullet-}$ production decreased bilaterally in the striatum compared to $AlCl_3$-injected rats (Fig. 2A). Thirty days after L-NAME injection, $O_2^{\bullet-}$ production decreased bilaterally in the striatum compared to control-injected rats and compared to $AlCl_3$-injected rats. In contrast, $O_2^{\bullet-}$ production increased bilaterally in this brain structure compared to the L-NAME+$AlCl_3$-treated group (Fig. 2B).

SOD activity in the rat striatum

After both 3 h and 30 days, $AlCl_3$ injection resulted in lower SOD activity, compared to the control group. However, the difference was not statistically significant (Fig. 3A,B). After both 3 h and 30 days of L-NAME+$AlCl_3$ injection, lower SOD activity was found, compared to both control and $AlCl_3$-injected rats ($p < 0.05$). After both 3 h and 30 days of L-NAME application, lower SOD activity was found bilaterally in the striatum compared to both control and $AlCl_3$-injected rats. In contrast, higher SOD activity was

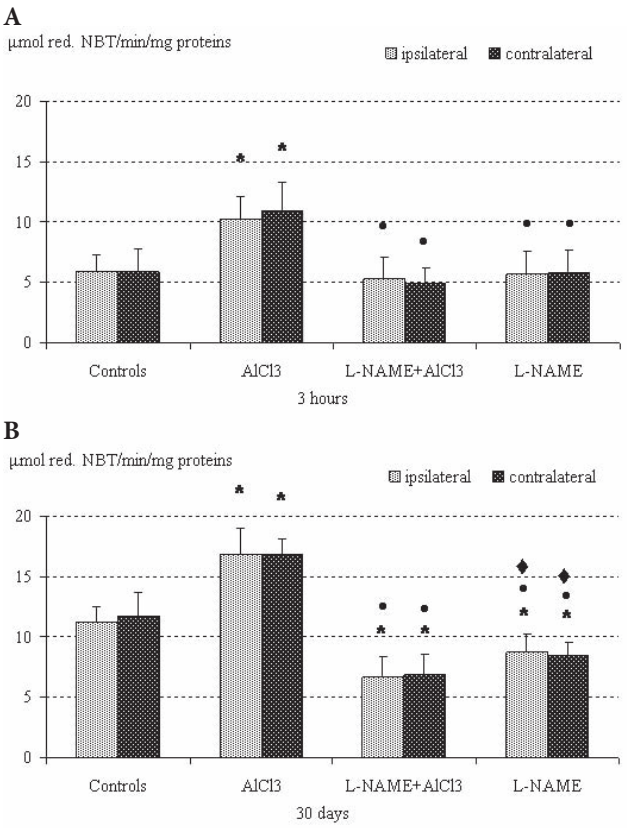

Figure 2. The effect of intrahippocampal drug administration on the concentration of $O_2^{\bullet -}$ (µmol/l red. NBT/min/mg proteins) in the rat ipsilateral and contralateral striatum at different survival times post injection: 3 h (A) and 30 days (B). Data are means ± S.D. of 10 animals. ✶ statistically significant difference between treated ($AlCl_3$-, L-NAME+$AlCl_3$- and L-NAME-treated) and control (sham-operated) animals ($p < 0.05$); ● statistically significant difference between treated (L-NAME+$AlCl_3$- and L-NAME-treated) and $AlCl_3$-treated animals ($p < 0.05$); ♦ statistically significant difference between L-NAME-treated and L-NAME+$AlCl_3$-treated animals ($p < 0.05$).

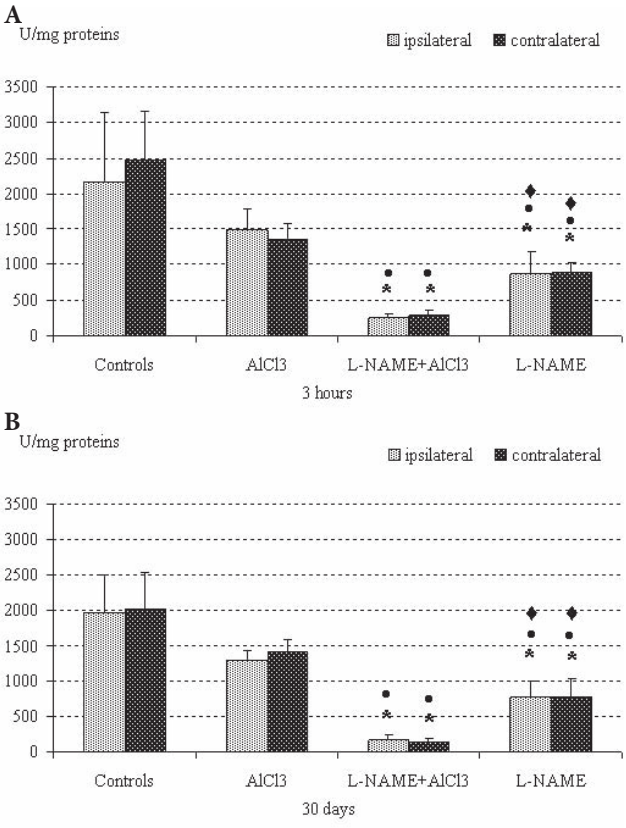

Figure 3. The effect of intrahippocampal drug administration on SOD activity (U/mg proteins) in the rat ipsilateral and contralateral striatum at different survival times post injection: 3 h (A) and 30 days (B). Data are means ± S.D. of 10 animals. ✶ statistically significant difference between treated (L-NAME+$AlCl_3$- and L-NAME-treated) and control (sham-operated) animals ($p < 0.05$); ● statistically significant difference between treated (L-NAME+$AlCl_3$- and L-NAME-treated) and $AlCl_3$-treated animals ($p < 0.05$); ♦ statistically significant difference between L-NAME-treated and L-NAME+$AlCl_3$-treated animals ($p < 0.05$).

found in both ipsi- and contralateral striatum compared to the L-NAME+$AlCl_3$-injected group of rats (Fig. 3A,B).

MDA concentration in the rat striatum

After both 3 h and 30 days post $AlCl_3$ injection, increased MDA concentration bilaterally in the striatum was apparent compared to control rats (Fig. 4A,B). L-NAME+$AlCl_3$ administration resulted in a decrease in the MDA concentration bilaterally in the same brain structure after both 3 h and 30 days compared to $AlCl_3$-injected rats. After 3 h, L-NAME administration resulted in a higher MDA concentration in the ipsilateral striatum compared to L-NAME+$AlCl_3$-injected rats and bilaterally in the same brain structure compared to control-treated rats. After 3 h, L-NAME resulted in a lower MDA concentration in both the ipsi- and contralateral striatum compared to $AlCl_3$-injected rats (Fig. 4A). After 30 days, L-NAME injection resulted in a lower MDA concentration compared to both control and $AlCl_3$-injected rats (Fig. 4B).

Reduced GSH content in the rat striatum

The GSH concentration was higher (bilaterally in the striatum) 3 h post $AlCl_3$ injection compared to control-injected rats (Fig. 5A). After 3 h, L-NAME+$AlCl_3$ administration resulted in a lower GSH concentration in both the ipsi- and contralateral striatum compared to the $AlCl_3$-treated group. In addition, 30 days after L-NAME+$AlCl_3$ administration, the GSH concentration decreased bilaterally in the striatum

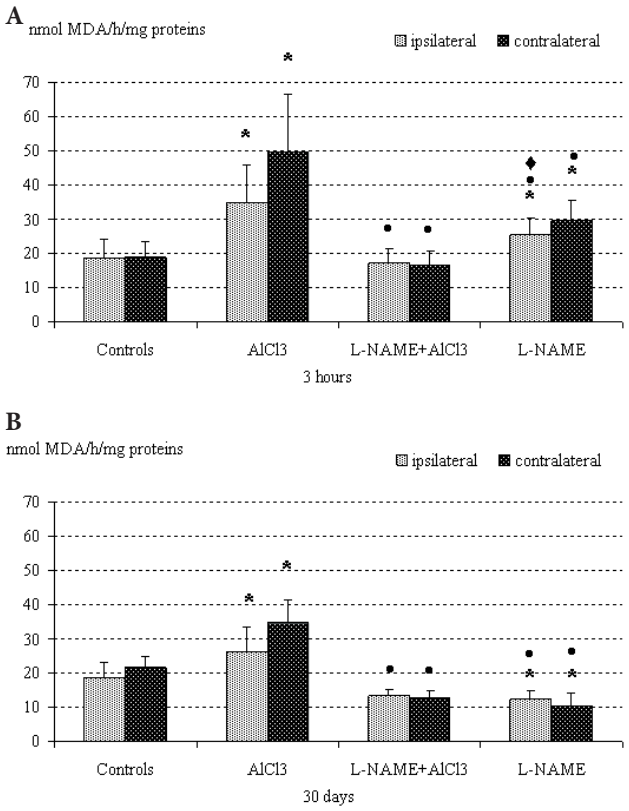

Figure 4. The effect of intrahippocampal drug administration on lipid peroxidation (nmol/l MDA/h/mg proteins) in the rat ipsilateral and contralateral striatum at different survival times post injection: 3 h (A) and 30 days (B). Data are means ± S.D. of 10 animals. ✶ statistically significant difference between treated ($AlCl_3$- and L-NAME-treated) and control (sham-operated) animals ($p < 0.05$); ● statistically significant difference between treated (L-NAME+$AlCl_3$- and L-NAME-treated) and $AlCl_3$-treated animals ($p < 0.05$). ♦ statistically significant difference between L-NAME-treated and L-NAME+$AlCl_3$-treated animals ($p < 0.05$).

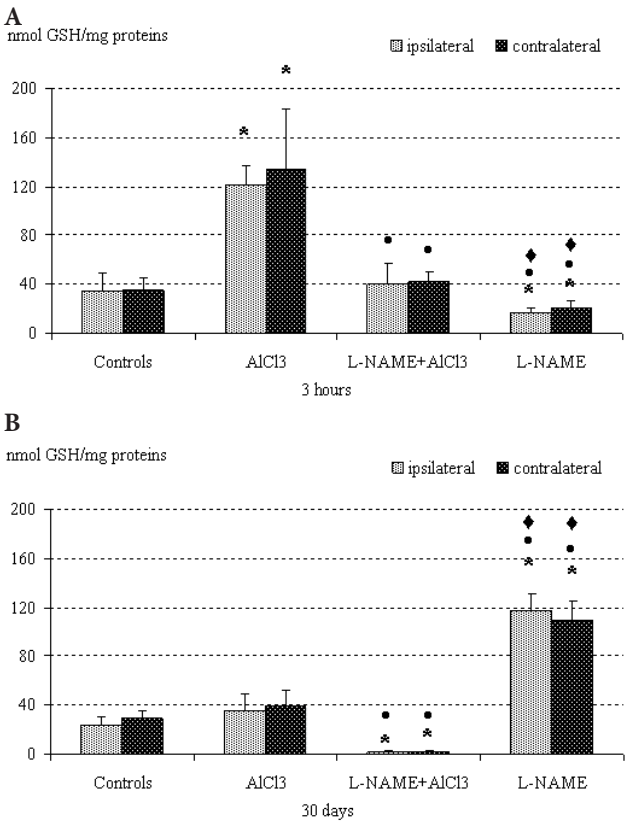

Figure 5. The effect of intrahippocampal drug administration on reduced GSH concentration (nM GSH/mg proteins) in the rat ipsilateral and contralateral striatum at different survival times post injection: 3 h (A) and 30 days (B). Data are means ± S.D. of 10 animals. ✶ statistically significant difference between treated ($AlCl_3$-, L-NAME+$AlCl_3$- and L-NAME-treated) and control (sham-operated) animals ($p < 0.05$); ● statistically significant difference between treated (L-NAME+$AlCl_3$- and L-NAME-treated) and $AlCl_3$-treated animals ($p < 0.05$); ♦ statistically significant difference between L-NAME-treated and L-NAME+$AlCl_3$-treated animals ($p < 0.05$).

compared to both control and $AlCl_3$-injected rats (Fig. 5B). After 3 h, L-NAME administration resulted in a lower GSH concentration bilaterally in the striatum compared to control, $AlCl_3$- and L-NAME+$AlCl_3$-injected rats. However, after 30 days, L-NAME injection resulted in a higher concentration of GSH bilaterally in the striatum compared to control, $AlCl_3$- and L-NAME+$AlCl_3$-injected rats (Fig. 5B).

Discussion

Extensive afferents from all areas of the cortex and the thalamus represent the most important source of excitatory amino acids, whereas the nigrostriatal pathway and intrinsic circuits provide the striatum with dopamine, acetylcholine, GABA, NO and adenosine. All these neurotransmitters interact in a voltage-dependent manner to regulate the efficacy of synaptic transmission within this circuit (Calabresi et al. 2000).

Our findings that $AlCl_3$ injection resulted in increased nitrite after 3 h bilaterally in the striatum but without change after 30 days bilaterally in this brain structure compared to control rats is in accordance with previously published data (Tohgi et al. 1998) demonstrating increased $NO^{\bullet}$concentration and oxidation in early stages of disease, while it was decreasing with elevating loss of neurons.

Increased $O_2^{\bullet -}$ production bilaterally in the striatum 3 h after $AlCl_3$ injection is in agreement with a published article regarding Al-mediated oxidative stress. Pro-oxidant properties of Aβ have been found in senile plaques and discussed by

Yang et al. (1999). In addition, free radical production in the brain could be stimulated by the presence of low molecular weight iron-containing compounds which are known Fenton reaction promoters.

The product of the reaction between $NO^{\bullet}$ and $O_2^{\bullet-}$ ($ONOO^-$) is a strong oxidising and nitrating agent which can react with all classes of biomolecules (Domico et al. 2007). In the central nervous system (CNS) it can be generated by microglial cells activated by pro-inflammatory cytokines or Aβ and by neurons when $ONOO^-$ directly contributes to the initiation of the neurodegenerative process (Torreilles et al. 1999; Wakselman et al. 2008).

Intracerebral administration of $AlCl_3$ resulted in increased $O_2^{\bullet-}$ production after 30 days in the ipsi- and contralateral striatum. A report has indicated that microglia are the CNS macrophages and are the primary cellular component of plaques that contribute to the oxidative stress associated with chronic neurodegeneration (Colton et al. 2000). The effect of Aβ peptides on $O_2^{\bullet-}$ production was not associated with a concomitant increase in $NO^{\bullet}$ concentration. Although statistically insignificant, $AlCl_3$ injection caused a decrease in SOD activity. The latter is in accordance with increased $O_2^{\bullet-}$ production in the same brain structure, indicating conditions favouring oxidative stress.

After both 3 h and 30 days post intrahippocampal $AlCl_3$ injection, the concentration of MDA increased bilaterally in the striatum. Previous data have demonstrated that Al affects Ca^{2+} flux and general homeostasis, increases ROS and facilitates membrane lipid peroxidation, which together can contribute to neurotoxicity induced by other neurotoxicants (Mundy et al. 1997).

Furthermore, we demonstrated that after 3 h $AlCl_3$ injection increased the concentration of GSH bilaterally in the striatum. All the detrimental effects of $ONOO^-$ can be successfully attenuated by the thiol-containing tripeptide antioxidant GSH (Burdo et al. 2008). Peroxynitrite is a powerful oxidant as it is capable of chemically modifying both membrane and cytosolic proteins which affects both their physical and chemical nature properties (Koppal et al. 1999). Not surprisingly, we found increased GSH concentration 3 h post $AlCl_3$ injection. Other parameters confirmed that oxidative stress processes were operative at this time point.

Our biochemical observations are of particular interest especially when taking in consideration the fact that interactions between basalocortical and intracortical NOS neurons are involved in the spatial and temporal regulation of cortical perfusion following basal forebrain activation (Tong and Hamel 2000). In addition, Al accumulation in the brain can modify neuronal signal transduction pathways associated with glutamate-induced activation of NOS and $NO^{\bullet}$-induced activation of the cGMP generating enzyme, guanylate cyclase. These findings suggest that glutathione-$NO^{\bullet}$-cGMP pathway impairment in the brain may be responsible for some Al-induced neurological alterations (Canales et al. 2001).

The decreased bilateral nitrite concentration in the striatum at 30 days post L-NAME+$AlCl_3$-injected rats (compared to $AlCl_3$-injected rats) suggests that L-NAME suppresses nitrite production and decreases neuron impairment through N-methyl-D-aspartic acid receptors.

Decreased $O_2^{\bullet-}$ production, decreased SOD activity and decreased MDA concentration bilaterally in the striatum at both 3 h and 30 days after L-NAME+$AlCl_3$ application (compared to $AlCl_3$-treated animals) confirm antioxidative effects if the NOS inhibitor. In the same experimental group of animals, we also noted decreased GSH content. Therefore, our results suggest the importance of GSH in the glutathionylation process as a crucial antioxidative defence mechanism against irreversible protein impairment (Giustarini et al. 2004).

The observed bilateral increase in NO concentration in the striatum, compared to the control group of rats, 3 h after L-NAME application was unexpected because of its inhibitory potential. However, in some circumstances L-NAME may contribute to $NO^{\bullet}$ donation, serving as an arginine analog (Chakraborti et al. 2008). Furthermore, the inhibition of inducible NOS expression by L-NAME prevented an increase in nitrogen intermediates and GABA release, but not in glutamate release (Waldmeier et al. 2008). In contrast, our results concerning reduced concentrations of both NO concentration and $O_2^{\bullet-}$ 30 days after L-NAME application, compared to $AlCl_3$-treated rats, suggest long-term inhibition of $NO^{\bullet}$ synthesis by L-NAME, which therefore fortifies its antioxidative potential.

Increased MDA concentration in tune with both decreased SOD activity and GSH concentration bilaterally in the striatum 3 h post L-NAME application, compared to control rats, all together contribute to oxidative development at such an early time point. Thirty days post L-NAME application resulted in an improvement in oxidative stress status development parameters (decreased MDA and increased GSH concentration). L-NAME could be a potential arginine analog, therefore it could have some toxic properties similar to those of $AlCl_3$. MDA may contribute to the protective effect of L-NAME in $AlCl_3$-treated rats, in contrast to $AlCl_3$'s and L-NAME's effects by themselves.

In conclusion, our results indicated that $NO^{\bullet}$-mediated neurotoxicity spread temporally and spatially in the striatum after intrahippocampal $AlCl_3$ administration and that L-NAME has potential neuroprotective roles.

References

Anderson M. E. (1986): Tissue glutathione. In: Handbook of Methods for Oxygen Radical Research. (Ed. R. A. Greenwald), pp. 317–323, CRC Press, Boca Raton, Florida

Auclair C., Voisin E. (1985): Nitroblue tetrazolium reduction. In: Handbook of Methods for Oxygen Radical Research. (Ed. R. A. Greenwald), pp. 123–132, CRC Press, Boca Raton, Florida

Burdo J., Schubert D., Maher P. (2008): Glutathione production is regulated via distinct pathways in stressed and non-stressed cortical neurons. Brain Res. **1189**, 12–22

Calabresi P., Centonze D., Gubellini P., Merfia G. A., Pisani A., Sancesario G., Bernardi G. (2000): Synaptic transmission in the striatum: from plasticity to neurodegeneration. Prog. Neurobiol. **61**, 231–265

Canales J. J., Corbalan R., Montoliu C., Liansola M., Monfort P., Erceg S., Hernandez-Viadel M., Felipo V. (2001): Aluminium impairs the glutamate-nitric oxide-cGMP pathway in cultured neurons and in rat brain *in vivo*: molecular mechanisms and implications for neuropathology. J. Inorg. Biochem. **87**, 63–69

Chakraborti A., Gulati K., Ray A. (2008): Age related differences in stress-induced neurobehavioral responses in rats: modulation by antioxidants and nitrergic agents. Behav. Brain Res. **194**, 86–91

Colton C. A., Chernyshev O. N., Gilbert D. L., Vitek M. P. (2000): Microglial contribution to oxidative stress in Alzheimer′s disease. Ann. N. Y. Acad. Sci. **899**, 292–307

Cucarella C., Montoliu C., Hermenegildo C., Saez R., Manzo L., Minana M. D., Felipo V. (1998): Chronic exposure to aluminium impairs the neuronal glutamate-nitric oxide-cyclic GMP pathway. J. Neurochem. **70**, 1609–1614

Domico L. M., Cooper K. R., Bernard L. P., Zeevalk G. D. (2007): Reactive oxygen species generation by the ethylene-bis-dithiocarbamate (EBDC) fungicide mancozeb and its contribution to neuronal toxicity in mesencephalic cells. Neurotoxicology **28**, 1079–1091

Drago D., Bettella M., Bolognin S., Cendron L., Scancar J., Milacic R., Ricchelli F., Casini A., Messori L., Tognon G., Zatta P. (2008): Potential pathogenic role of beta-amyloid(1-42)-aluminum complex in Alzheimer's disease. Int. J. Biochem. Cell Biol. **40**, 731–746

Exley C. (2007): Aluminium, tau and Alzheimer's disease. J. Alzheimers Dis. **12**, 313–315

Ferreira P. C., Piai K. A., Takayanagui A. M., Segura-Muñoz S. I. (2008): Aluminum as a risk factor for Alzheimer's disease. Rev. Lat. Am. Enfermagem **16**, 151–157

Giustarini D., Rossi R., Milzani A., Colombo R., Dalle-Donne I. (2004): S-glutathionylation-from redox regulation of protein functions to human diseases. J. Cell Mol. Med. **8**, 201–212

Gurd J. W., Jones L. R., Mahler H. R., Moore W. J. (1974): Isolation and partial characterization of rat brain synaptic plasma membranes. J. Neurochem. **22**, 281–290

Hara S., Mukai T., Kurosaki K., Mizukami H., Kuriiwa F., Endo T. (2007): Role of nitric oxide system in hydroxyl radical generation in rat striatum due to carbon monoxide poisoning, as determined by microdialysis. Toxicology **239**, 136–143

Johnson S. (2001): Gradual micronutrient accumulation and depletion in Alzheimer′s disease. Med. Hypotheses **56**, 595–597

Koppal T., Drake J., Yatin S., Jordan B., Varadarajan S., Bettenhausen L., Buttefield D. A. (1999): Peroxynitrite-induced alterations in synaptosomal membrane proteins: insight into oxidative stress in Alzheimer′s disease. J. Neurochem. **72**, 310–317

König J. F. R., Klippel R. A. (1963): A stereotaxic atlas of the forebrain and lower parts of the brain stem. In: The Rat Brain. The Williams and Wilkins company, Baltimore, USA

Lowry O. H., Rosenbrongh N. J., Farr A. L., Randall R. J. (1951): Protein measurement with the folin phenol reagent. J. Biol. Chem. **193**, 265–275

Luth H. J., Holzer M., Gartner U., Staufenbiel M., Arendt T. (2001): Expression of endothelial and inducible NOS-isoforms is increased in Alzheimer's disease, in APP23 transgenic mice and after experimental brain lesion in rat: evidence for an induction by amyloid pathology. Brain Res. **913**, 57–67

Mitsube K., Zackrisson U., Brännström M. (2002): Nitric oxide regulates ovarian blood flow in the rat during the periovulatory period. Hum. Reprod. **17**, 2509–2516

Miu A. C., Andreescu C. E., Vasiu R., Olteanu A. I. (2003): A behavioral and histological study of the effects of long-term exposure of adult rats to aluminium. Int. J. Neurosci. **113**, 1197–1211

Mundy W. R., Fraudenrich T. M., Kodavanti P. R. (1997): Aluminium potentiates glutamate-induced calcium accumulation and iron-induced oxygen free radical formation in primary neuronal cultures. Mol. Chem. Neuropathol. **32**, 41–57

Navarro-Gonzalvez J. A., Garcia-Benayas C., Arenas J. (1998): Semiautomated measurement of nitrate in biological fluids. Clin. Chem. **44**, 679–681

Platt B., Fiddler G., Riedel G., Henderson Z. (2001): Aluminium toxicity in the rat brain: histochemical and immunocytochemical evidence. Brain Res. Bull. **55**, 257–267

Rodella L., Rezzani R., Lanzi R., Bianchi R. (2001): Chronic exposure to aluminium decreases NADPH-diaphorase positive neurons in the rat cerebral cortex. Brain Res. **889**, 229–233

Scandalios J. G. (2005): Oxidative stress: molecular perception and transduction of signals triggering antioxidant gene defenses. Braz. J. Med. Biol. Res. **38**, 995–1014

Stanczyk M., Gromadzinska J., Wasowicz W. (2005): Roles of reactive oxygen species and selected antioxidants in regulation of cellular metabolism. Int. J. Occup. Med. Environ. Health **18**, 15–26

Stevanović I. D., Jovanović M. D., Jelenković A., Čolić M., Stojanović I., Ninković M. (2008): The effect of 7-nitroindazole on aluminium toxicity in the rat brain. Bulg. J. Vet. Med. **11**, 37–47

Sun M., Zigman S. (1978): An important spectrophotometric assay for superoxide dismutase based on epinephrine autooxidation. Analyt. Biochem. **90**, 81–89

Tanino H., Shimohama S., Sasaki Y., Sumida Y., Fujimoto S. (2000): Increase in phospholipase C-δ1 protein levels in aluminium-treated rat brains. Biochem. Biophys. Res. Commun. **271**, 620–625

Tohgi H., Abe T., Yamazaki K., Murata T., Isobe C., Ishizaki E. (1998): The cerebrospinal fluid oxidized NO metabolites, nitrite and nitrate in AD and vascular dementia of Binswanger type and multiple small infarct type. J. Neural. Transm. **105**, 1283–1291

Tong X. K., Hamel E. (2000): Basal forebrain nitric oxide synthase (NOS)-containing neurons project to microvessels and NOS neurons in the rat neocortex: cellular basis for cortical blood flow regulation. Eur. J. Neurosci. **12**, 2769–2780

Torreilles F., Salman-Tabcheh S., Guerin M., Torreilles J. (1999): Neurodegenerative disorders: the role of peroxynitrite. Brain Res., Brain Res. Rev. **30**, 153–163

Vasiljević I., Jovanović M., Ninković M., Maličević Ž. (2002): Nitric oxide synthase inhibition prevents acute QA-induced neurotoxicity. Acta Vet. **52**, 79–84

Villacara A., Kumami K., Yamamoto T., Mršulja B. B., Spatz M. (1989): Ischemic modification of cerebrocortical membranes: 5-hydroxytriptamine receptors, fluidity, and inducible *in vitro* lipid peroxidation. J. Neurochem. **53**, 595–601

Wakselman S., Béchade C., Roumier A., Bernard D., Triller A., Bessis A. (2008): Developmental neuronal death in hippocampus requires the microglial CD11b integrin and DAP12 immunoreceptor. J. Neurosci. **28**, 8138–8143

Waldmeier P. C., Kaupmann K., Urwyler S. (2008): Roles of GABA B receptor subtypes in presynaptic auto- and heteroreceptor function regulating GABA and glutamate release. J. Neural. Transm. **115**, 1401–1411

Yang S. N., Hsieh W. Y., Liu D. D., Tsai L. M., Tung C. S., Wu J. N. (1998): The involvement of nitric oxide in synergistic neuronal damage induced by beta-amyloid peptide and glutamate in primary rat cortical neurons. Chin. J. Physiol. **41**, 175–179

Yang E. Y., Guo-Ross S. X., Bondy S. C. (1999): The stabilization of ferrous iron by a toxic beta-amyloid fragment and by an aluminium salt. Brain Res. **839**, 221–226

Nitric oxide synthase inhibitors partially inhibit oxidative stress development in the rat brain during sepsis provoked by cecal ligation and puncture

Milica B. Ninković[1], Živorad M. Maličević[1], Ankica Jelenković[2], Mirjana M. Đukić[3], Marina D. Jovanović[1] and Ivana D. Stevanović[1]

[1] *Laboratory of Clinical Physiology, Institute of Medical Research, Military Medical Academy, Belgrade, Serbia*
[2] *Institute of Biology Research "Siniša Stanković", Belgrade, Serbia*
[3] *Department of Toxicological Chemistry, Faculty of Pharmacy, Belgrade, Serbia*

Abstract. Oxidative stress development in different brain structures and the influence of nitric oxide (NO) overproduction during sepsis was investigated using male Wistar rats. Rats were subjected to cecal ligation and puncture (CLP) or were sham-operated. To evaluate the source of NO production, 30 min before the operation septic and control animals were treated with single intraperitoneal doses of NO synthase (NOS) inhibitors: L-NAME and aminoguanidine (AG) (10, 30 or 90 mg/kg) and 7-nitroindazole (7-NI) (30 mg/kg). The concentration of GSH in the cortex, brain stem, cerebellum, striatum and hippocampus significantly decreased post CLP at both early and late stage sepsis. Lipid peroxidation also occurred in the cortex and cerebellum in late stage sepsis. Pre-treatment with a non-selective NOS inhibitor (L-NAME) and with selective inducible and neuronal NOS inhibitors (AG and 7-NI) revealed benefit effects on the GSH concentrations. Unexpectedly, NOS inhibition resulted in diverse effects on TBARS concentrations, suggesting the importance of specific quantities of NO in specific brain structures during sepsis.

Key words: Sepsis — Brain — Nitric oxide synthase inhibitors — Rat

Introduction

Sepsis and multiple organ dysfunctions are the leading causes of death among hospitalized patients in critical care units. Despite the availability of specialized therapy, mortality rates remain unacceptably high (Levy et al. 2003). Unfortunately, pathophysiological mechanisms underlying sepsis development (systemic inflammation, coagulopathy and systemic vascular dysfunction) are complex and are often undetectable until symptoms become visible at which time therapy is initiated (Rivers et al. 2005). One of the characteristic hallmarks of sepsis is tissue damage which is a consequence of gross systemic disturbance. A hyperactive immune system coupled with misbalanced overproduction of a number of endogenous mediators, are two examples of the host response (Hotchiss and Karl 2003).

Nitric oxide (NO) overproduction is a known occurrence in sepsis (Feihl et al. 2001). Due to the fact that NO is a key regulator of homeostasis in almost all known tissues, understanding both its direct and indirect actions are of particular interest during sepsis conditions (Poon et al. 2003). In addition to NO's well-documented roles in vascular homeostasis (vasodilatation, hemostasis, coagulation and imunommodulation) that influence septic processes, NO regulates a number of functions in the central nervous system (CNS) (Esplugues 2002).

NO serves as a neurotransmitter and a neuromodulatory mediator for inter-neuronal communication (Wiklund et al. 1997). Furthermore, NO participates in neuroendocrine regulation as well as in long-term potentiation that form the foundations for complex processes including learning, memory, sleep regulation, pain and appetite (Garthwaite and Boulton 1995). It is also crucial for correct cerebellar activity. The influence of NO on synaptic plasticity, long-term

Correspondence to: Milica B. Ninković, Laboratory of Clinical Physiology, Instititute of Medical Research, Military Medical Academy, Crnotravska 17, 11002 Belgrade, Serbia
E-mail: ninkomj@ptt.yu

potentiation, receptor neuromodulation as well as in the above-mentioned processes within blood vessels all together influence whole body homeostasis (Liaudet et al. 2000).

Brain complications during or after sepsis are not rare (Angus et al. 2001). Barichello and colleagues demonstrated that rats that survived sepsis showed decreased cognitive functions (Barichello et al. 2005). Reciprocal interactions between the immune and CNS seems to be the major components of the host response to sepsis. However, the dynamic of changes remain unresolved (Sharshar et al. 2005). They are related to neurochemical interaction complexity in the CNS, anatomical and functional brain defense that has developed throughout evolution as well as control of physiological functions that are crucial for maintaining homeostasis and orchestrating the host response at autonomic, neuroendocrine and behavioral levels (Sharshar et al. 2004). The oxidative milieu inside brain tissue reflects brain function during sepsis progression. Although brain tissue is approximately 2% of the total body weight, blood flow through the brain contributes to almost 15% of the total body blood flow. Cells within the blood brain barrier possess a high antioxidative capacity (consisting of enzymes: superoxide dismutase, catalase, glutathione peroxidase and glutathione reductase and non-enzyme components such as glutathione) (Ghersi-Egea et al. 1994). During sepsis, immune cells in the circulation exhibit features characteristic of an oxidative burst (as a defense mechanism) and contribute to conditions of enhanced oxidative stress at the blood brain barrier. At the same time, increased NO production can lead to nitrosative stress. Tissue homeostasis within the brain stem during system inflammation is of huge importance (Ninkovic et al. 2008). In addition, some brain structures possess selective vulnerability to oxidative as well as nitrosative stress development. These include the cerebral cortex (especially the third layer), the striatum (the caudate nucleus and the putamen), the hippocampus (CA1 and CA3 sector) and the cerebellum (Purkinje cells). Therefore, we sought to answer the following questions: In which brain regions do conditions of oxidative stress arise during sepsis progression? Does the blood brain barrier protect the oxidative milieu inside brain tissue during sepsis progression and what are NO's roles in such events?

Materials and Methods

The study was performed in accordance with the Guidelines for Animal Study No. 282-12/2002 (Ethics Committee of the Military Medical Academy, Belgrade, Serbia). Eleven-week-old male Wistar rats weighing between 250 and 300 g were purchased from the laboratory animal care centre located in the Military Medical Academy. *Escherichia coli* suspension – ATCC 25922 (33% agar in 0.7% saline solution) was manufactured in the Institute of Immunology and Virology, Torlak, Serbia.

The rats were housed five per cage with free access to food and water. For adaptation purposes they were maintained under standard laboratory conditions (room temperature and a circadian regime of light/dark ratio of 13 : 11 h) for at least seven days before the study.

Sepsis was induced by a modified method of cecal ligation and puncture (CLP) (Stojanovic et al. 2002). The procedure was performed in a sterile manner under brief diethylether anaesthesia. After midline laparotomy, the content of the cecum was squeezed towards the ileocecal valve. The cecum was tied with a 3-0 silk suture one centimetre from the distal end leaving the ileocecal valve free. *Escherichia coli* suspension (1 ml) was injected distal to the point of ligation using a 14-gauge needle. The above-mentioned procedure was performed inside the opened abdominal cavity ensuring that a small amount of *E. coli* suspension leaked from the puncture. The abdominal wall was then closed with silk sutures consisting of two layers. Sham operations were performed without CLP. After surgical procedures all animals had free access to food and water.

Animals were randomly assigned to the sepsis (CLP) group or to the sham-operated (control) group. Animals were also treated with non-selective/selective NO synthase (NOS) inhibitors before surgery. The non-selective NOS inhibitor, Lω-nitro-L-arginine methyl ester (L-NAME) (Sigma) and the selective inducible NOS (iNOS) inhibitor aminoguanidine (AG) (Sigma) were dissolved in 0.9% saline solution. The selective neuronal NOS (nNOS) inhibitor, 7-nitroindazole (7-NI) (Sigma) was dissolved in olive oil (Robert et al. 1997). All three inhibitors were administered intraperitoneally (i.p.) 30 min before surgery. The doses, the routes of administration and the pre-incubation times of the NOS inhibitors were chosen on the basis of published data and according to experience in our laboratory (Benjamim et al. 2002).

Experimental subgroups were defined according to the dose of the applied NOS inhibitor. Rats in the L-NAME 10 + CLP, the L-NAME 30 + CLP and the L-NAME 90 + CLP as well as those in the L-NAME 10 + control, the L-NAME 30 + control and the L-NAME 90 + control subgroups received L-NAME 30 min before surgery at a dose of 10, 30 or 90 mg/kg i.p.

Rats in the AG 10 + CLP, the AG 30 + CLP and the AG 90 + CLP as well as those in the AG 10 + control, the AG 30 + control and the AG 90 + control subgroups received AG 30 min before surgery at a dose of 10, 30 or 90 mg/kg i.p.

Rats in the 7-NI 30 + CLP and the 7-NI 30 + control subgroups received 7-NI 30 min before surgery at a dose of 30 mg/kg i.p.

To study the time-course of inflammation during sepsis, each subgroup was randomly subdivided into early and late stage sepsis, each consisting of 10 animals killed after 3 h or

48 h, respectively, after surgery. Rats were killed by decapitation. Their heads were immediately frozen in liquid nitrogen and stored at –70°C until use. Brain structures (cortex, brain stem, cerebellum, striatum and hippocampus) were removed on ice and then homogenised in cold buffered sucrose medium (0.25 mol/l sucrose (Serva Feinbiochemica), 10 mmol/l phosphate buffer (pH 7.0) and 1 mmol/l EDTA (Sigma)) (Gurd et al. 1974). Proteins were determined by the Lowry method using bovine serum albumin as a standard (Sigma) (Lowry et al. 1951).

Thiobarbituric acid reactive species (TBARS) were measured spectrophotometrically at 533 nm (Girotti 1991).

GSH in brain samples was measured spectrophotometrically at 412 nm (Ellman 1959).

Statistical analysis of the data was performed using Statistic 5.0 for Windows. Descriptive data are expressed as the mean ± standard deviation (SD). Data among the groups were analysed by two-way analysis of variance and the Students *t*-test. Differences were considered statistically significant when $p < 0.05$ and highly statistically significant when $p < 0.01$.

Results

A highly significant decrease in GSH in brain tissue was found in early stage sepsis when compared with control rats ($p < 0.01$) (Table 1). Pre-treatment with L-NAME followed by induction of sepsis led to a significant decrease in GSH in almost all the brain structures, (the exception being in the cortex in rats pre-treated with 90 mg/kg of L-NAME). L-NAME-mediated dose-dependent increase in brain stem GSH in septic rats

Table 1. Glutathione concentration in rat brain structures in early stage sepsis: effect of i.p. pre-treatment with NOS inhibitors

Group	Dose	Cortex	Brain stem	Cerebellum	Striatum	Hippocampus
Control	–	11.20 ± 4.70	15.17 ± 4.88	22.56 ± 7.58	16.36 ± 5.70	17.58 ± 4.84
CLP	–	3.45 ± 1.03**	2.75 ± 0.80**	4.35 ± 1.27**	4.21 ± 1.40**	4.73 ± 0.79**
L-NAME + CLP	10	5.74 ± 1.51**	5.83 ± 1.67**‡	7.07 ± 2.06**	5.62 ± 1.64**	6.13 ± 0.45**
	30	5.94 ± 1.89*	6.80 ± 2.12**‡	5.68 ± 1.43**	4.79 ± 1.23**	5.22 ± 1.36**
	90	8.13 ± 2.37^{+}	10.27 ± 0.83**‡	7.01 ± 1.53**	8.52 ± 1.67*$^{+}$	9.41 ± 2.58*‡
AG + CLP	10	8.50 ± 1.38‡	8.97 ± 2.62‡	8.74 ± 2.64*‡	4.94 ± 1.47**	7.36 ± 0.73**‡
	30	14.31 ± 4.73‡	17.70 ± 4.73‡	19.20 ± 5.44‡	10.76 ± 4.84*$^{+}$	16.97 ± 0.33‡
	90	10.40 ± 2.04*$^{+}$	8.20 ± 2.46‡	12.10 ± 2.92‡	12.37 ± 3.10‡	8.04 ± 2.17**‡
7-NI + CLP	30	13.75 ± 3.17‡	14.23 ± 3.21‡	17.72 ± 2.91‡	16.89 ± 2.50‡	15.01 ± 2.59‡

Data are expressed as mean ± SD nmol/mg protein ($n = 10$ for each group). Control, rats that underwent sham laparotomy; CLP, rats that underwent cecal ligation and puncture; L-NAME + CLP, rats that received L-NAME (10, 30 or 90 mg/kg b.w.) and underwent cecal ligation and puncture; AG + CLP, rats that received AG (10, 30 or 90 mg/kg b.w.) and underwent cecal ligation and puncture; 7-NI + CLP, rats that received 7-NI (30 mg/kg b.w.) and underwent cecal ligation and puncture. * $p < 0.05$, ** $p < 0.01$ compared with control; $^{+}$ $p < 0.05$, ‡ $p < 0.01$ compared with CLP.

Table 2. Glutathione concentration in rat brain structures in late stage sepsis: effect of i.p. pre-treatment with NOS inhibitors

Group	Dose	Cortex	Brain stem	Cerebellum	Striatum	Hippocampus
Control	–	20.04 ± 4.25	21.85 ± 5.35	21.38 ± 4.86	16.12 ± 4.14	20.18 ± 4.77
CLP	–	7.39 ± 2.25**	4.16 ± 1.22**	5.55 ± 0.64**	6.03 ± 1.13**	5.62 ± 1.61**
L-NAME+CLP	10	8.59 ± 2.47*	14.13 ± 1.40*‡	13.19 ± 1.52**‡	14.83 ± 3.22‡	12.80 ± 3.72**‡
	30	7.46 ± 2.07**	10.18 ± 3.37**‡	9.92 ± 2.82*$^{+}$	10.15 ± 2.55**‡	8.90 ± 2.01**$^{+}$
	90	11.63 ± 3.18*	17.89 ± 5.07**$^{+}$	9.47 ± 3.43*	5.69 ± 2.79**	10.35 ± 4.14*‡
AG+CLP	10	13.45 ± 1.38‡	7.37 ± 1.85**‡	10.65 ± 1.95**‡	9.70 ± 2.72*$^{+}$	15.44 ± 3.15**‡
	30	14.31 ± 4.73‡	16.40 ± 4.18‡	22.41 ± 7.00‡	15.35 ± 4.09‡	14.46 ± 2.25‡
	90	10.40 ± 2.04*$^{+}$	7.72 ± 1.65**$^{+}$	12.39 ± 1.99*‡	12.21 ± 3.03‡	15.14 ± 3.16‡
7-NI+CLP	30	13.75 ± 3.17‡	16.58 ± 2.38‡	17.32 ± 1.43‡	16.62 ± 1.71‡	15.14 ± 3.16‡

Data are expressed as mean ± SD nmol/mg proteins ($n = 10$ for each group). Control, rats that underwent sham laparotomy; CLP, rats that underwent cecal ligation and puncture; L-NAME+CLP, rats that received L-NAME (10, 30 or 90 mg/kg b.w.) and underwent cecal ligation and puncture; AG+CLP, rats that received AG (10, 30 or 90 mg/kg b.w.) and underwent cecal ligation and puncture; 7-NI+CLP, rats that received 7-NI (30 mg/kg b.w.) and underwent cecal ligation and puncture. * $p < 0.05$; ** $p < 0.01$ compared with control; $^{+}$ $p < 0.05$; ‡ $p < 0.01$ compared with CLP.

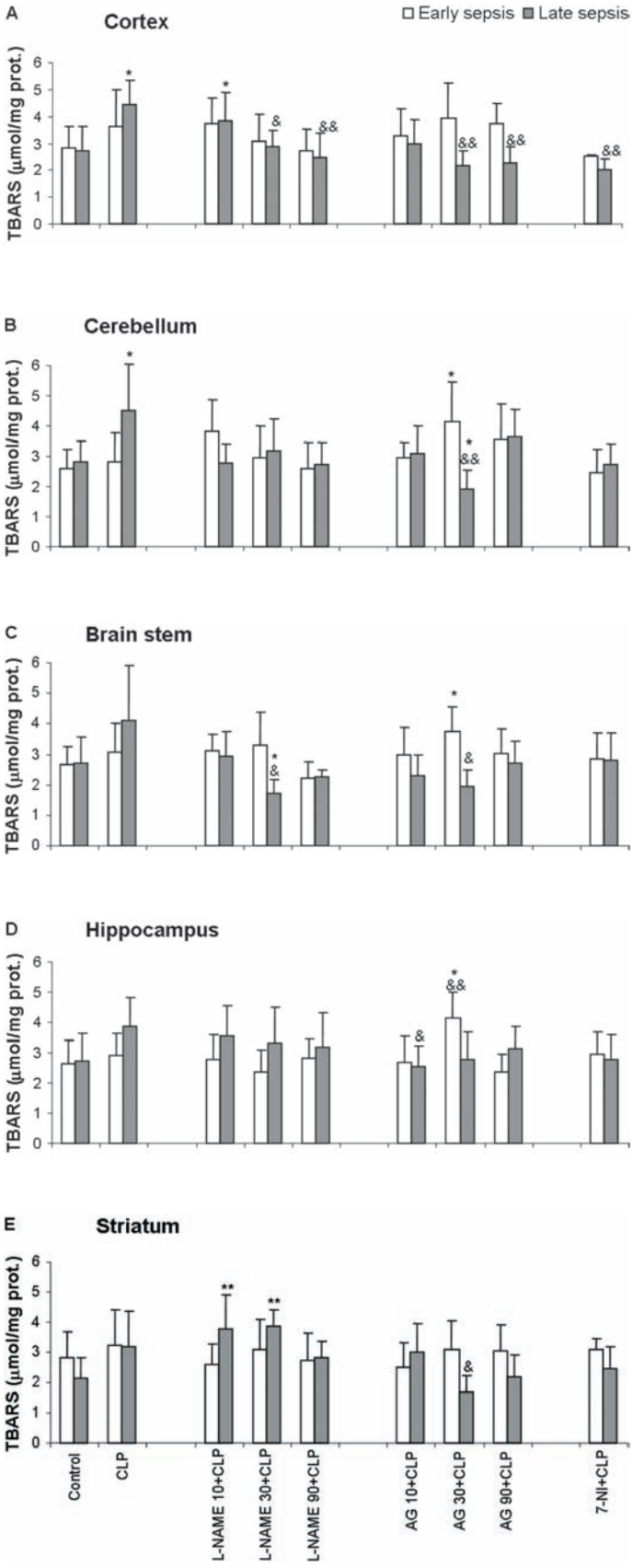

was apparent when compared with the CLP subgroup ($p < 0.01$). The increase in GSH was also evident in the cortex ($p < 0.05$), striatum ($p < 0.05$) and hippocampus ($p < 0.01$) in subgroups treated with 90 mg/kg of L-NAME. Increases in GSH concentrations were observed in other brain structures in septic rats pre-treated with L-NAME. However, these increases were not statistically significant when compared with the CLP subgroup. Pre-treatment with AG followed by induction of sepsis caused elevations in the GSH concentrations in almost all the investigated brain structures in early stage sepsis compared with the CLP subgroup. The exception was in the striatum from rats treated with 10 mg/kg AG, where the GSH concentration stayed low. Pre-treatment with 7-NI followed by induction of sepsis caused elevations in the GSH concentrations in all the investigated brain structures in early stage sepsis compared with the CLP subgroup ($p < 0.01$).

At a late (48 h) stage of sepsis, the concentration of GSH in brain structures stayed very low compared with control rats (Table 2). L-NAME pre-treatment prior to CLP increased the concentration of GSH compared with the CLP group. The exceptions were the cortex in all three septic groups pre-treated with L-NAME and both the cerebellum and striatum in septic groups pre-treated with 90 mg/kg L-NAME. Pre-treatment with AG led to an increase in the GSH concentration in all the investigated brain structures regardless of the applied AG dose. Moreover, pre-treatment with 30 mg/kg AG prior to CLP maintained the GSH concentration at a concentration found in control-treated rats. Similar effects were found in septic rats pre-treated with 7-NI. GSH concentrations in brain structures isolated from 7-NI-treated late stage septic rats were significantly elevated compared to the CLP group ($p < 0.01$) and were not significantly different to the concentrations found in control-treated rats.

To determine whether NOS inhibitors had any affect on oxidative stress development during sepsis, the levels of TBARS within brain tissue were examined during

◂ **Figure 1.** (A–E) TBARS concentrations in rat brain structures in early and late stage sepsis and the effect of i.p. pre-treatment with NOS inhibitors. Control, rats that underwent sham laparotomy; CLP, rats that underwent cecal ligation and puncture; L-NAME + CLP, rats that received L-NAME (10, 30 or 90 mg/kg b.w.) and underwent cecal ligation and puncture; AG + CLP, rats that received AG (10, 30 or 90 mg/kg b.w.) and underwent cecal ligation and puncture; 7-NI + CLP, rats that received 7-NI (30 mg/kg b.w.) and underwent cecal ligation and puncture. Each experimental group consisted of 10 rats ($n = 10$). * $p < 0.05$; ** $p < 0.01$ compared with control; $^{\&}$ $p < 0.05$; $^{\&\&}$ $p < 0.01$ compared with CLP.

both early and late stage sepsis in all experimental groups of rats. TBARS increased in the cortex (Figure 1A) and the cerebellum (Figure 1B) during late stage sepsis ($p < 0.05$).

In the two above-mentioned brain structures, pre-treatment with all three doses of L-NAME decreased TBARS, returning the levels back to control values. Only the lowest dose of L-NAME had no effect on the TBARS level in the cortex during the late sepsis period, causing it to remain significantly higher compared with control-treated rats ($p < 0.05$). All three doses of L-NAME maintained the control TBARS levels found after CLP in the hippocampus (Figure 1D). Non-elevated levels of TBARS were also found in the brain stem of septic rats. Surprisingly, pre-treatment with 30 mg/kg L-NAME led to a decrease in the level of TBARS in the brain stem (Figure 1C). Pre-treatment with 10 and 30 mg/kg L-NAME elevated the concentration of TBARS during the late stage of sepsis in the striatum. CLP itself failed to increase the concentration of TBARS in the striatum (Figure 1E).

The concentrations of TBARS in brain structures from AG pre-treated septic rats were different from L-NAME pre-treated septic rats. The most prominent effects observed were those in rats pre-treated with 30 mg/kg AG. This AG dose increased the concentration of TBARS in early sepsis in the cerebellum, brain stem and hippocampus compared to control-treated rats ($p < 0.05$). During late sepsis, the concentrations of TBARS in the cortex, cerebellum, brain stem and striatum of rats treated with 30 mg/kg AG decreased compared with the CLP group ($p < 0.05$). Septic rats pre-treated with AG (both 10 mg/kg as well as 90 mg/kg) presented no differences in the concentrations of TBARS in brain structures compared with control rats. The exceptions were the cortex isolated from rats pre-treated with 90 mg/kg and the hippocampus isolated from rats pre-treated with 10 mg/kg. Surprisingly, the concentration of TBARS decreased compared with CLP.

7-NI application before induction of sepsis did not affect the concentration of TBARS in almost all of the examined brain structures at both early and late stages of sepsis when compared with control rats. Only during late stage sepsis the concentration of TBARS was markedly reduced in the cortex in rats pre-treated with 7-NI when compared with the CLP group ($p < 0.01$).

The concentrations of TBARS in brain structures isolated from control-treated mice pre-treated with NOS inhibitors were not significantly different from each other (results not shown).

Discussion

The current study focused on oxidative stress development in brain structures as a consequence of CLP-induced sepsis. The major finding was a reduction in the concentration of GSH in both early and late stage sepsis. Lipid peroxidation, as revealed by the concentration of TBARS, is a common process in the cortex and cerebellum during late stage sepsis following CLP. Non-selective L-NAME-mediated NOS inhibition demonstrated the participation of the NO system in destructive events in the cortex during late stage sepsis. The lowest dose of L-NAME was not sufficient to abolish the increased TBARS in the cortex. Both 30 and 90 mg/kg b.w. L-NAME decreased TBARS accumulation back to control concentrations in late stage sepsis. Selective iNOS inhibition by AG and nNOS inhibition by 7-NI both inhibited CLP-induced TBARS elevation, suggesting the importance of eNOS in cortex homeostasis during late stage sepsis. In addition, non-selective L-NAME-induced NOS inhibition, as well as selective nNOS inhibition by 7-NI, stabilised the concentration of TBARS in the cerebellum during late stage sepsis.

The same effects caused selective iNOS inhibition induced by the lowest and the highest doses of AG. Unexpectedly 30 mg/kg b.w. AG pre-treatment increased TBARS in early stage sepsis and then decreased TBARS in late stage sepsis compared with controls. However, in the brain stem and the hippocampus simillar effects of increased TBARS in early stage sepsis were noted with 30 mg/kg b.w. AG pre-treatment. We cannot fully explain such an inverse effect. However, pharmacological effects of AG can be independent from iNOS inhibitory effects (Nilson 1999). Compared with other rat brain structures the cortex possesses the most effective system for cyclic guanosine monophosphate (cGMP) degradation. In addition, the granular layer of the cerebellum is sufficient for NOS activity as a high concentration of soluble guanylate cyclase exists (Pepicelli et al. 2004). The actions of the second messenger cGMP are largely under the influence of NO activity, underlining the importance of the correct functioning of the cortex and cerebellum. In addition to the apparent influence of the NO system on glutamatergic transmision, the unchanged concentration of TBARS in the hippocampus indicated its stabilty in both early and late stage sepsis. This could be a consequence of less cGMP-mediated signalling/activity, which has been suggested (Burgunder and Cheung 1994).

The most unpredictable results were obtained in the striatum. Besides decreased GSH, TBARS remained unchanged during sepsis. Non-selective NOS inhibition by low-dose L-NAME resulted in increased TBARS in late stage sepsis. While such changes were not as a consequence of selective iNOS and nNOS inhibition, they could be discussed of importance of endothelial NOS (eNOS) in striatum constancy. The striatum is a selectively excitable structure with a specific biochemical organisation containing robust antioxidant defence mechanisms as a consequence of it's high iron content which can be prooxidative in nature (Mizuno

and Ohta 1986). According to our results, non-selective NOS inhibition during sepsis could be detrimental to cell membranes, suggesting the importance of eNOS-mediated NO participation in the antioxidant defence system in the striatum.

Research aimed at understanding the pathophysiological mechanisms underlying sepsis are complicated due to hypotension during early stage sepsis (Matsuda and Hattori 2007). Among other endogenous mediators, NO participates in vasodilatation during sepsis. Most of the CLP models therefore use early saline resuscitation to abolish the hypotensive effect. According to our predictions, such action is too simple and does not sufficiently eliminate hypotension. At the same time, early saline resuscitation changes the natural defense mechanism reactions, which does not permit us to examine real time recovery and entry into early stage sepsis. There are sporadic and variable data concerning alterations in brain activity in early stage sepsis (Konsman et al. 1999), most of which are only related to the different models used and types of early saline resuscitation employed. Barichello and colleagues noted the oxidative stress development in the rat brain 6 h after CLP-induced sepsis with early saline resuscitation, prior to that found in other organs (Barichello et al. 2006). This time point fits in the stage of the developing sepsis, but not within early stage sepsis. We found a decrease in GSH 3 h post CLP, without any increase in TBARS in any of the examined brain structures. S-glutathionylation could have been a defence response to protect critical protein sulphydryl groups against irreversible destruction (Giustarini et al. 2004). Reactive oxygen species (ROS) interact, modify and inactivate numerous critical cells components including proteins, lipids and nucleic acids. In addition to lipid peroxidation, ROS can inactivate sulphydryl group-rich enzymes that participate in the Krebs cycle.

In all the investigated brain regions GSH concentrations remained very low in late stage sepsis. In the cortex and cerebellum TBARS increased. Our results are not totally consistent with those previously published concerning early changes in the cerebral capillaries of septic rats. However, they demonstrate that the detrimental process can pass the blood-brain barrier (Ninkovic et al. 2006). One could conclude that our results provide the basis for the effects of hypotension and consecutive brain ischaemia. However, published data has already demonstrated early oxidative stress development in several brain regions regardless of resuscitation and abolished hypotension (Barichello et al. 2006).

Non-selective NOS inhibition by L-NAME demonstrated a beneficial effect on the oxidative stress development, particularly at a dose of 90 mg/kg before CLP. This effect could have been due to suppression of hypotension. The same beneficial effect was also found in septic rats pre-treated with AG as well as 7-NI. Non-selective NOS inhibition by L-NAME indicated that the NO system participated in destructive events in the cortex. A low L-NAME dose was not sufficient enough to abolish NO´s effects. Doses of 30 and 90 mg/kg decreased late stage sepsis-induced TBARS elevation. Selective iNOS inhibition by all three doses of AG, and nNOS inhibition by 7-NI suppressed sepsis-induced TBARS elevation. This suggested the importance of constitutively active NOS activity in the homeostasis of the cortex during sepsis.

Due to its high affinity for both ROS and reactive nitrogen species, GSH participates in host defense mechanisms to combat oxidative/nitrosative stress during sepsis (Das and Maulik 2003). It is known that GSH depletion significantly increases NO cytotoxicity (Nelson et al. 2003). Nitrosothiols, including nitrosoglutathione, also serve as inhibitors of enzymes included in GSH storage (Wink and Mitchell 1998).

Moreover, AG's variable ability to decrease CLP-mediated oxidative stress was also dose-dependent which we mainly observed in late stage sepsis. Early time point discovered impaired oxidative status. Our results confirm the crucial role of both iNOS and eNOS. High concentrations of AG can be not only selective, but also a non-selective NOS inhibitor (Pheng et al 1995). In addition, it has been demonstrated that AG expresses pharmacological effects that are not related to NOS inhibition. These include inhibition of glycated end product production (typical in sepsis) and catalase inhibition, the latter leading to increased hydrogen peroxide production that could assist host defense mechanism during sepsis (Nilsson 1999).

Adjacent to neurons and nerve fibres which inervate larger brain arteries and pia blood vesels nNOS also exists in glial cells. It has been shown that dendrites and axons are the source of nearly 85% of nNOS activity in brain (Acki et al. 1993). nNOS activation is regulated by a number of factors, particularly glutamate (Huang et al. 1999). Besides eNOS participation in blood flow control, it is partly influenced by nNOS in physiological as well pathophysiological conditions (Estrada and Defelipe 1998).

One must consider that NO inhibition in all the investigated brain regions may suppress NO's hypotensive effect in early stage sepsis. However, in late stage sepsis the effect of NOS inhibition may be weaker due to the long distance time between NOS inhibitor application and animal sacrifice.

Despite the significant decrease in the hippocampal GSH concentration, the concentration of TBARS discreetly changed when NOS inhibitors were present. As the hippocampus is an extremely sensitive structure to oxidative stress the results were unexpected. However, mechanisms by which endotoxin-induced neuronal destruction are different from well-known mechanism of excitotoxicity (De Bock et al. 1998). This could be the explanation for the mild changes that occurred in the hippocampus during sepsis and in the presence of NOS inhibitors.

We conclude that the measured oxidative stress status parameters in the cortex, cerebellum, brain stem, hippocampus and striatum indicated oxidative stress development post CLP which resulted in a significant reduction in GSH concentration in both early and late stage sepsis. Lipid peroxidation was evident in late stage sepsis in both the cortex and the cerebellum. Pre-treatment with a non-selective NOS inhibitor (L-NAME) and with selective iNOS and nNOS inhibitors (AG and 7-NI) revealed benefit effects on the GSH concentrations. Unexpectedly, NOS inhibition resulted in diverse effects on TBARS concentrations, suggesting the importance of specific quantities of NO in specific brain structures during sepsis.

Acknowledgements. Supported by Military Medical Academy (VMA/08-10/B.3), Serbia, and by project No. 145010 of Ministry of Science and Environment Protection, Serbia. None of the authors have any financial interest to disclose.

References

Acki C., Fenstemaker S., Lubin M., Go C. G. (1993): Nitric oxide synthase in the visual cortex of monocular monkeys as revealed by light and electron imunocytochemistry. Brain Res. **620**, 97–113

Angus D. C., Musthafa A. A., Clermont G. (2001): Quality-adjusted survival in the first year after the acute respiratory distress syndrome. Am. J. Respir. Crit. Care Med. **163**, 1389–1394

Barichello T., Martins M., Reinke A., Feier G., Ritter C., Quevedo J., Dal-Pizzol F. (2005): Cognitive impairment in sepsis survivors from cecal ligation and perforation. Crit. Care Med. **33**, 221–223

Barichello T., Fortunato J. J., Vitali A. M., Feier G., Reinke A., Moreira J. C. F., Quevedo J., Dal-Pizzol F. (2006): Oxidative variables in the rat brain after sepsis induced by cecal ligation and perforation. Crit. Care Med. **34**, 886–889

Benjamim C. F., Silva J. S., Fortes Z. B., Oliveira M. A., Ferreira S. H., Cunha F. Q. (2002): Inhibition of leukocyte rolling by nitric oxide during sepsis leads to reduced migration of active microbicydal neutrophils. Infect. Immun. **70**, 3602–3610

Boveris A., Alvarez S., Navarro A. (2002): The role of mitochondrial nitric oxide synthase in inflammation and septic shock. Free Radic. Biol. Med. **33**, 1186–1193

Burgunder J. M., Cheung P. T. (1994): Expression of soluble guanylyl cyclase gene in adult rat brain. Eur. J. Pharmacol. **6**, 211–217

Das K. D, Maulik N. (2004): Conversion of death signal into survival signal by redox signaling. Biochemistry (Moscow) **69,** 10–17

De Bock F., Derijard B., Dornand J., Bockaert J., Rondouin G. (1998): The neuronal death induced by endotoxic shock but that induced by excitatory amino acids requires TNF-alpha. Eur. J. Neurosci. **10**, 3107–3114

Ellman G. L. (1959): Tissue sulphydril groups. Arch. Biochem. Biophys. 74, 443–450

Esplugues J. V. (2002): NO as a signalling molecule in the nervous system. Br. J. Pharmacol. **135**, 1079–1095

Estrada C., Defelipe J. (1998): Nitric oxide-producing neurons in the neocortex: morphological and functional relationship with intraparenchymal microvasculature. Cereb. Cortex **8**, 193–203

Feihl F., Waeber B., Liaudet L. (2001): Is nitric oxide overproduction the target of choice for the management of septic shock? Pharmacol. Ther. **91**, 179–213

Garthwaite J., Boulton C. L. (1995): Nitric oxide signalling in the central nervous system. Annu Rev. Physiol. **57**, 683–706

Ghersi-Egea J. F., Leininger-Muller B., Suleman G., Siest G., Minn A. (1994): Localization of drug-metabolising enzume activities to blood-brain interfaces and circumventricular organs. J. Neurochem. **62**,1089–1096

Ghafourifar B., Bringold U., Klein S. D., Richter C. (2001): Mitochondrial nitric oxide synthase, oxidative stress and apoptosis. Biol. Signals Recept. **10**, 57–65

Giustarini D., Rossi R., Milzani A., Colombo R., Dalle-Donne I. (2004): S-glutathionylation-from redox regulation of protein functions to human diseases. J. Cell. Mol. Med. **8**, 201–212

Gurd J. W., Jones L. R., Mahler H. R., Moore W. J. (1974): Isolation and partial characterization of rat brain synaptic membrane. J. Neurochem. **22**, 281–290

Hotchkiss R. S., Karl I. E. (2003): The pathophysiology and treatment of sepsis. N. Engl. J. Med. **348**, 138–150

Huang P. L., Gyurko R., Zhang L. (1999): Cardiovascular effects of nitric oxide: lessons learned from endothelial nitric oxide synthase knockout mice. In: Endothelium, Nitric Oxide and Atherosclerosis. (Eds. J. A. Panza and R. O. Cannon), pp. 37–48, Futura Publishing Co., Armonk, New York

Konsman J. P., Kelley K., Dantzer R. (1999): Temporal and spatial relationships between LPS-induced expression of FOS, inerleukin-1β inducible and inducible nitrit oxide synthase in rat brain. Neuroscience **89**, 535–548

Levy M. M., Fink M., Marshall J. C. (2003): SCCM/ESICM/ACCP/ATS/SIS international sepsis definitions conference. Crit. Care Med. **34**, 1250–1256

Liaudet L., Soriano F. G., Szabo C. (2000): Biology of nitric oxide signaling. Crit. Care Med. **28**, N37–52

Lowry O. H., Rosenbrough N. J., Farr A. L., Randall R. J. (1951): Protein measurement with the folin phenol reagent. J. Biol. Chem. **193**, 265–275

Matsuda N., Hattori Y. (2007): Vascular biology in sepsis: pathophisiological and therapeutic significance of vascular dysfunction. J. Smooth Muscle Res. **43**, 117–137

Girotti M. J. (1991): Early measurement of systemic lipid peroxidation products in the plasma of major blunt trauma patients. J. Trauma **31**, 32–34

Mizuno Y., Ohta K. (1986): Regional distributions of thiobarbituric acid-reactive products, activities of enzymes regulating the metabolism of oxygen free radicals, and some of the related enzymes in adult and aged rat brains. J. Neurochem. **46**, 1344–1352

Nelson J. E., Connolly J, McArthur P. (2003): Nitric oxide and S-nitrosylation: excitotoxic and cell signaling mechanism. Biol. Cell **95**, 3–8

Nilsson B. O. (1999): Biological effects of aminoguanidine: an update. Inflamm. Res. **48**, 509–515

Ninković M., Maličević Ž., Jelenković A., Jovanović D. M., Đukić M., Vasiljević I. (2006): Oxidative stress in the rats brain capillaries – the influence of 7-nitroindazole. Acta Physiol. Hung. **93**, 315–323

Ninković M., Maličević Ž., Stojanović D., Vasiljević I., Jovanović D. M., Đukić M. (2008): Brain stem and thalamus antioxidative defense in experimental sepsis. Acta Vet. (Belgrade) **58**, 129–137

Pepicelli O., Raiteri M., Fedele E. (2004): The NOS/sGC pathway in the rat central nervous system: a microdialysis overview. Neurochem. Int. **45**, 787–797

Pheng L. H, Francoeur C., Denis M. (1995): The involvment of nitric oxide in a mouse model of adult respiratory distress syndrome. Inflammation (N. Y.) **19**, 599–610

Poon B. Y., Raharjo, E., Patel, K. D., Tavener, S., Kubes, P. (2003): Complexity of inducible nitric oxide synthase. Cellular source determines benefit versus toxicity. Circulation **2**, 1107–1112

Rivers E. P., McIntyre L., Morro D. C., Rivers K. K. (2005): Early and innovative interventions for severe sepsis and septic shock: taking advantage of a window of opportunity. CMAJ **173**, 1054–1065

Robert P., Koedel U., Pfister H. (1997): 7-Nitroindazole inhibits pial arteriolar vasodilatation in a rat model of Pneumococcal meningitis. Metabolism **17**, 985–991

Sharshar T., Annane D., de la Grandmaison G. L., Brouland J. P., Hopkinson N. S., Gray F. (2004): The neuropathology of septic shock. Brain Pathol. **14**, 21–33

Sharshar T., Hopkinson N. S., Orlikowski D., Annane D. (2005): Science review: the brain in sepsis-culprit and victim. Crit. Care **9**, 37–44

Stojanović D., Maličević Ž., Ašanin M. (2002): The use of a new model for the investigation of sepsis. Acta Vet. (Belgrade) **52**, 125–132

Wiklund N., Cellek S., Leone A., Iversen H., Gustadsson L., Brundin L., Furst V., Flock A., Moncada S. (1997): Visualisation of nitric oxide released by nerve stimulation. J. Neurosci. Res. **47**, 224–232

Wink D. A., Mitchell J. B. (1998): Chemical biology of nitric oxide: insights into regulatory, cytotoxic and cytoprotective mechanisms of nitric oxide. Free Radic. Biol. Med. **25**, 434–456

Autonomic dysfunction in alcoholic cirrhosis and its relation to sudden cardiac death risk predictors

Branislav Milovanovic[1], Nikola Milinic[2], Danijela Trifunovic[3], Mirjana Krotin[1], Branka Filipovic[2], Vesna Bisenic[1] and Dragan Djuric[4]

[1] *Neurocardiology Laboratory, Department of Cardiology, Medical Centre Bezanijska Kosa, Belgrade, Serbia*
[2] *Department of Gastroenterology, Medical Centre Bezanijska Kosa, Belgrade, Serbia*
[3] *Institute for Cardiovascular Diseases, University Clinical Centre Serbia, Belgrade, Serbia*
[4] *Institute for Physiology, School of Medicine, University of Belgrade, Serbia*

Abstract. Patients with liver cirrhosis have autonomic dysfunction and complex cardiovascular changes. Increases risk for sudden cardiac death (SCD) was recently recognized in liver cirrhosis. This study analyzed risk predictors for SCD related to autonomic dysfunction in patients with alcoholic liver cirrhosis (ALC). Twenty five patients with ALC were examined and compared with healthy control group. Cardiovascular autonomic reflex tests, comprehensive ECG with QTc interval, late potentials, short-term heart rate variability (HRV) analysis (time domain, spectral and nonlinear-Poincare plot analysis) and 24-h Holter ECG with long-term HRV analysis were done. According to autonomic reflex tests patients with ALC had high incidence (56%) of severe autonomic dysfunction, manifested as pronounced damage of vagal function. Patients had significantly depressed HRV (SDNN, SDANN, triangular index, LF and HF) and more frequently had serious arrhythmias, prolonged QTc and Poincare plot in a shape of dot ($p < 0.001$). In patient group QTc significantly inversely correlated with spectral components from short-term HRV analysis (ln(LF): $r = -0.53$, ln(HF): $r = -0.47$; $p < 0.05$), and Lown class significantly correlated with total autonomic function score ($r = 0.64$, $p = 0.04$). This study indicates that in ALC autonomic neuropathy with vagal impairment and sympathetic predominance is related to SCD risk predictors and onset of serious ventricular arrhythmias.

Key words: Autonomic function — Alcoholic cirrhosis — Sudden cardiac death

Introduction

Liver cirrhosis is associated with complex cardiovascular changes, including hyperdynamic circulation with increased blood volume, increased cardiac output and reduced peripheral vascular resistance (Møller and Henriksen 2008). Autonomic dysfunction is common in liver cirrhosis, both in alcoholic and non-alcoholic and is associated with the severity of hepatic dysfunction (Dillon et al. 1994; Ates et al. 2006) and survival (Hendrickse et al. 1992; Fleckenstein et al. 1996). The pathogenesis of autonomic neuropathy in cirrhosis is not fully known and several mechanisms are suggested: circulatory changes in cirrhosis, metabolic and neurohormonal alterations including renin angiotensin aldosterone system, excessive nitric oxide production, oxidative stress and inflammatory mediators (interleukines) (Møller and Henriksen 2008). Autonomic dysfunction in cirrhotic patients has been evaluated by standard autonomic function test (Gonzalez-Reimers et al. 1991; Dillon et al. 1994; Szalay et al. 1998), heart rate variability (HRV) (Dillon et al. 1994; Fleisher et al. 2000; Ates et al. 2006) and 123I-metaiodobenzylguanidine myocardial scintigraphy (Iga et al. 2003). According to standard autonomic function tests, autonomic neuropathy in liver cirrhosis is characterized with predominately vagal impairment (Hendrickse et al. 1992; Dillon et al. 1994; Ates et al. 2006). Cirrhotic patients with

Correspondence to: Branislav Milovanović, Neurocardiology Laboratory, Department of Cardiology, Medical Centre Bezanijska Kosa, School of Medicine, University of Belgrade, Bezanijska Kosa b.b., 11080 Belgrade, Serbia
E mail: branislav_milovanovic@vektor.net

vagal neuropathy have a five-fold increased mortality compared to those without autonomic dysfunction (Hendrickse et al. 1992; Fleckenstein et al. 1996). However, mechanisms behind increased mortality related to autonomic dysfunction have not been evaluated. Recently, in patients with primary biliary cirrhosis unexplained excess mortality that remains even after accounting for liver and cancer-related deaths was recognized and potentially linked to increased risk of sudden cardiac death (SCD) (Newton et al. 2006).

Conversely, incidence of SCD is increased in chronic alcoholics (Moushmoush and Mansour 1991; Hémery et al. 2000; Spies et al. 2001). Chronic alcohol ingestion induces autonomic neuropathy, predominately of vagal origin (Duncan et al. 1980; Matikainen et al. 1986; Barter and Tanner 1987), potentially contributing to increased incidence of SCD in alcoholics (Yokoyama et al. 1992; Johnson and Robinson 1998), apart from heart muscle disease (alcoholic cardiomyopathy) often seen with chronic alcohol abuse.

Therefore, patients with alcoholic etiology of cirrhosis, at least from pathophysiological background, could be at increased risk of SCD. Autonomic dysfunction induced both by metabolic and homodynamic changes in cirrhosis and alcohol ingestion itself, could contribute to increased risk of SCD.

This study was aimed to evaluate presence and level of autonomic dysfunction in patients with alcoholic cirrhosis by standard cardiovascular autonomic function tests and to analyze risk predictors for sudden cardiac death related to autonomic dysfunction (HRV, late potentials and QTc interval).

Materials and Methods

Study population

The study was carried out on 25 patients with alcoholic hepatic cirrhosis and 17 healthy individuals similar in age and sex. Twenty five consecutive patients with previously proven liver cirrhosis and with the history of at least ten years of ethyl consumption more than 80 g per day were enrolled in this study. The diagnosis of cirrhosis was made histopathologically or based on clinical examination, laboratory parameters, ultrasonographic findings, and the presence of esophageal varices. Patients were admitted to Department of Gastroenterology of Clinical and Hospital Center "Bezanijska Kosa" for the further treatment (basic clinical data are shown in Table 1). Exclusion criteria were: coronary disease, heart failure, diabetes, chronic obstructive pulmonary disease and therapy with drug(s) known to influence autonomic function. The controls were healthy volunteers with no history of alcohol consumption and normal clinical and biochemical parameters. The study was approved by the Scientific Ethical Committee of Clinical Hospital Center "Bezanijska Kosa". Written informed consent was obtained from all subjects.

Table 1. Group characteristics

Alcoholics	$n = 25$
Gender (M/F)	20/5
Age (years, range)	54 (46–62)
EF (%)	58 ± 13
ESV (ml)	47 ± 11
EDV (ml)	117 ± 37
Control group	$n = 19$
Gender (M/F)	15/4
Age (years, range)	52 (44–60)

EF, ejection fraction; ESV, end systolic volume; EDV, end diastolic volume by 2D echocardiography.

Study protocol

All individuals were tested in the Neurocardiology Laboratory using the original protocol for the assessment of autonomic nervous system function and cardiovascular risk parameters related to cardiac death. Cardiovascular reflex tests were done first, followed by short-term ECG recording (10 min) with statistical, spectral and nonlinear (Poincare plot) analysis of HRV as well as late potentials analysis. Individuals were tested between 09:00 and 10:00 a.m., approximately 2 h after light breakfast, under ideal temperature conditions (23°C), without any previous consumption of alcohol, nicotine or coffee. In patients therapy was withdrawn 24 h before testing. After initial testing, at the same day 24-h Holter ECG was started and day after 24-h ambulatory blood pressure (BP) monitoring was done.

Cardiovascular reflex tests

We performed three parasympathetic tests (heart rate response to Valsalva maneuver, heart rate response to deep breathing and heart rate response to standing) and one test of sympathetic function (BP response to standing).

Heart rate response to Valsalva maneuver

Valsalva maneuver was performed using modified sphygmomanometer with blowing and holding a pressure of 40 mmHg for 15 s, with ECG recording. The results, expressed as a Valsalva ratio, measured the longest and the shortest RR interval using ruler and ECG trace.

Deep breathing test

Six deep inspirations and expirations were performed over one minute. The result is expressed as a difference between the highest and the lowest heart rate.

Heart rate response to standing test (30 : 15 ratio test)

Heart rate response after standing, expressed as a ratio between the longest RR interval corresponding with 30th beat after starting and the shortest RR interval corresponding with 15th beat.

BP response to standing

This test measured the subject's BP with a sphygmomanometer while he was lying quietly and one minute after he was made to stand up. The postural fall in BP was taken as the difference between the systolic pressure lying and the systolic BP standing.

Results of all four tests were expressed as a normal, borderline or abnormal, according to cut-off values given by Ewing and Clarke 1982). The patients were categorized as normal, if none of the tests was abnormal; with early parasympathetic damage, if results of one of the three tests of parasympathetic function was abnormal; with definite parasympathetic damage, if two or more of the three tests of parasympathetic function were abnormal; and with combined damage, if test of the sympathetic function was abnormal in addition to parasympathetic damage. For the purpose of the above-mentioned classification the borderline tests were interpreted as normal. A scoring system like the one suggested by Bellavere et al. (1983) was also used to assess the extent of autonomic nervous damage. For each test "0" score was given for normal, "1" for borderline, and "2" for an abnormal value. By adding the score of each of the five standard tests of autonomic function, total autonomic function score was determined for every subject.

Short-term ECG and short-term HRV analysis

Analysis of standard 12 leads ECG recording using commercially available softer (Schiller model AT-10, Austria) include ECG waves and interval analysis: duration of P wave, PQ interval, QRS complex, QT and QTc interval.

QT parameters were measured automatically from the 12-lead ECG recording (Schiller model AT-10, Austria) at a paper speed of 50 mm/s (gain, 10 mm/mV). The QT interval was measured from the onset of QRS complex to the end of T wave. Each QT interval was corrected for patient heart rate according to Bazett's formula: QTc = QT/$\sqrt{}$ (RR interval), where QT and RR interval are expressed in seconds.

Short-term HRV analysis was done from 512 consecutive RR intervals using commercial softer (Schiller model AT-10, Austria) according to previously published guideline (see in References: Task Force of the ESC 1996). Short-term HRV analysis includes: time domain analysis, frequency domain analysis and nonlinear HRV analysis (Poincare space plot). The following time domain variables were computed for each subject: average dRR interval, standard deviation of dRR intervals (SDRR), mean deviation of dRR (MDRR), square root of the mean of squared differences of two consecutive RR intervals (RMSSD), percent of beats with consecutive RR interval difference of more than 50 ms (pNN50). The following short-term frequency domain indices were determined using Hanning window type signal limitation before Fourier transformation: very low-frequency (VLF, 0.016–0.05 Hz), low-frequency (LF, 0.05–0.15 Hz), high-frequency (HF, 0.15–0.35 Hz) power, and LF/HF ratio. Late potential analysis was done based on data obtained from 12 standard ECG leads. Criteria for the presence of late potentials (frequency range of 40 to 250 Hz) were as follow: QRS duration >114 ms, LAHFd >38 ms, RMS-40 ms <20. In the presence of at least two parameters, late potential concerned as was positive. Nonlinear analysis (Poincare space plot): results of nonlinear Poincare space plot analysis were divided related to visual form (cigarette, cluster, comet or spot).

Holter ECG: rhythm analysis and long-term HRV analysis

24-h ambulatory ECG recordings were acquired by 3 leads ECG, sampling rate 1000 Hz per each lead (Biosensor, USA) and analyzed by an experienced analyst. Cardiac rhythms were screened for ventricular premature beats and supraventricular premature beats. The recordings were reviewed, and the beat classifications were manually checked, corrected, and readied for further analysis. After all of the artifacts and misclassified beats were corrected, time and frequency domain HRV analysis were carried out using the software package present in the system. The fast Fourier transformation and Hanning window were used for the analysis of the frequency (spectral) domain parameters.

In rhythm analysis total number of ventricular premature beats and supra ventricular premature beats for the whole period of recording was determined and number of ventricular premature beats per hour calculated. Also, the degree of arrhythmias was quantified according to Lown classification.

From time domain HRV analysis following time domain variables were computed: mean RR interval for 24 h (mean NN), standard deviation of normal RR intervals (SDNN), standard deviation of all 5-min mean normal RR intervals (SDANN), square root of the mean of the sum of the squares of differences between adjacent RR intervals (RMSSD). From frequency domain HRV analysis following 24-h frequency domain indices were determined: total power (TP, 0–0.4 Hz), HF (0.15–0.4 Hz), LF (0.04–0.15 Hz), and the (LF/HF ratio). Heart rate is measured in milliseconds; variance, which is referred to as the power in a portion of the total spectrum of frequencies, is measured in milliseconds squared. Triangular index was also determined from 24-h HRV analysis according to guidelines (Task Force of the ESC 1996 – see in References).

24-h ambulatory BP monitoring

Evaluation of 24 h profile of BP was done using recorder and commercial software for analysis (Mobil-O-graph). Monitoring began at approximately 11 a.m. and BP measurements were performed by oscillometric method every 15 min all day long. From these data following variables were calculated for each patient: average total (24 h), daytime (9 a.m.–9 p.m.) and nighttime (0 a.m.–6 a.m.) systolic BP, diastolic BP and pulls pressure; systolic and diastolic BP variability during day and during night expressed as standard deviation of all systolic and all diastolic BP measurements during daytime and during night (automatically calculated using the same software).

Statistics

All data were analyzed using computer software package SPSS 11.05 system for Windows. Beside the measures of the central tendency, parametric data were analyzed using independent *t*-test and Pearson chi-square (χ^2) test. Significance level was defined as $p < 0.05$. Since all components of HRV do not have normal distribution, ln transformation was done and parametric statistics applied afterward. Correlations between variables were tested using Pearson's coefficient.

Results

Cardiovascular reflex tests

Cardiovascular reflex tests were done in 16 out of 25 patients and in all controls. Parasympathetic dysfunction was present in 14/16 (87%) patients with alcoholic cirrhosis: seven patients (43%) have early and seven patients (43%) definitive parasympathetic damage. The result of Valsalva maneuver was abnormal in 5 patients, deep breathing test was abnormal in 9 patients and heart rate response on standing was abnormal also in 9 patients. Sympathetic dysfunction, manifested as orthostatic hypotension, was present in only 3 patients and only one of them did not have parasympathetic damage while rest two have parasympathetic dysfunction. Combined damage, parasympathetic and sympathetic dysfunction, was diagnosed in 2/16 (12.5%) patients. As expected, pathological results of cardiovascular reflex test were more common among patients with alcoholic liver diseases compared to control (Fig. 1). Total autonomic function score was higher in patients compared to control (4.70 ± 1.70 vs. 2.05 ± 1.50, $p < 0.001$) and nine out of sixteen patients (56%) have severe autonomic dysfunction (score >7) (Table 2).

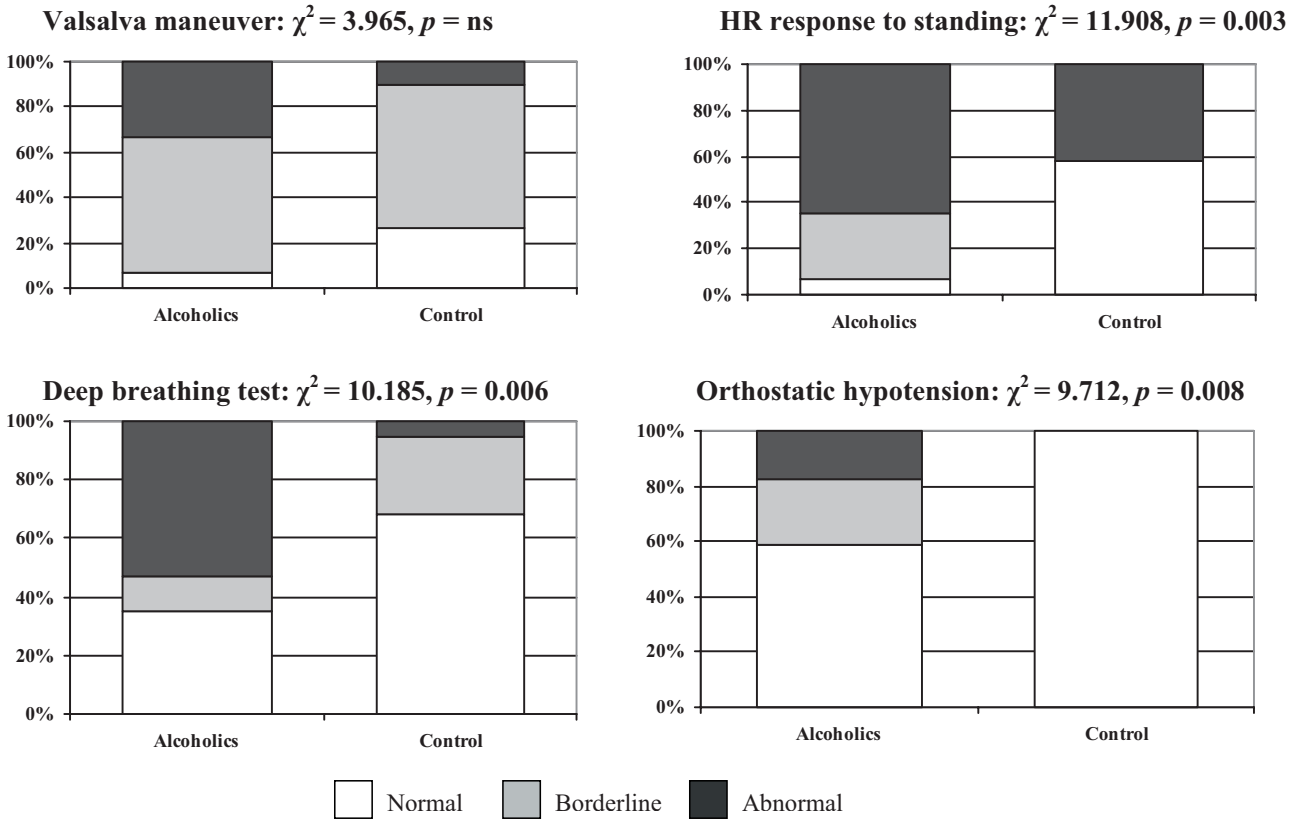

Figure 1. Cardiovascular reflex tests.

Table 2.

A. Distribution of autonomic dysfunction among alcoholics and control

	Parasympathetic damage			Sympathetic damage	Combined damage
	Without	Early	Definitive		
Alcoholics (n = 16)	2	7	7	3	2
Control (n = 19)	9	9	1	0	0

For parasympathetic damage: $\chi^2 = 9.014$, $p = 0.011$.

B. Extent of autonomic nervous damage based on total autonomic function score

	Autonomic nervous damage (autonomic neuropathy)			
	Without (0–1)	Mild (2–3)	Moderate (4–6)	Severe (7–10)
Alcoholics (n = 16)	0	1	6	9
Control (n = 19)	4	6	9	0

$\chi^2 = 17.039$, $p = 0.001$.

C. Distribution of autonomic dysfunction among alcoholics (n = 16)

		Parasympathetic damage			Total
		Without	Early	Definitive	
Sympathetic damage	Without	1	6	6	13
	With	1	1	1	3
Total		2	7	7	16

QT interval

The analysis of the QTc interval showed that it was significantly longer in patients with alcoholic liver disease, compared to healthy individuals (454.06 ± 25.33 vs. 419.72 ± 19.432 ms, $p < 0.001$). No significant difference was found between groups concerning duration of non-corrected QT interval, PQ interval, QRS complex and P wave. Prolonged QT (QTc > 440 ms) was present in 13/25 patients (52%) that is significantly more frequent compared to control group where only 3/19 individuals (6%) have prolonged QTc ($\chi^2 = 5.46$, $p = 0.026$).

Short-term HRV analysis

All spectral and time domain parameters were considerably lower in alcoholics. Values of RMSSD and HF reflecting vagal activity were significantly depressed in patients with alcoholic liver disease. LF spectral parameter reflecting sympathetic and vagal function was also lower in patients with the liver cirrhosis. LF/HF ratio, reflecting sympathovagal balance, was higher in alcoholics compared to control suggesting, however without statistical significance (Table 3).

Table 3. Short-term heart rate variability analysis

	Alcoholics	Control group	p
Average dRR (ms)	8.50 ± 8.78	25.22 ± 16.69	0.001
SDRR (ms)	8.56 ± 8.83	22.22 ± 12.54	0.001
MDRR (ms)	5.43 ± 5.36	16.33 ± 10.31	0.001
pNN50 (%)	1.43 ± 3.36	8.16 ± 9.90	0.014
RMSSD (ms)	12.37 ± 12.26	32.88 ± 21.36	0.002
ln(VLF)	3.60 ± 1.49	4.93 ± 1.13	0.007
ln(LF)	3.28 ± 1.40	4.81 ± 1.05	0.001
ln(HF)	2.26 ± 1.45	3.89 ± 1.26	0.002
LF/HF	5.02 ± 3.73	3.78 ± 3.64	n.s.

SDRR, standard deviation of dRR intervals; MDRR, mean deviation of dRR; RMSSD, square root of the mean of squared differences of two consecutive RR intervals; pNN50, percent of beats with consecutive RR interval difference of more than 50 ms; VLF, very low-frequency interval (0.016–0.05 Hz); LF, low-frequency interval (0.05–0.15 Hz); HF, high-frequency interval (0.15–0.35 Hz); n.s., non-significant.

Late potentials

Late potentials were positive only in one patient with alcoholic cirrhosis.

Nonlinear HRV analysis

Poincare plot in the shape of dot, indicating severe autonomic dysfunction, was present in 9/25 patients, 5/25 patients have Poincare plot in comet form and 11/25 in cigarette form. None of patients have Poincare plot in cluster form. In control group Poincare plot in dot for was not registered, 8/19 individuals have Poincare plot in cluster form, 10/19 in comet form and only 1/19 in cigarette form (for comparison between patients vs. control: $\chi^2 = 24.8$, $p < 0.001$).

Long-term HRV and arrhythmia analysis from 24 h

Analysis of time domain parameters indicated statistical significance for three important arrhythmia risk predictors. The SDNN, SDANN and triangular index had considerably lower values in alcoholics when compared to the control group. Power spectral analysis of long-term HRV revealed lower both ln(LF) and ln(HF). Supraventricular and ventricular premature beats were more common in alcoholics (Table 4).

Arrhythmia analysis from 24-h ECG monitoring revealed significantly different distribution according to Lown class between patients with alcoholic cirrhosis vs. control ($p = 0.011$). Among patients serious ventricular rhythm abnormalities (Lown class >2) were present in 10/25 (39%) patients, 12/25 (46%) patients were in Lown class 1 and 3/25 (15%) in Lown class 0. In control group 15/19 (76%) individuals have Lown class 0, 3/19 (16%) Lown class 1 and 1/19 (8%) person has Lown class >2.

Table 4. 24 h Holter ECG: long-term HRV analysis

	Alcoholics	Control group	*p*
VPB	758.3 ± 502.2	23.5 ± 20.3	0.04
SVPB	85.2 ± 38.1	4.4 ± 1.9	0.05
Mean RR (ms)	712.21 ± 157.00	782.76 ± 77.84	n.s.
SDNN (ms)	93.42 ± 42.69	463.15 ± 111.83	0.014
SDANN (ms)	71.80 ± 43.38	187.53 ± 85.74	0.000
RMSSD (ms)	53.00 ± 36.32	70.38 ± 30.78	n.s.
TRI INDEX	33.71 ± 17.17	50.61 ± 9.70	0.005
LF/HF	3.40 ± 2.11	3.55 ± 1.13	n.s.
ln(LF/HF)	0.99 ± 0.75	1.22 ± 0.30	n.s.
ln(LF)	6.85 ± 0.94	8.19 ± 0.98	0.002
ln(HF)	5.81 ± 1.17	7.00 ± 0.99	0.009

VPB, total number of ventricular premature beats during ECG monitoring; SPB, total number of supraventricular premature beats during ECG monitoring; SDNN, standard deviation of all the RR intervals; SDANN, standard deviation of all 5-min mean normal RR intervals; RMSSD, square root of the mean of squared differences of two consecutive RR intervals; TRI INDEX, triangular index; VLF, very low-frequency interval (0.016–0.05 Hz); LF, low-frequency interval (0.05–0.15 Hz); HF, high frequency interval (0.15–0.35 Hz); n.s., non-significant.

Correlations between autonomic function, repolarization abnormalities and arrhythmias in patients with alcoholic cirrhosis

In patients with alcoholic cirrhosis QTc significantly inversely correlated with spectral components from short-term HRV analysis: ln(LF) ($r = -0.53$, $p = 0.03$) and ln(HF) ($r = -0.47$, $p = 0.04$). We did not find significant correlation between HRV parameters from long-term HRV analysis and Lown class. In 16 patients in whom standard cardiovascular reflex tests were done Lown class significantly correlated with total autonomic function score ($r = 0.64$, $p = 0.04$).

Ambulatory BP monitoring

Detailed ambulatory BP analysis during 24 h including mean systolic and mean diastolic BP during 24 h, daytime, night-time, early in the morning, as well as systolic and diastolic BP variability, did not reveal statistically significant differences between patients with alcoholic cirrhosis and control.

Discussion

Autonomic dysfunction assessed by standard autonomic function tests in alcoholic cirrhosis

This study confirms that high percent of patients with alcoholic cirrhosis has abnormal autonomic function. In the current study in 16 out of 25 consecutive patients with alcoholic liver cirrhosis admitted to the hospital for further medical treatment, standard autonomic function tests were performed with satisfied patient's compliance and in more than 80% of these patients at least one or more parasympathetic function test was abnormal. Damage in sympathetic function was detected in lower percent. According to total autonomic function score 56% of evaluated patients in the current study have severe autonomic damage, comparable to findings of Fleckenstein et al. (1996).

Incidence of autonomic neuropathy based on traditional autonomic function test widely varies in chronic liver disease: from as low as 35% (Hendrickse and Triger 1990) to 45% (Hendrickse et al. 1992), 60% (Dillon et al. 1994) or even 80% (Bajaj et al. 2003). Higher frequency of neuropathy was found in studies involved higher proportion of patients with severe form of hepatic failure (80%) (Bajaj et al. 2003), compared to studies recruited patients with mild hepatic impairment (45%) (Hendrickse et al.1992). Cardiovascular autonomic dysfunction is significantly more frequent in

advanced liver disease compared with early liver disease (Hendrickse et al. 1992).

Using standard cardiovascular tests we, as others, found predominately vagal impairment in chronic alcoholic liver disease. Importance of vagal impairment for sodium and fluid retention has been shown in cirrhosis (Hendrickse and Triger 1994; Dillon et al. 1997; Trevisani et al. 1999). Neuromodulation with angiotensin II is proposed as one of the mechanism inducing parasympathetic dysfunction in cirrhosis and partly correction of vagal dysfunction in cirrhotic patients was achieved by captopril (Dillon et al. 1997).

In our study heart rate response to standing was the most frequently abnormal test. Barter and Tanner (1987) in their study also reported heart rate response to standing as the most sensitive test with high specificity, as well as Bajaj et al. (2003). Impaired cardiac and circulatory (BP) responses to orthostasis in cirrhosis are probably due to blunted baroreflex function (Laffi et al. 1997; La Villa et al. 2002; Newton et al. 2006). Impaired baroreflex function in cirrhosis can be related to activated renin angiotensin aldosterone system, since administration of canrenone, an aldosteron antagonist, in compensated cirrhotic patients normalizes cardiac response to postural changes (La Villa et al. 2002).

Clinical significance of vagal neuropathy detected by standard tests in liver cirrhosis is important. A strong correlation between the number of abnormal test and Child-Pugh score was demonstrated implying that with disease progression cardiovascular autonomic impairment also progress. In multiple regression analysis presence of vagal neuropathy in liver cirrhosis detected by standard autonomic tests is independent predictor of mortality (Hendrickse et al. 1992).

HRV in alcoholic cirrhosis

Cardiovascular reflex tests are relatively simple and useful to classify patients for the presence of autonomic neuropathy and its severity, but HRV potentially offers better accuracy (Malpas et al. 1991; Dillon et al. 1994) and is less dependent of patient compliance. Alcoholics without manifest cardiac disease have considerably lower HRV compared to control, even in cases with normal standard autonomic tests (Malpas et al. 1991). Malpas show that in chronic alcoholics SDSD index from statistical analysis of 24-h HRV (corresponding to HF from spectral analysis) can detect small changes in autonomic function, which may not be detectable by standard autonomic function test (Malpas et al. 1991).

In our study we could perform autonomic test in 16 out of 25 patients, because in the rest 9 patients adequate compliance was not achieved. However, HRV analysis was done in all, independently of patient condition, suggesting that in clinical practice HRV analysis is more feasible and applicable for autonomic function assessment than standard reflex tests.

In the present study we performed both short- and long-term HRV analysis, both time and frequency domain. By short-term HRV analysis in rest, we confirmed that patients with alcohol cirrhosis compared to control have decreased all time domain parameters (average dRR, SDRR, MDRR, RMSSD and pNN50). We also found that patients have all spectral components detected by short-term spectral analysis (VLF, LF and HF) significantly reduced compared to control, with trend towards increased LF/HF ratio. These results demonstrate impaired autonomic function in alcoholic cirrhosis with trend towards the sympathetic predominance. Fleisher et al. (2000) in patients awaiting liver transplantation found by short-term HRV analysis depressed SDNN, pNN50 (marker of parasympathetic activity) and ApEn (approximate entropy, a measure of regularity). During follow up ApEn was significantly lower in no survivors than in survivors. Iga et al. (2003) using spectral analysis of HRV shown that autonomic abnormalities appear early in the course of liver cirrhosis and that with progression of hepatic impairment LF/HF ratio increases, as well as blood level of norepinephrine, whereas HF power decreased.

Poincare plot offers exploration of non-linear phenomena involved in the genesis of HRV (Carrasco and Gaitan 2001; Piskorski and Guzik 2007). It is used for cardiac autonomic assessment and risk stratification in heart failure (Voss et al. 2007) and myocardial infarction (Milovanović et al. 2007). To the best of our knowledge there are no published data, related to the form of Poincare plot in alcoholics or in patients with alcoholic cirrhosis. In the present study we used visual analysis of the spatial form of Poincare plot and in 36% of patients found the dot shape. Dot shape of Poincare plot was previously shown to correspond with severe autonomic dysfunction and poor prognosis after myocardial infarction (Milovanović et al. 2007).

In the present study long-term time domain HRV analysis revealed in patients with alcoholic cirrhosis significantly reduced SDNN and SDANN parameters compared to the control. Ates et al. (2006) shown that severity of cirrhosis expressed using Child-Pugh classification scores is associated with reduced timed domain HRV measurements from 24-h ECG and that HRV was significantly lower in nonsurvivors than in survivors, suggesting prognostic significance of long-term time domain HRV analysis. Cooelho et al. (2001) found interesting positive correlations between SDNN and protrombin activity as well as with serum albumin but not with total bilirubin, indicating that autonomic dysfunction in liver cirrhosis is more closely related to hepatocellular dysfunction than cholestasis.

Triangular index is HRV parameter from geometric method and express overall HRV measured over 24 h. It was shown to be important prognostic marker for risk stratification after myocardial infarction (Kleiger et al. 1987), but has not been evaluated in liver cirrhosis. In the present study

we for the first time found in cirrhotic patients reduced triangular index. Prognostic value of HRV triangular index in cirrhosis remains to be determined.

The spectral analysis of long-term HRV assessment in the present study revealed significantly reduced both LF and HF component in cirrhotic patients compared to control, however, without significant difference in LF/HF ratio. Coelho et al. (2001) also reported in patients with cirrhosis decreased average total power with reduction of all components (VLF, LF, HF) in the absence of significant difference in LF/HF ratio. This spectral profile is characteristic for conditions with increased sympathetic activity and vagal impairment. Increased sympathetic activity in cirrhosis is demonstrated also by increased burst frequency and increased circulating cathecholamines and is in direct relation to the severity of the disease (Henriksen et al. 1998). The major triggers of the sympathetic overactivity seems to be baroreceptor- mediated stimulation, owing to the low arterial BP and hepatic dysfunction and a volume receptor mediated stimulation, owing to reduced central and arterial blood volume. Consequences of increased sympathetic activity in cirrhosis are important. Enhanced sympathetic tone with increased cellular exposure to noradrenalin for longer periods cause myocardial injury and impaired β adrenergic function (Opie 1998) with down regulation of β adrenergic receptor in cardiomyocytes and receptor desensitization with post receptor defects (Ma and Lee 1996), leading to cardiac dysfunction in liver cirrhosis (Møller and Henriksen 2002).

Arrhythmias in alcoholic liver cirrhosis and its correlation with autonomic disturbances

There is little data in literature regarding rhythm disturbances in patients with cirrhosis. The vast data are from case reports regarding ventricular arrhythmias, frequently torsade de points, occurs during or after liver transplantation (Lustik et al. 1998; Zaballos et al. 2005). The development of atrial fibrillation as well as episodes of supraventricular and ventricular tachycardia and even bradicardia associated with liver transplantation has also been described. There are several risk factors for arrhythmia and altered cardiac conduction in this specific situation: severe haemodynamic alterations, ion imbalance (hypokalemia, hypomagnesaemia), acid-base imbalance and hypothermia that accompany the reperfusion of a new organ.

In the present study in patients with severe, chronic alcoholic cirrhosis we found increased ectopic cardiac activity. Serious ventricular arrhythmias (Lown class >2) were present in 39% of patients and Lown class significantly correlated with total autonomic function score.

Several lines of evidence suggest that heavy drinking increase the risk of SCD with fatal arrhythmia as the most likely mechanism (Hémery et al. 2000; Spies et al. 2001; Newton et al. 2006). Although heart muscle disease induced by alcohol cardiotoxicity, i.e. alcoholic cardiomyopathy (clinically manifest or occult) is important arrhythmogenic substrate in chronic alcoholics, alcoholic autonomic neuropathy is at least contributing factor. In cirrhosis, independent of its etiology, fluidity of the plasma membrane and the function of membrane ion channels are impaired (Liu and Lee 1999). Electrophysiological abnormalities in cardiac excitation due to alteration in K^+ and Ca^{2+} channels were suggested that could potentially lead to serious ventricular arrhythmias (Moreau et al. 1994; Moreau and Lebrec 1995). However, link between cirrhotic autonomic neuropathy and cardiac rhythm disturbances was not evaluated.

In current study we found significant positive correlation between Lown class and total autonomic function score, robust index of global autonomic function, indicate potential association between ventricular arrhythmias and autonomic neuropathy. It should be noted that many other factors such as ion imbalance, and acid-base imbalance frequently present in advanced cirrhosis could be also potential proarrhythmogenic factors. Also, increased level of circulating cathecholamines could act as proarrhythmogenic agent. However, in the recent experimental study in cirrhotic rats reduced susceptibility to epinephrine-induced arrhythmias was shown and linked to potential protective effects of long-term NO overproduction (Tavakoli et al. 2007).

Prolonged QT interval in alcoholic cirrhosis and its relation with autonomic disturbances

In the present study QTc interval was much longer in cirrhotic patients compared to control and QTc > 440 ms was present in 52% of patients. A prolonged QTc interval has been previously described in 30–60% of patients with liver disease (Ishizaki et al. 1995; Mohamed et al.1996; Bal and Thuluvath 2003). Etiology of prolonged QTc in liver diseases is still unsettled. Ward et al. (1997) have shown decrease K^+ currents in ventricular cardiomyocytes from cirrhotic rats, which prolong the repolarization time and consequently QT interval (Day et al. 1993). The prolonged QTc interval could trigger sever ventricular arrhythmias, especially torsade de point and sudden cardiac death, but evidences from clinical studies are sparse. In cirrhotic patients the prolonged QT interval is significantly related to the severity of the liver disease, portal hypertension, portosystemic shunts, elevated BNP and proBNP, elevated plasma noradrenaline and reduced survival (Møller et al. 2002). The prolongation of QT interval is partly reversible after liver transplantation (Ward et al. 1997) and β-blocker treatment (Møller et al. 2002). We as well as Puthumana and co-workers could not find significant association between autonomic cardiovascular reflexes and QTc (Puthumana et al. 2001). However, we did found significant inverse correlation between duration of

QTc interval with LF and HF power spectral component. Since HRV is in some aspects more sensitive than standard autonomic cardiovascular tests, association between spectral components of HRV and QTc interval duration could suggest that autonomic dysfunction in alcoholic cirrhosis has some potential influence on delayed repolarization process in the myocardium. Also, in several studies QTc correlated with blood noradrenaline level confirming further association between autonomic function and QTc duration, as well as observation that QT is normalized with chronic β-blocker treatment in patients with prolonged baseline values (Zambruni et al. 2008). The importance of prolonged QTc interval in liver disease as independent prognostic parameter is still uncertain (Mohamed et al. 1996). Recently, QT dispersion and corrected QT dispersion parameters are suggested in to be better mortality indicators than QT intervals (Kosar et al. 2007).

Ambulatory BP recordings in cirrhotic patients

BP depends on cardiac output and the systemic vascular resistance.

Although total blood volume is increased in cirrhosis, as well as cardiac output, significant low systemic vascular resistance (arteriolar vasodilatation) with increased total vascular and arterial compliance maintain BP in low normal or even hypotensive range. There is a growing body of evidence that systemic nitric oxide over production in cirrhosis play a major role in the arteriolar and splanchnic vasodilatation and vascular hyporeactivity. However, in the present study using 24-h ambulatory BP monitoring we did not found significant difference in 24-h BP profile in cirrhotic patients compared to healthy individuals. Møller et al. (1995) report that arterial BP is reduced during the day, whereas at night the values are normal, indicating an abnormal BP regulation in cirrhosis.

It should be noted that new entity "cirrhotic cardiomyopathy" has been introduced recently (Møller and Henriksen 2008). According to this concept, patients with liver cirrhosis due to complex modifications of circulation, neurohormonal and metabolic changes have altered cardiac function. Cirrhotic cardiomyopathy is chronic cardiac dysfunction in cirrhotic patients characterized by blunted contractile responsiveness to stress, and/or altered diastolic relaxation, with electrophysiological abnormalities in the absence of other known cardiac disease (Møller et al. 2008). Heart rhythm and conduction disturbances as well as altered cardiovascular autonomic function in liver cirrhosis are considered to be a part of this complex entity. In the present study exclusion and inclusion criteria were not defined to include or exclude patients with cirrhotic cardiomyopathy, according to suggested diagnostic criteria. We did not include patents with over heart failure and patients with depressed ejection fraction by echocardiography. However, presence of some aspects of cirrhotic cardiomyopathy cannot be rolled out in the current study population.

Study limitation

The current study was performed on relatively small number of patients and in some of them classic cardiovascular autonomic function tests could not be performed with satisfied patient compliance, predominately due to patient's poor general condition. This could represent potential selection bias regarding analysis of autonomic function based on classical function tests, but at the same time represent limited feasibility of standard test when they are applied on severely ill patients. However, in the present study even on smaller number of relatively clinically better-preserved patients, we found severe form of autonomic dysfunction in high percent of patients.

In the present study we did not investigate links and associations between autonomic dysfunction and liver functional status, because it was not the aim of the current study.

Conclusion

Patients with alcoholic liver cirrhosis, according to the present study, have a severe form of autonomic dysfunction, manifested as more pronounced damage of vagal function and sympathetic predominance. Analysis of cardiovascular risk for the onset of sudden cardiac death revealed presence of several potentially important risk predictors, such as decreased SDNN value, Poincare plot in shape as dot, lower triangular index, serious arrhythmias, and prolonged QTc interval. Lown class and QTc interval are shown to be associated with the level of autonomic dysfunction. However, prognostic values of these risk predictors and their links to autonomic neuropathy in patients with liver cirrhosis are still to be firmly evaluated in longitudinal and larger studies.

References

Ates F., Topal E., Kosar F., Karincaoglu M., Yildirim B., Aksoy Y., Aladag M., Harputluoglu M. M., Demirel U., Alan H., Hilmioglu F. (2006): The relationship of heart rate variability with severity and prognosis of cirrhosis. Dig. Dis. Sci. **51,** 1614–1618

Bajaj B. K., Agarwal M. P., Ram B. K. (2003): Autonomic neuropathy in patients with hepatic cirrhosis. Postgrad. Med. J. **79**, 408–411

Bal J. S., Thuluvath P. J. (2003): Prolongation of QTc interval: relationship with etiology and severity of liver disease, mortality and liver transplantation. Liver Int. **23**, 243–248

Barter F., Tanner A. R. (1987): Autonomic neuropathy in alcoholic population. Postgrad. Med. J. **63**, 1033–1036

Bellavere F., Bosello G., Fedele D., Cardone C., Ferri M. (1983): Diagnosis and management of diabetic autonomic neuropathy. Br. Med. J. **287,** 61

Carrasco S., Gaitan M. J. (2001): Correlation among Poincare plot indexes and time and frequency domain measures of heart rate variability. J. Med. Eng. Technol. **25**, 240–248

Coelho L., Saraiva S., Guimaräes H., Freitas D., Providência L. A. (2001): Autonomic function in chronic liver disease assessed by heart rate variability study. Rev. Port. Cardiol. **20**, 25–36

Day C. P., James O. F., Butler T. J., Campbell R. W. (1993): QT prolongation and sudden cardiac death in patients with alcoholic liver disease. Lancet **341,** 1423–1428

Dillon J. F., Plevris J. N., Nolan J., Ewing D. J., Neilson J. M., Bouchier I. A., Hayes P. C. (1994): Autonomic function in cirrhosis assessed by cardiovascular reflex tests and 24-hour heart rate variability. Am. J. Gastroenterol. **89**, 1544–15447

Dillon J. F., Nolan J., Thomas H., Williams B. C., Neilson J. M., Bouchier I. A., Hayes P. C. (1997): The correction of autonomic dysfunction in cirrhosis by captopril. J. Hepatol. **26**, 331–335

Duncan G., Johnson R. H., Lambie D. G., Whiteside E. A. (1980): Evidence of vagal neuropathy in chronic alcoholics. Lancet **2**, 1053–1057

Ewing D. J., Clarke B. F. (1982): Diagnosis and management of diabetic autonomic neuropathy. BMJ **285**, 916–919

Fleckenstein J. F., Frank S., Thuluvath P. J. (1996): Presence of autonomic neuropathy is a poor prognostic indicator in patients with advanced liver disease. Hepatology **23**, 471–475

Fleisher L. A., Fleckenstein J. F., Frank S. M., Thuluvath P. J. (2000): Heart rate variability as a predictor of autonomic dysfunction in patients awaiting liver transplantation. Dig. Dis. Sci. **45**, 340–344

Gonzalez-Reimers E., Alonso-Socas M., Santolaria-Fernandez F., Hernandez-Peña J., Conde-Martel A., Rodriguez-Moreno F. (1991): Autonomic and peripheral neuropathy in chronic alcoholic liver disease. Drug Alcohol. Depend. **27**, 219–222

Hémery Y., Broustet H., Guiraudet O., Schiano P., Godreuil C., Plotton C., Ollivier J. P. (2000): Alcohol and rhythm disorders. Ann. Cardiol. Angeiol. (Paris) **49**, 473–479 (in French)

Hendrickse M. T., Thuluvath P. J., Triger D. R. (1992): Natural history of autonomic neuropathy in chronic liver disease. Lancet **339**, 1462–1464

Hendrickse M. T., Triger D. R. (1990): Autonomic dysfunction and hepatic function in chronic liver disease. Gut **31**, A1164

Hendrickse M. T., Triger D. R. (1992): Peripheral and cardiovascular autonomic impairment in chronic liver disease: prevalence and relation to hepatic function. J. Hepatol. **16**, 177–183

Hendrickse M. T., Triger D. R. (1994): Vagal dysfunction and impaired urinary sodium and water excretion in cirrhosis. Am. J. Gastroenterol. **89**, 750–757

Henriksen J. H., Møller S., Ring-Larsen H., Christensen N. J. (1998): The sympathetic nervous system in liver disease. J. Hepatol. **29**, 328–341

Iga A., Nomura M., Sawada Y., Ito S., Nakaya Y. (2003): Autonomic nervous dysfunction in patients with liver cirrhosis using 123I-metaiodobenzylguanidine myocardial scintigraphy and spectrum analysis of heart-rate variability. J. Gastroenterol. Hepatol. **18**, 651–659

Ishizaki F., Harada T., Yamaguchi S., Mimori Y., Nakayama T., Yamamura Y., Murakami I., Nakamura S. (1995): Relationship between impaired blood pressure control and multiple system involvement in chronic alcoholics. No To Shinkei **47**, 139–145 (in Japanese)

Johnson R. H., Robinson B. J. (1988): Mortality in alcoholics with autonomic neuropathy. J. Neurol. Neurosurg. Psychiatry **51**, 476–480

Kleiger R. E., Miller J. P., Bigger J. T., Moss A. J. (1987): Decreased heart rate variability and its association with increased mortality after acute myocardial infarction. Am. J. Cardiol. **59**, 256–262

Kosar F., Ates F., Sahin I., Karincaoglu M., Yildirim B. (2007): QT interval analysis in patients with chronic liver disease: a prospective study. Angiology **58**, 218–224

La Villa G., Barletta G., Romanelli R. G., Laffi G., Del Bene R., Vizzutti F., Pantaleo P., Mazzocchi V., Gentilini P. (2002): Cardiovascular effects of canrenone in patients with preascitic cirrhosis. Hepatology **35**, 1441–1448

Laffi G., Barletta G., La Villa G., Del Bene R., Riccardi D., Ticali P., Malani L., Fantini F., Gentilini P. (1997): Altered cardiovascular responsiveness to active tilting in nonalcoholic cirrhosis. Gastroenterology **113**, 891–898

Liu H., Lee S. S. (1999): Cardiopulmonary dysfunction in cirrhosis. J. Gastroenterol. Hepatol. **14**, 600–608

Lustik S. J., Eichelberger J. P., Chhibber A. K., Bronsther O. (1998): Torsade de pointes during orthotopic liver transplantation. Anesth. Analg. **87**, 300–303

Ma Z., Lee S. S. (1996): Cirrhotic cardiomyopathy: getting to the heart of the matter. Hepatology **24**, 451–459

Malpas S. C., Whiteside E. A., Maling T. J. (1991): Heart rate variability and cardiac autonomic function in men with chronic alcohol dependence. Br. Heart J. **65**, 84–88

Matikainen E., Juntunen J., Salmi T. (1986): Autonomic dysfunction in long-standing alcoholism. Alcohol Alcohol. **21,** 69–73

Milovanović B., Krotin M., Bisenić V., Vuković D., Nikolić S., Mirjanić T. (2007): Prognostic value of Poincare plot as nonlinear parameter of chaos theory in patients with myocardial infarction. Srp. Arh. Celok. Lek. **135,** 15–20 (in Serbian)

Mohamed R., Forsey P. R., Davies M. K., Neuberger J. M. (1996): Effect of liver transplantation on QT interval prolongation and autonomic dysfunction in end-stage liver disease. Hepatology **23**, 1128–1134

Møller S., Henriksen J. H. (2002): Cirrhotic cardiomyopathy: a pathophysiological review of circulatory dysfunction in liver disease. Heart **87**, 9–15

Møller S., Henriksen J. H. (2008): Cardiovascular complications of cirrhosis. Gut **57**, 268–278

Møller S., Wiinberg N., Hernriksen J. H. (1995): Noninvasive 24-hour ambulatory arterial blood pressure monitoring in cirrhosis. Hepatology **22**, 88–95

Moreau R., Komeichi H., Kirstetter P., Ohsuga M., Cailmail S, Lebrec D. (1994): Altered control of vascular tone by adenosine triphosphate-sensitive potassium channels in rats with cirrhosis. Gastroenterology **106**, 1016–1023

Moreau R., Lebrec D. (1995): Endogenous factors involved in the control of arterial tone in cirrhosis. J. Hepatol. **22**, 370–376

Moushmoush B., Mansour P. A. (1991): Alcohol and the heart. Arch. Intern. Med. **151**, 36–40

Newton J. L., Allen J., Kerr S., Jones D. E. (2006): Reduced heart rate variability and baroreflex sensitivity in primary biliary cirrhosis. Liver Int. **26**, 197–202

Opie L. H. (1998): The Heart: Physiology, from Cell to Circulation. Lippincott, Philadelphia

Piskorski J., Guzik P. (2007): Geometry of the Poincare plot of RR intervals and its asymmetry in healthy adults. Physiol. Meas. **28,** 287–300

Puthumana L., Chaudhry V., Thuluvath P. J. (2001): Prolonged QTc interval and its relationship to autonomic cardiovascular reflexes in patients with cirrhosis. J. Hepatol. **35,** 733–738

Spies C. D., Sander M., Stangl K., Fernandez-Sola J., Preedy V., Rubin E., Andreasson S., Hanna E. Z., Kox W. J. (2001): Effects of alcohol on the heart. Curr. Opin. Crit. Care **7,** 337–343

Szalay F., Marton A., Keresztes K., Hermányi Z. S., Kempler P. (1998): Neuropathy as an extrahepatic manifestation of chronic liver diseases. Scand. J. Gastroenterol. Suppl. **228**, 130–132

Task Force of the European Society of Cardiology and the North American Society of Pacing and Electrophysiology (1996): Heart rate variability: standards of measurement, physiological interpretation and clinical use. Circulation **93**, 1043–1065

Tavakoli S., Hajrasouliha A. R., Jabehdar-Maralani P., Ebrahimi F., Solhpour A., Sadeghipour H., Ghasemi M., Dehpour A. (2007): Reduced susceptibility to epinephrine-induced arrhythmias in cirrhotic rats: the roles of nitric oxide and endogenous opioid peptides. J. Hepatol. **46**, 432–439

Trevisani F., Sica G., Mainquà P., Santese G. De Notaris S., Caraceni P., Domenicali M., Zaca F., Grazi G. L., Mazziotti A., Cavallari A., Bernardi M. (1999): Autonomic dysfunction and hyperdynamic circulation in cirrhosis with ascites. Hepatology **30**, 1387–1392

Voss A., Schroeder R., Truebner S., Goernig M., Figulla H. R., Schirdewan A. (2007): Comparison of nonlinear methods symbolic dynamics, detrended fluctuation, and Poincare plot analysis in risk stratification in patients with dilated cardiomyopathy. Chaos **17,** 151–120

Ward C. A., Ma Z., Lee S. S., Giles W. R. (1997): Potassium currents in atrial and ventricular myocytes from a rat model of cirrhosis. Am. J. Physiol. **273**, G537–544

Yokoyama A., Ishii H., Takagi T., Hori S., Matsushita S., Onishi S., Katsukawa F., Takei I., Kato S., Maruyama K., Tsuchiya M. (1992): Prolonged QT interval in alcoholic autonomic nervous dysfunction. Alcohol. Clin. Exp. Res. **16,** 1090–1092

Zaballos M., Jimeno C., Jiménez C., Fraile J. R. (2005): Dual atrioventricular nodal conduction and arrhythmia with severe hemodynamic alterations during liver retransplantation. Rev. Esp. Anestesiol. Reanim. **52**, 355–358 (in Spanish)

Zambruni A., Trevisani F., Di Micoli A., Savelli F., Berzigotti A., Bracci E., Caraceni P., Domenicali M., Felline P., Zoli M., Bernardi M. (2008): Effect of chronic beta-blockade on QT interval in patients with liver cirrhosis. J. Hepatol. **48**, 415–421

Preconditioning with glucose-insulin-potassium solution and restoration of myocardial function during coronary surgery

Miomir Jovic[1], Sinisa Gradinac[1], Ljiljana Lausevic-Vuk[1], Dusko Nezic[1], Predrag Stevanovic[2], Predrag Milojevic[1] and Bosko Djukanovic[1]

[1] *Clinic for Anesthesia and Critical Care, "Dedinje" Cardiovascular Institute Belgrade, Serbia*
[2] *Clinical Center "Dr. Dragisa Mišović" Belgrade, Serbia*

Abstract. The administration of glucose-insulin-potassium (GIK) solution has beeen shown to exert cardioprotective and immunomodulatory properties in coronary disease.

49 patients (pts.) for coronary surgery were randomly assigned to receive high-dose GIK treatment (30% glucose, insulin 2 IU·kg^{-1}·l^{-1} and K^+ 80 mmo/l solution; 1 ml/kg/h); low-dose GIK treatment (10% glucose, insulin 32 IU l^{-1} and K^+ 80 mmol/l solution; 1 ml/kg/h) or control treatment (Ringer solution 1 ml/kg/h). Haemodynamic measurements were done for four time points: T1 – after induction of anaesthesia; T2 – after the operation; T3 – 6 h after the operation and T4 – 24 h after the operation.

Significant recovery of cardiac function was evident in high-dose GIK (H-GIK) and low-dose GIK (L-GIK) groups after 24 h (cardiac index improved considerably ($p = 0.0002$)), with a statistically significant difference between the groups ($p = 0.005$). LVSWI covariated with PCWP, improved over time in group H-GIK ($p = 0.0008$) and between the groups ($p = 0.046$). Oxygen supply-consumption ratio evidently improved in the GIK groups, while inotropic drug support was used in 5.5% pts. in group H-GIK vs. 13% in group L-GIK and 31% pts. in control (C) group.

Glucose-insulin treatment has a potential cardioprotective effect in coronary surgery. The effect is independent of the glucose-insulin concentration and amount.

Key words: Coronary surgery — GIK — Haemodynamic parameters — Oxygen profile

Introduction

From the first clinical investigation by Sodi-Pallares and colleagues, clinical trials were directed to assess the influence of the glucose-insulin-potassium (GIK) solution on myocardium in acute ischemic event (Sodi-Pallares et al. 1962). Early studies found that GIK treatment in patients (pts.) with acute myocardial ischemia reduces electrocardiographic changes, decreases infarct size and improves ventricular function. Subsequent multicentric studies, ECLA (Dias et al. 1998) as well as DIGAMI (Malmberg et al. 1996) study in diabetic pts., documented favorable effect of the GIK solution in pts. with acute ischemic syndrome. They reported a remarkable decrease in the mortality rate in pts. treated with GIK solution. The idea of GIK's protective role and beneficial effect on myocardium during coronary surgery was revitalized (Gradinac et al. 1989; Svedjeholm et al. 1991; Lazar et al. 1997). Some experimental and some clinical studies suggested that the viability of ischaemic myocardium depends on the glucose supply. Providing glucose to the critically ischaemic cell has been hypothesized to have multiple beneficial effects, and despite the inhibition of fatty acid metabolism, it increases the production of anaerobic ATP while maintaining a protective role on the threatened cell membrane (Opie 1998). Many clinical reports were strongly suggestive of the protective effect of GIK administration on myocardial function, during acute myocardial ischaemia, coronary angioplasty or coronary surgery. The importance of insulin for coronary blood supply and its role on vasodilatation have been implicated in some experimental studies (Downing et al. 1977). Recently,

Correspondence to: Miomir Jovic, Clinic for Anesthesia and Critical Care, "Dedinje" Cardiovascular Institute Belgrade, Milana Tepića 1, 11000 Belgrade, Serbia
E-mail: drjovic@ikvbd.com

a clinical study by Laine et al. (2000) has also reported that insulin acts as a true vasodilatory horomone in the myocardial vasculature. The sensitivity of GIK echocardiography (GIK solution administration during echocardiography) in detection of myocardial viability seems to be very similar to low-dose dobutamine stress echocardiography (Van Wezel et al. 2006).

GIK treatment has been used in cardiac surgery, mainly because of its potentially beneficial effects on myocardial metabolism during ischaemia. Lazar et al. (1997) reported results from a random study of urgent coronary bypass grafting for unstable angina. GIK infusion was given prior to bypass and for 12 h afterwards. Cardiac indexes (CI) of the GIK groups improved significantly with less inotropic support and with dramatically reduced incidence of perioperative atrial fibrillation. Results in another blind, controlled study conformed that GIK initiated prior to the bypass produced marked improvement in CI with the most beneficial effect in those pts. with the worst left ventricular function (Girard et al. 1992). Our study was primarily based on the encouraging results from earlier trials, where GIK was infused during the coronary surgery. Even in diabetic pts., this treatment had a supportive effect on left ventricular function and postoperative outcome (Szabo et al. 2001). Furthermore, recent human (Hansen et al. 2003) and experimental studies (Brix-Christiansen et al. 2008) have shown that the administration of insulin may also have immunomodulation effects and potential to reduce the production of proinflamatory cytokines. Our hypothesis states that a high-dose GIK treatment could enhance myocardial preconditioning as well as improve the postischaemic recovery and restoration of myocardial function.

Materials and Methods

The aim of the study

The aim of the study was: i) to evaluate the beneficial effect of GIK on left ventricular performances and haemodynamics during and after the coronary artery bypass surgery in pts. with poor left ventricular function, ii) to determine whether the difference in glucose-insulin amount and concentration has an impact on left ventricular recovery and haemodynamics restoration.

Open, prospective, randomized study was performed in 49 pts. for coronary artery bypass graft (CABG) surgery with poor left ventricular function (EF < 40%). All pts. were clinically examined. Following the usual examination, coronarography with ventriculography, evaluation was completed with dobutamine-stress test echocardiography on myocardial viability in 56 pts. Forty nine pts. with positive dobutamine-stress test and conformed myocardial viability in one or more segments were included in study and divided in three groups, a high-dose GIK (H-GIK), low-dose GIK (L-GIK) and a control (C) .

Table 1. Patients' assessment

	H-GIK group	L-GIK group	C group
Sex m/f	17/0	12/3	15/2
Age	58.5 ± 6.5	58.2 ± 4.61	54.75 ± 9
Smoking (%)	94.4	46.6	68.75
Hypertension (%)	72.2	73. 3	68.75
Diabetes (%)	44.4	12.5	37.5
Arrhythmia (%)	11.1	20.0	0
COPD (%)	11.1	0	31.25
MI (%)	83.3 (22.2*)	73.3	93.75 (6.24*)
AICS (%)	0	0	0

m, male; f, female; COPD, chronic obstructive pulmonary disease; MI, preoperative myocardial infarction; AICS, preoperative acute coronary syndrome; * percentage of pts. with two or more preoperative myocardial infarctions.

There were no significant differences between groups. The majority were male pts., while only 10.2% were female. About two thirds were treated of hypertension and most of them were smokers. Most of the pts. had a previous history of myocardial infarctions (83.3% in group H-GIK and 73.3% in group L-GIK and 93.75 in group C) and about 40% were on oral medication due to diabetes (Table 1).

Dobutamine stress echocardiography protocol

After usual transthoracic echocardiography examination, pts. received dobutamine 5 $\mu g/kg^{-1}\cdot min^{-1}$ during 3 min with additional 10 $\mu g\cdot kg^{-1}\cdot min^{-1}$ for next 3 min. During the test, global and regional left ventricular function and wall motion was assessed. Hypokinesia was defined as systolic left ventricular wall thickening less then 40%, while systolic left ventricular wall thickening less then 10% was defined as akinesia. Dyskinesia was observed as lateral wall movement with wall thinning. Regional wall movement analyses were done according to the American Society of Echocardiography Recommendations.

Anaesthesia

Premedication for all pts. included: atropine 0.5 mg, midazolam 0.1 $mg\cdot kg^{-1}$, and dolantin 50 mg intramuscularly, thirty minutes prior to operation. After preoxygenation FiO_2 1.0 and induction of anaesthesia with midazolam 0.3–0.4 $mg\cdot kg^{-1}$, fentanil 10–15 $\mu g\cdot kg^{-1}$ and pancuronium 0.1 $mg\cdot kg^{-1}$ pts. were intubated endotrachealy. Intermittent doses of the same drugs were used for anaesthesia

maintenance. Arterial pressure was measured *via* arterial catheter inserted into the left radial artery. Central venous catheter (three ports) was inserted trough the right subclavian vein while the pulmonary artery catheter (five lead Arrow 7.5 F) was inserted through right internal jugular vein.

Haemodynamic study

Haemodynamic measures and calculations were done for four time points. First (T1) – before the surgery, after the induction of anaesthesia (pre OP), the second (T2) – at the end of the surgery (after the chest closure) (post OP), the third (T3) – 6 h after the operation (6 h post OP) and the fourth (T4) – 24 h after the operation (24 h post OP). Cardiac output was measured three times at every time point, the average value was used as a definitive value for the actual time point. Calculated haemodynamic parameters included: cardiac output, CI, stroke volume, stroke volume index (LVSWI), left ventricular stroke work index, right ventricular stroke work index (RVSWI), systemic vascular resistance, and pulmonary vascular resistance simultaneously with oxygen profile parameters: arterial oxygen content, venous oxygen content, arterio-venous oxygen difference, oxygen consumption (VO_2), oxygen delivery (DO_2) and oxygen extraction.

Study design – GIK protocol

Pts. were divided, prospectively, in three groups:

H-GIK group – 17 pts. received a GIK infusion, 30% glucose, insulin 2 IU·kg^{-1}·l, K^+ 80 mmol/l at 1 ml/kg/h rate, after the induction of anaesthesia until aortic cross-clamping. After the distal anastomoses has been completed, and aortic cross-clamp has been released, GIK infusion was continued until the end of surgery. Prior aortic cross-clamping, additional doze of insulin 24 IU was given. After initial 500 ml 30% GIK infusion was terminated, additional 10% glucose, 32 IU·l^{-1} of insulin and K^+ 80 mmol/l was infused up to 24 h after operation at same rate 1 ml/kg/h.

L-GIK group – 17 pts. received a GIK infusion, 10% glucose, insulin 32 IU·kg^{-1}·l, K^+ 80 mmol/l at 1 ml/kg/h rate, after the induction of anaesthesia until aortic cross-clamping. After the distal anastomoses has been completed, and aortic cross clamp has been released, low-GIK infusion was continued until the end of surgery and up to 24 h after operation at same rate 1 ml/kg/h.

C group – 15 pts. received Ringer solution 1 ml/kg/h during the operation and 24 h postoperatively. St. Thomas cold crystalloid cardioplegia was used in all pts. after aortic cross-clamping.

Blood glucose and potassium levels were assessed simultaneously every 60 min.

Statistical analysis

Statistical analyses were performed with a statistical software package for Windows (Statistic 4.5). Data are presented as the mean ± S.D. Mann-Whitney U test was used for simple comparison of clinical and haemodynamic data. ANOVA for repeated measures and Newman-Keuls *post hoc* analysis were used to study the trend, of haemodynamic parameter data. Significance was defined as a p value less then 0.05.

Ethical aspects

The study was performed according to the principles of the Helsinki Declaration of Human Rights and the Ethics Committee, "Dedinje" Cardiovascular Institute, Medical School, University of Belgrade approved the protocol of the study. Signed informed consent was obtained from each patient.

Results

Echocardiography

There were no differences between the groups on preoperative echocardiography examination. Average left ventricular end-diastolic diameter, average left ventricular end-systolic diameter was 40.8 in H-GIK group vs. 44.5 in L-GIK group vs. 41.8 mm in C group; left atrial diameter 39 mm with mitral insufficiency $1–2^+$. Average left ventricular ejection fraction was 34%.

Operative procedures

There were no significant differences between the groups. Average grafts number was 2.6 in group H-GIK, vs. 2.3 in group L-GIK vs. 2.8 in group C. Bypass duration was as follows: group H-GIK 76.7 min; group L-GIK 73.6 min vs. group C 69.1 min with cross-clamping time 43.6 min in group H-GIK, 47.2 min in group L-GIK and 38.8 min in group C.

Hemodynamic data

There was no difference between groups at first (pre OP) measurement. CI changes for the GIK groups were insignificant during the first six postoperative hours, with a significant improvement between the third and fourth time point measurement ($p = 0.002$). Total improvement was found to be 2.14 ± 0.36 l·min^{-1}·m$^{2-1}$ to 3.05 ± 0.55 l·min^{-1}·m$^{2-1}$ ($p = 0.00002$) in H-GIK group vs. 2.24 ± 0.40 l·min^{-1}·m$^{2-1}$ to 3.16 ± 0.43 l·min^{-1}·m$^{2-1}$ ($p = 0.00003$) in L-GIK group.

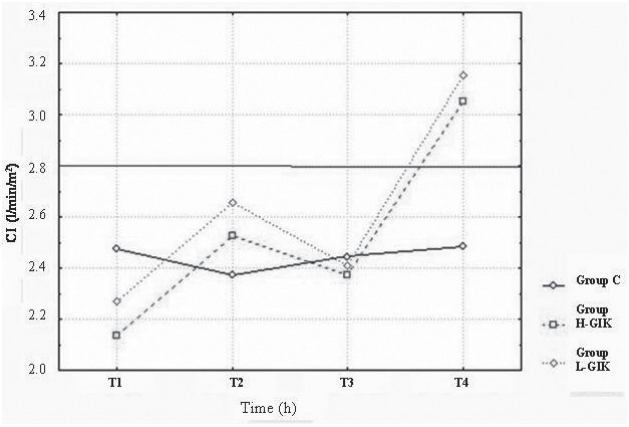

Figure 1. In GIK groups were significant cardiac index (CI) improvement between T3–T4 (p = 0.002). Total improvement was found to be 2.14 ± 0.36 l·min^{-1}·m$^{2-1}$ to 3.05 ± 0.55 l·min^{-1}·m$^{2-1}$ (p = 0.00002) in H-GIK group vs. 2.24 ± 0.40 l·min^{-1}·m$^{2-1}$ to 3.16 ± 0.43 l·min^{-1}·m$^{2-1}$ (p = 0.00003) in L-GIK group. Four time points: T1 – before the surgery (after the induction of anaesthesia), T2 – at the end of the surgery (after the chest closure), T3 – 6 h after the operation, T – 24 h after the operation.

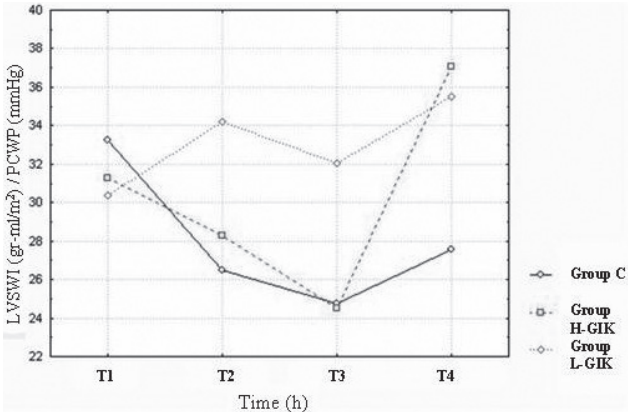

Figure 2. Trend of changes over time was more significant (p = 0.0016) then the difference between the groups (p = 0.014). The improvement in H-GIK group was significant in the interval between T3–T4 (p = 0.0039). LWSWI, left ventricle stroke work index; PCWP, pulmonary capillary wedge pressure. Four time points: T1 – before the surgery (after the induction of anaesthesia), T2 – at the end of the surgery (after the chest closure), T3 – 6 h after the operation, T4 – 24 h after the operation.

In the C group, CI changes had a linear trend 2.47 ± 0.39 l·min^{-1}·m$^{2-1}$ to 2.48 ± 0.50 l·min^{-1}·m$^{2-1}$. Difference between the groups were found to be statistically significant in the postoperative period, during last two time points, 6 h to 24 h post OP (p = 0.005) (Figure 1).

We assessed the GIK influence on the global left ventricular function by comparing LVSWI as an index of left ventricular work and pulmonary capillary wedge pressure (PCWP) as an index of ventricular loading. Covariation of LVSWI with PCWP was performed. Calculated values were individually more sensitive than each parameter by itself. Trend of LVSWI-PCWP changes over time was more significant (p = 0.0016) then the difference between the groups (p = 0.014). Segmental analyses emphasizes the improvement in H-GIK group in interval between 6 and 24 h after surgery (p = 0.0039) (Figure 2).

By comparing right ventricle work and loading (RVSWI/CVP) we found a significant improvement in GIK groups (p = 0.000017), with a considerable deference between groups during the time interval (p = 0.015). Significant improvement was observed in H-GIK group between T1 and T4 (p = 0.019) vs. L-GIK group between T1 and T4 (p = 0.022) vs. stagnation in group C (Figure 3).

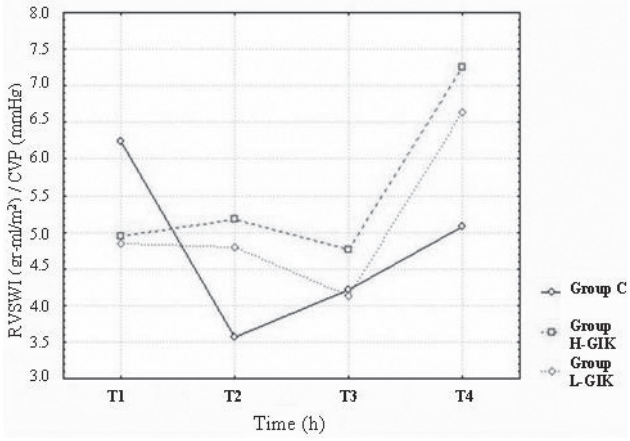

Figure 3. Remarkable deference between groups during the time interval (p = 0.015). Significant improvement in H-GIK group between T1–T4 p = 0.019 vs. L-GIK group between T1–T4 p = 0.022 vs. stagnation in group C. RVSWI, right ventricle stroke work index; CVP, central venous pressure. Four time points: T1 – before the surgery (after the induction of anaesthesia), T2 – at the end of the surgery (after the chest closure), T3 – 6 h after the operation, T4 – 24 h after the operation.

Oxygen delivery-consumption relationship

Analysis of the DO_2-VO_2 relationship during the time intervals and comparing the differences between groups resulted in interesting results. Shift to the left of the DO_2-VO_2 relationship curve to the critical, supply dependent VO_2, was evident immediately after the surgery in both groups. In an interval between 6 and 24 h after operation, we observed a shift to the right and a marked improvement in GIK groups, from baseline values DO_2-VO_2

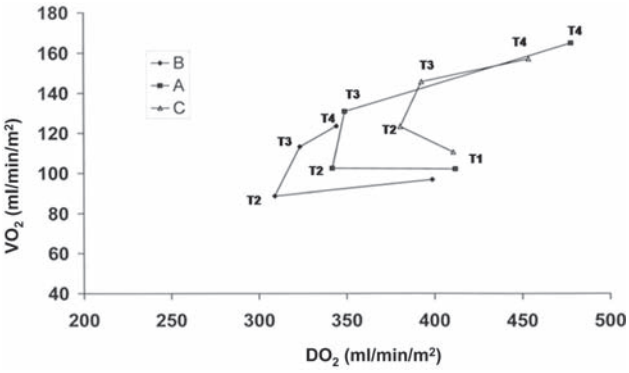

Figure 4. There was no difference in the behavior between groups during the time intervals. The difference in achieved levels of DO_2-VO_2 balance between groups was extremely significant (p = 0.00073). There was no difference between H-GIK and L-GIK groups. VO_2, oxygen consumption; DO_2, oxygen delivery. Four time points: T1 – before the surgery (after the induction of anaesthesia), T2 – at the end of the surgery (after the chest closure), T3 – 6 h after the operation, T4 – 24 h after the operation.

(430–101 ml·m$^{2-1}$·min^{-1}) toward normal ratio (500–156 ml·m$^{2-1}$·min^{-1}). There was no difference in the behavior between groups during the time intervals, but the difference in achieved levels of DO_2-VO_2 balance between groups was extremely significant (p = 0.00073). There was no difference between H-GIK and L-GIK groups, while the group C ratio DO_2-VO_2 was at the borderline level, 349–136 ml·m$^{2-1}$·min^{-1} (Figure 4).

Blood glucose and serum potassium levels were assessed every 4 h. Only in three pts., in group H-GIK and group C, glucose level was over 12 mmol/l at the second reading, while the potassium levels in both groups were between 3.77–4.29 mmol/l.

Postoperative treatment

During the ICU treatment, duration of mechanical ventilation was same for all pts., 15.58 ± 3.09 h in H-GIK group vs. 16.78 ± 4.04 h in L-GIK group vs. 17.40 ± 2.41 h in C group. The difference was in ICU stay, 1.14 days for group H-GIK vs. 1.73 for group L-GIK vs. 2.3 days for group C. The inotropic support (dopamine 5–10 μg·kg^{-1}·min^{-1} or epinephrine 0.03–0.1 μg·kg^{-1}·min^{-1}) was needed in 5.5% of pts. in H-GIK group vs. 13% of pts. in L-GIK group vs. 31% of pts. in C group. Statistical significance was determined using the binomial sampling distribution analysis, such that the exact probability was calculated to be p = 0.01391 for the H-GIK group and p = 0.05 for the L-GIK group. The mechanical assist device was not necessary.

Morbidity-mortality rate was the same for all three groups. One patient in H-GIK group died 34 h postoperatively, after reintervention due to surgical bleeding and consequent myocardial insufficiency. Another patient in the C group died on 13th postoperative day due to the myocardial infarction and subsequent cardiorespiratory insufficiency.

Discussion

During prolonged coronary insufficiency, myocardial hibernation overcomes the persistent energy deficit through adaptation to reduced myocardial blood flow. Reduced energy reserves act to maintain myocardial integrity and viability (Opie 1988).

Myocardial stunning and reperfusion injury during the coronary surgery as well as a great number of incorporated intracellular mechanisms and disorders all occur due to the energy deficit. The anaerobic metabolism with reduced energy production in mitochondria and deterioration in energy consumption in myofibrils are critical for this process (Opie 1988). Cascade of intra-mitochondrial events, namely calcium ion metabolism disorders, oxygen free radicals production, free fatty acids mobilization, pyruvate dehydrogenase inactivation and Krebs cycle dysfunction, all have an influence on myocardial contractility (Downing et al. 1977; Svedjeholm et al. 1991; Laine et al. 2000; Van Wezel 2006). The role for mitochondria during preconditioning and reperfusion is becoming increasingly clear. During ischemia, oxidative phosphorylation is maintained while the process of oxidation is impaired (mitochondrial uncoupling). During reperfusion, energy production is restored. Restored energy stimulates the calcium overload, with the consequence of uncontrolled force generation followed by hypercontractility of myofibrils (mitochondrial paradox). Subsequently it leads to self-destruction and myocyte dysfunction after prolonged ischemia (Lazar et al. 1997).

In extensive coronary disease with preserved myocardial viability, detection of hibernated myocardium and its protection can be extremely beneficial during the reperfusion or revascularization procedures. Hibernated myocardium must be recognized and identified by appropriate diagnostic procedures. In our study we preferred a dobutamine-stress echocardiography for detection and assessment of hibernated myocardium. This was potentially advantageous in evaluating the myocardial functional reserve (Girard et al. 1992) and as such was important for the study. The restoration and protection of high-energy phosphate stores in the viable myocardium was the target of the GIK protective action.

Previous studies with GIK

Many of GIK studies assessed GIK effects on myocardium in acute myocardial infarction (Sodi-Pallares et al. 1962;

Malmberg et al. 1996; Dias et al. 1998; Bertrand et al. 2008; Nesto and Lago 2008), during PTCA (percutaneous transluminal coronary angioplasty) (Van der Horst et al. 2003) or during the CABG surgery (Svedjeholm et al. 1991; Girard et al. 1992; Lazar et al. 1997; Szabo et al. 2001), considering mortality rate, heart failure or recurrence of ischemic event. Following the initial study and experience with GIK solution of Sodi-Pallares and coworkers (1962), many studies have been performed. Most of them were nonprospective and nonrandomized, with modest design. Controversial results in these studies are the consequence of the employed strategy. They reported various criteria for GIK usage, difference in glucose concentration and insulin doses as well as in selection of the proper moment for the treatment. In some of them glucose was given peroraly with subcutaneous insulin while in others GIK infusion was induced 48 h after the onset of angina. In a meta-analysis of randomized, placebo-controlled trials, the benefits of GIK therapy in acute myocardial infarction have been demonstrated. In the four studies GIK has been administered intravenously at a high-dose resulting in mortality reduction of 48% relative to the placebo group (Szabo et al. 2001). In nonrandomized study pts. with acute myocardial infarction were treated with thrombolysis. Some of them were given GIK, carnitin and magnesium by peripheral venous infusion. Pts. treated with metabolic support had significantly lower incidence of heart failure development or death, compared to control pts. treated only with thrombolysis (Ganc and Braunwald 1997). Despite the controversy of the GIK beneficial effects (Kloner and Nesto 2008) and results of some clinical studies, in pts. with ST elevation myocardial infarction (Rasoul et al. 2007) and on diastolic dysfunction after coronary-bypass grafting (Tsang et al. 2007) where GIK infusion did not improve the outcome, metabolic modulation still attracted attention (Yetkin et al. 2002).

Ischemia and reperfusion lead to desirable pharmacological effects of metabolic modulation with GIK infusion such as decreased fatty acid oxidation, increased glucose oxidation, maintaining the coupling of glycolysis to glucose oxidation with increased glycolysis, increased efficiency in oxygen utilization for supporting ATP synthesis and increased efficiency of ATP utilization for contractile function (Bolli et al. 1989; Bolli 1990). Aforementioned processes are associated with simultaneous improvement in the cardiac contractile function.

Recent evidence was strongly suggestive of the insulin signaling K_{ATP} channel activation. K_{ATP} channels are crucial and critical mediators of ischaemic preconditioning, the process of importance for powerful protection against myocardial infarction, ischaemia-reperfusion injury and apoptosis (Gross 1992; Akao et al. 2001). Their activity is modulated by several intracellular kinases as well as by insulin (Chai et al. 2008). Insulin has also been shown to regulate K_{ATP} channel activity by increasing the open-state probability of the channel and by decreasing the channel sensitivity to ATP (Tricarico et al. 1997). Recent studies have suggested that under pathological conditions, such as type-2 diabetes, myocardial ischaemia, and cardiac hypertrophy, insulin signal transduction pathways and action are modified (Bertrand et al. 2008). Results of the recent experimental study confirm protective effects of GIK administration immediately before the reperfusion independently of blood glucose level (Laine et al. 2000). However, presented findings support previous observations in rats that GIK or insulin administered immediately before reperfusion reduced the ischemic area. High-dose insulin treatment was known to have potential anti-inflammatory properties in coronary revascularization surgery (Koskenkari et al. 2006). The efficacy of GIK may be modulated under these conditions because of the glucose-impaired K^+ channel activation or due to metabolic effects of insulin and glucose.

This idea was an inspiration for our study. Pts. about to undergo the coronary artery bypass surgery with poor left ventricular function and detected hibernated myocardium were selected in order to evaluate efficiency of GIK infusion on preconditioning and intraoperative protection of myocardial function. The intention was to evaluate haemodynamic parameters and DO_2-VO_2 relationship as direct effect of left ventricular function. The primary function of the left ventricle is to generate a flow and distribution of oxygenated blood to sustain aerobic metabolism. The relationship between DO_2 and VO_2 is in very sensitive balance. Oxygen can not be stored and any disturbances in haemodynamics with consequences on perfusion, affect the delivery/consumption ratio. Cardiac output and left ventricular pump function are essential in achieving this goal. With that in mind our intention was to evaluate the left ventricular function indirectly, considering that the oxygen supply becomes limited with depressed left ventricular performances, resulting in VO_2 becoming almost supply dependent. Furthermore, simultaneously with haemodynamic calculations, DO_2, VO_2 and their respective ratios were calculated.

In this study we used high concentration glucose (30%) insulin 1 IU·kg^{-1}·h^{-1} and single dose 24 IU of insulin prior to aortic cross-clamping, without any extreme blood glucose values during the study. Only in three pts. in each group's blood glucose level was over 12 mmol/l at T2.

Considering an importance and influence of the GIK infusion on haemodynamic and intraoperative outcome, difference between groups is evident and significant. Postoperative improvement of CI, LVSWI and LVSWI/PCWP in GIK groups is emphasized during last hours, between T3–T4 (6 to 24 h after the surgery). During the ICU treatment, duration of mechanical ventilation was

same for all pts. The difference was in ICU stay, 1.14 days for group H-GIK vs. 1.73 for group L-GIK vs. 2.3 days for group C what is in correlation with inotropic support. A significant difference in the need for inotropic support was demonstrated (5.5 vs. 13 vs. 31%; $p = 0.01391$ for the H-GIK group and $p = 0.05$ for the L-GIK group) which may indicate favorable effects of GIK. Advanced surgical skills, modern anesthetic techniques and improved myocardial protection are essential to achieving a better outcome of coronary artery by pass surgery in advanced left ventricular dysfunction (Trachiotis et al. 1998). However, surgical coronary revascularization in pts. with poor left ventricle still remains a challenge for a surgical team. Two large studies of postoperative treatment after coronary artery bypass surgery in pts. with low EF, reported usage of IABP in 10.7–20% of pts. with intrahospital mortality rate 3.8–10% (Elefteriadis and Kron 1995; Kaul et al. 1996; Trachiotis et al. 1998). Considering this, metabolic modulation might serve as an alternative to standard procedures in intraoperative myocardial protection used in our study.

The importance of DO_2-VO_2 relationship has been investigated as a predictive factor for an outcome in critically ill and septic pts. for years (Boyd et al. 1993). Shoemaker et al. reported the importance of increasing blood volume, CO, DO_2 and VO_2 in treatment of oxygen debt and for the postoperative outcome (Shoemaker et al. 1988, 1992a). This poses a dilemma whether the DO_2-VO_2 ratio can be used as an outcome-prediction factor in CABG surgery and it can be interpreted as a supplement to haemodynamic parameters (Shoemaker et al. 1992b). Despite the difficulties of evaluating regional blood flow, distribution and regional DO_2-VO_2 relationship, our idea was to test DO_2-VO_2 relationship in the context of haemodynamics, considering that left ventricular function and cardiac output are the main contributing factors to oxygen metabolism balance in a tissue.

Preoperatively all pts. exhibited a borderline level of DO_2-VO_2 relationship. During the postoperative period it deteriorated, shifted to the left, and near to the critical levels (VO_2 supply-dependent). Six hours after the operation improvement was obvious, with a rightward shift observed in all three groups. Pts. in group C retained near-initial levels while the GIK groups exhibited DO_2-VO_2 ratios (shifted to the right), significantly above the starting levels, and close to the normal levels.

In the presented study we have performed an assessment of haemodynamic parameters during and after the surgery. Considering the volume loading, LVSWI, DO_2-VO_2 ratio and the need for inotropic support, evaluation of myocardial working capabilities were provided during reperfusion period, 24 h after surgery. The difference between GIK groups and control were significant.

Study limitations

The present results should be interpreted within the constraints of several potential limitations. With the observed low mortality rates in the GIK groups and control group, our study could not detect a significant difference in mortality. Nevertheless, myocardial VO_2 was not directly measured in the current study; DO_2-VO_2 ratio was measured as factor dependent on haemodynamics and left ventricular pump capability.

This is a report of clinical experience and not a formal scientific trial. The comparatively earlier haemodynamic recovery, improvement of oxygen supply-consumption relationship and minimal inotropic support in GIK groups, are consistent with the assumption that the course of recovery was influenced by metabolic support.

Results of our study should be an encouragement for further randomized, controlled metabolic and clinical studies, even multicentric, in order to define metabolic strategies for intraoperative myocardial protection and for broader use of GIK metabolic support.

Acknowledgements. Authors thank Igor Todorovski for expert technical assistance, Branka Ilić and Drena Beraković for the assistance in the collection of data.

References

Akao M., Ohler A., O'Rourke B., Marban E. (2001): Mitochondrial ATP-sensitive potassium channels inhibit apoptosis induced by oxidative stress in cardiac cells. Circ. Res. **88**, 1267–1275

Bertrand L., Horman S., Beauloye C., Vanoverchelde L. J. (2008): Insulin signaling in the heart. Cardiovasc. Res. **79**, 238–248

Bolli R., Jeroudi M. O., Patel B. S., Arouma I. O., Halliwell B., Lai K. E., McCay B. P. (1989): Marked reduction of free radical generation and contractile dysfunction by antioxidant therapy begun at the time of reperfusion: evidence that myocardial "stunning" is a manifestation of reperfusion injury. Circ. Res. **65,** 607–622

Bolli R. (1990): Mechanism of myocardial "stunning". Circulation **82**, 723–738

Boyd O., Grounds R. M., Bennett E. D. (1993): A randomized clinical trial of the effect of deliberate perioperative increase of oxygen delivery on mortality in high-risk surgical patients. JAMA **270,** 2699–2707

Brix-Christiensen V., Andersen S. K., Andersen R., Mengel R., Dyhr T., Andersen N. T., Larsson A., Schmitz O., Orskov H., Tonnesen E. (2004): Acute hyperinsulinemia restrains endotoxine-induced systemic inflammatory response: an experimental study in a porcine model. Anesthesiology **100,** 861–870

Chai W., Wu Y., Li G., Cao W., Yang Z., Liu Z. (2008): Activation of p38 mitogen-activated protein kinase abolishes insu-

lin-mediated myocardial protection against ischemia-reperfusion injury. Am. J. Physiol., Endocrinol. Metab. **294**, E183–189

Diaz R., Paolasso A. E., Piegas S. L., Tajer D. C., Moreno G. M, Corvalan R., Isea E. J., Romero G. (1998): Metabolic modulation of acute myocardial infarction. The ECLA glucose-insulin-potassium pilot trial. Circulation **98**, 2227–2234

Downing S. E., Lee J. C., Rieker R. P. (1977): Mechanical and metabolic effects of insulin on newborn lamb myocardium. Am. J. Obstet. Gynecol. **127**, 649–656

Elefteriadis J. A., Kron I. L. (1995): CABG in advanced left ventricular dysfunction. Cardiol. Clin. **13**, 1036–1045

Ganc P., Braunwald E. (1997): Coronary blood flow and myocardial ischemia. In: Heart Diseases. (5th edition), pp. 1161–1183, W. B. Saunders Company, Philadelphia

Girard C., Quentin P., Bouvier H., Blanc P., Bastien O., Lehot J. J., Mikealoff P., Estanove S. (1992): Glucose and insulin supply befor cardiopulmonary bypass in cardiac surgery: a double blind study. Ann. Thorac. Surg. **54,** 259–263

Gradinac S., Coleman G. M., Taegtmeyer H., Sweeny M., Frazier H. O. (1989): Improved cardiac function with glucose-insulin-potassium after aortocoronary bypass grafting. Ann. Thorac. Surg. **48**, 484–489

Gross G. J., Auchampach J. A. (1992): Blockade of ATP-sensitive potassium channels prevents myocardial preconditioning in dogs. Circ. Res. **70**, 223–233

Hansen T. K., Thiel S., Wouters P. J., Christiansen J. S., Van den Berhe G. (2003): Intensive insulin therapy exerts antiinflammatory effects in critically ill patients and counteracts the adverse effect of low mannose-binding lecithin levels. J. Clin. Endocrinol. Metab. **88**, 1082–1088

Kaul K. T., Agnihtory K. A., Fields L. B., Riggins S. L., Wyatt A. D., Jones R. C. (1996): Coronary artery bypass grafting in patients with ejection fraction of twenty percent or less. J. Cardiovasc. Surg. **5**, 1001–1012

Kloner A. R., Nesto W. R. (2008): Glucose-insulin-potassium for acute myocardial infarction: continuing controversy over cardioprotection. Circulation **117**, 2523–2533

Koskenkari K. J., Kaukoranta K. P., Rimpilainen J., Vainionpaa V., Ohtonen P. P., Surcel M. H. Juvonen T., Ala-Kokko I. T. (2006): Anti-inflammatory effect of high-dose insulin treatment after urgent coronary revascularization surgery. Acta Anaesthesiol. Scand. **50,** 962–969

La Disa F. J., Krolikowski G. J., Pagel S. P., Warltier C. D., Kersten R. J. (2004): Cardioprotection by glucose-insulin-potassium: dependence on K_{ATP} channel opening and blood glucose concentration before ischemia. Am. J. Physiol., Heart. Circ. Physiol. **287,** H601–607

Laine H., Nuutila P., Loutalahti M., Meyer C., Elomaa T., Koskinene P., Ronnemaa T., Knuuti J. (2000): Insulin-induced increment of coronary flow reserve is not abolished by dexamethasone in healthy young men. J. Clin. Endocrinol. Metab. **85**, 1868–1873

Lazar L. H., Philippides G., Fitzgerald C., Lancaster D., Shemin J. R., Apstein C. (1997): Glucose-insulin-potassium solutions enhance recovery after urgent coronary artery bypass grafting. J. Thorac. Cardiovasc. Surg. **113**, 354–360

Malmberg K., Ryden L., Hamsten A., Herlitz J., Waldenstrom A., Wedel H. (1996): Effects of insulin treatment on cause-specific one-year mortality and morbidity in diabetic patients with acute myocardial infarction. DIGAMI study group. Diabetes-insulin-glucose in acute myocardial infarction. Eur. Heart. J. **17,** 1337–1344

Nesto W. R., Lago M. R. (2008): Glucose: a biomarker in acute myocardial infarction ready for prome time? Circulation **117**, 990–992

Opie L. (1988): Hypothesis: glycolytic rates control cell viability in ischemia. J. Appl. Cardiol. **3**, 407–414

Rasoul S., Ottervanger J. P., Timmer J. R., Svilaas T., Henriques J. P., Dambrink J. H., van der Horst I. C., Zijlstra F. (2007): One year outcomes after glucose-insulin-potassium in ST elevation myocardial infarction. The glucose-insulin-potassium study II. Int. J. Cardiol. **122**, 52–55

Shoemaker W. C., Kram K. B., Appel P. L., Kram B. H., Waxman K., Lee S. T.(1988): Prospective trial of supranormal values of survivors as therapeutic goals in high-risk surgical patients. Chest **94**, 1176–1188

Shoemaker W. C., Appel P. L., Kram H. B. (1992a): Role of oxygen debt in the development of organ failure, sepsis, and death in high-risk surgical patients. Chest **102**, 208-215

Shoemaker W. C., Patil R., Appel P. L., Kram H. B. (1992b): Hemodynamic and oxygen transport patterns for outcome prediction, therapeutic goals, and clinical algorithms to improve outcome. Feasibility of artificial intelligence to customize algorithms. Chest **102**, 617–625

Sodi-Pallares D., Testelli M., Fishleder F. (1962): Effects of an intravenous infusion of a potassium-insulin-glucose solution on the electrocardiographic signs of myocardial infarction. Am. J. Cardiol. **9**, 166–181

Svedjeholm R., Hallhagen S., Ekroth R., Joachimsson P. O., Ronquist G. (1991): Dopamine and high-dose insulin infusion (glucose-insulin-potassium) after a cardiac operation: effects on myocardial metabolism. Ann. Thorac. Surg. **51**, 262–270

Szabó Z., Arnqvist H., Håkanson E., Jorfeldt L., Svedjeholm R. (2001): Effects of high-dose glucose-insulin-potassium on myocardial metabolism after coronary surgery in patients with Type II diabetes. Clin. Sci. **101**, 37–43

Tricarico D., Mallamaci R., Barbieri M., Conte Camerini D. (1997): Modulation of ATP-sensitive K^+ channels by insulin in rat skeletal muscle fibers. Biochem. Biophys. Res. Commun. **232**, 536–539

Trachiotis D. G., Weintraub S. W., Johnston S. T., Jones L. E., Guyton A. R., Craver M. J. (1998): Coronary artery by pass grafting in patients with advanced left ventricular dysfunction. Ann. Thorac. Surg. **66**, 1632–1639

Tsang W. M., Davidoff R., Korach A., Apstein S. C., Hesselvik F. J., Nguyen H., Shemin J. R., Shapita M. O. (2007): Diastolic dysfunction after coronary artery bypass grafting-the effect of glucose-insulin-potassium infusion. J. Card. Surg. **22**, 185–191

van der Horst I. C. C., Zijlstra F., van't Hof A. W. J., Doggen C. J. M., de Boer M.-J., Suryapranata H., Hoorntje J. C. A., Dambrink J.-H. E., Gaus R. O. B., Bilo H. J. G. (2003): Glucose-insulin-potassium infusion in patients treated with primary angioplasty for acute myocardial infarction. J. Am. Coll. Cardiol. **42**, 784–791

van Wezel B. H. (2006): Glucose-insulin-potassium techniques in cardiac surgery: historical overview and future perspectives. Semin. Cardiothorac. Vasc. Anesth. **10**, 224–227

Yetkin E., Senen K., Ileri M., Atak R., Yetkin O., Tandogan I., Turhan H., Cehreli S. (2002): Comparison of low-dose dobutamine stress echocardiography during glucose-insulin-potassium infusion for detection of myocardial viability after anterior myocardial infarction. Coron. Artery Dis. **13**, 145–149

Predictive value of serum bicarbonate, arterial base deficit/excess and SAPS III score in critically ill patients

Maja Surbatovic[1], Sonja Radakovic[1], Miodrag Jevtic[1], Nikola Filipovic[1], Predrag Romic[1], Nada Popovic[2], Jasna Jevdjic[3], Krasimirka Grujic[4] and Dragan Djordjevic[1]

[1] *Military Medical Academy, Belgrade, Serbia*
[2] *Clinical Center of Serbia, Belgrade, Serbia*
[3] *Clinical Center, Kragujevac, Serbia*
[4] *Clinical Center, Kosovska Mitrovica, Serbia*

Abstract. Arterial base deficit/excess (BD/E) is commonly used marker of metabolic acidosis in critically ill patients, but requires an arterial puncture and blood gas analysis. We hypothesized that serum bicarbonate (HCO_3), which can be routinely obtained, strongly correlates with arterial BD/E and provides equivalent predictive information. In addition, we evaluated predictive value of simplified acute physiology score III (SAPS III). Total of 152 critically ill surgical patients were included in retrospective analysis. On admission to intensive care unit sets of simultaneously obtained paired laboratory data, including an arterial blood gas and serum chemistry panel with serum HCO_3 were obtained. Very strong correlation between BD/E and simultaneously measured serum HCO_3 levels was found ($r = 0.857$, $R^2 = 0.732$, $p < 0.01$). The serum HCO_3 level reliably identified a significant metabolic acidosis (AUC = 0.761, $p < 0.05$). BD and SAPS III were good predictors of mortality (AUCs 0.70 and 0.74, respectively). Serum HCO_3 may be used as substitute to detect severe metabolic acidosis. BD and SAPS III score were good predictors of mortality.

Key words: Serum bicarbonate — Base deficit — Critically ill — SAPS III score

Introduction

The association between acidosis and increase in multiple organ dysfunction and mortality for intensive care patients has been long known. To assist in the resuscitation of critically ill patients, clinicians have developed the concept of endpoints of therapy or resuscitation, most importantly in the early stage of critical illness (Rivers et al. 2007). One of the most commonly used endpoints of therapy or resuscitation is arterial base deficit/excess (BD/E). Despite acid-base imbalance being an integral aspect of ongoing pathologic processes in a large number of critically ill patients, the importance of understanding the fundamental principles behind the physiology has been largely ignored. Measurement of the standard bicarbonate and BD/E has been used for decades as indicators of metabolic acid-base disturbances (Rhodes and Cusack 2000). The standard bicarbonate is the concentration of bicarbonate (HCO_3) in the plasma when the hemoglobin in the whole blood has been fully oxygenated, at a temperature of 37°C and corrected to arterial partial pressure of CO_2 ($PaCO_2$) of 40 mm Hg (5.33 kPa). These corrections remove the influence of the respiratory component upon measurement. BD/E is directly calculated from the blood gas analyzer from $PaCO_2$, pH and serum HCO_3 values as applied to a standard nomogram and represents the amount of acid or base required to normalize the pH in a liter of blood. Unfortunately, BD/E determination generally requires an arterial puncture and often necessitates multiple arterial punctures or placement of an indwelling arterial catheter. This procedure is painful, invasive, costly and can be associated with complications such as infection, pseudoaneurysm, distal embolization, and, in rare cases, hand or limb loss. Moreover, arterial blood gas measurement is not routinely performed in all intensive care unit (ICU) patients early enough, that fact could result in a failure or delay in the

Correspondence to: Maja Surbatovic, Clinic of Anesthesiology and Intensive Therapy, Military Medical Academy, Crnotravska 17, Belgrade 11000, Serbia
E-mail: MAYA@EUnet.rs

diagnosis of significant acidosis. The increased concentrations of plasma hydrogen ions with metabolic acidosis are buffered by a variety of homeostatic mechanisms, including plasma bicarbonates (Kellum 2000). Serum HCO_3 levels have been shown to decrease in a linear fashion with increasing acid load and theoretically should provide information similar to the arterial BD/E (Sterns 2003; Wiederseiner et al. 2004). Also, serum bicarbonate is routinely obtained as a part of chemistry panel on most ICU admissions, it does not require any separate equipment to perform analysis, and does not require arterial puncture or catheterization. We hypothesized that serum HCO_3 strongly correlates with arterial BD/E and provides equivalent predictive information.

In addition, simplified acute physiology score III (SAPS III) (Moreno et al. 2008) on ICU admission and SAPS II (Le Gall et al. 1993), sepsis-related organ failure assessment (SOFA) score (Moreno et al. 1999) and acute physiology and chronic health evaluation score II (APACHE II) (Knaus et al. 1985) at 24 h after ICU admission were calculated and recorded.

SAPS III is newly developed score and it was design to empirically test, based on a large multicenter multinational database, whether a modified PIRO (predisposition, insult, response and organ dysfunction) concept could be applied to predict mortality in patients with infection and sepsis and our objective was to determine its predictive value in critically ill patients and to compare this score with SAPS II, SOFA and APACHE II scores.

Materials and Methods

This study was designed as a retrospective analysis to compare the use of serum HCO_3 levels with the standard measure of arterial BD/E in a surgical ICU population. Four hospitals were included; all of them were tertiary care facilities. About one quarter of patients were transferred from other hospitals where they were previously treated but failed to improve, and developed severe complications. The study population included adult (>18 years) patients admitted to the surgical ICU from January 2007 to August 2008. They were admitted by either Emergency Departments or one of the general surgical specialty services with one of the following diagnosis: peritonitis, pancreatitis, pneumonia and all were in ICU longer than 24 h. Reason for the admission of patients with pneumonia in surgical ICU was severe complication of pneumonia (gangrenous lesions) which required thoracic surgical treatment.

Patients who met the foregoing criteria and had at least 1 simultaneously drawn arterial blood gas determination (with BD/E) and serum chemistry panel (with HCO_3) were included. The SAPS III on ICU admission, SAPS II, APACHE II and SOFA score at 24 h after ICU admission were calculated and recorded. The correlation between HCO_3 and BD/E was assessed by calculation of the Pearson correlation coefficient r and coefficient of determination R^2, and linear regression analysis was used to develop a predictive equation for BD. The predictive ability of HCO_3 and pH of severe metabolic acidosis and predictive ability of BD, base excess, HCO_3, pH and four above mentioned scores of mortality were examined by calculating the area under the receiver operating characteristic curve (AUC). Severe metabolic acidosis is defined as BD greater than –5, for example –6, –7 etc. Linear variables are reported as the mean value ±1 SD and AUC with 95% confidence intervals. All statistical analysis was performed with SPSS 12.0 for Windows (SPSS Inc., Chicago, IL, USA) and statistical significance was set at $p < 0.05$. This study was reviewed and approved with waiver of informed consent by the hospital's institutional review boards.

Results

In this study total of 152 critically ill surgical patients were included. In all of them, on admission to ICU, sets of simultaneously obtained paired laboratory data, including an arterial blood gas and serum chemistry panel with serum HCO_3 were obtained. The patient's demographics are shown in Table 1.

All patients with pneumonia were male, frequency of pancreatitis was 5-fold higher in males, numbers of male and female patients with peritonitis were similar (42 and 39, respectively). Overall ICU mortality rate was 73.7%, but it varied according to diagnosis: peritonitis 81.5%, pancreatitis 67.2% and pneumonia 50%. Mechanical ventilation was most

Table 1. Patient demographics

Characteristic	Finding
Patients	152
Age (years)[a]	62.4 ± 13.7
Sex (%)	
Male	103 (67.8)
Female	49 (32.2)
Mechanical ventilation (%)	82 (54)
SAPS II[a]	39.66 ± 11.12
APACHE II[a]	17.19 ± 5.78
SOFA[a]	5.32 ± 3.05
SAPS III[a]	62.34 ± 10.36
Reason for ICU admission (%)	
Peritonitis	81 (53.3)
Pancreatitis	61 (40.1)
Pneumonia	10 (6.6)
ICU mortality (%)	112 (73.7)

[a] mean ± SD.

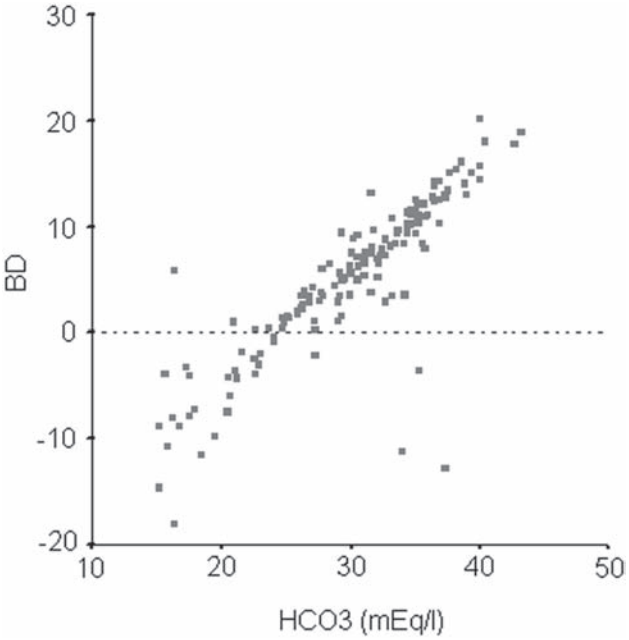

Figure 1. Scatterplot of the admission BD/E vs. the admission serum HCO_3 level.

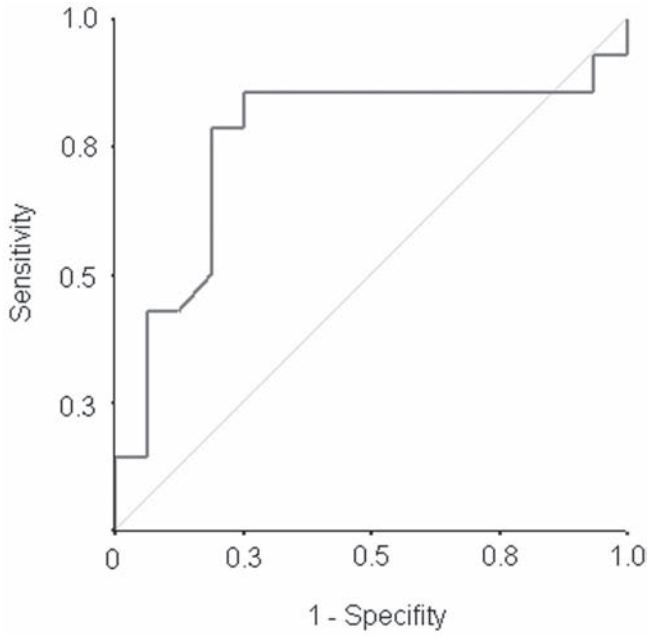

Figure 2. Receiver operating characteristic curve for the prediction of significant metabolic acidosis (BD < –5) by serum HCO_3 level.

frequently performed in patients with pneumonia (70%), then in patients with peritonitis (67.9%) and pancreatitis (30%) with statistically highly significant difference (Pearson Chi-square test: 18.379, p <0.01).

Table 2 shows the mean relevant laboratory and score values for study population according to diagnosis on admission. Statistical analysis (ANOVA) showed statistically significant to highly significant difference.

Correlation and regression analysis demonstrated a very strong correlation between the arterial BD/E and simultaneously measured serum HCO_3 levels. Fig. 1 shows the strong linear correlation between the BD/E and serum HCO_3 level drawn at the time of ICU admission with a correlation coefficient r of 0.857 ($R^2 = 0.732$, $p < 0.01$).

The regression equation derived from this analysis allows prediction of the arterial BD/E from the serum HCO_3 level by the following formulas: BD = 0.125 – (8.9 × HCO_3) and base excess = 0.885 – (20.296 × HCO_3).

From these equations, two important cutoff points for clinical use would be a serum HCO_3 level of 20.3 mEq/l, which equals a BD/E of 0, and serum HCO_3 level of 17 mEq/l, which equates to a BD of –5.

Assessment of accuracy and reliability of serum HCO_3 level for the identification of significant metabolic acidosis (BD greater than –5) and comparison with other conventional measures of acidosis such as pH was performed. The serum HCO_3 level reliably and accurately identified the presence of a significant metabolic acidosis, with AUC of 0.761 ($p < 0.05$). Cutoff point of 20 mEq/l had sensitivity of 78.6% and specificity of 75%. Values lower than 20 mEq/l suggested that significant metabolic acidosis is present and *vice versa* (Fig. 2).

Table 2. Mean relevant laboratory and score values for study population according to diagnosis on admission

	Peritonitis	Pancreatitis	Pneumonia	*p*
pH	7.44 ± 0.10	7.46 ± 0.05	7.38 ± 0.06	<0.05
HCO_3 (mEq/l)	30.45 ± 6.64	30.45 ± 5.71	23.63 ± 6.98	<0.01
BD/E	5.11 ± 8.06	6.45 ± 5.98	–0.09 ± 6.85	<0.05
SAPS II	43.56 ± 7.84	33.93 ± 12.86	43.00 ± 7.38	<0.01
APACHE II	20.02 ± 4.93	13.05 ± 4.19	19.50 ± 5.80	<0.01
SOFA	6.00 ± 3.33	4.23 ± 2.41	6.50 ± 2.27	<0.01
SAPS III	64.48 ± 11.68	59.05 ± 7.94	65.10 ± 6.77	<0.01

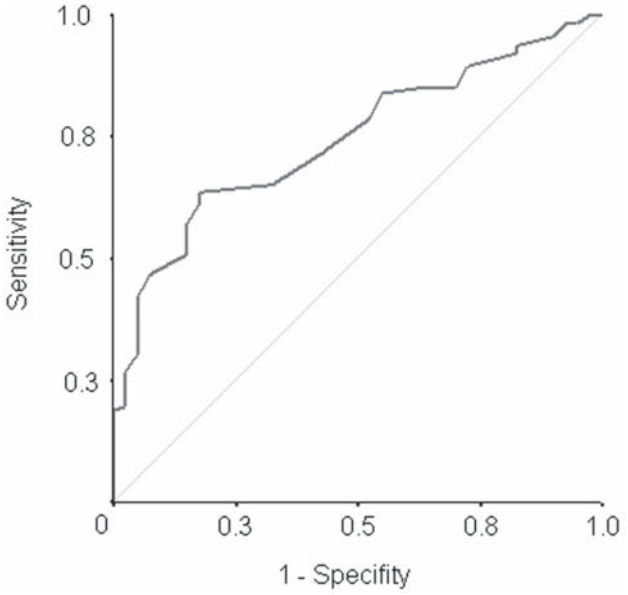

Figure 3. Receiver operating characteristic curve for outcome prediction by SAPS III.

Various laboratory and score values were then analyzed for their ability to predict mortality. The receiver operating characteristic curves for mortality prediction demonstrated that the arterial BD performed better than base excess, serum HCO_3 and pH. For BD, AUC was 0.70, with sensitivity of 82% (chance of dying: 8 out of 10) and specificity of 63% (chance of survival) for cutoff point of –8.3. In those patients (with BD) AUC for serum HCO_3 was 0.67, with sensitivity of 91% and specificity of 63% for cutoff point of 17 mEq/l. In patients with base excess, AUC for BE was 0.64, with sensitivity of 60% and specificity of 60% for cutoff point of 7.7. In the same group of patients AUC for serum HCO_3 was 0.64, with sensitivity of 60% and specificity of 65% for cutoff point of 32 mEq/l. pH value is not good predictor of outcome, AUC was 0.54.

Nonsurvivors were older, had a higher SAPS II, SAPS III, APACHE II and SOFA scores, pH, HCO_3 and lower BD at the time of ICU admission compared to survivors (Table 3).

Table 3. Comparison of survivors and nonsurvivors

Variable	Survived (n = 40)	Died (n = 112)	p
Age (years)	55.1 ± 13.1	64.9 ± 13.0	<0.01
pH	7.43 ± 0.12	7.45 ± 0.07	n.s.
HCO_3 (mEq/l)	28.62 ± 6.00	30.49 ± 6.61	n.s.
BD	–11.55 ± 4.02	–9.14 ± 2.39	n.s.
SAPS II	33.50 ± 9.80	41.86 ± 10.76	<0.01
APACHE II	12.88 ± 4.40	18.73 ± 5.44	<0.01
SOFA	3.65 ± 1.54	5.91 ± 3.23	<0.01
SAPS III	55.98 ± 6.69	64.62 ± 10.51	<0.01

The receiver operating characteristic curves for mortality prediction demonstrated that the all four scores performed well as predictors of outcome ($p < 0.01$). For SAPS II, AUC was 0.71, with sensitivity of 66% and specificity of 63.5% for cutoff point of 36.5. For APACHE II, AUC was 0.79, with sensitivity of 85% and specificity of 63% for cutoff point of 13.5. For SOFA, AUC was 0.72, with sensitivity of 60% and specificity of 73% for cutoff point of 4.5. For SAPS III, AUC was 0.74, with sensitivity of 61% and specificity of 83% for cutoff point of 60 (Fig. 3).

Discussion

Systemic arterial pH is maintained between 7.35 and 7.45 by extracellular and intracellular chemical buffering together with respiratory and renal regulatory mechanisms. The control of $PaCO_2$ by central nervous system and respiratory system and the control of the plasma bicarbonate by the kidneys stabilize the arterial pH by excretion or retention of acid or alkali. The metabolic and respiratory components that regulate systemic pH are described by the Henderson-Hasselbalch equation. Under most circumstances, CO_2 production and excretion are matched, and the usual steady-state $PaCO_2$ is maintained at 40 mm Hg. The development of metabolic acidosis is a common occurrence during critical illness (DuBose 2005). Early and accurate identification and correction of significant metabolic acidosis are particularly relevant to patients in the surgical ICU. But arterial blood gas sampling carries all the risks associated with arterial puncture. Contraindications to this procedure are numerous: cellulites or the infections over the radial artery, absence of palpable radial artery pulse, various coagulopathies, history of arterial spasms following previous punctures, severe peripheral vascular disease, arterial graft (Rodriguez Montalban et al. 2000; Crawford 2004; Wallach 2004). Particular attention should be paid to negative results of an Allen test (collateral circulation test), indicating that only one artery supplies the hand. In that case, another extremity as the site for arterial puncture should be selected. The substitution of an easily measured value from a venous sample, such as the serum HCO_3, would overcome most of these drawbacks if it provided clinical information equivalent to the arterial BD/E.

There are only several published studies examining the utility of using the serum HCO_3 to provide information equivalent to arterial BD/E in the ICU. The most important two studies were performed by Martin (in surgical ICU) and FitzSullivan (in trauma ICU) with co-workers (FitzSullivan et al. 2005; Martin et al. 2005). Martin found that serum HCO_3 levels showed significant correlation with arterial

BD levels both at admission ($r = 0.85$, $R^2 = 0.72$, $p < 0.01$) and throughout the ICU stay ($r = 0.88$, $R^2 = 0.77$, $p < 0.01$). He concluded that serum HCO_3 reliably predicted the presence of significant metabolic acidosis (BD greather than –5) with an AUC of 0.93 at admission ($p < 0.01$), outperforming pH, anion gap and lactate and that admission serum HCO_3 level predicted ICU mortality as accurately as the admission arterial BD (AUCs of 0.68 and 0.70, respectively) and more accurately than either admission pH or anion gap. Our study showed similar findings. We found strong linear correlation between the BD/E and serum HCO_3 level at ICU admission ($r = 0.857$, $R^2 = 0.732$, $p < 0.01$). Also, in our study serum HCO_3 level reliably and accurately identified the presence of significant metabolic acidosis (BD greather than –5) with an AUC of 0.761 at admission ($p < 0.05$), outperforming pH. FitzSullivan presented similar results in trauma patients: serum HCO_3 showed a significant linear correlation with BD ($r = 0.80$, $p < 0.01$) on admission, and reliably predicted the presence of significant metabolic acidoses, with an AUC of 0.96 ($p < 0.01$). Unlike Martin's and FitzSullivan´s study, in our investigation difference in BD and serum HCO_3 levels between survivors and nonsurvivors did not reach statistical significance. Eachempati with co-workers (2003) also performed the study in which correlation of serum bicarbonate with BD in a cohort of surgical ICU patients was evaluated. They found strong linear inverse correlation between two measures ($r = 0.91$, $R^2 = 0.83$, $p < 0.01$).

But, critically ill patients might present complex acid-base disorders, even when the pH, $PaCO_2$, HCO_3 and BD/E levels are normal. Lactic acidosis is primarily suspected because of presence of metabolic acidosis. Nevertheless, serum HCO_3 and BD/E levels might be normal despite the presence of hyperlactatemia, as a result of simultaneous alkalinizing processes that normalize the BD/E. Three widely accepted methods are used to analyze and classify acid-base disorders, yielding mutually compatible results. The approaches differ only in assessment of the metabolic component (i.e., all three treat $PaCO_2$ as an independent variable): 1. HCO_3 concentration; 2. standard base excess; 3. strong ion difference (SID). All three yield virtually identical results when used to quantify the acid-base status of a given blood sample. There are three mathematically independent determinants of blood pH. First, there is the difference between the sum of the concentrations of strong cations (e.g., Na^+ and K^+) and the sum of the concentrations of strong anions (e.g. Cl^-, lactate); this difference is called the SID. Second, the total weak acid buffers concentration (A_{tot}), which is mostly composed of the concentrations of albumin and phosphate and third is $PaCO_2$. Only these three variables can independently affect blood pH (Stewart 1993). Concentrations of H^+ and HCO_3^- are dependent variables, being functions of SID, A_{tot} and $PaCO_2$. Changes in plasma H^+ concentrations occur as a result of changes in the dissociation of water and A_{tot} brought about by the electrochemical forces produced by changes in SID and $PaCO_2$. The standard base excess is mathematically equivalent to the change in SID required to restore pH to 7.4 given a $PaCO_2$ of 40 mm Hg and the prevailing A_{tot}. Thus, a standard base excess of –10 mEq/l means that the SID is 10 mEq/l less than the SID that is associated with a pH of 7.4 when $PaCO_2$ is 40 mm Hg (Kellum 2005). Fencl and colleagues (2000) showed that in 152 critically ill patients, Stewart's (1983) approach could detect metabolic acidosis in some patients with normal HCO_3 and BD/E level. In those patients, the metabolic acidosis with a low SID was counterbalanced by alkalinizing processes. Low SID was undetected through changes in BD/E because the low SID acidosis was masked by the alkalinizing effect of hypoalbuminemia present in all patients. This study also showed that the traditional analysis frequently failed to identify severe metabolic acidosis. But, concept of "primary hypoproteinemic alkalosis" in hypoalbuminemic ICU patients with positive BE and elevated HCO_3 levels were recently challenged (Dubin et al. 2007). Tuhay and colleagues (2008) found that 20% of the critically ill patients with severe hyperlactatemia showed normal pH, HCO_3, BD/E and SID levels because of the simultaneous presence of hypochloremic metabolic alkalosis. Nevertheless, the presence of metabolic acidosis in critical patients has prognostic implications. Gunnerson and colleagues (2006) demonstrated that patients with metabolic acidosis (BD greather than –2) had a higher mortality rate than those without this disorder: 45% versus 25%. Some authors stated that the relationship between the bicarbonate and BD/E is only valid if the pH is held constant, that is the case when patients have preserved at least some of the compensatory mechanisms to correct acid-base disorders (Lujan and Howard 2006). In our study, pH changed very little, there was not even significant difference in pH between survivors and nonsurvivors.

SAPS III score performed well as predictor of outcome (AUC 0.74), slightly better than SAPS II (AUC 0.70) and SOFA (AUC 0.72), but slightly worse than APACHE (AUC 0.79). So, SAPS III could be used by physicians to stratify patients at ICU admission or shortly thereafter, contributing to a better selection of treatment regimen according to the risk of death. Mortality rates in our patients were somewhat higher than expected in critically ill patients. We believe that the main reason for this difference is the fact that about one quarter of patients were transferred from other hospitals where they were previously treated but failed to improve, and developed severe complications. That means that precious time for their optimal treatment was lost, so in spite of all our efforts, mortality rate was high.

In conclusion, in our study serum HCO_3 may be used as substitute to detect severe metabolic acidosis because there is a strong linear correlation with arterial BD/E. But, it has

to be done with a caution because critically ill patients might present complex acid-base disorders, even when the pH, $PaCO_2$, HCO_3 and BD/E levels are normal.

References

Crawford A. (2004): An audit of the patient's experience of arterial blood gas testing. Br. J. Nurs. **13**, 529–532

Dubin A., Menises M., Masevicius F. D., Moseinco M., Kutscherauer D., Ventrice E., Laffaire E., Estenssoro E. (2007): Comparison of three different methods of evaluation of metabolic acid-base disorders. Crit. Care Med. **35**, 1264–1270

DuBose T. D. (2005): Metabolic acidosis and alkalosis. In: Textbook of Critical Care. (5th edition), (Eds. M. P. Fink, E. Abraham, J. L. Vincent and P. M. Kochanek), pp. 1069–1083, Elsvier Saunders, Philadelphia

Eachempati S. R., Reed R. L., Barie P. S. (2003): Serum bicarbonate concentration correlates with arterial base deficit in critically Ill patients. Surg. Infect. **4**, 193–197

Fencl V., Jabor A., Kazda A., Figge J. (2000): Diagnosis of metabolic acid-base disturbances in critically ill patients. Am. J. Respir. Crit. Care Med. **162,** 2246–2251

FitzSullivan E., Salim A., Demetriades D., Asensio J., Martin M. J. (2005): Serum bicarbonate may replace the arterial base deficit in trauma intensive care unit. Am. J. Surg. **190**, 941–946

Gunnerson K. J., Saul M., He S., Kellum J. A. (2006): Lactate versus non-lactate metabolic acidosis: a retrospective outcome evaluation of critically ill patients. Crit. Care. **10,** R22

Kellum J. A. (2000): Determinants of blood pH in health and disease. Crit. Care. **4**, 6–14

Kellum J. A. (2005): Acid-base disorders. In: Textbook of Critical Care. (5th edition), (Eds. M. P. Fink, E. Abraham, J. L. Vincent and P. M. Kochanek), pp. 51–65, Elsvier Saunders, Philadelphia

Knaus W. A., Draper E. A., Wagner D. P., Zimmerman J. E. (1985): APACHE II: a severity of disease classification system. Crit. Care Med. **13**, 818–829

Le Gall J. R., Lemeshow S., Saulnier F. (1993): A new simplified acute physiology score (SAPS II) based on a European/North American multicenter study. JAMA **270**, 2957–2963

Lujan E., Howard R. (2006): Venous bicarbonate correlates linearly with arterial base deficit only if pH is constant. Arch. Surg. **141**, 105

Martin M. J., FitzSullivan E., Salim A., Berne T. V., Towfigh S. (2005): Use of serum bicarbonate measurement in place of arterial base deficit in the surgical intensive care unit. Arch. Surg. **140,** 745–751

Moreno R. P., Metnitz B., Adler L., Hoechtl A., Bauer P., Metnitz P. G. (2008): Sepsis mortality prediction based on predisposition, infection and response. Intensive Care Med. **34**, 496–504

Moreno R. P., Vincent J. L., Matos R., Mendonca A., Cantraine F., Thijs L., Takala J., Sprung C., Antonelli M., Bruining H., Willatts S. (1999): The use of maximum SOFA score to quatify organ dysfunction/failure in intensive care. Results of a prospective multicentre study. Intensive Care Med. **25**, 686–696

Rhodes A., Cusack R. J. (2000): Arterial blood gas analysis and lactate. Curr. Opin. Crit. Care **6**, 227–231

Rivers E. P., Krause J. A., Jacobsen G., Shah K., Loomba M., Otero R., Childs E. W.(2007): The influence of early hemodynamic optimization on biomarker patterns of severe sepsis and septic shock. Crit. Care Med. **35**, 2016–2024

Rodriguez Montalban R., Martinez de Guerenu Alonso M. A., Perez-Cerda Silvestre F., Cortes Guerrero M., del Campo Sanchez I., Real Navacerrada M. I., Davila Munoz P. (2000): Acute ischemia of the hand as a complication of radial artery catheterization: apropos of 2 cases following abdominal sarcoma surgery. Rev. Esp. Anestesiol. Reanim. **47**, 480–484 (in Spanish)

Sterns R. H. (2003): Fluid, electrolyte, and acid-base disturbances. J. Am. Soc. Nephrol. **2**, 1–33

Stewart P. A. (1983): Modern quantitative acid-base chemistry. Can. J. Physiol. Pharmacol. **61**, 1441–1464

Tuhay G., Pein M. C., Masevicius F. D., Olmos Kutscherauer D. O., Dubin A. (2008): Severe hyperlactatemia with normal base excess: a quantitative analysis using conventional and Stewart approaches. Crit. Care **12**, R66

Wallach S. G. (2004): Cannulation injury of the radial artery: diagnosis and treatment algorithm. Am. J. Crit. Care **13**, 315–319

Wiederseiner J. M., Muser J., Lutz T., Hulter H. N., Krapf R. (2004): Acute metabolic acidosis: characterzation and diagnosis of the disorder and the plasma potassium response. J. Am. Soc. Nephrol. **15**, 1589–1596

Screening of vascular calcifications in patients with end-stage renal diseases

Tatjana Damjanovic[1], Zivka Djuric[1], Natasa Markovic[2], Sinisa Dimkovic[2], Zoran Radojicic[3] and Nada Dimkovic[1]

[1] *Clinical Department for Renal Diseases, Zvezdara University Medical Center, Belgrade, Serbia*
[2] *Clinical Department for Cardiology, Zvezdara University Medical Center, Belgrade, Serbia*
[3] *Faculty of Organizational Sciences, Institute for Statistics, Belgrade, Serbia*

Abstract. Vascular calcifications (VC) are a major contributor to the massively increased mortality in hemodialysis (HD) patients. The present study aimed to detect arterial media and intima calcifications in HD patients and to evaluate potential risk factors.

214 patients aged 59.0 ± 11.0 years on HD for 6.39 ± 4.59 years were studied. VC were scored based on to plain radiographs. Potential risk factors were assessed.

Out of the 214 patients studied, only 14% did not display any detectable VC. Using plain radiographs calcifications could be detected in 136 (63.6%) patients. Calcified plaques on carotid arteries were detected in 168 (78.4%) patients. There was the highest frequency of patients with the most pronounced calcifications. Calcifications of heart valves were detected in 89 (44.1%) patients. Univariante analysis indicate that risk to develop VC is present in older patients, patients with longer dialysis vintage, thicker intima media, higher lumen diameter and mitral valve calcifications. Multivariate multinomial logistic regression analysis revealed these factors as independent predictors of VC in dialysis patients.

Our data confirm a high prevalence of VC in HD patients, their association with older ages, longer dialysis vintage, and presence of valvular calcifications and early markers of atherosclerosis.

Key words: Hemodialysis — Arterial calcifications — Atherosclerosis — Cardiovascular disease — Conventional radiography — Echosonography

Introduction

Cardiovascular disease is common among patients with end-stage renal disease (ESRD), accounting for approximately half of the deaths in those treated with regular hemodialysis (HD) (Go et al. 2004; Brancaccio and Zoccali 2006). Arterial disease due to vascular calcifications (VC) and left ventricular hypertrophy are two principal risk factors for the high rate of cardiovascular mortality. There are two types of arterial calcifications: atherosclerotic vascular lesions with calcium accumulation in the intimal layer of arteries, usually together with localized accumulations of lipid, macrophages and fibrous tissue; medial calcifications – Moenckeberg's sclerosis, typically affects the medial wall of arteries, not usual in general population, but only in diabetic and uremic patients (Kimura et al. 1999; Davies and Hruska 2001; O´Hare et al. 2002; Goodman 2004; Yildiz et al. 2004).

The underlying cause of VC remains uncertain, but there is now strong evidence that it is an active cellular and regulated process. Beside traditional risk factors, hyperparathyroidism, isolated hyperphosphataemia, administration of calcium-containing phosphate binders and vitamin D analogues, inflammation, deficiency in circulating inhibitors of calcification and adynamic bone disease have all been proposed to contribute to VC (Hayden et al. 2005; Shanahan 2005; Qunibi 2005).

Consequences of medial VC include diminished arterial compliance and arterial wall thickening, which can adversely

Correspondence to: Tatjana Damjanovic, Clinical Department for Renal Diseases, Zvezdara University Medical Center, Dimitrija Tucovića Street 161, Belgrade, Serbia
E-mail: damtanja@beotel.yu

affect systemic blood pressure and modify hemodynamic stresses upon the myocardium and large arteries (London et al. 2002; Tozawa et al. 2002). Consequences of intimal VC include reductions in blood flow, vascular occlusion and thrombosis (O´Hare et al. 2002; Tozawa et al. 2002; Yildiz et al. 2004; Okamoto et al. 2006). Calcifications of the myocardium and cardiac valves represent additional serious cardiovascular complications (Wang et al. 2005).

The arterial tree has considerable variability in the susceptibility and the type of calcification. In older patients with ESRD, calcification in the aortic wall and radial artery consistently involves both the intima and media, whereas in younger patients, isolated mediasclerosis predominates especially in blood vessels of lower extremities (Moe et al. 2002).

Several radiographic techniques have been used to detect soft-tissue and VC in patients with chronic renal failure, but none has gained widespread acceptance as a method to reliably assess the prevalence, extent or progression of VC in this patient population. Conventional radiographs often reveal calcifications within medium-sized and large arteries (Adragao et al. 2004; Goodman 2004; Hernandez et al. 2005). Improvements in the spatial resolution achievable with ultrasound have led to the widespread use of this noninvasive method for evaluating the cardiovascular system. Measurements of intimal medial wall thickness in large arteries can be obtained, and atherosclerotic plaques can be visualized in the aorta, common femoral arteries and common carotid arteries. Localized calcium deposits can be detected in the walls of arteries and in atherosclerotic plaques (O´Hare et al. 2002; London et al. 2003; Goodman 2004). Echocardiography can also be used to document the presence of calcium deposits within cardiac valves, and to assess the impact of this abnormality on valve motion and function (Goodman and Salusky 2001; Bellasi and Raggi 2007). Electron-beam computed tomography (EBCT) and spiral computed tomography have been developed as noninvasive, sensitive, but very expensive techniques to screen for the presence of coronary artery calcifications (Moe et al. 2002; Moe and Chen 2008). Braun et al. (1996) showed that coronary artery calcium score revealed by EBCT was from 2.5-fold to 5-fold higher in the dialysis patients as compared with non-dialysis patients with coronary artery disease .

The aim of this study was screening of VC in patients undergoing chronic HD using sensitive, non-invasive radiographic methods and evaluation of the risk factors for their appearance.

Materials and Methods

Population

This single-center cross-sectional study included 214 patients, 116 males and 98 females, on HD for at least six months (mean 6.39 ± 4.59 years) and with a mean age of 59.0 ± 11.0 years. Patients were maintained on bicarbonate HD, three times per week for 12–15 h. Etiologies for ESRD were hypertensive nephrosclerosis, 118 (54.6%); glomerulonephritis, 31 (14.4%); autosomal-dominant polycystic kidney disease, 20 (10.2%); pyelonephritis 22 (10.2%), tubulointerstitial disease and obstructive nephropathy, 3 (1.4%); diabetic nephropathy, 12 (5.6%) and Balkan endemic nephropathy, 8 (3.7%). The following phosphate binders and vitamin D medications were given: calcium carbonate, 159 (75%); aluminum hydroxide, 21 (10%); calcium carbonate/aluminum hydroxide, 24 (11%); no phosphate binder, 8 (4%); 1,25-OH-vitamin D3, 146 (69%); 1α-OH-vitamin D3, 14 (6.6%); warfarin, 5 (2.4%); calcium antagonists, 89 (42%). Cumulative dose of calcium carbonate for six months was 686.2 ± 280.4 g. Viral hepapitis B was detected in 21(9.7%) and viral hepatitis C infection in 61 (28.2%) patients. Due to local circumstances, no patient used lipid lowering drugs, and anti-hypertensive drugs were prescribed as necessary to maintain a post-weekend pre-dialysis blood pressure below 140/90 mmHg. The study protocol was approved by the Ethics Committee of the Zvezdara University Medical Centre (Belgrade, Serbia) and each patient gave informed consent.

Calcification assessment

Common carotid arteries were investigated by B-mode ultrasonography (using the ALOCA SSD 2000 system equipment with 7.5 MHz linear transducers). A trained sonographer evaluated intima media thickness (IMT) and carotid plaques in both common carotid arteries 4 cm from the bulbs, within carotid bulbs and the first 2 cm of the internal and external carotid arteries (Kawagishi et al. 1995). Plaques were defined as echogenic structures showing protrusion into the lumen with focal widening that was 50% greater than the IMT of adjacent sites. Highly echogenic plaques producing bright white echoes with shadowing were considered to be calcifications (Hunt et al. 2001). Such plaques were defined as representing arterial intima calcification (AIC) pattern. To determine the intraobserver variability of IMT measurements, one experienced investigator examined 30 randomly selected patients twice within 14 days. Intraobserver variability was 8%.

Arterial media calcifications (AMC) were detected by plain radiography of the pelvis, both hands and the region of the vascular access. The presence of linear VC was defined as a pattern indicating AMC. Extent of calcifications on plain radiography was analyzed semi-quantitatively by an overall score (Adragao plus region of vascular access score). X-rays of pelvis and one hand were divided into 4 sections by a median vertical line and horizontal line just above the upper rim of the femoral heads and the metacarpal bones, respectively. The presence of linear VC in

each quadrant was counted as 1 point, thus a maximum of 8 points could be achieved (Hunt et al. 2001). In addition to the Adragao score, calcifications detected by X-ray of the fistula arm (fistula itself, ulnar and radial artery) were counted as 1 point each. The investigations were performed by three experienced physicians blinded to patient's information.

Baseline echocardiography was performed with an Aspen-Acuson device equipped with a 2.5 MHz probe allowing M-mode, two-dimensional, and pulsed Doppler measurements. Measurements were made according to the recommendations of the American Society of Echocardiography (Feigenbaum 1994). To determine the intraobserver variability of echocardiographic detection of valvular calcification, one experienced investigator examined 30 randomly selected patients twice within 14 days. Intraobserver variability was 4%.

Biochemistry

Average values of plasma total protein, total cholesterol and triglycerides during the previous year were assessed as traditional risk factors and average values of plasma calcium, phosphorus, intact parathormon (iPTH) and calcium x phosphate product, C-reactive protein (CRP), as non-traditional factors. Inhibitors of VC (fetuin-A and matrix-Gla protein (MGP)) were also detected. All parameters were analyzed by standard laboratory procedures using an automated analyzer. iPTH was assessed by chemiluminescence's assay (Diagnostic Product Corporation, USA). Serum analysis for high sensitivity CRP was performed by particle-enhanced immunonephelometry using a standard 'CardioPhase hsCRP' for 'BNII' (Dade Behring Holding GmbH, Liederbach, Germany). The nephelometric method for association of serum fetuin-A was adopted from a serum ELISA method (Dade Behring Holdings, Liederbach, Germany). The ELISA measurement of undercarboxylated MGP (ucMGP) was conducted as previously described (Schurgers et al. 2005).

Statistics

Statistical calculations were performed using the SPSS software. Data were expressed as percentages for discrete factors, and mean values for continuous variables. Statistical analyses include descriptive statistics and exploratory analyses. Mantel-Haenszel Common Odds Ratio Estimate test was used for risk estimation for VC. Multinominal logistic regression analyses were used to determine odds ratios for calcifications associated with clinical and biological parameters. In all comparisons, $p < 0.05$ was considered statistically significant.

Results

Prevalence of calcification patterns

Out of the 214 patients studied, only 30 did not display any detectable VC (14%). Using plain radiographs calcifications of pelvis, hands and vascular access, calcifications could be detected in 136 (63.6%) patients (Figure 1). Calcified plaques on carotid arteries were detected in 168 (78.4%) patients. Mean value of IMT was 0.79 ± 0.09 mm and lumen diameter 7.27 ± 0.86 mm. There was the highest frequency of patients with the most pronounced calcifications (AIC plus AMC) (Figure 2). Calcifications of heart valves were detected in 89 (44.1%) patients. Mitral valves calcifications were detected in 68 (33.8%), and aortic valves calcifications in 42 (20.9%) patients.

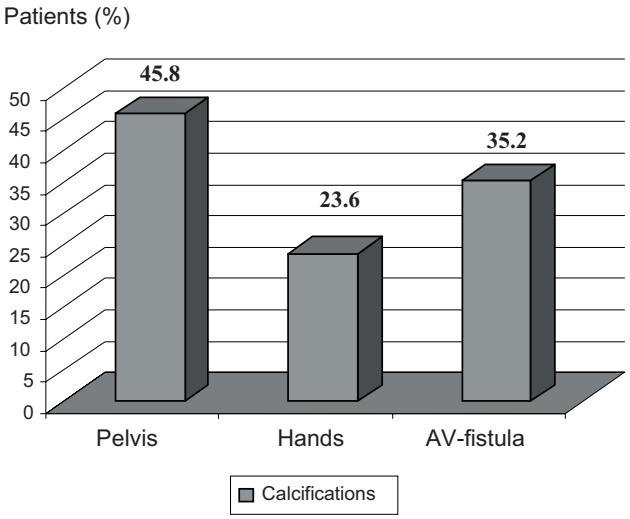

Figure 1. Distribution of VC detected by plain radiography. Calcifications of pelvis, hands and vascular access were detected in 136 (63.6%) of patients. Most of them have calcifications in two or all analyzed regions. The most frequent calcifications were in region of pelvis (45, 8%). AV, arteriovenous.

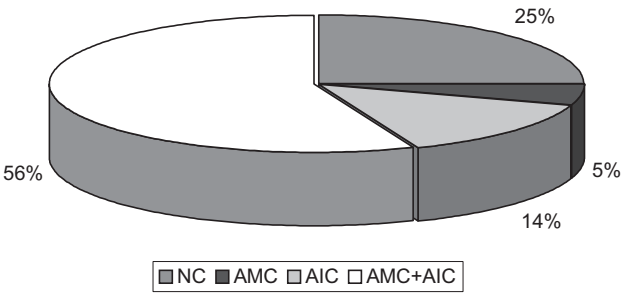

Figure 2. Distribution of different localizations of VC. There is the highest frequency of patients with mixed calcifications (isolated AMC plus AIC, 56%). NC, non-calcifying group of patients; AMC, arterial media calcifications; AIC, arterial intima calcifications

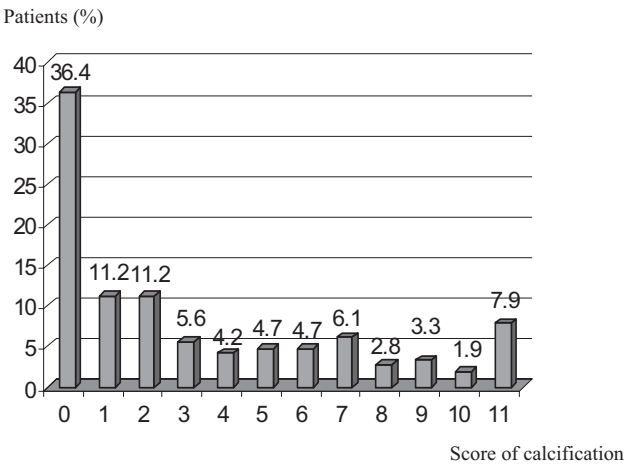

Figure 3. Frequency of patients with different overall score of calcifications detected by plain radiography. Overall score included Adragao score of blood vessels from pelvis and both hands (description in the text), plus blood vessels of arteriovenous fistula.

Extent of calcifications using owerall score is presented in Figure 3. Biochemical parameters of dialysis populations are presented in Table 1.

Risk factors for VC

Using receiver operating characteristic analysis, four out of 16 parameters tested (age, dialysis vintage, body mass index (BMI), phosphates, calcium, calcium-phosphate product, total proteins, bicarbonates, hemoglobin, total cholesterol, triglycerides, CRP, fetuin-A, ucMGP, IMT and lumen diameter of common carotid arteries), were found to be significat risk factors for VC: age (area under curve (AUC) = 0.723, p = 0.000, 95% confidence interval (CI) = 0.64–0.81, positive/negative ratio (P/N) = 54), dialysis vintage (AUC = 0.632, p = 0.020, 95% CI = 0.53–0.73, P/N = 4), IMT (AUC = 0.756, p = 0.000, 95% CI = 0.68–0.84, P/N = 0.75) and lumen diameter of common carotid arteries (AUC = 0.654, p = 0.007, 95% CI = 0.56–0.75, P/N = 6.98).

Results of the univariante analysis (Mantel-Haenszel Common Odds Ratio Estimate test) are shown in Table 2. Risk to develop VC is present in older patients (odds ratio (OR) = 2.45; relative risk (RR) = 1.6), patiens with longer dialysis vintage (OR = 5.6; RR = 2.4), thicker intima media (OR 3.94; RR 2.0), higher lumen diameter (OR 2.28; RR 1.5) and mitral valve calcifications (OR 3.7; RR = 2.7).

Multivariate multinomial logistic regression analysis reveled age, dialysis vintage, IMT, lumen diameter and valvular calcifications as an independent predictors of VC in dialysis patients (Table 3).

Table 1. Laboratory parameters in dialysis population. Data include main parameters that may be significant in the pathogenesis of VC

Variables	Values	Normal rang
Calcium (mmol/l)	2.29 ± 0.18	2.20–2.7
Phosphorous (mmol/l)	1.62 ± 0.42	0.60–1.5
iPTH (pg/ml)	363 ± 456	10–69
Ca x PO4 ($mmol^2/l^2$)	3.74 ± 1.10	<4.50
Hemoglobin (g/dl)	9.40 ± 1.50	12–18
Serum protein (g/l)	67.20 ± 4.99	64–83
Serum cholesterol (mmol/l)	5.13 ± 1.20	3.6–5.2
Serum triglycerides (mmol/l)	2.28 ± 1.28	0.4–1.7
Bicarbonates (mmol/l)	21.20 ± 2.70	21–31
CRP (mg/l)	9.46 ± 17.33	0–5
Fetuin-A (g/l)	0.55 ± 0.14	0.5–1.0
ucMGP(nmol/l)	185.4 ± 100.8	not defined

iPTH, intact parathormon; CRP, C-reactive protein; ucMGP, undercarboxylated matrix-Gla protein.

Table 2. Results of the univariante analysis (Mantel-Haenszel Common Odds Ratio Estimate test) of factors predicting VC

Parameter	OR	p	OR 95% CI	RR
Age Cutoff point – 54 years	2.45	0.028	1.1–5.5	1.6
Dialysis vintage Cutoff point – 4 years	5.62	0.000	2.4–13.0	2.4
Calcifications of mitral valve	3.70	0.020	1.2–11.1	2.7
IMT Cutoff point – 0.75 mm	3.94	0.001	1.7–8.9	2.0
Lumen diameter Cutoff point – 6.98 mm	2.28	0.039	1.05–5.0	1.5

Factors of significance are: age above 54 years, dialysis vintage longer then 4 years, calcifications of mitral valve, intima media thickness (IMT) above 0.75 mm and lumen diameter of common carotid arteries higher of 6.98 mm. OR, odds ratio; CI, confidence interval; RR, relative risk.

Table 3. Multivariate multinomial logistic regression analysis of the calcification risk in dialysis patients. Several factors were recognized to be associated with calcifications risk

Parameters	Score	p
Age	17.833	0.000
Dialysis vintage	4.994	0.025
IMT	18.555	0.000
Lumen diameter	5.289	0.021
Aortic valve calcifications	7.787	0.005
Mitral valve calcifications	6.600	0.010
Presence of valvular calcifications	11.768	0.001

Model R^2 (Nagelkerke) = 0.806. IMT, intima media thickness.

Discussion

In the present study, we found that of 214 randomly selected patients undergoing chronic HD, 86% have their arteries calcified. High prevalence of both media and intima calcifications (56 %) may be explained by similar pathogenetic mechanism proposed by some authors (Goodman 2004; Cozzolino et al. 2005) and this may also be an explanation for small percent of patient with isolated media calcifications (5%). Literature reports on this issue are not uniform. Salgeira et al. (2003) found VC in 67.5% dialysis patients using plain radiography of thorax, abdomen and pelvis. Study from Japan (Okamoto et al. 2006) included 515 patients on maintenance HD and by radiography of the left abdomen, abdominal aortic calcification was found in 56.5%. Also, London et al. (2003) found 36% of HD patients to be free of VC using plain radiography. Chertow et al. (2004) found that 17% of HD subjects had no coronary calcifications and 20% had no aortic calcifications using EBCT. Stompor et al. (2003) found that 29% of their peritoneal dialysis population remained calcium-free after 12 months. Moe et al. (2003) found 28% of HD patients had no evidence of coronary calcification using spiral CT. Oh et al. (2003) using CT scan, found coronary calcifications in 92% young adult ESRD patients with childhood-onset chronic renal failure either undergoing dialysis or after transplantation. Difference between reports may probably be explained by different methodology used and different population of patients that were included into studies.

Valvular calcifications were detected in 44% patients (mitral and aortic valve). Ix et al. (2007) detected mitral valve calcifications in 20% cardiovascular patients without renal disease. Braun et al. (1996) were detected aortic valve in 55%, and mitral valve calcifications in 59% dialysis patients using more sensitive method – EBCT.

Recently Muntner et al. (2007), revealed the importance of simple method including demographic information, dialysis vintage, abdominal aorta calcification and mitral and aortic valve calcification in predicting of coronary artery calcifications with very good accuracy. Furthermore, they concluded even simpler method warrants consideration and that omitting the echocardiogram would result in substantially reduced test cost and feasibility. It seems that every dialysis center search for the most available, feasible, less costly and, on the first place, most accurate diagnostic method for VC. Our intention was to follow the NKF-DOQI (National Kidney Foundation Disease Outcomes Quality Initiative) recommendation about screening dialysis patients for VC.

For better accuracy, standard Adragao score was strengthened by using additiononal scores (for fistula calcifications). Evaluation of media calcifications by using extended Adragao score provided us additional information about the distribution and extent of VC. We believe that follow-up data will be more conclusive about the role of scoring of calcifications in evaluation of calcifications progression.

For many years, calcifications of soft tissues and arteries were considered to passively result from calcium and phosphate precipitation due to a high calcium-phosphate ion product leading to supersaturated plasma. However, at least in the case of VC there is now strong evidence that it is an active and regulated process that may be initiated by a number of different mechanisms. Human and mouse genetic findings have determined that blood vessels normally express inhibitors of mineralization, such as pyrophosphate, MGP, fetuin/2-HS-glycoprotein and osteoprotegerin, and that lack of these molecules leads to spontaneous VC and increased mortality. The presence of bone proteins such as osteopontin, osteocalcin, and BMP2, matrix vesicles, and outright bone and cartilage formation in calcified vascular lesions, has suggested that osteogenic mechanisms may also play a role in VC. Cells derived from the vascular media undergo bone- and cartilage-like phenotypic change and calcification *in vitro* under various conditions. Bone turnover leading to release of circulating nucleation complexes (aggregates of calcium-phosphate and proteins released from remodeling bone that may initiate ectopic mineralization), and cell death can provide phospholipids rich membranous debris and apoptotic bodies that may serve to nucleate apatite, especially in diseases where necrosis and apoptosis are prevalent, such as atherosclerosis. Abnormalities in mineral metabolism that enhance the calcium-phosphate product may further exacerbate VC initiated by any of these mechanisms (Giacheli 2004; Johnson et al. 2006; Ketteler and Floege 2006).

In the present study univariate analysis indicated that risk for VC increases in older patients, patients with longer dialysis vintage, thicker intima media, higher lumen diameter and detected valvular calcifications. In multivariate regression analysis the same factors remained as independent predictors of VC.

Krasniak et al. (2007) evaluated several risk factors for coronary artery calcifications in univariate analysis (age, BMI, serum iPTH, CRP, interleukin-6, 25-OH-vitamin D3, transforming growth factor-β, plateled derived growt factor and carotid artery IMT), but in multivariate regression analysis only age and carotid artery IMT remained as independent predictors of coronary artery calcifications. Hermans et al. (2007) evaluated the relation between serum fetuin-A and arterial stiffness, as a feature of predominant VC. Fetuin-A, well known inhibitor of VC, appeared not to be an independent predictor of aortic stiffness in a dialysis population with a low level of inflammatory activity. All above suggest a great complexity of VC process and more clinical and basic research data in that field are still needed.

The current study needs to be considered in the context of its limitations. At the moment, there are no enough data

to confirm advantage or inferiority of "classic" X-ray and echosonography imaging over more modern and sophisticated (but also less available) diagnostic procedures. Unless we are provided with those data, dialysis patients should be regularly monitored according to currently accepted guidelines. The cross-sectional character of present study assessing most serum parameters at only one single time point, decreases the potential predictive power of individual serum parameters. This is, why, at least in the case of rapidly fluctuating parameters such as phosphate and calcium, we used time-averaged values for the analyses.

In summary, the data presented reveal an extremely high percentage of dialysis patients with VC and most of them exhibited both intimal and medial localizations. By multivariate analysis, significant risk factors for VC were older age, longer dialysis vintage, thicker intima media, higher lumen diameter and presence of valvular calcifications. Further studies are needed for better understanding calcification process and its consequences.

References

Adragao T., Pires A., Lucas C., Birne R., Magalhaes L., Gonçalves M., Negrao A. P. (2004): A simple vascular calcification score predicts cardiovascular risk in haemodialysis patients. Nephrol. Dial. Transplant. **19**, 1480–1488

Amann K., Tyralla K., Gross M. L., Eifert T., Adamczak M., Ritz E. (2003): Special characteristics of atherosclerosis in chronic renal failure. Clin. Nephrol. **60**, S13–21

Bellasi A., Raggi P. (2007): Techniques and technologies to assess vascular calcification. Semin. Dial. **20**, 129–133

Brancaccio D., Zoccali C. (2006): The continuous challenge of cardiovascular and bone disease in uraemic patients: clinical consequences of hyperphosphatemia and advanced therapeutic approaches. J. Nephrol. **19**, 12–20

Braun J., Oldendorf M., Moshage W., Heidler R., Zeitler E., Luft F. C. ((1996): Electron beam computed tomography in the evaluation of cardiac calcification in chronic dialysis patients. Am. J. Kidney Dis. **27**, 394–401

Chertow M. G., Raggi P., Chasan-Taber S., Bommer J., Holzer H., Burke S. K. (2004): Determinants of progresive vascular calcification in haemodialysis patients. Nephrol. Dial. Transplant. **19**, 1489–1497

Cozzolino M., Brancaccio D., Gallieni M., Slatopolsky E. (2005): Pathogenesis of vascular calcification in chronic kidney disease. Kidney Int. **68**, 429–436

Davies R. M., Hruska A. K. (2001): Patophisiological mechanisms of vascular calcification in end stage renal disease. Kidney Int. **60**, 472–480

Feigenbaum H. (1994): Echocardiographic evaluation of cardiac chambers (wall thickness, mass and stress). In: Echocardiography. (5th edition), pp. 134–173, Philadelphia

Giacheli C. M. (2004): Vascular calcification mechanisms. J. Am. Soc. Nephrol. **15**, 2959–2964

Go A. S., Chertow G. M., Fan D., McCulloch C. E., Hsu C. Y. (2004): Chronic kidney disease and the risks of death, cardiovascular events, and hospitalisation. N. Engl. J. Med. **351**, 1296–1305

Goodman W. G., Salusky I. B. (2001): Non invasive assessments of cardiovascular disease in patients with renal failure. Curr. Op. Neph. Hyp. **10**, 365–369

Goodman W. G. (2004): Importance of hyperphosphataemia in the cardio-renal axis. Nephrol. Dial. Transplant. **19**, (Suppl.) i4–8

Hayden M. R., Tyagi S. C., Kolb L., Sowers J. R., Khanna R. (2005): Vascular ossification – calcification in metabolic syndrome, type 2 diabetes mellitus, chronic kidney disease, and calciphylaxix – calcific uremic arteriolopathy: the emergening role of sodium thiosulfate. Cardiovasc. Diabetol. **4**, 4

Hermans M. M., Vermeer C., Kooman J. P., Brandenburg V., Ketteler M., Gladziwa U., Rensma P. L., Leunissen K. M., Schurgers L. J. (2007): Undercarboxylated matrix GLA protein levels are decreased in dialysis patients and related to parameters of calcium-phopsphate metabolism and aortic augmentation index. Blood Purif. **25**, 395–401

Hernandez D., Rufino M., Bartolomei S., González-Rinne A., Lorenzo V., Cobo M., Torres A. (2005): Clinical impact of preexisting vascular calcifications on mortality after renal transplantation. Kidney Int. **67**, 2015–2020

Hunt K. J., Sharrett A. R., Chambless L. E., Folsom A. R., Evans G. W., Heiss G. (2001): Acustic shadowing on B-mode ultrasound of the carotid artery predicts ischemic stroke: the atherosclerosis risk in communities (ARIC) study. Stroke **32**, 1120–1126

Ix J. H., Chertow G. M., Shlipak M. G., Brandenburg V. M., Ketteler M., Whooley M. A. (2007): Association of fetuin-A with mitral annular calcification and aortic stenosis among persons with coronary heart disease: data from the heart and soul study. Circulation **15**, 2533–2539

Johnson J. L., Baker A. H., Oka K., Chan L., Newby A. C., Jackson C. L., George S. J. (2006): Suppression of atherosclerotic plaque progression and instability by tissue inhibitor of metalloproteinase-2: involvement of macrophage migration and apoptosis. Circulation **113**, 2435–2444

Kawagishi T., Nishizawa Y., Konishi T., Kawasaki K., Emoto M., Shoji T., Tabata T., Inoue T., Morii H. (1995): High resolution B-mode ultrasonography in evaluation of atherosclerosis in uremia. Kidney Int. **48**, 826–838

Ketteler M., Floege J. (2006): Calcification and the usual suspect phosphate: still guilty but there are other guys behind scenes. Nephrol. Dial. Transplant. **21**, 33–35

Kimura K., Saika Y., Otani H., Fujii R., Mune M., Yukawa S. (1999): Factors associated with calcification of the abdominal aorta in haemodialysis patients. Kidney Int. **56**, 238–240

Krasniak A., Drozdz M., Pasowicz M., Chmiel G., Michałek M., Szumilak D., Podolec P., Klimeczek P., Konieczyńska M., Wicher-Muniak E., Tracz W., Khoa T. N., Souberbielle J. C., Drueke T. B., Sulowicz W. (2007): Factors involved in vascular calcifications and atherosclerosis in maintenance haemodialysis patients. Nephrol. Dial. Transplant. **22**, 515–521

London G. M., Marchais S. J., Guerin A. P., Metivier F., Adda H. (2002): Arterial structure and function in end stage renal disease. Nephrol. Dial. Transplant. **17**, 1713–1724

London G. M., Guérin A. P., Marchais S. J., Métivier F., Pannier B., Adda H. (2003): Arterial media calcification in end-stage rebal disease: impact on all – cause and cardiovascular mortality. Nephrol. Dial. Transplant. **18**, 1731–1740

Moe S. M., O'Neill K. D., Duan D., Ahmed S., Chen N. X., Leapman S. B., Fineberg N., Kopecky K. (2002): Medial artery calcification in ESRD patients is associated with deposition of bone matrix proteins. Kidney Int. **61**, 638–647

Moe S. M., O'Neill K. D., Fineberg N., Persohn S., Ahmed S., Garrett P., Meyer C. A. (2003): Assessment of vascular calcification in ESRD patients using spiral CT. Nephrol. Dial. Transplant. **18**, 1152–1158

Moe S. M., Chen N. X. (2008): Mechanisms of vascular calcification in chronic kidney disease. J. Am. Soc. Nephrol. **19**, 213–216

Muntner P., Ferramosca E., Bellasi A., Block G. A., Raggi P. (2007): Development of a cardiovascular calcification index using simple imaging tools in haemodialysis patients. Nephrol. Dial. Transplant. **22**, 508–514

Oh J., Wunsch R., Turzer M., Bahner M., Raggi P., Querfeld U., Mehls O., Schaefer F. (2002): Advanced coronary and carotid arteriopathy in young adults with childhood-onset chronic renal failure. Circulation **106**, 100–105

O´Hare A. M., Hsu C. Y., Bacchetti P., Johansen K. L. (2002): Peripheral vascular disease risk factors among patients undergoing hemodialysis. J. Am. Soc. Nephrol. **13**, 497–450

Okamoto K., Oka M., Maesato K., Ikee R., Mano T., Moriya H., Ohtake T., Kobayashi S. (2006): Peripheral arterial occlusive disease is more prevalent in patients with hemodialysis: comparison with the findings of multidetector-row computed tomography. Am. J. Kidney Dis. **48**, 269–276

Qunibi W. Y. (2005): Dyslipidemia and progresion of vascular calcifications in patients with end-stage renal diseases. Kidney Int. **67**, S43–50

Salgueira M., del Toro N., Moreno-Alba R., Jiménez E., Aresté N., Palma A. (2003): Vascular calcification in uremic patients: a cardiovascular risk? Kidney Int. **63**, 119–121

Schurgers L. J., Teunissen K. J., Knapen M. H., Kwaijtaal M., van Diest R., Appels A., Reutelingsperger C. P., Cleutjens J. P., Vermeer C. (2005): Novel conformation-specific antibodies against matrix gamma-carboxyglutamic acid (Gla) protein: undercarboxilated matrix Gla protein as a marker for vascular calcification. Arterioscler. Thromb. Vasc. Biol. **25**, 1629–1633

Shanahan C. M. (2005): Mechanisms of vascular calcification in renal disease. Clin. Nephrol. **63**, 146–157

Stompor T., Pasowicz M., Sułłowicz W., Dembińska-Kieć A., Janda K., Wójcik K., Tracz W., Zdzienicka A., Klimeczek P., Janusz-Grzybowska E. (2003): An association between coronary artery calcification score, lipid profile, and selected markers of chronic inflammation in ESRD patients treated with peritoneal dialysis. Am. J. Kidney Dis. **41**, 203–211

Tozawa M., Iseki K., Iseki C., Takishita S. (2002): Pulse pressure and risk of total mortality and cardiovascular events in patients on chronic hemodialysis. Kidney Int. **61**, 717–726

Wang A.Y., Ho S. S., Wang M., Liu E. K., Ho S., Li P. K., Lui S. F., Sanderson J. E. (2005): Cardiac valvular calcifications as a marker of atherosclerosis and arterial calcifications in end stage renal diseases. Arch. Intern. Med. **165**, 327–332

Yildiz A., Tepe S., Oflaz H., Yazici H., Pusuroglu H., Besler M., Ark E., Erzengin F. (2004): Carotid atherosclerosis is a predictor of coronary calcification in chronic haemodialysis patients. Nephrol. Dial. Transplant. **19**, 885–891

The righting reflex from a supine to a prone position in the guinea pig fetus

Slobodan Sekulić[1], Damir Lukač[2], Miodrag Drapšin[2], Vesna Suknjaja[1], Goran Keković[3], Gordana Grbić[3] and Ljiljana Martać[3]

[1] *Department of Neurology, University Clinics, Clinical Center of Vojvodina, Novi Sad, Serbia*
[2] *Department of Physiology, Medical Faculty, University of Novi Sad, 21000 Novi Sad, Serbia*
[3] *Institute of Biological Research "Dr. Siniša Stanković", 11000 Beograd, Serbia*

Abstract. The aim of this study was to examine the righting reflex from a supine to a prone position in the albino guinea pig fetus. Ultrasound examinations of one-fetus gestations were performed in the period from the 31st to the 66th day of gestation. The experimental and control group each encompassed 6 fetuses. Fetuses were brought into supine positions relative to the gravity vector by manipulating the pregnant females into the appropriate positions. The control group received 15 mg/kg of diazepam intraperitoneally before the examination to show whether changes in fetal position occurred as the result of passive rotation. In the experimental group, each fetus was examined every other day (summary results: absent 69 times, prone position 10 times, lateral position 29 times). In the control group, each fetus was examined every five days (summary results: absent 42 times). The absence of the righting reflex in the control group was statistically significant (χ^2 = 18.66, df = 1, p = 0.000, $p < 0.05$). The experimental group fetuses assumed a prone position more frequently in the period from the 51st to the 66th day of gestation than in the period from the 31st to the 50th day of gestation (χ^2 = 4.17, df = 1, p = 0.0412, $p < 0.05$), suggesting maturation of the righting reflex.

Key words: Fetus — Reflex — Gestation — Guinea pig

Introduction

The righting reflex from a supine position to a prone position occurs when an individual returns to standing position after being positioned supine. There are two forms of this reflex: air-righting and contact-righting. A variant of the air-righting reflex may be induced in water. The contact-righting reflex can be triggered with tactile and vestibular stimuli, whereas the air-righting reflex and its water variant are prompted by vestibular and visual stimulation (Watt 1976; Pellis et al. 1989). This reflex is important for a fetus because it enables physiological delivery; it was observed in cattle and sheep that the fetus changes its position from a lateral or supine position to a prone position during delivery (Husa et al. 1988; Fraser 1989). To induce this reflex, it is necessary to position an experimental animal into a supine position relative to the gravitational vector. Accordingly, a study of the prenatal presence of the reflex would provide evidence that gravity, as an environmental factor, affects fetal development (Sekulić 2000).

Guinea pigs belong to the group of mammals that display precocious development. Gestation lasts an average of 66 days. Ultrasound observations of the guinea pig fetus have shown that fetal movements first occur around the 26th day of gestation (Sekulić et al. 2009). Studies of exteriorized guinea pig fetuses suggest that the fetuses open their eyes between the 46th and the 50th day of gestation. They become covered with fur from the 52nd to the 57th day of gestation. The righting reflex of moving from a supine to a prone position is present from the 60th day of gestation, as is crawling. Standing and walking are present from the 63rd day of gestation (Avery 1928). The period from the 35th to the 40th day of gestation is characterized by an established

Correspondence to: Slobodan Sekulić, Department of Neurology, Clinical Center of Vojvodina, Hajduk Veljkova 1–7, 21000 Novi Sad, Serbia
E-mail: turija@EUnet.rs; nadlak@yahoo.com

link between the sensory epithelium of the vestibular apparatus and the vestibular ganglion (Heywood et al. 1976; Sobin and Anniko 1983). Myelination of the vestibular nerve begins on approximately the 40th day of gestation (Heywood et al. 1976). The authors of this paper found no data in available literature about cutaneous and proprioceptive receptor maturation in guinea pigs.

Intrauterine examination of the reflex has so far been attempted in a single study in which a pregnant guinea pig with two fetuses was observed on the 63rd day of gestation. No changes were detected with X-rays examination of the two fetuses that had been brought into supine positions during the 15-min observation. A possible explanation for the study's failure is its small sample size. Furthermore, the study's technique of fixing the pregnant female involved pressing the female's abdomen and hence also pressing fetuses, which may have prevented the rotation of the fetuses (Avery 1928).

The aim of this study was to examine the righting reflex from a supine to a prone position in the albino guinea pig fetus. The hypothesis was that when fetuses were brought into supine position, they would return to a prone position.

Materials and Methods

The study subjects were albino guinea pigs (*Cavia porcellus*) obtained from the Department of Biochemistry of the Faculty of Medicine, Novi Sad. The experiments with the animals were approved by the Ethics Committee of the Institute of Neurology in Novi Sad. The guinea pigs were kept in 400 (wide) × 1000 (length) × 300 (hight) mm plastic containers in a harem system: each container held three or four females and one male. Pregnant females were moved to 300 × 300 × 300 mm plastic containers after the 60th day of gestation, where they were kept separate until delivery and, with their respective offspring, for the first 15 days after delivery. The animals were fed a standard commercial-pellet diet and *ad libitum* water enriched with vitamin C (30 mg/100 ml water). Artificial cycles with 12 h of light (08:00–20:00) and 12 h of dark were provided.

Inspection of the vaginal introitus was performed daily, and the day that the vaginal membrane was perforated was considered to be the first day of gestation. The study included only pregnant guinea pigs that bore one fetus each. The number of fetuses was determined by ultrasound examination, and the pregnant guinea pigs were randomly selected for the experimental and control groups. Each group (experimental and control) included 6 pregnant females and 6 fetuses.

The shaving of the abdominal region was conducted during a short-term inhalatory ether narcosis on the 25th day of gestation. The pregnant guinea pigs were supported in a supine position on a 15 × 30 cm board using plastic strips with clasps that were fastened over the thoracic area and the inguinal region from both sides. The strips were pulled through holes in the board near the body of the animal and were fastened on the other side of the board (Figure 1). Pregnant females were calm during examination and showed no signs of distress due to immobilization.

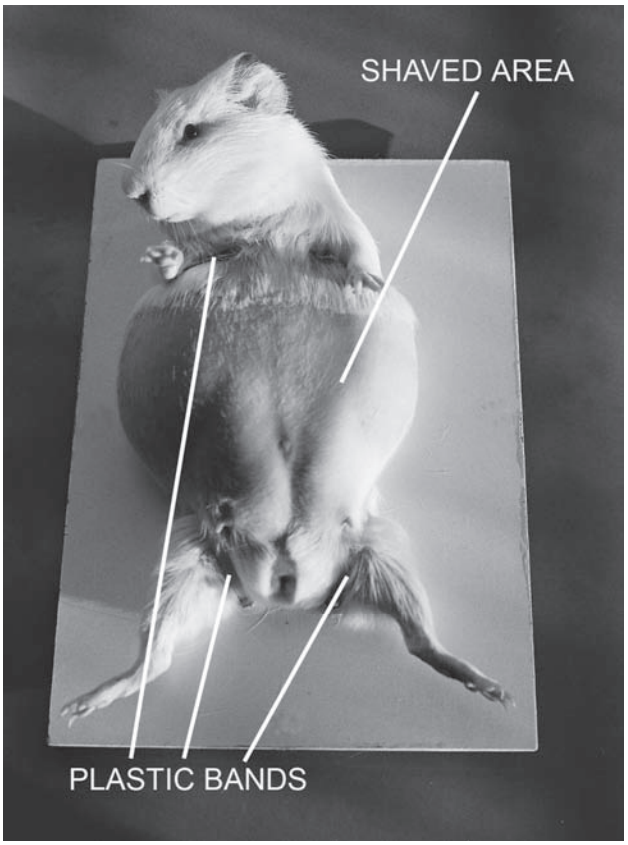

Figure 1. Guinea pig prepared for ultrasonic examination.

Ultrasound examinations were performed using a Toshiba Nemio SSA-550A apparatus with a 6–11 Hz linear probe. Pregnant females were brought into supination by manipulating the boards to which they were fastened. The fetuses' orientations were then determined by tracking them with the ultrasound probe along the longitudinal and transversal axes of the fetuses. The position of each fetus's trunk was determined by the positions of its heart, forelimbs, and hind legs (Figure 2). Next, the board was rotated until the fetus was brought into a supine position relative to gravity, and the examination was then repeated. If a fetus was initially observed in a supine position, then the pregnant female's position was not changed.

During the examinations, the following parameters were observed: absence of any changes in position, rotation to

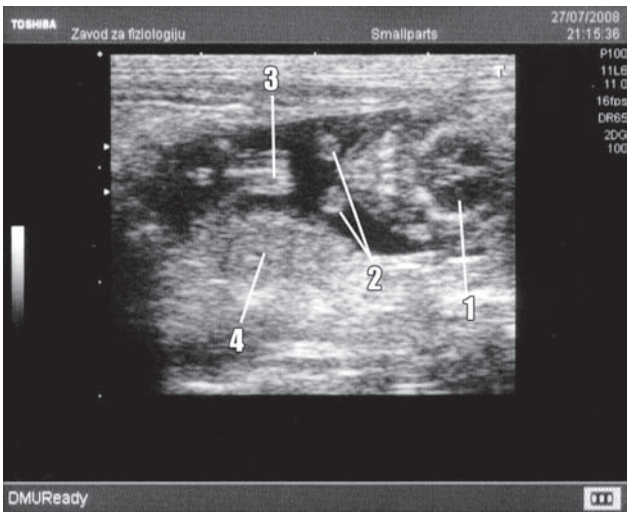

Figure 2. Longitudinal image of a fetus on the 35th day of gestation. 1, head; 2, forelimbs; 3, hind limbs; 4, placenta.

a lateral position, and rotation to a prone position. Rotation to a lateral position was considered an incomplete reflex reaction. The examination was continued until a change in the fetus's position was registered or until the end of the arbitrarily set period of 2 min, whichever came first. The ultrasound examinations began on the 31st day of gestation and lasted until the 66th day of gestation. Each pregnant female in the experimental group had a total of 18 ultrasound examinations during gestation. Examinations were performed every other day.

The control group was formed to show whether changes in fetal positioning occurred as the result of passive fetal rotation. Diazepam has been used to immobilize the human fetus during nuclear magnetic resonance studies (Huisman et al. 2002). In the guinea pig, diazepam passes through the fetoplacental barrier; residual diazepam and its metabolite nordiazepam can be found in the brain of the guinea pig fetus (Ungar and Ecobichon 1986). Diazepam increases the latency of the righting reflex from supine to prone position in adult guinea pig (Scott et al. 1994). For this reason, each animal in the control group received 15 mg/kg of diazepam (Bensedin 10 mg; Galenika, Serbia) intraperitoneally 15 min before each examination. The dosage was determined in a pilot study, when absence of maternal movement and tonus as well as fetal movement was observed only at the dose of 15 mg/kg. Pregnant females weighed from 480 to 750 g each, and the respective administered diazepam dosages ranged from 7.2 to 11.25 mg. In this group, examinations were performed once in every period of 5 days, for a total of 7 examinations during each gestation. Because pregnant females from the control group did not move and were hypotonic for couple hours after examination, in order to avoid their possible injury, they were placed in separate plastic containers measuring 300 × 300 × 300 mm each for the following 24 h.

For statistical analysis, the chi-square test (χ^2-test) was used. When the expected values were less than 5, Fisher's exact test was used instead of the χ^2-test. The level of $p < 0.05$ was adopted in order to determine statistical significance.

Results

The results for each gestation period are shown in Table 1. The χ^2-test shows the statistically significant absence of the righting response (turning to lateral and prone positions) in the experimental group for the entire gestation period ($\chi^2 = 18.66$, df = 1, $p = 0.000$, $p < 0.05$). Comparison of the experimental and control group for the period from the 31st day to the 50th day of gestation shows a statistically significant absence of the righting reflex (turning to a lateral or prone position) ($\chi^2 = 8.10$, df = 1, $p = 0.004$, $p < 0.05$). This difference was also present for the period from the 51st day to the 66th day of gestation (Fisher's exact test $p = 0.002$, df = 1, $p < 0.05$). A comparison of positive responses (turning to a lateral or prone position) in the experimental group between gestation days 31–50 and 51–66 did not show any significant difference ($\chi^2 = 0.76$, df = 1, $p = 0.382$, $p > 0.05$). In the experimental group, significantly more fetuses rotated from supine positions to prone positions in the period from the 51st to the 66th day of gestation than in the period from the 31st to the 50th day of gestation ($\chi^2 = 4.17$, df = 1, $p = 0.0412$, $p < 0.05$). Turning from a supine to lateral position did not

Table1. Distribution of responses in experimental (Exp) and control (Con) groups

Fetal responses after being placed in supine position	Gestation days								Total	
	31–40		41–50		51–60		61–66			
	Exp	Con	Exp	Con	Exp	Con	Exp	Con	Exp	Con
Negative response	21	12	20	12	18	12	10	6	69	42
Fetuses turning to prone position	2	0	0	0	3	0	5	0	10	0
Fetuses turning to lateral position	7	0	10	0	9	0	3	0	29	0

decrease significantly as gestation advanced ($\chi^2 = 0.83$, df = 1, $p = 0.3616$, $p > 0.05$).

In both the experimental and the control group, the contact-righting reflex was present in all newborns. All newborns rotated immediately after being placed in a supine position, without any latency.

Discussion

Ultrasound observation of the fetuses in this study showed that fetuses change their positions by pushing their legs against the intrauterine walls and by stretching their trunks while leaning against the intrauterine walls. In addition, it was observed that after the 40th day of gestation, the fetus does not float in the intrauterine cavity but rather leans with a great portion of its body against the intrauterine wall. This suggests that the fetus changes its position from a supine to prone using the contact-righting form of the reflex. A more detailed study of fetal movements will be possible only with real-time three-dimensional ultrasound imaging.

Although there was no difference in the frequency of positive responses (rotation to a lateral or prone position) between the observed gestation periods in the experimental group (gestation days 31–50 vs. 51–66), the proportion of successful rotations to prone positions significantly increased in the second part of gestation. This corresponds with the results of an earlier study in which, as mentioned before, this reflex was present after the 60th day of gestation among prematurely born offspring. In the period from the 51st to the 66th day of gestation, compared with the period from the 31st to the 50th day of gestation, there were less frequent lateral rotations, which could also suggest maturation of the reflex. However, the difference was not statistically significant. Similar results showing that the incidence of prone rotation increases among older specimens have also been found in the field mouse, the Norway rat, the roof rat, and the cat (Pellis et al.1991)

The righting reflex from a supine to a prone position was present in all offspring on the first day of extrauterine life. This finding is substantially different from the intrauterine frequency of the reflex in the period from the 61st to the 66th day of gestation (27.7%). A possible explanation is that fetuses are less mobile than preterm offspring of the same age because increased restraint *in utero* (Robinson and Smotherman 1992). Additionally, the shape of the intrauterine cavity, which remains the same despite any changes in the orientation of the gravitational vector, may favor certain fetal positions.

The complete absence of any change in fetal positioning in the control group suggests that the changes in the experimental group did not result from passive fetal movements during the manipulation of the pregnant females. In order to achieve extended righting-reflex latency in the adult guinea pig, administration of a new dose of diazepam is needed before every examination (Scott et al. 1994). Daily intraperitoneal administration of diazepam in pregnant rats in the second half of gestation has no effect on the maturation of the righting reflexes in their offspring (Laitinen et al. 1986; Schlumpf et al. 1989). This shows that the administration of diazepam in the control group had only a temporary effect on the inhibition of the righting reflex. The positive contact-righting reflex in all litters from the control group supports this conclusion.

The results of our study demonstrate that fetal behavior may be partly gravity-dependent, as suggested earlier (Sekulić 2000). The results also indicate the presence of the prenatal and postnatal continuity of the influence of gravity. Likewise, the results of this study are in agreement that the development of the righting reflex from a supine position to a prone position is retarded in microgravity conditions (Ronca and Alberts 2000; Walton et al. 2005).

Acknowledgement. This study was supported by the Serbian Ministry of Science and Environmental Protection, grant No. 143021/2006.

References

Avery G. T. (1928): Responses of foetal guinea pigs prematurely delivered. Genet. Psychol. Monogr. **3**, 245–331

Fraser A. F. (1989): A monitored study of major physical activities in the perinatal calf. Vet. Rec. **125**, 38–40

Heywood P., Pujol R., Hilding D. A. (1976): Development of the labyrinthine receptors in the guinea pig, cat and dog. Acta. Otolaryngol. **82**, 352–367

Huisman T. A., Martin E., Kubik-Huch R., Marincek B. (2002): Fetal magnetic resonance imaging of the brain: technical considerations and normal brain development. Eur. Radiol. **12**, 1941–1951

Husa L., Bieger D., Fraser A. F. (1988): Fluroscopic study of the birth posture of the sheep fetus. Vet. Rec. **123**, 645–648

Laitinen K., MacDonald E., Saano V. (1986): Effects of diazepam, tofiyopam or phenytoin during foetal development on subsequent behaviour and benzodiazepine receptor characteristics in rats. Arch. Toxicol. Suppl. **9**, 51–54

Pellis S. M., Pellis V. C., Chen Y. C., Barzci S., Teitelbaum P. (1989): Recovery from axial apraxia in the lateral hypothalamic labyrinthectomized rat reveals three elements of contact-righting: cephalocaudal dominance, axial rotation, and distal limb action. Behav. Brain. Res. **35**, 241–251

Pellis V. C., Pellis S. M., Teitelbaum P. (1991): A descriptive analysis of the postnatal development of contact-righting in rats *(Rattus norvegicus)*. Dev. Psychobiol. **24**, 237–263

Robinson S. R., Smotherman W. P. (1992): Fundamental motor patterns of the mammalian fetus. J. Neurobiol. **23**, 1574–1600

Ronca A. E., Alberts J. R. (2000): Effects of prenatal spaceflight on vestibular responses in neonatal rats. J. Appl. Physiol. **89**, 2318–2324

Schlumpf M., Ramseier H., Abriel H., Youmbi M., Baumann J. B., Lichtensteiger W. (1989): Diazepam effects on the fetus. Neurotoxicology **10**, 501–516

Scott S. J., Smith P. F., Darlington C. L. (1994): Quantification of the depressive effects of diazepam on the guinea pig righting reflex. Pharmacol. Biochem. Behav. **47**, 739–741

Sekulić S. R. (2000): Possible explanation of cephalic and non-cephalic presentation during pregnancy: a theoretical approach. Med. Hypotheses **55**, 429–434

Sekulić S. R., Lukač D., Drapšin M., Čapo I., Lalošević D., Novakov-Mikić A. (2009): Ultrasonographic observations of the maturation of basic movements in guinea pig fetuses. Cent. Eur. J. Biol. **4**, 58–61

Sobin A., Anniko M. (1983): Embrionic development of the specific vestibular hair cell pathology in a strain of the waltzing guinea pig. Acta. Otolaryngol. **96**, 397–405

Ungar W., Ecobichon D. J. (1986): Diazepam metabolism in the guinea pig materno- fetal model: effects of cigarette smoke. Drug. Chem. Toxicol. **9**, 205–221

Walton K. D., Harding S., Anschel D., Harris Y. T., Llinás R. (2005): The effects of microgravity on the development of surface righting in rats. J. Physiol. **565**, 593–608

Watt D. (1976): Responses of cats to sudden falls: an otolith-originating reflex assisstinf landing. J. Neurophysiol. **39**, 257–265

General Physiology and Biophysics

An International Journal

General Physiology and Biophysics appears quarterly and is devoted to the publication of original research papers concerned with general physiology, biophysics and biochemistry at the cellular and molecular level. The coverage of the journal includes:

- membrane physiology and biophysics (ion channels, receptors, transporters, protein-lipid interactions, surface phenomena, model membranes),
- intercellular and intracellular signalling (neurotransmission, endocrine regulations, messengers, secretory mechanisms, regulatory proteins, calcium signalling pathways, nitric oxide),
- excitability and contractility (neurophysiology, smooth, cardiac and skeletal muscle physiology, excitation-contraction coupling, cellular motility),
- biophysical analysis of cellular function (bioenergetics, volume regulation, thermodynamics, mathematical models),
- metabolic regulations (enzymology, ATPases, plant and microbial metabolism),
- cellular aspects of pharmacology, toxicology and pathology (receptor-drug interaction, the action of drugs and toxins on signalling and regulatory functions, free radicals, lipid peroxidation, ischemic preconditioning, calcium paradox),
- accounts of advances in relevant techniques and methodology.

Mini Reviews should not exceed 15 pages. *Review* articles will generally be published by invitation only. Theoretical contributions are acceptable as long as they formulate testable hypotheses. *Short Communications* will be published as quickly as possible. *Letters to the Editor* with comments on findings published in the journal will be also accepted. The language of the journal is English.

INSTRUCTIONS FOR AUTHORS

A. General

Manuscripts should be submitted electronically as an e-mail attachment preferentially to one of the **Editors** according to their fields of expertise (see the list of the Editors) or to the **Editorial Office**. Authors unable to submit the manuscript electronically for technical reasons should contact the Editorial Office, General Physiology and Biophysics, Institute of Molecular Physiology and Genetics, Slovak Academy of Sciences, 833 34 Bratislava, Vlárska 5, Slovakia.

Tel.: +421-2-5932 7705; Fax: +421-2-5477 3666; E-mail: gpb@savba.sk

Website: http://www.gpb.sav.sk

Both Word and PDF versions are required.

The text of the manuscript (including title, Abstract, Key words, main text, References and Figure legends) should be submitted as a single text file (.doc or .rtf). Tables should be uploaded as text (.doc or .rtf) and Figures separately as .jpg, .eps or .tiff files. Standard fonts should be used (Times New Roman or Courier for the general text and Arial for the figures). Authors are required to keep the format and arrangement of the whole text as described in section Preparation of manuscripts.

It is presumed that manuscripts have not been published and have not been simultaneously submitted elsewhere.

B. Preparation of manuscripts

1. *Manuscripts* should be in English, typed double-spaced with 2.5 cm margins, and an unjustified right margin. Use a standard 12 point typeface (e.g., Times, Arial, or Courier) throughout the manuscript. Number each page at the bottom. Use hard return only at the end of paragraphs. Do not use any hyphenation to divide words at the right margin. Please take care to distinguish properly between digit "1" and letter "l" (also 0 and O).
2. Abbreviations in parentheses should be preceded by the full term when first used (except for those which are very common).
3. If you use symbols or special characters the PDF of the corresponding text file must show exactly how they have to look like.
4. Numbers, constants and mathematical operators (sin, cos, log, etc.) should be in regular font as distinguished from variables, which should be written in italics (d*y*/d*x*, not *dy*/*dx*).
5. Scientific investigations involving humans or animals must have approval of the appropriate ethics committee. Animal experiments should be carried out in accordance with EU (86/609/EEC) or the NIH guidelines. Investigations involving humans must be accompanied by a statement that informed consent was obtained from all subjects.
6. The text should be arranged under the following headings: Introduction; Materials and Methods; Results; Discussion; Acknowledgement and References.
7. Title page should include the title of the article, authors' names (first name in full and initials of the middle names), without academic degrees, the name of the institutions, addresses and e-mail address for the first author (in case he (she) is not the corresponding author). Give a short title which should be printed at the head of the right-hand pages of the article. On the bottom give a full name, address and e-mail address of the corresponding author.
8. An *Abstract* of not more than 200 words together with up to 5 key words should be submitted on a separate sheet. If needed, the abbreviations used in the text with their full explanations could be listed here, too.
9. The *References* should be in alphabetical order according to the following format:

   a) *Articles from journals:*

   Hodgkin A. L., Huxley A. F., Katz B. (1952): Measurement of current-voltage relations in the membrane of the giant axon of *Loligo*. J. Physiol. (London) **116**, 424–448

   b) *Monographs:*

   Zachar J. (1971): Electrogenesis and Contractility in Skeletal Muscle Cells. University Park Press, Baltimore and London

c) *Chapters from monographs:*

Haggis G. H. (1964): The structure and function of membranes. In: Introduction to Molecular Biology. (Eds. G. H. Haggis, D. Michie, A. R. Muir, K. B. Roberts and P. M. B. Walker), pp. 151–192, Longmans, London

Abbreviation of journal titles should correspond to those used in Current Contents. In case of any doubt the way how the journal quotes itself should be used. Personal communications or unpublished papers should not be included in the list of references. In the text the name of the author should be followed by the year of publication. Where there are more than two authors, only the first should be named, followed by "et al.".

Articles may only be cited as "in press" when a copy of the acceptance notice is supplied at the time of submission.

10. *Illustrations:*

a) *Tables* including appropriate headings must be typed on separate sheets and numbered in consecutive order as cited in the text. Other data or legends should be given as footnotes below the tables.

b) *Graphs* and *diagrams* should be in a form suitable for reproduction. Use quality graphic programs such as Adobe Photoshop, Adobe Illustrator, Corel Draw, or Freehand. Line graphic should be saved as .eps, .tiff or .jpg files (600 dpi).

c) *Halftone photographs* should be arranged in layouts and submitted in the exact size for printing and saved as .tiff or .jpg (300 dpi).

d) *Colour photographs* will be only printed at the discretion of the Editors. The publisher will provide the author with the precise cost estimate when the figures are received (the cost per a single page containing picture(s) printed in colour is Euro 100).

11. *Figure legends* should be typed on a separate page.

12. Numerical data should be expressed in SI units (Système International d'Unités). When expressing concentrations mol/l or $mol \cdot l^{-1}$ instead of M should be used.

13. *Short Communications* should be limited to six pages without section headings including a maximum of three figures and an Abstract of not more than 100 words.

14. The Editors will not accept a series of papers with the same main title followed by "part I", "part II", etc. Each paper should have its own title.

15. Authors not entirely familiar with English should seek a native English-speaking colleague or professional service for advice on correct syntax and word usage. Correct style and word usage, however, are the responsibility of the author(s). Spelling may be British or American, but it must be consistent throughout the text. Manuscripts submitted in poor English may be returned to the author(s) and there will be a delay in publication.

16. All contributions get carefully reviewed by our Field Editors. The final decision whether a specific manuscript may be accepted for publication in General Physiology and Biophysics will be made by the Editors. Authors are encouraged to suggest up to three names (including postal address, phone and e-mail address) to be added to our list from which referees will be selected. Authors may exclude referees as well.

17. The corresponding author will receive proofs by e-mail in PDF format. Authors are requested to check the proofs and return any corrections within 48 hours. The corresponding author, at no cost, will obtain a PDF file of the article *via* e-mail. Reprints are available, provided the order to *koresp@aepress.sk* is received with the corrected proofs.